Final Report

A STUDY ON THE PROPERTIES OF SOLID ADSORBENTS FOR THE DESIGN OF REGENERATIVE CO$_2$ REMOVAL SYSTEMS

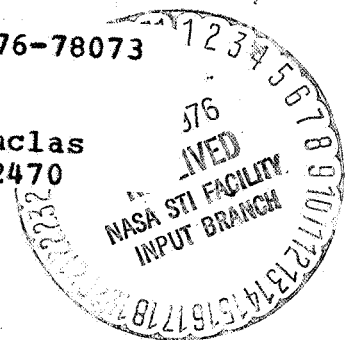# APOLLO APPLICATIONS PROGRAM ENVIRONMENTAL CONTROL/LIFE SUPPORT SYSTEM

Contract NAS 9-3541

67-1751
February 1968

Prepared for

The National Aeronautics and Space Administration
Manned Spacecraft Center
Houston, Texas

GARRETT

AIRESEARCH MANUFACTURING DIVISION
Los Angeles, California

FOREWORD

This report was prepared by the AiResearch Manufacturing Division of The Garrett Corporation, Los Angeles, California, to summarize and report the findings of Task B-3 of Phase IB, "Regenerative CO_2 Removal R&D," of Contract NAS 9-3541.

The program was sponsored by the National Aeronautics and Space Administration, Manned Spacecraft Center, Houston, Texas, and was monitored by Mr. Wilbert Ellis of the Crew Systems Division.

The study and research work was performed by AiResearch under the direction of J. P. Byrne, Program Manager. Experimental Studies were conducted by S. Steinberg, J. Littman, and R. Haug; and analytical investigations by P. Fukunaga and Dr. K. C. Hwang of AiResearch and Drs. J. Winnick, S. Davis, and L. Dell'Osso of NASA.

CONTENTS

CONTENTS (Continued)

CONTENTS (Continued)

CONTENTS (Continued)

ILLUSTRATIONS

ILLUSTRATIONS (Continued)

ILLUSTRATIONS (Continued)

ILLUSTRATIONS (Continued)

ILLUSTRATIONS (Continued)

ILLUSTRATIONS (Continued)

ILLUSTRATIONS (Continued)

ILLUSTRATIONS (Continued)

ILLUSTRATIONS (Continued)

TABLES

SECTION I

INTRODUCTION

The Apollo Applications Program Environmental Control and Life Support System (AAP EC/LSS) development contract, NAS 9-3541, has as its objective the identification and development of the new subsystems and components necessary to extend the life and performance of the present Block II Apollo environmental control and life support system for potential AAP missions. One of the major new subsystems identified in the Phase IA study portion of the program was a regenerative CO_2 removal system to replace the expendable LiOH absorbent CO_2 control method presently used.

This report summarizes the results of a one-year research program conducted by AiResearch on the fundamental properties of solid adsorbents and methods for design and performance prediction of systems using these materials.

The work was conducted with the help and direction of personnel of the Crew Systems Division of the NASA Manned Spacecraft Center, particularly Mr. Wilbert Ellis, Dr. Samuel Davis, and Dr. Jack Winnick.

The basic objective of this work was to provide the data and analytical techniques necessary to design a regenerative CO_2 removal unit for the AAP EC/LSS. Successful conclusion of the task has provided a unique capability to predict, with digital computation techniques, the performance of these previously empirical systems.

SECTION 2

SUMMARY AND CONCLUSIONS

The initial study and analysis activity of this task identified the basic design of the regenerative CO_2 removal unit as one that would utilize the synthetic zeolites, known as molecular sieves, as the CO_2 adsorbent. It was obvious, however, early in the research program that the water vapor always present in the spacecraft atmosphere would degrade to a marked degree the CO_2 adsorption capability of the molecular sieve. Thus, the parallel investigation of silica gel as a regenerative predryer was conducted.

The equilibrium capacity of these materials for CO_2 and water was measured over a wide range of temperatures and pressures, and the performance under dynamic conditions duplicating the adsorption and desorption modes in a real system studied. At the same time a mathematical model was developed, after a review of present-day adsorption theory, that best described the results of testing. This model was developed into a transient digital computer program which predicts the performance of a given design.

One of the most important findings of the program was the profound influence of water vapor on the design. The affinity of the molecular sieve for water, its degradation of CO_2 removal capability, and the extreme difficulty in removing this water once adsorbed by the sieve became a major consideration in system design. It was determined that the understanding of, and design treatment to prevent, the "poisoning" of molecular sieve by water was the secret to a successful regenerative CO_2 removal system.

The report that follows has been organized into five basic sections, each reporting upon a distinct part of the research program.

Section 3 describes and lists the extensive bibliography built up over the course of the program, to provide the reader with a view of the extensive literature on the subject, and divert him to specific areas of interest.

Section 4 provides, as background information, a summation of the present-day theory of fixed bed adsorption, indicating the general mathematical models that have been developed.

Section 5 describes the initial R&D effort devoted to the fundamental properties and performance of molecular sieves and silica gel and summarizes the results obtained.

Section 6 describes the next step undertaken in the laboratory, where a full-scale adsorbent bed was operated under conditions simulating the real installation to confirm and expand the knowledge already developed.

Section 7 describes the digital computer program developed from the analytical investigation, and shows its applicability to the test data and design problems. The appendixes contain additional test data obtained as well as Fortran listings and typical input and output of the computer program.

SECTION 3

BIBLIOGRAPHICAL REVIEW OF SORBENT TECHNOLOGY

RESUME OF LITERATURE

An extensive review of the literature was instituted to determine insights into the problems various investigators had encountered in developing solutions to the complex phenomena of fixed bed sorption analyses.

Examination of the cited papers will show that there are numerous gas-solid contacting operations whose mathematical analysis is quite analogous, if not identical, to that of fixed bed adsorption. Consequently, techniques of solution developed in those fields are directly applicable to adsorption bed analysis.

The following references emphasize these points:

A1, G8, G9, H10, H12, K5, K6, L5, M13, M14, O2, S4, V1, V7, V8

The fundamental review of the whole field of subject matter introduced in this report is:

H10, H11, H12, H17, K8, K9, M5, O2, T3, T1, V7, V8

The ground work for processes exhibiting second-order kinetics was provided by the following references:

A4, H6, T2, T3, W6

Detailed or exacting treatments of intraparticle diffusion are contained in the following references. (Some of these also establish what justification there is for the approximation of Equation (4-1) by a simply formulated kinetic rate law.)

E1, G1, K2, R4, R5, T4, T5, T6, T7

When equations of Table 4-1 are solved neglecting the axial dispersion in Equation (4-1) and substituting kinetic rate laws in place of the full expression for intraparticle diffusion in Equation (4-16), the resulting partial differential equation system is of the hyperbolic type and thus can be solved numerically by means of the method of characteristics as well as by the method of the usual finite differences.

The method of characteristics is discussed in A1, D11, L6, V1.

Finite difference methods are discussed by D11, L6, O1, O2, V1.

The treatment of the full system reduces to a parabolic system. Some general numerical and computational techniques that are available are:

L6, L12, O1, R7, S9

The numerical solution for the full treatment of pore or intraparticle diffusion exemplified by Equation (4-16) and its attendant equations is presented and/or discussed by the following:

E1, G7, U3, R4, R5, T4, T5, T6, T7; the series solution to (4-16) is correlated by: G7, H6, R2.

The following references discuss multicomponent adsorption, adiabatic adsorption, adsorption with reaction, distorted velocity profile, or pressure drop influence:

A1, H16, H17, W1

Standard and current references describing the application to diffusion of mass transfer, pressure drop, axial dispersion studies, and correlations and computational techniques are:

B8, C3, C4, G2, G3, G5, G11, H4, H18, R3, R6, S7, V1, Y2

Basic references for diffusion, especially for the partial specific volume average stressed in Appendix B, are:

B8, C5, C6, D9, S8, S9 (multicomponent systems)

Treatments of longitudinal diffusion, i.e., axial dispersion, are contained in these references:

A2, H3, H17, L3, W2

Reference M4 makes a particular point of isolating surface diffusion from the more usual kind of intraparticle diffusion. Reference B2 is basic for an understanding of the phenomenology of this process. References K10 and K11 present the kinetic viewpoint. The influence of surface migration on adsorption equilibrium is given in the following series of articles:

D2, D3, D4, D5, D6, D7

In fact, in Reference D8, a two dimensional van der Waals equation of state, is developed to characterize a specific adsorption system.

Surprisingly enough, the Polanyi potential theory for adsorption equilibrium (P1) is still finding use today (see G13; also L9 and L10).

Early work on adsorption beds that employed simple or restrictedly applicable equations and references that extend or review these treatments are:

B12, D1, K8, K9, M9, M10 ___/

The following are fairly recent articles that use sorption processes to determine basic fixed bed phenomena such as intraparticle diffusion, heats of adsorption, etc:

G1, G10, H1

BIBLIOGRAPHY

A1 Acrivos, A., "Method of Characteristic Technique: Application to Heat and Mass Transfer Problems," _Ind. Eng. Chem._ 48, 703(1956)

A2 Acrivos, A., "On the Combined Effect of Longitudinal Diffusion and External Mass Transfer Resistance in Fixed Bed Operations," _Chem. Eng. Sci._ 13, 1(1960)

A3 Amundson, N. R., "Mathematics of Adsorption in Beds, Part I," _J. Phys. Colloid Chem._ 52, 1153(1948)

A4 Amundson, N. R., "Mathematics of Adsorption in Beds, Part II," _J. Phys. Colloid Chem._ 54, 812(1950)

A5 Anzelius, A., "Uber Erwärmung vermittels durchströmender Medien," _Z. Angew. Math. Mech._ 6, 291(1926)

B1 Baddour, R. F., and R. D. Hawthorn, "Chromatographic Separation by Ion Exchange," _Ind. Eng. Chem._ 47, 2517(1955)

B2 Barrer, R. M., "A New Approach to Gas Flow in Capillary Systems," _J. Phys. Chem._ 57, 35(1953)

B3 Barrer, R. M., Peterson, D. I. and B. P. Schoenborn,"Separation of Gases by Zeolites," _Science_ 153, 556(1966)

B4 Beaton, R. H., and C. C. Furnas, "Concentration of Dilute Solutions of Electrolytes by Base-Exchange Materials," _Ind. Eng. Chem._ 33, 1500(1951)

B5 Benson, S. W. and J. W. King, Jr.,"Electrostatic Aspects of Physical Adsorption; Implications for Molecular Sieves and Gaseous Anesthesia," _Science_ 150, 1710-1713, December 1965.

B6 Bertsch, L., and H. W. Habgood, "An Infrared Spectroscopic Study of the Adsorption of Water and Carbon Dioxide by Linde Molecular Sieve X", _J. Phys. Chem.,_ 67, 1621-8, (August 1963).

B7 Bieber, H., F. E. Steidler, and W. A. Selke, "Ion Exchange Rate Mechanism," _Chem. Eng. Prog. Symposium Ser._ 50, No. 14, 17(1954)

B8 Bird, R. B., C. F. Curtiss, and J. D. Hirschfelder, "Fluid Mechanics and the Transport Phenomena," _Chem. Eng. Prog. Symposium Ser._ 51, No. 16, 69(1955)

B9 Bird, R. B.,"Theory of Diffusion," Advances in Chemical Engineering, Vol. I, Drew, T. B. and J. W. Hoopes, Jr. eds., Academic Press, N. Y. 1956

B10 Bird, R. T.,"The Equations of Change and the Macroscopic Mass,"_Chem. Eng. Sci._ 6, 123(1957)

BIBLIOGRAPHY (Continued)

B11 Bird, R. B., Stewart, W. E., and E. N. Lightfoot, Transport Phenomena, Wiley, N. Y. 1960

B12 Bohart, G. S., and E. Q. Adams, "Some Aspects of the Behavior of Charcoal with Respect to Chlorine," J. Am. Chem. Soc. 42, 523(1920)

B13 Bowman, J. R. and R. C. Briant, "The Theory of the Performance of Packed Rectifying Columns," Ind. Eng. Chem. 39, 746(1947)

B14 Boyd, G. E., A. W. Adamson, and L. S. Meyers, Jr., "The Exchange Adsorption of Ions from Aqueous Solutions by Organic Zeolites, Part II: Kinetics," J. Am. Chem. Soc. 69, 2836(1947)

B15 Brinkley, Jr., S. R., "Heat Transfer Between a Fluid and a Porous Solid Generating Heat," J. Applied Phys. 18, 582(1947)

B16 Brunauer, S., Emmelt, P. H. and E. Teller, J. Am Chem. Soc. 60, 309 (1938) Adsorption of Gases in Multimolecular Layers

C1 Caddel, J. R., and R. L. Moison, "Mixed-Bed Deionization at High Flow Rates," Chem. Eng. Prog. Symposium Ser. 50, No. 14, 1(1954)

C2 Campbell, M. L., and L. N. Canjar, "Adsorption of Methane from Hydrogen on Fixed Beds of Silica Gel," A. E. Ch. E. J. 8, 540(1962)

C3 Carberry, J. L., and M. W. Wendel, "A Computer Model of the Fixed Bed Catalytic Reactor: The Adiabatic and Quasi-adiabatic Cases," A. I. Ch. E. J. 9, 129(1963)

C4 Chilton, T. H., and A. P. Colburn, "Heat Transfer and Pressure Drop in Empty, Baffled and Packed Tubes, Part II: Pressure Drop in Packed Tubes," Trans. A. I. Ch. E. 26, 178(1931)

C5 Cussler, E. L., Jr. and E. N. Lightfoot, Jr., "Multicomponent Diffusion in Semi-Infinite Systems," A. E. Ch. E. J. 9, 783(1963)

C6 Cussler, E. L., Jr. and E. N. Lightfoot, Jr., "Multicomponent Diffusion in Restricted Systems," A. I. Ch. E. J. 9, 702(1963)

D1 Danby, C. J., J. G. Davoud, R. H. Everett, C. N. Hinshelwood, and R. M. Lodge, "The Kinetics of Adsorption of Gases from an Air Stream by Granular Reagents," J. Chem. Soc. 98 (1946)

D2 DeBoer, J. H., and S. Kruyer, "Entropy and Mobility of Adsorbed Molecules, Part I: Procedure, Atomic Gases on Charcoal," Proc. Kon. Ned. Ad. v. Wet., 55B, 45(1952)

D3 DeBoer, J. H., and S. Kruyer, "Entropy and Mobility of Adsorbed Molecules, Part II: Nitrogen on charcoal," Proc. Kon. Ned. Ak. v. Wet. 56B, 67(1953)

D4 DeBoer, J. H., and S. Kruyer, "Entropy and Mobility of Adsorbed Molecules, Part III: Hydrogen and Oxygen on Charcoal," Proc. Kon. Ned. Ak. v. Wet. 56B, 236(1953)

BIBLIOGRAPHY (Continued)

D5   DeBoer, J. H., and S. Kruyer, "Entropy and Mobility of Adsorbed Molecules, Part IV: Aliphatic Hydrocarbons on Charcoal," Proc. Kon. Ned. Ak. V. Wet. 56B, 415(1953)

D6   DeBoer, J. H., and S. Kruyer, "Entropy and Mobility of Adsorbed Molecules, Part V: CO, CO_2, and CS_2 on Charcoal,""Proc. Kon. Ned. Ad. v. Wet. 57B, 92(1954)

D7   DeBoer, J. H., and S. Kruyer, "Entropy and Mobility of Adsorbed Molecules, Part VI: Polar Gases on Charcoal," Proc. Kon. Ned. Ak. v. Wet. 58B, 61(1955)

D8   DeBoer, J. H., and S. Kruyer, "The Two-Dimensional van der Waals Constants of Molecules Adsorbed on Charcoal and Graphite," Trans. Faraday Soc. 54, 540(1958)

D9   DeGroot, S. R., and P. Mazur,"Non-Equilibrium Thermodyanmics,"Interscience, N. Y., 1962

D10   Devault, D., "The Theory of Chromatograph," J. Am. Chem. Soc. 65, 532(1943)

D11   Dranoff, J. S., and L. Lapidus, "Multicomponent Ion Exchange Column Calculations," N.Y.U. - I.B.M. Symposium on Digital Computing in the Chemical and Petrochemical Industries P. 63 1958 N.Y.

E1   Edeskuty, F. J., and N. R. Amundson, "Mathematics of Adsorption, Part IV: Effect of Intraparticle Diffusion in Agitated Static Systems," J. Phys. Chem. 56, 148(1952)

F1   Fitts, D. D., Nonequilibrium Thermodynamics, McGraw-Hill, N.Y., 1962

F2   Ford, F. E., and D. D. Perlmutter, "Mass Transfer Effects in Surface Catalysis," A. I. Ch. E. J. 9, 371(1963)

F3   Frish, N. W., and F. X. McGarvey, "Application of Ion Exchanger Equilibrium Relationships to Process Design," Chem. Eng. Prog. Symposium Ser. 55, No. 24, (1959)

F4   Frisch, N. W., and R. Kunin, "Kinetics of Mixed-Bed Deionization, Part I," A. I. Ch. E. J. 6, 640(1960)

F5   Funk, J. E.,and G. Houghton,"A Mathematical Model for Gas-Liquid Partition Chromatography," Nature 188, 389(1960)

F6   Funk, J. E. and G. Houghton,"A Lumped-Film Model for Gas-Liquid Partition Chromatography, Part I Numerical Methods of Solution," J. Chromatog. 6, 193(1961)

BIBLIOGRAPHY (Continued)

F7   Funk, J. E. and G. Houghton, "A Lumped-Film Model for Gas-Liquid Partition Chromatography, Part II Experimental Evaluation of Analytical Solutions," J. Chromatog. 6, 281(1961)

F8   Furnas, C. C., "Heat Transfer from a Gas Stream to a Bed of Broken Solids," Trans. A. I. Ch. E. 24, 142(1930)

F9   Furnas, C. C., "Heat Transfer from a Gas Stream to a Bed of Broken Solids," Ind. Eng. Chem. 22, 26(1930)

F10   Furnas, C. C., "Heat Transfer from a Gas Stream to a Bed of Broken Solids," Ind. Eng. Chem. 22, 721(1930)

G1   Gale, R. L., and R. A. Beebe, "Determination of Heats of Adsorption on Carbon Blacks and Bone Mineral by Chromatography Using the Eluted Pulse Technique," J. Phys. Chem. 68, 555(1964)

G2   Gamson, B. W., G. Thodos. and D. A. Hougen, "Heat, Mass and Momentum Transfer in the Flow of Gases through Granular Solids," Trans. A. I. Ch. E. 39, 1(1943)

G3   Gamson, B. W., "Heat and Mass Transfer: Fluid Solid Systems," Chem. Eng. Prog. 47, 19(1951)

G4   Geser, J. J., and L. N. Canjar, "Adsorption of Methane and Hydrogen on Packed Beds of Activated Carbon," A. I. Ch. E. J. 8, 494(1962)

G5   Giddings, J. C., and S. L. Seager, "Method for Rapid Determination of Diffusion Coefficients, Theory and Application," Ind. Eng. Chem. Fund 1, 277(1962)

G6   Gilliland, E. R., and R. F. Baddour, "The Rate of Ion Exhcnange," Ind. Eng. Chem. 45, 330(1953)

G7   Glueckauf, E., "Theory of Chromatography, Part 10: Formulae for Diffusion into Spheres and their Application to Chromatography," Trans. Faraday Soc. 51, 1540(1955)

G8   Goldstein, S., "On the Mathematics of Exchange Processes in Fixed Columns, Part I: Mathematical Solutions and Asymptotic Expansions," Proc. Roy. Soc. A, 219, 15(1953)

G9   Goldstein, S., "On the Mathematics of Exchange Processes in Fixed Columns, Part II: The Equilibrium Theory as the Limit of the Kinetic Theory," Proc. Roy. Soc. A, 219, 171(1953)

G10   Gorring, R. L., and A. J. DeRosset, "Gas Diffusion in Porous Catalysts: Diffusion-Controlled Elution of Physically Adsorbed Hydrocarbons," J. Catalysis 3, 341(1964)

BIBLIOGRAPHY (Continued)

G11 Gottschlich, C. F., "Axial Dispersion in a Packed Bed," <u>A. I. Ch. E. J. 9</u>, 88(1963)

G12 Grapham, D., "Adsorption Equilibrium," <u>Chem. Prog. Symposium Ser. 55,</u> No. 24(1959)

G13 Grant, R. J., and M. Manes, "Correlation of Some Gas Adsorption Data Extending to Low Pressures and Supercritical Temperatures," <u>Ind. Eng. Chem. Fund.</u>3, 221(9164)

H1   Habgood, H. W., and J. F. Hanlan, "A Gas Chromatographic Study of the Adsorptive Properties of a Series of Activated Charcoals," <u>Can J. Chem. 31,</u> 843(1959

H2   Harkins, W. D. and Jura, G., "Surfaces of Solids. XII An Absolute Method for the Determination of the Area of a Finely Divided Crystalline Solid," <u>J. Am. Chem. Soc. 66</u>, 1362(1944)

H3   Hashimoto, I., Deshpande, K. B. and H. C. Thomas, "Peclet Numbers and Retardation Factors for Ion Exchange Columns," <u>Ind. Eng. Chem. Fund.</u>3, 216(1964)

H4   Hatfield, M. R., "Fluid Flow Through Porous Carbon," <u>Ind. Eng. Chem. 31</u>, 1419(1959)

H5   Heifferick, F., and M. S. Plesset, "Ion Exhange Kinetics: A Nonlinear Diffusion Problem," <u>J. Chem. Phys. 28</u>, 418(1958)

H6   Heitner-Wirguin, C., and G. Markovits, "Kinetics of Ion Exchange in the Chelating Resin Bio-Chelex 100, Part I: The Exchange of the Alkaline Earth Ions," <u>J. Phys. Chem. 67</u>, 2263(1963)

H7   Hellums, J. D., and S. W. Churchill, "Simplification of the Mathematical Description of Boundary and Initial Value Problems," <u>A. I. Ch. E. J. 10</u>, 110(1964)

H8   Hersh, C. K., Molecular Sieves, Reinhold Publishing Corp., N. Y., (1961)

H9   Hiester, N. K., and T. Vermeulen, "Elution Equations for Adsorption and Ion Exchange in Flow Systems," <u>J. Chem. Phys. 16</u>, 1087(1948)

H10 Hiester, N. K., and T. Vermeulen, "Saturation Performance of Ion-Exchange and Adsorption Columns," <u>Chem. Eng. Prog. 48,</u> 505(1952)

H11 Hiester, N. K., S. B. Radding, R. L. Nelson, Jr., and T. Vermeulen, "Interpretation and Correlation of Ion Exhcnage Column Performance under Nonlinear Equilibia," <u>A. I. Ch. E. J. 2,</u> 404(1956)

H12 Hiester, N. K., and T. Vermeulen, and G. Klein, "Adsorption and Ion Exchange," Section 16, Chemical Engineers' Handbook, (Perry), 4th edition (1963)

H13 Hill, T. L.,"Theory of Physical Adsorption," Advances in Catalysis, Vol. IV, Academic Press, N. Y. (1952)

H14 Hill, T. L., Thermodynamic of Small Systems, 2 vols., Benjamin, N. Y. (1963-1964)

H15 Hobson, J. P. and R. A. Armstrong, A Study of Physical Adsorption at Very Low Pressures Using Ultrahigh Vacuum Techniques, J. Phys. Chem. 67, 2000(1963)

H16 Hougen, D. A., and W. R. Marshall, Jr., "Adsorption from a Fluid Stream Flowing through a Stationary Granular Bed," Chem. Eng. Prog. 43, 197(1947)

H17 Houghton, G., "Band Shapes in Non-Linear Chromatography with Axial Dispersion," J. Phys. Chem. 67, 84(1963)

H18 Huang, C. J., and C. H. Kuo, "General Mathematical Model for Mass Transfer Accompanied by Chemical Reaction," A. I. Ch. E. J. 9, 161(1963)

K1 Kasten, P. R., and N. R. Amundson, "An Elementary Theory of Adsorption in Fluidized Beds: Mathematics of Adsorption in Beds," Ind. Eng. Chem. 42, 1342(1950)

K2 Kasten, P. R., L. Lapidus, and N. R. Amundson, "Mathematics of Adsorption in Beds, Part V: Effect of Interparticle Diffusion in Flow Systems in Fixed Beds," J. Phys. Chem. 56, 683(1952)

K3 Kel'tsev, N. V., Kinetics of Desorption of Water Vapor and Carbon Dioxide from Zeolites under Vacuum, Gazovaya Promyshlennost' (Gas Industry) 4 51-54(1964)

K4 Kington, G. L., and A. C. Macleod, Trans. Faraday Society, 55, 1799 (1959)

K5 Klinkenberg, A., "Numerical Evaluation of Equations Describing Transient Heat and Mass Transfer in Packed Solids," Ind. Eng. Chem. 40, 1992(1948)

K6 Klinkenberg, A., "Heat Transfer in Cross Flow Heat Exchangers and Packed Beds: Evaluation of Equations for Penetration of Heat or Solutes," Ind. Eng. Chem. 46, 2285(1954)

K7 Klinkenberg, A., "Equations for Transient Heat Transfer in Packed Beds," A.I. Ch. E. J. 8, 703(1962)

K8 Klotz, I. M., "The Adsorption Wave," Chem. Revs. 39, 241(1946)

K9 Klotz, I. M., "The Adsorption Wave," Chapter 1 in Handbook on Aerosols, (TID-4500, 27 ed.), U.S.A.E.C., Washington, D.C., 1950, Reissued 1963

K10 Kovach, J. L., Principles of Adsorption, Barneby-Cheney Co., Columbus, Ohio

K11 Kruyer, S., "Hopping Molecules and Surface Migration," Proc. Kon. Ned. Ak. v. Wet. 56B, 274(1953)

K12 Kruyer, S., "The Time of Adsorption and the Time of Oscillation," Proc. Kon. Ned. Ak. v. Wet. 58B, 73(1955)

L1 Lapidus, L., and N. R. Amundson, "Mathematics of Adsorption in Beds, Part III," J. Phys. Chem. 54, 821(1950)

L2 Lapidus, L., and N. R. Amundson, "The Rate-Determining Steps in Radial Adsorption Analysis," J. Phys. Chem 56, 373(1952)

L3 Lapidus, L., and N. R. Amundson, "Mathematics of Adsorption in Beds, Part VI: The Effect of Longitudinal Diffusion in Ion Exchange and Chromatographic Column," J. Phys. Chem. 56, 984(1952)

L4 Lapidus, L., and J. B. Rosen, "Experimental Investigations of Ion Exchange Mechanisms in Fixed Beds by Means of an Asymptotic Solution," Chem. Eng. Prog. Symposium Ser. 50, No. 14, 97(1954)

L5 Lapidus, L., "Sorption Processes: Granular Processes-Adsorption," Chem. Eng. Prog. 53, 517(1957)

L6 Lapidus, L., Partial Differential Equations in Digital Computation for Chemical Engineers, McGraw-Hill, N.Y. (1962)

L7 Ledoux, E., Vapor Adsorption, Industrial Applications and Competing Processes, Chemical Publishing Co., N.Y.(1945)

L8 Ledoux, E., "Dynamic Cooling of Adsorbent Beds," Ind. Eng. Chem. 40, 1970(1948)

L9 Lewis, W. K., E. R. Gilliland, B. Chertow, and W. P. Cadogan, "Adsorption Equilibria: Hydrocarbon Gas Mixtures," Ind. Eng. Chem. 42, 1319(1950)

L10 Lewis, W. K., E. R. Gilliland, B. Chertow, and W. P. Cadogan, "Adsorption Equilibrium: Pure Gas Isotherms," Ind. Eng. Chem. 42, 1326(1950)

L11 Löf, G. O. G., and R. W. Hawley, "Unsteady-State Heat Transfer Between Air and Loose Solids," Ind. Eng. Chem. 40, 1061(1948)

L12 Lundberg, J. L., M. B. Wilk, and M. J. Huyett, "Sorption Studies Using Automation and Computation," Ind. Eng. Chem. Fund. 2, 37(1963)

M1 Mantell, C. L., Industrial Carbon, Van Nostrand, N. Y. (1946) 2nd edn.

M2 Mantell, C. L., Adsorption, McGraw-Hill, N. Y. (1951) 2nd edn.

M3 Marks, D. E., Robinson, R. J., Arnold, C. W., and Hoffmann, A. E., "Dynamic Behavior of Fixed-Bed Adsorbers," J. Petrol. Technol. 15, 433(1963)

BIBLIOGRAPHY (Continued)

M4 Masamune, S., and J. M. Smith, "Pore Diffusion in Silver Catalysts," <u>A. I. Ch. E. J. **8**</u>, 217(1962)

M5 Masamune, S., and J. M. Smith, "Adsorption Rate Studies: Significance of Pore Diffusion," <u>A. I. Ch. E. J. 10</u>, 247(1964)

M6 Masamune, S., and J. M. Smith, "Adsorption Rate Studies: Interaction of Diffusion and Surface Processes," <u>A. I. Ch. E. J. 11</u>, 34(1965)

M7 Masamune, S., and J. M. Smith, "Adsorption of Ethyl Alcohol on Silica Gel," <u>A. I. Ch. E. J. 11</u>, 41(1965)

M8 McConnachie, J.T.L., and G. Thodos, "Transfer Processes in the Flow of Gases Through Packed and Distended Beds," <u>A. I. Ch. E. J. 9,</u> 60(1963)

M9 Mecklenburg, W., "Über Schichtenfiltration, ein Beitrag zur Theorie der Gasmaske," <u>Z. Elecktrochem. 31</u>, 488(1925)

M10 Mecklenburg, W., "Über Schichtenfiltration, ein Beitrag zur Theories der Gasmaske, II," <u>Kolloid Z. 52</u>, 88(1930)

M11 Michaels, A. S., "Simplified Method of Interpreting Kinetic Data in Fixed-Bed Ion Exchange," <u>Ind. Eng. Chem. 44</u>, 1922(1952)

M12 Moison, R. L., and H. A. O'Hern, Jr., "Ion Exchange Kinetics," <u>Chem. Eng. Prog. Symposium Ser. 55</u>, No. 24, 71(1959)

M13 Monet, G. P., "Adsorption, Dialysis and Ion Exchange," <u>Chem. Eng. Prog. 53,</u> 514(1957)

M14 Monet, G. P., "Similarities in Adsorption, Dialysis, and Ion Exchange," <u>Chem. Eng. Prog. Symposium Ser. 55,</u> No. 24 (1959)

N1 Nutter, J. I., and G. Burnet, Jr., "Drying of Air by Fixed Bed Adsorption with Molecular Sieves," <u>A. I. Ch. E. J. 9</u>, 202(1963)

O1 O'Brien, G. G., M. A. Hyman, and S. Kaplan, "A Study of the Numerical Solution of Partial Differential Equations," <u>J. Math. Phys. 29</u>, 223(1951)

O2 Opler, A., and N. K. Hiester, <u>Tables for Predicting the Performance of Fixed-Bed Ion Exchange</u>, Stanford Research Institute, Stanford, California

P1 Polanyi, M., "Adsorption and the Origin of Adsorption Forces," <u>Z. Electrochem. 26</u>, 370(1920)

R1 Rao, M. R., and J. M. Smith, "Diffusion Resistances in Alumina and Silica Catalysts," <u>A. I. Ch. E. J. 9</u>, 485(1963)

R2 Reichenberg, D., "Properties of Ion-Exchange Resins in Relation to their Structure, Part III: Kinetics of Exchange," <u>J. Am. Chem. Soc. 75</u>, 589(1953)

R3 Roemer, G., J. S. Dranoff, and J. M. Smith, "Diffusion in Packed Beds at Low Flow Rates," <u>Ind. Eng. Chem. Fund. 1</u>, 284(1962)

BIBLIOGRAPHY (Continued)

R4   Rosen, J. B., "Kinetics of a Fixed Bed System for Solid Diffusion into Spherical Particles," J. Chem. Phys. 20, 387(1952)

R5   Rosen, J. B., "General Numerical Solution for Solid Diffusion in Fixed Beds," Ind. Eng. Chem. 46, 1590(1954)

R6   Rothfeld, L. B., "Gaseous Counterdiffusion in Catalyst Pellets," A. I. Ch. E. J. 9, 19(1963)

R7   Round, G. F., R. Newton, and P. J. Redberger, "Variable Mesh Size in Iteration Methods of Solving Partial Differential Equations and Application to Heat Transfer," Chem. Eng. Prog. Symposium Ser. 58, No. 37, 29(1962)

S1   Schmelzer, E. R., M. C. Molstad, and P. F. Hagerty, "Selective Adsorption of Toluene and n-Heptane by Silica Gel," Chem. Eng. Prog. Symposium Ser. 55, No. 24, 209(1959)

S2   Schumann, T. E. W., "Heat Transfer: A Liquid Flowing Through a Porous Prism," J. Franklin Inst. 208, 405(1929)

S3   Selke, W. A., and H. Bliss, "Application of Ion Exchange Copper-Amberlite IR-120 in Fixed Beds," Chem. Eng. Prog. 46, 509(1950)

S4   Selke, W. A., "Sorption Processes, Granular Processes-Ion Exchange," Chem. Eng. Prog. 53, 601(1957)

S5   Sherry, H. S., "Separation of Gases by Zeolites," Science 153, 555(1966)

S6   Smith, S. B., A. X. Heltgen, and A. J. Juhola, "Kinetics of Batch Adsorption of Dichlorophenol on Activated Carbon," Chem. Eng. Prog. Symposium Ser. 55, No. 24(1959)

S7   Stahel, E. P., and C. J. Geankoplis, "Axial Diffusion and Pressure Drop of Liquids in Porous Media," A. I. Ch. E. J. 10, 174(1964)

S8   Stewart, W. E., "Forced Convection in Three-Dimensional Flows, Part I: Asymptotic Solutions for Fixed Interfaces," A. I. Ch. E. J. 9, 528(1963)

S9   Stewart, W. E., and R. Prober, "Matrix Calculation of Multicomponent Mass Transfer in Isothermal Systems," Ind. Eng. Chem. Fund. 3, 225(1964)

S10   Stone, H. L., and P. L. T. Brian, "Numerical Solution of Convective Transport Problems," A. I. Ch. E. J. 9, 68(1963)

T1   Thiele, E. W., "Material or Heat Transfer Between a Granular Solid and Flowing Fluid, Present Status of Theory," Ind. Eng. Chem. 38, 646(1946)

BIBLIOGRAPHY (Continued)

T2   Thomas, H. C., "Heterogeneous Ion Exchange in a Flowing System," J. Am. Chem. Soc. 66, 1664(1944)

T3   Thomas, H. C., "Chromatography: A Problem in Kinetics," Ann. N. Y. Acad. Sci. 49, 161(1948)

T4   Thomas, H. C., "Solid Diffusion in Chromatography," J. Chem. Phys. 19 1213(1951)

T5   Tien, C., and G. Thodos, "Ion Exchange Kinetics for Systems of Nonlinear Equilibrium Relationships," A. I. Ch. E. J. 5, 373(1959)

T6   Tien, C. and G. Thodos, "Ion Exchange Kinetics for Systems of Linear Equilibrium Relationships," A. I. Ch. E. J. 6, 364(1960)

T7   Tien, C., "Adsorption Kinetics of a Nonflow System with Nonlinear Equilibrium Relationship," A. I. Ch. E. J. 7, 410(1961)

T8   Treybal, R. E., Mass Transfer Operations, McGraw-Hill, N. Y. (1955)

V1   Van Arsdel, W. B., "Simultaneous Heat and Mass Transfer in a Nonisothermal System: Through-Flow Drying in the Low-Moisture Range," Chem. Eng. Prog. Symposium Ser. 51, No. 16, 47(1955)

V2   Vasishth, R. C., and M. M. David, "Rate Studies in Concentrated Solutions," A. I. Ch. E. J. 5, 394(1959)

V3   Vassiliou, B., and J. S. Dranoff, "The Kinetics of Ion Exclusion," A. I. Ch. E. J. 8, 248(1962)

V4   Vermeulen, T., and N. K. Hiester, "Ion-Exchange Chromatography of Trace Components," Ind. Eng. Chem. 44, 636(1952)

V5   Vermeulen, T., "Theory for Irreversible and Constant-Pattern Solid Diffusion," Ind. Eng. Chem. 45, 1664(1953)

V6   Vermeulen, T., and N. K. Hiester, "Ion-Exchange and Adsorption Column Kinetics with Uniform Partial Presaturation," J. Chem. Phys. 22, 96(1954)

V7   Vermeulen, T., "Separation by Adsorption Methods," Advances in Chemical Engineering, Vol II, (T. B. Drew and J. W. Hoopes, Jr., eds.), Academic Press. N. Y. (1958)

V8   Vermeulen, T., and N. K. Hiester, "Kinetic Relationships for Ion Exchange Processes," Chem. Eng. Prog Symposium Ser. 55, No. 24, 61(1959)

W1   Walter, J. E., "Multiple Adsorption from Solutions," J. Chem. Phys. 13, 229(1945)

BIBLIOGRAPHY(Continued)

W2   Wicke, E., "Empirische und theoretische Untersuchungen der Sorptionsgesch-
      windigkeit von Gasen an porösen Stoffen II," Kolloid Z. 86, 295(1939)

W3   Wilke, C. R., and O. A. Hougen, "Mass Transfer in the Flow of Gases
      through Granular Solids Extended to Low Modified Reynolds Numbers,"
      Trans. A. I. Ch. E. 61, 445(1945)

W4   Wernick, M. Task No. 33 in Report CB-1004, Collective Protection
      Against CB Agents by Makowski, J., et al., AD 462, 636 Garrett
      Corporation, AiResearch Manufacturing Company Division, Los Angeles,
      California. Contract DA-18-035-AMC-279(A) for Chemical Research and
      Development Laboratories, U.S. Army Edgewood Arsenal, Maryland,
      April 1965.

W5   Wernick, M., Task No. 33 in Report CB-1006, Collective Protection Against
      CB Agents by Makowski, J., et al., AD473,535 Garrett Corporation, AiResearch
      Manufacturing Company Division, Los Angeles, California. Contract
      DA-18-035-AMC-279(A) for Chemical Research and Development Laboratories,
      US Army Edgewood Arsenal, Maryland, September 1965.

W6   Wernick, M. AiResearch Manufacturing Company Proposal SS-3094, Vol. 2,
      Section 2, Exhibit A Technical Discussion, 1964.

W7   Wheeler, A., Task No. 12 in Report CB 1008, vol. 1, Collective Protection
      Against CB Agents by Makowski, J., et. al., AD 480511. Garrett
      Corporation, AiResearch Manufacturing Company Division, Los Angeles,
      Califronia. Contract DA-18-035-AMC-279(A) for Physical Research Laboratory,
      U.S. Army Edgewood Arsenal, Maryland, February 1966.

Y1   Yoshida, F., "Gas-Film Mass Transfer in a Packed Column," Chem. Eng.
      Prog. Symposium Ser. 51, No. 16, 59(1955)

Y2   Yoshida, F., Ramaswami, D., and O. A. Hougen, "Temperatures and Partial
      Pressures at the Surfaces of Catalyst Particles," A. I. Ch. E. J. 8,
      5(1962)

SECTION 4

FUNDAMENTAL BASIS OF THERMODYNAMICS AND KINETICS FOR FIXED BED SORPTION PROCESSES

INTRODUCTION

Adsorption processes that occur in fixed beds can be studied from two general points of view. If the process is allowed to take place over a relatively long period of time for a fixed amount of gas, i.e., a batch process, then equilibrium considerations are of first importance. On the other hand, if a flow or cycling process is of practical interest, i.e., a gas flows over the solid which may alternately adsorb or desorb constituents from the stream, then dynamical or transport considerations may also become important.

Historically, the static process has received prior study; data correlations at constant temperatures between concentration in the gas phase and on the solid surface have been made. These isotherms, and their alternative variants, isobars and isosteres were explained by means of various theories concerning solid surfaces and the molecular forces that were involved. Speculation proceeds even today as to the underlying physical explanation of these data correlation curves. Some mention will be made here of some of these highlights along with the thermodynamics of the equilibrium process before moving on to the dynamical or transport considerations. For the sake of fixing attention on the overall view of the problem the following summary of basic phenomena should be kept in mind.

BASIC PHENOMENA

The adsorption-desorption process in a fixed granular bed involves the following sequence:

(a) Mass transfer of contaminants and other gaseous components from the bulk of the flowing gas stream to the proximity of the interstices and pores of the granular bed

(b) Diffusion through the porous substructure of the solid until encounter with the surface

(c) Retention at the surface by means of condensation or reaction with it

(d) Disengagement of the contaminants or reaction products from the solid surface

(e) Diffusion out of the porous substructure

(f) Mass transfer into the bulk gas stream

Steps 1 and 2, and 5 and 6, have been differentiated for the sake of empha-
sizing a serious difference in the mechanisms of the diffusional transport in
or out of the pores. In Steps 3 and 4, the components may stick to the surface
or be freed from it either by means of long-range forces akin to those of
intermolecular attraction that produce condensation or vaporization (physical
adsorption), or by means of stronger interactions of a more energetic kind
leading to reactivity with components on the surface of the solid (chemisorp-
tion). The latter components may be quite different from those found in the
bulk of the solid. These may be impurities that lead to electrical-charge
which may have been introduced during formulation of the adsorbent material;
these defects may have been formed by retention of gases during activation or
pretreatment of the sorbent.

A quantitative treatment of the adsorption process requires that the
kinetics of Steps 1 through 6 be examined in detail; in the general case, this
leads to mathematical complexities. All of the mass transport mechanisms and
surface reaction steps must be incorporated into the unsteady-state behavior
of the bed. The energy balance for this transient behavior must be considered
together with the material balance for each contaminant. Most analytical
expressions assume that one step is rate-controlling and that the other steps
are of negligible importance. Such analyses are usually inaccurate when
applied to predicting bed behavior over a wide range of operating conditions.
Also, the neglect of heat effects in the adsorption process (where these are
significant) can introduce serious analytical deficiencies.

Following is a sketch of what is observed in a fixed bed of adsorbent
material during flow-through of the gaseous medium. Let t be the total time
since the inception of contaminant flow and y the concentration of the contam-
inant in the effluent. The effluent stream exhibits the following schematic
variation of y with t:
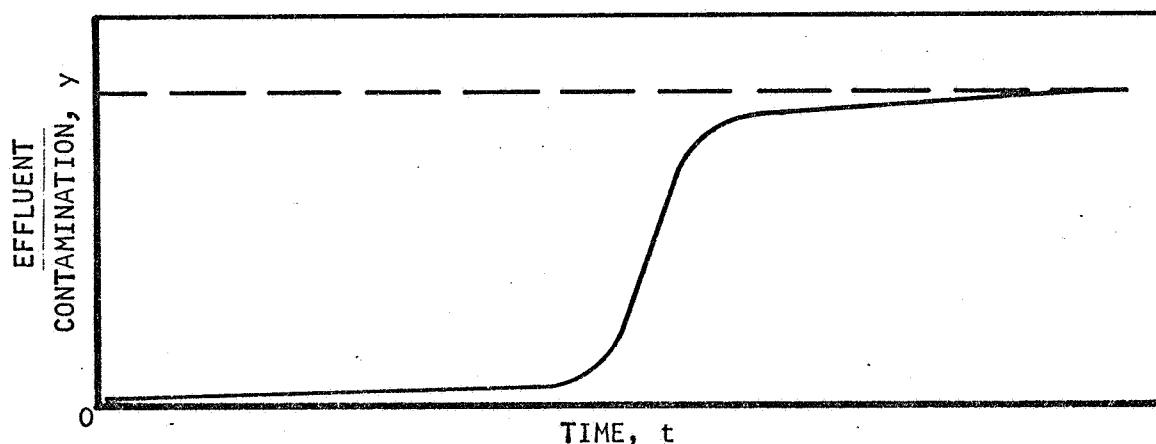
The effluent will at first have a small concentration of the contaminant; then
y will increase until it reaches the current value of the inlet y, and no
removal is afforded by the bed.

A similar situation will develop in the bed prior to observance of these phenomena in the effluent. If w is the concentration of the contaminant in the bed, the same wave pattern as in the above figure will move down the length of the bed until its subsequent appearance in the effluent stream. The latter occurrence is termed breakthrough, and the wave pattern is called the adsorption wave. More detailed descriptions are given later in this section.

One of the major purposes of any study is the development of accurate mathematical models incorporating the more important factors involved in adsorption-desorption processes. These models, used to characterize adsorption bed behavior, provide an invaluable basis for design and optimization of improved beds.

ADSORPTION STEP

Adsorption may be defined as a phenomenon involving concentration of the adsorbable species at an interface. The interface is the thin region (on the order of molecular dimensions) between two bulk phases. The discussion below is concerned with the adsorption of a gas at the interface between a solid and the gas. In the extreme, the adsorption of a gas on a solid surface may be classified as (1) chemisorption and (2) physical adsorption. These are extremes; in some systems, neither category is entirely suitable. Both chemisorption and physical adsorption may occur simultaneously.

Chemisorption may be defined as a process in which a chemical bond is formed between a gas molecule, atom, or ion on the surface of the solid. Thus, chemisorption is a process involving a major electron transfer. The energetics of chemisorption are those characteristic of chemical bond formulation; the enthalpies of chemisorption may range upwards from 40 kcal per mole. Once the primary valence forces of the surface atoms or ions are satisfied, no further bonding can occur; chemisorption is thus restricted to the formation of a monomolecular layer of adsorbed gas on the surface of the solid. The thermodynamics of chemisorption are essentially reaction thermodynamics. The kinetics of chemisorption involve rate expressions in the concentration of gas and of surface sites; activation energies may be calculated from the variation of rate constant with temperature.

In physical adsorption the forces of interaction between the surface and the adsorbed gas molecule are those responsible for the formation of a condensed phase from a gas phase. The forces (van der Waal's forces) are considerably lower in magnitude than those responsible for bond formation and are shorter range forces. Physical adsorption occurs when the interaction energies are large with respect to thermal energy and is most pronounced at temperatures below the condensation temperature of the gas. The enthalpy of physical adsorption (except at extremely low surface coverage) is on the order of the enthalpy of condensation. Physical adsorption is usually polymolecular in nature. These two extreme types of adsorption are considered in further detail below, and attempts are made to point out the relation between thermodynamic properties, reaction kinetics, and adsorption and desorption phenomena.

The determination of these relationships will permit a better understanding of the basic phenomena involved in the adsorption processes and, therefore, will make possible the utilization of adsorbents particularly efficient in removing selected contaminants.

There exist basically two complementary avenues leading to the exploration and better understanding of the adsorption and desorption phenomena. One is concerned with the macroscopic equilibrium or statistical aspect of adsorption (thermodynamics and chemical kinetics), while the other deals with the microscopic aspect in which the individual adsorbate molecules are considered in relation to the adsorbent as a semiconductor (electronic theory of chemisorption) or as polarization and surface dispersion (physical adsorption).

Examples of the first approach follow below, which will yield some insight concerning the heats of adsorption. The microscopic aspect with regard to molecular sieves has been thrown open to controversy. For example, Benson and associates maintain that an electrostatic rather than a molecular size effect governs the adsorption selectivity of the molecular sieves. Others contest this assertion. The designated references B5, S5, and B3* contain the details of this discussion.

Thermodynamics of Adsorption

The thermodynamics of the reversible adsorption step are outlined in Appendix C for systems consisting of one adsorbate, and employing the method of "adsorption thermodynamics"** which is equivalent to the method of "solution thermodynamics"*** and the Gibbsian "surface excess" method.

The variety of different treatments and the differing interpretations of surface energy and quantities of experimental significance arise from difficulties in suitably defining the surface of separation or surface of tension. As a case in point, some workers recently determined that the interfacial thickness and composition in it are not independent variables, but are governed by the thermodynamic necessity of minimizing the surface layer free energy. A comprehensive treatment of these problems is found in a monograph by Hill, H14.

The remainder of this discussion supplements Appendix A in the light of the aforementioned viewpoints.

Equations (A-11) and (A-12) of Appendix A furnish the thermodynamic bases for phase equilibrium and the adsorption isotherm, respectively. They will now be related to practical measurement of heats of adsorption.

---

*The designated references are listed in the Bibliography part of Section 3.

**Adsorption thermodynamics deals only with the adsorbate; i.e., the adsorbent is considered inert.

***Solution thermodynamics considers both components, i.e., the adsorbent and the adsorbate.

Define

$$dA_{\lambda} = -S_{\lambda}dT - PdV_{\lambda} - \Phi da + \mu dn \qquad \boxed{*}$$

for the adsorbed phase.

By a Maxwell relation, neglecting changes in V_s or properly locating the surface in the Gibbsian manner,

$$\left(\frac{\partial \mu}{\partial T}\right)_{\Gamma} = -\left(\frac{\partial S_{\lambda}}{\partial n}\right)_{T, a}$$

Where constant a and n are replaced by their equivalent, Γ.

For the gas phase

$$d\mu = -\Delta_G dT + \upsilon_G dP$$

$$\left(\frac{\partial \mu}{\partial T}\right)_{\Gamma} = -\Delta_G + \upsilon_G \left(\frac{dP}{dT}\right)_{\Gamma} = -\left(\frac{\partial S_{\lambda}}{\partial n_{\lambda}}\right)_{T, a}$$

Consequently,

$$\left(\frac{\partial P}{\partial T}\right)_{\Gamma} = \frac{\left[\Delta_G - \left(\frac{\partial S_{\lambda}}{\partial n}\right)_{T, a}\right]}{\upsilon_G}$$

This is the analogue of Gibb's expression. T times the quantity in the numerator is the isosteric heat of adsorption (q_{st}). The same and other ensuing results follow from solution thermodynamics when the constant "a" condition is visualized as arising from the pure solid condition in the same state of subdivision as the adsorbent, Reference (H-13); i.e., the specific surface (cm^2/gm) remains constant with the addition of more adsorbent.

Utilizing Equations (A-2) and (A-14) of Appendix A, q_d, the isothermal heat of adsorption with no PV work, can be expressed as follows:

Neglecting V_s as before,

$$\left(\frac{\partial E_{\lambda}}{\partial n}\right)_{T, a} - T\left(\frac{\partial S}{\partial n}\right)_{T, a} = \mu = e_G - T\Delta_G + P\upsilon_G$$

or

$$T\left[\Delta_G - \left(\frac{\partial S}{\partial n}\right)_{T, a}\right] = q_{st} = \left[e_G - \left(\frac{\partial E_{\lambda}}{\partial n}\right)_{T, a}\right] + P\upsilon_G$$

*The symbols used in this discussion are introduced in Appendix A and are taken from the thermodynamical presentation found there.

or

$$q_{st} = q_d + P v_G$$

The quantity q_d is commonly called the differential heat of adsorption. For isothermal reversible measurement of the heat of adsorption with external PV work, as is the common situation, q_{th} is obtained. Proceeding in a fashion similar to the last case,

$$\left(\frac{\partial H_s}{\partial n}\right)_{T,a} - T\left(\frac{\partial S}{\partial n}\right)_{T,a} = \mu = h_G - T s_G - V_G \left(\frac{\partial P}{\partial n}\right)_{T,a}$$

$$h_G - \left(\frac{\partial H_s}{\partial n}\right)_{T,a} = q_{th} = q_{st} + V_G \left(\frac{\partial P}{\partial n}\right)_{T,a}$$

Multicomponent adsorption relations can be dealt with in a fashion analogous to that in Appendix A if Equation (A-2) is now written

$$dE = Td s + PdV - \phi da + \Sigma \mu_i dn_i$$

Surface Kinetics and Equilibrium (Isotherms)

The velocity of adsorption depends basically on three factors:

The rate of collision with the surface

The probability of collision on available sites

The activation energy E involved in adsorption

Several theories have been advanced for the adsorption process. One such theory, developed by DeBoer and coworkers, References D2 through D7, K10 and K11, deals with the residence time of an adsorbed molecule on the surface of the adsorbent; it is limited to very low surface coverages. Theories of the Langmuir type define the rate of adsorption in the following manner.

$$\mu = \frac{\sigma P}{\sqrt{2\pi m kT}} \cdot f(\theta) \cdot e^{-E/RT}$$

Similarly, for the rate of desorption

$$\mu' = K f'(\theta) e^{-E/RT}$$

where u   = velocity of adsorption

   u'   = velocity of desorption

   σ = condensation coefficient

   p   = partial pressure of the adsorbate gas

   m   = mass of the gas molecule

   k   = gas constant

   T   = absolute temperature

   $f(\theta)$ = probability of collision at available sites

   $f'(\theta)$ = probability of escape from the sites

   E   = activation energy

   θ = fraction of surface covered

   K   = velocity constant

   E'   = sum of activation energy and heat of adsorption, $E' = E + q$

   a   = coefficient depending on temperature alone

   q   = heat of adsorption = $q(\theta)$, in general

At equilibrium $u = u'$, and the equation of the adsorption isotherm may be written:

$$P = \frac{K}{\sigma}\sqrt{2\pi m k T}\;\frac{f'(\theta)}{f(\theta)}\cdot e^{-q/RT}$$

Specific isotherms may be derived from this expression by inserting appropriate expressions for $f(\theta)$ and $f'(\theta)$.

Among the assumptions Langmuir made in his work were:

(a) The surface is homogeneously available.

(b) No interference exists between adsorbed neighbors.

As a consequence, $f'(\theta)/f(\theta)$ was taken equal to $\theta/(1-\theta)$ and q independent of θ and any inhomogeneities of the surface. The resulting expression, after combining the various constants together, is

$$\theta = \frac{cp}{1 + cp}$$

If it is further assumed, in the multilayer case, that q for the successive layers is the heat of liquefaction, the result is the BET equation, upon which one of the standard methods of surface area determination is based. If it is assumed that q falls logarithmically as θ increases, another characteristic isotherm is obtained which describes better the adsorption phenomena in the case of surface heterogeneity (Freundlich isotherm). If, moreover, it is assumed that the heat of adsorption decreases linearly with θ, a Tempkin isotherm is obtained which better describes the adsorption phenomena in particular cases. For substances with small pore radii such as some forms of silica gel, capillary-condensation becomes important at fairly high coverages. The appropriate expression for this phenomena is given by Equation (A-12) (see the presentation of the thermodynamics of adsorption in Appendix A).

These brief considerations illustrate the relationship between the shape of the adsorption isotherms and the phenomena of adsorption in relation to such parameters as number of vacant sites, number of adsorbed layers, etc. A fairly recent and complete review of these relationships is contained in Reference KI0.

The following paragraphs constitute a brief review of the microscopic picture.

Chemisorption

Chemisorption may be considered as a process involving the formation of a chemical bond between the adsorbed gas molecule and an atom or ion on the surface of the solid. The enthalpy of adsorption is high; consequently, at equilibrium, there is a large difference in entropy between the adsorbed molecules and those in the gas phase. Chemisorption possesses the specificity characteristic of chemical reactions. If the chemisorption process is reversible, it may be treated by the conventional technics of classical thermodynamics; if the process is irreversible, the thermodynamic treatment must be based upon the energetics of chemical bond formation and an estimate of the nature of the bond formed in the adsorption process. Calorimetric methods are suitable for the determination of enthalpies for both the reversible and irreversible processes. Normally, chemisorption occurs slowly at very low gas pressures (less than 10^{-7} torr); the kinetics are a function of the pressure. At pressures exceeding 10^{-6} torr, the adsorption process is usually complete in a matter of seconds. Chemisorption, it is again emphasized, is restricted to the formation of a monomolecular layer of adsorbed gas.

The magnitude of the heat of adsorption is the most significant single property of a particular adsorption phenomenon because the determination of the entropies and enthalpies of chemisorption gives important information on the structure of the solid adsorbent, the nature of the surface bond, the amount of coverage, the possible catalytic activity, etc. Moreover, it must be noticed that there is evidence that each of the three main types of chemical bonds (the ionic, covalent, and co-ionic) may be formed in chemisorption. For ionic bonds, the ease of passage of electrons across the surface plane, i.e., the magnitude of the work function, may decide both the ease of formation and strength of the bond. Covalent bonds can be formed only if the adsorbent possesses orbitals with unpaired electrons capable of entering into covalence.

Coordination, with electron donation to the adsorbent, requires the latter to have a vacant orbital capable of receiving the pair. For this reason, the nature of the surface bond formed in the adsorption of a particular molecule depends very largely upon the electronic structure of the adsorbent.

The high heat of adsorption of CO_2 on the natural zeolite chabazite (ca 409 to 573 Btu per lb) reported by Kington and Macleod (Reference K4) appears consistent with the findings of Bertsch and Hubgood (Reference B6), i.e., that carbon dioxide is chemisorbed on the Linde X zeolites in the low coverage region. It is interesting to note that for a fully dehydrated Linde Type 13X molecular sieve, the adsorption of CO_2 is extremely slow at $25^{\circ}C$ below 0.3 mm Hg (i.e., each isotherm point requires periods in excess of 60 hr to equilibrate). However, when a small quantity of water is initially present, true equilibrium is reached within minutes, probably as a result of the water molecules acting as a catalyst for the chemisorption step.

Physical Adsorption

The short-range forces responsible for physical adsorption may be further classified according to their origin into (1) dispersion forces, (2) dipole (or quadrapole)-dipole forces, (3) dipole-induced dipole forces, (4) ion-dipole forces, etc. Although the pair dispersion forces vary with the inverse sixth power of the distance between centers, the total interaction of a gas molecule with all the atoms in a solid is described in terms of an inverse fourth power relation (inverse third power in energy). The enthalpies of physical adsorption processes are on the order of enthalpies of vaporization. Physical adsorption is normally appreciable only at temperatures below the critical temperature of the adsorbate; the extent of adsorption increases with decreasing temperature. Adsorption generally leads to the formation of polymolecular layers at higher equilibrium pressures, and the pressure range in which appreciable physical adsorption occurs is generally considerably greater than the range for chemisorption.

Many theories have been advanced to explain physical adsorption.. These theories cover a wide range. At one extreme is the establishment of a detailed model on a molecular basis and the application of statistical methods to obtain the observed thermodynamic functions; at the other, analogies are drawn between the behavior of films on solids and monomolecular films on liquid subphases. Here only a few of these theories are listed:

The Hill theory, which eventually leads to the partition function for the adsorbed molecule placed in the perturbing field of the surface. Reference H14.

The potential theory, which is especially useful in correlating adsorption behavior as a function of temperature; the approach is quasi-thermodynamic. Reference P1.

The theory of Brunauer, Emmett, and Teller, which is actually an extension of the Langmuir treatment to polymolecular adsorption. This theory forms the basis for the most commonly employed method in the determination of the specific surface areas of solids. Reference B15.

The theory of Harkins and Jura, which is essentially a thermodynamic description of the surface phase in terms of an equation of state; this theory also affords a means for measuring the specific surface area of a solid. Reference H2.

Mention has already been made of the electrostatic theories of molecular sieves by Benson and coworkers, Reference B5.

ANALYSES OF ADSORPTION BED DYNAMICS

The six basic phenomena listed in the introduction will now be examined from the dynamic point of view.

The basic theories of material, energy and mass transport for a homogeneous phase, are fairly well understood. The understanding of interphase transport is not as well established, References B8, B9, B10, and B11. Most of the ideas of transport theory are derived from the thermodynamics of irreversible processes, References D9 and F1.

Many of the physical phenomena encountered in sorption bed analysis depend upon transport theory. Mass transport by diffusion and convection are among the most critical phenomena for the analysis. A general review of the literature (see Section 3, Resume of Literature), indicates that many operations carried out in fixed beds in which there is fluid-solid contact (such as ion-exchange, chromatography, and regeneration heat exchange with a bed of broken solids) involve similar phenomena and are directly applicable to sorption problems, since the fundamental mathematical analysis is the same.

Mass Balances

Based upon transport theory referred to above, mass balances in the fluid stream will be considered first. In considering the flow through the granular bed, overall macroscopic balances such as are detailed in Reference B9 are in order. However no information as to the adsorption process would be forthcoming. In the chapter on macroscopic balances of Reference B10, however, a further refinement is made in which the volume space is subdivided into a fluid space and the solid space. Mass balances can then be written for each.

A general theoretical approach to diffusional mass transfer has been summarized in Appendix B for a homogeneous isotropic fluid with regular phase boundaries. In this case of the fixed bed, the same analysis has been applied to flow in the interstices of the packed bed.

Consider the flow of fluid through the bed whose fraction of voids is ϵ*. Let the average superficial velocity be v, i.e., the volumetric flow rate per unit cross-sectional area of the cylindrically shaped bed. It is assumed here that v is constant and in the direction of the cylindrical axis. As discussed in Appendix B, v, the average velocity based upon the partial specific volume average, can be taken to be constant in the axial direction, since the local acceleration terms vanish; and the pressure gradient is assumed not too great.

Further, let C be the mass concentration in the bulk fluid stream and R the overall rate of contaminant disappearance into the stationary phase per unit volume of bed. The rate of change of diffusive flux with distance postulated only in the axial direction was computed. In these calculations, the diffusion coefficient, which will be designated here as E, is differentiated from others discussed in Appendix B, when a regularly bounded phase was considered. E is commonly called the longitudinal dispersion coefficient for transport processes in packed beds and is frequently measured by tracer techniques. In general, it may be due to both molecular and turbulent transport.

By means of a mass balance analogous to the one described in Appendix B, the following is the most general equation written.

$$\epsilon \frac{\partial C}{\partial t} + v \frac{\partial C}{\partial X^2} + R_T = E \frac{\partial^2 C}{\partial Z^2} \qquad (4\text{-}1)$$

Dispersion in all but the X direction is neglected. This equation states that the rate of change of the adsorbate in an element of bulk stream fluid plus the amount convected out, plus the rate of disappearance out of the bulk stream, is equal to the net diffusive influx into the element. Equation (4-1) is similar to most of the "one dimensional" diffusion equations. The critical term is R_T, the rate of disappearance from the bulk stream. The manner in which R_T is written varies throughout the literature depending upon the assumptions and simplifications that are made. An initial unified approach will be sketched here, and then the variations on the input variables will serve to introduce the approaches and simplifications reported in the references.

Before going on to examine this rate in detail, some variations of the preceding mass equation will be reviewed. Funk and Houghton, References F5, F6, and F7, in their analysis of gas-liquid partition chromatography rewrote Equation (4-1) above in terms of the mole fraction N and total pressure P.

$$\epsilon \frac{\partial N}{\partial t} = E \frac{\partial^2 N}{\partial X^2} - \left(v - \frac{2E}{P} \frac{\partial P}{\partial X} \right) \frac{\partial N}{\partial X} - R_M + \frac{EN}{P} \frac{\partial^2 P}{\partial X^2} \qquad (4\text{-}2)$$

---

*Symbols are listed and systematically defined in the Nomenclature at the end of this section for the dynamical equations written henceforth.

This result is obtained if ideal gas laws are used in substitution for the concentration C where

$$C = \frac{PMN}{R_G T} \qquad (4-3)$$

where M is the molecular weight of the contaminant and R_G the universal gas constant. R_M is the disappearance rate now in terms of the mole fraction.

The assumption is made, of course, of isothermal operation. In addition, v is treated as a constant and the substantive derivative of P is assumed to be zero.

$$\frac{DP}{DT} = \frac{\partial P}{\partial t} + v\frac{\partial P}{\partial X} = 0 \qquad (4-4)$$

The pressure drop gradient, $\frac{\partial P}{\partial X}$, is related by the authors to Darcy's law for the flow of fluids through porous media, Reference B11, p. 150.

$$v = const \frac{\partial P}{\partial X} \qquad (4-5)$$

Another approach in which the effects of pressure change are incorporated into the mass balance is the one used in AiResearch computer program S9960 and described in Section 7. In it the time variation of pressure is not neglected so as to provide a basis of analysis for vacuum induced desorption. Pressure effects are introduced partly through the ideal gas laws and partly by incorporation of the factor F which relates the pressure drop in packed beds to the flow velocity by means of the Ergun equation, Reference B10, p. 200. For our purposes

$$F = \frac{1}{v}\frac{\partial P}{\partial X} \qquad (4-6)$$

While the initial material balance is written in terms of total fluid stream molar concentration C_M.

$$\epsilon\left(\frac{\partial C_M}{\partial t}\right) = -\epsilon\frac{\partial}{\partial X}\left(C_M v\right) + m \qquad (4-7)$$

By ideal gas law

$$C_M = \frac{P}{R_G T} \qquad (4-8)$$

The last expression is substituted for C_M in the left hand side of $(4-7)$, while v is rewritten in terms of F as in $(4-6)$. The velocity v' is based upon flow in the void space.

The resulting expression is

$$\frac{\partial P}{\partial t} = \frac{P}{3} \frac{\partial^2 P}{\partial X^2} + \frac{P}{C_M} \frac{\partial}{\partial X}\left(\frac{C_M}{3}\right) \frac{\partial P}{\partial X} + \frac{P}{C_M \epsilon} m + \frac{P}{T} \frac{\partial T}{\partial t} \qquad (4-9)$$

Longitudinal dispersion, as can be seen, has been neglected. The dependence upon temperature called for explicitly by $\frac{\partial T}{\partial t}$ and implicitly by m is provided by a simultaneous energy balance equation.

Both treatments involving pressure drop go on to link the transfer rates embodied in R_T or m to conditions in the stationary phase in manners fairly typical of the literature summarized in Section 3, Resume of Literature. However, because of the linking of pressure drop and temperature variation directly into the fluid phase mass balance in a nonlinear fashion, the solutions are necessarily numerical and obtainable practically only by computer programs.

The rest of this section will be devoted to developing expressions for the material balance solution when changes in pressure drop and temperature can be neglected as during the adsorption part of a regenerable bed cycle. The interphase mass transfer concepts in the literature will also be illustrated thereby, and in addition, the analytical, closed form solutions will provide some insight as to the relative importance of the various dynamical steps.

Interphase Mass Transfer

Three major steps that remain to be examined are summarized in the introduction. They are repeated and amplified upon here for purposes of clarity.

1. Mass Transfer Between the Fluid Stream and the Particles of the Adsorbent Bed

   This process is termed "interparticle diffusion" by Masamune and Smith, Reference M5. It is usually written as a first order or linear rate law employing a rate constant that is the familiar "film coefficient" for interphase mass transfer at low transfer rates, Reference B11, Chapter 21.

2. Diffusion Through the Pores of the Sorbent

   This phenomena is termed "intraparticle diffusion" in Reference M5 by way of contrast with the preceding one. The major portion of the particle surfaces consists of an intricate network of pores whose boundaries constitute the extended surface area of the sorbents. Diffusion equations are written usually in terms of a pore diffusion coefficient. This coefficient can

usually be determined only experimentally, Reference M4. It is a true transport property only in the case of very fine and uniform pores (Knudsen diffusion, see Chapter XV of Reference D9). In most of the treatments in the literature, the particles are assumed to be of uniform size, spherical in shape, and with uniform pore structure. Diffusion equations are written in which only radial concentration gradients are taken into account. Kel'tsev, Reference K3, however, considers diffusion in cylindrically shaped particles in his studies of desorption of carbon dioxide and water from molecular sieves. Concentration gradients are formulated for both the cylindrically radial and the axial directions in the particles. He considers this mechanism exclusively.

3. Adsorption/Desorption Rates at the Extended Surfaces

This step of the process deals with the kinetics of alternately sticking or evaporating from the extensive surface area of the particles. Some approximations, in the literature assume such rapidity to this dynamic step that equilibrium relations as discussed in the beginning of this section are written for it (see Section 3, Resume of Literature). Other treatments assign either a first or second order rate law such as Langmuir kinetics to this step. Hill, Reference H13, p. 217, shows that in the limit of low gas phase partial pressures the adsorption step is linear. The thermodynamics of irreversible processes also asserts that at states not too far from equilibrium, kinetic rate laws should be linear. It should be noted, however, that Hobson and Armstrong, Reference H15, in their ultrahigh vacuum investigations were not readily able to confirm Hill's theorem.

Figures 4-1 and 4-2 contain sketches of the steps and some of the customary analytical simplifications. Symbols are defined in succeeding text and the Nomenclature Section. Figure 4-3 represents a typical equilibrium isotherm at low surface coverage.

Remainder of Interphase and Granular Particle Mass Transfer Analysis

Let k_F be the mass transfer coefficient from the bulk stream to the particle pores. The concentration of fluid diffusing through the pores of the particles that make up the bed is designated by $\bar{C}$. Then the following equation describes the transfer from the bulk stream to the fluid in the pores:

$$R_T = k_F A (C - C_a)$$

(4-10)

where A is the total gross geometric area of the bed particles per unit volume and C_a is the concentration at the interface.

INTERSTITIAL VOID VOLUME ϵ

PARTICLE RADIUS a

C_o
INLET FLUID CONCENTRATION

C
OUTLET FLUID CONCENTRATION

X
BED LENGTH COORDINATE
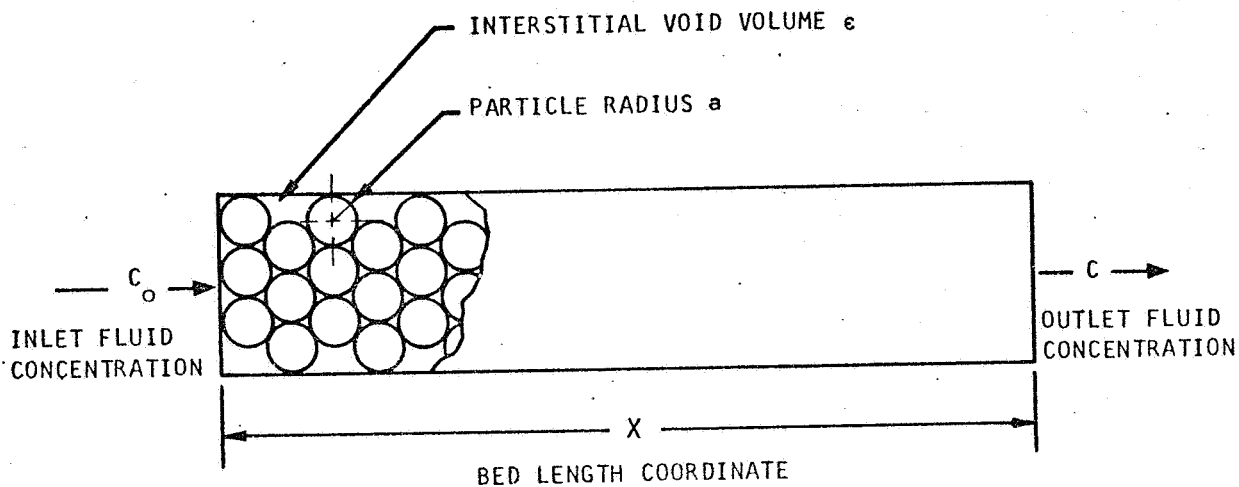
A-8581

Figure 4-1. Particle Arrangement in Fixed Bed (Particles of Sorbent Are Assumed to Be of Uniform Size and Arrangement in Bed)
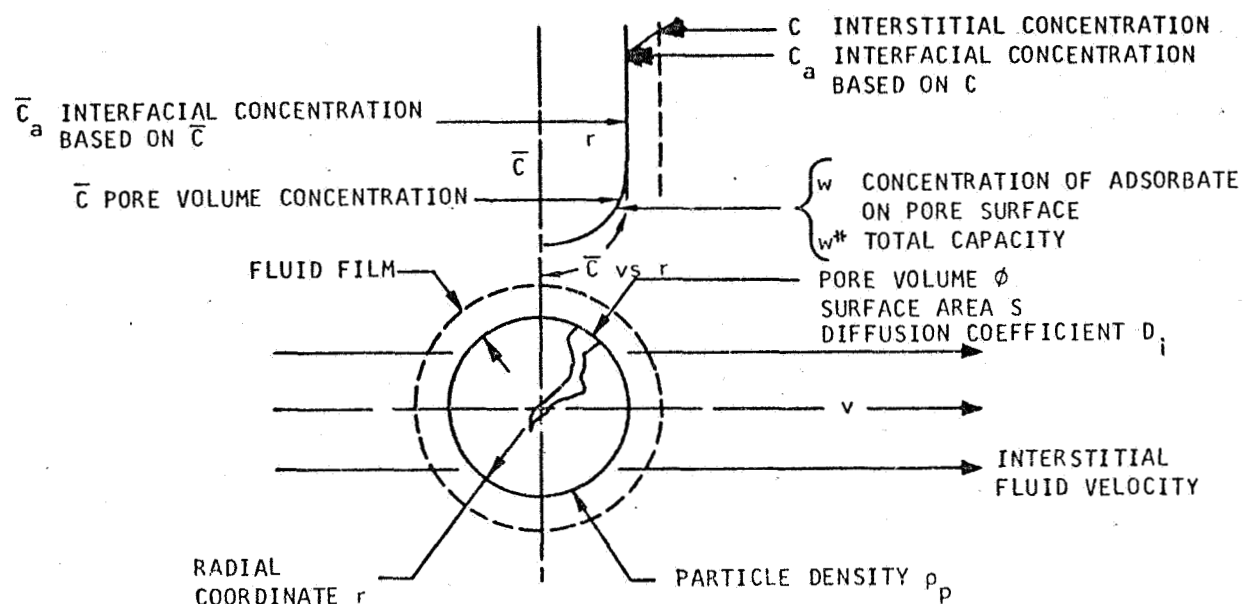
Figure 4-2.   Single-Particle Physical Parameters
and Related Concentrations

A-8582-A

SLOPE = K, EQUILIBRIUM CONSTANT

$\dfrac{W^*}{W}$

0.10

0.05

0

0.1

$\overline{C}$
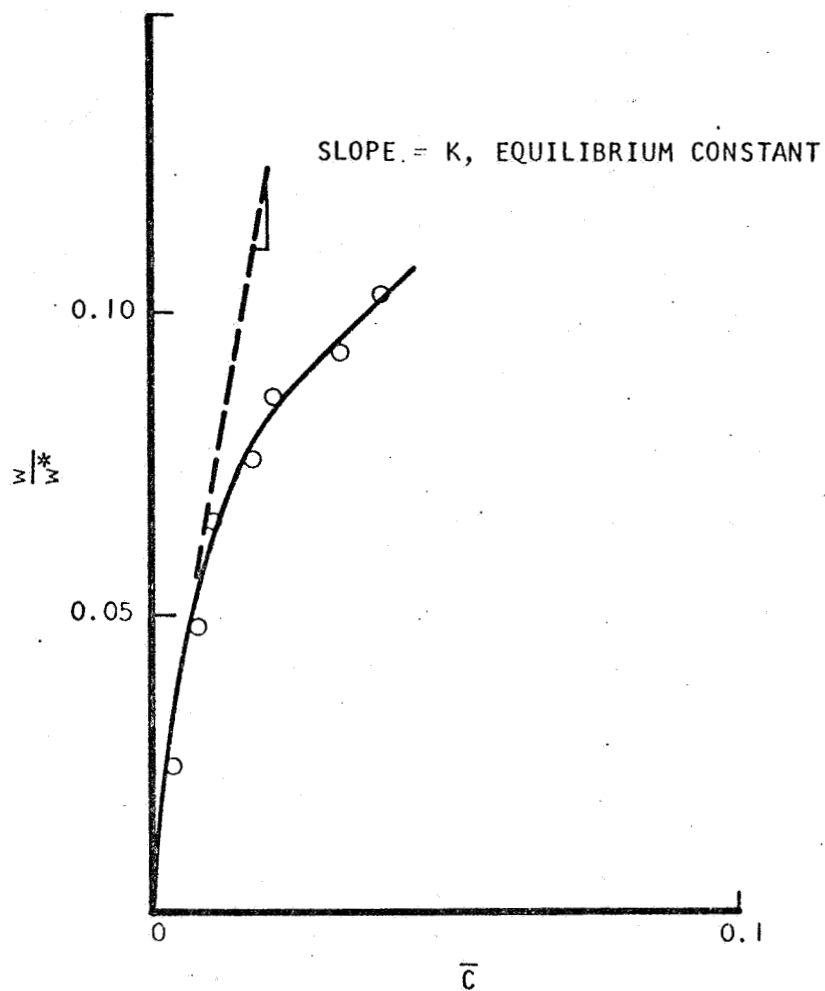
A-8579

Figure 4-3. Schematic of Typical Adsorption Equilibrium
Isotherm at Low Coverage (Proportionate Law)

The mean external area of the particles per total volume of bed is expressed in the following manner.

$$A = \frac{4\pi a^2 (1-\epsilon)}{\frac{4}{3}\pi a^3}$$

or

$$A = \frac{3(1-\epsilon)}{a} \qquad (4-11)$$

Consequently,

$$R_T = k_F \frac{3(1-\epsilon)(c-c_a)}{a} \qquad (4-12)$$

The next step of the process is diffusion within or along the pores while matter is constantly adsorbing or desorbing on the surfaces of the pores.

In general in diffusion through the pores, $\bar{c}$ is a function of the radial distances in a pellet as well as of the length along the bed X and the time t.

$$\bar{c} = \bar{c}(r, X, t) \qquad (4-13)$$

The usual approximation that is made is that the diffusion in the pores is spherical and r, therefore, is the radial coordinate. What is meant, then, by the notation $\bar{C}_a$ is the following:

$$\bar{c}_a = \bar{c}(a, X, t) \qquad (4-14)$$

where a is the mean particle size radius in the bed. $\bar{C}_a$ is the interfacial concentration corresponding to the bulk fluid stream.

At steady state, the boundary condition on the pore diffusion from the surface can be related to $\bar{C}$ in the pores by the familiar relation

$$\phi D_i \frac{\partial \bar{c}_a}{\partial r} = k_F (c - c_a) \qquad (4-15)$$

where D_i is the coefficient of pore diffusion. It may depend upon surface migration as well as volume movement through the pores, References M4 and M5.

The mass balance of the diffusing substance in the pores is similar to the one written for the bulk stream, except that spherical symmetry is now assumed and the average convective velocity is zero.* If ϕ is the porosity of the bed particle and ρ_p its density, the following may be written

$$\phi \frac{\partial \bar{c}}{\partial t} + \rho_p \frac{\partial w}{\partial t} = \phi D_i \left(\frac{\partial^2 \bar{c}}{\partial r^2} + \frac{2}{r} \frac{\partial \bar{c}}{\partial r} \right) \qquad (4\text{-}16)$$

where w is the mass adsorbed at the pore surface per unit mass of adsorbent.

Finally, the rate of change of w can be expressed in the equation that follows. (In this equation, w is given by a functional relation between C and w and includes some other possible parameters, such as the rate constant for adsorption k, the surface area per unit mass of adsorbent S, the monomolecular capacity w^*, and the adsorption equilibrium constant k.)

$$\frac{\partial w}{\partial t} = f\left(\bar{c}, w, w^*, k, K, S \right)$$

To give the preceding equation some substance, a particular example is set forth below. Assume a process of Langmuir kinetics. The rate of adsorption is proportional to the fraction of unoccupied surface and also to the concentration of adsorbate in the fluid. The rate of desorption is proportional to the amount of surface that is covered. The net rate of adsorption is then

$$\frac{1}{w^*} \frac{\partial w}{\partial t} = \frac{kS}{w^*} \left[\bar{c}(w^* - w) - \frac{1}{K} w \right] \qquad (4\text{-}17)$$

For the case of low coverage depicted in Figure 4-3,

$$\frac{w}{w^*} \ll 1$$

---

*Appendix B develops some of the justification for this assumption.

and for this approximation, the preceding equation assumes the linear form

$$\frac{1}{w^*} \frac{\partial w}{\partial t} = \frac{kS}{Kw^*} \left(Kw^* \bar{c} - w \right) \qquad (4\text{-}18)$$

For boundary and initial conditions, the foregoing system of equations must be completed by assuming or postulating the initial and boundary conditions for the whole column of adsorbent bed.

In their more general form, these conditions are as follows: (1) at the beginning of the process the adsorbent particles may have some initial concentration distribution, and (2) the inlet stream may also have a time variation. As a consequence, the most general set of boundary and initial conditions is developed now.

For the concentration of the mobile bulk stream, the general initial condition may be written as

$$C\left(X, o\right) = C_i\left(X\right) \qquad (4\text{-}19)$$

where $C_i(X)$ is its initial concentration distribution. Also, the following relationship may be written

$$C\left(o, t\right) = C_o\left(t\right) \qquad (4\text{-}20)$$

The preceding equation states that the inlet concentration is $C_o(t)$, in general, a function of time.

A natural assumption for the case where the fixed bed column is very long is that the concentration should approach zero at the exit, viz:

$$C\left(\infty, t\right) = o \qquad (4\text{-}21)$$

For the adsorbed species, the general initial condition could be taken as follows:

$$w(r, X, o) = w_i\left(\bar{c}_i\right) \qquad (4\text{-}22)$$

where the initial distribution w_i is a function of r and X and can be related to that of the diffusing species concentration in the porous substructure.

For the concentration of diffusing species in the pores,

$$\bar{C}(r,X,o) = \bar{C}_i(r,X) \tag{4-23}$$

already has been implied as the initial condition, and

$$\frac{\partial}{\partial r}\bar{C}(o,X,t) = 0 \tag{4-24}$$

since $\bar{C}$ is symmetrical with respect to the radius r of the porous bed particle. This last condition also assumes that Equation (4-16) will have a bounded solution at r = 0. Finally, the boundary condition on C at the particle exterior r = a is Equation (4-15), where $\bar{C}_a$ is defined by Equation (4-14).

Table 4-1 is a summary of the general equations for fixed bed adsorption given thus far, plus some variations of them that are easily derived. These generalities, although formidable enough in their appearance, result nevertheless from the following simplifying assumptions.

The process is isothermal. The effects of heats of adsorption are neglected.

Only the adsorption of one component is considered. Thus, the effects of humidity, for example, have been ignored.

The density of the gas flowing through the bed is assumed constant.

The velocity is assumed to be constant over a cross-section normal to the longitudinal axis.

The velocity is unaffected by the rate of mass transfer to the stationary bed.

Radial diffusion of mixing in the mobile phase is neglected.

The effects of pressure drop on velocity are neglected.

Effective averages of particle size and pore volume are assumed.

On the basis of Equation (4-14), Equation (4-25) is an expression of the continuity of fluid phase interfacial concentration whether based upon the bulk stream or on the pore spaces.

TABLE 4-1

SUMMARY OF GENERAL EQUATIONS FOR ADSORPTION IN FIXED BEDS

$$\epsilon \frac{\partial c}{\partial t} + v \frac{\partial c}{\partial x} + R = \epsilon \frac{\partial^2 c}{\partial x^2} \tag{4-1}$$

$$R = \frac{3(1-\epsilon)}{a} k_F (c - c_a) \tag{4-12}$$

$$c(x,0) = c_i(x) \tag{4-19}$$

$$c(0,t) = c_0(t) \tag{4-20}$$

$$c(\infty,t) = 0 \tag{4-21}$$

$$\phi \frac{\partial c}{\partial t} + \rho_p \frac{\partial w}{\partial t} = \phi D_i \left(\frac{\partial^2 \bar{c}}{\partial r^2} + \frac{2}{r} \frac{\partial \bar{c}}{\partial r} \right) \tag{4-16}$$

$$\bar{c}(r, x, 0) = \bar{c}_i(r, x) \tag{4-23}$$

$$\frac{\partial}{\partial r} \bar{c}(0, x, t) = 0 \tag{4-24}$$

$$\bar{c}_a = \bar{c}(a, x, t) \tag{4-14}$$

$$\phi D_i \frac{\partial}{\partial r} \bar{c}_a = k_F (c - c_a) \tag{4-15}$$

$$w(r, x, 0) = w_i(\bar{c}_i) \tag{4-22}$$

$$\frac{\partial w}{\partial t} = \frac{kS}{w^*} \left[\bar{c}(w^* - w) - \frac{w}{K} \right] \tag{4-17}$$

$$\epsilon C_a = (1-\epsilon) \phi \bar{c}_a \tag{4-25}$$

General Analytic Solution for Isothermal Sorption

Based upon the discussion just concluded for the various mass balances involved in sorption bed dynamics, the following is a resume of the analytic solution obtained keeping most of the generalities of Table 4-1. The details of how the solution was obtained are presented in References W4 and W6. Linear surface kinetics are assumed as in Equation (4-18) except that allowance

is made for a <u>linear isotherm</u> with possible nonzero intercept, w_b. Also, since total length of axial flow is assumed large compared to the width of the bed, the longitudinal dispersion term involving E has been neglected. If in addition one converts the time t to

$$t \rightarrow t - \frac{\partial X}{v}$$

Equation (4-1) then becomes

$$v \frac{\partial c}{\partial X} + R_T = 0 \qquad\qquad (4-26)$$

The restatement of the problem for the general analytic solution is presented in Reference W4.

NOMENCLATURE

Symbols

A A Exterior surface area of particles, length^2

a a Average particle size radius in bed, length

c C Interparticle (external void space) concentration, mass/length^3

$\bar{c}$ $\bar{C}$ Intraparticle (pore volume) concentration, mass/length^3

c_a C_a Interparticle concentration at $r = a$ defined by (4-14), mass/length^3

$\bar{c}_a$ $\bar{C}_a$ Intraparticle concentration at $r = a$, mass/length^3

$\bar{c}_o$ $\bar{C}_o$ Constant intraparticle concentration at $X = 0$, mass/length

c_o C_o Constant interparticle concentration at $X = 0$, mass/length^3

c_i C_i Reference interparticle distribution, mass/length^3

$\bar{c}_i$ $\bar{C}_i$ $\bar{C}$ taken in reference to w_i, mass/length^3

c_M C_M Molar concentration of fluid phase, mole/length^3

D D Cumulative dosage (concentration integrated over time) of exit fluid stream, dimensionless

D_i D_i Intraparticle diffusion coefficient, length^2/time

D_{AB} D_{AB} Fluid stream (regularly bounded passages) diffusion coefficient for a binary system, length^2/(time)

E E Interparticle diffusion (axial dispersion) diffusion coefficient, length^2/(time)

f f Functional symbol such as $y = f(x)$, dimensions: as defined

F F Factor relating pressure drop in (4-6) for packed beds to flow velocity, pressure/(length velocity)

K K Equilibrium constant for the surface reaction (adsorption) based on the pore volume, length^3/mass

k k Rate constant for adsorption based on the pore surface, length/time

k_F k_F Fixed bed bulk stream mass transfer (film) coefficient based on the external surface of the bed particles, length/time

NOMENCLATURE (Continued)

Symbols

M   ʍ   Molecular weight, mass/mole

m   ʍ   Mass of a diffusing component or mixture, mass

m   ʍ   Rate of decrease of total moles in the fluid stream, moles/(volume time)

N   N   Number of moles of a diffusing component or mixture

P   P   Pressure of a mass transport system, force/length^2

R   R   Cumulative retention on fixed bed, dimensionless

R_G R_G Universal gas constant, energy/(mole, deg abs)

R_T R_T Overall rate of removal of material from the interparticle bulk stream based upon the volume of the empty bed, mass/(length^3 time)

r   ʀ   Spherical radial coordinate of bed particle, length

S   S   Surface area (specific), length^2/mass

T   T   Absolute temperature of a mass transport system, temperature

t   t   Time variable, physical time less time for fluid stream to penetrate bed, $\varepsilon X/v$, time

υ   V   Superficial velocity of flow through bed, length/time

V   V   Total volume, length^3

v^0 v^0 Partial specific volume fraction average velocity, length/time

W   W   Reduced form of w based upon bed standard condition, defined by (4-40), dimensionless

w   w   Amount adsorbed on fixed bed, mass/mass adsorbent, dimensionless

w_b w_b Intercept of general linear isotherm, mass/mass adsorbent, dimensionless

w_i w_i Average bed standard condition, mass/mass adsorbent, dimensionless

w^* w^* Maximum value of w, total mass of adsorbate that can be adsorbed in a monolayer per unit mass of adsorbent, dimensionless

NOMENCLATURE (Continued)

Symbols

.X ⋋   Coordinate for axial position along bed, length

ε   ∈   Gross void volume of packed bed, empty volume/total volume, dimensionless

ρ_p ρ_p Density of bed particles (average), mass/length^3

ϕ ϕ Average pore volume of bed particles, pore volume/gross particle volume, dimensionless

SUBSCRIPTS

a   α   Denotes boundary condition at $r = a$

av αv Denotes average over radius of bed particles

o   o   Denotes boundary condition at either $X = 0$ or $t = 0$

i   ι   Denotes scale factor at $t = 0$

A   A   Component A in binary mixture

B   B   Component B in binary mixture

Overhead Symbols

−   −   In Appendix A, a partial molal quantity. Otherwise, it denotes concentrations in the pore volume where the mass fluxes are assumed to be relative to the specific volume average velocity (assumed to be negligible)

Superscripts

o   o   Designates specific volume average for a quantity; used in Appendix A

SECTION 5

BASIC LABORATORY STUDIES

APPARATUS AND EXPERIMENTAL TECHNIQUE

Equilibrium Isotherms

The adsorption equilibrium isotherms and differential heats of adsorption were determined by means of a gravimetric (McBain balance type) sorption apparatus. This apparatus is essentially a system in which the adsorbate is added incrementally at constant temperature to the adsorbent. In this system, the adsorbent is suspended on a quartz spring balance and the change in weight of the sorbent and the system pressure are measured, thus obtaining adsorption isotherms. For the nonequilibrium desorption rate and isotherm, the system is opened slightly to vacuum.

The gravimetric sorption apparatus used in these studies is shown schematically in Figure 5-1, and a photograph of the apparatus appears in Figure 5-2. This apparatus consists of a vacuum system, a gas reservoir supply system, a liquid-vapor reservoir supply system, a weighing system, and a pressure measuring system. It should be noted that the liquid-vapor reservoir supply system is also used to purify the liquid. By means of distilling, freezing out, and evacuation, any absorbed gases were removed from the distilled water used for the water equilibrium adsorption studies.

In all of the tests, equilibrium, mass transfer, and vacuum desorption, the carbon dioxide used was high purity grade supplied by Liquid Carbonic Co. It had an analysis of 99.99 percent carbon dioxide, 32 ppm oxygen, and 1.1 ppm water.

The weighing system is essentially a helical quartz spring balance which extends with added weight. This quartz spring is kept at constant temperature by means of constant temperature water flowing through a jacket surrounding the spring. The linear expansion of the quartz spring is observed by means of a cathetometer which is capable of reading to 0.005 cm. Before any tests were made, the spring was calibrated with known analytical (Class S) balance weights placed in the quartz sample bucket. Calibrations were performed in both vacuum and air in order to determine any variation due to buoyancy; none were observed. For these tests two different springs were used because of accidental breakage of one of the springs in the middle of the series of tests. The first spring gave an average extension of 0.025 cm per milligram weight change over the weight range to 1 g, which is equivalent to 4 mg per millimeter extension, while the second gave an average extension of 0.0256 cm/mg, equivalent to 3.9 mg/mm.

The vacuum system, which is capable of obtaining pressures to 10^{-5} mm Hg, consists of a Kinney vacuum forepump and a mercury diffusion pump. Pressure was monitored in the vacuum manifold by a Veeco thermocouple and ion gauge.
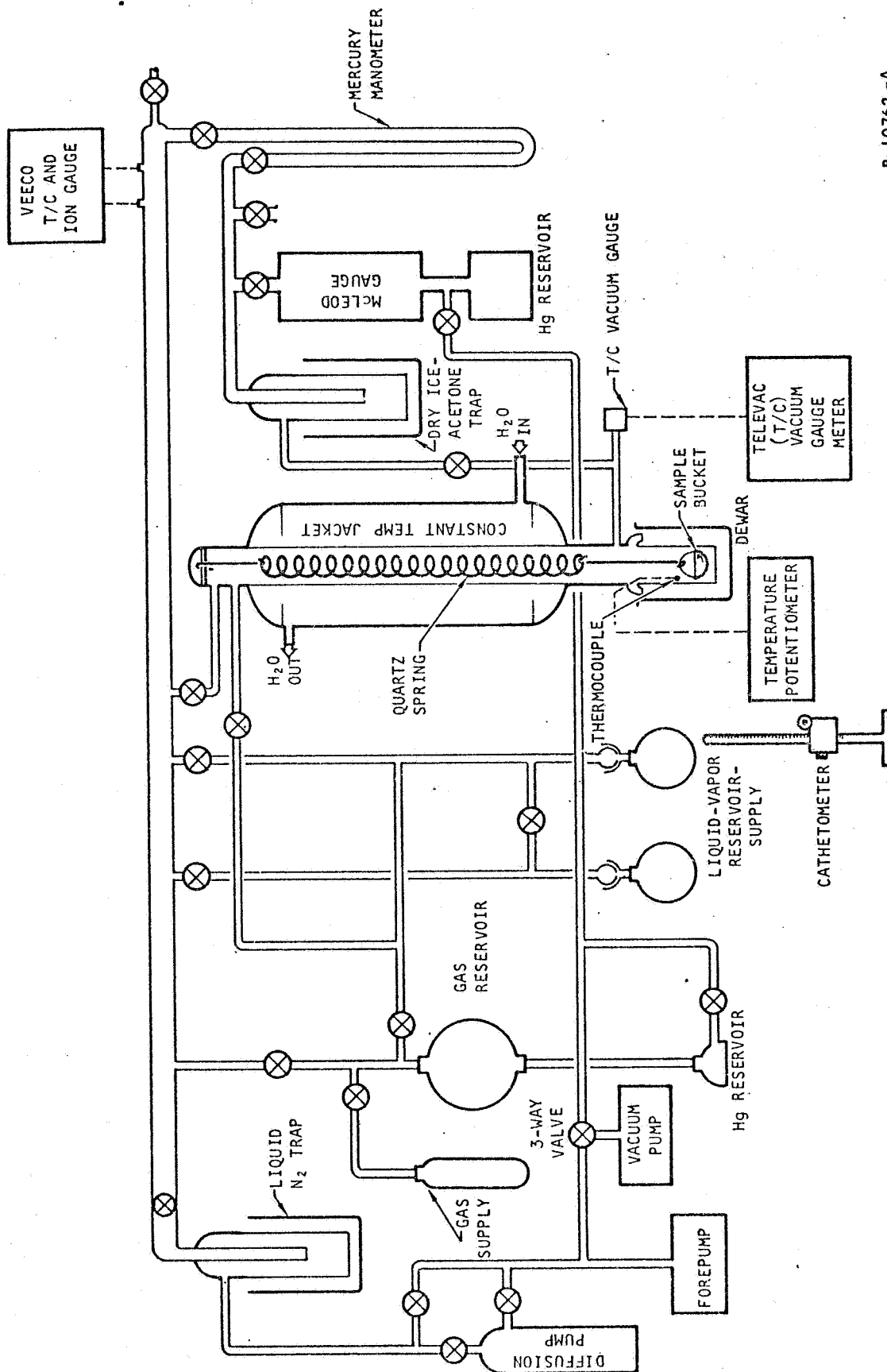
Figure 5-1. Schematic of Gravimetric Equilibrium Sorption Apparatus

B-10762 -A
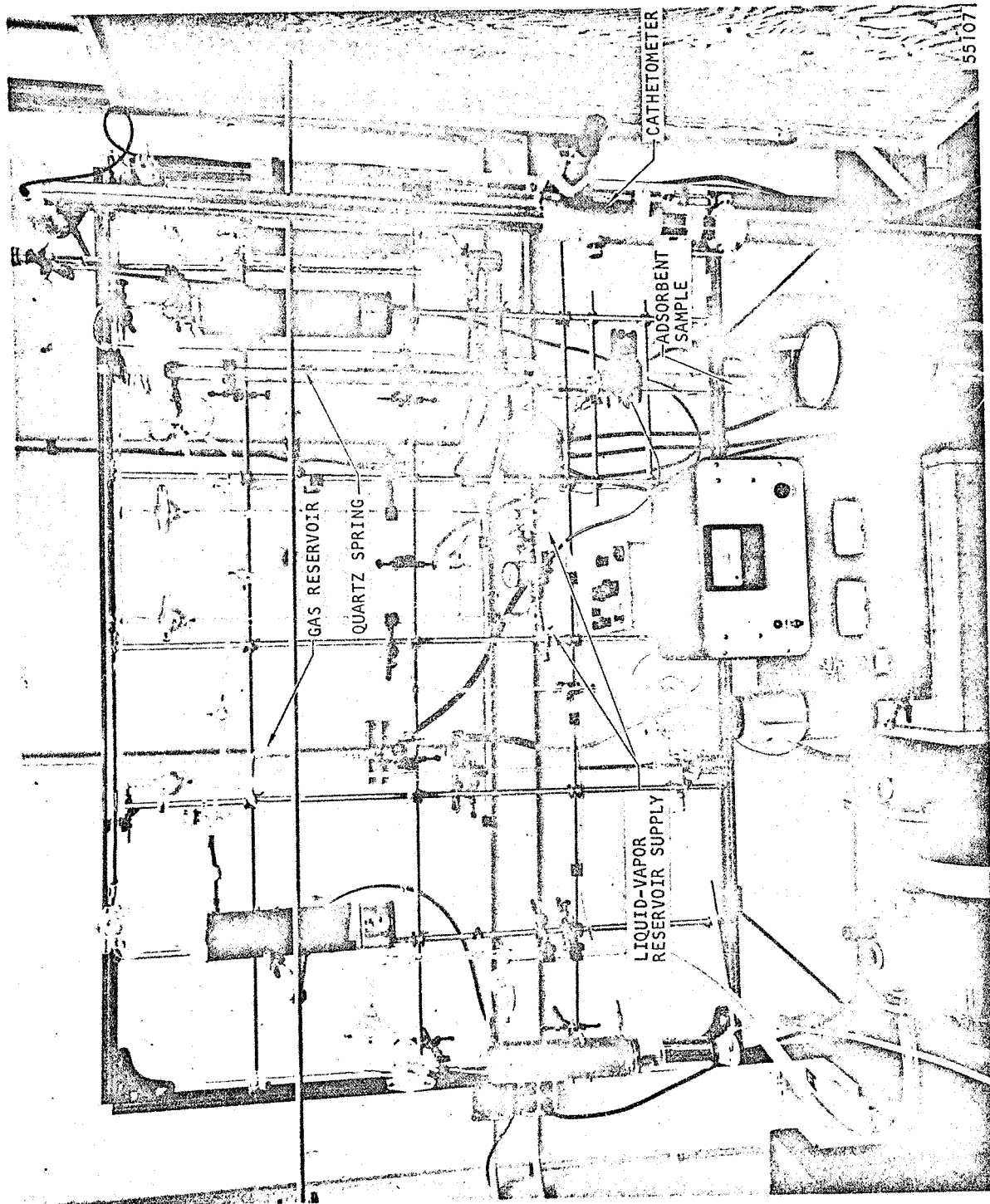
Figure 5-2. Photograph of Gravimetric Sorption Apparatus

Labels on figure: CATHETOMETER, ADSORBENT SAMPLE, GAS RESERVOIR, QUARTZ SPRING, LIQUID-VAPOR RESERVOIR SUPPLY

55107

F-5579

Three pressure measuring devices, (1) a McLeod gauge, i.e., a standard for measuring gas pressure (Figure 5-3a), (2) a Televac thermocouple gauge (Figure 5-3b), and (3) a mercury manometer, were used to sense the system sample pressure. A dry ice-acetone trap was placed between the sample and the McLeod gauge and mercury manometer to prevent mercury contamination of the sample and thermocouple pressure gauge. The McLeod gauge was used for measuring system pressure in the carbon dioxide studies. Since the McLeod gauge cannot be used for condensables, the thermocouple pressure gauge and the mercury manometer were used in the water vapor studies. The Televac thermocouple gauge was calibrated against the McLeod gauge with dry nitrogen and corrections were made to the thermocouple readings for water vapor effects according to manufacturer's instructions. The Televac was used in the range of 0 to 600 microns (0.6 mm Hg); the mercury manometer was used to 13.1 mm Hg.

Operation of the gravimetric adsorption apparatus is relatively simple. As an example, a typical adsorption isotherm determination is performed as follows. Adsorbent is placed on the sample pan. A heating tape is wound around the sample tube and the unit is brought to the required regeneration temperature. At the same time that the sample is heated, it is also evacuated by the pumping system. The temperature is monitored by the thermocouple near the sample pan. After regeneration is complete, i.e., when there is no rise in system pressure after it has been closed off from the pumping system for at least 1/2 hour, the heating tape is removed, sample allowed to cool to room temperature, and the Dewar flask is placed in position. The proper refrigerant is placed in the Dewar flask, and the sample is cooled to the temperature of the refrigerant. After the sample is at the proper temperature, the sample weight is determined from readings of the expansion of the spring by the cathetometer. A small increment of gas or vapor is now added from the respective reservoir-supply system. After addition of the gas or vapor, periodic readings are made of the system pressure and position of the spring. After equilibrium is reached (i.e., when there is no change in system pressure and position of the spring over a period of time), another increment of gas or vapor is added to the sample system. This procedure is repeated until the entire pressure range of interest has been covered.

Adsorption

As described in Section 4, the mechanism controlling adsorption may be film-diffusion, pore-diffusion, or surface reaction. The purpose of the dynamic study was to determine the simplest analytical technique for description of the process and the variation in the necessary coefficients with the experimental parameters.

Data required for determining the mechanism of mass-transfer and the appropriate coefficients were obtained by use of a dynamic adsorption apparatus. This type of apparatus consists of a system where gas or vapor is permitted to flow at known flow rates through a bed of adsorbent of known dimensions at constant temperature and pressure. In this apparatus there is an analytical instrument to determine the inlet and outlet concentrations of the gas or vapor.
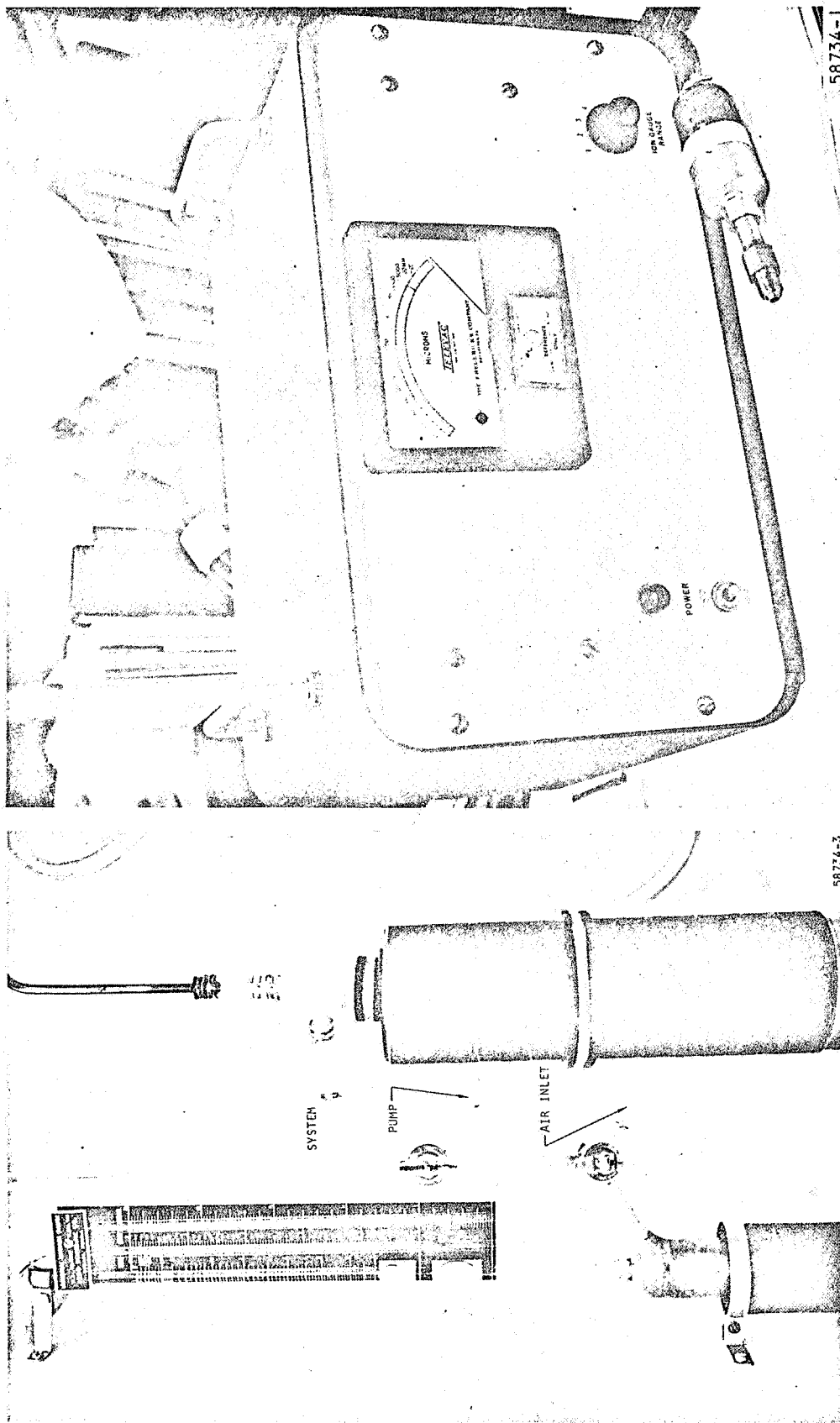
Figure 5-3. (a) McLeod Gauge (Standard) and
(b) Televac Model 2C-M Thermocouple
Gauge

The dynamic adsorption apparatus used in the mass transfer tests is shown schematically in Figure 5-4 and photographically in Figure 5-5. This apparatus consists of a vacuum system, a gas or vapor supply system, an analysis system, and a sample system. A schematic diagram of the sorbent bed system is given in Figure 5-6 and a close-up photograph is shown in Figure 5-7. The copper tube bed is 10 in. long and has an internal diameter of 5/8 in. Its interior is outfitted with 0.010-in.-thick copper fins for good heat transfer; to avoid channeling, the fins are alternately offset by 45 deg for each 1-in. section throughout the bed. Pressure probes and thermocouples were placed at 1-in. intervals throughout the length of the bed starting at 1/2 in. above the retainer screen at the bottom of the bed. Because of the high regeneration temperature and presence of water vapor, chromel-alumel thermocouples were used. Small open beads were exposed to the bed and were checked to ensure that they were not in contact with any metal surfaces. The lead wires were insulated with close packed magnesium oxide and sheathed with stainless steel tubing. The thermocouples of the bed were attached to an eight-channel Offner recorder with an ice bath as the reference junction.

The nitrogen and carbon dioxide flowmeters used were Fischer-Porter instruments with capacities of 2900 cc of nitrogen per min. and 30 cc of carbon dioxide per min., respectively. The accuracy of these flowmeters is 2 percent of full scale.

Inlet and outlet carbon dioxide concentrations were determined by two Beckman IR 15A infrared carbon dioxide analyzers. These analyzers monitored both inlet and outlet concentrations throughout the entire run. The output of the analyzers was recorded on a Brown two-pen recorder. Periodically during the series of tests the two IR analyzers were checked for calibration with known gas mixtures of carbon dioxide and dry nitrogen. Further, at the beginning and end of each run, the instrument zero, gain, and the calibration at the upper end of the scale were checked.

System pressure was determined by a Wallace and Tiernan absolute pressure gauge. This gauge was checked against a McLeod gauge prior to use. The system was kept at a reduced pressure by means of a Kinney vacuum pump in series with a Kinney blower. The combined vacuum system has a design capability of 1000 cfm at 10 microns of pressure.

Water vapor concentrations were determined by means of an AiResearch Dewpointer. This instrument measures dew point with an accuracy of $\pm 3°F$, and has a range of $+150°F$ to less than $-100°F$.

Prior to placement in the sample bed holder, the adsorbent was heat treated at $150°C$ under vacuum in a vacuum furnace for two days and then carefully placed in a capped bottle in a desiccator to prevent contamination with water vapor. The capped bottle containing the adsorbent was weighed and then a portion of the adsorbent was placed in the sample bed holder until proper bed height was attained. The capped bottle was then reweighed and the sample weight in the bed was determined by the difference in weight. In this manner, sample weight could be obtained with a minimum of error due to contamination from water vapor in the air. The bed was packed with the aid of a vibrator to ensure a fairly uniform particle distribution.
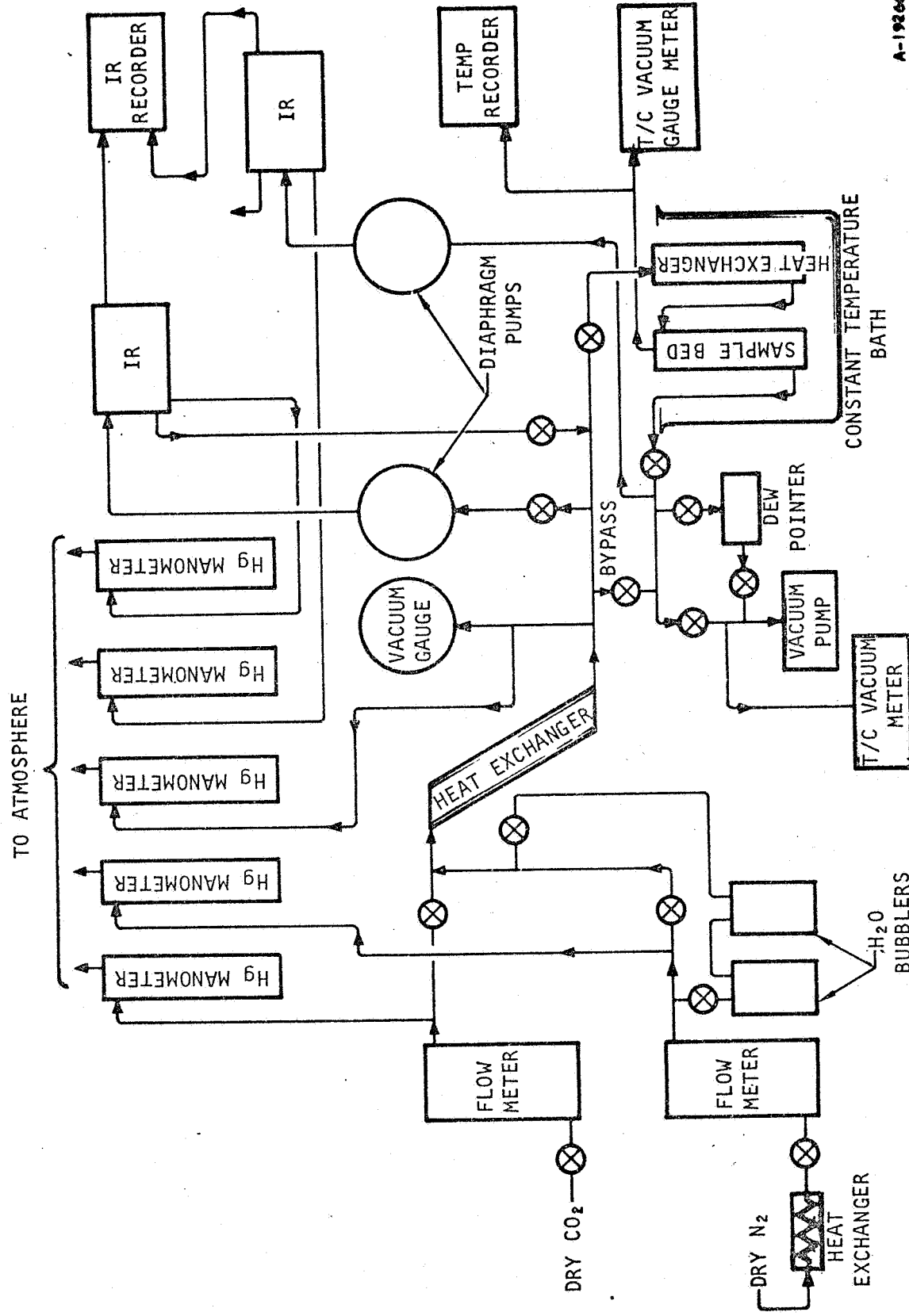
Figure 5-4. Schematic of Dynamic Adsorption Apparatus
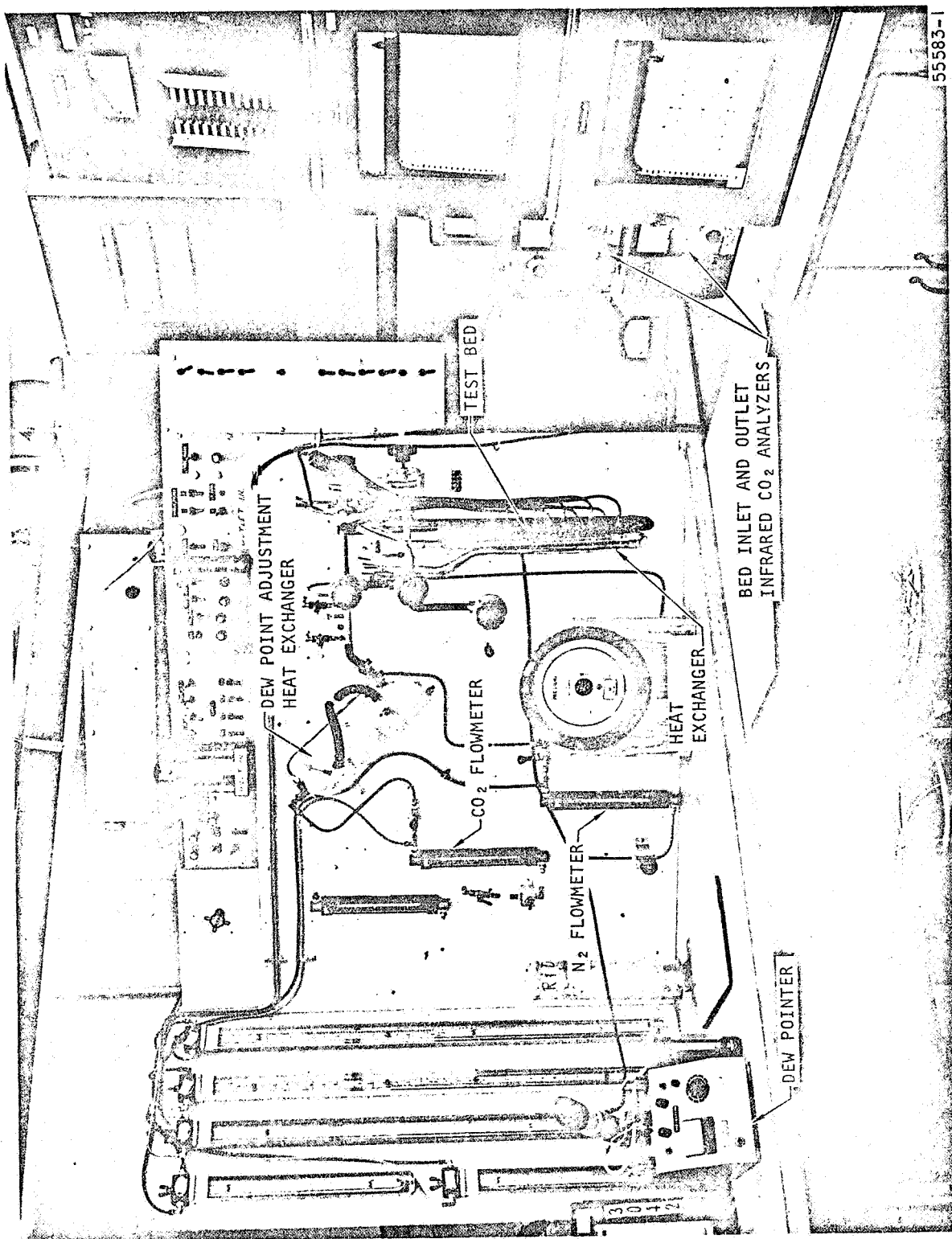
Figure 5-5. Photograph of Dynamic Adsorption Apparatus

GAS/VAPOR INLET

0.010 IN. THICK
COPPER FIN

CHROMEL
ALUMEL
THERMOCOUPLE

ADSORBENT

PRESSURE PROBES

TO
VACUUM

2.0 IN.

P_2

RETAINING SCREEN

TO
PRESSURE
PICKUP (P_1

0.5 IN.

A-22063
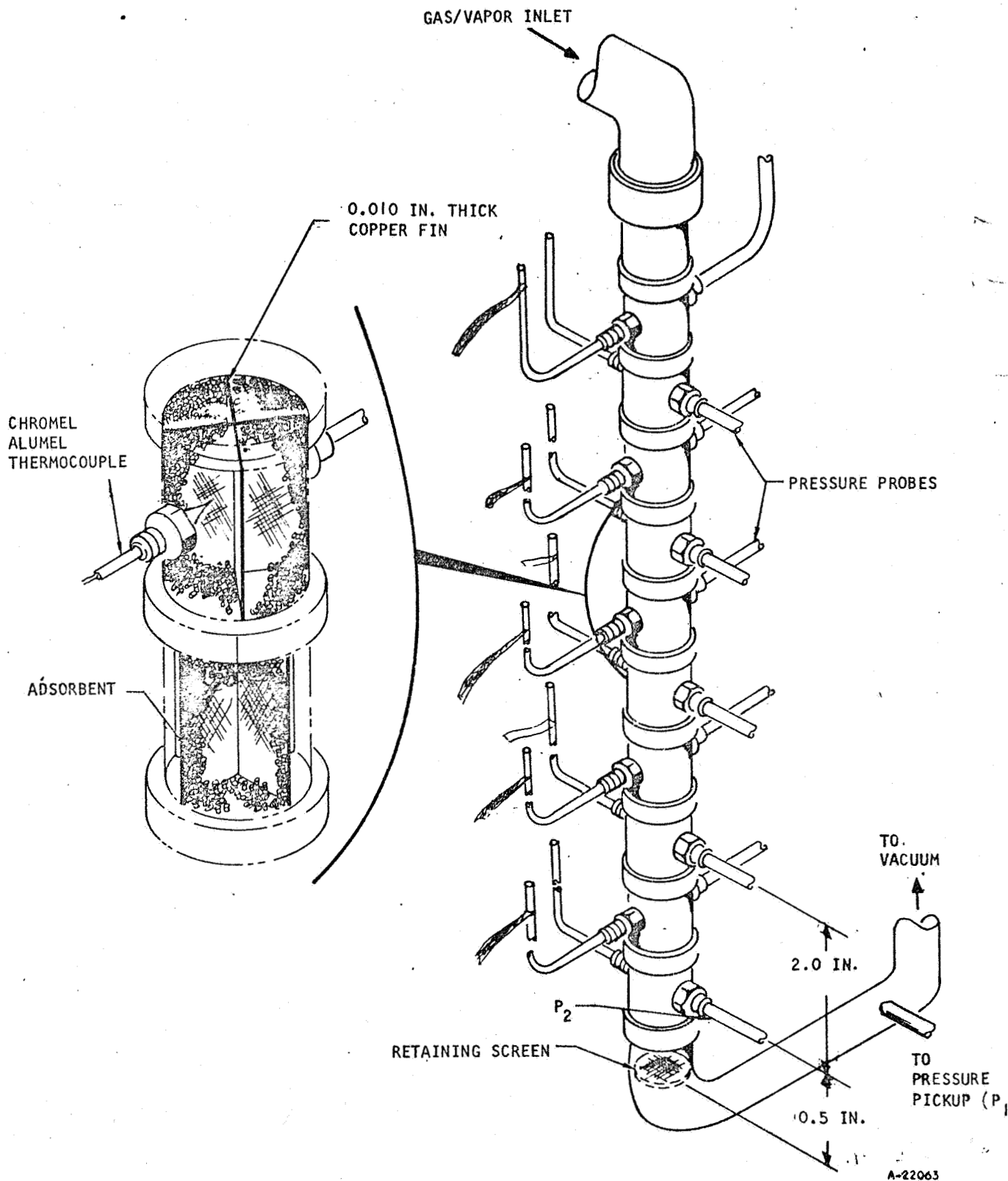
Figure 5-6. Dynamic Sorption Test Bed

PACKED TEST BED

HEAT
EXCHANGER

PRESSURE PORT (TYPICAL)

THERMOCOUPLE
(TYPICAL)

55583-2
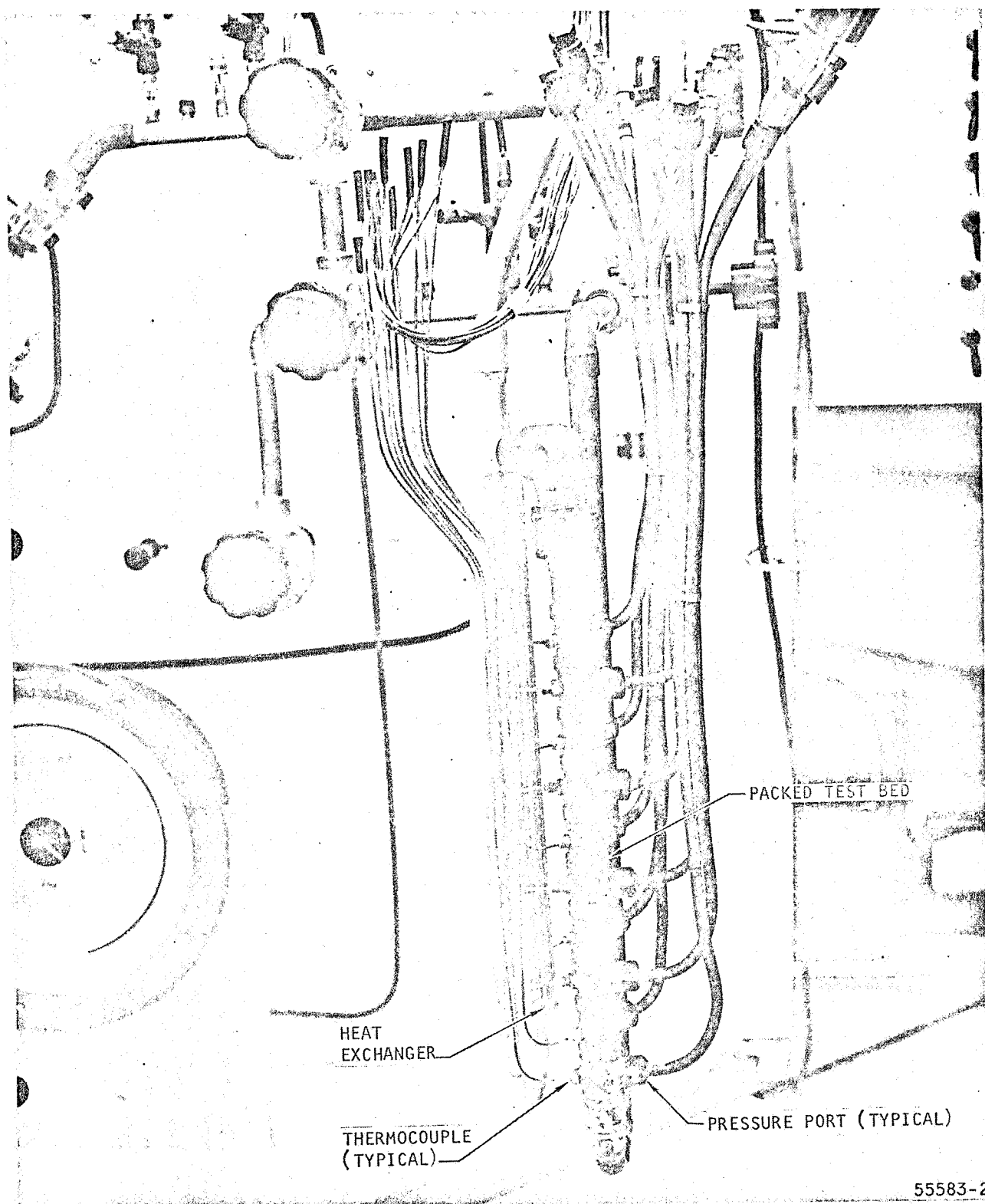
F-5580

Figure 5-7.   Instrumented Packed Adsorbent Bed

Desorption

The process of vacuum desorption occurs in a somewhat different manner than does adsorption. During desorption, no inert gas is present after the first few seconds. Thus, there can be no film-diffusional resistance. Further, the pressure in the bed is an unknown function of axial distance and time. This pressure history may affect both the mass-transfer and heat-transfer rates, the latter due to the drop in gas phase conduction at low pressures.

For the above reasons, a detailed stepwise experimental program was required for the desorption studies--one which would first allow the identification of the rate-controlling step and then permit the determination of the parameters involved.

The dynamic desorption characteristics of water vapor and carbon dioxide from molecular sieve and water vapor from silica gel were determined using the sample bed and dynamic system described above. For these tests, only the sample bed system and the vacuum system portions of the dynamic adsorption apparatus were required. To provide a low-impedance vacuum system, the sample bed was modified. The test bed tubing was cut at a section below the retainer screen, a plug was inserted, and the unit was sealed with silver solder. The top section of the packed bed was modified to accept a 3/4-in. male AN fitting, and the unit was connected directly to the 3-in. vacuum manifold. The pressure pickup formerly located below the retainer screen, was installed in the vacuum manifold elbow section, directly above the bed. Flex-O-Lite glass beads with a 1-% 12 mesh (0.062 to 0.079 in.) were used to fill the bottom void volume of the sample bed; the remaining 5-in. upper section of the bed was packed with the test sorbent. Figure 5-9 shows the system as modified.

Pressures in the bed and manifold were measured using a four-channel CVC Magnevac GMA 140 thermal conductivity gauge (Figure 5-8a). Since this type of gauge is affected by the characteristics of the vapor measured, it was calibrated and monitored by a Texas Instruments precision quartz pressure gauge (Figure 5-8b). This instrument, which is not affected by the characteristics of the vapor being measured, was used to calibrate the Magnevac pressure gauges using pure carbon dioxide or water vapor, respectively. The accuracy of the Texas Instruments gauge was periodically checked by calibrating it against a McCleod gauge with dry nitrogen.

To conduct a desorption experiment, the glass beads and the test sorbent were initially outgassed (for a period over 16 hr) in a 150°C vacuum oven. After the sample bed was packed, the top retainer screen emplaced, and the glass bead and sorbent weights noted, the system was checked for leakage with a Vecco model MS-9 mass spectrometer leak detector. The volume occupied by the sorbent and the free volume of the test system were obtained by initially calibrating a pressure vessel with water and subsequently pressurizing the known volume source with helium and permitting it to expand into the bed and manifold. The relationship is expressed as follows:

$$P_1 V_i \cong P_2 (V_1 + V_f) \tag{5-1}$$

58734-2

58786

F-6539
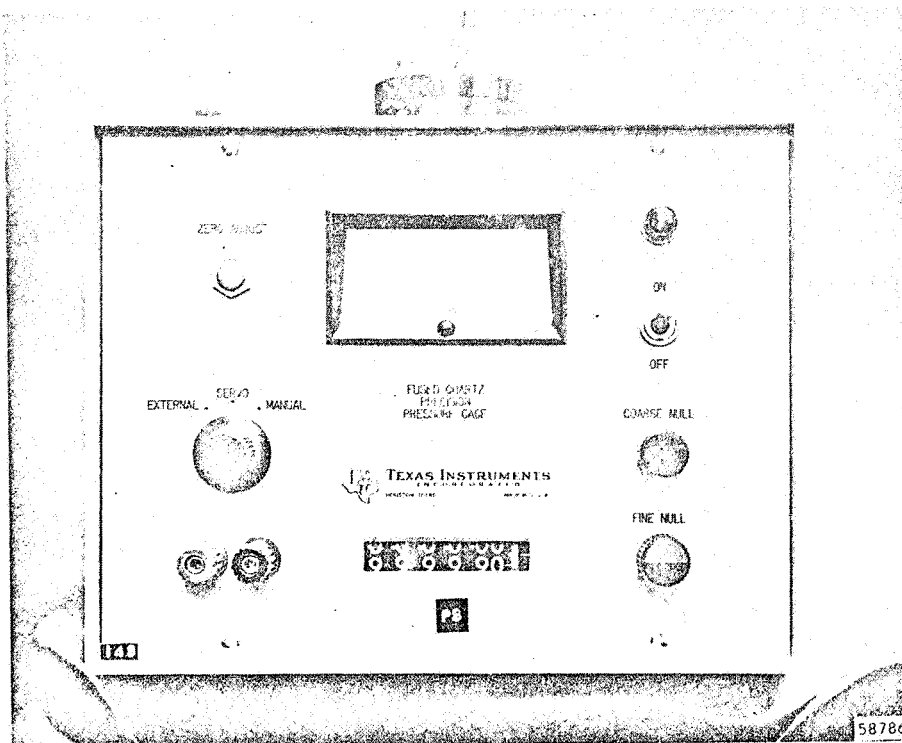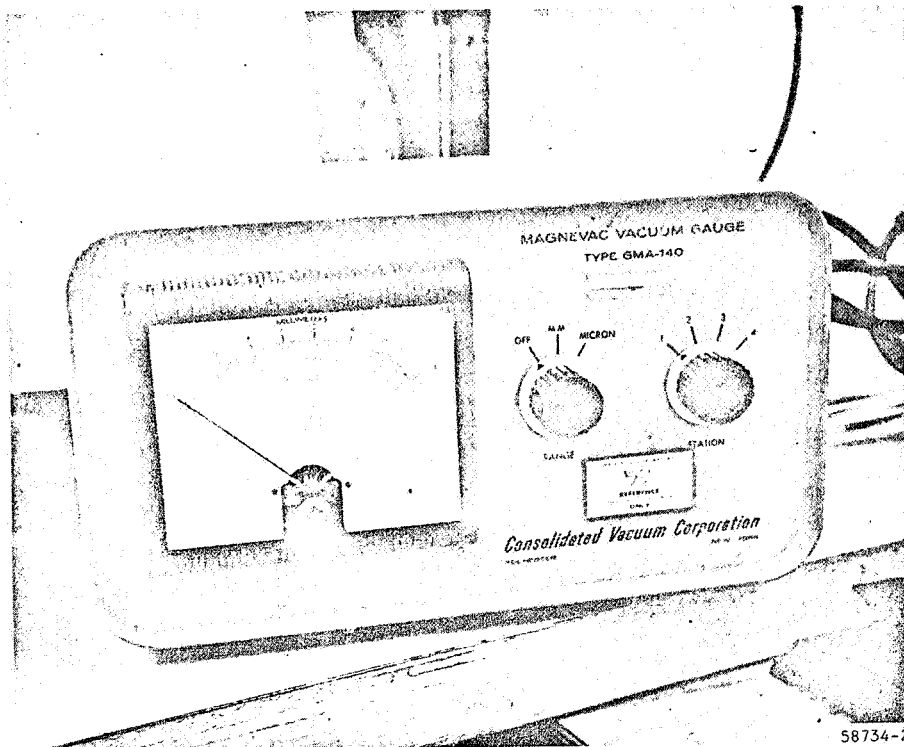
Figure 5-8. (a) CVC Magnevac GMA-140
             Thermal Conductivity Gauge and
             (b) Texas Instruments Quartz Tube
             Gauge
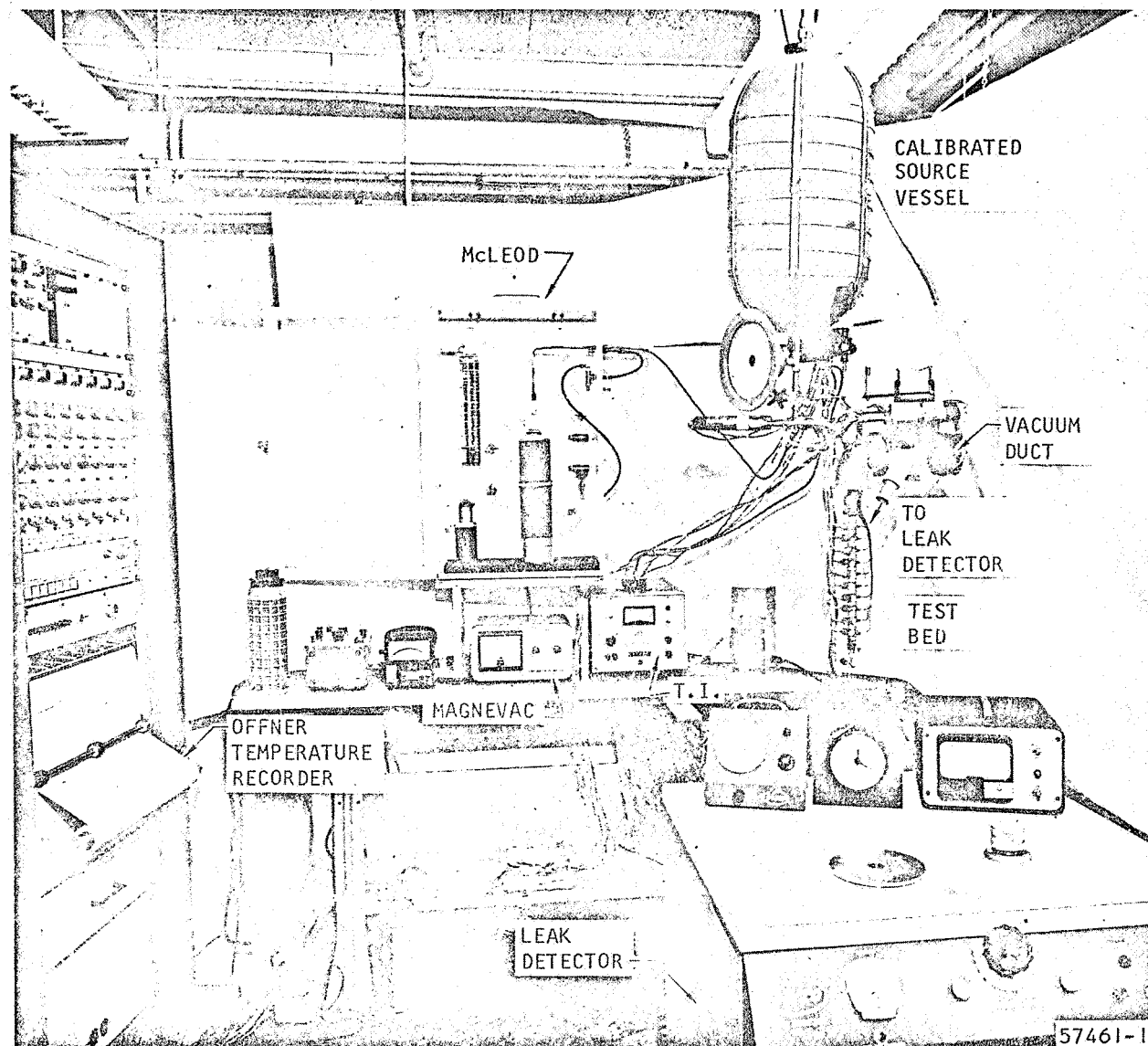
Figure 5-9.   Modified Desorption Apparatus

where P_1 = initial helium source pressure

V_1 = calibrated source vessel volume

V_2 = system pressure after expansion

V_f = free volume of the packed bed

Upon completion of calibration, the bed would be regenerated (Figure 5-10) at a temperature of 600°F for molecular sieve and 350°F for silica gel and at a pressure of 7 microns, for a duration of several hours. The adsorbent was then brought to test temperature by means of a constant temperature bath (Figure 5-11). Pure carbon dioxide or water vapor was introduced to the sample bed through one of the unused pressure probes by means of a valve arrangement, and the bed was brought to a predetermined pressure. The bed and gas or vapor were allowed to come to equilibrium overnight; the temperature of the bath and bed were kept constant.

During initial studies, a known quantity of adsorbate gas or vapor was metered into the adsorbent bed by using the calibrated vessel technique. The amount of gas adsorbed was then checked by allowing for the vapor in the free volume previously determined, the difference between the amount discharged from the calibrated vessel and the amount in the free volume of the bed being the amount adsorbed in the bed. The amount of gas adsorbed was found to check quite closely with the equilibrium value obtained from the equilibrium data previously determined; thus, this procedure was simplified for most runs by using the loading values obtained from equilibrium data.

After equilibrium had been established and initial loading determined, the temperature desired for the desorption run was established in the bath surrounding the bed. The vacuum valve was then opened to vacuum and pressure readings were made at all four stations at frequent time intervals. Temperature data were recorded simultaneously and continuously on the Offner recorder. To determine loading at various times during the desorption run, the vacuum valve was closed, the bed allowed to equilibrate, and from pressure and temperature readings, loading was determined using equilibrium data. The run was then reinitiated. Final bed loading was again generally checked by allowing an overnight equilibrium.
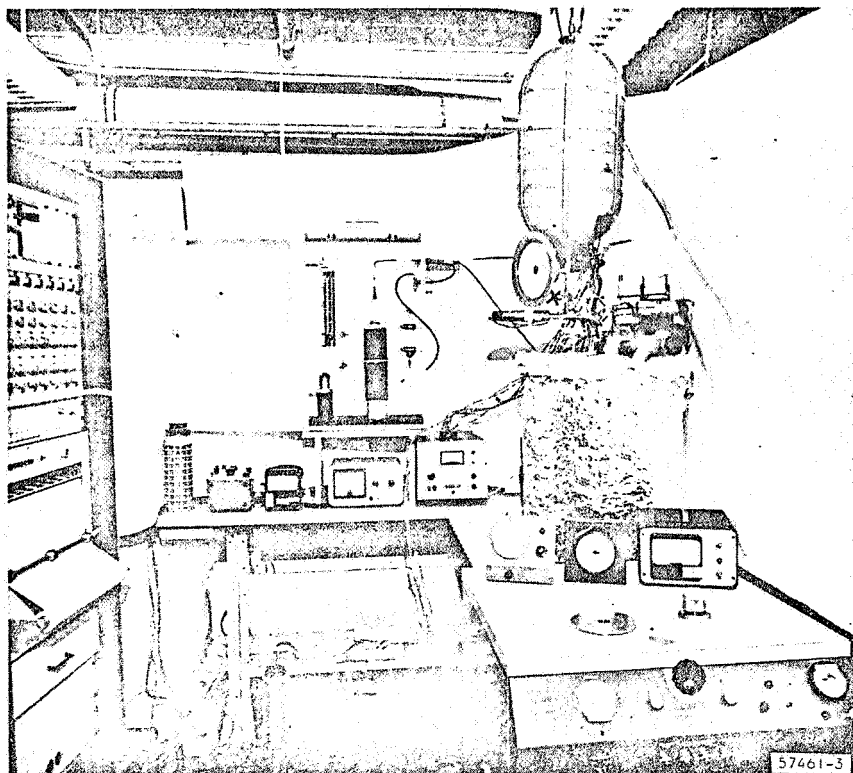
Figure 5-10.   Desorption Bed with Regenerator

F-6432
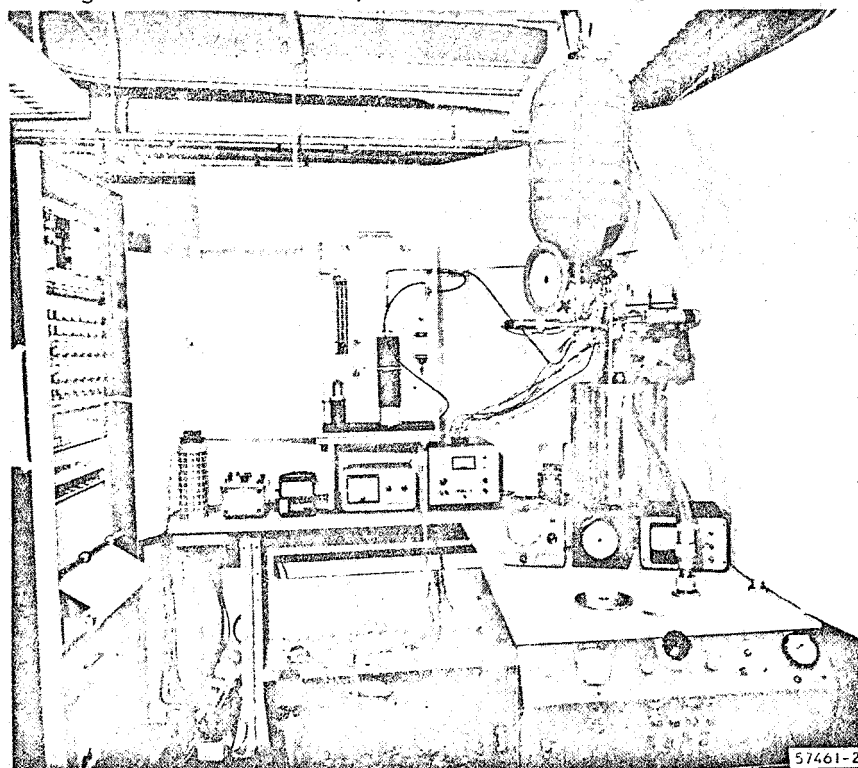
Figure 5-11.   Desorption Bed with Constant Temperature Bath

EQUILIBRIUM ISOTHERMS

Equilibrium isotherms were determined for the adsorption of (1) carbon dioxide on Linde Co. molecular sieve, Type 5A [$Ca_{4.5}Na_3[(AlO_2)_{12}(SiO_2)_{12}] \cdot 30 H_2O$] and Type 5AXW; (2) water vapor on Type 5A molecular sieve; (3) carbon dioxide on water pretreated Type 5A molecular sieve; and (4) water vapor on Davison Co. silica gel (97 percent SiO_2), Grade 05, 6-16 mesh. All molecular sieve tests were performed with 1/16 in.-diameter pellets. For the equilibrium determinations, prior to each adsorption run, the molecular sieve samples were desorbed, in situ, at 600°F under vacuum conditions (10^{-5} mm Hg), and the silica gel samples were desorbed, in situ, at 350°F under vacuum conditions.

Carbon Dioxide Adsorption on Molecular Sieves

Initially, a preliminary isotherm was determined for carbon dioxide adsorption on Type 5A molecular sieve that had been regenerated at 400°F under vacuum conditions. The resultant data gave lower adsorption capacities than reported by Linde (Reference 5-1). Since Linde states that water may be removed, without damage to the molecular sieve by heating to 600°F, it was decided to regenerate at that temperature.

All of the molecular sieve equilibrium isotherms determined have been plotted with actual adsorption capacities obtained vs pressure; test data points appear in the figures presented in Appendix C.

Figures 5-12 and C-1 through C-4 give the four equilibrium isotherms obtained at 0°, 10.5°, 25°, and 50°C (32°, 50.9°, 77° and 122°F), (Run Nos. 5 and 6, 7, 1-4, and 10, respectively) for the adsorption of carbon dioxide on Linde Type 5A molecular sieve 1/16-in.-dia pellets (Lot No. 551194). These isotherms are typical of the equilibrium data obtained, and as expected (1) adsorption capacity increases with lowering of temperature and (2) the general shape of the isotherms undergoes no discontinuity as the critical temperature of CO_2 (31°C) is approached and passed. A comparison of the isotherms determined at AiResearch with isotherms given in Linde publications indicates that the former gave lower adsorption capacities than the latter. Further, data reported by Minneapolis-Honeywell (Reference 5-2) at 25°C seems to be between Linde and AiResearch's data. Due to the differences between the various sources of data, a sample of the same lot tested by AiResearch was sent to an outside laboratory (Pacific Sorption Service, Chico, California) for an adsorption isotherm determination at 25°C. The outside laboratory performed its determination using a volumetric technique by means of a B.E.T. apparatus. Their results gave adsorption capacities slightly lower than that obtained by AiResearch. A comparison of the 25°C isotherms determined by the four different sources is given in Figure 5-13. Also included are the capacities at approximately 1 and 7 mm Hg pressure determined by the dynamic breakthrough tests.

The discrepancies in the isotherms of Linde, Minneapolis-Honeywell, and AiResearch are probably due to differences in the production of the molecular sieve. Over the years, there have been changes in the manufacture of molecular sieves which gave different adsorption capacities. For example, different Linde publications have given different isotherms. Pacific Sorption Service's lower adsorption capacity data may be due to their desorbing the sample at
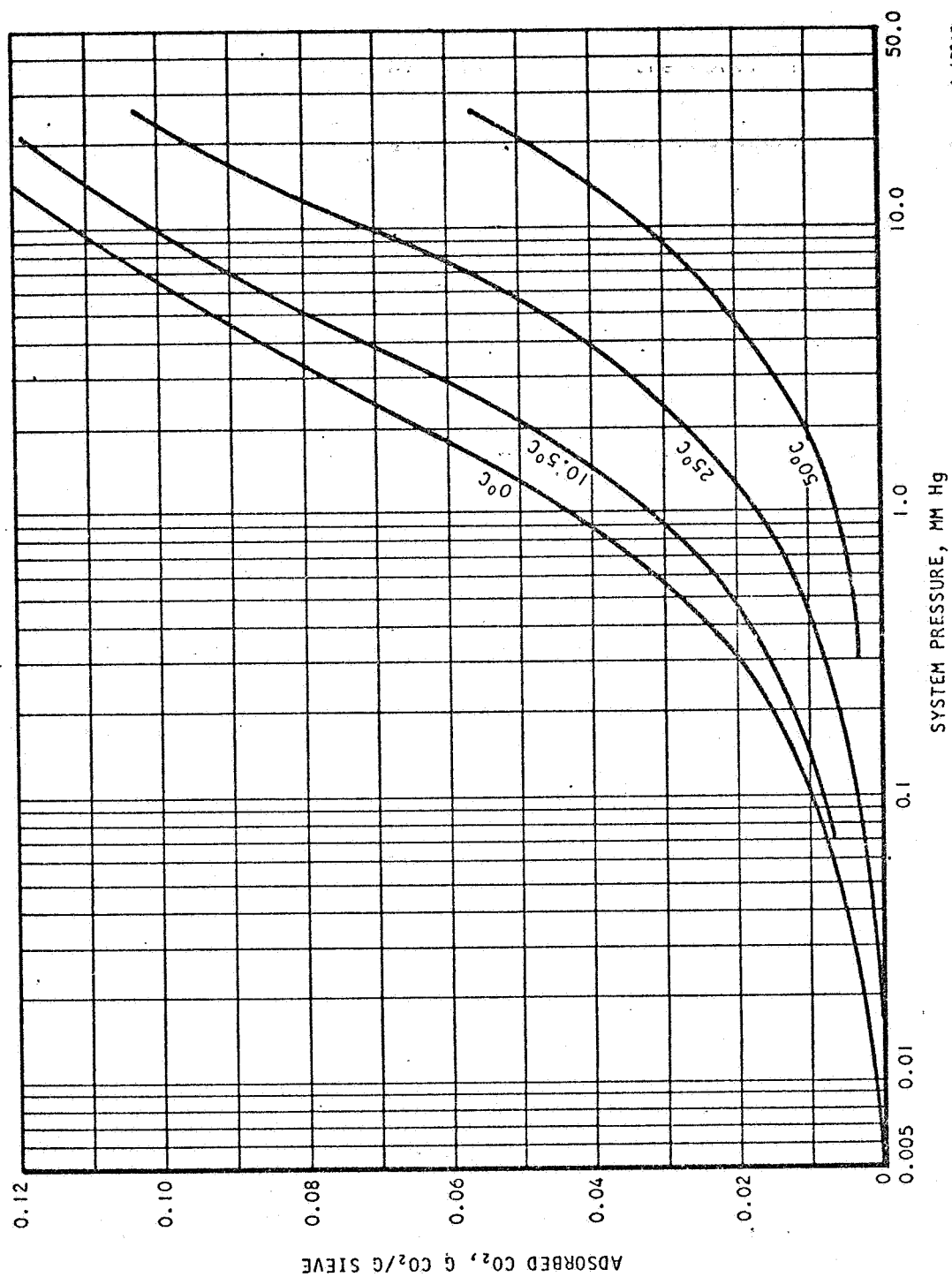
Figure 5-12. Equilibrium Isotherms of Carbon Dioxide Adsorption on Linde Molecular Sieve, Type 5A, 1/16-in.-dia Pellets

A-19269
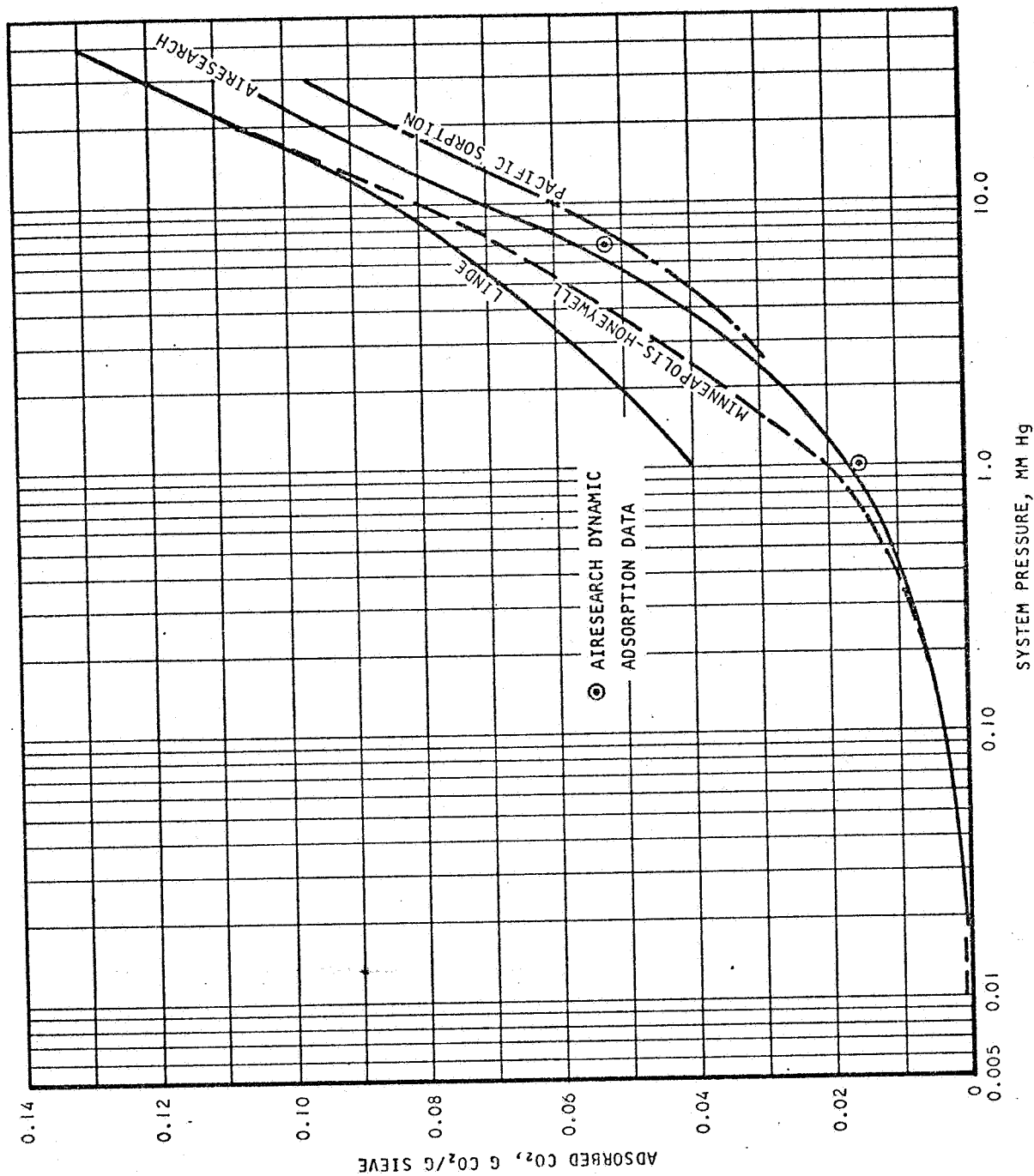
Figure 5-13. Comparison of 25°C Equilibrium Isotherms of Adsorption of Carbon Dioxide on Linde Type 5A Molecular Sieve

AIRESEARCH MANUFACTURING DIVISION
Los Angeles, California

600°F for only one hour under vacuum conditions and, thus, not completely desorbing the pellets. At AiResearch, the pellets are desorbed at 600°F for several hours under high-vacuum conditions.

In an effort to determine any difference in adsorption capacities of different lots supplied by Linde, a carbon dioxide adsorption isotherm at 25°C was determined for a sample of Type 5A, 1/16-in.-dia pellets of Lot No. 541259 (Run No. 8). This isotherm gave adsorption capacities just slightly larger than the previous lot. It is still considerably less than that reported by Linde. A new sample of the original Lot No. 551194 was also tested (Run No. 9). Here, the 25°C carbon dioxide adsorption isotherm was identical to the previous isotherms obtained for this lot.

From the four isotherms shown in Figure 5-12, isobars and isosteres were plotted (Figures 5-14 and 5-15, respectively). Using these plots, new isotherms were calculated for 5°C, 18°C, and 37°C. Both isobar and isostere plots gave identical isotherms indicating consistent data. This comparison is given in Figure 5-16. An attempt to do this with isobars and isosteres obtained from Linde isotherms gave inconsistent data; two different curves were obtained.

The equilibrium isotherm at 25°C Figure 5-17, for Type 5AXW (Run No. 12) molecular sieve, 1/16-in.-dia pellets (Linde Lot No. 556313) gave higher adsorption capacities than Type 5A. These capacities varied from about 4 percent higher at 20 mm Hg pressure to about ten percent higher at a pressure of 1 mm Hg. At still lower pressures there was a further increase in percentage of greater CO_2 adsorption capacity. Even with the higher capacity obtained, this data was lower than that reported by Linde Company for Type 5A molecular sieve. At the present time, Linde could not provide equilibrium adsorption isotherm data for Type 5AXW molecular sieve. Although both types of material contain the same adsorbent, the amount of nonactive inert binder differs. The Type 5A material contains 20 percent binder, while Type 5AXW contains 7 percent binder.

The properties of the two types should be similar except that the higher density adsorbent in Type 5AXW pellets should give higher capacities than Type 5A pellets for the same weight of pellets. There is a difference in color of pellets; Type 5A is white, while Type 5AXW is yellow. Little was known about the stability of Type 5AXW pellets on long-duration cycling; it was felt that the lower amount of binder present in Type 5AXW would eventually result in powdering and breakdown upon continuous regeneration.

Water Adsorption on Molecular Sieve

An equilibrium isotherm of the adsorption of degassed distilled water on Type 5A, 1/16-in.-dia pellets (Linde Lot No. 51194) at 25°C was made (Run No. 11) (Figure 5-18 and Figure C-5). The adsorption data obtained gave an isotherm with lower water adsorption capacities than Linde reported. This difference again may be due to differences in production of the different lots tested; the Linde data are several years old.
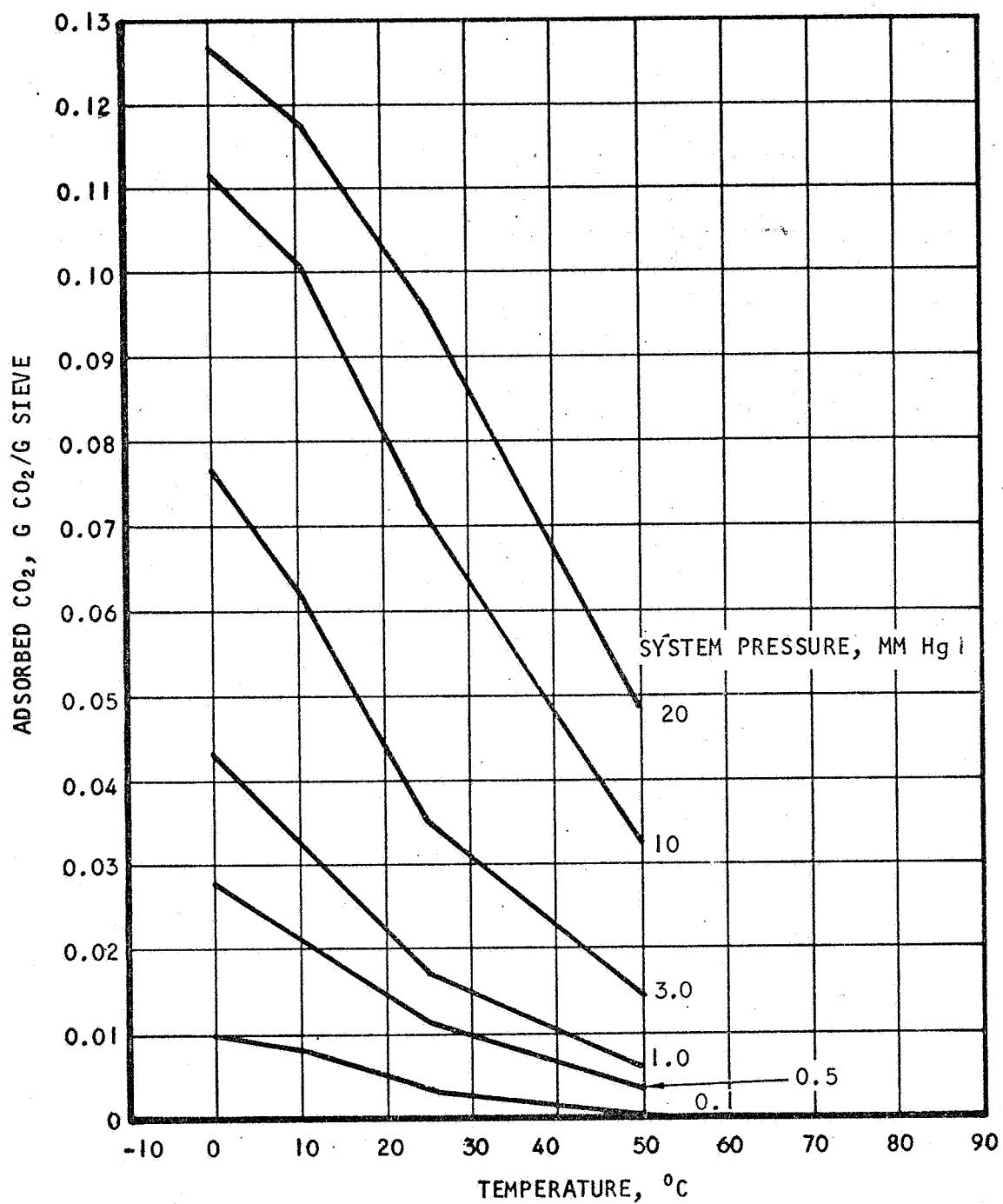
A-22035

Figure 5-14. Equilibrium Isobars of Carbon Dioxide Adsorption on Linde Molecular Sieve Type 5A, 1/16-in.-dia Pellets Obtained from Figure 5-12
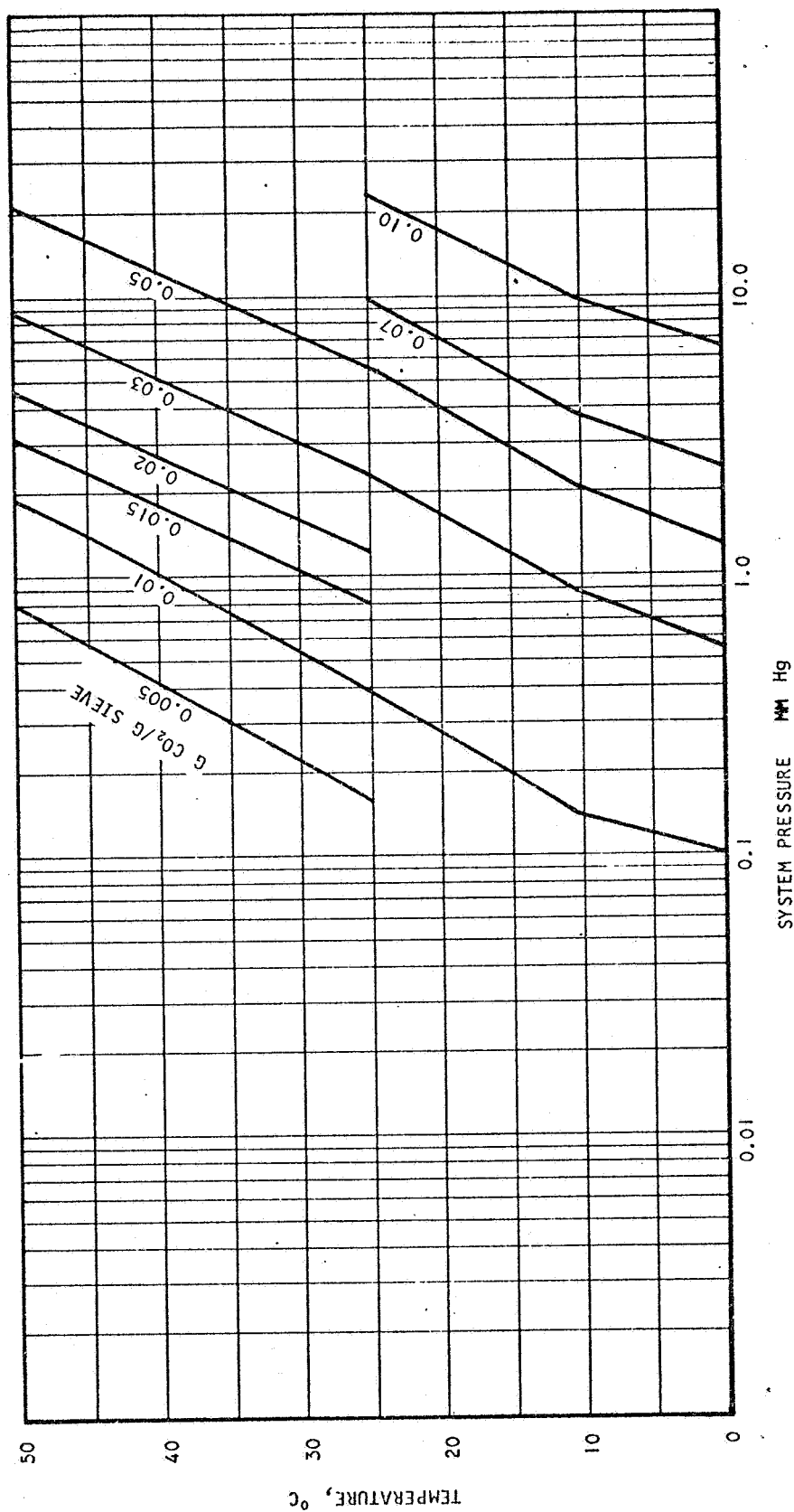
Figure 5-15. Equilibrium Isosteres of Carbon Dioxide Adsorption on Linde Molecular Sieve Type 5A, 1/16-in.-dia Pellets Obtained from Figure 5-12

B-11135
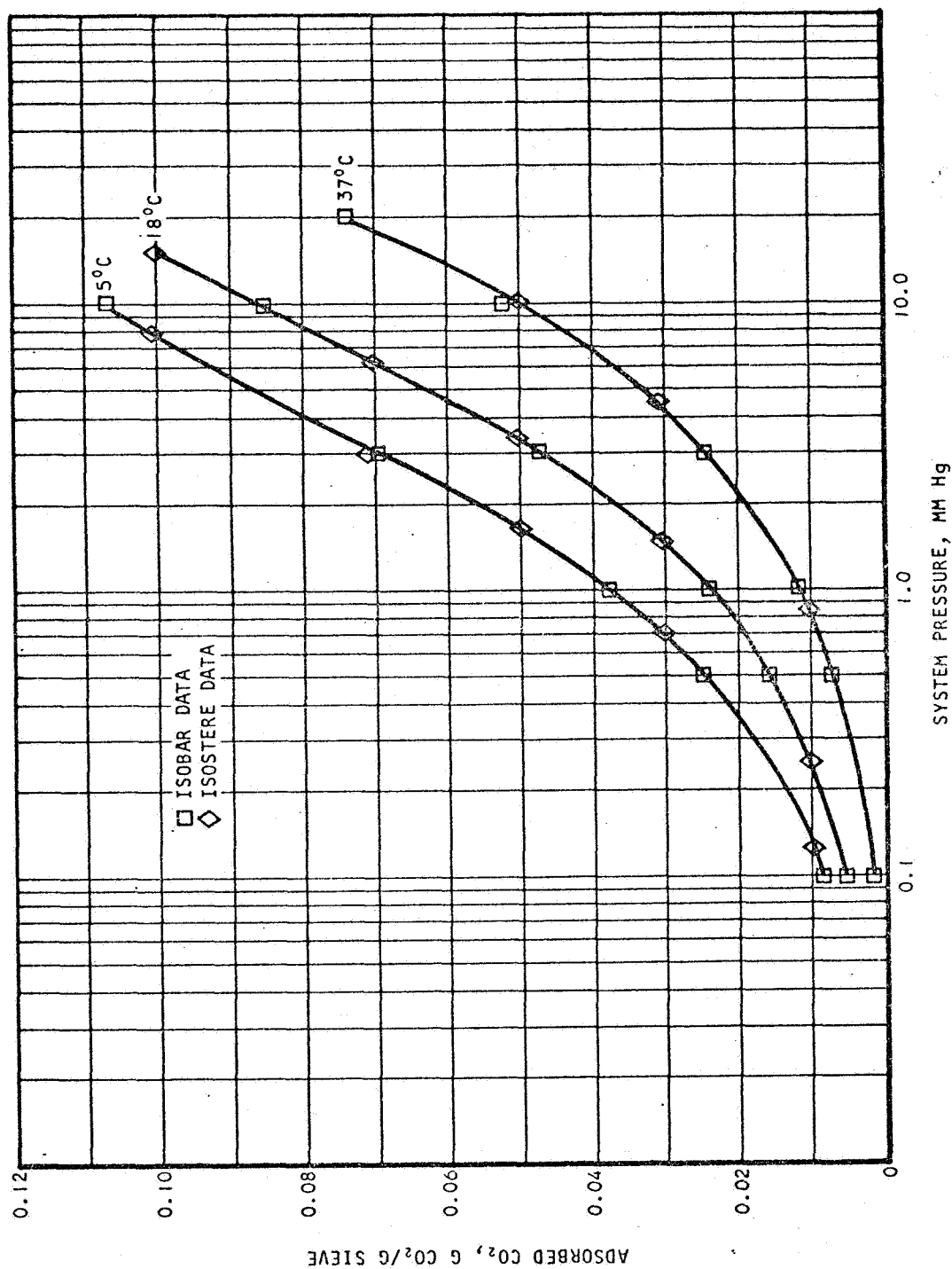
Figure 5-16. Equilibrium Isotherms Obtained From Isobar and Isostere Cross Plots
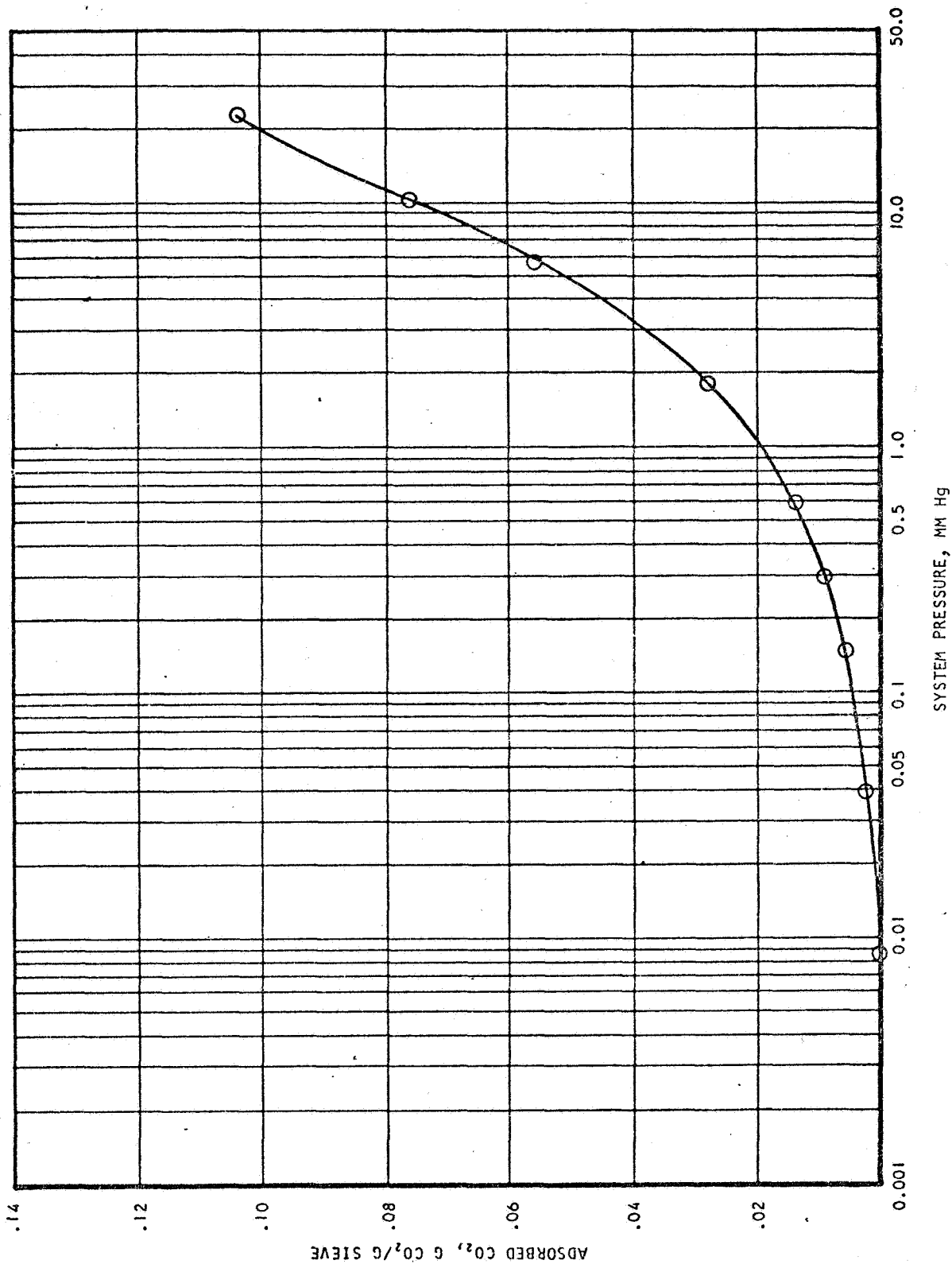
Figure 5-17. Equilibrium Isotherm of Carbon Dioxide Adsorption on Linde Molecular Sieve Type 5AXW, 1/16-in.-dia Pellets at 25°C

A-21999
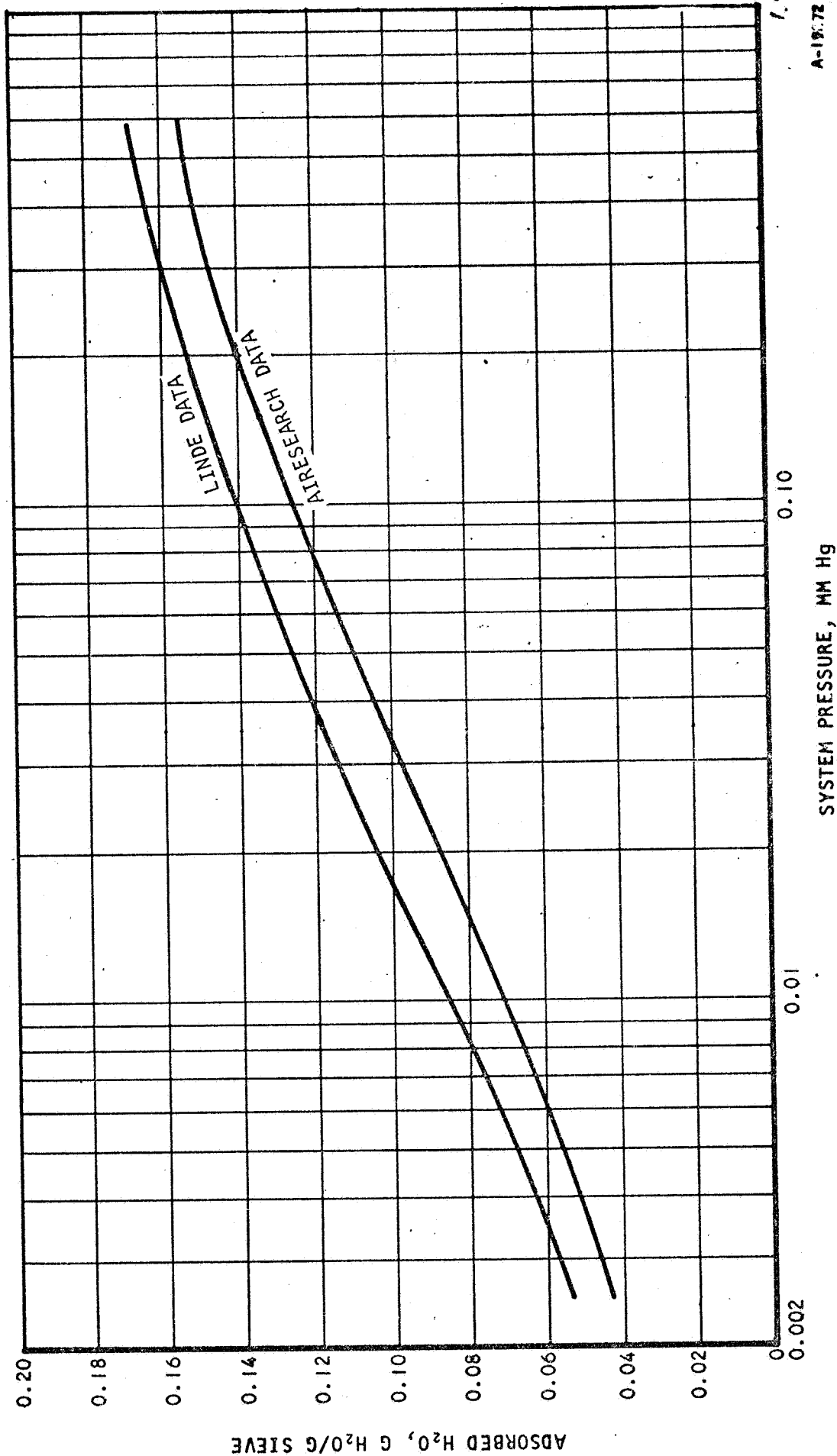
Figure 5-18. Equilibrium Isotherm of Water Vapor Adsorption on Linde Molecular Sieve Type 5A, 1/16-in.-dia Pellets at 25°C

Effect of Residual Water on Carbon Dioxide Capacity of Molecular Sieve

In an effort to determine the effect of previously adsorbed water on molecular sieve on the further adsorption of carbon dioxide, an equilibrium carbon dioxide adsorption isotherm at 25°C was determined (Run No. 11A) on Type 5A, 1/16-in.-dia pellets containing a known amount of water (see Figure 5-19). Only a small amount of carbon dioxide was capable of being coadsorbed on the molecular sieve in this determination. For example, the sample containing 0.076 g H_2O/g sieve, corresponding to an equilibrium partial pressure of water vapor of 0.0125 mm Hg, only adsorbed 0.0185 g CO_2/g sieve at a system pressure of 23 mm Hg, while dry molecular sieve adsorbed 0.10 g CO_2/g sieve at a system pressure of 23 mm Hg.

Water Vapor Adsorption on Silica Gel

As a result of differences in experimental equilibrium data by various sources encountered during the molecular sieve phase of the program, an equilibrium isotherm at 25°C (Figure 5-20) was obtained for the adsorption of water vapor on silica gel (Davison Chemical, Lot No. 1807, 6-16 mesh, Grade 05) over a pressure range of 0.02 to 13 mm Hg. The isotherm obtained gave similar adsorption capacities for water vapor when compared with data presented by Davison (Reference 5-3). Additional equilibrium data for Davison silica gel with water vapor (Reference 5-4) is shown in Figure 5-21.

In an effort to quickly determine cycle reproducibility, four cycles of adsorbing water on silica gel at 25°C and approximately 7 mm Hg pressure and then desorbing at 50°C to approximately 0.2 mm Hg pressure were performed.

The results, summarized in Table 5-1, indicate that similar bed loads were obtained for both adsorption and desorption for all four cycles at equilibrium conditions.

TABLE 5-1

CYCLING DATA FOR ADSORPTION OF WATER VAPOR AT 25°C
ON SILICA GEL AND DESORBING AT 50°C

Cycle No.	Adsorption at 25°C		Desorption at 50°C	
	P (mm Hg)	Capacity (g H_2O/g gel)	P (mm Hg)	Capacity (g H_2O/g gel)
1	6.8	0.1843	0.220	0.0064
2	6.5	0.1788	0.218	0.0064
3	6.7	0.1745	0.228	0.0064
4	6.8	0.1814	0.183	0.0055
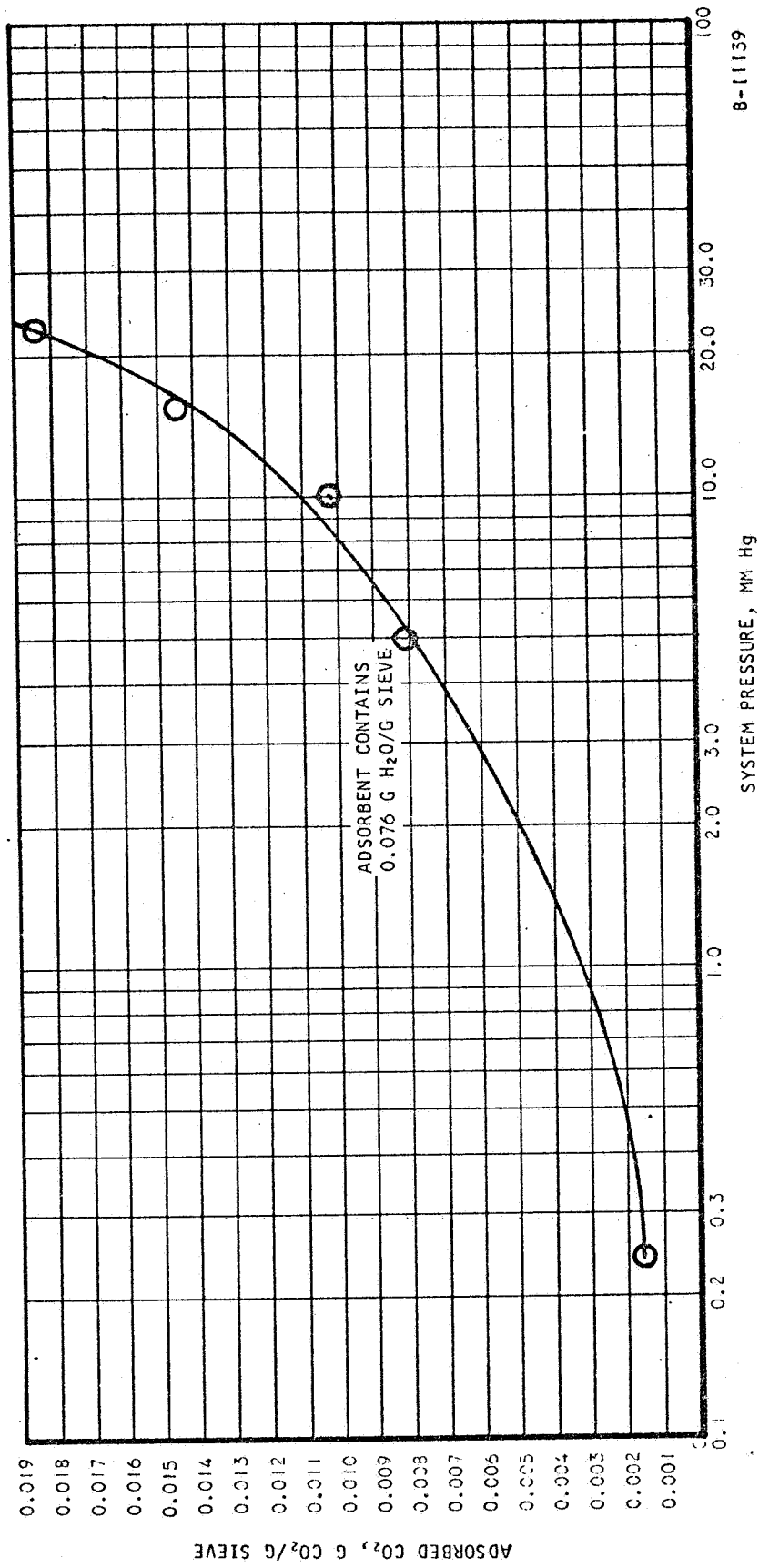
Figure 5-19. Equilibrium Isotherm of Carbon Dioxide Adsorption on Water Treated Linde Molecular Sieve Type 5A, 1/16-in.-dia Pellets at 25°C
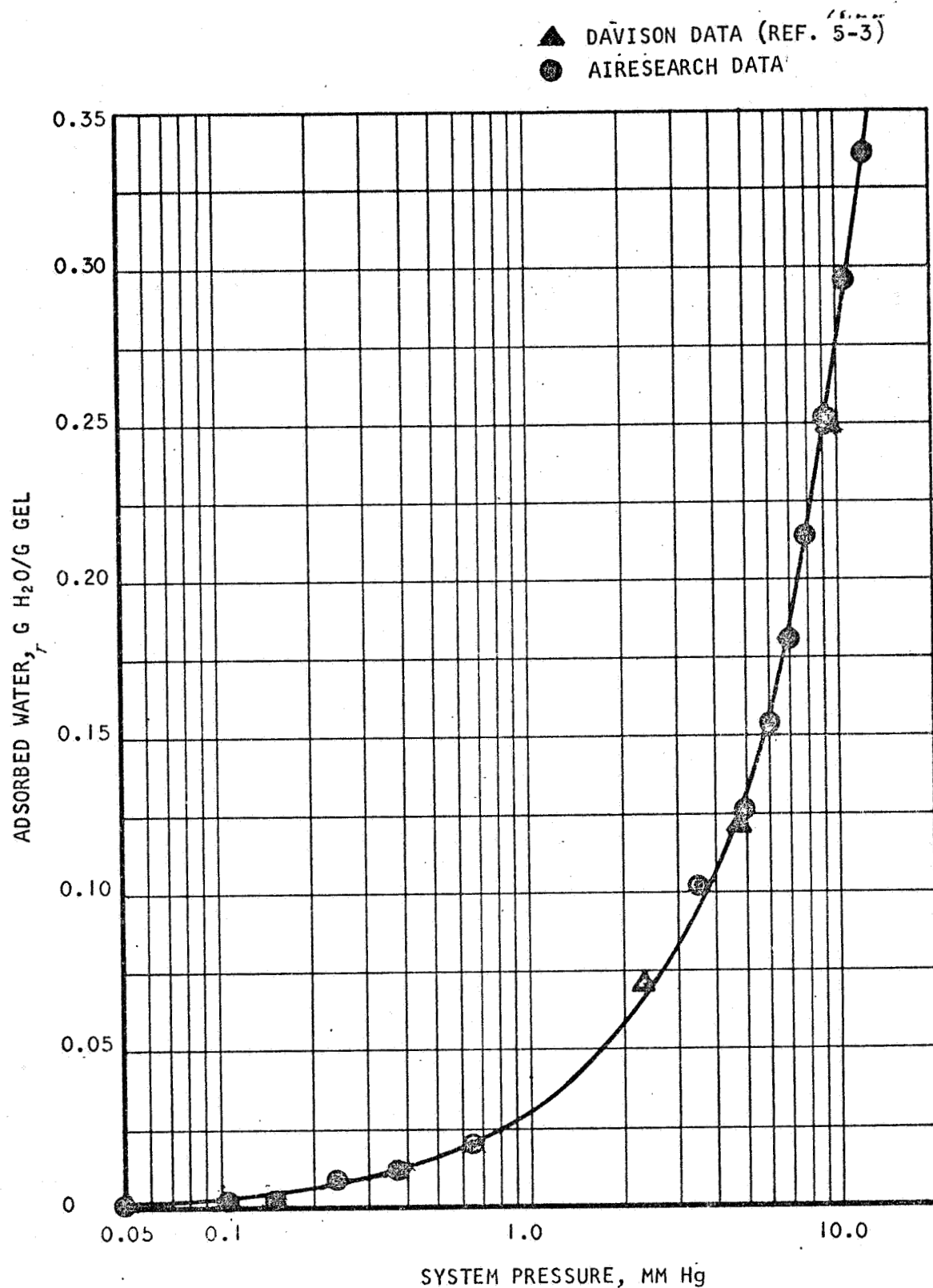
Figure 5-20. Equilibrium Isotherm of Water Vapor Adsorbed on
Davison Grade 05, 6-16 Mesh Silica Gel at 25°C

The graph axes and labels:

- Y-axis: ADSORBED WATER, G H_2O/G GEL (0 to 40)
- X-axis: SILICA GEL TEMPERATURE, °F (40 to 200)

Text within graph: DEW POINTS CORRESPONDING TO PARTIAL PRESSURES ARE GIVEN IN PARENTHESES ON ISOPIESTIC LINES (*, **)

Isopiestic line labels: 0.20 (35°), 0.40 (53°), 0.70 (68°), 1.00 (79°), 1.50 (92°), 2.00 (101°), 3.00 (115°), 4.00 (125°), 6.00 (141°), 8.00 (152°), 12.00 (169°), 16.00 IN. Hg (182°F DP)

Lower isopiestic lines: 0.10 (20), 0.06 (9), 0.02 (-11), 0.007 (-30), 0.002 (-50), 0.001 (-57), 0.0003 IN. Hg (-77)
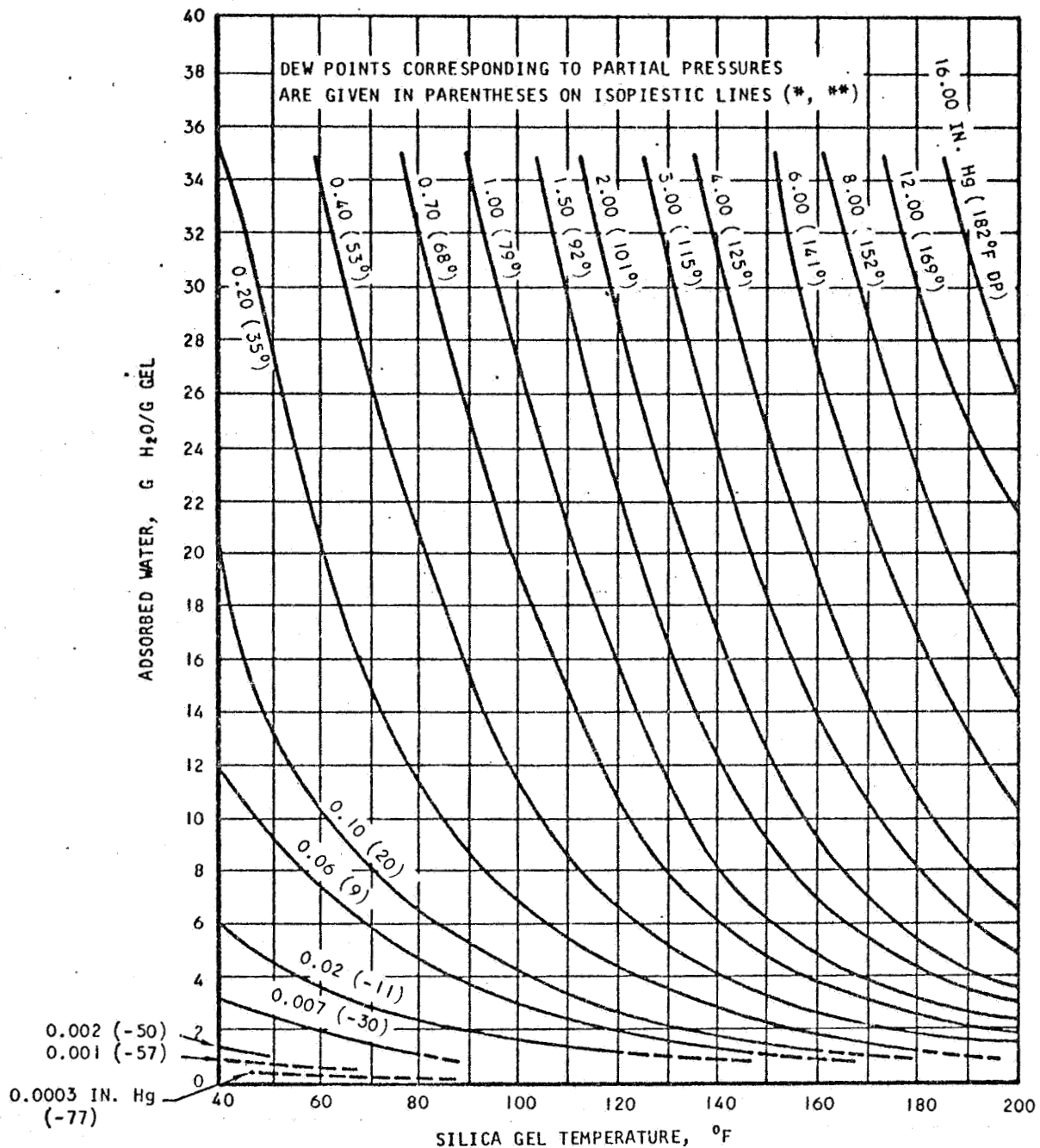
A-6558-8

*THE CONCEPT OF A DEW POINT BELOW 32°F, ALTHOUGH WIDELY ACCEPTED BY THE INDUSTRY, IS A MISNOMER; A SUBLIMATION POINT WOULD BE A MORE APPROPRIATE TERM.

**THE SATURATION TEMPERATURES CORRESPONDING TO PRESSURES BELOW 0.20 INCHES OF Hg HAVE BEEN CORRECTED ACCORDING TO REFERENCE 5-5.

Figure 5-21. Water Vapor Capacity of Silica Gel as a Function of Temperature at Various Partial Pressures, in. Hg (Equilibrium Isopiestics) as Reported by Davison Co. (Reference 5-4)

Differential Heat of Adsorption

When a gas or vapor is adsorbed on the surface of a solid, or when a liquid wets an adsorbent, heat is released. The heats evolved are usually referred to as integral heats when a definite quantity of fluid and a bare surface are involved. The term differential heat is used to describe a process conducted at constant temperature whereby a unit quantity of fluid contacts a large quantity of solid that has been previously exposed to the fluid, i.e., a constant concentration (isosteric) process. In most instances the total heat evolved during adsorption is greater than the heat of liquefaction of an equivalent amount of vapor; this difference is referred to as a net heat of adsorption, or the heat of wetting.

As developed in Section 4, the isosteric or differential heat of adsorption may be determined from the Clausius-Clapyron equation (A-17), assuming ideal vapor behavior;

$$\frac{d \ln P}{d \left(\frac{1}{T}\right)} = \frac{\Delta H}{R} \qquad (5-2)$$

where

P = partial pressure, psia

T = absolute temperature, $^{\circ}R$

ΔH = isosteric or differential heat of adsorption, Btu/lb

R = gas constant, 1.987 Btu/lb mole $^{\circ}R$

by plotting the log P vs $1/T$ and determining the slope of the isostere. If the equation is integrated and rearranged as follows

$$\Delta H = R \frac{T_1 T_2}{T_2 - T_1} \ln \frac{P_2}{P_1} \qquad (5-3)$$

the differential heat of adsorption may be determined from two close adsorption isotherms at T_1 and T_2 at the same adsorbent loading, for a range of loadings.

From the isosteres plotted for the adsorption of carbon dioxide on Type 5A molecular sieve pellets (Figure 5-15), differential heats of adsorption at T_1 = 32.2 (90°F) and T_2 = 37.8°C (100°F) were calculated for various bed loadings. This temperature regime is approximately the expected system design temperature for the desorption of carbon dioxide from molecular sieve. Figure 5-22 gives the relationship of the calculated differential heats of adsorption with bed loading. Initially, at low bed loadings (0.5 percent), the differential heat of adsorption is high, 511 Btu lb. This value drops rapidly with an increase of carbon dioxide loading until a loading of about 1.5 percent. Thereafter, the heat of adsorption value decreases very slowly, giving almost a constant heat of adsorption from 1.5 to 5 percent loading; the heat of adsorption values in this range only decreased from 419 Btu/lb to 414 Btu/lb.
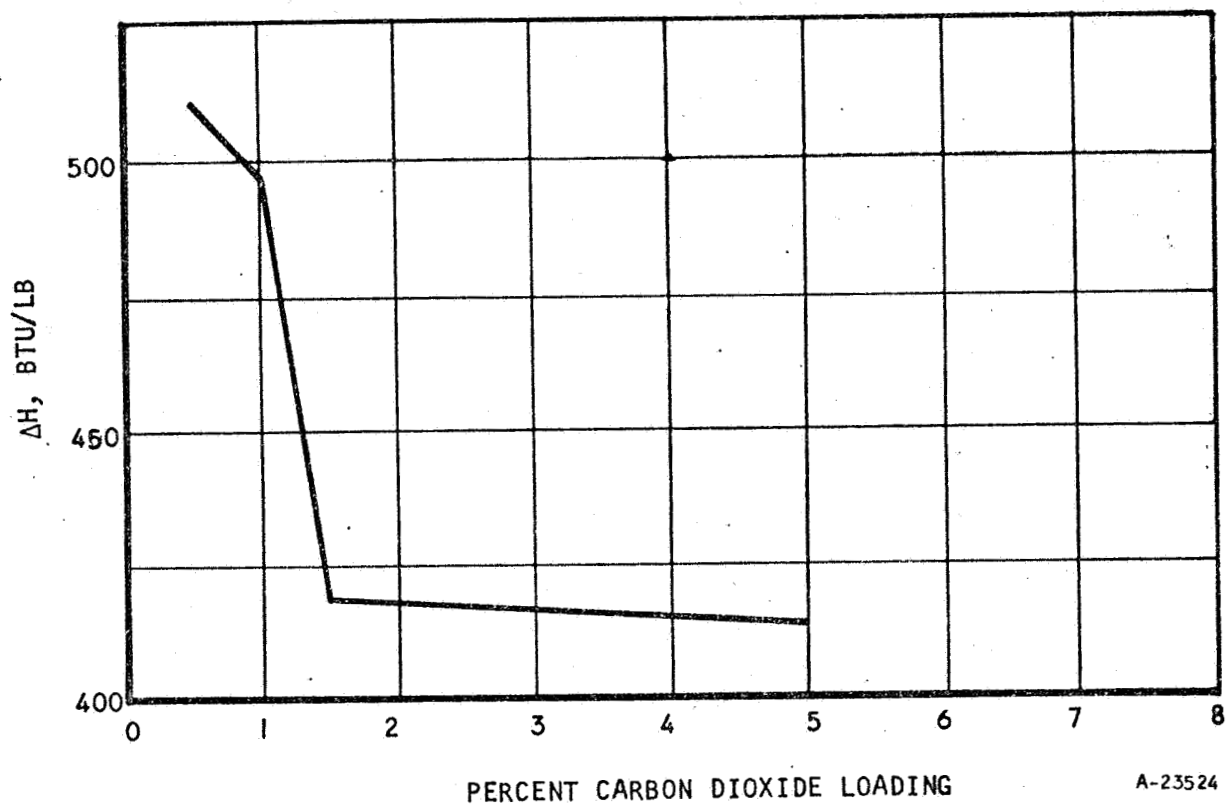
PERCENT CARBON DIOXIDE LOADING   A-23524

Figure 5-22.   Differential Heat of Adsorption at 95°F
               Based on Isosteres of Carbon Dioxide
               Adsorption on Linde Type 5A Molecular
               Sieve Pellets

DYNAMIC ADSORPTION STUDIES

Breakthrough curves were determined for (1) carbon dioxide adsorption on Linde Type 5A molecular sieve pellets for a variety of test conditions and (2) water adsorption on Davison Co. Grade 05 silica gel. When treated mathematically (see Section 7), these curves allow the evaluation of the controlling transfer coefficients. Originally it had been hoped that dynamic adsorption data for CO_2 on water loaded molecular sieve might be obtained; but results obtained during the equilibrium studies showed that very little capacity for CO_2 adsorption exists when even small amounts of water are present on the sieve, thus dynamic studies of molecular sieve were limited to adsorption of CO_2.

Carbon Dioxide Adsorption on Molecular Sieves

The dynamic adsorption of carbon dioxide on Type 5A molecular sieve 1/16-in.-dia pellets (Linde Lot No. 551194) was determined under the following varied conditions: (1) mass velocity, (2) total pressure, (3) inlet carbon dioxide partial pressure, (4) bed temperature, (5) bed length, and (6) carrier gas. As in the equilibrium adsorption determinations, the molecular sieve sample was regenerated in situ at 600°F under vacuum conditions prior to each test.

Test data and results are summarized in Table 5-2 and are supplemented by the plots in the Appendix (Figures C-7 through C-38). There are two separate plots in the Appendix for each run; one gives the carbon dioxide concentration at sorbent bed inlet and outlet as a function of time and the other gives the percent breakthrough as a function of time. A typical plot of the inlet and outlet carbon dioxide concentrations with time, shown in Figures 5-23 and 5-24, gives the typical breakthrough curve obtained from such data.

The initial dynamic breakthrough tests were performed with a bed of about 7 in. in length. A comparison of the adsorption capacity of the bed obtained at 100 percent breakthrough with that obtained in the equilibrium isotherms indicated lower capacity in the dynamic tests. Preliminary analysis of the breakthrough data seemed to indicate that the mass transfer zone (MTZ) was about the same length as the bed. The mass transfer zone is designated as that portion of the bed in which adsorption currently occurs, and this zone of fixed length travels along the bed as the bed becomes saturated with adsorbate. A bed requiring a given capacity for adsorbate without allowing any unadsorbed material to leave the column must have, in addition to the amount of adsorbent necessary for the desired capacity at saturation, a length of bed where the mass transfer zone can travel without allowing absorbate to break through.

Mass transfer zone length can be calculated from the breakthrough curve, according to Trybal (Reference 5-9), by the following equation:

$$Z_a = Z \frac{\theta_a}{\theta_E - (1-f) \theta_a} \qquad (5-4)$$

TABLE 5-2

SUMMARY OF DYNAMIC CARBON DIOXIDE ADSORPTION
ON MOLECULAR SIEVE TEST DATA AND RESULTS

Run No.	Carrier Gas	Average Inlet Mass Velocity, lb/ft² min	Av. Inlet CO_2 Partial Press., mm Hg	Total Pressure, psia	Bed Temp., °C (°F)	Bed Length, inch	Sample wt., g	Time to Initial Breakthrough, Min	Time to 100% Breakthrough, Min	CO_2 Adsorbed, G CO_2/G Sieve	Percent of Equilibrium CO_2 Adsorbed
2	N_2	1.54	7.15	5.07	25 (77)	7.2	24.5	10.3	40	0.0529	90.9
3	N_2	0.67	7.13	5.10	25 (77)	7.2	24.5	30.5	95	0.0492	84.7
4	N_2	1.55	7.12	5.08	0 (32)	7.2	24.5	23.5	70	0.0997	97.3
5	N_2	0.68	7.03	7.05	25 (77)	7.2	24.5	41.3	120	0.0504	87.7
6	N_2	1.54	7.18	5.08	25 (77)	10.1	35.4	20	70	0.0525	89.7
7	N_2	0.69	7.14	5.08	25 (77)	10.1	35.4	53	105	0.0524	90.0
8	N_2	1.50	7.13	5.08	0 (32)	10.1	35.4	43.5	80	0.0986	96.2
9	O_2	1.75	7.19	5.08	25 (77)	10.1	35.4	19	65	0.0493	84.3
10	O_2	1.75	7.25	5.08	0 (32)	10.1	35.4	40.3	105	0.0926	89.9
11	He	0.28	7.20	5.08	25 (77)	10.1	35.4	22.5	65	0.0526	89.9
12	N_2	0.68	6.91	7.07	25 (77)	10.1	35.4	74	165	0.0489	85.8
13	N_2	0.67	7.21	5.08	50 (122)	10.1	35.4	22.5	75	0.0235	89.4
14	N_2	1.54	7.01	5.08	9.1 (48.4)	10.1	35.4	34	65	0.0802	89.1
15	N_2	1.48	1.03	5.06	25 (77)	10.1	35.4	43	120	0.016	90.4
16	N_2	1.49	1.04	5.07	50 (122)	10.1	35.4	17	40	0.0065	100.0
17	N_2	1.47	1.01	5.08	0 (32)	10.1	35.4	116	220	0.0394	91.0

B-12564

INLET

OUTLET

PERCENT CO₂ BY VOLUME

TIME, MIN
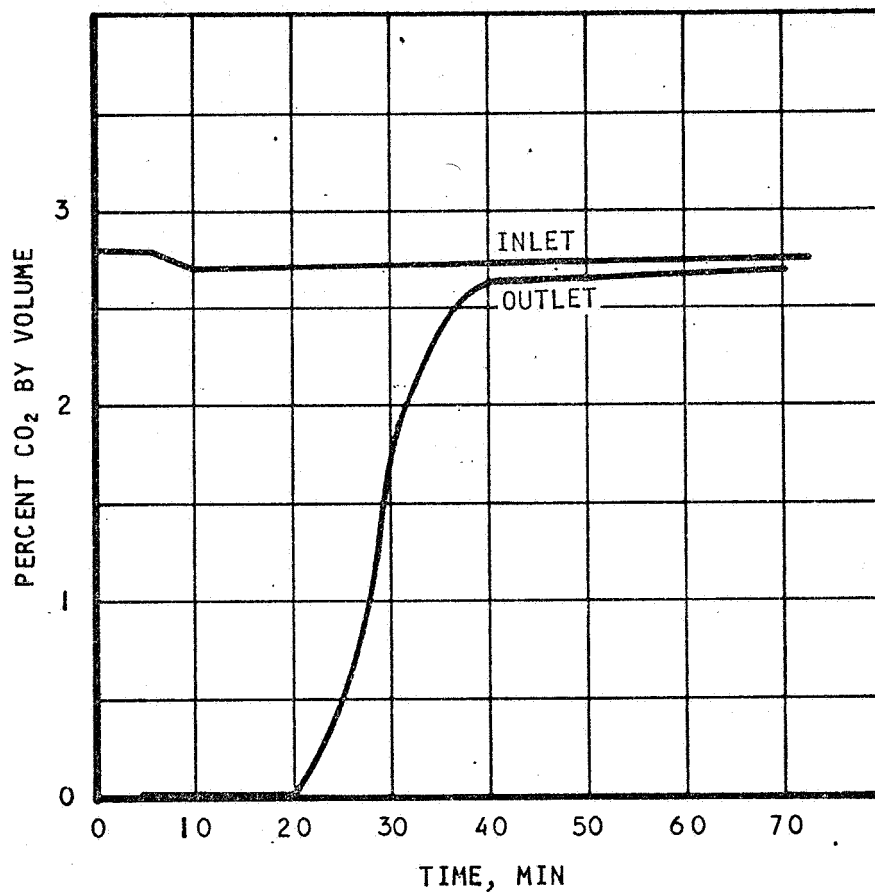
A-19274

Figure 5-23. Typical Plot Obtained from Experimental Data. This is Adsorption of CO_2 on Linde Type 5A Molecular Sieve Pellets at 25°C
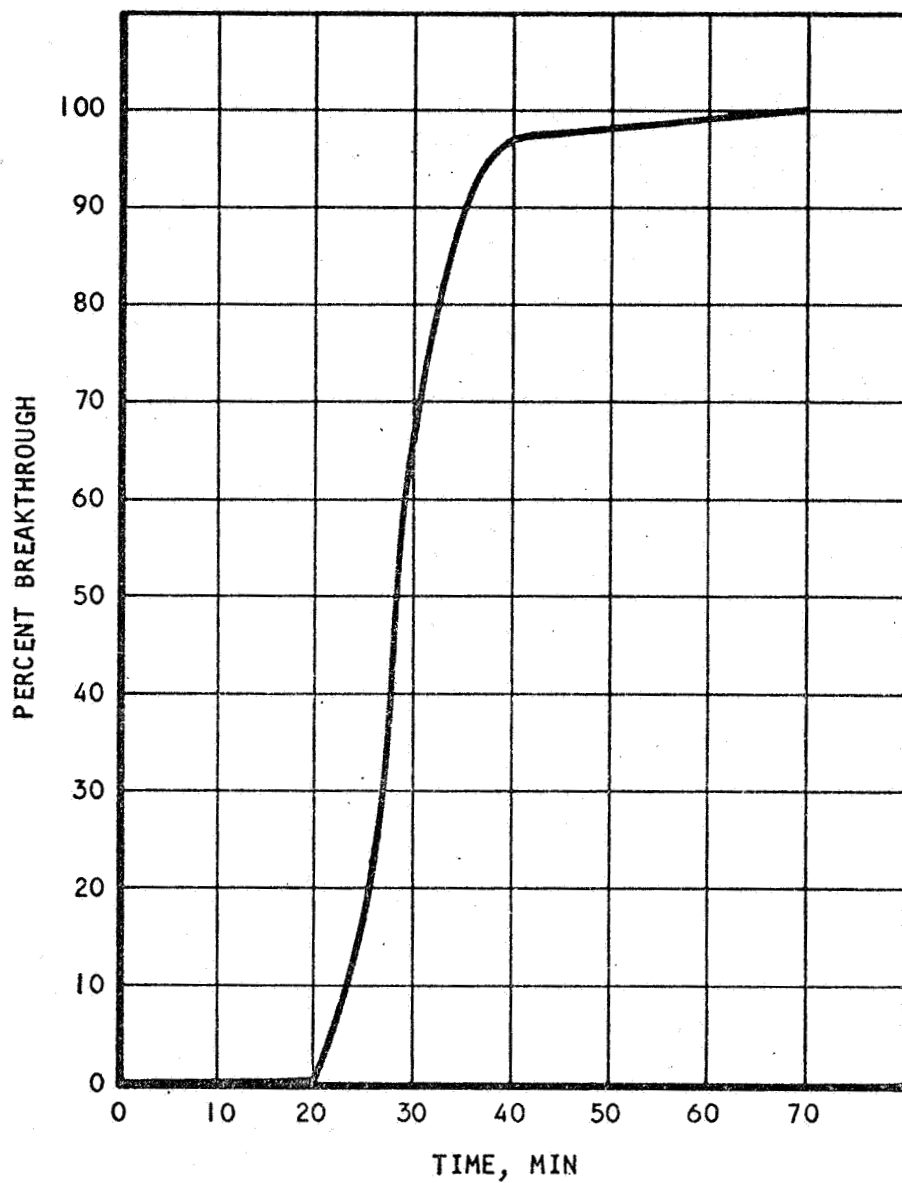
Figure 5-24. Typical Breakthrough Curve Obtained from Experimental Data. This is Percent Breakthrough of CO_2 from Linde Type 5A Molecular Sieve Pellets at $25^\circ C$

where Z_a = MTZ length

Z = packed bed length

θ_E = time to bed exhaustion

θ_a = time from initial breakthrough to bed exhaustion

f = fraction of the MTZ not loaded with adsorbate and is equal to the ratio of the area under the breakthrough curve to the total area between start of breakthrough and bed exhaustion.

In practice, one uses as start of breakthrough the time of 5 percent breakthrough and bed exhaustion when the breakthrough reaches 95 percent.

The MTZ length calculated by Equation (5-4) for Run No. 2 is 6.2 in., which is very close to the actual bed length. After increasing the packed column to about 10 in., the MTZ length calculated for Run No. 6, which was performed under the same test conditions as Run No. 2 except for bed length, gave a value of 5.3 in.

Increase of bed length, however, still gave the same lower adsorption capacity (approximately 10 percent) for the dynamic tests compared with the equilibrium studies. In order to determine if this difference in adsorption capacities is due to difference in the molecular sieve sample or test configuration, a volumetric determination was made of the equilibrium carbon dioxide adsorption capacity of the dynamic test bed, in situ. The results (0.0458 g CO_2/g sieve adsorbed, P = 4.5 mm Hg, T = 23.7°C) is the same as that obtained in the equilibrium studies. This indicates that the capacity differences are not due to either the sample or test configuration.

Since the possible effect of coadsorption of the carrier gas could explain the evident reduction in dynamic adsorption capacity, other carrier gases were investigated. Linde Company reported that Type 5A molecular sieve has an adsorption capacity for helium, oxygen, and nitrogen (at 0°C and 300 mm Hg) of 0.001, and 0.16, and 1.0 wt. percent, respectively. A series of dynamic tests, therefore, was performed with oxygen and helium, respectively, as carrier gases. The test results show that there was no difference in dynamic adsorption capacities between helium and nitrogen as carrier gases.

There was, contrary to expectations, a lower adsorption capacity (0.0493 g CO_2/g sieve at 25°C and 0.0926 g CO_2/g sieve at 0°C) for oxygen as carrier gas than for nitrogen (0.0525 g CO_2/g sieve at 25°C and 0.0986 g CO_2/g sieve at 0°C) under the same pressure and flow conditions. An explanation for this phenomenon may be attributed to the velocity at which molecules traverse the zeolite channels; it appears to be remarkably fast and depends to a large degree on the size of the molecule concerned. Although the nitrogen molecule is only 0.2 Å larger than the oxygen molecule, this difference might allow greater oxygen coadsorption, causing a reduction in CO_2 capacity when using oxygen as the carrier gas (Reference 5-10). This effect should also occur since the helium molecule is smaller than the nitrogen molecule, but may be

offset in this case by the extremely low capacity of the molecular sieve for helium. As expected, the dynamic test data, summarized in Table 5-2, give higher adsorption capacities with lowering of temperature.

There appears to be no difference in capacity due to mass flow rates. Both tests at mass velocities of 1.54 and 0.69 lb/ft^2-min at $25°C$ with nitrogen as carrier gas in the 10-in. packed bed gave the same adsorption capacity, 0.0525 and 0.0524 g CO_2/g sieve.

System pressure, on the other hand, seemed to have an effect. There is a lowering in capacity of 7 psia (0.0489 g CO_2/g sieve) over that at 5 psia (0.0525 g CO_2/g sieve) at the same test conditions (mass flow 0.69 lb/ft^2-min; temperature, $25°C$; nitrogen, carrier gas; 10-in. packed bed; and approximately 7.0 mm Hg partial pressure of inlet CO_2). This descrease in CO_2 adsorption capacity as a result of an increase in the nitrogen partial pressure would tend to support the case for nitrogen coadsorption as a contributor to lower dynamic adsorption capacity.

Tests performed with inlet carbon dioxide partial pressures of about 1 mm Hg gave the same lowering of adsorption capacity, approximately 10 percent, at complete breakthrough as the 7mm Hg inlet carbon dioxide partial pressure tests.

Water Vapor Adsorption on Silica Gel

The dynamic adsorption of water vapor on silica gel (Davison Chemical Lot No. 1807, 6-16 mesh, Grade 05) was determined at two different temperatures. Prior to each determination the silica gel bed was regenerated at $350°F$ under vacuum conditions. Since Hougen and Marshall (Reference 5-11) have performed an extensive theoretical analysis of the adsorption of water vapor from air by silica gel, a corroboration of the experimental data of two different temperatures was considered adequate at this time.

Test data and results are summarized in Table 5-3 and are supplemented by the plots in the Appendix (Figure C-39 through Figure C-42). There are two separate plots in the Appendix for each run; one gives the dew point at sorbent bed inlet and outlet as a function of time and the other gives the percent breakthrough as a function of time. These plots are similar to the typical plots shown in Figures 5-23 and 5-24 for carbon dioxide adsorption.

Although data are given for only two runs (Run No. 1W and 4W) in Table 5-3, there were actually four determinations made. In Run No. 2W, the inlet dew point varied considerably during the determination and analysis of the data; therefore, it did not give any meaningful information. At the conclusion of Run No. 3W it was found that the dew point measuring device had become defective some time during the run and was giving erroneous dew points.

As expected, the dynamic adsorption capacity at 100 percent breakthrough decreased with temperature from 0.354 g H_2O/g gel at $15.6°C$ to 0.235 g H_2O/g gel at $25°C$. A comparison of the adsorption capacity at $25°C$ with the experimental equilibrium adsorption isotherm indicates that dynamic water vapor adsorption on silica gel exhibits the same lowering of capacity shown by

dynamic adsorption of carbon dixoide by molecular sieve. The dynamic adsorption data for silica gel were lower than the equilibrium adsorption data (0.295 b H_2O/g gel) obtained by AiResearch.

TABLE 5-3

SUMMARY OF DYNAMIC WATER VAPOR ADSORPTION ON SILICA GEL TEST DATA AND RESULTS

Run Number	IW	4W
Carrier Gas	N_2	N_2
Average Inlet Mass Velocity, (lb/ft^2-min)	1.53	1.50
Average Inlet Dew Point, $^{\circ}F$	53.5	49.3
Average Inlet H_2O Partial Pressure, mm Hg	10.41	8.89
Total Pressure, psia	5.14	5.08
Bed Temperature, $^{\circ}C$ ($^{\circ}F$)	25 (77)	15.6 (60)
Bed Length, in.	10	10
Sample Wt, g	33.75	33.75
Time to Initial Breakthrough, minutes	126	255
Time to 100% Breakthrough, minutes	300	460
H_2O Adsorbed, g H_2O/g gel	0.235	0.354

DYNAMIC DESORPTION STUDIES

Scope

While the techniques for evaluating the controlling parameters for mixed-gas adsorption are reasonably well known (see Section 4), the same is not true for vacuum desorption. A preliminary series of runs yielded a qualitative estimate of the desorption rates. The more controlled series of experimentation was specifically designed to identify the controlling desorption step.

Preliminary Runs

A summary of the vacuum desorption test conditions for the preliminary series of runs conducted is reported in Table 5-4.

TABLE 5-4

VACUUM DESORPTION TEST CONDITIONS

Run No.	Adsorbent	Adsorbate	Bed Height in.	Bed Weight g	Initial P mm Hg	Desorption Bath Temperature °C
3 SG	Silica Gel	H_2O	10	33.75	~22*	50
4 SG	Silica Gel	H_2O	10	33.75	7.4	25
1 MS	Molecular Sieve	CO_2	5	17.05	8.8	25
2 MS	Molecular Sieve	CO_2	5	17.05	~20*	50

*The bed was loaded with adsorbate at 25°C, and then, at the start, a 50°C bath was placed around the sample bed.

Figures 5-25 through 5-28 give the pressure histories of the test bed for each run. Adsorption of the adsorbate for each case was performed at 25°C; for the 50°C desorption tests, the constant temperature bath around the sample bed was changed prior to the start of the run to one containing water at 50°C.

The temperature profiles of both silica gel (Figures 5-29 and 5-30) and molecular sieve (Figures 5-31 and 5-32) beds suggest, as expected, that the vacuum end of the bed is desorbed first and a "desorption wave" propagates through the bed. Tests were performed to ensure that the thermocouples were not in contact with the metal heat transfer surfaces.
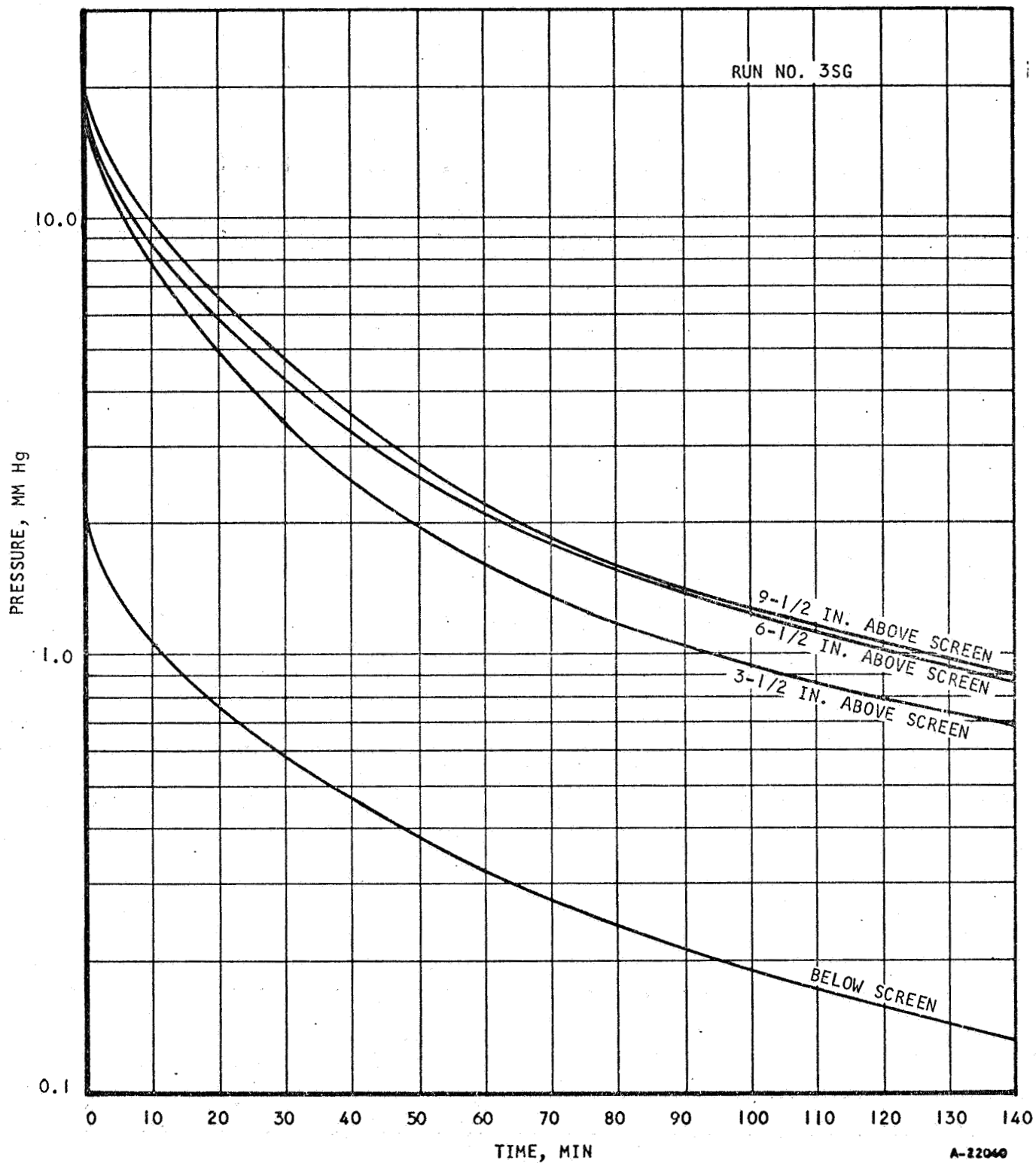
Figure 5-25. Bed Pressure Profile for the Isothermal Vacuum Desorption of Water Vapor from Davison Grade 05, 6-16 Mesh Silica Gel at 50°C
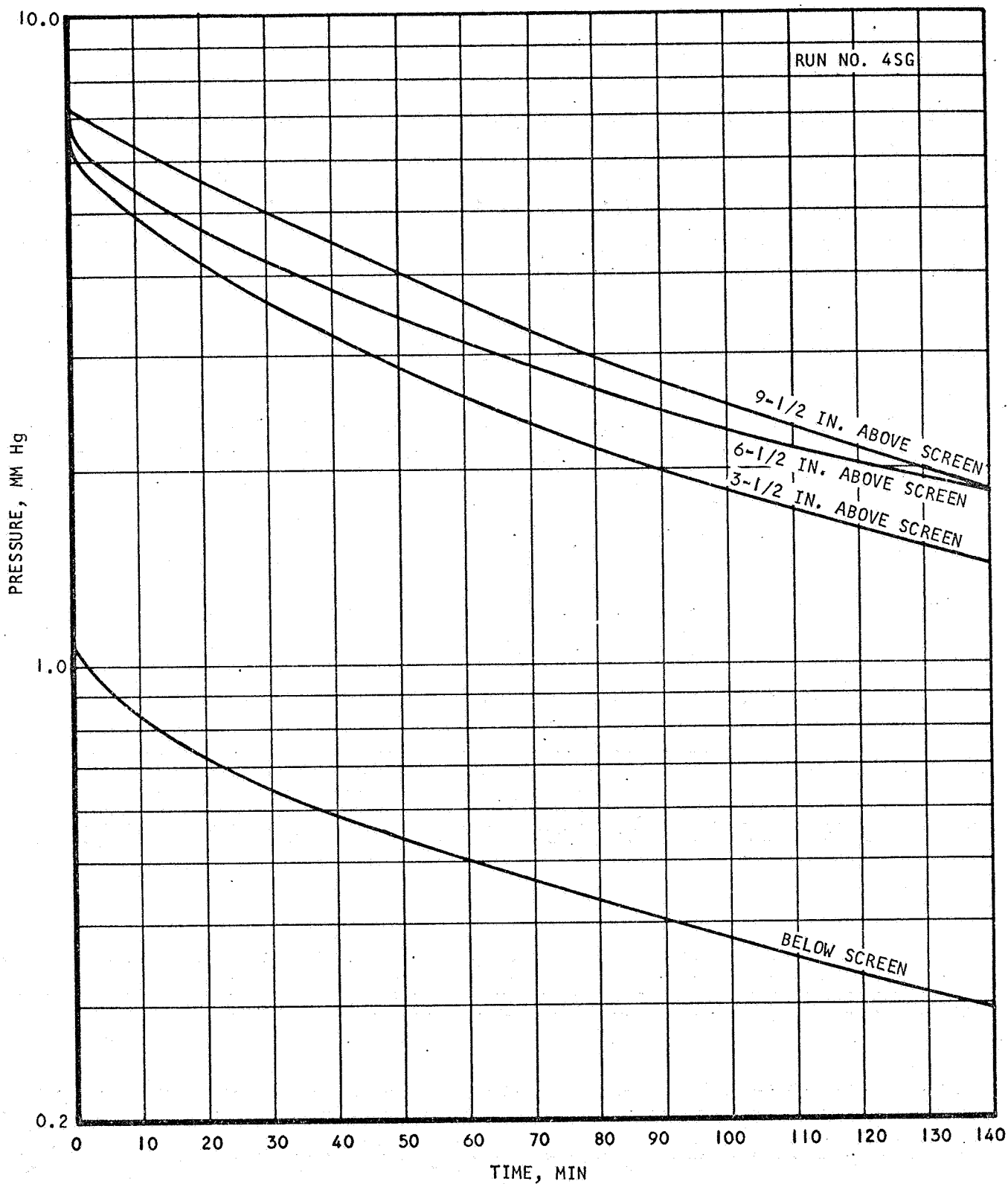
Figure 5-26. Bed Pressure Profile for the Isothermal Vacuum Desorption of
Water Vapor from Davison Grade 05, 6-16 Mesh Silica Gel at 25°C

A-22041
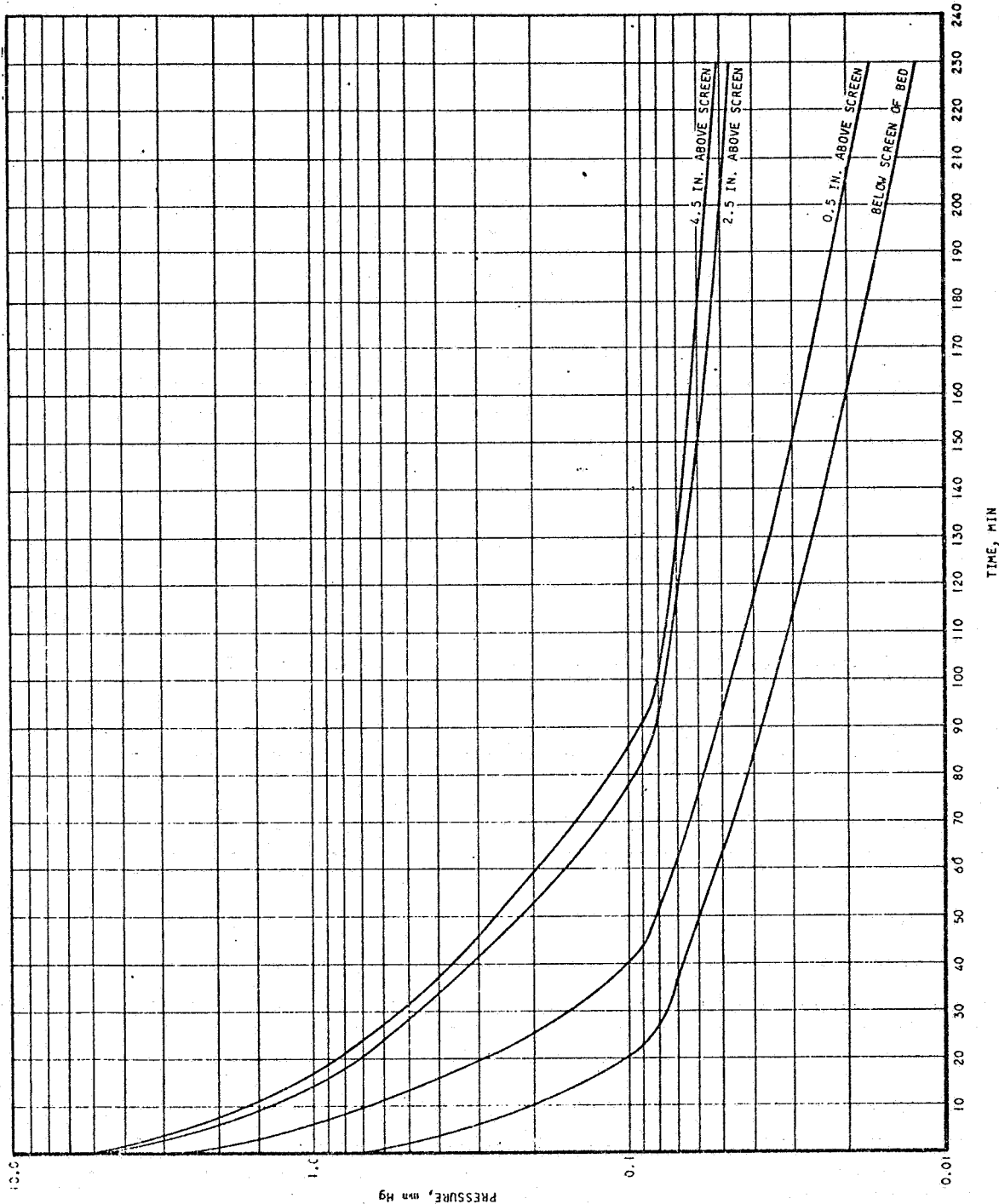
Figure 5-27.   Bed Pressure Profile for the Isothermal Vacuum Desorption of CO_2 from Type 5A, Linde Molecular Sieve, 1/16-in.-dia Pellets at 25°C
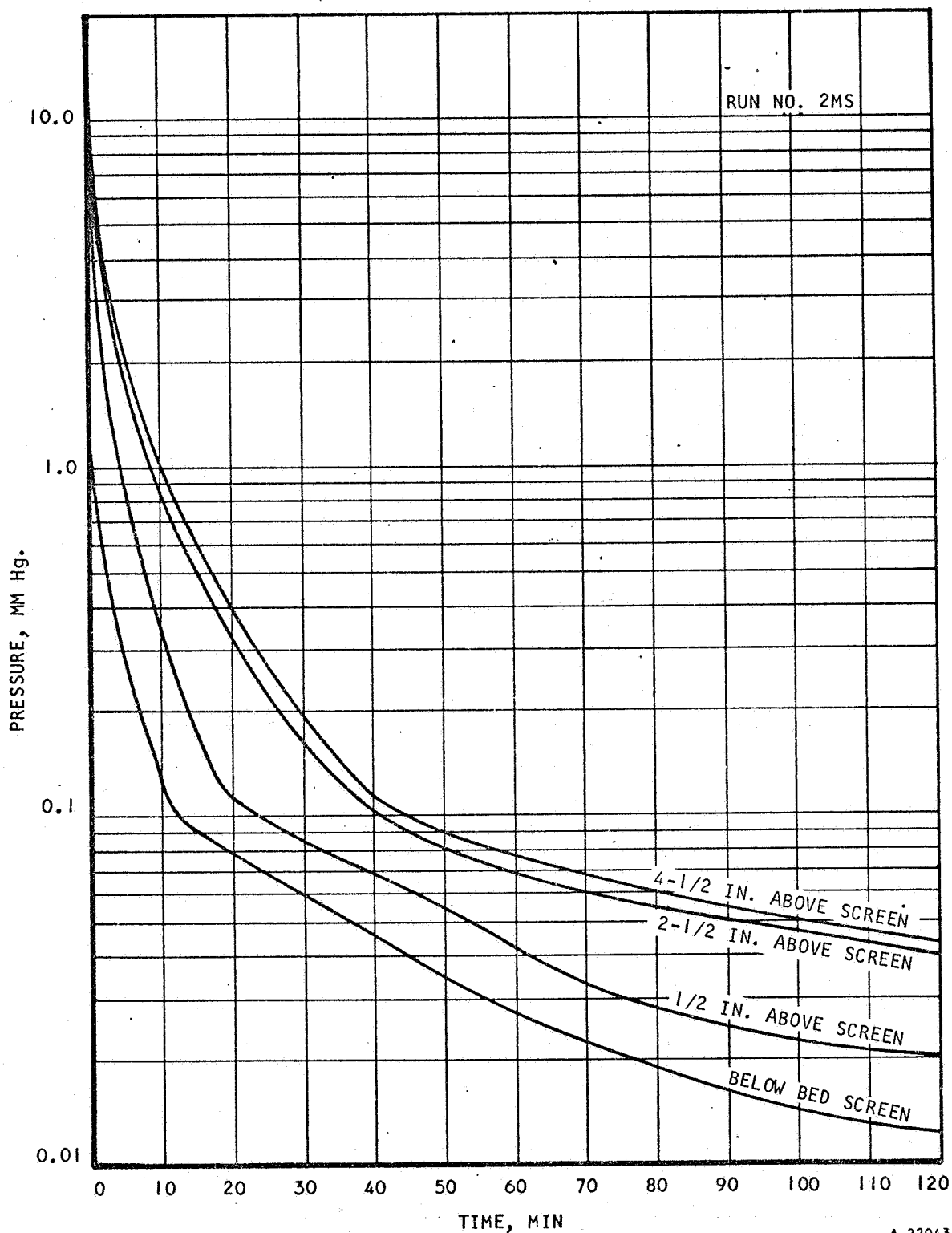
Figure 5-28. Bed Pressure Profile for the Isothermal Vacuum Desorption of CO_2 from Type 5A, Linde Molecular Sieve, 1-16-in.-dia Pellets at $50^\circ C$
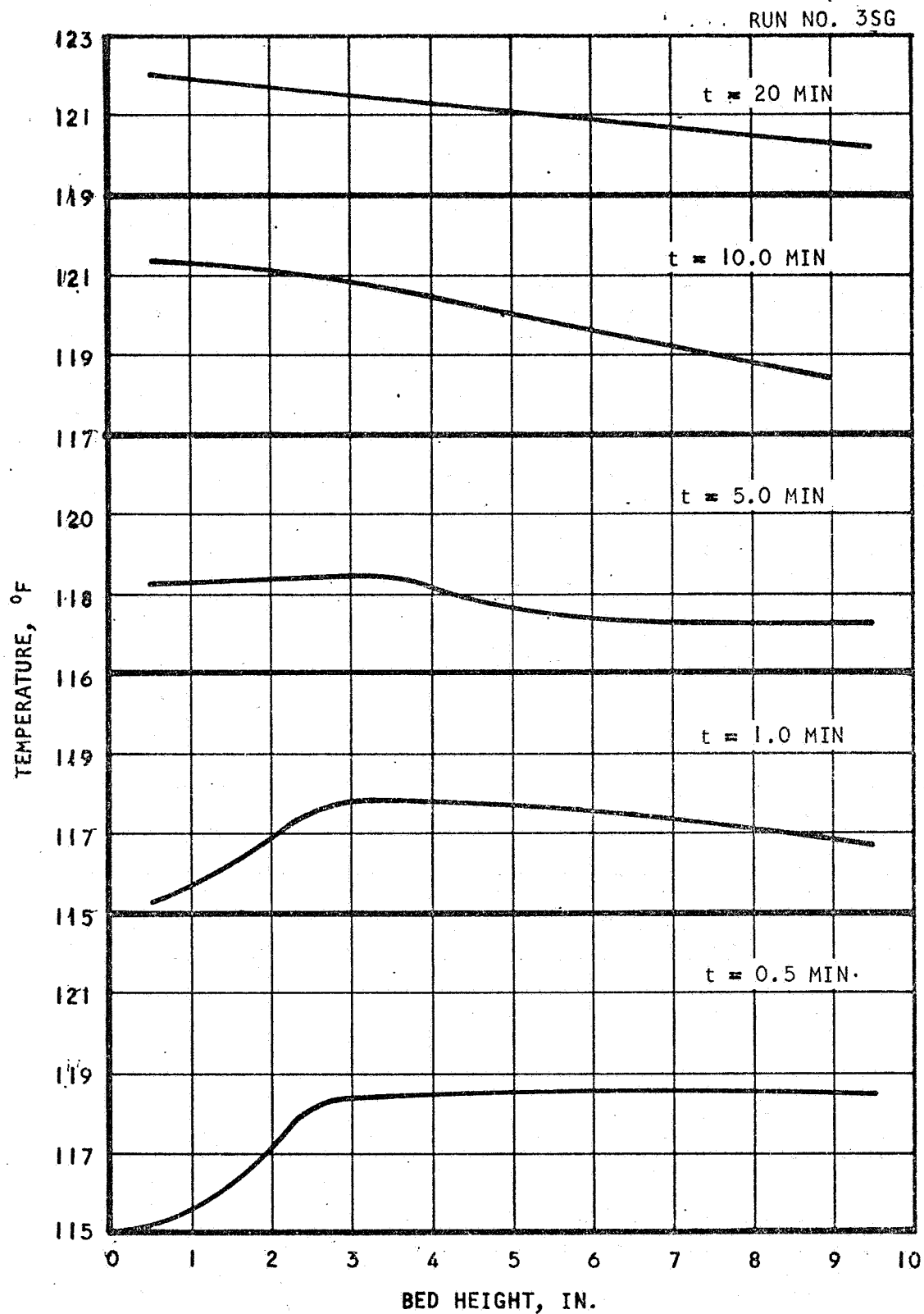
Figure 5-29.   Bed Temperature Profile for the Isothermal
Vacuum Desorption of Water Vapor from Davison
Grade 05, 6-16 Mesh Silica Gel at 122°F

A-22039
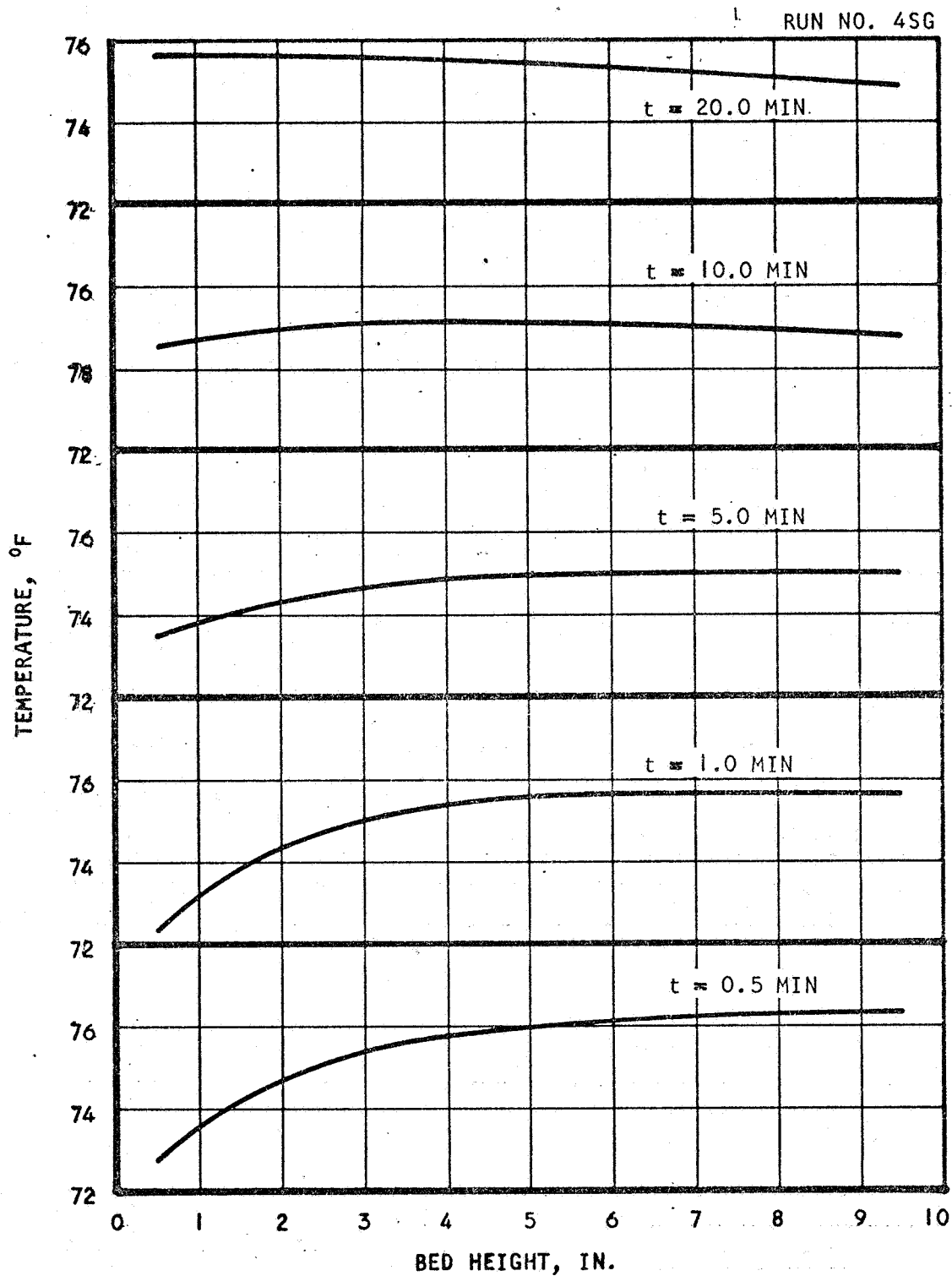
A-22042

Figure 5-30. Bed Temperature Profile for the Isothermal Vacuum
Desorption of Water Vapor from Davison Grade 05,
6-16 Mesh Silica Gel at 77°F

RUN NO. IMS

t = 10.0 MIN

t = 5.0 MIN

t = 1.0 MIN

t = 0.5 MIN

TEMPERATURE, °F

BED HEIGHT, IN.
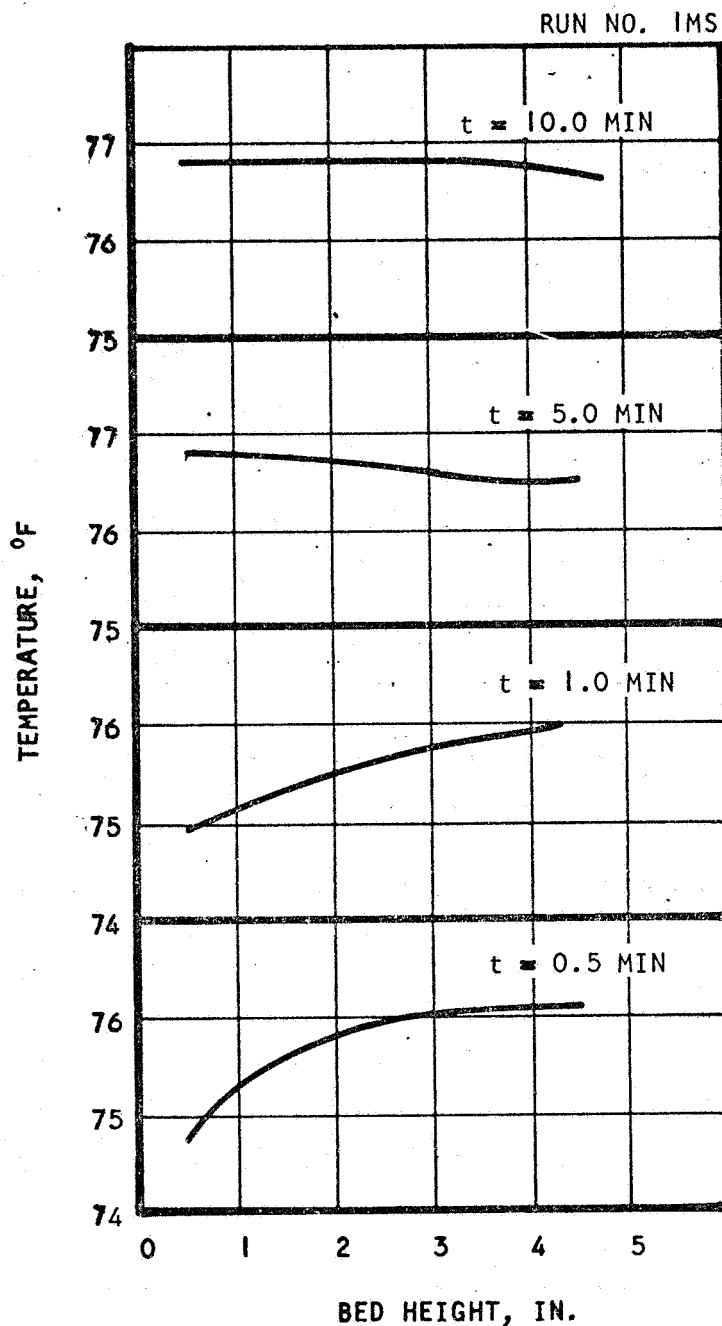
A-22033

Figure 5-31.   Bed Temperature Profile for the Isothermal Vacuum Desorption of CO_2 from Type 5A Linde Molecular Sieve, 1/16-in.-dia Pellets at 77°F
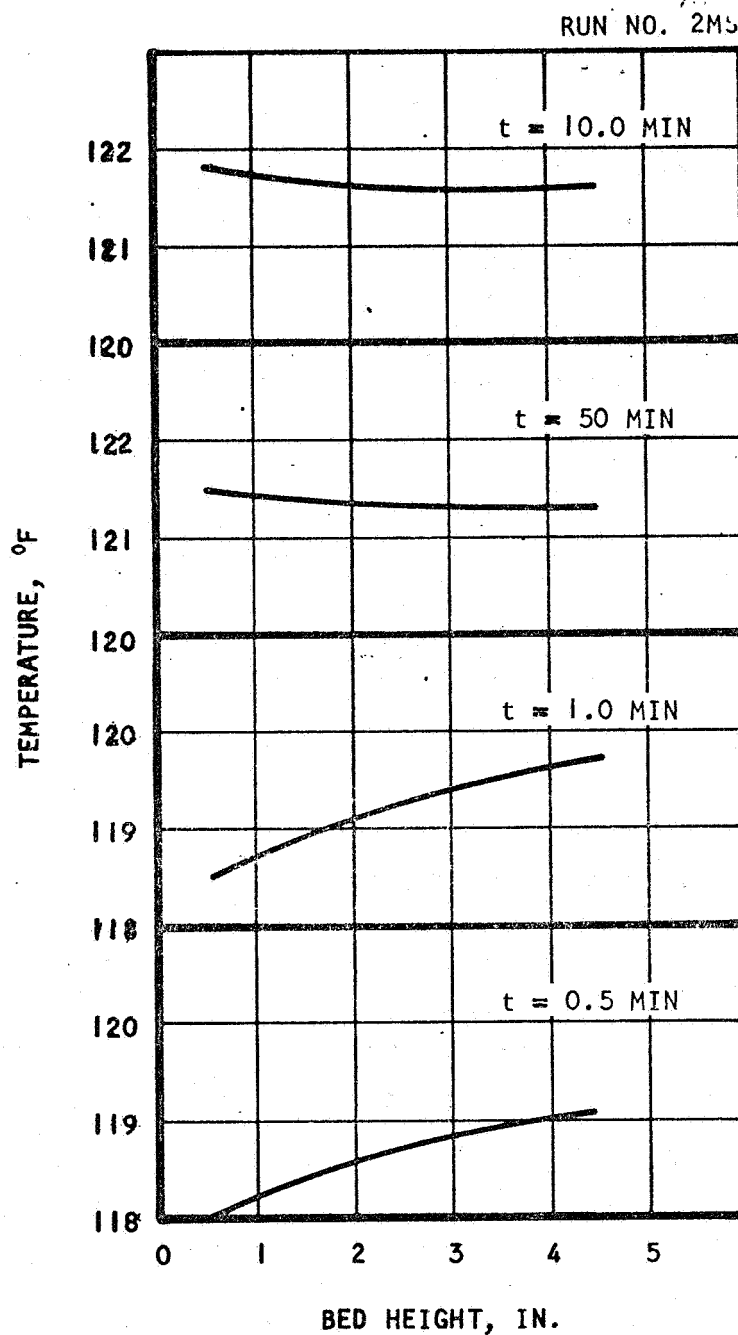
Figure 5-32. Bed Temperature Profile
for the Isothermal Vacuum
Desorption of CO_2 from
Type 5A Linde Molecular
Sieve, 1/16-in.-dia
Pellets at 122°F

A-22032

Desorption at the higher temperature ($50^\circ C$), of course, gave higher desorption rates and, consequently, larger temperature changes in the bed than desorption at $25^\circ C$. The initial temperature change at the vacuum end of the bed is greater in the desorption of water vapor from silica gel than in the desorption of the carbon dioxide from molecular sieve. This is understandable since the heat of adsorption of water vapor on silica gel is about three times greater than the heat of adsorption of carbon dioxide on molecular sieve.

Determination of Controlling Step

At the conclusion of this preliminary series it was clear that some understanding of the controlling phenomena during vacuum desorption was needed. A series of tests was structured to provide a measure of the importance of mass transfer, heat transfer, desorption pressure (momentum), temperature level, and particle size. Thus, a matrix of tests was arranged for CO_2 desorption from molecular sieve, as shown in Table 5-5, to provide comparative data with which to assess the influence of these variables.

TABLE 5-5

TEST MATRIX

Test	Bath Temperature $^\circ C$	Initial Loading Percent	Particle Size, in.	Vacuum Source
A	50	8	1/16	Low
B	25	8	1/16	Low
C	50	1	1/16	Low
D	Insulated adiabatic bed	8	1/16	Low
E	50	8	1/16	Throttled
F	50	8	1/8	Low

By comparing the results of tests A and C, the influence of mass transfer could be determined; A and D, heat transfer; A and E, desorption pressure, A and B, temperature level; and A and F, intraparticle diffusion.

Carbon Dioxide Vacuum Desorption from Molecular Sieve

The individual tests are displayed in Appendix C, Figures C-43 to Figure C-53; the results are summarized in Table 5-6 and Figure 5-33. Examination of the data shows the relative ease of CO_2 removal from molecular sieve by vacuum desorption. Over 70 percent of the initial quantity of CO_2 present on the sieve is removed during the first 10 min of a 30 min run at $25^\circ C$. This percentage of CO_2 removal (within the first 10 min) increases to almost 90 percent when the temperature is raised to $50^\circ C$. Specifically, the influences of the variables outlined previously were as follows:

TABLE 5-6

VACUUM DESORPTION OF CO_2 FROM LINDE TYPE 5A MOLECULAR SIEVE PELLETS

Test No.	Pellet Diameter, inch	Initial CO_2 Loading, g CO_2/g Sieve (mm Hg)	Desorption Temperature, °C	Final CO_2 Loading, g CO_2/g Sieve (mm Hg)	Desorption Time, Min.
1	1/16	0.062 (7.98)	25	0.007 (.241)	30
2	1/16	0.0625 (8.1)	50	0.001 (0.027)	30
3	1/16	0.0625 (8.1)	50	0.004 (0.120)	10
4	1/16	0.065 (8.74)	50	0.0035 (0.085)	30
5	1/16	0.0135 (0.69)	50 (Throttled Vacuum)	0.001 (0.030)	30
6	1/16	0.0625 (8.15)	(Adiabatic(Ambient))	0.007 (0.258)	30
7a	1/16	0.066 (8.9)	25	0.038 (3.48)	2
b		(Accidently bled air into system)	25	0.027 (1.97)	2
c		0.027 (1.97)	25	0.019 (1.15)	2
d		0.019 (1.15)	25	0.0155 (0.84)	2
8a	1/16	0.0625 (8.17)	25 (Throttled Vacuum)	0.025 (1.74)	5
b		0.025 (1.74)	25	0.007 (0.251)	25
9a	1/16	0.0625 (8.15)	25	0.0175 (1.04)	8
b		0.0175 (1.04)	25	0.010 (0.399)	9
c		0.010 (0.399)	25	0.0055 (0.188)	13
d		0.0055 (0.188)	25	0.0035 (0.094)	15
10	1/16	0.062 (8.0)	25 / 50	0.001 (0.025)	2 / 28
11a	1/8	0.0625 (8.15)	25	0.035 (3.04)	2
b		0.035 (3.04)	25	0.013 (0.64)	8
c		0.013 (0.64)	25	0.007 (0.258)	9
d		0.007 (0.258)	25	0.0037 (0.109)	13
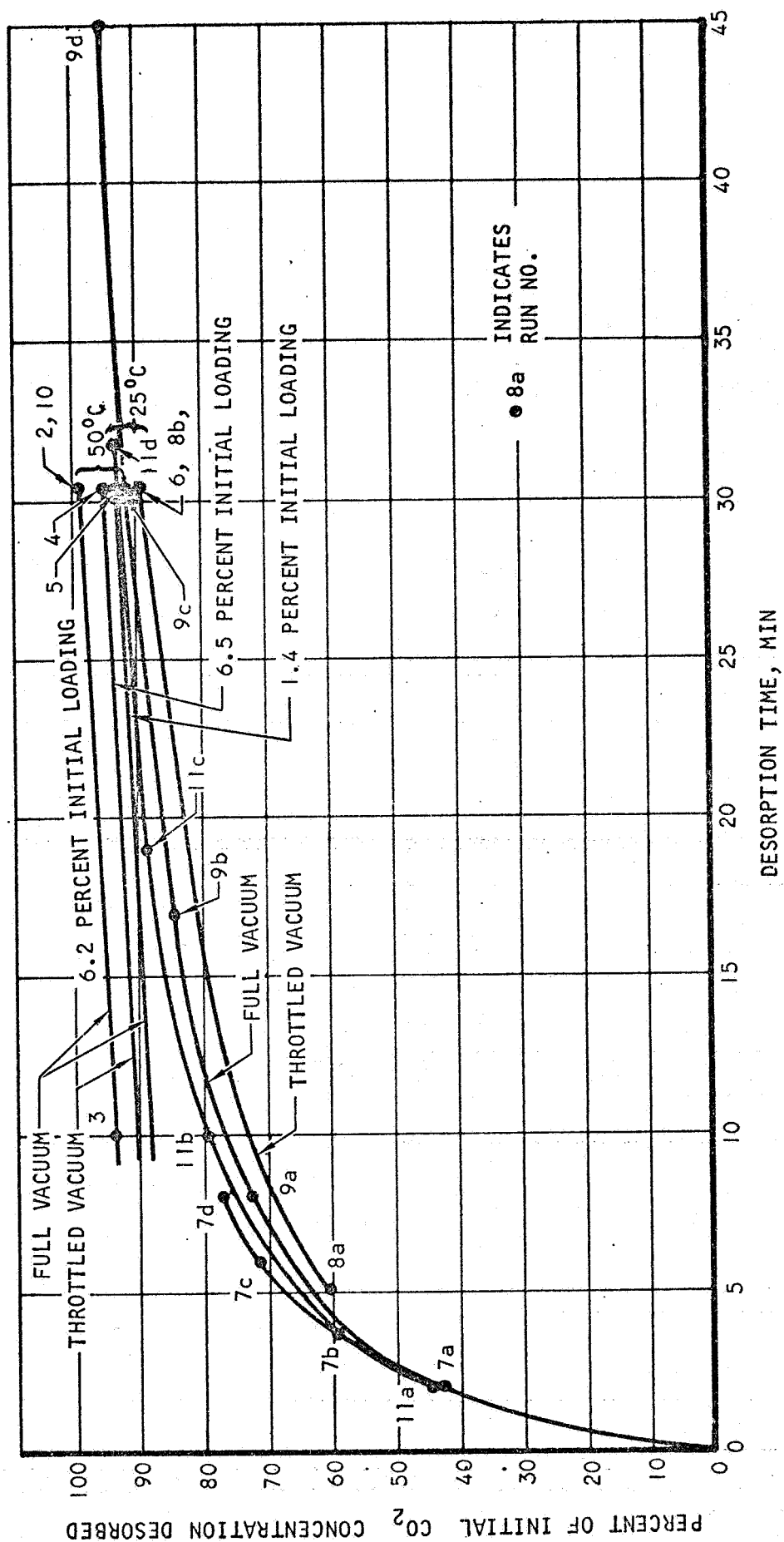
Figure 5-33. Vacuum Desorption of CO_2 from Linde Type 5A Molecular Sieve

(a) Mass Transfer--Comparison of Runs 2 and 5 showed no difference in final loading between an initial loading of 8 percent and I percent.

(b) Heat Transfer--Comparison of Runs 2 and 6 showed the influence of heat transfer (which actually reflects the dependence on temperature level). At the end of 30 min the adiabatically desorbed bed had 0.7 percent loading while the bed held at $50^{\circ}C$ had 0.1 percent loading.

(c) Desorption Pressure--Very little difference was detected between Runs 2 and 4. As can be seen in Figures C-44 and C-46, pressure in the vacuum manifold during Run 2 was approximately 10 microns, while during Run 4 pressure was held above 350 microns. Pressures within the bed during Run 4 is correspondingly higher, with minor influence on desorption. Later, test series 8 (Figure C-50) using a lower flow vacuum pump, while maintaining manifold pressures in the 40 to 100 micron range, again showed only minor difference.

(d) Temperature Level--This parameter has the most influence of those measured. Differences between $50^{\circ}C$ and $25^{\circ}C$ runs, such as Runs I and 2, show this dependence.

(e) Particle Size--Comparison of the final loading after desorption between Runs 9 and II shows very little difference. It had been theorized that if the basic phenomenon was pore diffusion-limited, the larger particle having longer pores would exhibit a lower rate. Actually, a slightly higher rate was detected.

The quantitative determination of the parameters necessary for description of the desorption process is described in Section 7.

Water Vapor Vacuum Desorption from Silica Gel

A series of desorption tests of water vapor from silica gel was conducted using the same test bed and test technique used to study the desorption of CO_2 from molecular sieve. Test data are summarized in Table 5-7 and Figure 5-34. The individual test results appear in Appendix C, Figures C-54 to Figure C-61. Temperature appears to be the most significant factor in the removal of water vapor from silica gel by vacuum desorption. With a H_2O vapor concentration of approximately 6 wt percent present on the gel, a 30 minute desorption at 25°, 38°, and $50^{\circ}C$ reduced the initial water vapor concentration by 55, 79, and 88 percent, respectively. A change in the particle size produced results similar to that encountered during the molecular sieve, CO_2 removal test series; i.e., water vapor was removed at a slightly higher rate for the larger (3-8 mesh) granules then the 6-16 mesh gel.

TABLE 5-7

VACUUM DESORPTION OF H_2O VAPOR FROM DAVISON SILICA GEL GRANULES

Test No.	Granule, Grade, Mesh	Initial H_2O Vapor Loading g H_2O/g GEL (mm Hg)	Desorption Temperature, °C	Final H_2O Vapor Loading g H_2O/g GEL (mm Hg)	Desorption Time, Min.
1	05 6-16	0.0575 (1.8)	25	0.046 (1.25)	5
2	05 6-16	0.046 (1.25)		0.035 (0.82)	10
3a	05 6-16	0.035 (0.82)		0.026 (0.525)	15
b					
c					
4a	05 6-16	0.0575 (7.9)	50	0.0314 (3.4)	5
b		0.0314 (3.4)		0.015 (1.05)	10
c		0.015 (1.08)		0.007 (0.066)	15
5a	05 6-16	0.062 (1.94) 25°C	50 Throttled Vacuum	0.033 (3.6) 50°C	5
b	05 6-16	0.033 (3.6) 50°C		0.0155 (1.13) 50°C	10
c		0.0155 (1.13) 50°C		0.007 (0.050) 25°C	15
6a	05 6-16	0.060 (8.6)	50 Throttled Vacuum	0.034 (3.7)	5
b		0.034 (3.7)		0.016 (1.2)	10
c		0.016 (1.2)		0.007 (0.060) 25°C	15
7a	05 6-16	0.058 (1.8) 25°C	38	0.05 (2.5) 38°C	5
b		0.05 (2.5) 38°C		0.028 (1.08) 38°C	10
c		0.028 (1.08) 38°C		0.012 (.155) 25°C	15
8a	05 6-16	0.058 (1.81) 25°C	Adiabatic (Ambient)	0.044 (1.14) 25°C	5
b		0.044 (1.14) 25°C		0.036 (0.86) 25°C	10
c		0.036 (0.86) 25°C		0.027 (0.550) 25°C	15
9a	05 6-16	0.059 (8.5)	50	0.0445 (5.6)	2
b		0.0445 (5.6)		0.0207 (1.82)	8
c		0.0207 (1.82)		0.008 (0.425)	20
d		0.008 (0.425)		0.006 (0.015) 25°C	15
10a	01 3-8	0.062 (9.2)	50	0.0322 (3.5) 25°C 5	10
b		0.0322 (3.5)		0.0130 (0.86)	15
c		0.0130 (0.86)		0.0054 (0.20)	

Figure 5-34. Vacuum Desorption of H_2O Vapor from Davison Silica Gel

Water Vapor Vacuum Desorption from Molecular Sieve

Preliminary studies indicated that the desorption of water vapor from a poisoned molecular sieve bed would present a fundamental problem in rate kinetics and would have to be investigated to complete the regenerable CO_2 removal system design analysis. The series of tests conducted, involving the vacuum desorption of water vapor from molecular sieve, is listed and the results are summarized in Table 5-8 and Figure 5-35. The individual test results are presented in Appendix C, Figures C-62 through C-73. Examination of Figure 5-35 shows the pronounced effect of temperature and vacuum desorption time on the removal of vapor from a water vapor poisoned molecular sieve. Temperatures in excess of 200°C are required for regeneration of a water vapor poisoned molecular sieve bed. It is interesting to note that in studies conducted by Kel'tsev (Reference 5-12), the water vapor removal rate from synthetic zeolites was inversely proportional to the squares of the grain diameters, indicating that pore diffusion is the controlling factor in the removal of water vapor from pure molecular sieve granules. The present studies, on molecular sieve suspended in an inert matrix, do not yield these results.

It should be noted that, although the level to which the sorbent is loaded with water remains rather high, the initial rate of desorption is high. Also, the final loading is within experimental error of being exactly that at equilibrium.

Discussion of Test Results

As described in the review of dynamic adsorption tests, a consistent reduction in capacity was noted when compared with equilibrium data for both CO_2 on molecular sieve and water vapor on silica gel. While the type and total pressure of the carrier gas had an effect, a fundamental reduction below equilibrium capacity always occurred. It became obvious that this reduction was a mechanism limitation peculiar to the dynamic adsorption process, i.e., rate dependent. The adsorption of carbon dioxide on molecular sieve zeolites appears to be of three different types (Reference 5-11): physical adsorption, chemisorption, and adsorption by an ion-dipole interaction or polarization (Reference 5-12) caused by the actions in the zeolite. In the current area of interest, i.e., pressures and temperatures exceeding 0.3 mm Hg and 0°C, respectively, physical adsorption is of primary importance in the adsorption of carbon dioxide on molecular sieve. In general there are three rate-determining mechanisms (1) gas phase external mass transfer diffusion from the fluid stream to the outer surface of the particle, (2) gas-phase pore diffusion, and (3) surface adsorption (or sticking) in the pores. In desorption tests conducted with 1/8th and 1/16th-in. O D particles, no significant difference in the rate of desorption was observed using CO_2 and Type 5A molecular sieve. Thus, mechanism (2) would not seem important.

If mechanism (1) is controlling, the mass transfer rate would be expected to increase inversely within the 1.5 power of the particle diameter. If mechanism (2) is controlling, one would expect the mass transfer rate to vary inversely with the square of the particle diameter. During the laboratory test program it was noted that the time required to reach equilibrium was fairly

TABLE 5-8

DESORPTION OF WATER VAPOR FROM A 5/8-IN.-DIA BED OF 1/16-IN.-DIA LINDE TYPE 5A MOLECULAR SIEVE PELLETS

Test No.	Initial Loading, percent	Desorption Temperature, ^{0}C	Desorption Time	Final Loading, percent	End of Desorption, Bed Face Pressure, μ
1	5	200	Unsuccessful due to leakage		---
2a	8.2	150	5 min	5.3	44
b	5.3	150	10 min	4.3	32
c	4.3	150	15 min	3.5	25
3a	10.0	100	5 min	8.5	33
b	8.5	100	10 min	7.0	26
c	7.0	100	30 min	5.2	17
4	9.9	100	30 min	6.4	Vacuum throttled to 215
5a	6.4	100	17 hr	4.15	16
b	4.15	100	19 hr	3.3	16
6a	5.0	200	30 min	2.0	23
b	2.0	200	4.75 hr	1.1	16
c	1.1	200	16.5 hr	1.0	14
7a	5.2	100	30 min	4.5	18
b	4.5	100	64.4 hr	3.0	18
8	5.2	100	30 min N$_2$		Dry GN$_2$ purge at 5 psia
			5 min vac	3.6	
			25 min vac	3.6	
9	10.1	100	30 min N$_2$		Dry GN$_2$ purge at 5 psia
			5 min vac	7.75	
			25 min vac	5.4	
10	6.1	100	1 hr N$_2$		Dry GN$_2$ purge at 5 psia
			5 min vac	5.3	
11	5.0	200	2 min	3.2	65
	3.2	200	8 min	2.15	37
	2.15	200	90 min	1.35	17
	1.35	200	18.2 hr	1.4	19
	1.4	200	3 hr	X	13
	X	200	16.6 hr	0.4* 1.1**	10
12	5.0	200	30 min N$_2$		Dry GN$_2$ purge at 5 psia
			5 min vac	2.2	

*1.9 hr at equilibrium
**24.1 hr at equilibrium
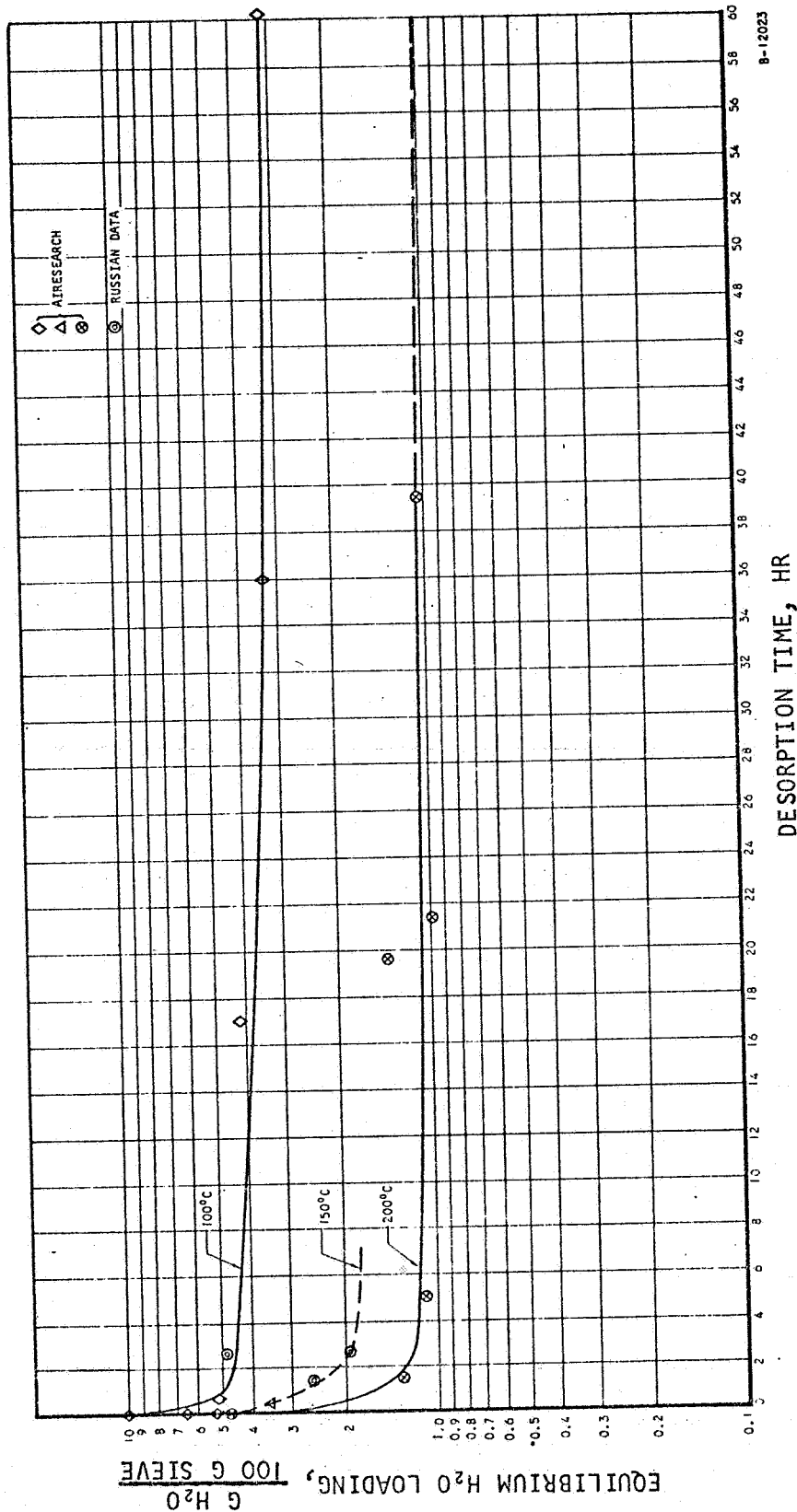
Figure 5-35. Vacuum Desorption of H_2O Vapor from Linde Type 5A Molecular Sieve

AIRESEARCH MANUFACTURING DIVISION
Los Angeles, California

long in many instances; for this reason mechanism (3); i.e., the "sticking" phenomenon, is presently considered the controlling step and accounts for the lower dynamic adsorption capacity. Further, more quantitative bases for this conclusion are arrived at in Section 7, where the data are evaluated by means of detailed analysis.

REFERENCES

5-1. <u>Molecular Sieves for Selective Adsorption, Non-Hydrocarbon Materials Data Sheets</u>, Linde Co., New York, New York, Linde Form 9691-E, February 1959.

5-2. Willard, T. L., <u>Research and Development on Closed Respiratory System Accessories, Molecular Sieves for Carbon Dioxide Adsorption</u>, Report No. ASD-TR-527, Wright-Patterson Air Force Base, Ohio, October 1961.

5-3. <u>Davison Granular Silica Gels</u>, Davison Chemical Division, Baltimore, Maryland, Davison Technical Bulletin No. 303, p8.

5-4. <u>Dehydration of Air and Gas with Davison Silica Gel</u>, Davison Chemical Division, Baltimore, Maryland, Davison Technical Bulletin 202, January 1965, p2.

5-5. <u>Chemical Engineers' Handbook</u>, edited by John H. Perry, 3rd Edition, McGraw-Hill, New York, 1950, pgs769-770.

5-6. Ledoux, E., <u>Vapor Adsorption</u>, Chemical Publishing Co., New York, 1945, pgs109-128.

5-7. Hougen, O. A., Watson, K. M. and R. A. Ragatz, <u>Chemical Process Principles, Part I</u>, 2nd Ed. John Wiley and Sons, New York, 1958, pgs382-3.

5-8. Tsuji, J. and S. Steinberg, <u>Test Proposal, Study on the Properties of Solid Adsorbents for the Design of Regenerable Carbon Dioxide Removal Systems</u>, AiResearch Manufacturing Co., Div. of The Garrett Corporation, Los Angeles, Calif. Report SS-3406, July 5, 1965, p2-20.

5-9. Treybal, R. E., <u>Mass Transfer Operations</u>, McGraw-Hill Book Co., New York, 1955, p497-511.

5-10. Breck, D. W., "Crystalline Molecular Sieves," <u>J. Chem. Education</u>, <u>48</u>, 678 (December 1964).

5-11. Hougen, O.A., and W. R. Marshall, Jr., "Adsorption from a Fluid Stream Flowing Through a Stationary Granular Bed," <u>Chem. Eng. Progress, 43</u>, (1947), p 197.

5-12. Kel'tsev, N. V., "Kinetics of Desorption of Water Vapor and Carbon Dioxide from Zeolites under Vacuum," <u>Gazovaya Promyshlennost' (Gas Industry)</u>, No. 4, 1964, pgs 51-54.

SECTION 6

PROTOTYPE EXPERIMENTAL TEST PROGRAM

INTRODUCTION

To provide information on the performance of full-scale silica gel and molecular sieve beds a series of tests was conducted on a 6 in. by 6 in. by 6 in. aluminum plate fin heat exchanger packed with varying amounts of silica gel and molecular sieve. A photograph of the experimental system appears in Figure 6-1. The test bed and valve assembly appears in Figure 6-2, and a photograph of the sorbent bed and heat exchanger core is shown in Figure 6-3.

WATER VAPOR ON SILICA GEL

Purpose

Expermients were performed to investigate the influence of desorption pressure and temperature upon the adsorption performance of the silica gel bed. Preliminary analysis had indicated that a 2-in. bed depth would be sufficient to reduce the water vapor concentration from a dew point of $52^\circ F$ (10 mm Hg partial pressure) to a dew point of $-54^\circ F$ (0.04 mm Hg partial pressure) for mass velocity of 0.30 lb/ft^2-min at a total pressure of 5 psia; these results were anticipated for a 30-min adsorption cycle when the previous 30-min desorption cycle was performed at a nominal $100^\circ F$ bed temperature, and a pressure of 200 mm Hg at the face (directly exposed to the vacuum manifold) of the desorbing bed. This test series was conducted to confirm this analysis and to determine the importance of such variables as desorption coolant temperature and desorption pressure.

Technique

The heat exchanger was packed with a 2-in. layer (1.75 lb) of Grade 05, 6-16 mesh Davidson silica gel. The balance of the depth of the heat exchanger was filled with 5 lb of 3-4 mm pyrex glass beads. The bed was then installed in the test setup as shown in Figure 6-4, with the silica gel section adjacent to the gas valve.

Flow was induced through the bed by operation of the gas vacuum pump. Nitrogen gas flow was established at the desired flow rate by regulating the N_2 injection valve and observing flow meter readings. Pressure in the bed was then adjusted by regulating the throttling valve in the line to the gas vacuum pump. Inlet dew point was adjusted by varying the temperature of the coolant flow to the heat exchanger downstream of the water bubbling chamber. During adsorption, the gas valve upstream of the bed was positioned for flow through the bed, and the bed heat exchanger valve was positioned to feed cool glycol through the heat exchanger core. When desorption was desired, the gas valves and coolant valves were switched simultaneously; the bed vapors were directed to the liquid nitrogen cold trap and vacuum pumping system, and warm coolant was permitted to enter the test bed heat exchanger core. For some

FREEZE TRAP
STEAM CONDENSER

SORBENT TEST
BED ASSEMBLY

AIR SUPPLY

HEAT EXCHANGER

DIFFUSION
PUMP

GAS
VACUUM
PUMP

SURGE TANK

CONTROL
CONSOLE

58052-4
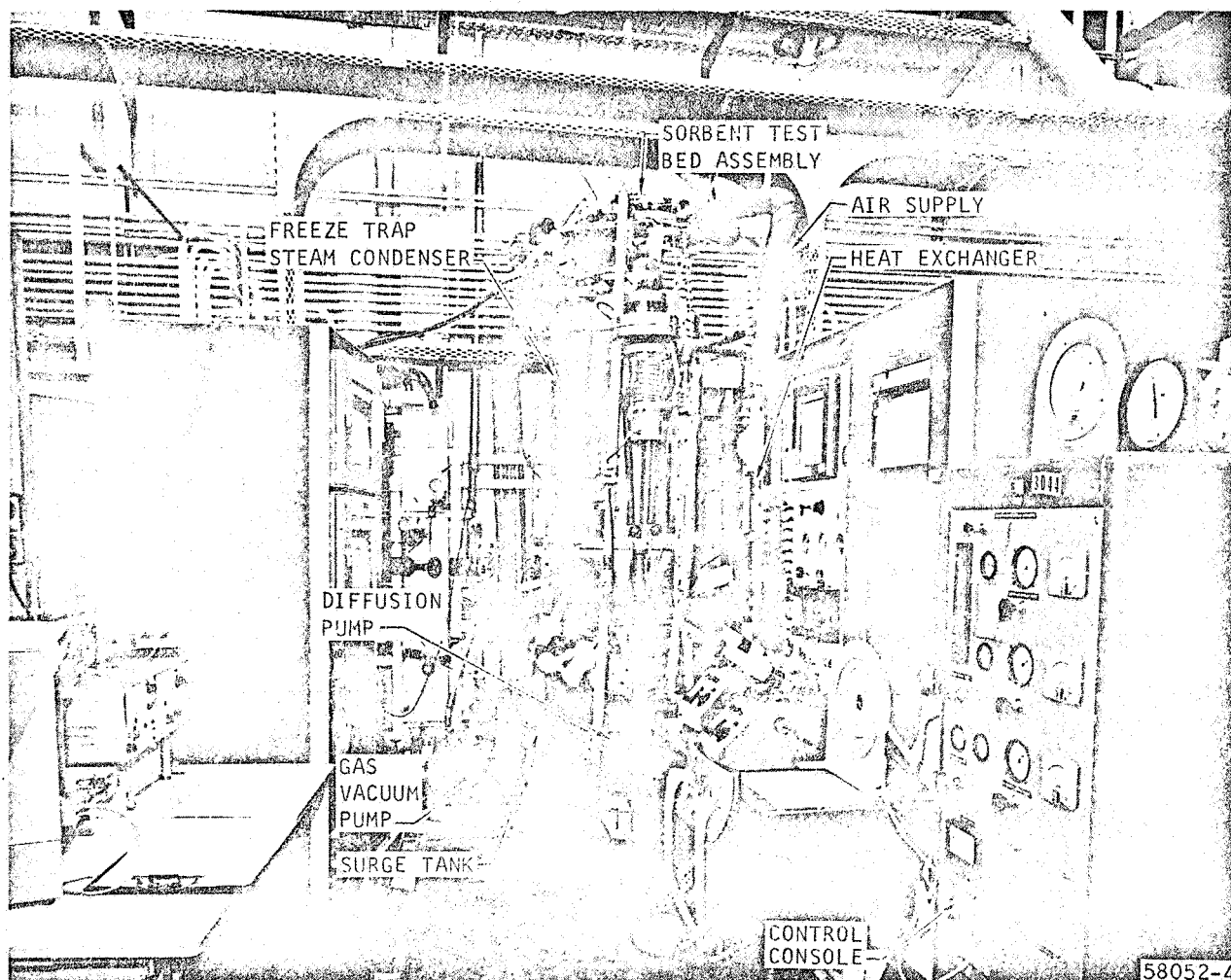
Figure 6-1. Prototype Test System

GAS VALVE AND
ACTUATOR

AIR INLET

GLYCOL
INLET

AIR OUTLET
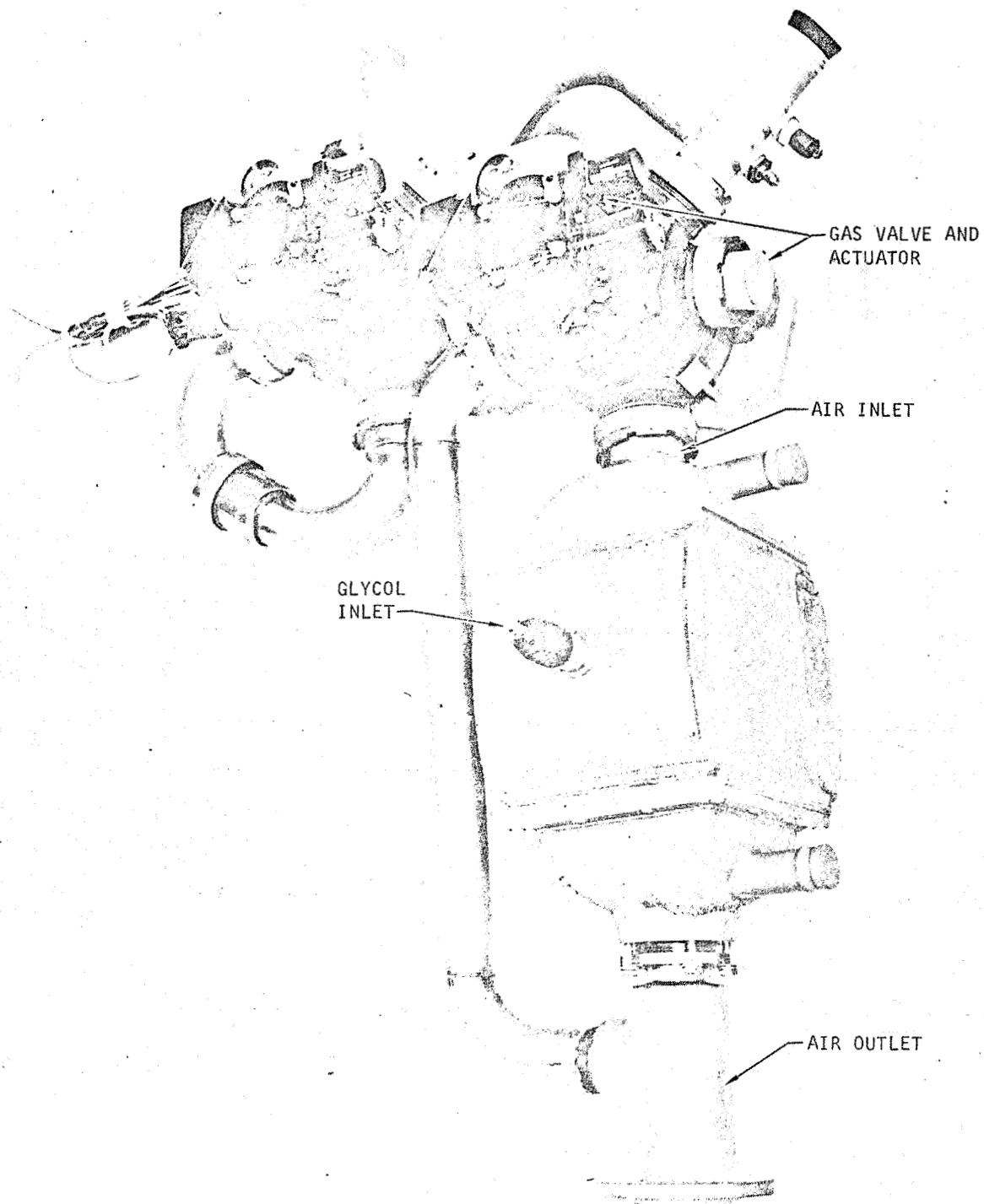
57267-3

Figure 6-2.   Prototype Sorbent Test Bed and Valve Assembly
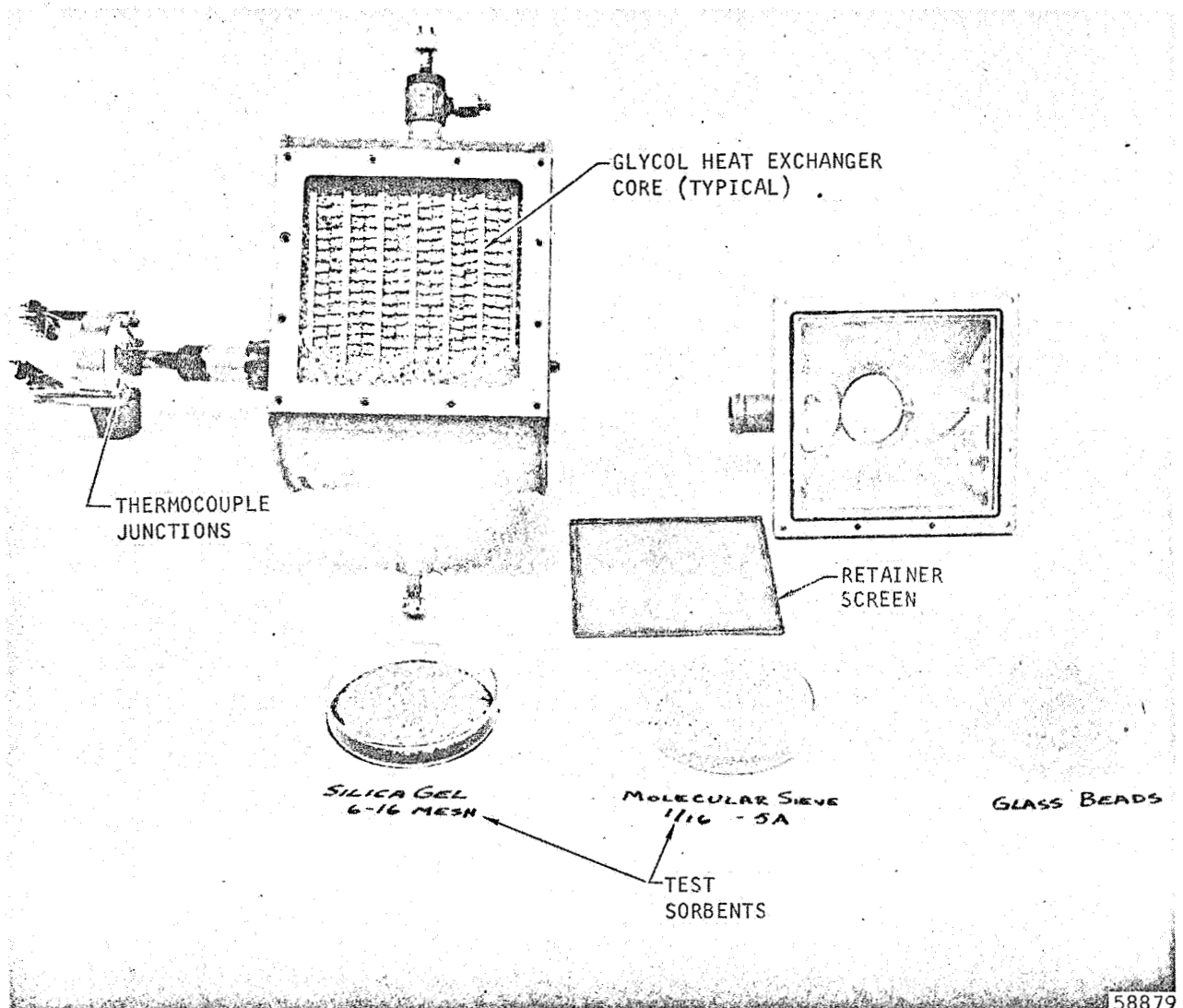
Figure 6-3.   Prototype Sorbent Bed and Heat Exchanger Core

Labels within figure:
- GLYCOL HEAT EXCHANGER CORE (TYPICAL)
- THERMOCOUPLE JUNCTIONS
- RETAINER SCREEN
- SILICA GEL 6-16 MESH
- MOLECULAR SIEVE 1/16 - 5A
- GLASS BEADS
- TEST SORBENTS
- 58879
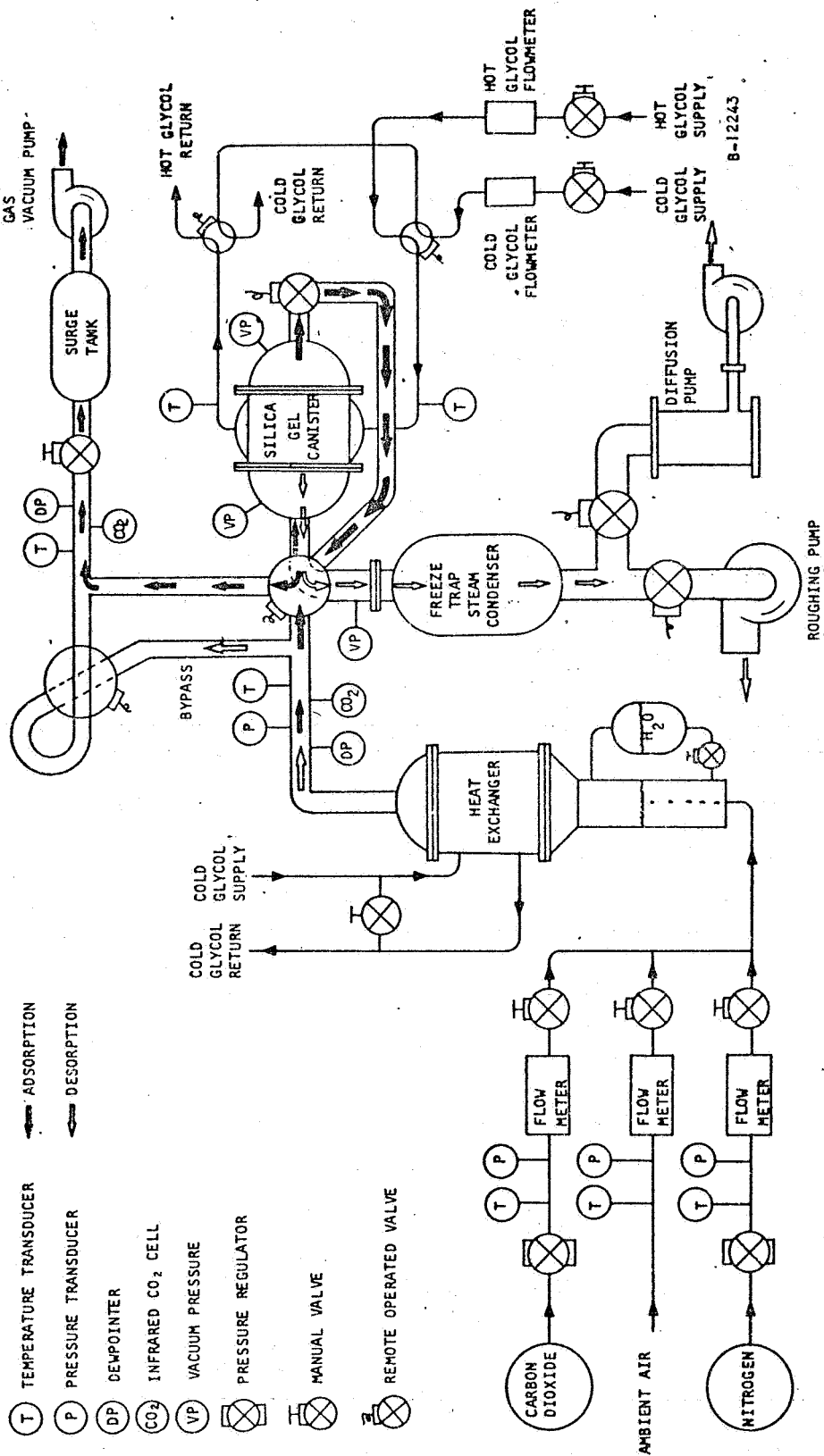
Figure 6-4. Prototype Silica Gel Test System Configuration Schematic

Legend:

- (T) TEMPERATURE TRANSDUCER
- (P) PRESSURE TRANSDUCER
- (DP) DEWPOINTER
- (CO₂) INFRARED CO_2 CELL
- (VP) VACUUM PRESSURE
- PRESSURE REGULATOR
- MANUAL VALVE
- REMOTE OPERATED VALVE

ADSORPTION
DESORPTION

runs the desorption pressure was adjusted by bleeding dry nitrogen into the vacuum pumping system to essentially decrease its pumping rate from the bed, thus increasing the desorption bed face pressure.

During each run, temperatures were recorded by a Brown Multipoint Recorder; pressures and inlet and outlet dew points were measured and recorded manually.

Test Results

Table 6-1 summarizes the tests conducted. Figure 6-5 shows results obtained during Run No. 2-2, which is typical for all runs. The outlet dew point as reasured was compared to that computed, using the technique described in the next section. For purposes of simplicity, the bed was assumed to be isothermal during adsorption and also during desorption. The temperatures were determined primarily by the coolant temperatures. Figures 6-6, 6-7, and 6-8 show the comparison. The adsorption mass transfer coefficient used was 0.7 by 10^{-3} in all cases. It had, however, very little effect since the predicted outlet dew point depended almost exclusively on the water loading at the end of desorption. This loading is a function of bed temperature and water partial pressure during desorption. The consistently better performance of the bed over that calculated, then, must be due to better desorption than is indicated. Inspection of the bed pressures during desorption shows an unusually high drop between the face and back for the flow of water vapor occurring (Figure 6-9). This suggests a higher gas flow rate, which could only be caused by a leak at the back of the bed. The gas leaking in would be essentially dry and would act as an effective purge, thus improving the adsorption performance.

A better method for determining the adsorption mass-transfer coefficient is the use of the breakthrough performance. Figure 6-10 shows the effect of the adsorption mass-transfer coefficient on the predicted outlet dew point. The initial load was assumed to be nearly zero, since the breakthrough was performed immediately following a bakeout.

The coefficient will be a strong function of how the bed is packed around the heat exchanger core. A tight pack will eliminate channeling, provide high interstitial velocities, and yield a high mass-transfer coefficient. This is the case of the 2-in. prototype bed, where a rather high value of 1.0 by 10^{-3} along with a high contact area, ASG, of 935, was best. This area was estimated by ratio from the packed densities of this bed and the 5/8-in. bed, where an ASG of 700 was used.

Discussion of Test Results

Outlet dew point data obtained confirmed initial predictions of full-scale bed performance to a considerable degree. As mentioned earlier, the most important variable in obtaining high-efficiency predryer sections for a regenerative CO_2 removal unit is desorption temperature and pressure. The water vapor outlet partial pressures recorded during adsorption as shown are almost constant for the entire adsorption run, indicating that the adsorption mass transfer zone is within the 2-in. depth for the entire run. Thus, the outlet

TABLE 6-1

SILICA GEL PERFORMANCE

Tests of a 2-in.-deep 6-16 mesh (1.75 lb) silica gel bed in a 6-in. by 5.8-in. face heat exchanger.

Carrier gas	Nitrogen at 5 psia
Gas flow	3.5 lb/hr (0.302 lb/ft^2-min)
Adsorbent coolant temperature	58°F
Coolant flow	200 lb/hr
Inlet dew point	52°F, 10 mm Hg
Half cycle time	30 min

Test Series	Total Time, Hr	Desorb Coolant Temp, °F	Outlet Water Vapor Concentration		Bed Face Pressure At End Of Desorption, μ	Remarks
			Dew Point, °F	Partial Pressure, MM Hg		
2-1	5-1/2	115 to 120	-70 to -75	0.012	40	
2-2	12	97 to 100	-75 to -80	0.0072	40	Outlet dew point appears low
3-1	6-1/2	80	-40 to -50	0.07	40	
3-2	6	80	-30 to -35	0.15	500	
2-3	7-1/2	100	-55 to -60	0.03	175	
2-4	2-1/2	100	-50 to -55	0.042	500	
4-1	6	70 ads	-30 to -35	0.15	40	70°F Adsorbent coolant
5-1	8-1/2	100	-50 to -55	0.042	200	Gas flow increased to 3.75 lb/hr

TABLE 6-1 (continued)

Test Series	Total Time, Hr	Desorb Coolant Temp, °F	Outlet Water Vapor Concentration		Bed Face Pressure At End Of Desorption, μ	Remarks
			Dew Point, °F	Partial Pressure, MM Hg		
5-2	10	100	-40 to -45	0.08	200	Desorb coolant flow decreased to 31 lb/hr
6-1*	3.0	None	-	-	-	Run to breakthrough

*Run on modified bed: 2-7/16-in. deep (1.0 lb) silica gel in 4.3 in. by 4.8 in. face area. Gas flow 5.5 lb/hr.
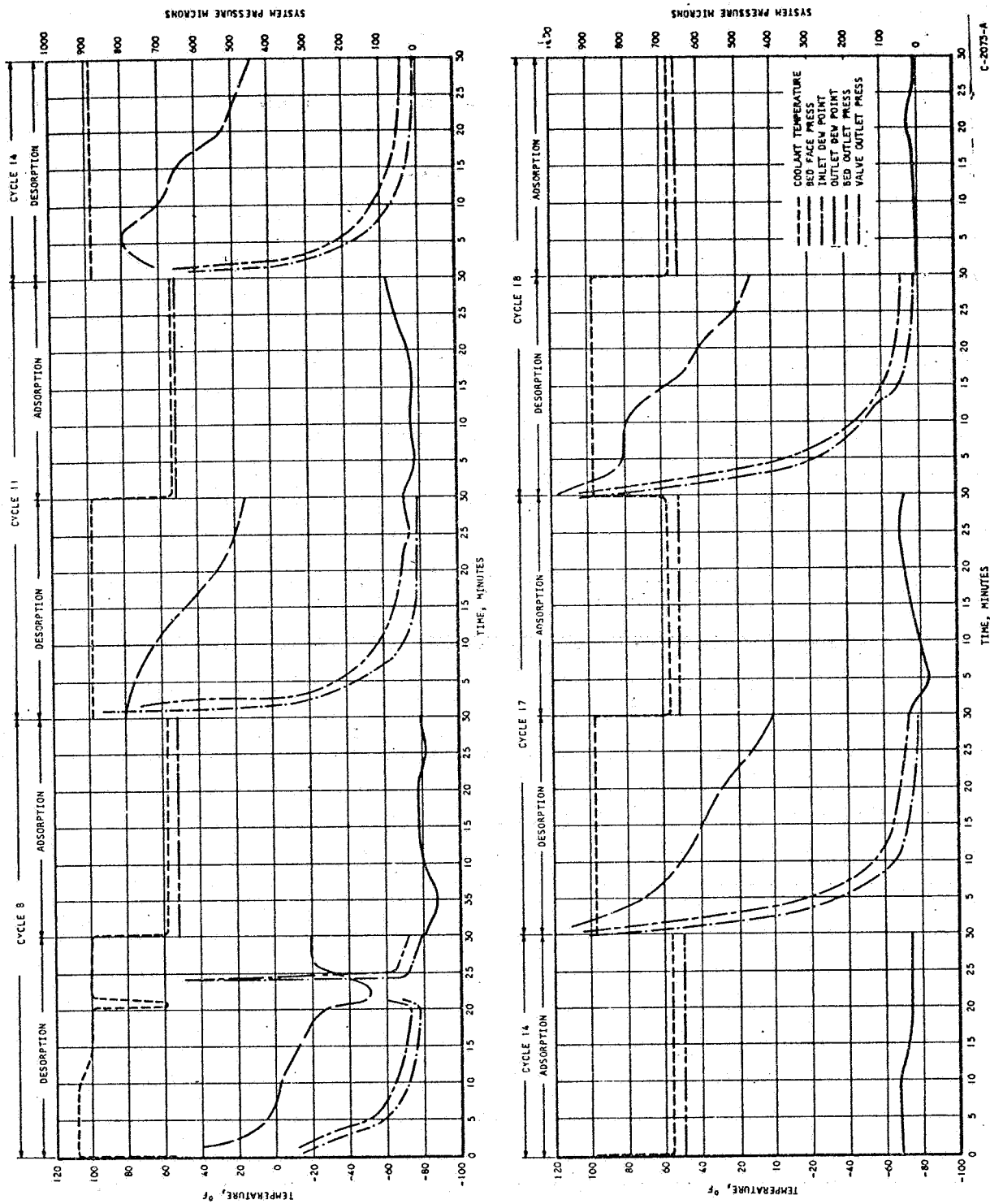
Figure 6-5. Test Results for a Silica Gel/H_2O Typical. (Run No. 2-2) Desorption-Adsorption Cycle Series
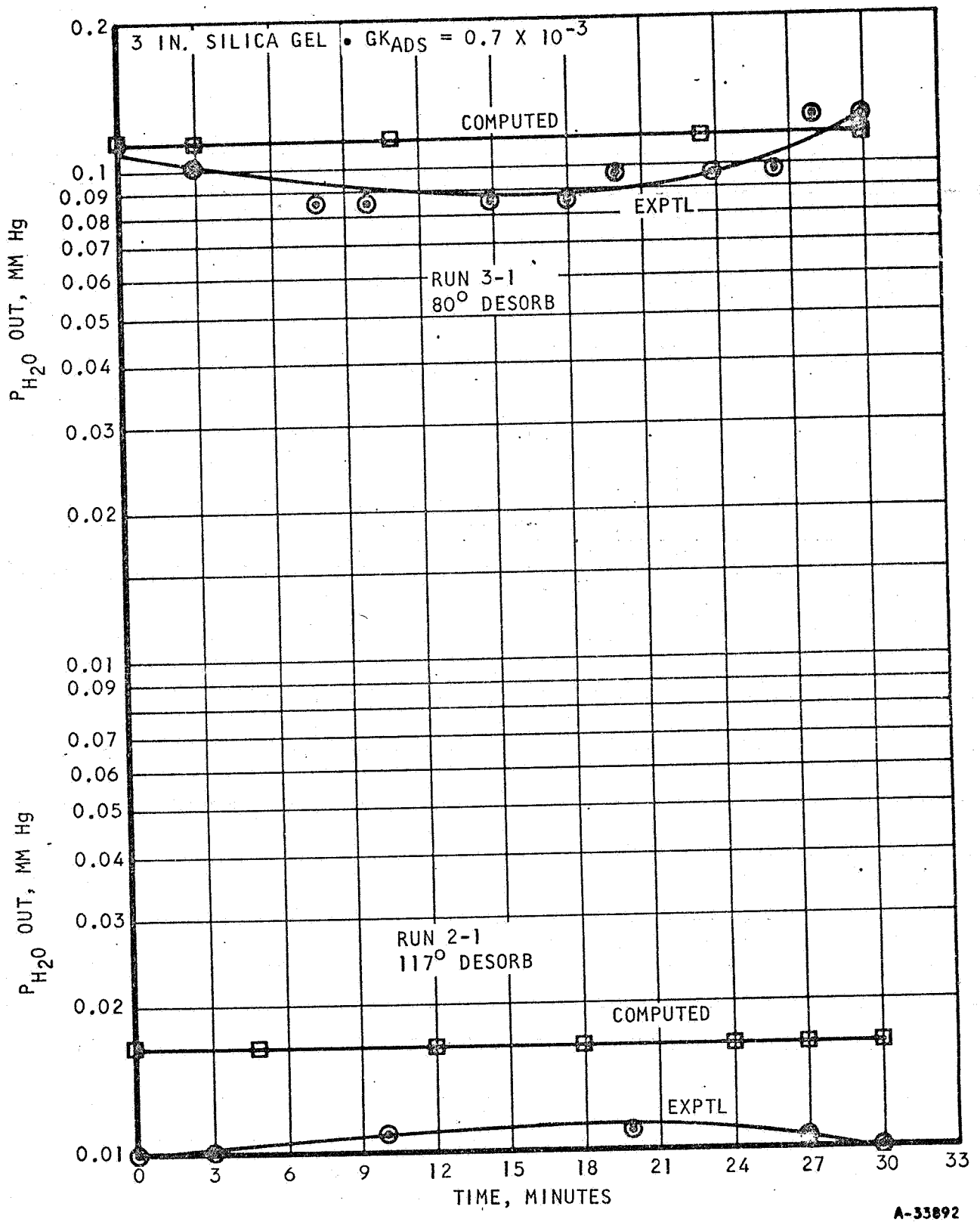
Figure 6-6. 3-In. Silica Gel Tests

A-33892
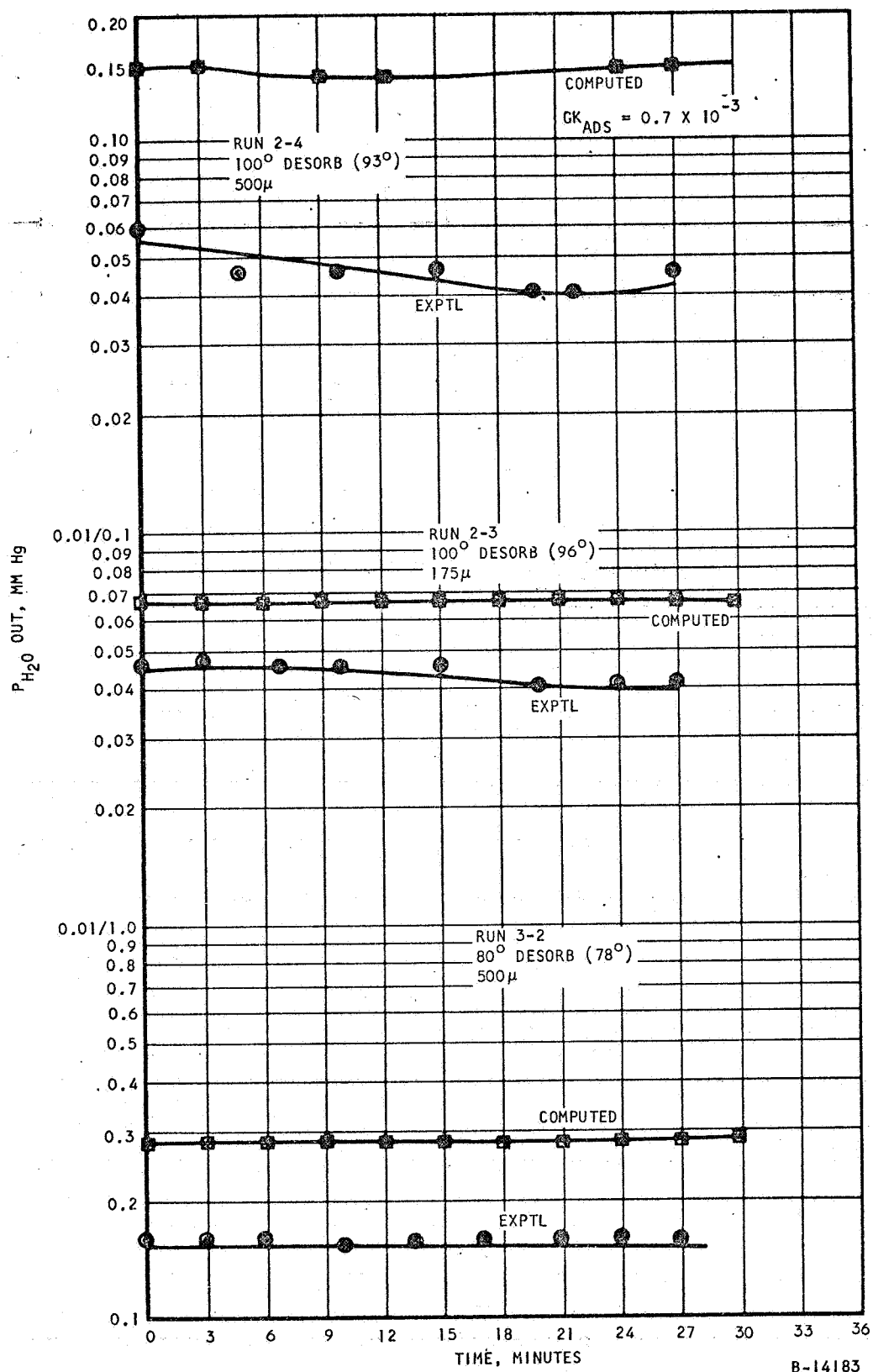
Figure 6-7. 1-in. Silica Gel Tests
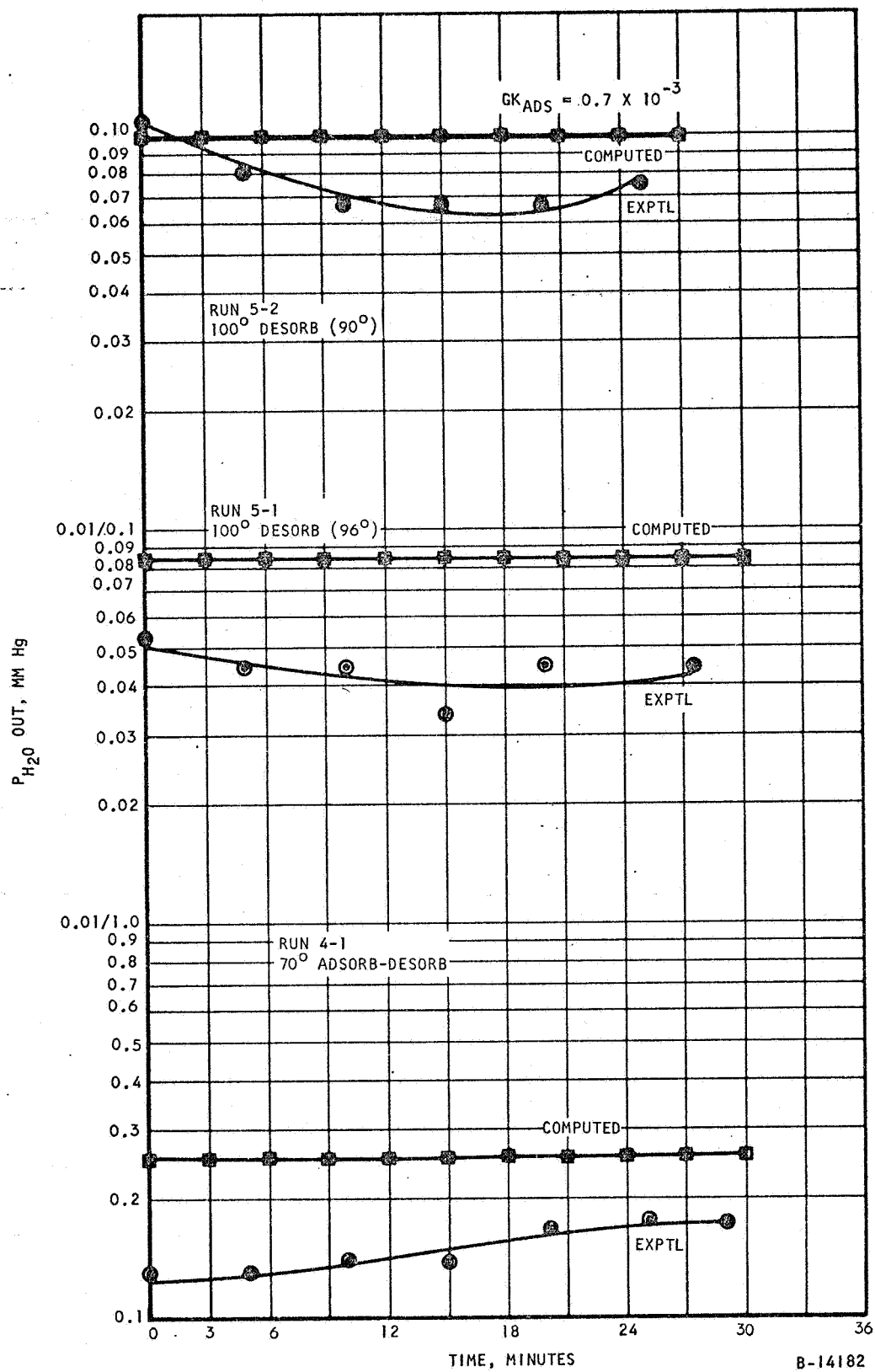
Figure 6-8. 2-in. Silica Gel Tests
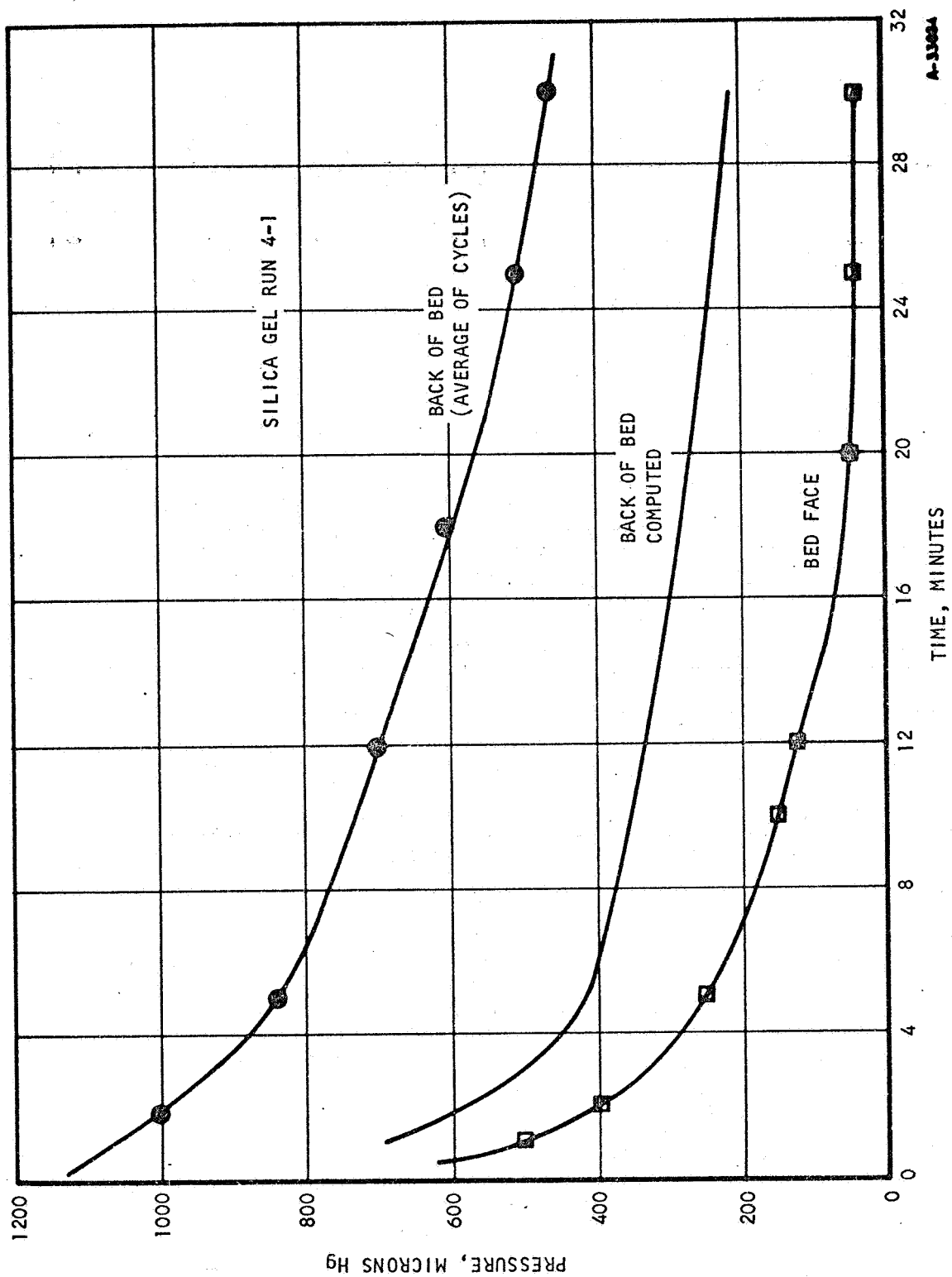
Figure 6-9. Desorption Pressure Comparison Showing Apparent Leak
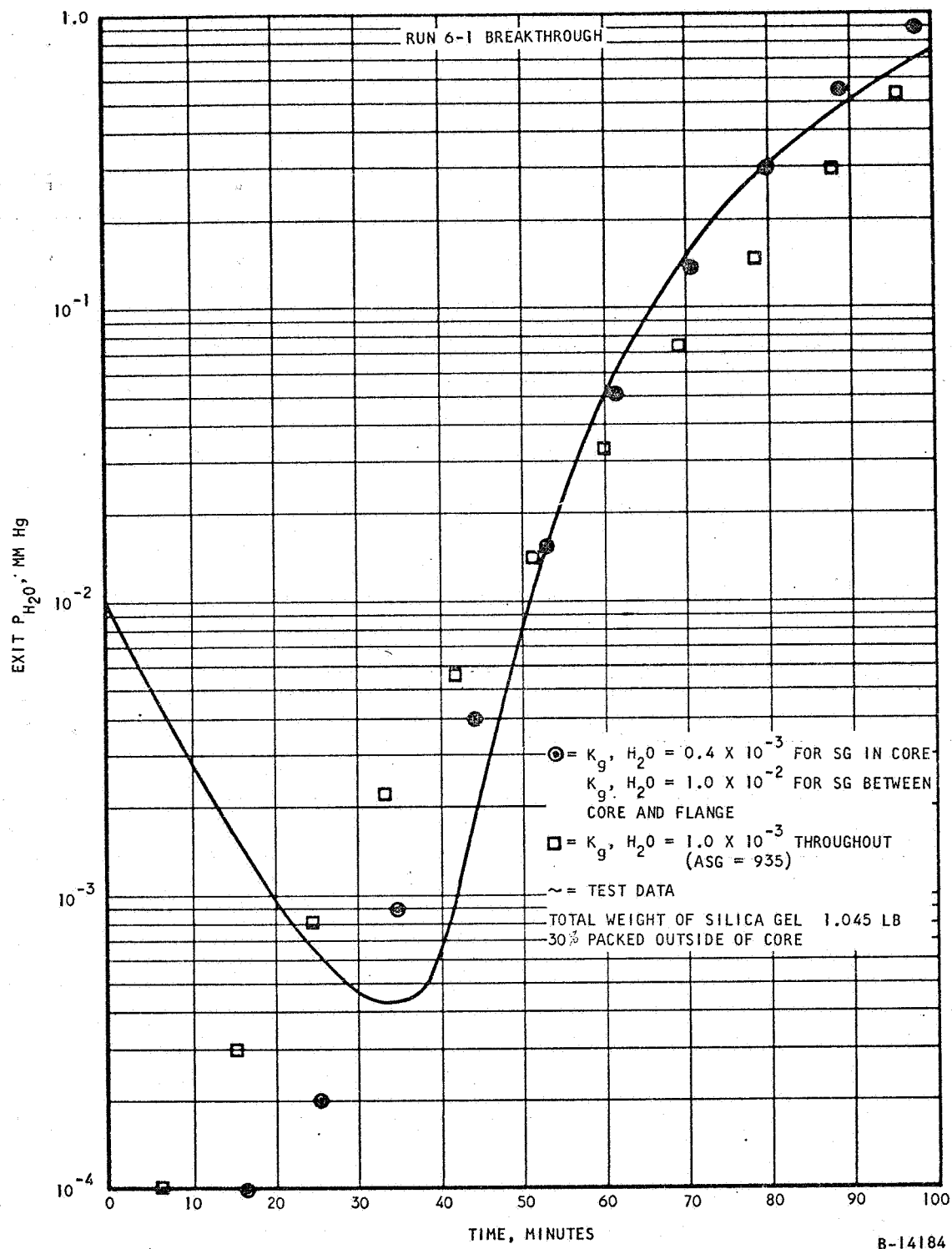
Figure 6-10. Water Breakthrough on 3-in. Silica Gel Bed

partial pressure is influenced almost exclusively by the residual loading of the bed from the previous desorption. This will be characteristic of all predryer designs, since the important factor in these units is absolute maximum water removal to protect the molecular sieve bed downstream.

CO$_2$ AND WATER VAPOR ON MOLECULAR SIEVE

Purpose

This test series was initiated to provide confirmation of predicted CO$_2$ removal efficiency of molecular sieves, by investigating the effect of bed size, bed temperature, and coadsorbed water during adiabatic and thermal swing operation.

Technique

The heat exchanger was packed with varying depths of 1/16-in. pellet, Linde Type 5A molecular sieves. The balance of the heat exchanger was filled with glass beads. The bed was then installed in the test setup as shown in Figure 6-11 with the molecular sieve section adjacent to the gas valve.

Operation and procedures were the same as during the silica gel tests, except that pure CO$_2$ was injected in the nitrogen carrier gas upstream of the bed, and the inlet and outlet CO$_2$ concentration was monitored by an infrared CO$_2$ analyzer. H$_2$O injection was restricted to low levels typical of that anticipated from the silica gel predryer (below -50°F dew point). Injection of this very small amount of water vapor was accomplished by bleeding into the circuit small amounts of laboratory ambient air.

Test Results

1. Test Series 6 and 7 (1-in.-deep test bed)

A total of 219 hr of cyclic operation was conducted on the test unit packed with a 1-in. depth (0.5 lb) of 1/16-in.-dia pellet, Linde Type 5A molecular sieve. The series of tests conducted, outlined in Table 6-2, provided information on thermal swing and adiabatic operation of the bed, at conditions simulating anticipated final design conditions. In addition, an accelerated water poisoning test was conducted, with periodic measurement of CO$_2$ removal performance as water buildup accumulated. The initial portions of this test were repeated twice following extended bakeout periods to confirm findings. Figures 6-12 and 6-13 show representative CO$_2$ breakthrough curves for the various runs, in all cases after sufficient cycles had been run to establish stability. The differences in performance between runs is attributed to differences in residual water loading, with best performance occurring during runs 6-8 and 7-3, after a 30-hr bakeout. Water loading at this point is estimated to be less than 1 percent, with other runs shown indicating residual water up to 2 percent.
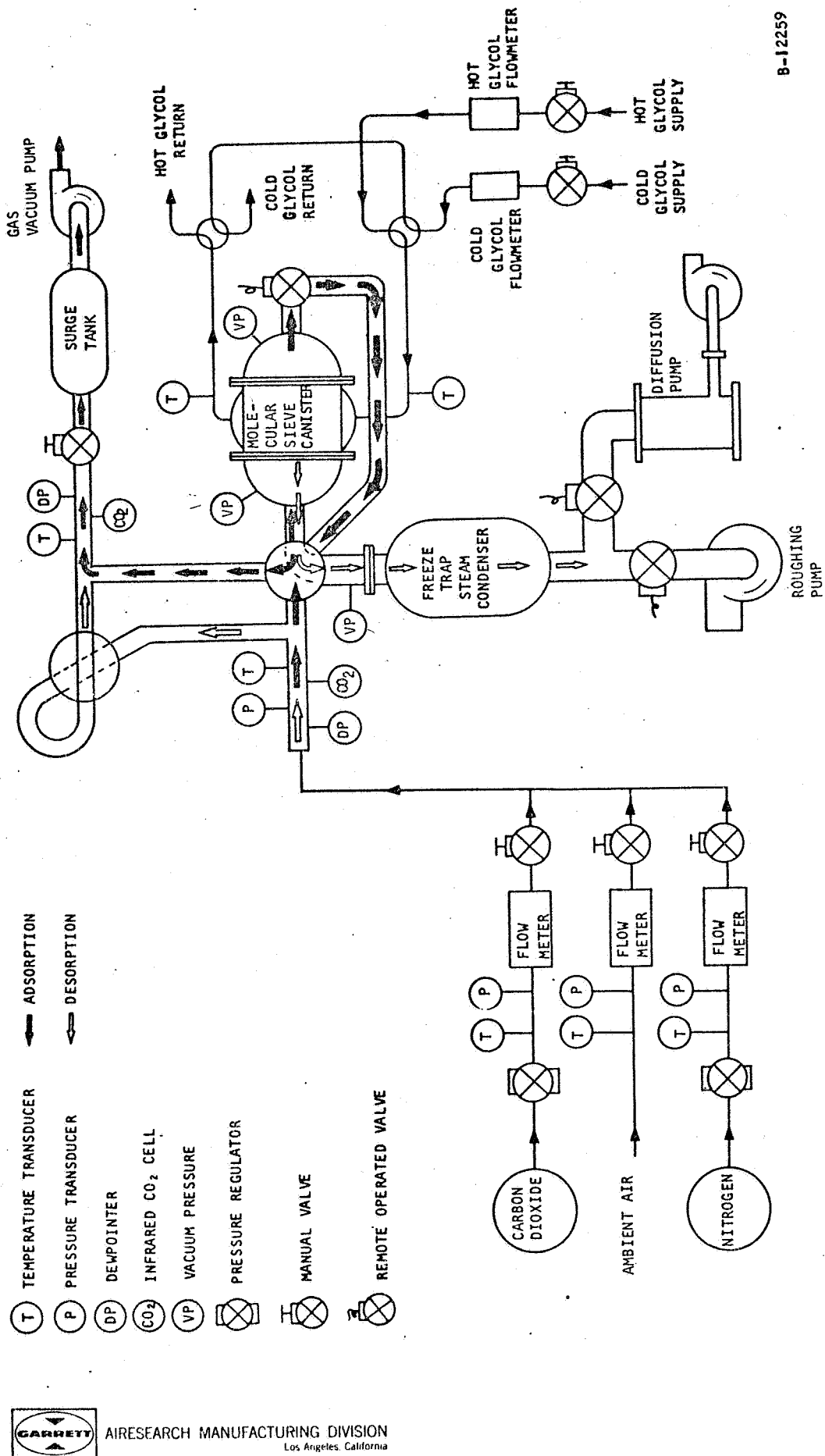
Figure 6-11. Prototype Molecular Sieve Test System Configuration Schematic

B-12259

TABLE 6-2

SUMMARY OF TESTS ON 1-IN.-DEEP MOLECULAR SIEVE BED

Test No.	No. Cycles/ Adsorb. Hr	Half Cycle Time, Min	Gas Flow Rate, lb/hr	Coolant Temp Adsorb/Desorb, °F	Desorb Pressure, μ	Inlet Dewpoint, °F	Outlet pCO_2 End of Cycle, MM Hg	Remarks
Initial Bakeout								Leakage suspected
				Hours at 400°F with < 10μ Vacuum				
6-1	13/6.5	30	3.7	58/85	550	-50	6.2 to 6.95	Poor CO_2 removal, poor bakeout suspected
6-2	2/1	30	3.7	58/85	550	-50	---	IR calibration in error, data discarded
Bakeout			10 Hours at 240°F, 8 Hours dry GN_2 Purge at 240°F					
6-3	4/2	30	3.8	58/95	150	-80	6.45	Initial check with dry gas
6-4	54/101*	30	3.8/7.7**	58/95	550	-50	See Fig.	First H_2O poisoning check
Bakeout			30 Hours at 185°F					
6-5	5/2.5	30	3.8	58/95	700	-80	6.6	Run with dry gas, poor bakeout due to low temperature
Bakeout			12 Hours at 400°F					
6-6	23/11.5	30	3.8	58/95	550	-50	5.7 to 6.6	Repeat of H_2O poisoning check
6-7	3/1.5	30	3.8	58/95	550	-50	5.7 to 6.6	
7-1	14/3.5	15	4.0	None	550	-65	5.9 to 6.1	Adiabatic operation
7-2	4/2	30	4.0	None	550	-65	6.7	Adiabatic operation
Bakeout			30 Hours at 400°F					
6-8	28/14	30	3.8	58/95	550	-50	5.5 to 6.7	Third H_2O poisoning check
7-3	10/2.5	15	4.0	None	550	-65	5.75	

*Excess adsorb time shown is due to noncyclic adsorption of H_2O only to accelerate water loading.
**Gas flow is increased to accelerate water loading.
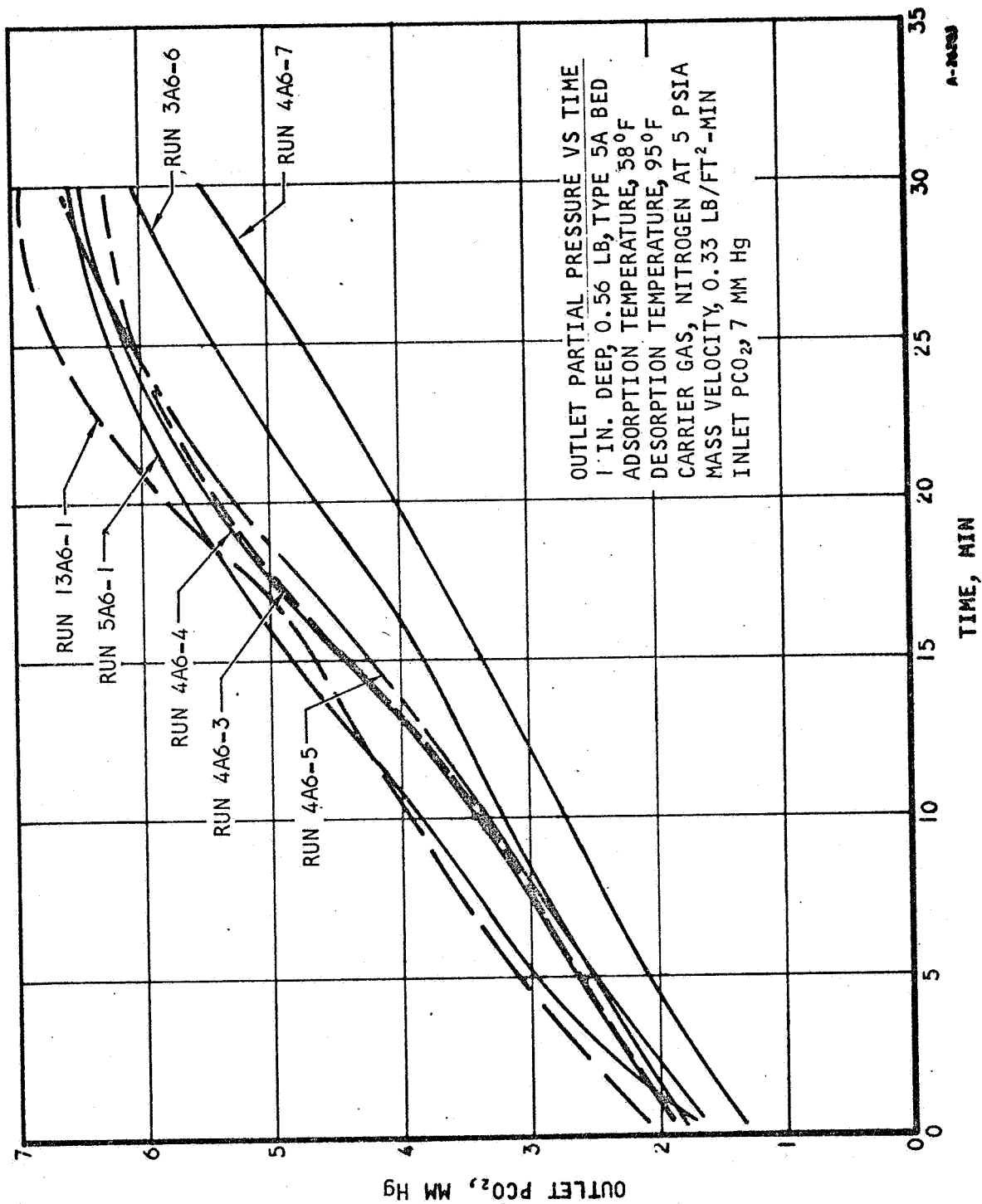
Figure 6-12. Thermal Swing CO$_2$ Removal of a 1-in. Bed

The graph shows OUTLET PCO$_2$, MM Hg versus TIME, MIN.

Curves labeled: RUN 3A6-6, RUN 4A6-7, RUN 13A6-1, RUN 5A6-1, RUN 4A6-4, RUN 4A6-3, RUN 4A6-5

OUTLET PARTIAL PRESSURE VS TIME
1 IN. DEEP, 0.56 LB, TYPE 5A BED
ADSORPTION TEMPERATURE, 58°F
DESORPTION TEMPERATURE, 95°F
CARRIER GAS, NITROGEN AT 5 PSIA
MASS VELOCITY, 0.33 LB/FT^2-MIN
INLET PCO$_2$, 7 MM Hg

A-24893
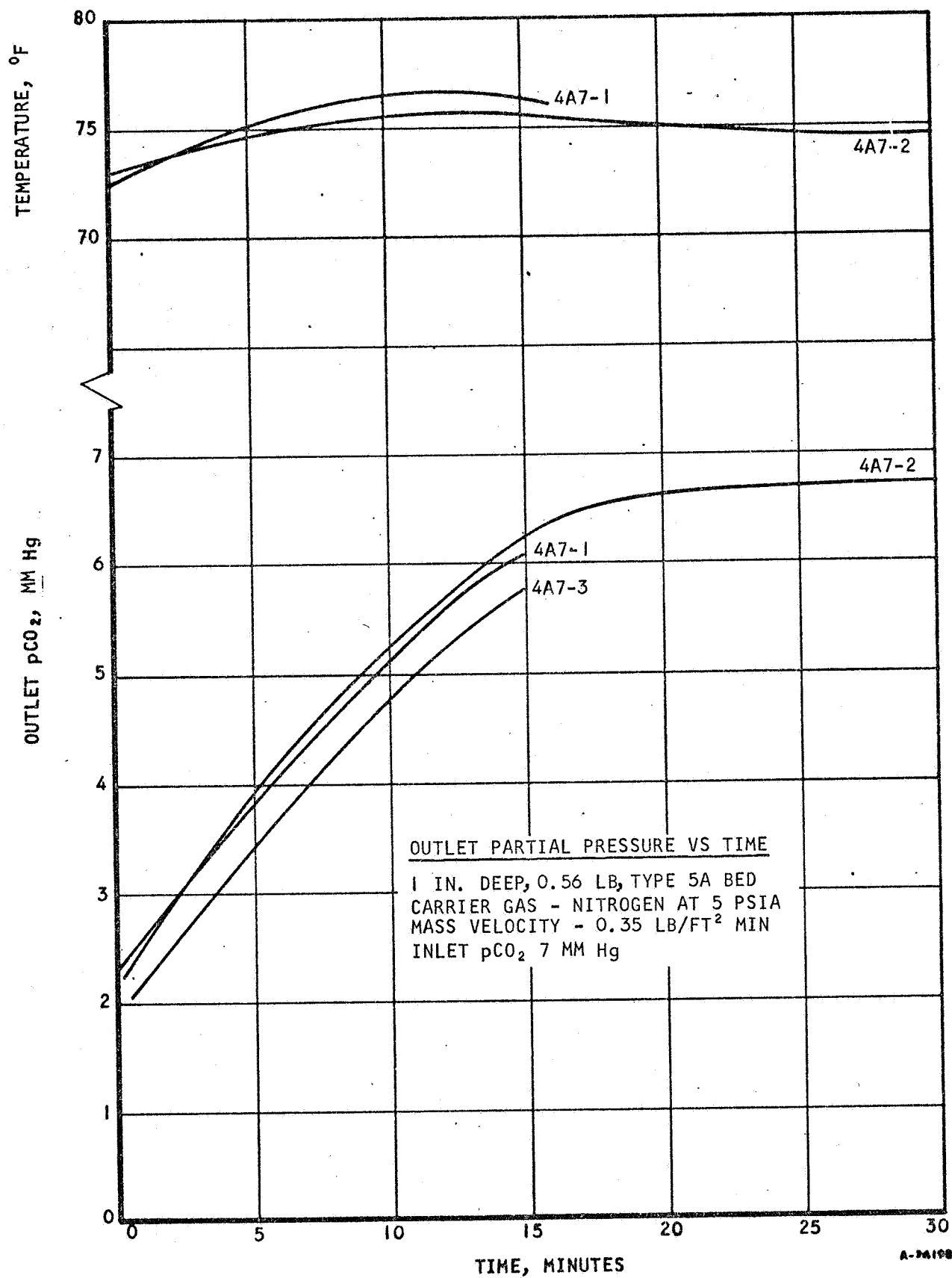
Figure 6-13. Adiabatic CO_2 Removal of a 1-In. Bed

2. Test Series 8 (2-in.-deep test bed)

Following the l-in. bed tests, a short series of runs was conducted to determine the CO_2 removal performance with a 2-in. (1.7-lb) bed. Table 6-3 summarizes the tests conducted, and Figure 6-14 shows typical CO_2 breakthrough curves.

3. Test Series 9, 10, and 11 (3-in.-deep test bed)

Following the 2-in. bed tests, the test heat exchanger was loaded with about 2 lb of molecular sieve to a 3-in. depth. Test series 9 was conducted. During these tests considerable difficulty was experienced in attaining a leak-tight system during desorption. The test setup was revised as shown in Figure 6-15, eliminating the extensive adsorption ducting. Following this revision to the test setup, a series of tests was conducted, particularly to provide further data on water poisoning. Run 11-1 was a continuous H_2O injection with periodic CO_2 adsorption performance measurement; in addition, three CO_2 adsorption breakthrough curves to equilibrium were obtained at various inlet partial pressures, shown in Figure 6-16. Table 6-4 summarizes this test series, and Figure 6-17 shows typical results on a fresh bed.

Calculations and Water Poisoning

In order to find the best constants for predicting bed performance and also to examine methods for estimating the effect of water poisoning, computer comparisons were made with the data from the tests.

1. One-In. Bed

a. Dry Bed Performance

Although the mass of molecular sieve loaded into the bed was measured, it contained an unknown amount of adsorbed material, mostly water. For use in calculations, the dry mass or mass available for CO_2 must be known. The best way to obtain this is from the amount of CO_2 actually adsorbed under known pressure and temperature conditions. Comparison of this result, calculated from the known flow rate and inlet and effluent CO_2 pressure, with the equilibrium loading at those conditions yields the bed weight. Run 6-3 to breakthrough was used. A bed weight of 0.375 lb was calculated. The fourth adsorb cycle is compared to the steady-state computed results in Figure 6-18. A mass-transfer coefficient for adsorption of 0.9 by 10^{-4} was used along with 5.0 by 10^{-4} for desorption. The desorption coefficient is the same formed for all testing, on the 5/8-in.-dia bed as well as the large prototype bed. However, the coefficient for adsorption is much smaller than that formed for the 5/8-in. bed. As will be discussed in Section 7, the effect of channeling is considered most responsible for the decreased coefficient in a highly finned bed.

b. Water Poisoning

An accurate description of CO_2 performance on a bed exposed to some water vapor would require knowledge of coadsorption equilibrium as well as rate data.

TABLE 6-3

SUMMARY OF TESTS ON 2-IN.-DEEP MOLECULAR SIEVE BED

Test No.	No. Cycles/Adsorb, hr	Half Cycle Time, min	Gas Flow Rate, lb/hr	Coolant Temp, Adsorb/Desorb, °F	Desorb Pressure, μ	Inlet Dewpoint, °F	Outlet pCO_2 end of Cycle, MM Hg	Remarks
Bakeout				25 hr at 400°F				
8-1	8/4	30	3.8	58/95	400	-50	2.9 to 3.0	Adiabatic operation
8-2	3/.75	15	4.0	None	550	-75	2.75	
8-1 (cont)	7/11.5*	30	3.8	58/95	400	-50	3.0 to 3.4	Short H_2O poisoning check
8-3	6/1.5	15	4.0	None	500	-50	3.5 to 3.6	Adiabatic operation

*Noncyclic H_2O adsorption included
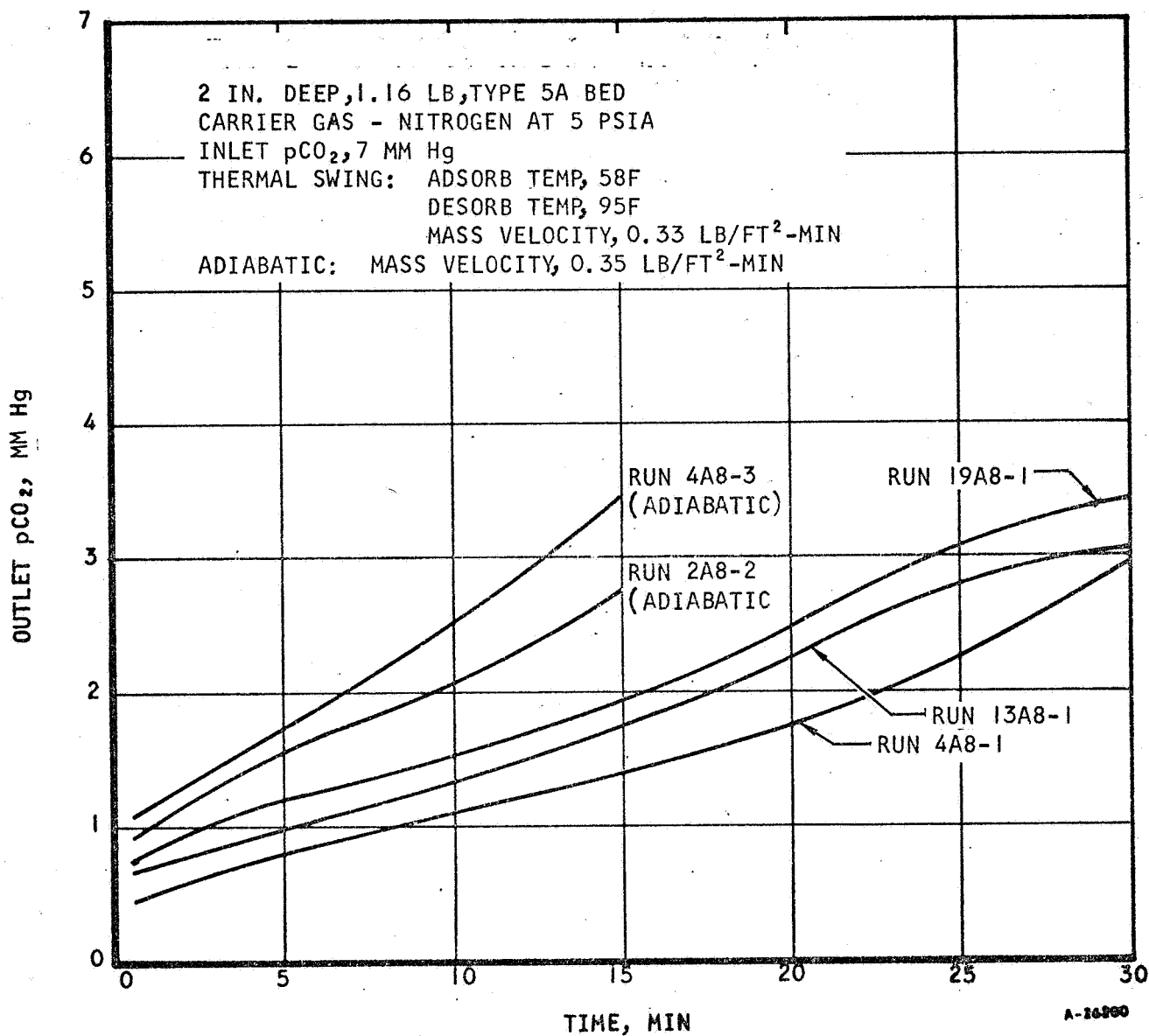
Figure 6-14. CO₂ Adsorption Performance of a 2-in. Bed
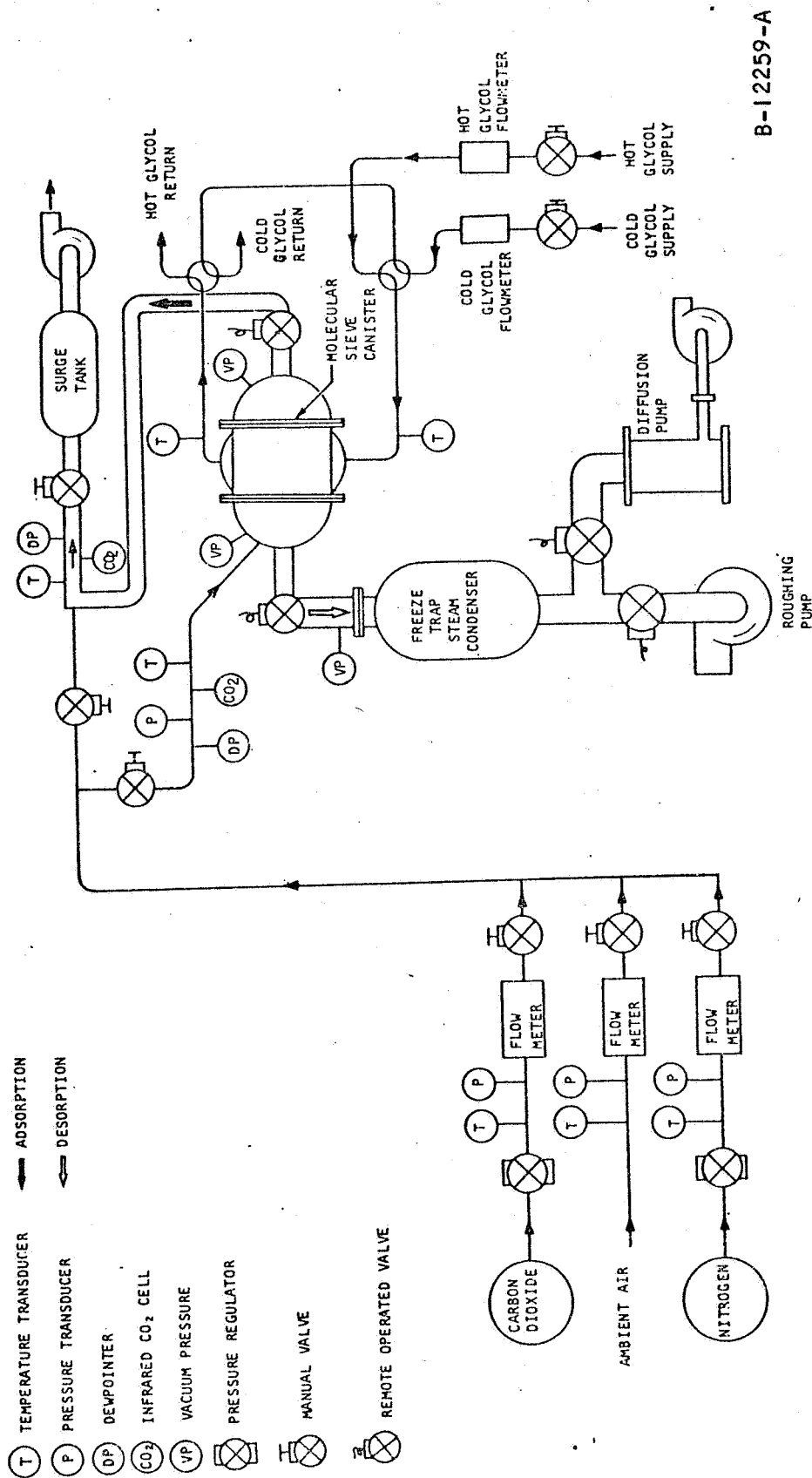
Figure 6-15. Modified Molecular Sieve Test System Configuration

B-12259-A

KEY:

- T — TEMPERATURE TRANSDUCER
- P — PRESSURE TRANSDUCER
- DP — DEWPOINTER
- CO_2 — INFRARED CO_2 CELL
- VP — VACUUM PRESSURE
- PRESSURE REGULATOR
- MANUAL VALVE
- REMOTE OPERATED VALVE

ADSORPTION
DESORPTION
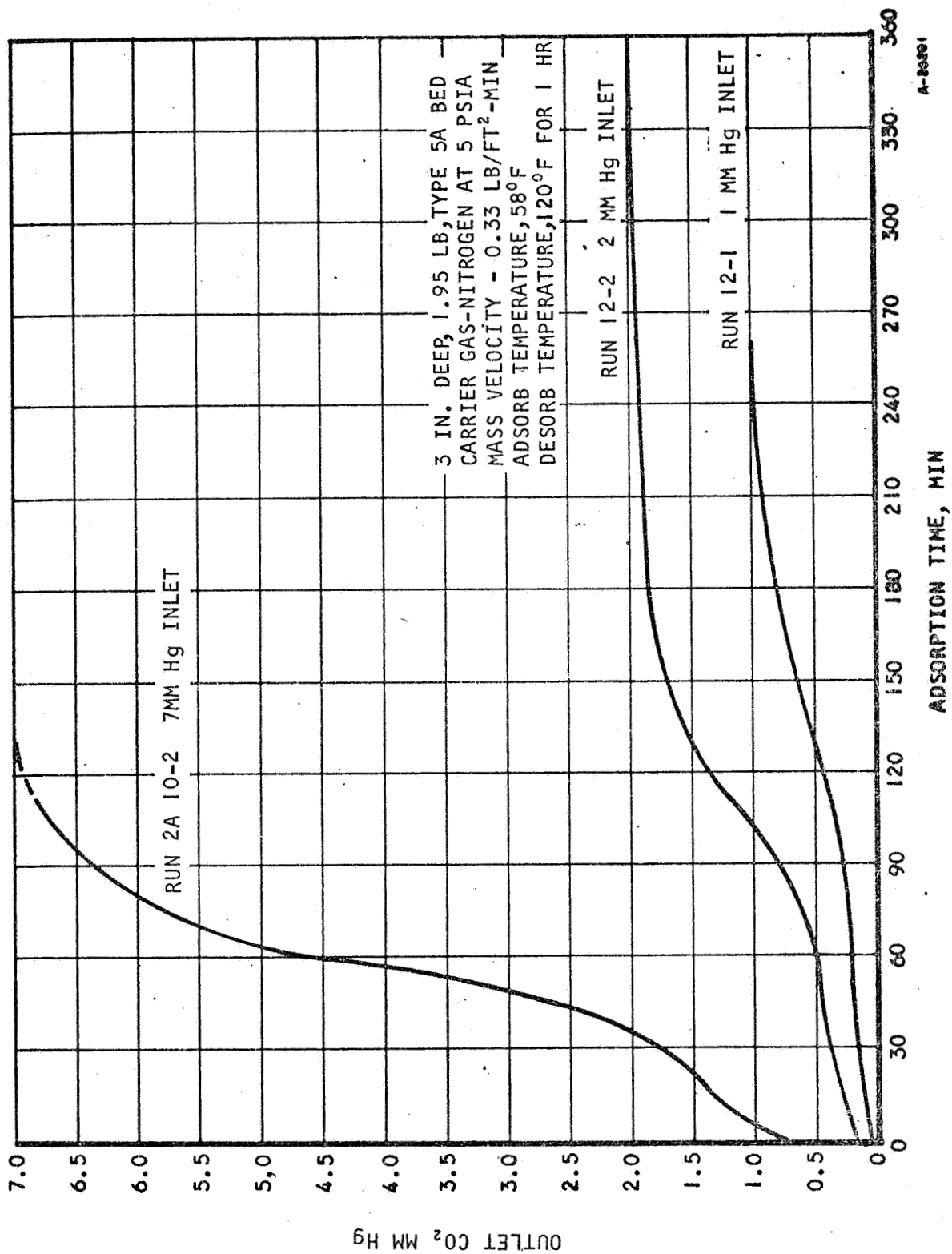
Figure 6-16. CO₂ Breakthrough in a 3-in.-Deep Bed.

A-26391

TABLE 6-4

SUMMARY OF TESTS ON 3-IN.-DEEP MOLECULAR SIEVE BED

Test No.	No. Cycles/ Adsorb, hr	Half Cycle Time, min	Gas Flow Rate, lb/hr	Coolant Temp, °F Adsorb/Desorb	Desorb Pressure, μ	Inlet Dewpoint, °F	Outlet pCO$_2$ End of Cycle, MM Hg	Remarks
Bakeout				20 hr at 400°F				
9-1	10/5	30	3.8	58/95	450	-50	1.7	
9-2	10/2.5	15	4.0	None	500	-65	2.0	
9-3	2/1	30	4.0	None	400	-65	3.5	
				Revised Test Setup, Bakeout 35 hr at 400°F				
10-1	9/4.5	30	3.8	58/95	450	-60	1.8	
Bakeout				13 hr at 400°F				
10-2	2/6.5	30	3.8	58/95	500	-50	See Figures 6-14 and 6-15	Second adsorb cycle run until complete bed breakthrough
11-1	1/	--	3.9	58/	--	+20	--	H$_2$O breakthrough run
Bakeout				5 hr at 400°F				
10-3	7/1.5	15	4.0	None	500	-65	2.2	
10-4	10/5	30	3.8	58/95	500	-50	1.75 to 1.9	
11-2	7/17	30	3.8	58/95	500	+20	See Figure 6-18	H$_2$O injection and periodic CO$_2$ removal performance
Bakeout				14 hr at 400°F				
12-1	1/	--	3.8	58/110	10	<-75	See Figure 6-14	Breakthrough run - 1mm pCO$_2$ inlet
12-2	1/	--	3.8	58/100	10	<-75	See Figure 6-14	Breakthrough run - 2mm pCO$_2$ inlet
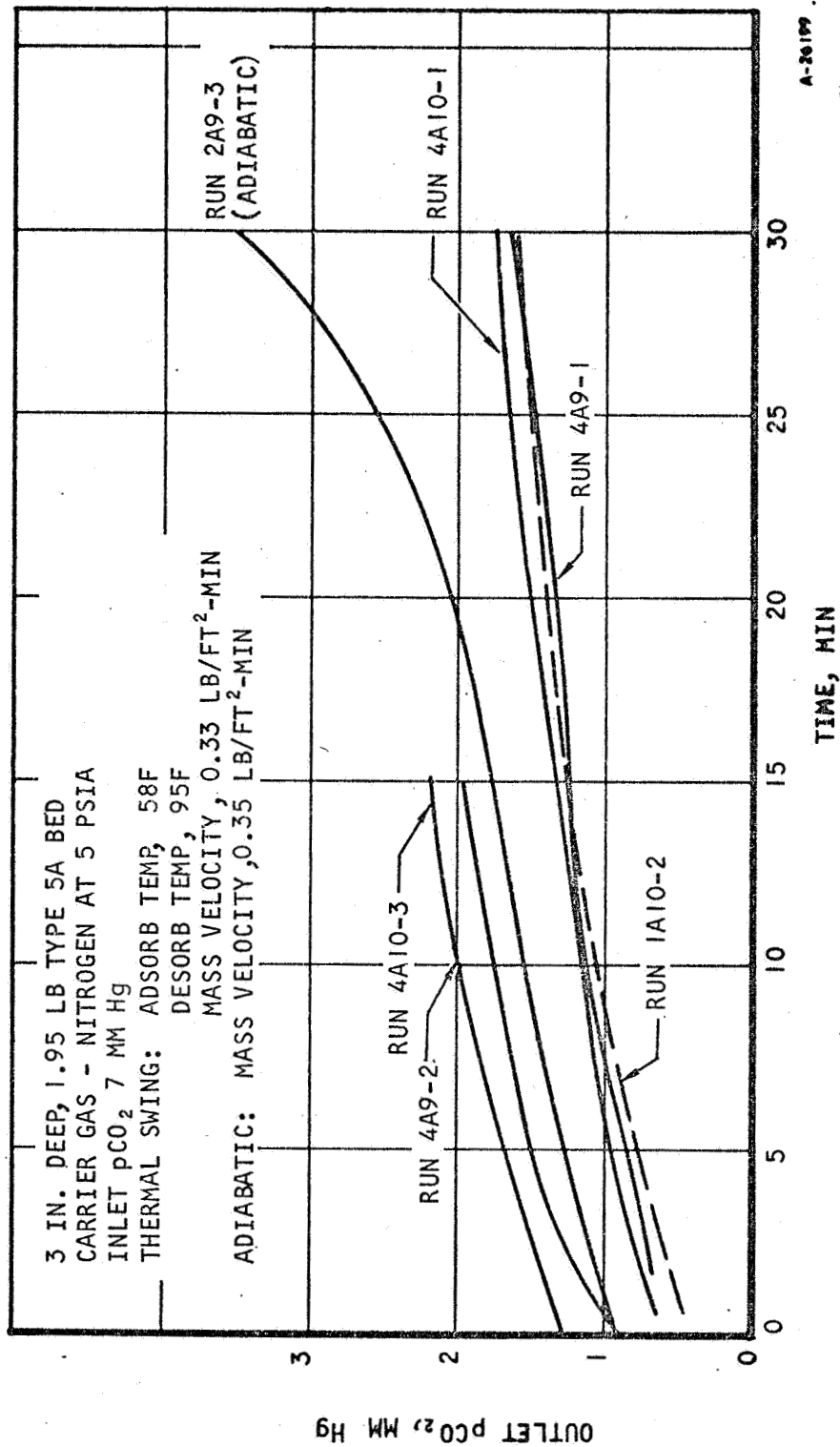
Figure 6-17. CO₂ Adsorption Performance of a 3-in.-Deep Bed

3 IN. DEEP, 1.95 LB TYPE 5A BED
CARRIER GAS - NITROGEN AT 5 PSIA
INLET pCO₂ 7 MM Hg
THERMAL SWING: ADSORB TEMP, 58F
DESORB TEMP, 95F
MASS VELOCITY, 0.33 LB/FT²-MIN
ADIABATIC: MASS VELOCITY, 0.35 LB/FT²-MIN

RUN 2A9-3 (ADIABATIC)
RUN 4A10-1
RUN 4A9-1
RUN 4A10-3
RUN 4A9-2
RUN 1A10-2

TIME, MIN

OUTLET pCO₂, MM Hg

A-26199
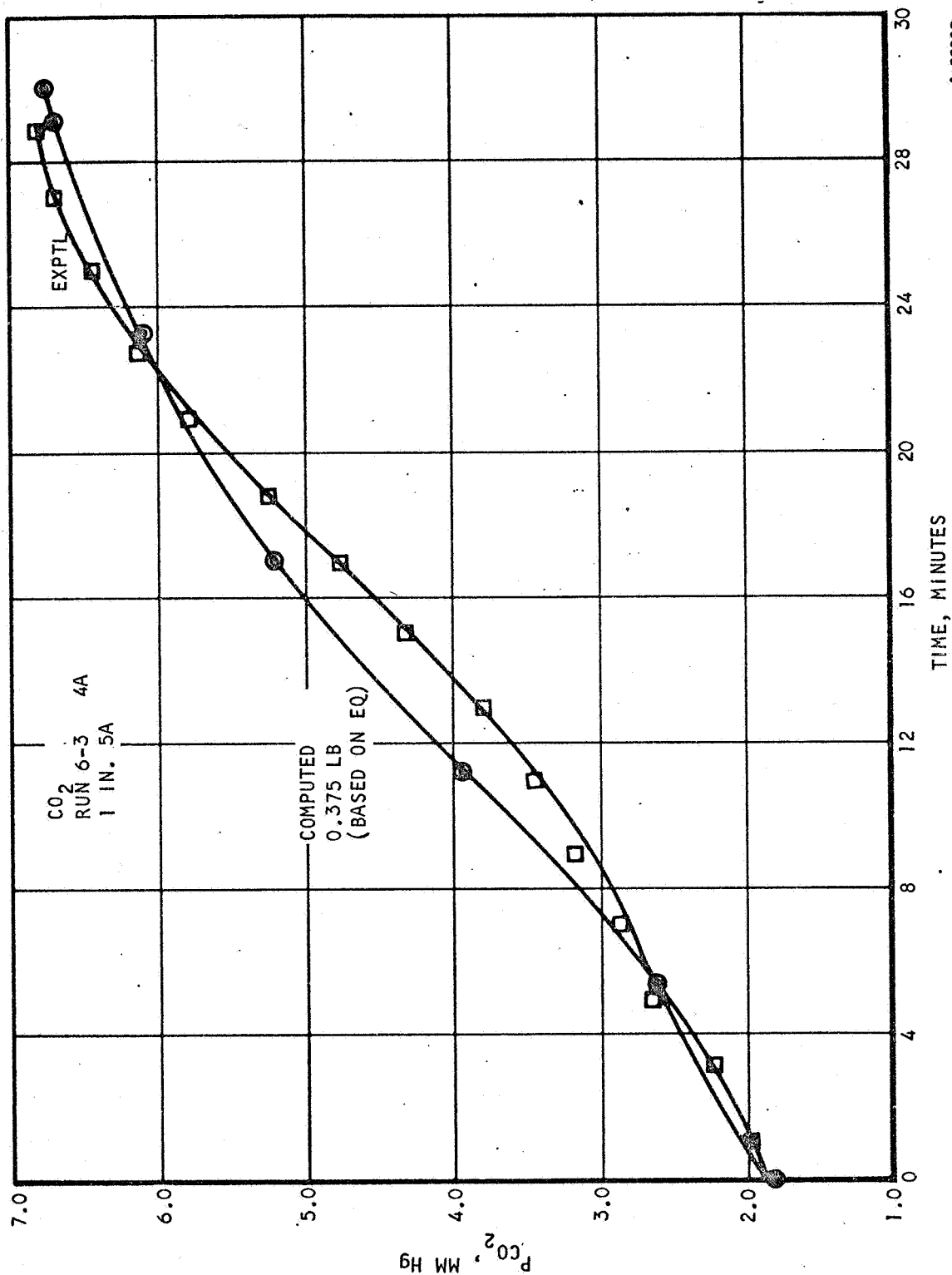
Figure 6-18. Computed and Experimental Results for CO_2 on Dry 1-in. 5A Bed

A-33967
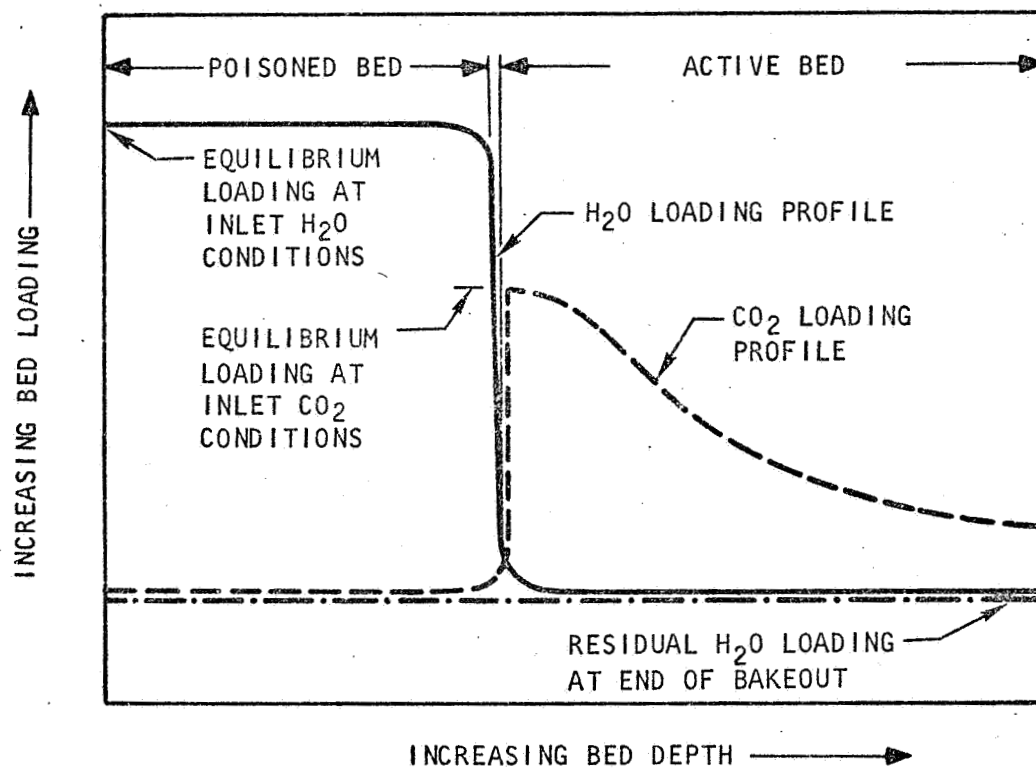
Figure 6-19. Prediction Model for Water Poisoning Effect on Molecular Sieve Bed
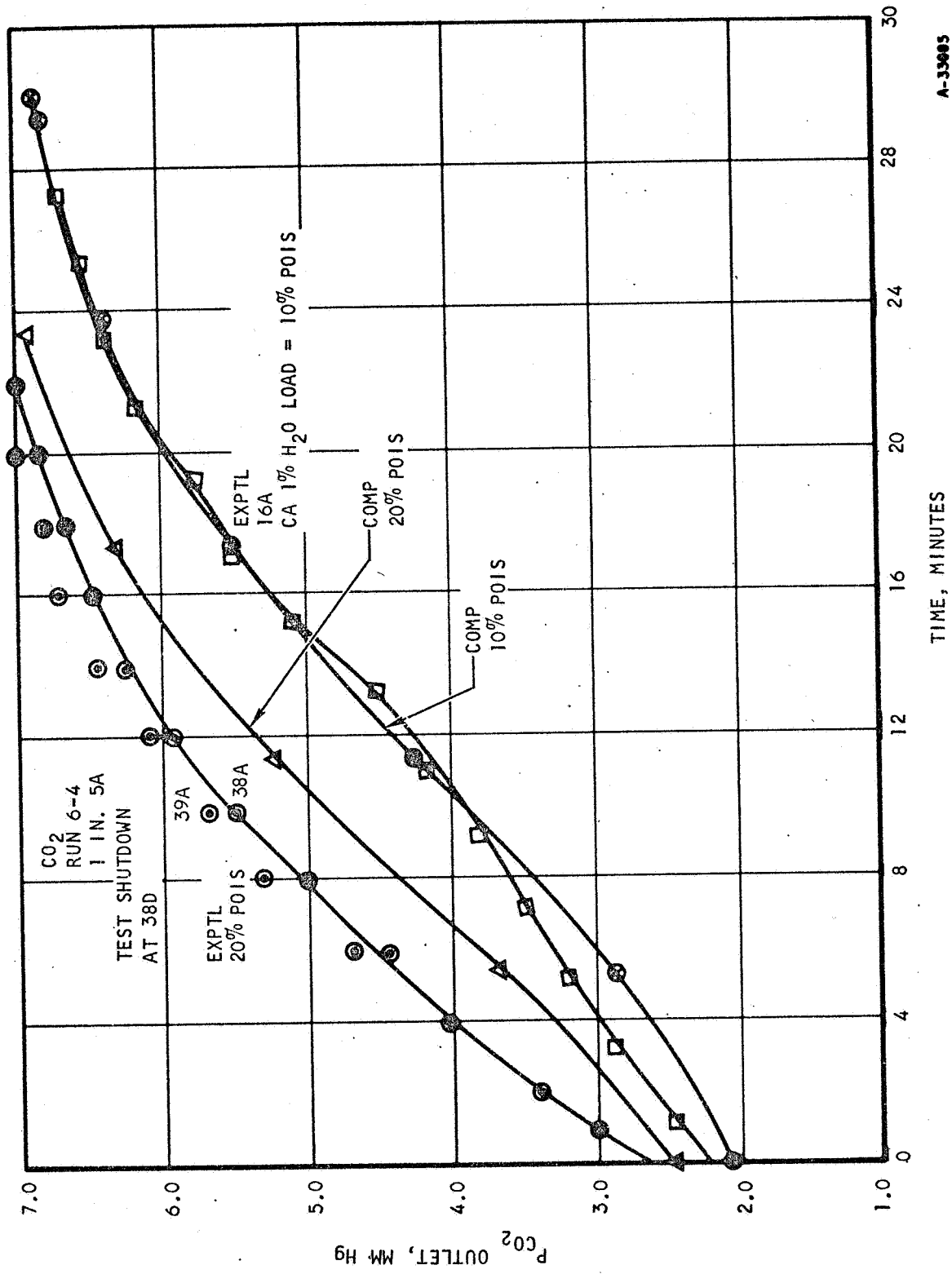
Figure 6-20. Comparison of 1-in. 5A Bed Results with Poisoning Prediction

A-33005
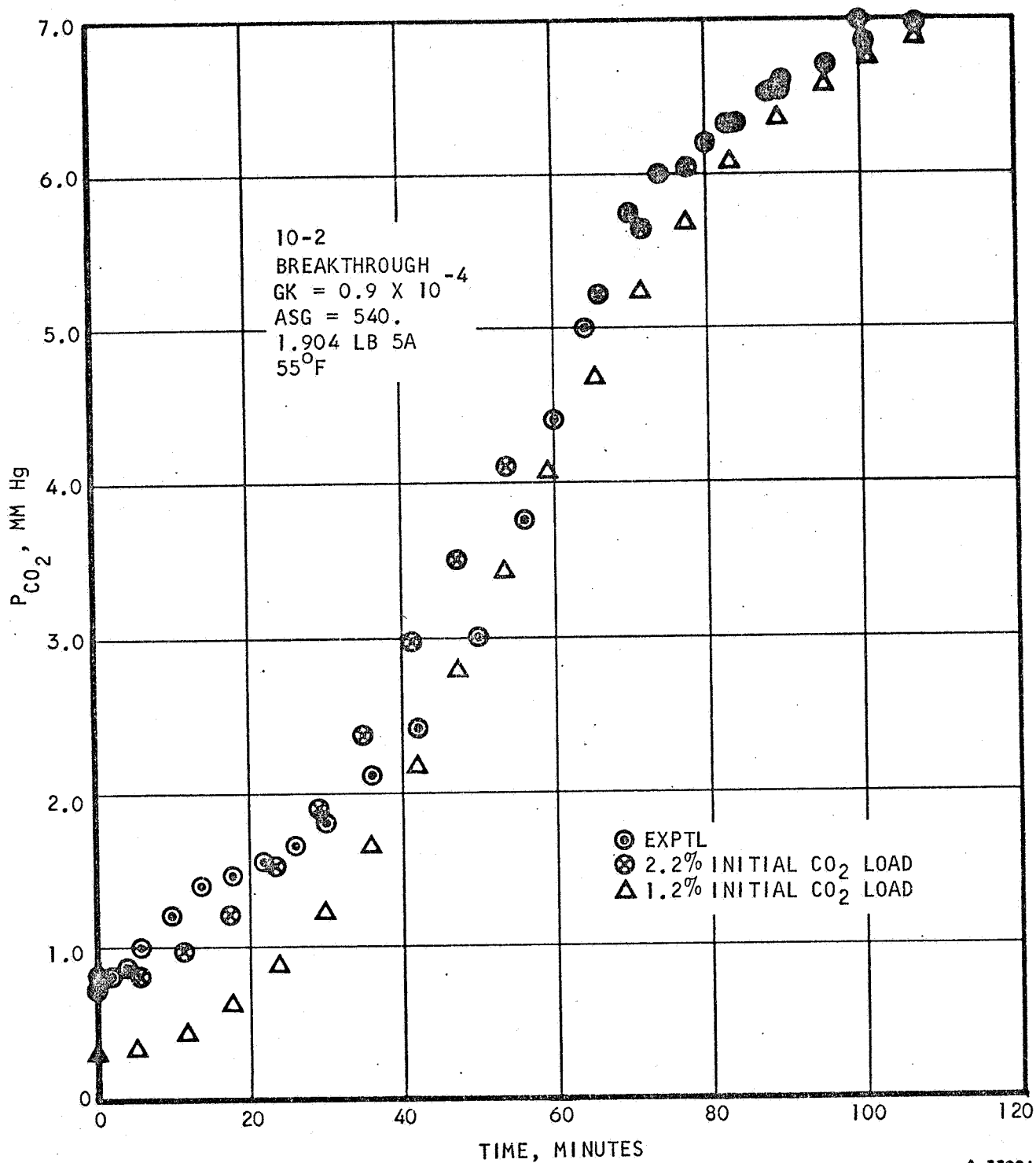
Figure 6-21. Computed and Experimental Results for CO_2 Breakthrough on Dry 3-in. Bed

The chart shows P_{CO_2}, MM Hg (0 to 7.0) versus TIME, MINUTES (0 to 120).

Annotations on chart:
10-2
BREAKTHROUGH
GK = 0.9 X 10^{-4}
ASG = 540.
1.904 LB 5A
55°F

Legend:
EXPTL
2.2% INITIAL CO_2 LOAD
1.2% INITIAL CO_2 LOAD

A-33891
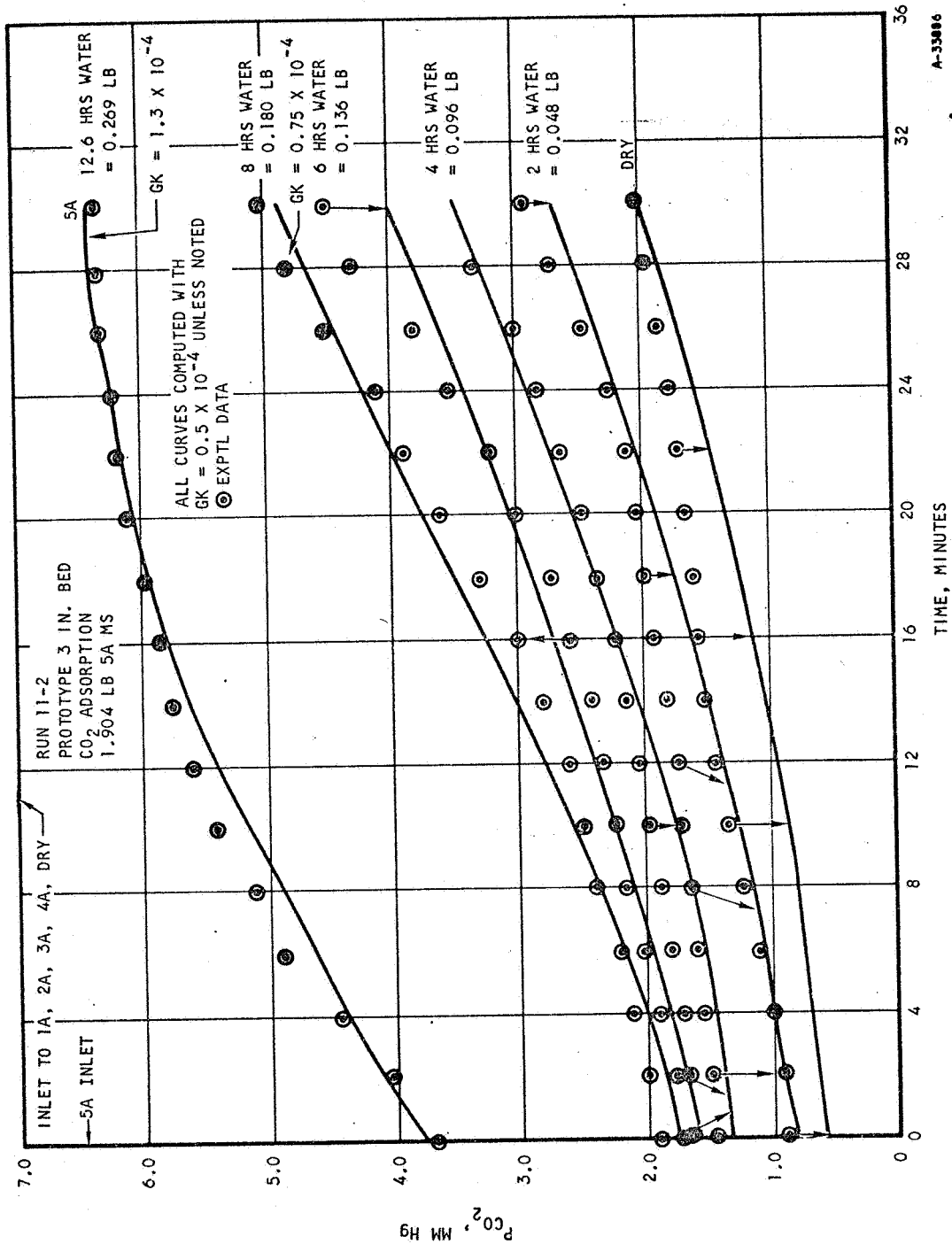
Figure 6-22. Calculated and Experimental 3-in. 5A Bed CO_2 Results with Intermittent Metered Water Poisoning

3. Water Breakthrough on Molecular Sieve

In order to check the idea of a flat H_2O adsorption profile and also to check the equilibrium data, the breakthrough Run 11-1 on the 3-in.-deep bed was compared with computed results for the same run. The Linde equilibrium data was fit for this purpose with the analytical representation:

$$\log_{10}P = \frac{2.85\ln T - 16.4 - \ln(\log_{10}W - 1.255)}{2.29 - 0.0113T + 1.54 \times 10^{-5}T^2}$$

$$200^\circ F \geq T \geq 20^\circ F$$

where   P = pressure, mm Hg

         W = loading, lb/lb

         T = temperature, $^\circ F$

The best match is shown in Figure 6-23. The sharp breakthrough was confirmed, but either the mass of sorbent calculated earlier or the equilibrium data would seem to be slightly in error. A mass-transfer coefficient of 3.0×10^{-4} yielded a slope similar to that of the experimental data.

Discussion of Test Results

1. CO_2 on Molecular Sieve

Two fundamental characteristics of the molecular sieve were confirmed during this test series. First, basic adsorption data were obtained and compared to analytical predictions based on small bed tests. These comparisons, as outlined in Section 7, were generally quite close, and confirmation of constants to be used in performance prediction was thus obtained. Second, and of equal importance, the influence of residual or coadsorbed water on CO_2 removal performance was obtained.

2. Influence of Water on the Molecular Sieve

As shown in Figures 6-20 and 6-22, a marked reduction in CO_2 removal capability occurs as the molecular sieve picks up water. Absolute accuracy of the H_2O loading data for these test runs is open to some doubt since initial loading could only be estimated from bakeout conditions, and some difficulties were experienced in maintaining the system leak-tight throughout the runs. However, the indication of rapid decay of CO_2 removal capability is obvious and confirms data obtained in the small-bed test program. To provide further data on water poisoning, test series 11-1 and 11-2 were conducted on the 3-in. deep bed. To accelerate water loading, a high inlet partial pressure was used, 2.6 mm Hg ($+20^\circ F$ dew point). To check accuracy of water loading measurement, Run 11-1 (Figure 6-23) was carried to complete breakthrough without interruption. A total of 0.32 lb of H_2O was adsorbed in the bed during this run giving a 16.4 percent delta loading. With the assumed 1 percent initial loading, this gives a total loading at complete breakthrough of 17.4
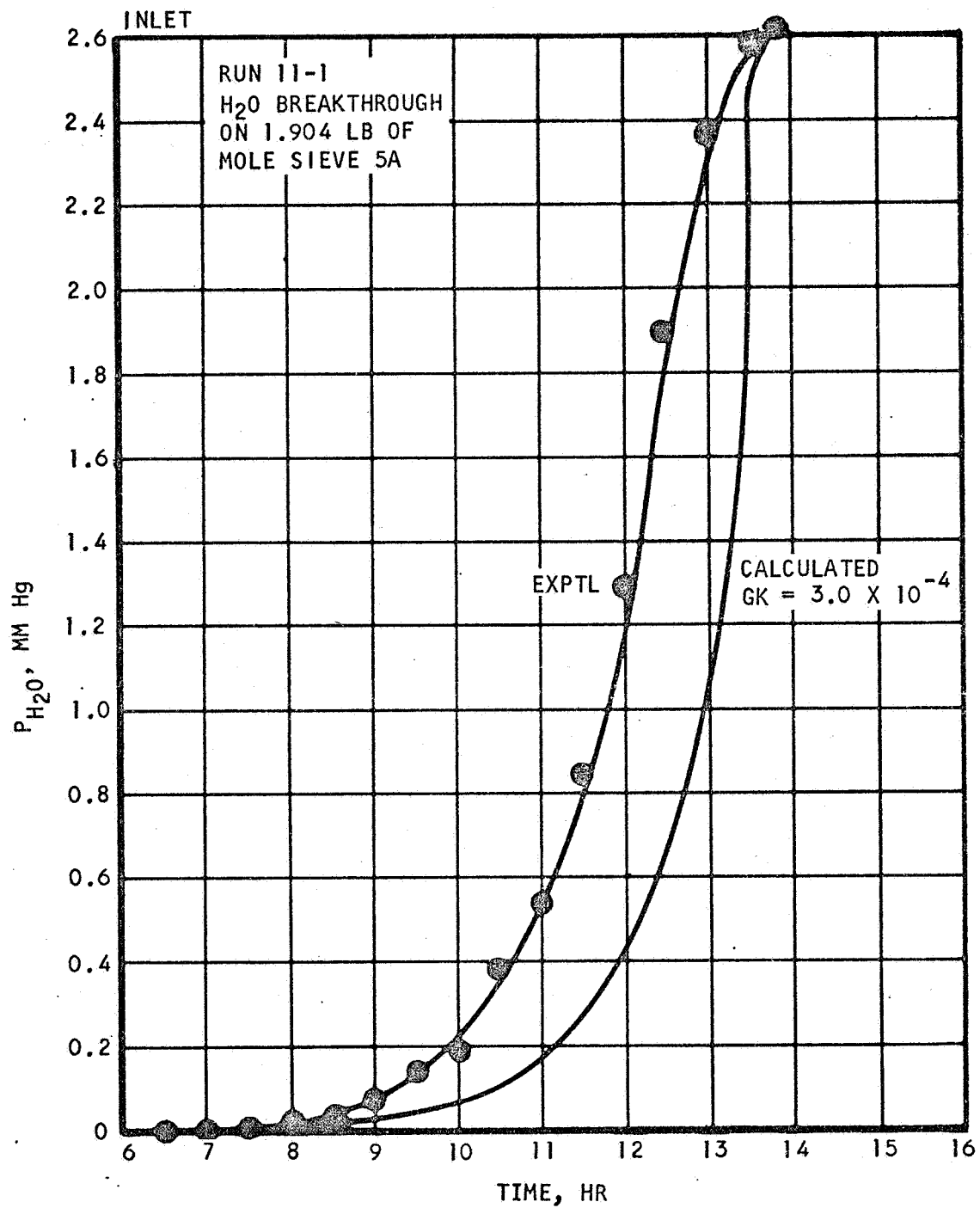
Figure 6-23. Water Breakthrough on 3-in. Molecular Sieve Bed

percent, which agrees reasonably well with Linde equilibrium data of 18 to 18.5 percent. Run 11-2 (Figure 6-16) was interrupted at arbitrary times, and CO_2 removal performance measured. Total water buildup in the molecular sieve during the run was 0.33 lb of H_2O or 17 percent delta loading. Again this agrees favorably with a residual loading of approximately 1 percent giving a total load at complete breakthrough of 18 percent. Figure 6-22 shows CO_2 removal performance measured during the water injection run. These runs indicate a slow degradation of CO_2 removal performance as water buildup occurs in the molecular sieve.

3. Predicting the Influence of Water on Molecular Sieve

As mentioned previously, a method of predicting this slow degration of the CO_2 adsorption capability of molecular sieve might require an exhaustive analysis of the coadsorption phenomena. The difficulty in obtaining fundamental rate data of two or three gas mixtures, as well as the complex mathematical model required for computer prediction of coadsorption, precluded the use of this approach. Rather, an attempt has been made to correlate the data obtained in the tests outlined in this section and Section 5, and establish an approximate analysis method with reasonable accuracy. With this model it is possible to predict CO_2 removal performance using the analytical model developed for single gas adsorption. The active zone is always considered the minimum bed depth for CO_2 removal; and an additional depth of bed is provided to adsorb the small but significant amount of H_2O which is discharged from the silica gel predryer. It is assumed that very little of this water is desorbed from the molecular sieve during normal cyclic operation since data presented in Section 5 show that the relatively low temperature and short duration of cyclic desorption (not over $100°F$, or 30 min) will desorb very little H_2O. Thus, production of poisoning rate is accomplished by decreasing bed depth at a rate equal to water injection rate divided by bed loading capability for H_2O. CO_2 removal performance is estimated by considering this bed depth as not being available for CO_2 adsorption. Plotted in Figures 6-20 and 6-22 are results of such a prediction, showing the expected CO_2 removal performance as the bed is poisoned by the increasing amounts of water added.

SECTION 7

DIGITAL COMPUTER PREDICTION DEVELOPMENT

INTRODUCTION

The present computer program package for the Univac 1107 computer, S9950 through S9999, was developed to predict the transient performance of a composite molecular sieve, silica gel bed for CO_2 removal, which may be operated either under adiabatic or thermal swing conditions. A schematic drawing of such a CO_2 removal system is shown in Figure 7-1.

An attempt was made to solve the actual physical problem as rigorously and as generally as was feasible. Thus, transient pressure variations during a desorption cycle are not arbitrarily set, but are calculated from the AiResearch test data for the flow of nitrogen gas under low pressures through a 5/8-in.-ID molecular sieve bed. These data are shown in this section. To make the program flexible, most of the physical properties and transfer rate constants are allowed to vary as a function of the bed location. Such a flexibility allows for the use of different heat exchanger configurations and different modes of operation for the molecular sieve bed and the silica gel bed.

The mass-transfer equations are written to permit both intraparticle diffusion and surface resistance. Either process can be made to control by proper choice of the appropriate coefficients in the input. A major goal for the computer program was the determination from the data of the proper values of the mass transfer coefficients for adsorption and desorption, for water and CO_2, in both silica gel and molecular sieve 5A. When all experimental data can be fit with reasonable accuracy, operation of proposed designs can be simulated with an equal degree of confidence.

To minimize the running time of the program, an implicit scheme as proposed by Hwang (Reference 7-1) was employed for transient mass transfer calculation, and a method somewhat similar to the one proposed by DuFort and Frankel (Reference 7-2) for solving a diffusion equation was used to handle the coupling terms of the energy equations for the transient temperature changes of the metal parts, the sorbent, and the coolant. The program, therefore, permits the use of as large time increments as are allowable for accuracy considerations.

Program S9960 does adsorption and desorption calculations for a specified number of complete cycles. Programs S9950 and S9951 perform adsorption and desorption calculations respectively for just one-half-cycle. With all physical properties and operation parameters inputted through two block data subprograms, the programs will compute and print out temperature and bed loading changes as a function of time. Average bed loadings and average rates of adsorption and desorption are also printed.

The differential equations which describe the adsorption problem, and a brief description of how the equations are solved by the program, will be given later. Determination of the various transfer coefficients to be used in final bed design will be described also. Example input and output and a complete listing of the Fortran source program will follow.
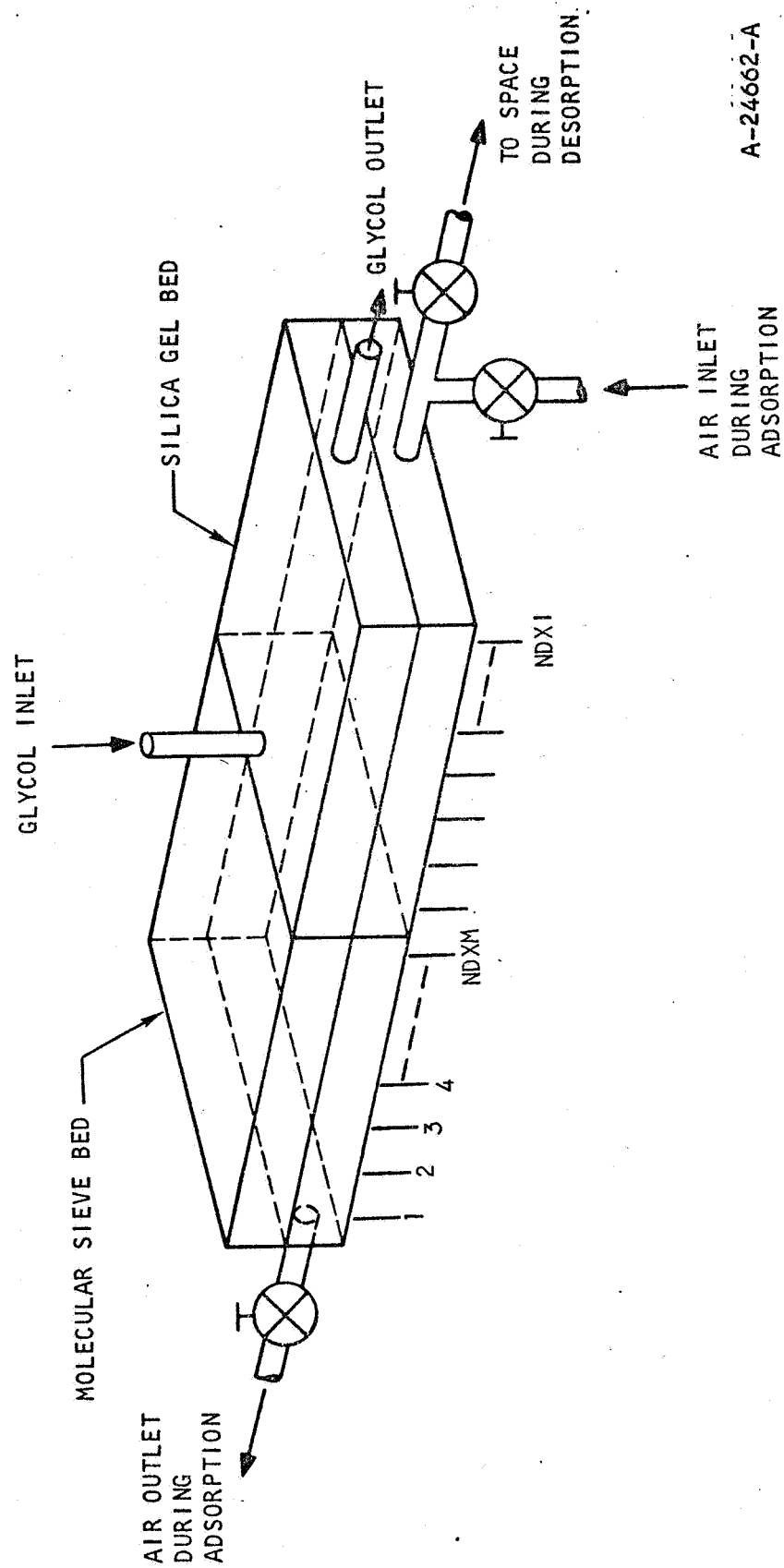
Figure 7-1. A Composite Molecular Sieve, Silica Gel Bed for CO_2 Removal

A-24662-A

MATHEMATICAL MODEL

General Assumptions Made

In addition to some minor approximations which will be mentioned with the derivation of equations, the following general assumptions were made in deriving the differential equations which were employed in the present programs.

- **Assumption A**--Temperature gradient in the pellet interior is negligible.

- **Assumption B**--Adsorption occurs by the diffusion of an adsorbate through the stagnant surface film at the exterior surface of an adsorbent particle, condensing at the surface and then diffusion into the interior of the particle. Desorption occurs in a reverse fashion. This assumption should be completely valid for the adsorption of CO_2 on a molecular sieve bed, as the size of the CO_2 molecules and that of the micropores of the adsorbent are roughly the same-- $<4\overset{0}{A}$ for the former and $5\overset{0}{A}$ for the latter.

- **Assumption C**--Adsorbent pellets can be represented by spherical particles for mass transfer calculations.

- **Assumption D**--Heats of adsorption and desorption do not depend on temperature or concentration.

- **Assumption E**--In the adsorption half-cycle, the total flow rate and density of the gas stream are constant.

- **Assumption F**--No variations exist in the direction perpendicular to the direction of the gas flow.

The test of all the above assumptions is whether the program can indeed describe the test data without the need for indiscriminant variations in the coefficients.

Differential Equations Describing Transient Behavior of an Adsorption Bed System

In the following, only those equations which are not obvious will be given their derivations. The equations which are assumed to be obvious or easily derived by the reader are listed with appropriate boundary conditions without proof. Initial conditions of the equations are omitted, as their existence should be apparent.

1. Diffusion Equation for Interior of Sorbent Pellet in Finite Difference Form

Dividing the pellet into elements with equal volume except the center and the surface nodes, which are half nodes, a material balance similar to Equation (4-16) gives

$$(\Delta V)\, \rho_s \frac{dW_k}{dt} = \left(4\pi\, r_{M-\frac{1}{2}}^2\right) \frac{\rho_s D_k}{r_M - r_{M-1}} \left(W_{M-1} - W_M\right)$$

$$- \left(4\pi\, r_{M+\frac{1}{2}}^2\right) \frac{\rho_s D_k}{r_{M+1} - r_M} \left(W_M - W_{M+1}\right) \qquad * \qquad (7\text{-}1)$$

At the outside surface of the pellet, Equation (4-15) becomes for the transient situation

$$\frac{(\Delta V)}{2}\, \rho_s \frac{dW_k}{dt} = \left(4\pi\, r_{s-\frac{1}{2}}^2\right) \frac{\rho_s D_k}{r_s - r_{s-1}} \left(W_{s-1} - W_s\right)$$

$$- \left(4\pi\, r_s^2\right) M_{Wk} \cdot K_g \cdot \left(P_{k_s} - P \cdot X_k\right) \qquad (7\text{-}2)$$

where the mass-transfer condition of Equation (4-12) has been used.

At the center, Equation (4-24) is modified to allow surface migration in place of pore-diffusion:

$$\frac{(\Delta V)}{2}\, \rho_s \frac{dW_k}{dt} = -\left(4\pi\, r_{1\frac{1}{2}}^2\right) \frac{\rho_s D_k}{r_2 - 0} \left(W_1 - W_2\right) \qquad (7\text{-}2a)$$

2. Energy Equation for Gas Stream

As the thermal capacitance of the gas in the void space of the bed is negligible compared with those of the sorbent bed or the heat exchanger core, a quasi-steady-state assumption can be made and there is obtained, as energy equation for the gas stream,

---

* Symbols are listed and systematically defined in the Nomenclature at the end of this section.

$$\frac{dT_g}{dx} = \frac{1}{f \rho_g \, C_{pg} \cdot u_g} \quad a_{sg} \cdot h_{sg} \, (T_s - T_g) + a_{xg} \cdot h_{xg} \cdot$$

$$(T_x - T_g) \tag{7-3}$$

For the adsorption half cycle, $f \cdot \rho_g \cdot C_{pg} \cdot u_g = (G_t \cdot C_{pg})/A$

Equation (7-3) is subject to a boundary condition

$$T_g = T_{gi} \quad \text{at } x = x_o \tag{7-4}$$

for the adsorption half cycle, while for the desorption half cycle, the condition to be satisfied is

$$T_g = T_s \quad \text{at } x = 0 \tag{7-5}$$

3. **Energy Equation for Sorbent**

$$\frac{\partial T_s}{\partial t} = \left(\frac{k_s}{C_{ps} \, \rho_{sb}} \right) \frac{\partial^2 T_S}{\partial x^2} + \left(\frac{a_{sg} \cdot h_{sg}}{C_{ps} \cdot \rho_{sb}} \right) (T_g - T_s) + \left(\frac{a_{xs} \cdot h_{xs}}{C_{ps} \cdot \rho_{sb}} \right) (T_x - T_s)$$

$$+ \left(\frac{a_{sg} \cdot K_g}{C_{ps} \cdot \rho_{sb}} \right) (P \cdot X_k - P_{ks}) \cdot (\Delta H_k) \tag{7-6}$$

This equation is subject to the conditions

$$\frac{\partial T_s}{\partial x} = 0 \quad \text{at } x = 0, \; x = x_o,$$

$$x = x_{MS \; max} \quad \text{and } x = x_{SG \; min} \tag{7-7}$$

4. **Energy Equation for Glycol Stream**

$$\frac{\partial T_c}{\partial t} = -u_c \frac{\partial T_c}{\partial x} + \left(\frac{a_{vc} h_{xc}}{C_{pc} \cdot \rho_c} \right) (T_x - T_c) \tag{7-8}$$

The boundary condition for this equation is

$$T_c = T_{268} \quad \text{at } x = x_{glycol \; inlet} \tag{7-9}$$

5. Energy Equation for Metal Portion of Heat Exchanger

$$(C_{px} \, \rho_x) \frac{\partial T_x}{\partial t} = k_x \frac{\partial^2 T_x}{\partial x^2} + a_{vx} \cdot \left[h_{xs}(T_s - T_x) + \right.$$

$$\left. h_{xg}(T_g - T_x) + h_{xc}(T_c - T_x) \right] \tag{7-10}$$

Boundary conditions for this equation are

$$\frac{\partial T_x}{\partial x} = 0 \qquad \text{at } x = 0 \text{ and} \tag{7-11}$$

$$\text{at } x = x_o$$

6. Adsorption Material Balance Equation for k-th Component in Gas Stream

By assuming that quasi-steady-state conditions exist for the gas phase material balance, there is obtained from Equations (4-1) and (4-12) with the conditions of steady-state and no axial diffusion:

$$\frac{dP_k}{dx} = \left(\frac{P \, M_{wg}}{f \rho_g u_g} \right) a_{sg} \cdot K_g \cdot (P_{ks} - P_k) \tag{7-12}$$

This has an inlet condition

$$P_k = P_{k, \text{ inlet}} \qquad \text{at } x = x_o \tag{7-13}$$

7. Pressure Equation for Desorption

During the desorption cycle, both the bed pressure and gas flow rate vary with time and the axial location in the bed, and a method of calculating instantaneous pressures at various bed locations is desired. Although a quasi-steady-state assumption could be made regarding pressure calculations, the simplified problem so obtained would still be a boundary value problem which requires an iterative method of solution. An alternative approach would be to solve a transient equation describing pressure changes. The latter approach was taken in the present program, and the derivation of the pressure-equation employed in the program will be given below.

A material balance for a unit volume of bed gives

$$A f \left(\frac{\partial C}{\partial t} \right) = - \frac{\partial}{\partial x} (f \, C \, A \, u_g) + A \, M_{sg} \tag{7-14}$$

where

$$\dot{M}_{sg} = a_{sg} \cdot K_g \cdot (P_{ks} - P.X_k) \qquad (7-15)$$

and u_g is related to pressure gradient by Equation (4-6);

$$u_g = -\frac{1}{F}\left(\frac{\partial P}{\partial x}\right) \qquad (7-16)$$

Also, by differentiating the perfect gas law

$$C = \frac{P}{RT_g} \qquad (7-17)$$

one obtains

$$\frac{\partial C}{\partial t} = \frac{1}{RT_g}\left(\frac{\partial P}{\partial t}\right) - \frac{P}{RT_g^2}\left(\frac{\partial T_g}{\partial t}\right) \qquad (7-18)$$

By combining with equations (7-16), (7-17) and (7-18), and dropping the term $\frac{P}{RT_g^2}\left(\frac{\partial T_g}{\partial t}\right)$, Equation (7-14) can be converted to Equation (4-9) in a quasi-isothermal condition:

$$\frac{\partial P}{\partial t} = \frac{P}{F}\left(\frac{\partial^2 P}{\partial x^2}\right) + \frac{P}{f \cdot C \cdot A}\ \frac{\partial}{\partial x}\left(\frac{A \cdot f \cdot C}{F}\right)\left(\frac{\partial P}{\partial x}\right) + \frac{P}{C \cdot f}\dot{M}_{sg} \qquad (7-19)$$

Equation (7-19) is used in the program for calculating pressure changes during the desorption half cycle.

The proportionality constant F in Equation (7-16) is a strong function of pressure, as the gas flow during desorption lies in the slip flow region. The pressure drop data for the flow of nitrogen gas through a 5/8-in.-ID molecular sieve bed were reduced by using the equation

$$\frac{F_{N_2} \cdot G.R.T_g}{M} = \frac{(P_1^2 - P_2^2)}{2.(x_2 - x_1)} \qquad (7-20)$$

to obtain F_{N_2} at various mean pressures. The result is plotted in Figure 7-2, and a best straight line fit of the data gives

$$F_{N_2} = 2.494 \times 10^{-4} \times P^{0.795} \qquad (7-21)$$
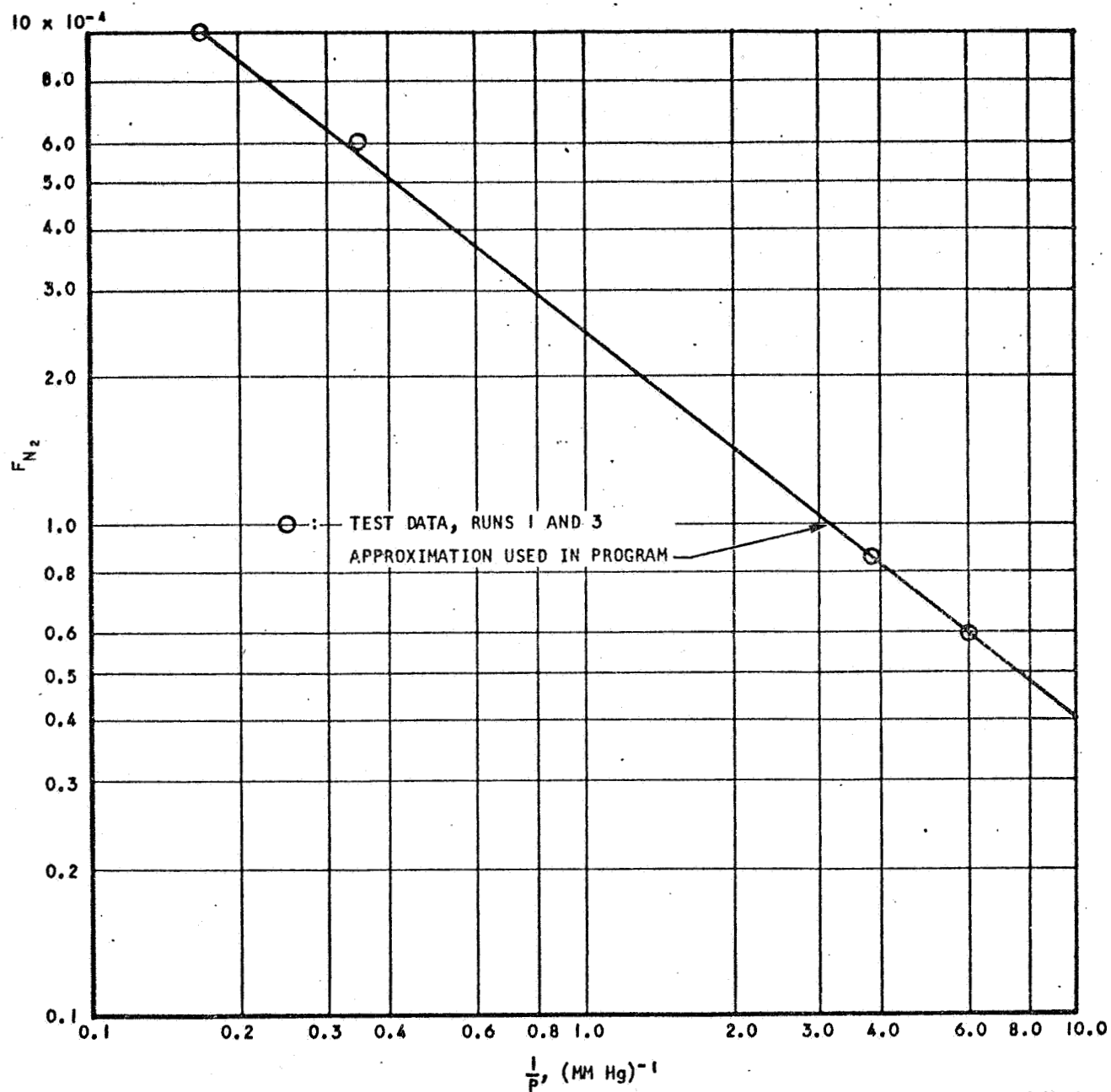
Figure 7-2. Correlation of F_{N_2} vs $\left(\frac{1}{P}\right)$ From Test Data

A-24666

Equation (7-21) is applicable only for nitrogen gas at 70°F, which has a viscosity of 0.0174 cp. In the desorption program, F is linearly corrected for the difference in viscosity as predicted by the Blake-Kozeny equation. Thus

$$F = \left(\frac{Avg\ Viscosity}{0.0174}\right) \times 2.494 \times 10^{-4} \times P^{0.795} \qquad (7-22)$$

It would seem reasonable to use a molal average viscosity for the gas mixtures in the Silica-Gel bed section; however, it was found that the use of the CO_2 viscosity for that of H_2O vapor resulted in a better pressure predictions.

Equation (7-19) is subject to a boundary condition

$$\frac{\partial P}{\partial X} = 0 \qquad at\ x = 0 \qquad (7-23)$$

At the bed exit, the pressure can be specified as a function of time, or else the vacuum duct resistance to gas flow will play a role in fixing the pressure and flow rate. The boundary condition will then be

$$f \cdot \rho_g \cdot u_g \cdot A = W_D(P) \qquad (7-24)$$

Where $W_D(P)$ can be approximated by the following expression which corresponds to the straight line shown in Figure 7-3 for a 3-in. duct.

$$W_D(P) = 11.2\ P^{1.715} \qquad (7-25)$$

Combination of Equations (7-16), (7-24), and (7-25) gives

$$\frac{1}{F}\frac{\partial P}{\partial X} = \left(\frac{11.2\ P^{0.715}}{f \cdot \rho_g \cdot A}\right) P \qquad (7-26)$$

8. Equilibrium Relationship

For CO_2 molecular sieve systems, adsorption isotherms results, reported in Section 5, were reduced to the expression

$$P_{CO_2} = exp\left[-\frac{9166.56}{T_s + 460} + 1.678\ log_e(W_{CO_2}) + 23.823\right] \qquad * \qquad (7-27)$$

---

*This relation should be relied upon only within the temperature range of 20° to 50°C.
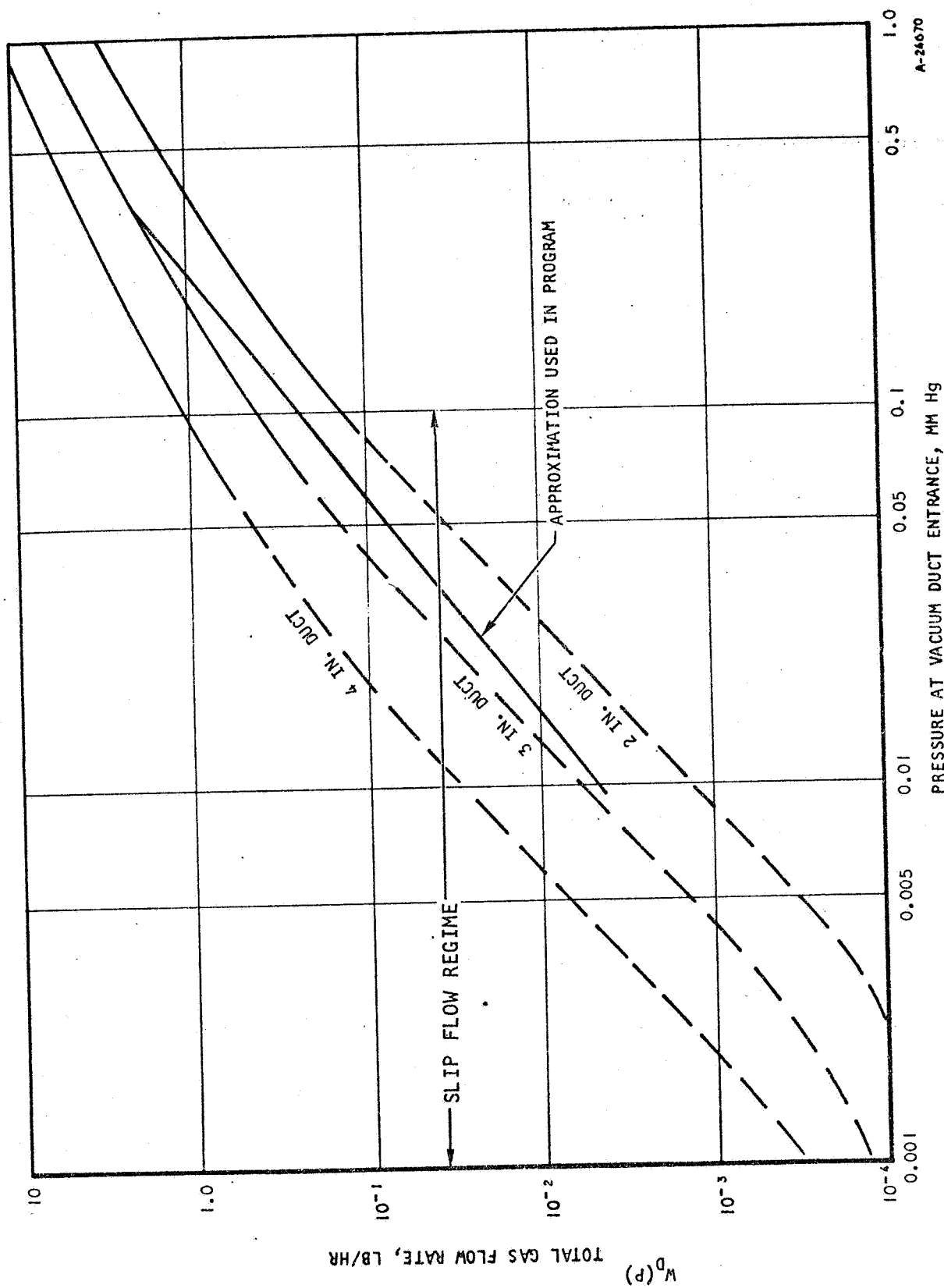
Figure 7-3. Vacuum Duct Capacities for Various Duct Sizes and Duct Inlet Pressures

For the H_2O silica gel system, the equilibrium vapor pressure data published by W. R. Grace & Co. (Reference 7-3) were used to give

$$P_{H_2O} = \exp\left[21.08 - \frac{1.075 \times 10^4 \ (0.852 - 0.3215 \ \ln W)}{T_s + 460} \right.$$

$$\left. +0.394 \ \ln W - 0.0592 \ (\ln W)^2 \right] \qquad (7-28)$$

Equations (7-27) and (7-28) are used in the program, and are compared with test data in Figures 7-4 and 7-5.

PROGRAM DESCRIPTION

The main structure of Program S9960, which performs cyclical adsorption-desorption calculations, is depicted in Figure 7-6. The functions of each subroutine will be explained to help the user understand the program better.

MAIN PROGRAM (S9960)

This is a main program which coordinates all the subroutines required for predicting the performance of a composite molecular sieve-silica gel bed. The program is executed by the control card

7/8 XQT S9960

All the input data must be inputed via two Block Data subprograms S9973 and S9993.

MADSOR (S9970)

This subroutine monitors the adsorption half cycle calculations. It prints the total quantities of molecular sieve and silica gel pellets in the composite bed for input data check-out purposes. The routine, then, calls STARTA. The time increment size for the next time step is selected such that TI and WI specified in the input data are satisfied. Subroutine ADSORB is then called to advance one time step, and the results are printed if this should be done according to NPRINT.

STARTA (S9978)

Everything which stays constant throughout the entire adsorption half cycle is evaluated in this subroutine. A, RS, CRI, CR2, CR3 are evaluated in the subroutine.

ADSORB (S9971)

This subroutine simultaneously integrates Equations (7-1), (7-6), and (7-12) by a backward difference method, except that the term $\frac{\partial^2 T_s}{\partial x^2}$ is evaluated
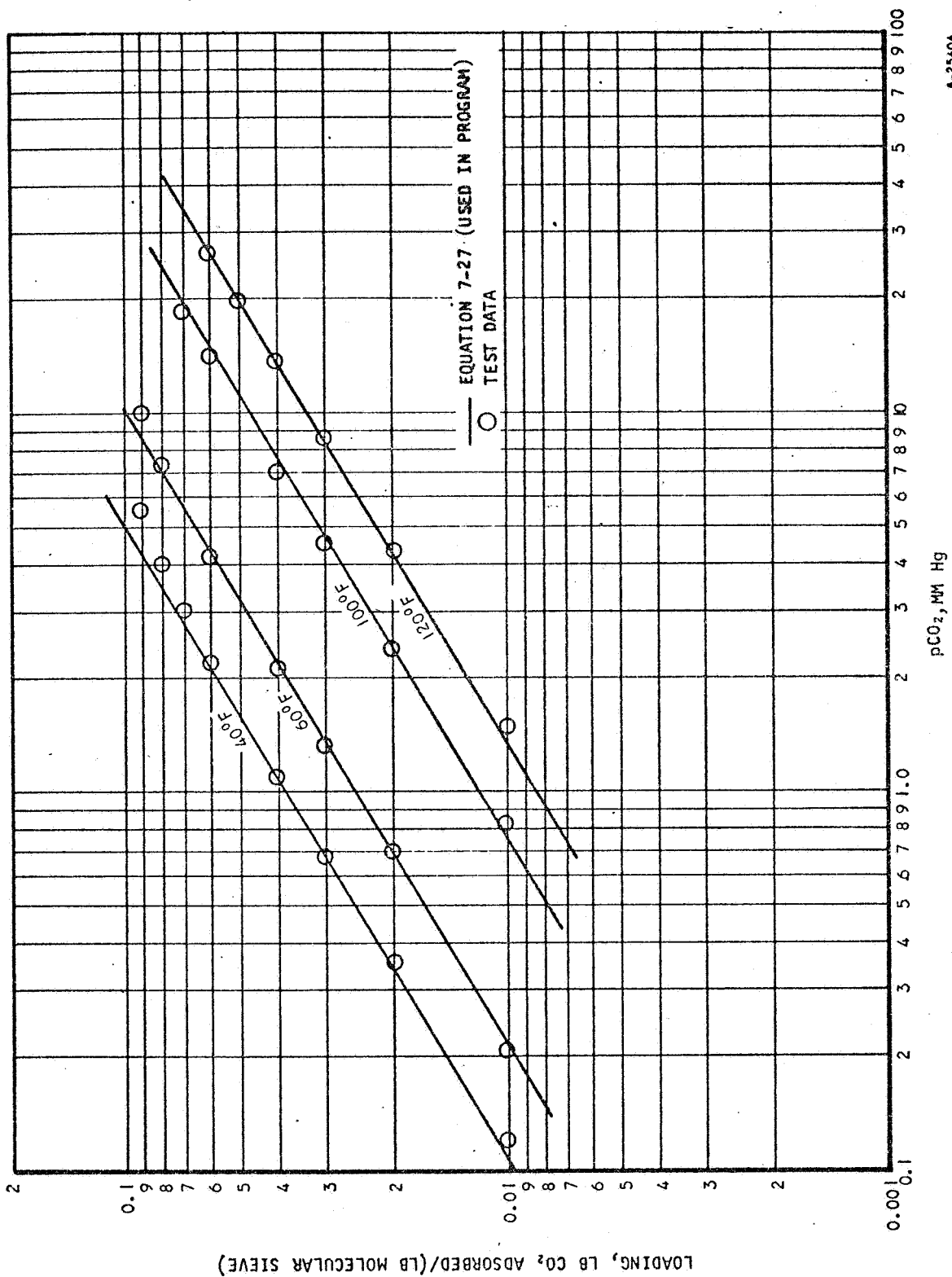
Figure 7-4. Adsorption Isotherms for CO_2 on Molecular Sieve

GARRETT AIRESEARCH MANUFACTURING DIVISION
Los Angeles, California
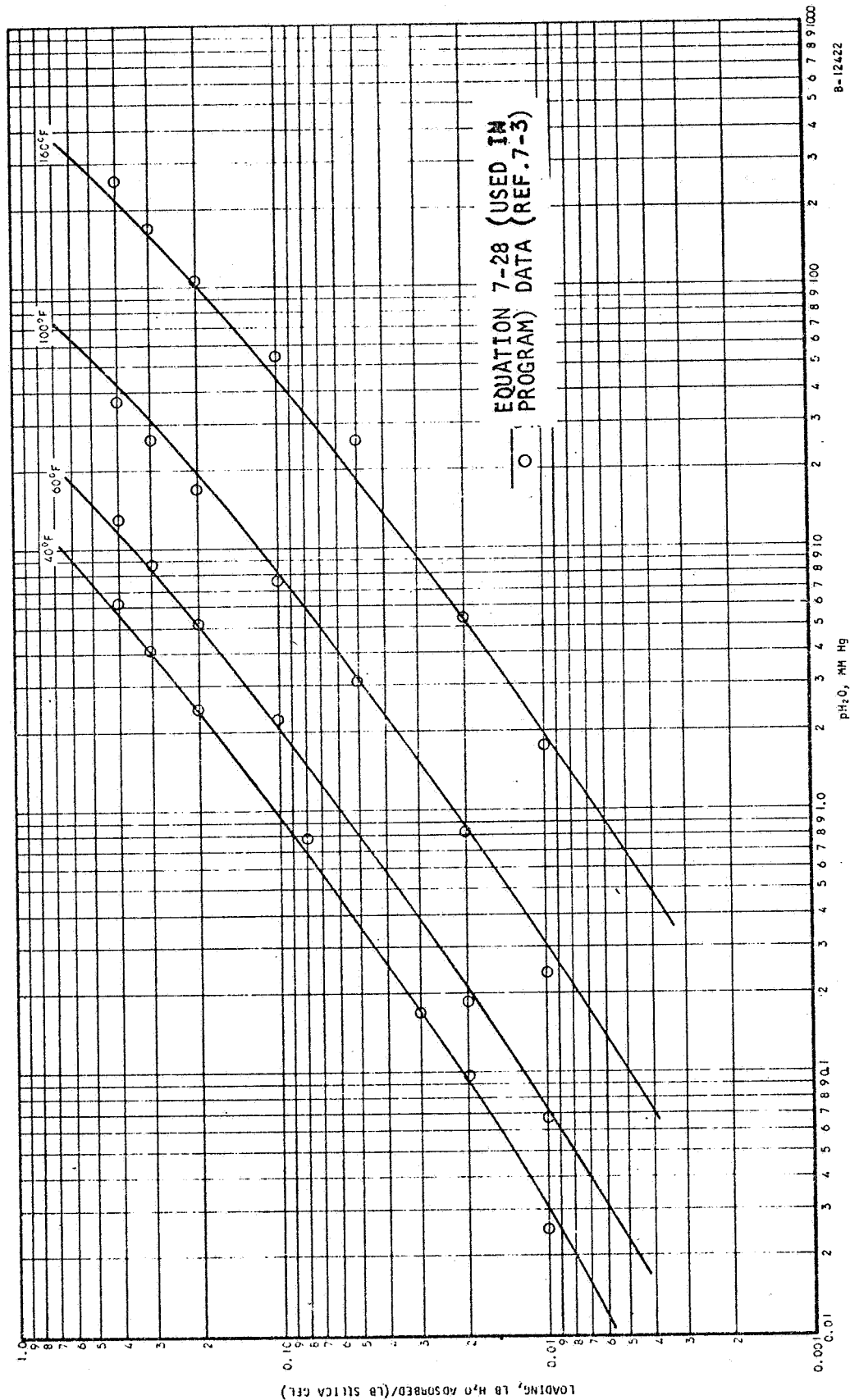
Figure 7-5. Adsorption Isotherms for Water on Silica Gel

B-12422
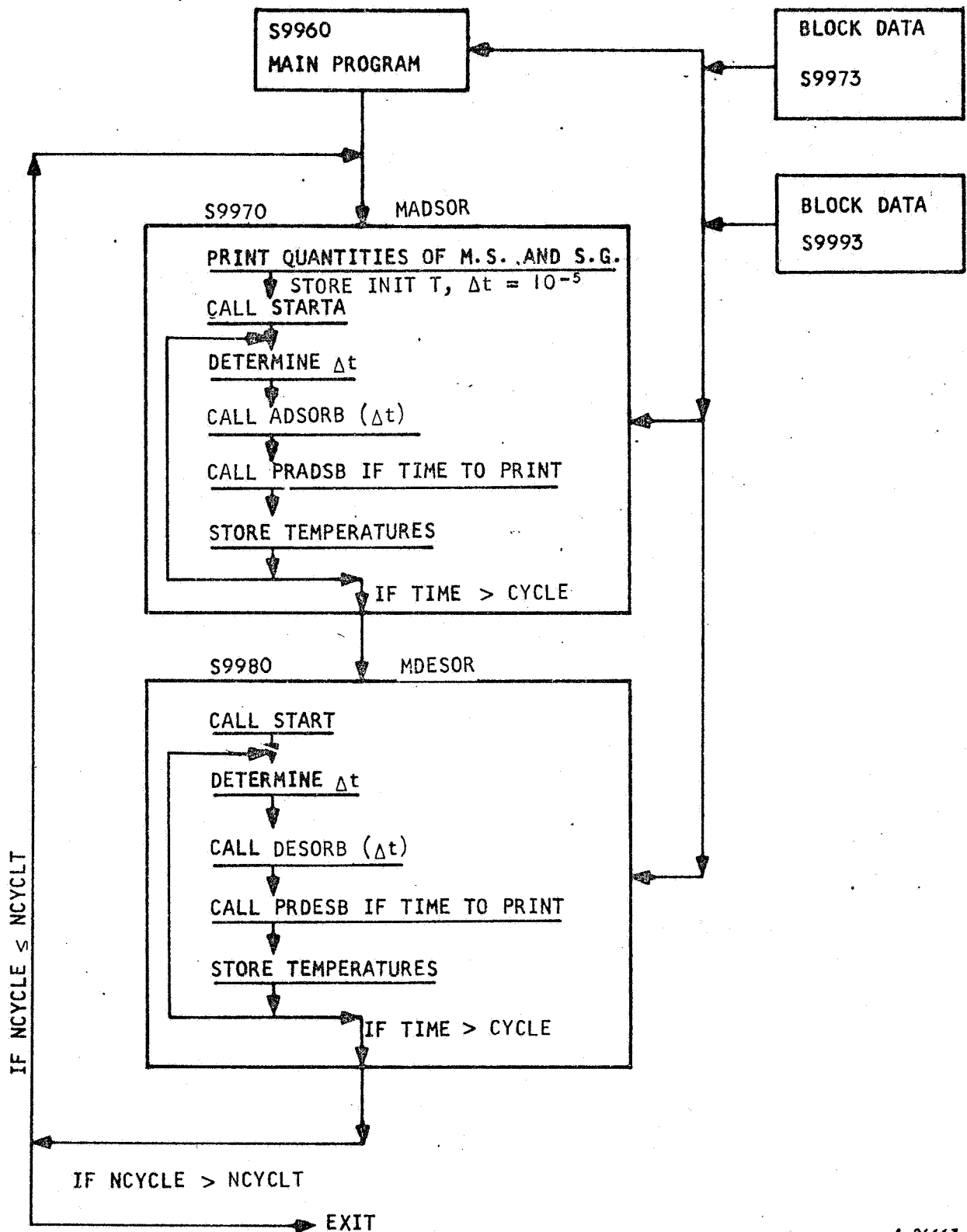
Figure 7-6. Structure of Program S9960

A-24663

at the beginning of a time increment, such that no iterations will be required. The use of a complicated scheme like this is to avoid numerical instability at large time increment sizes.

After P_k's and W_K's at the end of the (Δt) have been found, TSORBA, TGLCOL, HXCORE, GASTA are called to calculate the various temperatures.

In solving a one-dimensional diffusion equation, finite difference equations of the form

$$C_{1,N} \cdot T_{N-1} + C_{2,N} \cdot T_N + C_{3,N} \cdot T_{N+1} = D_N \text{ for } N = 1 \text{ to NDX1} \qquad (7-29)$$

are written.

The coefficients C_1, C_2, C_3 are set such that all boundary conditions are satisfied.

The system of equations represented by Equation (7-29) belongs to a special class of equations where a tri-diagonal matrix is involved. Inversion of the matrix is not required, and the method proposed by (Reference 7-4) is employed in solving the set of equations. Both subroutines FDEQIM and FDEQID do the same job of solving the system of equations, the only difference being that the latter uses a double-precision arithmetic.

The coupling of temperatures appearing in the source terms of Equations (7-6), (7-8), and (7-10) are handled by a method similar to the one suggested by DuFort and Frankel (Reference 7-2) for a single diffusion equation. For example, the source term in Equation (7-8) is approximated by

$$\left(\frac{a_{vc} h_{xc}}{C_{pc} \cdot \rho_c} \right) \cdot \left[T_{x,t} - \frac{T_{c,t-\Delta t} + T_{c,t+\Delta t}}{2} \right] \qquad (7-30)$$

TSORBA (S9977)

This routine integrates the energy equation for the sorbent during the adsorption half cycle. In other words, Equation (7-6) is integrated.

TGLCOL (S9987)

Equation (7-8) is solved.

HXCORE (S9991)

Equation (7-10) is solved.

GASTA (S9976)

The routine solves Equation (7-3) for the adsorption half cycle.

PRADSB (S9979)

This is a print routine for the adsorption program.

MDESOR (S9980)

The routine controls desprotion calculations much as MADSOR does the adsorption counterpart. It calls START, picks up a Δt, calls DESORB, PRDESB, and stores temperatures.

START (S9988)

Similar to STARTA for the adsorption, this subroutine generates all the constants which stay unchanged for the entire desorption half cycle.

PRDESB (S9989)

This is a print routine for the desorption program.

DESORB (S9983)

Equations (7-1), (7-6), and (7-19) are solved simultaneously. Because of extremely large coefficients involved, Equation (7-19) is solved by a double precision arithmetic to avoid accumulation of errors. The gas flow rate, density, and composition are then found at each axial location. TSORB, TGLCOL, HXCORE, GAST are called to solve for temperatures.

TSORB (S9997)

The routine solves for sorbent temperatures in the desorption period.

GAST (S9986)

Gas temperatures in the desorption period are calculated by the subroutine.

PKEQ (S9992)

Equations (7-27) and (7-28) are used to obtain the equilibrium P_{CO_2} over the molecular sieve bed, and the equilibrium P_{H_2O} over the silica gel bed, respectively.

IFN (S9981)

The function determines whether a given axial node belongs in the molecular sieve bed or silica-gel bed.

FDEQIM (S9984)

The routine solves a system of finite difference equations by the method of Thomas (Reference 7-4).

FDEQID (S9985)

The subroutine is a double precision version of FDEQIM.

LAGIN2 (S9996)

This routine performs a Lagrangian polynomial interpolation.

MAIN PROGRAM (S9950)

This main program just calls MADSOR to perform one adsorption half-cycle calculation. It is executed by

7/8 XQT S9950

MAIN PROGRAM (S9951)

This main program calls MDESOR to carry out one desorption half-cycle calculation. It is executed by

7/8 XQT S9951

VARIOUS OPTIONS OF USING THE PROGRAM PACKAGE

The various options allowed by the present program package are tabulated below.

How Executed	Characteristics of Option
7/8 XQT S9950	One half-cycle adsorption.
7/8 XQT S9951	One half-cycle desorption.
7/8 XQT S9960	NCYLT full cycles of adsorption and desorption.
NTEMP = 0	No temperature calculations, with all temperatures set equal to T_{268}. No heat transfer area or thermal property data are required for this option.
NBCOUT = 1	Bed exit pressure calculated from vacuum duct capacity and total desorption rate.
NBCOUT = 2	Bed exit pressure specified in the input data.
NPSET = I, J, K	Specify modes of applied vacuum.

PROGRAM INPUT

Data input required by the program is executed by block data subprograms, S9973 and S9993. Subprogram S9973 inputs all data required to execute the adsorption analysis; subprogram S9993 inputs all data required to execute the desorption analysis. Both block data subprograms must be compiled at execution time if cyclic system performance is desired. If only adsorption or desorption performance is required, then only the respective block data subprogram need be compiled at execution time. The following lists the variables which are inputted via the block data subprograms.

Variables Common to Both S9973 and S9993

Fortran Symbol	Maximum Dimension	Definition
RHOS	(2)	Sorbent particle density, lb/(cu ft) RHOS(1) = M.S. particle density RHOS(2) = S.G. particle density
WM	(2)	Adsorbate molecular weight WM(1) = 44 (CO_2) WM(2) = 18 (H_2O)
RHOSB	(41)	Sorbent bulk density, lb/(cu ft)
W	(21,41)	Initial sorbent loading, lb/lb (double precision)
TG	(41)	Initial gas temperature, ^0F
TS	(41)	Initial sorbent temperature, ^0F
TC	(41)	Initial coolant temperature, ^0F
TX	(41)	Initial heat exchanger temperature, ^0F
NPRINT		Integer control variable which determines the frequency of printout occurrence; e.g., if NPRINT = 2, printout occurs after every TWO time steps, if NPRINT = 5, printout occurs after every five time steps, etc.
DTMAX		Maximum allowable time step size, usually 0.01 hr for isothermal analysis and 0.005 hr for nonisothermal analysis.

Fortran Symbol	Maximum Dimension	Definition
NTEMP		Integer control variable; if NTEMP = 0, isothermal analysis; the energy equations are ignored, and the bed temperature is set equal to T268. If NTEMP $\neq$ 0, non-isothermal analysis.
ABED	(41)	Sorbent bed cross-section area normal to flow of process gas, sq ft
AVX	(41)	Primary heat exchanger plate area per unit volume of heat exchanger core metal, sq ft/(cu ft)
TKX	(41)	Heat exchanger metal thermal conductivity, TKX (K) denotes that between node K-1 and node K
CPX	(41)	Heat exchanger specific heat, Btu/(^{0}F)(lb)
RHOX	(41)	Heat exchanger metal density, lb/(cu ft)
HXC	(41)	Heat transfer doefficient, heat exchanger to coolant, Btu/(sq ft) (hr) (^{0}F)
HXS	(41)	Heat transfer coefficient, heat exchanger to sorbent, Btu/(sq ft) (hr) (^{0}F)
ASX	(41)	Heat exchanger primary area per unit volume of sorbent bed, sq ft/(cu ft)
AGX	(41)	Identical to ASX
CPG	(41)	Specific heat of the process gas, Btu/(lb) (^{0}F)
NDXM		Integer denoting total number of M.S. nodes
NDXI		Integer denoting total number of axial nodes
NDR4		Integer denoting total number of radial sorbent pellet nodes (interior nodes)
DX		Axial node dimension, ft
UC	(41)	Coolant velocity, ft/hr
CPC	(41)	Coolant specific heat, Btu/(lb) (^{0}F)
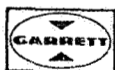
Fortran Symbol	Maximum Dimension	Definition
RHOC	(41)	Coolant density, lb/(cu ft)
T268		Coolant inlet temperature, °F
DH	(41)	Differential heat of adsorption, Btu/(lb adsorbed)
CYCLE		Cycle time per one adsorption or one desorption half-cycle, hr
DIF	(41)	Internal diffusivity, sq ft/hr
GK	(41)	External surface mass transfer coefficient, lb-mole/(hr) (sq ft) (mm H_g)
SK	(41)	Effective sorbent thermal conductivity, Btu/(hr) (sq ft) (°F/ft)
ASG	(41)	Sorbent specific surface area, sq ft/(cu ft of bed)
NOG		Node to which coolant is added
HXG	(41)	Heat transfer coefficient, heat exchanger to process gas, Btu/(sq ft) (°F) (hr)
HSG	(41)	Heat transfer coefficient, sorbent to gas, Btu/(hr) (sq ft) (°F)
NDXMAC		Integer denoting number of active M.S. nodes, i.e., (NDXM - NDXMAC) represents the number of M.S. nodes which have been inactivated by water-poisoning
TI		Maximum temperature change allowable per time increment in selecting Δt, °F
WI		Maximum loading change allowable per time increment in selecting Δt, lb/lb
NCYCLT		Total number of complete adsorption-desorption cycle calculations desired
CPS	(41)	Sorbent specific heat, Btu/(lb) (°F)
AVC	(41)	Primary heat exchanger plate area per unit volume of coolant held up in HX, sq ft/(cu ft)

NOTE: Variables W, TG, TS, TC, TX, NPRINT, DTMAX, NTEMP, CYCLE, NCYCLT, WI, TI, NDXMAC need to appear only once either in S9973 or S9993.

Input Variables Required by S9973 Only

Fortran Symbol	Definition
GMR	Process gas flow rate, lb/hr
GMW	Process gas molecular weight
PA	System total pressure, mm Hg
PCO2C	Initial CO_2 partial pressure in cabin, mm Hg
PH2OI	Inlet H_2O partial pressure, mm Hg
TGI	Inlet process gas temperature, $^{\circ}F$
VOLCAB	Cabin volume for atmosphere, cu ft; use $VOLCAB = 10^{20}$, for constant PCO2C
RCO2C	Rate of CO_2 generation in cabin, lb CO_2 per hr
NDTCϕN	$I_f = 1$, internal Δt calculations . $I_f = 2$, fixed Δt calculations.

Input Variables Required by S9993 Only

Fortran Symbol	Definition
NBCOUT	Integer control variable, if NBCOUT = 2, the outlet manifold pressure is specified as a function of time; NBCOUT = 1, the manifold pressure is computed from vacuum duct resistance.
POUT (10), TIMET (10)	10 pairs of exit pressure vs time data to be used if NBCOUT = 2; POUT = vacuum end manifold pressures (mm Hg), TIMET = times (hr).
NPSET (3)	Denotes nodes to which vacuum applied.

I. Molecular Sieve, CO_2 Adsorption GK and DIF

As discussed in Section 5, it was evident that the controlling factor in CO_2 adsorption by molecular sieves was the lumped value of gas stream to particle boundary mass transfer (plus, possibly, the reaction at the surface of the material). Diffusion through the pore, or internal resistance, was not controlling. Thus, a relatively large value of DIF was selected, 4 by 10^{-3} (sq ft)/hr.

Initially the variation of GK during adsorption was thought to be a result of the different residual water loading generally maintained in the two test programs. In the basic laboratory studies the bed was carefully baked at high temperature ($600^\circ F$) for a number of hours to assure absolute dryness. In the prototype program lower temperatures were used ($400^\circ F$), reflecting actual bakeout procedures contemplated in the final design. These lower temperatures result in an estimated 1 percent residual water loading in the molecular sieve, and it was theorized that the presence of this water could have an effect on the mass transfer coefficient. Later study of this phenomenon has altered this view, somewhat, and it is felt that actual bed configuration may be the controlling factor. Of particular significance is the probable channeling occurring in shallow beds with small, straight fin structure providing many short bypass paths along the surface of each fin element. Best values of GK were found ranging from a high of 5 by 10^{-4} for shallow finned beds. Figures 7-7 and 7-8 compare CO_2 breakthrough curves obtained from the deep basic studies beds with prediction using a GK of 5 by 10^{-4}. Comparison of GK selection with test results from the 3-in.-deep fresh prototype bed is shown in Figure 7-9. It was found that mixing caused by the use of a small number of axial increments is significant and, therefore, strictly speaking, precise values for constants must depend upon axial increment sizes chosen in calculations. Best values of GK were found for various (ΔX)'s and plotted in Figure 7-9. Plot of this variation of GK with (ΔX) is shown in Figure 7-10.

Later, as shown in Section 6, the adsorbed water was found to raise the effective mass-transfer coefficient as the loadings became high. The exact value, then, is seen to be rather difficult to establish under highly variant bed conditions.

Determination of Constants GK and DIF

Breakthrough curves obtained in the laboratory test programs described in Section 5 and Section 6 were reviewed and used to determine, through a matching procedure, these constants. Two types of beds were tested. In the basic laboratory studies a small, high-aspect-ratio bed was used, with offset fin structure. In the prototype program the bed condiguration was nearer to the final bed design; relatively shadow or low-aspect-ratio beds with continuous fins. A study of the breakthrough curves and desorption pressure vs time profiles from these two test programs indicated that best match of computer prediction with test results was obtained with the following constants.

CO$_2$ ADSORPTION RUN NO. 2 1.265 L/MIN (STD), 7.15 MM PCO$_2$ INLET, 25^{0}C

▲ PREDICTION WITH GK 5 x 10^{-4}, DIF 4 x 10^{-3}
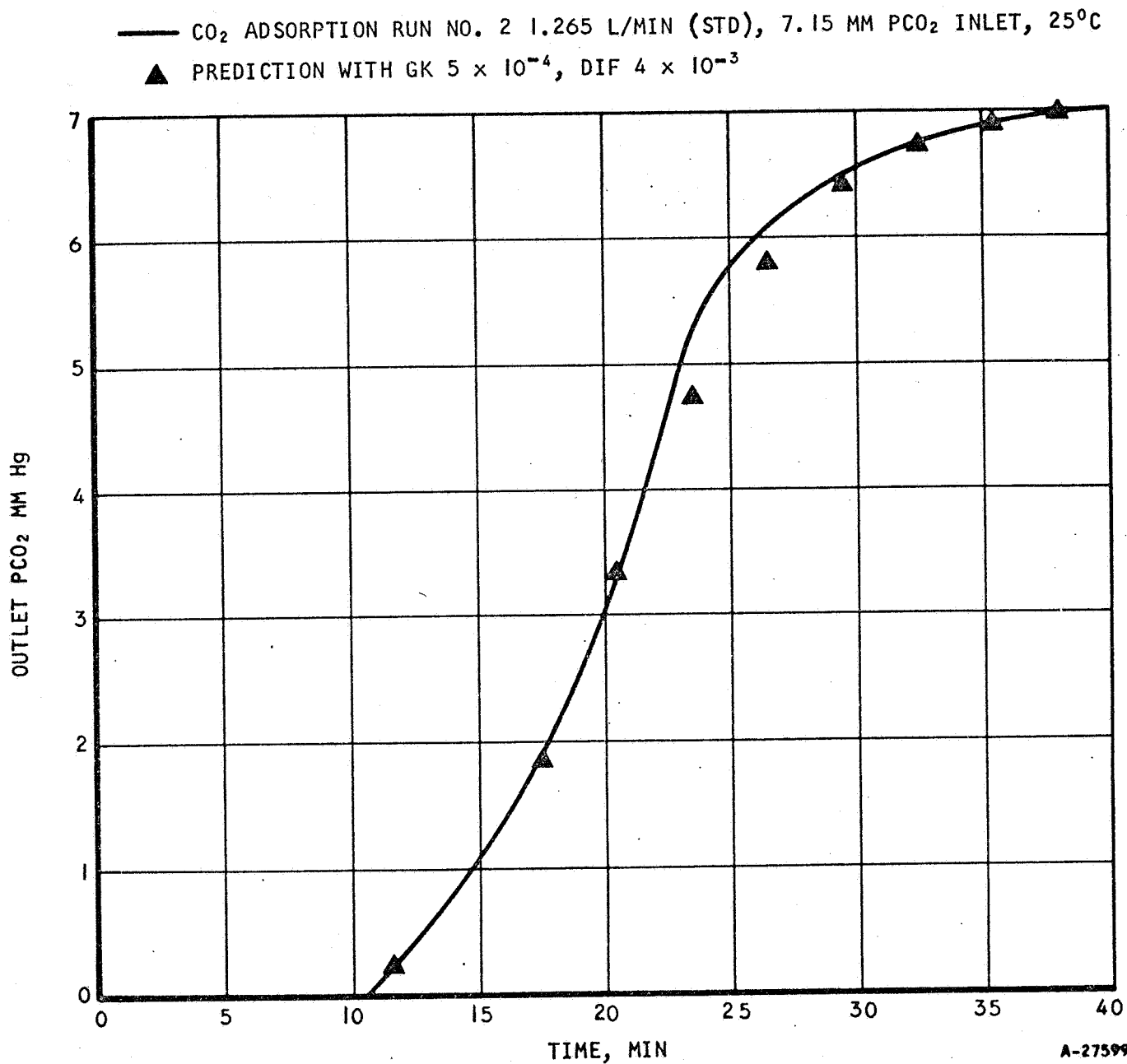
Figure 7-7. Computer Comparison of 5/8-in. Bed CO$_2$ Performance at High Gas Flow

A-27599

—— CO_2 ADSORPTION RUN NO. 3 0.557 L/MIN (STD), 7.13 MM PCO_2 INLET, 25°C

▲ PREDICTION WITH GK 5 x 10^{-4}, DIF 4 x 10^{-3}

OUTLET P_{CO_2}, MM Hg

TIME, MIN
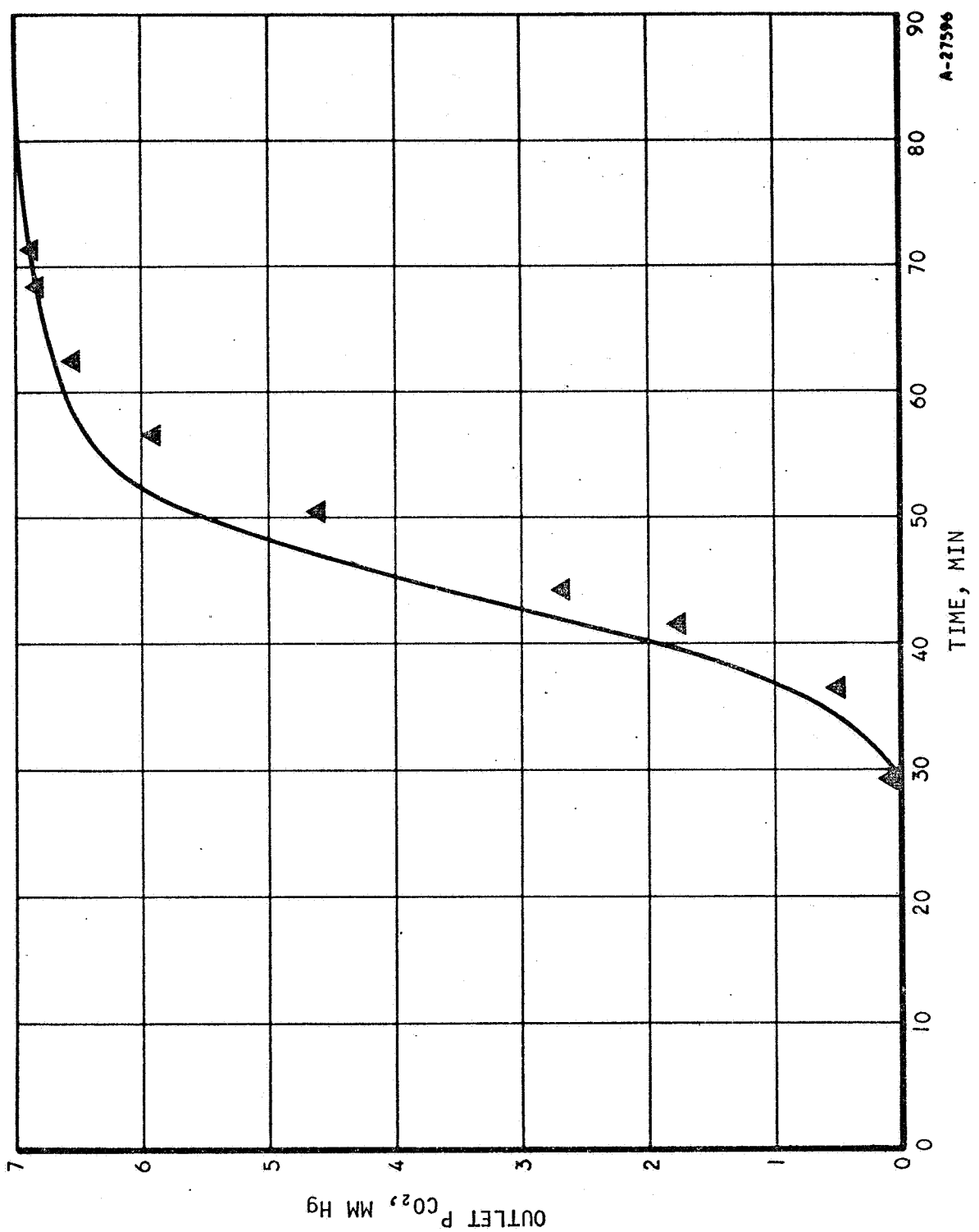
A-27596

Figure 7-8. Computer Comparison of 5/8-in. Bed CO_2 Performance at Low Gas Flow
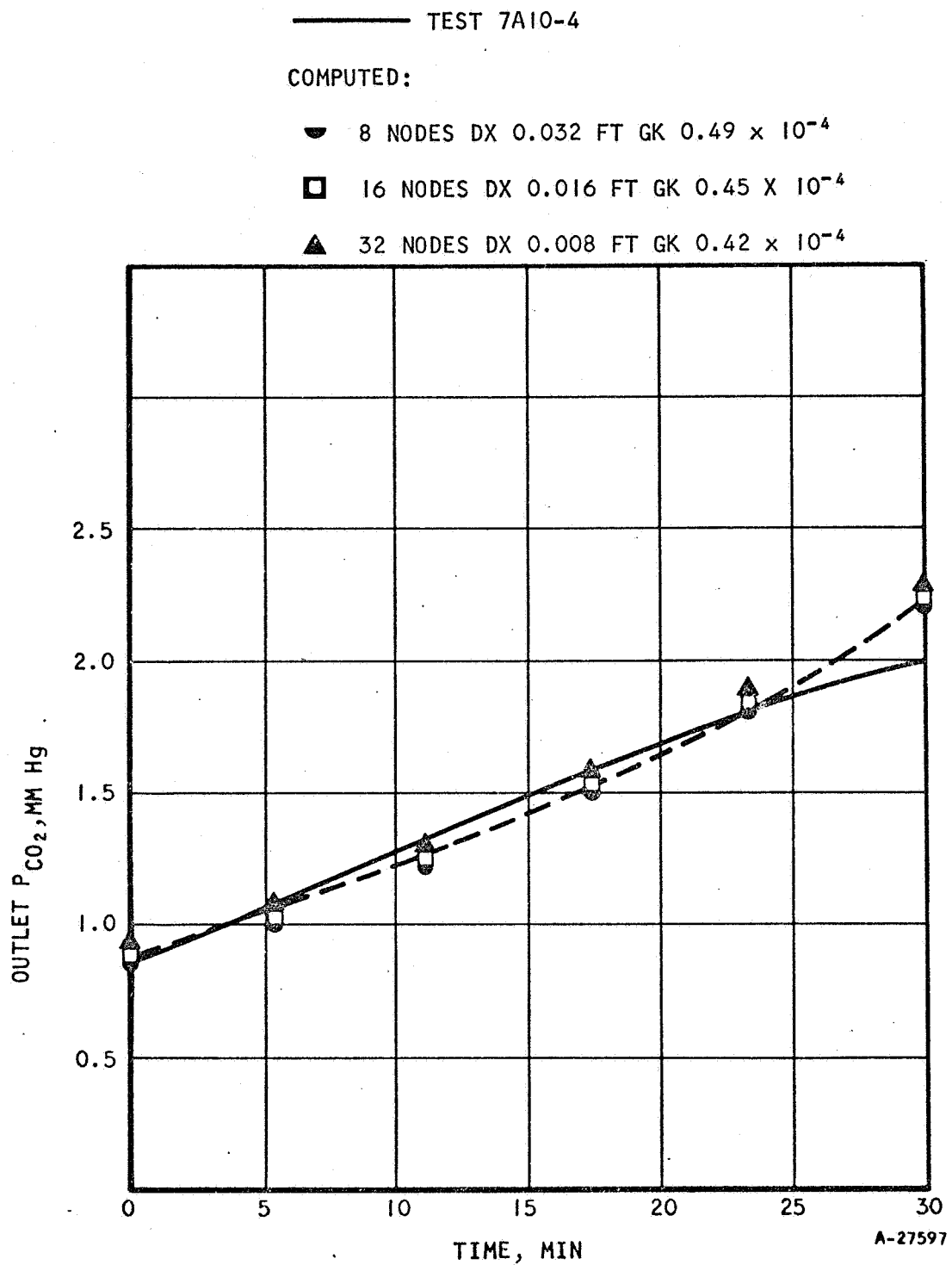
Figure 7-9. Effect of Computer Nodal Size on Predicted CO_2 Performance
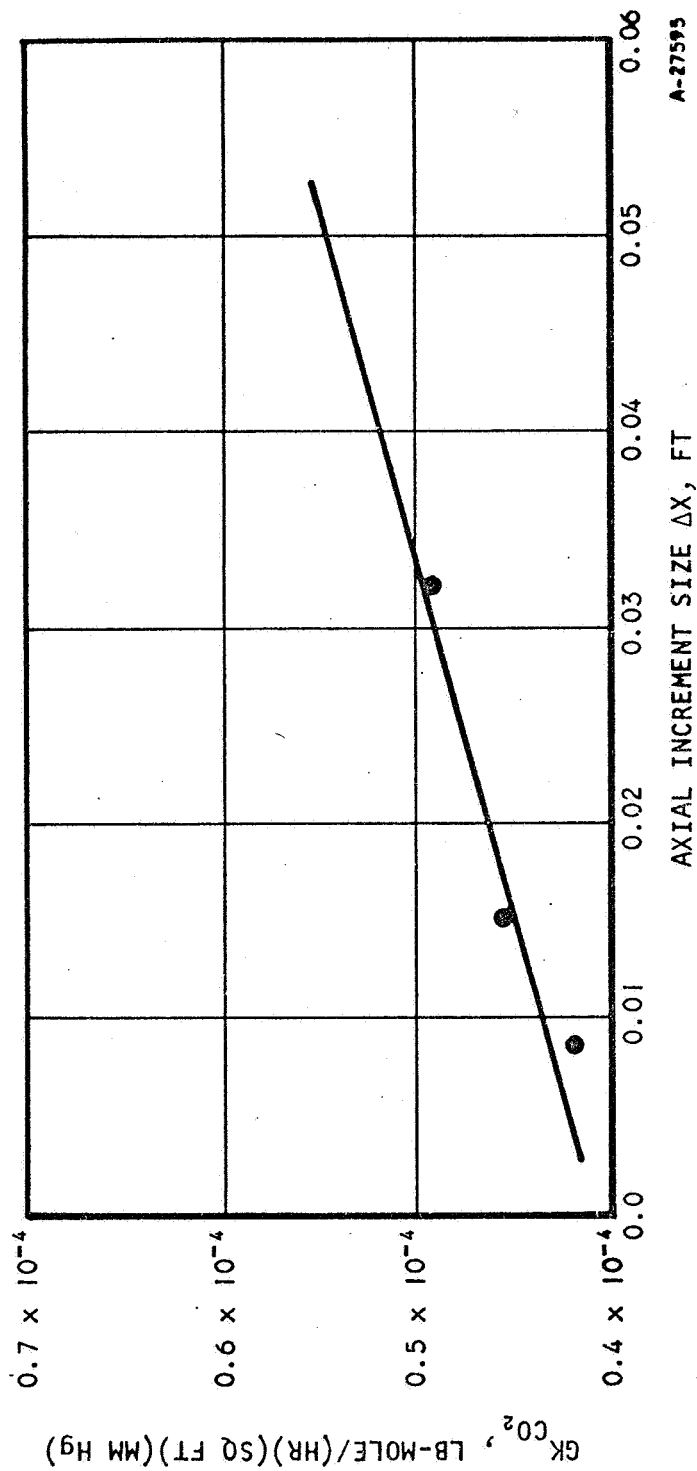
Figure 7-10. Effect of Nodal Size on Best Adsorption Mass-Transfer Coefficient

A-27595

	GK lb-mol/(hr)(sq ft)(mm Hg)	DIF sq ft/hr
Molecular sieve, CO_2 adsorption	0.4×10^{-4} to 5×10^{-4}	4×10^{-3}
Molecular sieve, CO_2 desorption	5×10^{-4}	4×10^{-3}
Silica gel, H_2O adsorption	0.7×10^{-3} to 1.0×10^{-3}	1×10^{-5}
Silica gel, H_2O desorption	1×10^{-3}	1×10^{-5}

From this analysis a range of GK's is evident, depending upon at least two factors: (1) actual bed configuration as it affects the adequacy of contact between the flowing gas stream and the molecular sieve and (2) water-loading. The values plotted in Figure 7-10 will be conservative for almost all cases, with values of around at least 100 percent larger being possible.

2. Molecular Sieve, Desorption GK and DIF

Best fit with desorption data in both test configurations was found with the higher value of GK, 5×10^{-4} (lb-mol) (hr) (sq ft) (mm Hg), which is not surprising since the variation found in adsorption due to "channeling" would not be prevalent during a vacuum desorption process. Again a high value of DIF was selected, 4×10^{-3} (sq ft)/hr. Figure 7-11 compares the desorption pressure profiles measured during the basic studies in a deep bed with calculations using the selected constants. Figure 7-12 shows the same comparison with prototype bed data. Further configuration of both adsorption and desorption constants was obtained by comparison of predicted cyclic performance of the prototype bed operated adiabatically with test results, as shown in Figure 7-13. As can be seen from Figure 7-13, a general trend toward conservation will be obtained when using these constants.

3. Silica Gel, Adsorption and Desorption GK and DIF

Matching of GK and DIF for the deep bed used in the basic studies work resulted in the following constants for both adsorption and desorption:

GK 1×10^{-3} (lb-mol) (hr) (sq ft) (mm Hg)

DIF 1×10^{-5} (sq ft)/hr

Figures 7-14, 7-15, and 7-16 compare the calculated performance of the 5/8-in.-dia silica gel bed vs test results. Figure 7-17 shows the comparison of calculated observed performance of a 3-in.-deep silica gel bed. The test description was given in Section 6.

Matching of the silica gel test results for the prototype bed is described in Section 6.
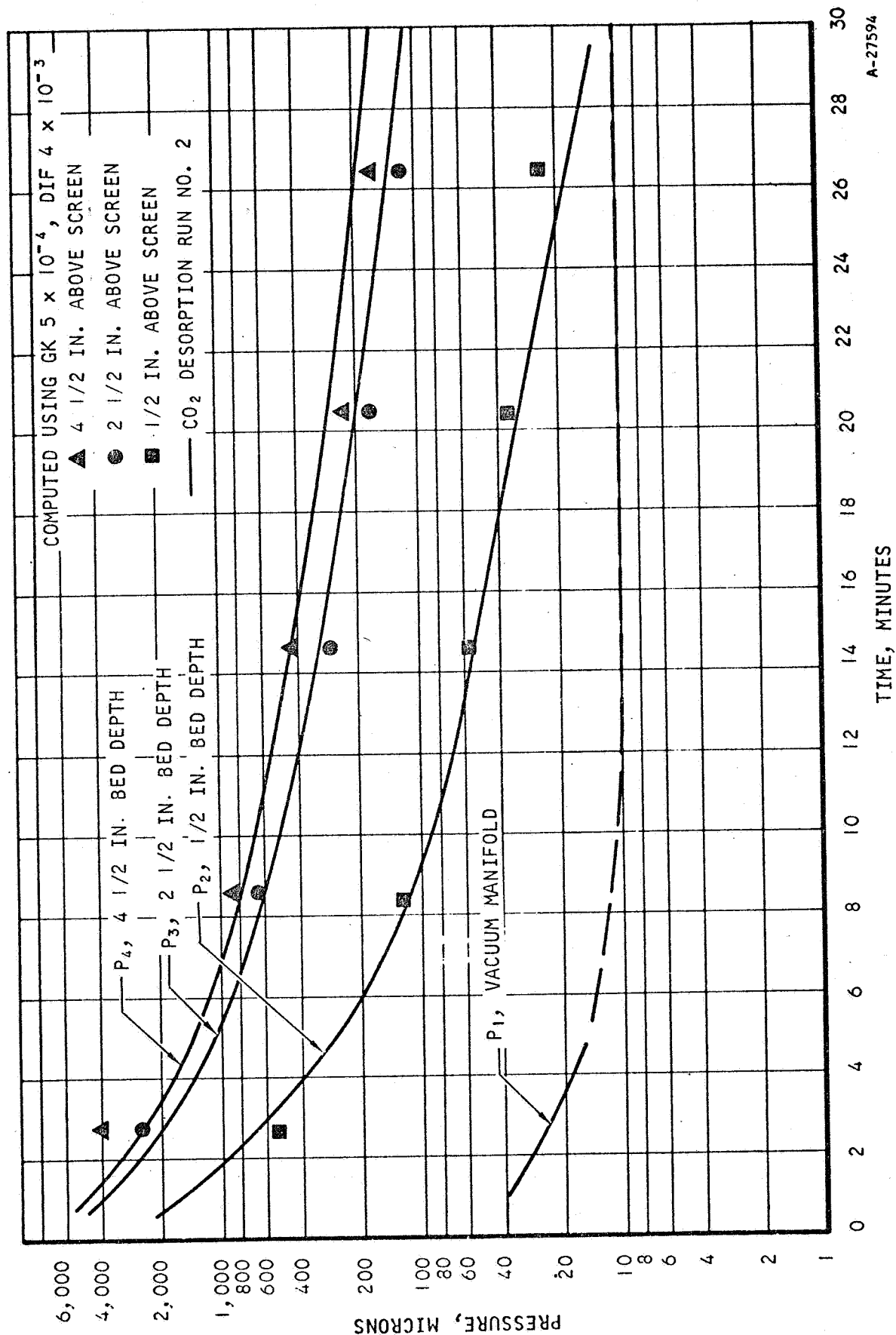
Figure 7-11. Pressure Histories During CO_2 Desorption from a 5/8-in.-dia Molecular Sieve Bed
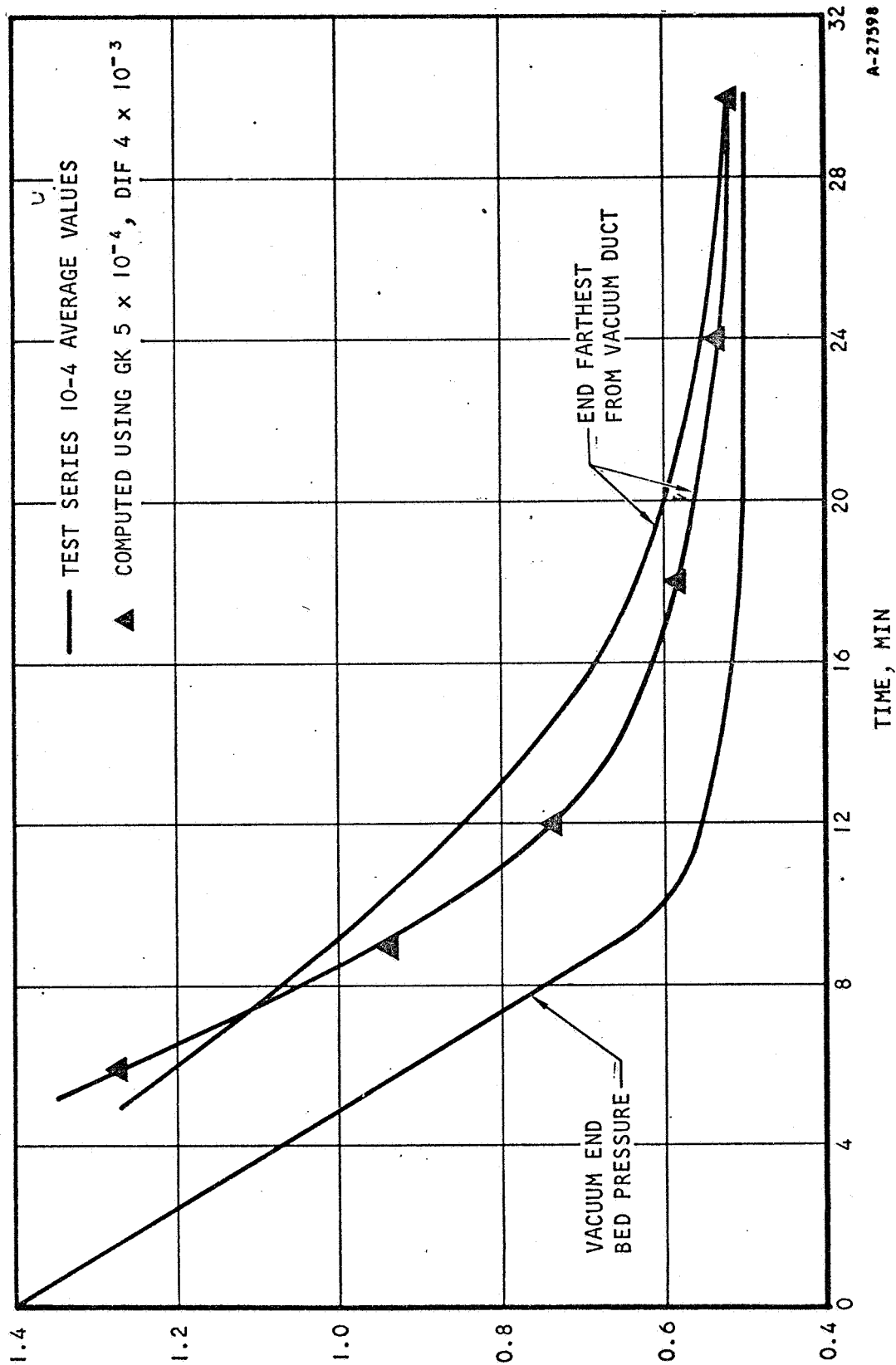
A-27594

Figure 7-12. Pressure Histories During CO_2 Desorption from the Portotype Molecular Sieve Bed

Figure 7-13. Adiabatic CO_2 Performance of Prototype Bed

TEST DATA, TEST SERIES NO. 10-3

—— TEST DATA, TEST SERIES NO. 10-3

● COMPUTED WITH GK, CO_2, ads $= 0.49 \times 10^{-4}$, GK, CO_2, des $= 5.0 \times 10^{-4}$

DIF, CO_2, ads $= 4 \times 10^{-3}$, DIF, CO_2, des $= 4 \times 10^{-3}$

OUTLET P_{CO_2}, MM Hg

TIME, MIN

CYCLE 1   CYCLE 2   CYCLE 3   CYCLE 4

A-27595
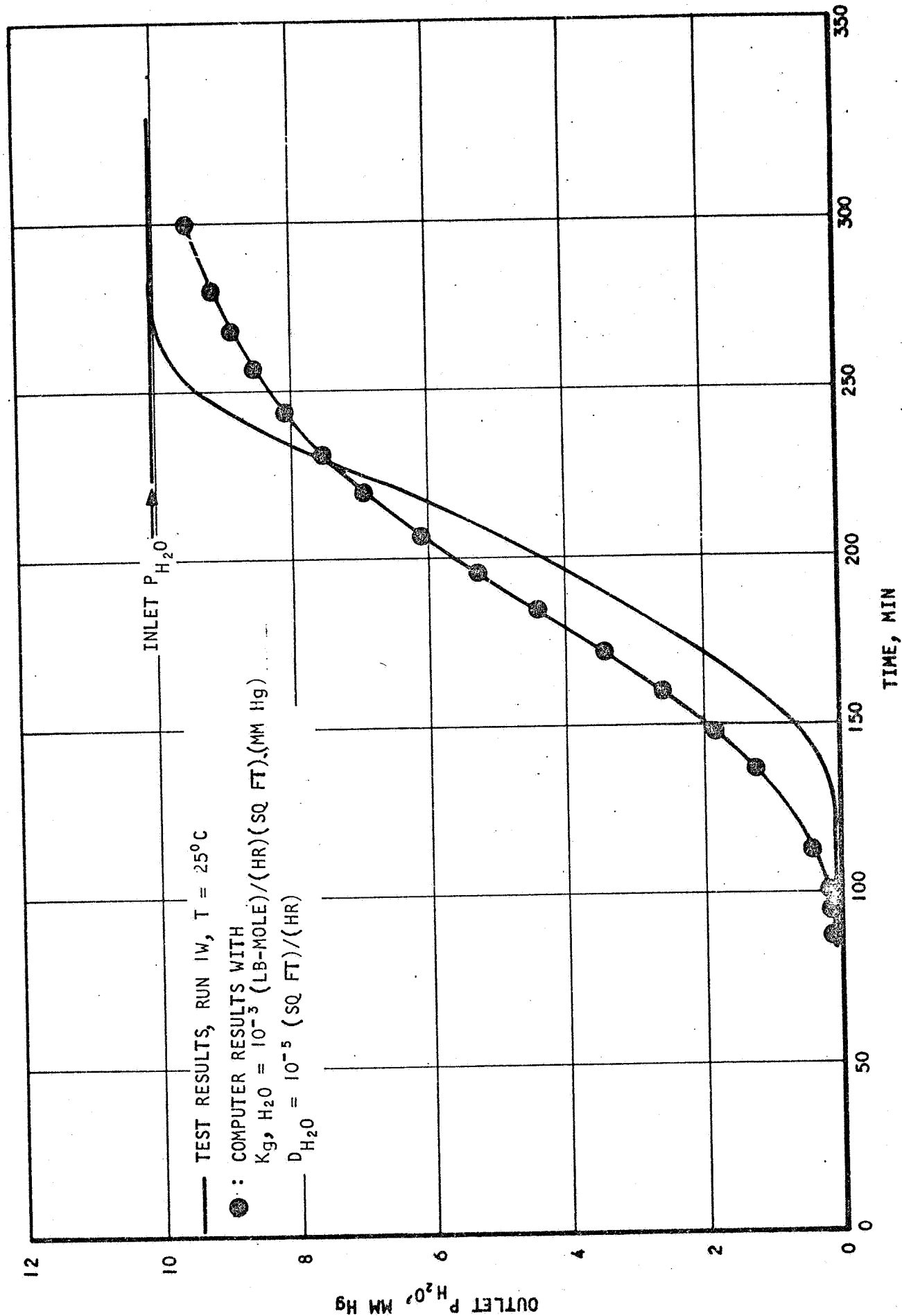
Figure 7-14. Comparison of Predicted and Measured Adsorption Performance of a 5/8-in.-dia Silica Gel Bed

The figure plots OUTLET P_{H_2O}, MM Hg (vertical axis, 0 to 12) against TIME, MIN (horizontal axis, 0 to 350).

Legend:
- — TEST RESULTS, RUN 1W, T = 25°C
- ● : COMPUTER RESULTS WITH K_g, H_2O = 10^{-3} (LB-MOLE)/(HR)(SQ FT)(MM Hg)
- D_{H_2O} = 10^{-5} (SQ FT)/(HR)

INLET P_{H_2O}

A-24064

The graph shows:
- Y-axis: PERCENTAGE LOADING, LB H_2O/100 LB S.G. (0 to 6)
- X-axis: TIME, MINUTES (0 to 35)

Legend:
- ▲ COMPUTER PREDICTIONS WITH $K_g = 10^{-3}$ LB-MOLE/(HR)(FT^2)(MM Hg), $D_{H_2O} = 10^{-5}$ FT^2/HR
- —— TEST DATA

Curve labels: 25°C (RUN 3), 50°C (RUN 4)

A-24665-A

Figure 7-15. Comparison of Predicted and Measured Changes in H_2O Loading on a 5/8-in.-dia Silica Gel Bed During Desorption

$= $ RUN NO. 3 AT 25°C
5/8-IN.-DIA BED AT A.4 1/2-IN. DEPTH
$= $ COMPUTER RESULTS WITH
$K_{g,H_2O} = 10^{-3}$ LB-MOLE (HR)(FT^2)(MM Hg)
$D_{H_2O} = 10^{-5}$ FT^2/HR

PRESSURE, MM Hg

2.0
1.8
1.6
1.4
1.2
1.0
0.8
0.6
0.4
0.2
0.0

BED EXIT

0   5   10   15   20   25   30

TIME, MIN
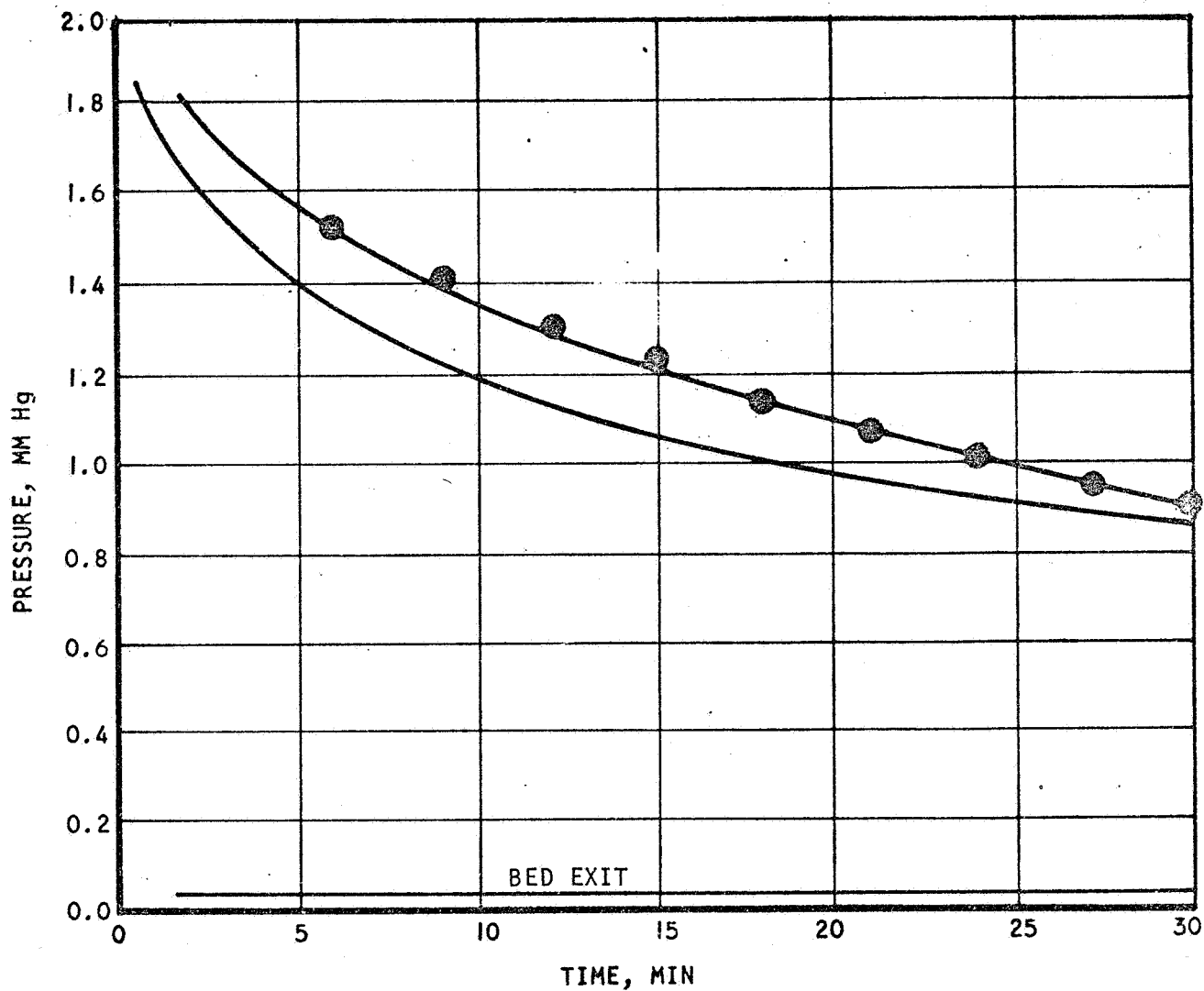
A-24669

Figure 7-16. Pressure History During Desorption of H_2O from a 5/8-in.-dia Silica-Gel Bed (77°F)
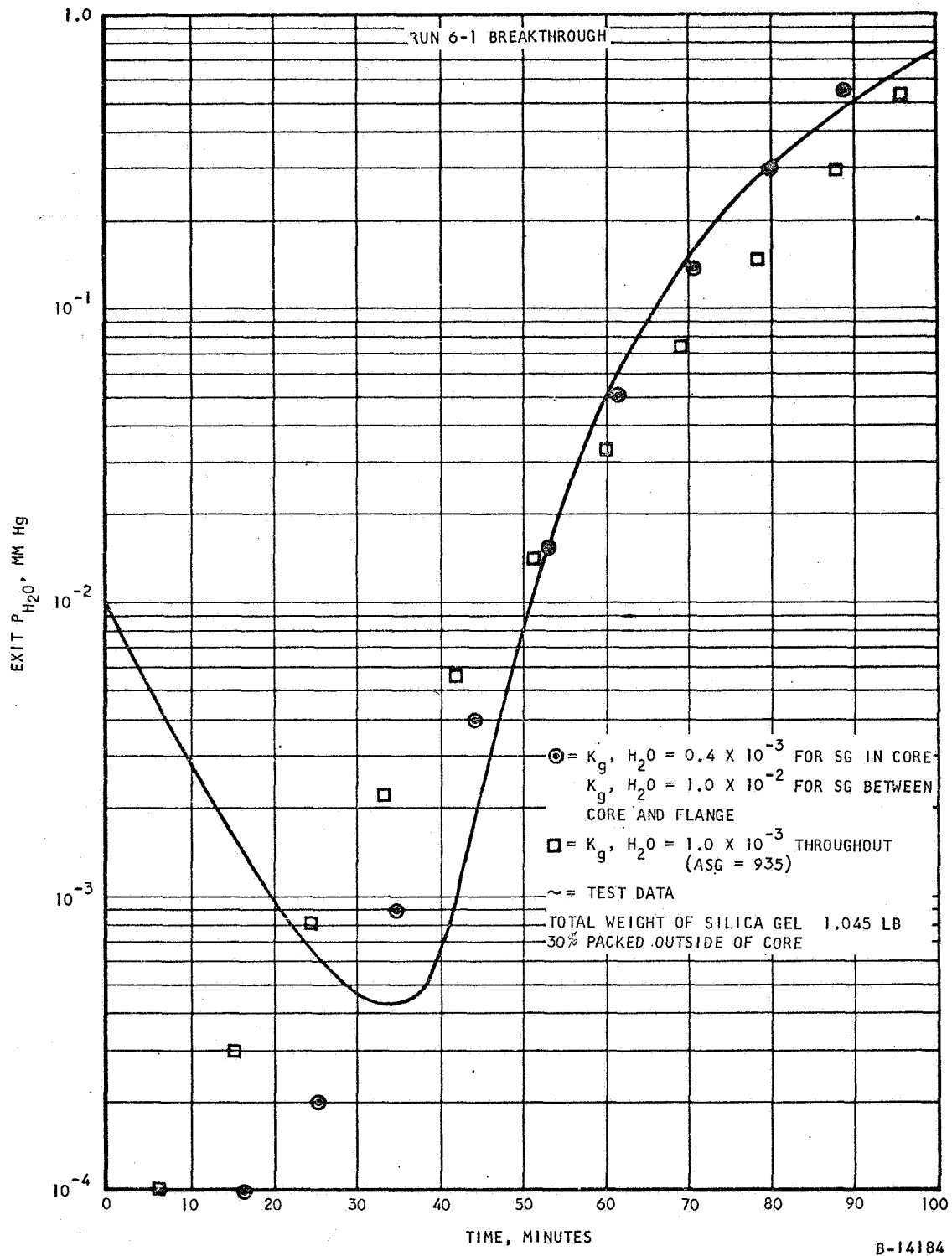
Figure 7-17. Water Breakthrough on 3-in. Silica Gel Bed

Various Heat Transfer Coefficients for the Final Bed

In estimating the heat transfer coefficients to be used in the final bed design calculations, the following bed properties are used:

$$\rho_x, \text{ M.S.} = 64 \text{ lb/cu ft}$$

$$\rho_{sb}, \text{ M.S.} = 34.2 \text{ lb/cu ft}$$

$$a_{sg}, \text{ M.S.} = 540 \text{ sq ft/cu ft}$$

Apparent molecular sieve particle diameter is

$$d_{M.S.} = \frac{6 \times 34.2}{64 \times 500} = 0.00642 \text{ ft}$$

$$f = 0.46$$

$$\rho_{s, \text{ S.G.}} = 75 \text{ lb/cu ft}$$

$$\rho_{sb, \text{ S.G.}} = 37 \text{ lb/cu ft}$$

$$a_{sg, \text{ S.G.}} = 700 \text{ sq ft/cu ft}$$

Apparent silica gel particle diameter is

$$d_{S.G.} = \frac{6 \times 37}{75 \times 700} = 0.00423 \text{ ft}$$

$$f = 0.5$$

i. Sorbent-to-Gas Heat Transfer Coefficient

Using a correlation given by Pfeffer and Happel (Reference 7-5), at Peclet number of 2.5 and void fraction of about 0.5, one obtains a Nusselt number of roughly 10. Using this and the thermal conductivity of 0.01475 Btu/(hr) (sq ft) (^{o}F/ft) for O_2, there are obtained

$$h_{sg, \text{ M.S. adsorption}} = 23 \text{ Btu/(hr) (sq ft) } (^o\text{F})$$

$$h_{sg, \text{ S.G. adsorption}} = 35 \text{ Btu/(hr) (sq ft) } (^o\text{F})$$

During the desorption period, thermal conductivities of CO_2 and that of CO_2-H_2O mixture are corrected for pressure effect by the method given by Schotte (Reference 7-6). By assuming an average pressure of 1 mm Hg in the M.S. bed, and 0.5 mm Hg in the S.G. bed, the gas phase thermal conductivities are found to be 0.00194 and 0.00079 Btu/(hr) (sq ft) (^{o}F/ft). Using these values, particle surface film heat transfer coefficients are found to be

h_{sg}, M.S., desorption = 3.02 Btu/(hr) (sq ft) ($^\circ$F)

h_{sg}, S.G., desorption = 1.87 Btu/(hr) (sq ft) ($^\circ$F)

2. Heat Exchanger-to-Gas Heat Transfer Coefficient

Assuming that the sorbent-to-gas film transfer coefficients obtained in the preceding part can be employed for the film coefficients in the present case, after correcting for the fin effectiveness and area factor (Reference 7-7), we obtain

h_{xg}, M.S. adsorption = 66

h_{xg}, S.G., adsorption = 95

h_{xg}, M.S., desorption = 9.5

h_{xg} S.G., desorption = 6.0

It should be noted that the above heat transfer coefficients are based on the primary plate area, which does not include fin areas.

3. Effective Thermal Conductivity of Sorbent Bed

Phillips, et al, experimentally obtained a correlation for the effective thermal conductivity of a 1/8-in. molecular sieve bed as a function of gas thermal conductivity and gas flow rate (Reference 7-8). Assuming their results can be applied to our final composite bed, which is made up of 1/16-in. molecular sieve pellets and 10-16 mesh silica gel pellets, we obtain

During adsorption k_s = 0.10 Btu/(hr) (sq ft) ($^\circ$F/ft)

During desorption k_s = 0.08 Btu/(hr) (sq ft) ($^\circ$F/ft)

4. Heat Exchanger-to-Sorbent Heat Transfer Coefficient

Assuming an effective length of conductance of 0.1 in. between the heat exchanger core metal and the sorbent, and using a bed conductivity of 0.08, we readily obtain

h_{xs} = 9.6 Btu/(sq ft) (hr) ($^\circ$F)

NOMENCLATURE

Algebraic	Fortran	Definition
A	ABED(41)	Cross-sectional area of adsorbent bed, sq ft
a_{sg}	ASG(41)	External surface area of sorbent, sq ft/ (cu ft of bed)
a_{vc}	AVC(41)	Primary heat transfer area for coolant, sq ft/ (cu ft of coolant volume)
a_{vx}	AVX(41)	Primary heat transfer area for heat exchanger, sq ft plate area/(cu ft of metal)
a_{xg}	AXG(41)	Primary heat transfer area between heat exchanger and gas stream, sq ft/cu ft of sorbent bed
a_{xs}	AXS(41)	Primary heat transfer area between heat exchanger and sorbent, identical to a_{xg}
C	C(41)	Molal density of gas mixture lb moles/ (cu ft)
C_{pc}	CPC(41)	Heat capacity of coolant, Btu/(^{0}F) (lb)
C_{pg}	CPG(41)	Heat capacity of gas mixture, Btu/(^{0}F) (lb)
C_{px}	CPX(41)	Heat capacity of heat exchanger metal, Btu/(^{0}F) (lb)
D_k	DIF(41)	Mass diffusivity of component k through the interior of sorbent, sq ft/hr
F	F(41)	Factor defined by Equation (7-16), a function of pressure
F_{N_2}		Factor F for the flow of N_2 gas through M.S. bed
f	VϕIDF(41)	Void fraction of bed
G		Mass flux = $u_g \rho_g$, lb/(hr) (sq ft void area)
G_t	GMR	Total mass flow rate, lb/(hr)

Algebraic	Fortran	Definition
ΔH_k	DH(41)	Heat of adsorption at each node Btu/(lb adsorbed)
h_{sg}	HSG(41)	Heat transfer coefficient between sorbent and gas, based on a_{sg}, Btu/(sq ft) ($^{\circ}$F) (hr)
h_{xc}	HXC(41)	Heat transfer coefficient between heat exchanger primary plate and coolant, Btu/(sq ft) ($^{\circ}$F) (hr)
h_{xg}	HXG(41)	Heat transfer coefficient between heat exchanger primary plate and gas stream, Btu/(sq ft) ($^{\circ}$F) (hr)
h_{xs}	HXS(41)	Effective heat transfer coefficient between heat exchanger primary plate and sorbent Btu/(sq ft) ($^{\circ}$F) (hr)
K_g	GK(41)	Mass transfer coefficient between bulk stream and the surface of adsorbent. Surface kinetic rate can be incorporated in this coefficient, lb-moles/(hr) (sq ft) (mm Hg)
k_s	SK(41)	Effective thermal conductivity of sorbent bed, Btu/(hr) (sq ft) ($^{\circ}$F/ft)
k_x	TKX(41)	Thermal conductivity of heat exchanger core metal, Btu/(hr) (sq ft) ($^{\circ}$F/ft)
M_{sg}		Molal rate of mass transfer into bulk gas stream/unit bed volume, lb-moles per (cu ft of bed) (hr); See Eq. (7-15)
M		Index denoting interior radial node in sorbent
M_s		Interior node corresponding to the surface of pellet
M_{wk}	SM(K)	Molecular weight of component K. K = 1 and 2
P	P(41)	Total pressure in bulk gas stream, mm Hg
P_k	PK(K,41)	$=P \cdot X_k$; Partial pressure of component k in bulk gas stream, mm Hg

Algebraic	Fortran	Definition
P_{ks}		Equilibrium pressure of component k at surface of sorbent, mm Hg
R	RGAS	Gas constant, 554 (mm Hg)(cu ft)/(lb-mole)($^\circ$R)
r		Radial distance from center of sphere, ft
r_M		r at interior node M, ft
r_s		Average particle radius found from ρ_{sb} and a_{sg}, ft
t		Time, hr
Δt		Time increment, hr
T_c	TC(41)	Coolant temperature, $^\circ$F
T_g	TG(41)	Gas temperature, $^\circ$F
T_s	TS(41)	Sorbent temperature, $^\circ$F
T_x	TX(41)	Heat exchanger core metal temperature, $^\circ$F
T_{gi}	TGI	Inlet gas temperature for adsorption cycle, $^\circ$F
T_{268}	T268	Inlet glycol temperature, $^\circ$F
u_c	UC(41)	Coolant velocity, ft/hr
u_g	UG(41)	Interstitial gas velocity, i.e., true gas velocity, ft/hr
ΔV		Size of each sorbent interior node, cu ft
W_k	W(21, 41)	Local loading of component k in sorbent, lb adsorbate k/lb sorbent
$W_d(P)$		A function of pressure which represents the capacity of vacuum duct, lb/hr
x		Distance from molecular sieve bed end, ft
X_k	X(41)	Mole fraction of component k in gas stream. k refers to CO_2 in M.S. bed gas stream, and H_2O in S.G. bed gas stream

Algebraic	Fortran	Definition
x_o		Total combined bed depth, ft

Greek Letters

Algebraic	Fortran	Definition
ρ_c	RHϕC(41)	Coolant density, lb/(cu ft)
ρ_g	RHϕG(41)	Gas density, lb/(cu ft)
ρ_s	RHϕS(2)	Sorbent density, lb/(cu ft particle)
ρ_{sb}	RHϕSB(41)	Sorbent bulk density, lb/(cu ft bed volume)

Subscripts

b	Bulk
c	Coolant
g	Gas stream
i	Inlet
k	Component k
M	Sorbent interior node
s	Surface of sorbent
s	Sorbent
t	At time t
v	Volume
x	Heat exchanger

EXAMPLE INPUT AND OUTPUT

As an example of the program usage, the input data required for predicting the performance of the composite bed, which is described in Section 8, are given in Appendix D. Example outputs of the adsorption period are given in Appendix E, and those of the desorption period are given in Appendix F.

COMPLETE LISTING OF SOURCE PROGRAM

A complete listing of the Fortran source program is given in Appendix G.

REFERENCES

7-1.   Hwang, K.C., "A Mathematical Study of the Transient Behavior of a Fixed-Bed Catalytic Reactor," A PhD Dissertation, University Microfilms, Inc., Ann Arbor, Michigan.

7-2.   DuFort, E.C. and S.P. Frankel, Math. Tables and Other Aids to Computation, 7, p. 135, 1953.

7-3.   W.R. Grace and Co., Davison Chemical Division, Technical Bulletin 202, January 1965.

7-4.   J. Todd, "Survey of Numerical Analysis," pp 395, McGraw-Hill Book Company, Inc., 1962.

7-5.   Pfeffer, R. and J. Happel, A.I.Ch.E. Jour. 10, 605, 1964.

7-6.   Schotte, W., "Thermal Conductivity of Packed Beds," A.I.Ch.E. Jour., 6, 63-67, March 1960.

7-7.   Kays, W.M., and A.L. London, "Compact Heat Exchangers," 2 ed., McGraw-Hill Book Company, 1964.

7-8.   Phillips, B.D., F.W. Leavitt and C.Y. Yoon, "Heat Transfer with Molecular Sieve Adsorbent," Chem. Engrg. Progr. Symposium Series, 56, 219-228.

SECTION 8

BED DESIGN

The data taken on the small, 5/8-in.-diameter bed and on the 3-in.-deep prototype bed were used to identify the mass and heat transfer parameters necessary to describe the mixed gas adsorption and desorption processes. Using these parameters it was possible to simulate any bed configuration with any gas flow, coolant flow, cabin size, and CO_2 or H_2O production rate. The computer program, which simulates bed performance under the operating conditions input to it, then revealed the CO_2 and H_2O removal rate under these conditions. From simple mass balances the program also calculated the instantaneous change in cabin CO_2 pressure and the poisoning rate of the moelcular sieve bed due to the water effluent from the silica gel predryer.

The total bed size, including the silica gel and molecular sieve and the ducting was fixed by the geometry of the enclosure in the spacecraft. Bed design became a matter of choosing the best division of total sorbent volume between silica gel and molecular sieve, the gas flow rate, the heat exchanger configuration, the heat transfer fluid flow rates and temperatures, and the cycle time. The design performance criteria were a cabin CO_2 level of no higher than 7.6 mm Hg at a production of 0.264 lb CO_2/hr and a bed life until bakeout of at least 45 days. The design was accomplished by varying one operating parameter at a time to find the approximate optimum of all.*

Several computer calculations were made to determine the effect of each parameter. Because the silica gel bed performance seemed difficult to predict with a great degree of certainty, a length of 3 in. was assumed great enough to prevent breakthrough at any operating conditions being considered and also to prohibit channeling. This fixed the molecular sieve bed length at 7.63 in. The predicted outlet dew point was fairly constant all through the cycle and depended primarily on desorption performance. This, in turn, depended on the amount of stripping provided by the desorbing CO_2 from the molecular sieve bed.

The molecular sieve bed must be initially baked out before flight. An electric heating matrix was provided in the major portion of the bed (see Figure 8-1). This unit would also be used for regeneration in the case of accidental water poisoning in flight. To regenerate the sieve to acceptably low residual water requires temperatures of 400°F. A glycol or water heat exchanger would not withstand this, so were not permitted in this molecular sieve section. However, since the heat of adsorption of CO_2 is low, the adverse temperature swing in an adiabatic bed is not large. Also, without a liquid heat exchanger, more volume remains for sorbent material.

---

*A more sophisticated optimization approach was not felt justified due to the approximate nature of several of the coefficients and also because of the complexity of the process.
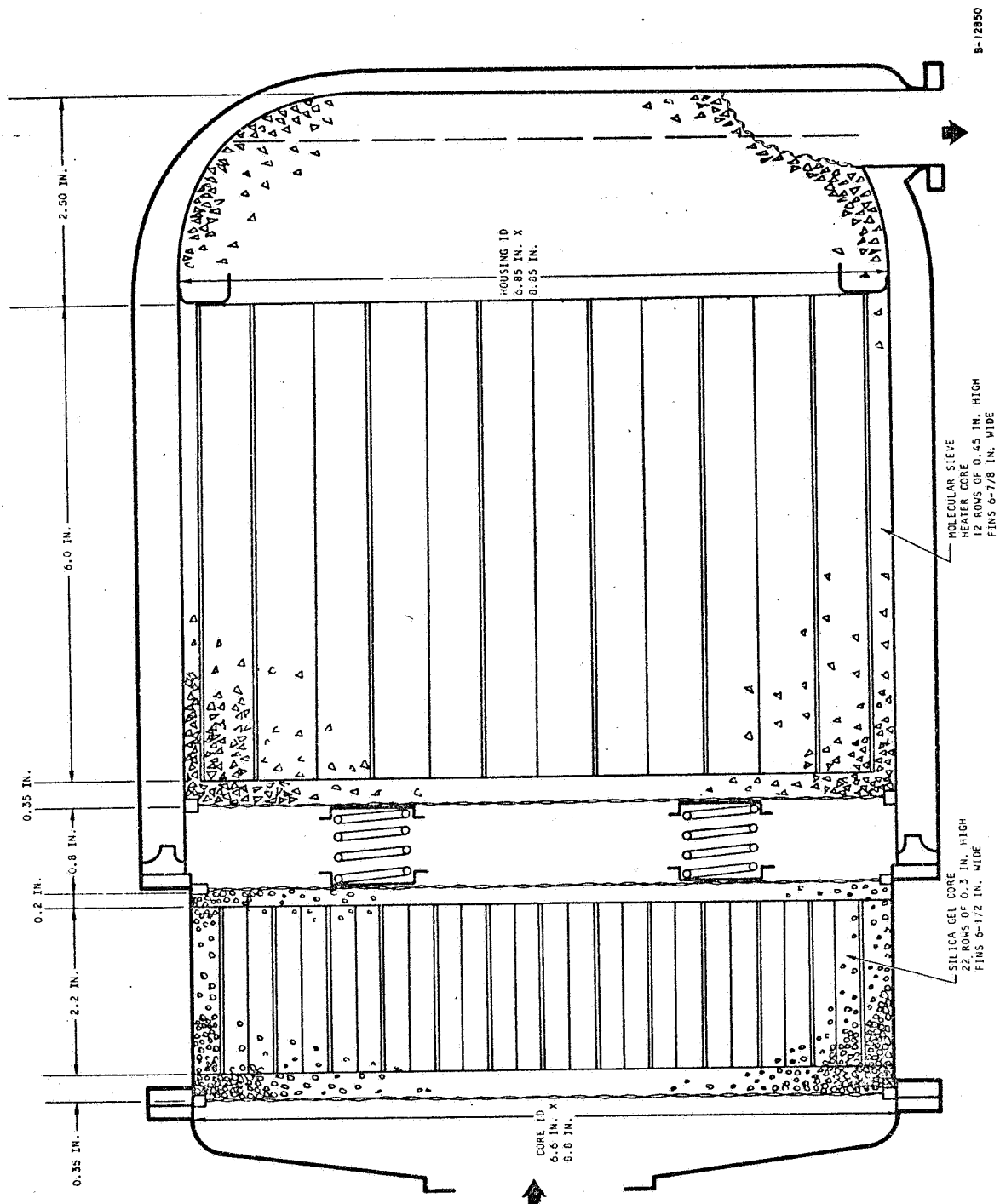
Figure 8-1. Adsorbent Cannister

Labels within figure:

B-12850

2.50 IN.

6.0 IN.

HOUSING ID
6.85 IN. X
0.05 IN.

MOLECULAR SIEVE
HEATER CORE
12 ROWS OF 0.45 IN. HIGH
FINS 6-7/8 IN. WIDE

SILICA GEL CORE
22 ROWS OF 0.3 IN. HIGH
FINS 6-1/2 IN. WIDE

0.35 IN.

0.8 IN.

0.2 IN.

2.2 IN.

0.35 IN.

CORE ID
6.6 IN. X
6.0 IN.

GARRETT

For purposes of calculation, the molecular sieve bed was divided into an active portion and a water-poisoning "dump," adjacent to the silica gel bed. The life of a given bed is determined by how long it will take to completely fill the "dump" section of the molecular sieve with the water vapor effluent from the silica gel bed. Thus, with a fixed total molecular sieve bed size, a larger active bed means a smaller "dump," and hence shorter bed life. But the longer active bed naturally increases the CO_2 removal rate. So conditions must be found where the bed life is at least 45 days, at which time the CO_2 removal rate remains at least 0.264 lb/hr. In reality, the active bed decreases in size all during the days of operation. The calculations are performed, in effect, at the worst possible time, when the entire section allotted for water poisoning has been poisoned. Additional conservatism was achieved by initially subtracting from the active bed 1 in. of sieve to account for a water loading profile not as sharply defined as anticipated.

The predicted effect of flow rate on CO_2 performance is shown in Figure 8-2 at one cycle time, 15 min. The bed length is that length of sieve not water poisoned. Increasing flow rate increases the CO_2 removal rate, but also increases the water poisoning rate due to the faster breakthrough of the silica gel. The effect of active molecular sieve depth is also shown. At a given active bed length, the higher flow rates produce better CO_2 removal rates but also lower bed life. Increasing the active bed length increases the removal rate.

The effect of cycle time on CO_2 performance and poisoning is shown in Figure 8-3. Here the effects of varying the active and "dump" sections of the molecular sieve bed become apparent. The total molecular sieve bed is composed of 18 equal sized nodes for computation purposes. The total weight is 9.56 lb. The curves referred to the left-hand ordinate show the effects of increasing active bed size and gas flow rate on CO_2 removal. Increases in either aid the removal rate. However, increasing the active bed lowers the available "dump" size. The curves referred to the right-hand ordinate show this effect. The lower "dump" size lowers the days of operation until the dump is completely filled with water. Longer cycle time is seen to decrease both bed life and CO_2 removal performance. However, longer cycle times are desirable from the viewpoint of wear on switching components such as gas and coolant valves.

The operating point was chosen in Figure 8-2 as 10 lb/hr gas flow with 13 nodes considered active. The 5 nodes left for water poisoning yield as predicted bed life of 45 days at a cycle time of 20 min. However, because the curves are very flat, the precise values awaited performance testing. Confidence was gained in the design chosen even though it was not possible to specify exactly operation parameters. The calculations did show the range of these parameters which would yield the desired bed performance.

Bed Physical Characteristics

The final bed design is shown as Figure 8-1. A photograph of the two beds mounted in their frame is Figure 8-4. Figure 8-5 shows the integration into the command module. Figure 8-6 is the schematic of the ducting arrangement for the system.
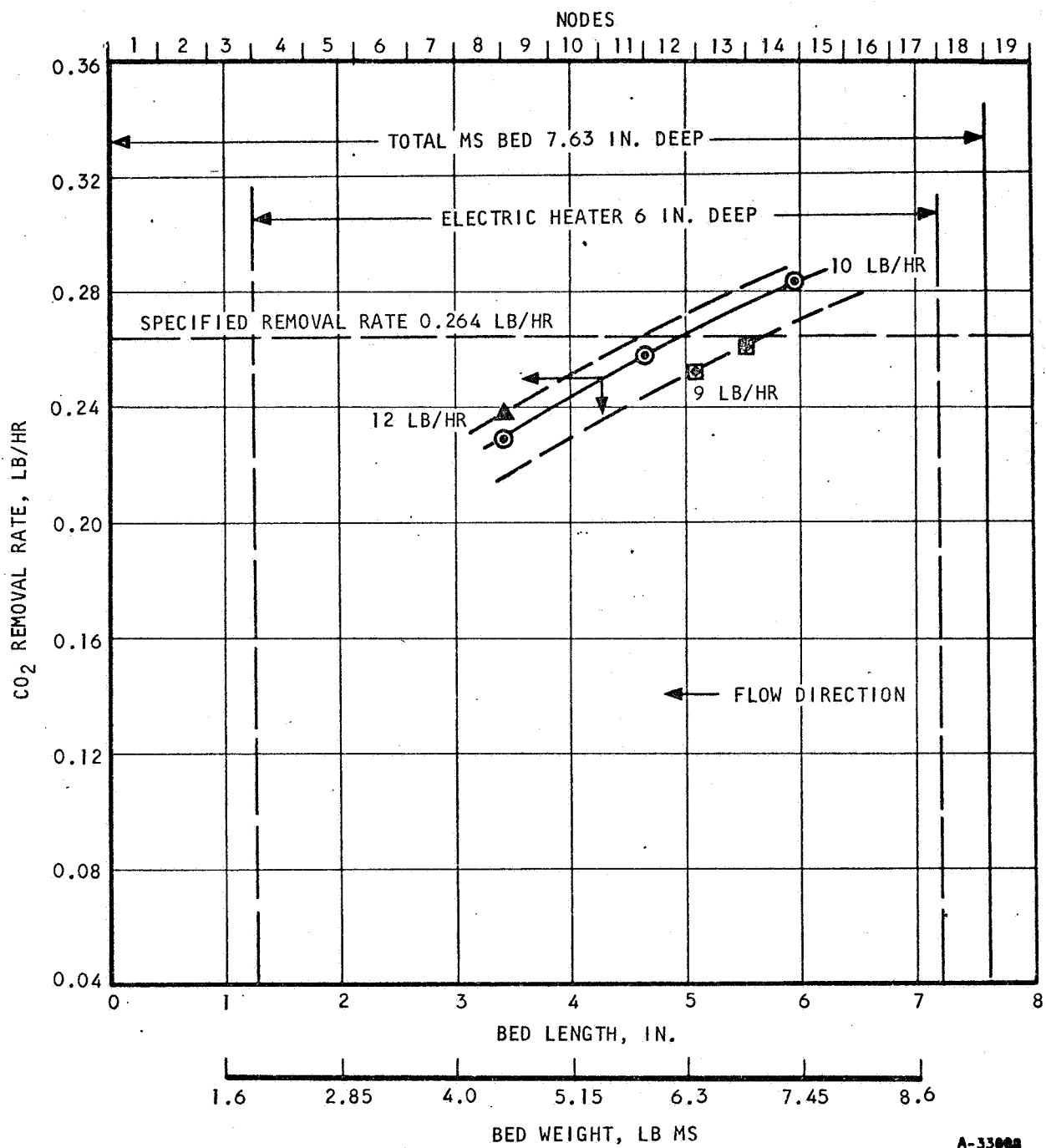
Figure 8-2. Predicted Effect of Bed Size and Gas Flow on CO_2 Removal
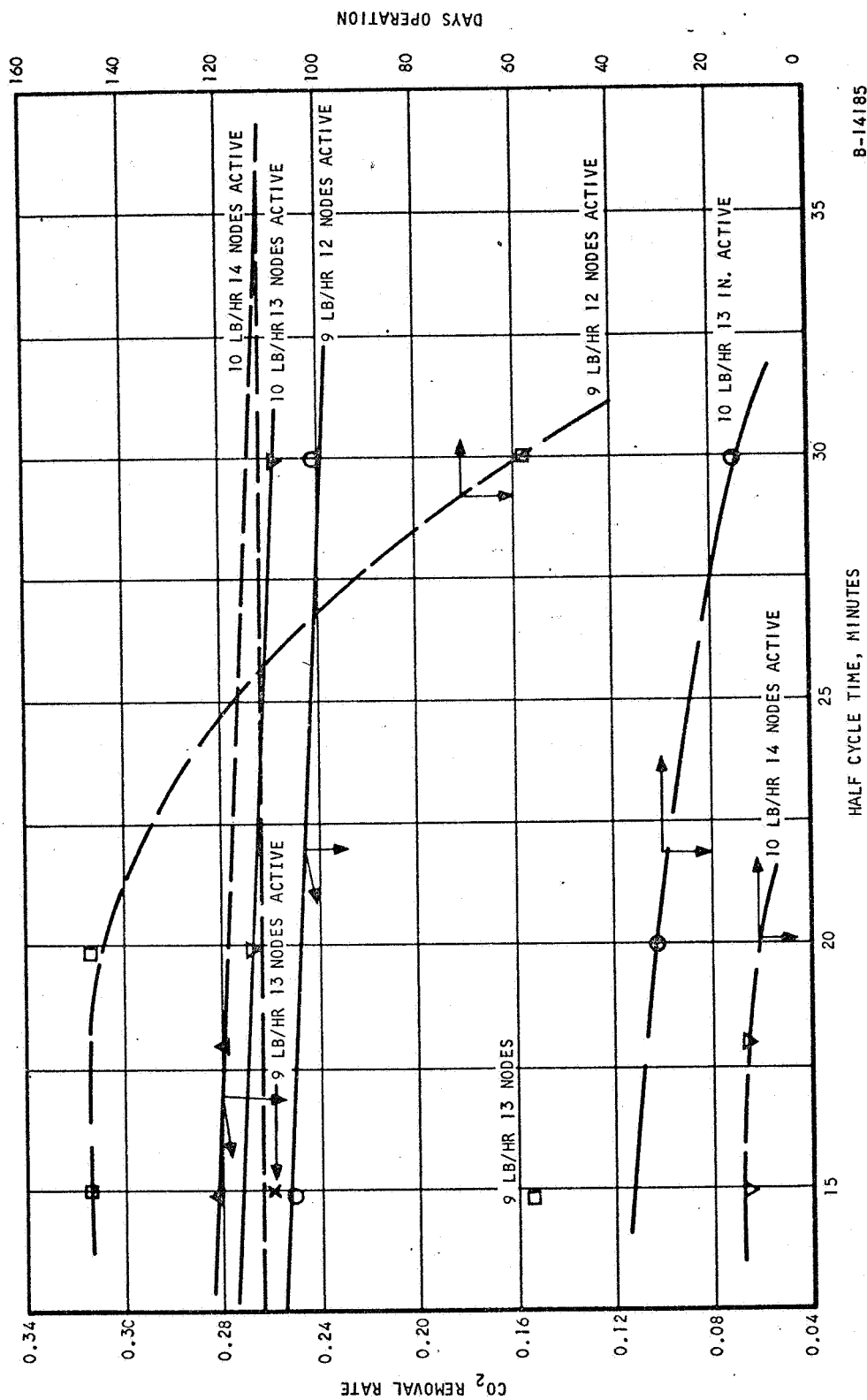
Figure 8-3. Predicted Effects of Cycle Time and Gas Flow on CO_2 Removal and Bed Life

B-14185

GARRETT AIRESEARCH MANUFACTURING DIVISION
Los Angeles, California

67-1751
Page 8-5

COOLANT
VALVE
ASSEMBLY

ADSORBENT
CANISTER
NO. 2

ODOR
ADSORBER

GAS VALVE
ASSEMBLY

ADSORBENT
CANISTER
NO. 1

PARTICULATE
FILTER
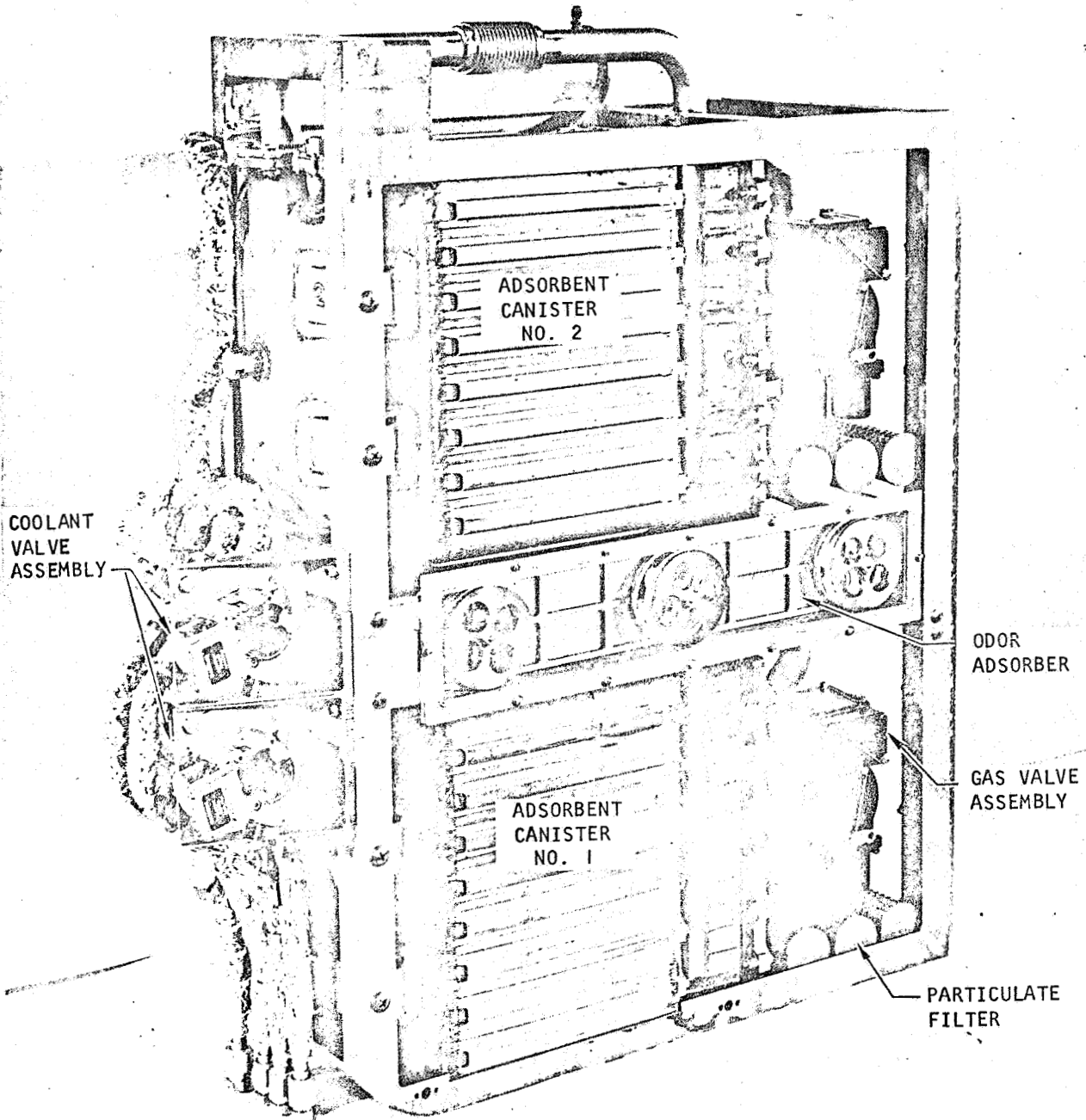
60018-46

F-8468

Figure 8-4. Regenerable CO_2 Removal System
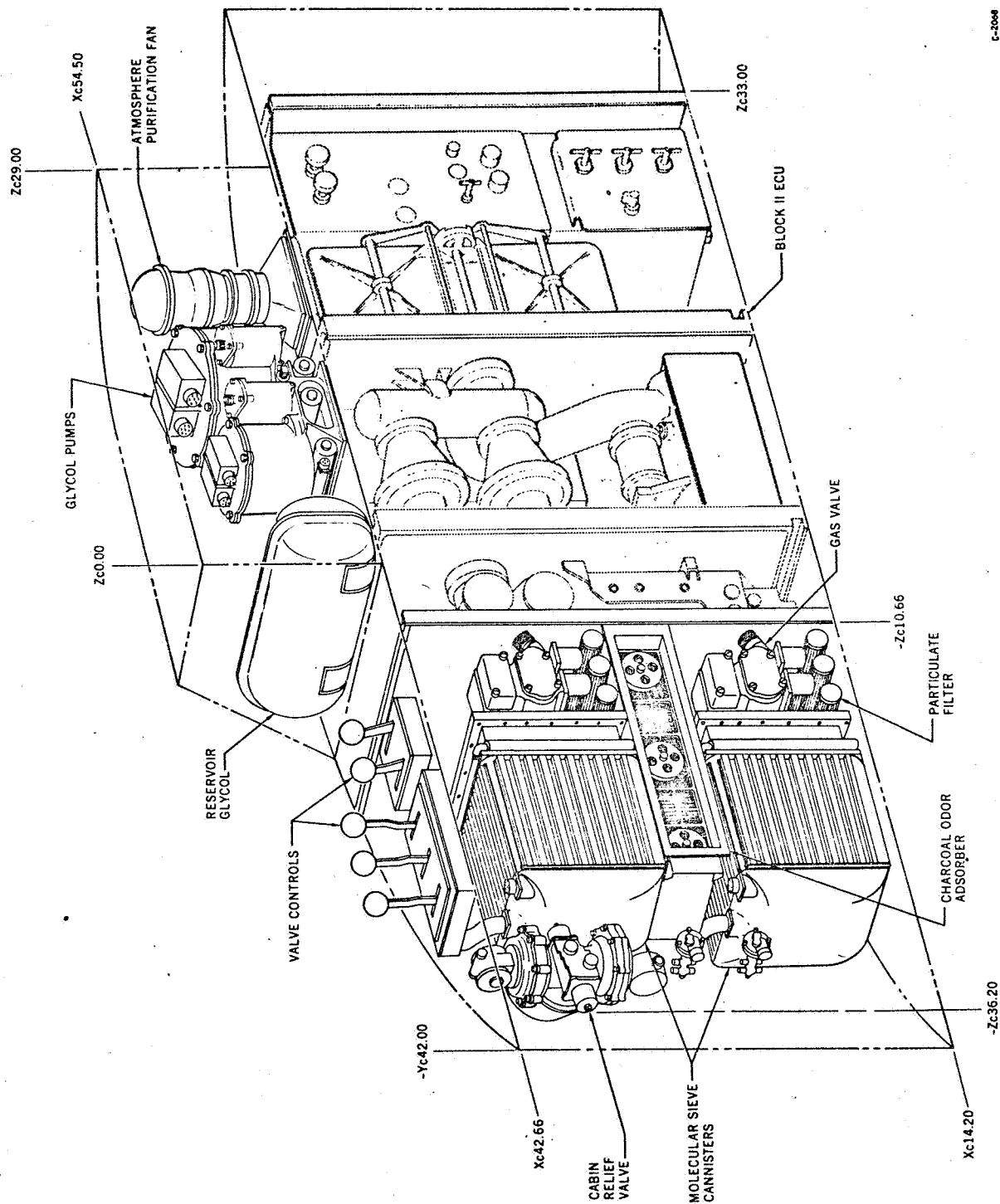
Figure 8-5. Regenerative CO_2 Removal System Integrated with the Apollo Block II ECS
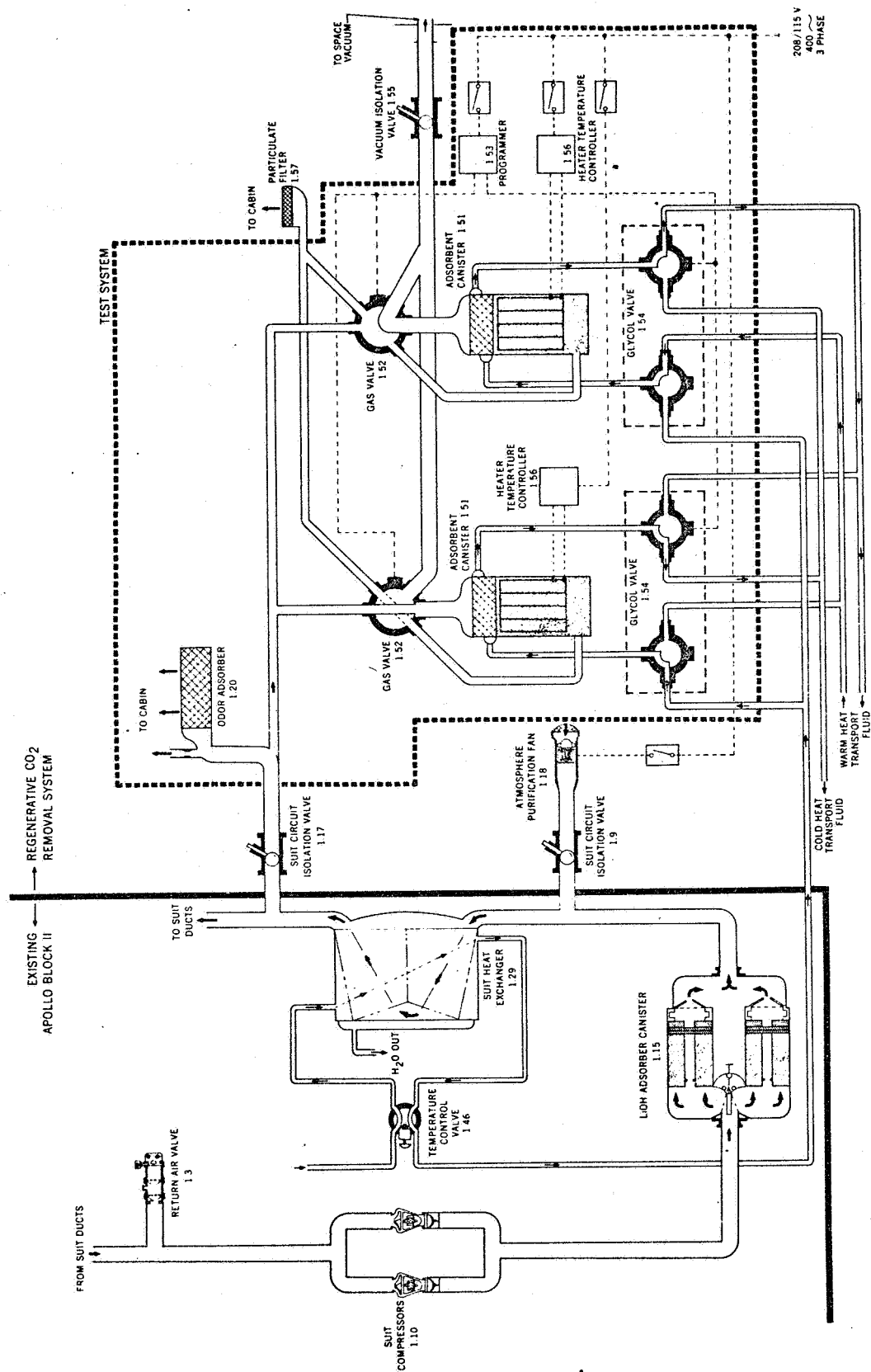
Figure 8-6. Schematic of AAP Regenerative CO_2 Removal System

APPENDIX A

THERMODYNAMICS OF ADSORPTION

Consider n moles of gas physically adsorbed upon an inert adsorbent and having energy E_s, entropy S_s, volume V_s, and area a. This adsorption, except for hysteresis, is then reversible. The energy of the system, by the first law of thermodynamics, is a perfect differential, and can be written as a function of the aforementioned extensive variables in the following manner:

$$dE = \left(\frac{\partial E}{\partial S}\right)_{V,n,a} dS + \left(\frac{\partial E}{\partial V}\right)_{S,n,a} dV + \left(\frac{\partial E}{\partial a}\right)_{S,V,n} da + \left(\frac{\partial E}{\partial n}\right)_{S,V,a} dn \qquad (A-1)$$

For simplicity, the subscripts s referring to the adsorbed phase have been omitted and will be understood implicity henceforth.

The differential coefficients are defined, respectively, to be the temperature, T, pressure, P, surface pressure, ϕ, and chemical potential μ, of the adsorbate with algebraic signs designated as follows:

$$dE = TdS - PdV - \phi da + \mu dn \qquad (A-2)$$

Since E is a homogeneous function of the first degree in extensive variables S, V, a, and n, Equation (A-2) integrates directly to

$$E = TS - PV - \phi a + \mu n \qquad (A-3)$$

Taking the total differential of each term in the preceding equation, the next relationship follows:

$$dE = TdS + SdT - PdV - VdP - \phi da - ad\phi + \mu dn + nd\mu \qquad (A-4)$$

If Equation (A-2) is subtracted from Equation (A-4), the result is

$$nd\mu = -SdT + VdP + ad\phi \qquad (A-5)$$

Let $\quad \Gamma_1 = \frac{a}{n},\ s = \frac{S}{n},$ and $v = \frac{V}{n}$; also $\Gamma = \frac{n}{a}$ and $e = \frac{E}{n}$ $\qquad (A-6)$

Then $\quad d\mu = -sdT + vdP + \Gamma d\phi \qquad (A-7)$

Consider now the gaseous phase in equilibrium with the adsorbate. It will be assumed that the pressure and temperature of this phase has become equal to those that have been designated T and P in the adsorbed layer. Then by a similar sequence of steps, the following applies to the gas phase where the subscript G refers to its state.

$$d\mu_G = -s_G dT + v_G \, dp \tag{A-8}$$

At equilibrium

$$\mu_G = \mu \tag{A-9}$$

consequently,

$$-sdT + vdP + \Gamma d\phi = -s_G dT + v_G \, dP \tag{A-10}$$

constant ϕ

$$\left(\frac{\partial P}{\partial T}\right)_\phi = \frac{(s_G - s)}{(v_G - v)} \tag{A-11}$$

At constant T

$$\left(\frac{\partial \phi}{\partial P}\right)_T = (v_G - v)\Gamma_1 \tag{A-12}$$

The preceding equation shows how to obtain ϕ from isothermal data which is the familiar Gibbs Isotherm for spreading of surface layers. Equation (A-11), on the other hand, is the analog of the usual change of phase equation such as the Clapeyron one. In fact, it can be written in more familiar form by means of Equation (A-3) and its counterpart for the gas phase.

Rewrite Equation (A-3) as follows for n = 1

$$\mu = e + Pv - Ts + \phi\Gamma_1 \tag{A-13}$$

Similarly, for the gas phase

$$\mu_G = e_G + Pv_G - Ts_G \tag{A-14}$$

Utilizing Equation (C-9)

$$e + Pv - Ts + \phi\Gamma = e_G + Pv_G - Ts_G \tag{A-15}$$

Then

$$T(s_G - s) = h_G - (h + \phi\Gamma_1) \tag{A-16}$$

where $h = e + Pv$.

The right-hand side of the preceding can be designated as a generalized Δh. Then Equation (A-11) can be written

$$\left(\frac{\partial P}{\partial T}\right)_\phi = \frac{\Delta h}{T\Delta v} \tag{A-17}$$

where $\Delta v = v_G - v$

Closer scrutiny of Equation (A-2) shows that the adsorbate state is really the difference between that of the pure solid and solid plus adsorbed phase, provided the subdivision and specific surface are retained. Then ϕ receives its interpretation as follows:

$$\phi a = (\gamma_o - \gamma)a \qquad (A-18)$$

where γ_o and γ represent the surface tensions before and after adsorption.

This is the equivalent of the spreading pressure encountered in other surface systems. As another consequence, the remaining variables of Equation (A-2) acquire their customary interpretation; e.g., P is the hydrostatic pressure.

As corollaries, if the solid is still assumed to be inert, the phase boundary can be rigidly designated as the solid surface and the quantities treated in the counterpart of Equation (A-2). The Gibbsian form of the suceeding relations derivable from Equation (A-2), dealing with surface excesses only, is indistinguishable from the foregoing results. On the other hand, if the solid plus adsorbate is treated as one phase and the treatment following Equation (A-2) is parallel, allowances for changes in dimensions in the adsorbant plus adsorbate can be allowed for. The results would still have the same form.

For changes in dimension, use Equation (A-7) with the understanding that it refers to the last named system. Then

$$\left(\frac{\partial \mu}{\partial v}\right)_{T,\phi} = \left(\frac{\partial \mu}{\partial p}\right)_{T,\phi} \left(\frac{\partial p}{\partial v}\right)_{T,\phi} \qquad (A-19)$$

or

$$\left(\frac{\partial \mu}{\partial v}\right)_{T,\phi} = v\left(\frac{\partial p}{\partial v}\right)_{T,\phi} = -B \qquad (A-20)$$

utilizing the usual definition of bulk modulus.

If Equation (A-7) is integrated at constant T and P employing the same technique as with Equation (A-2),

$$\mu \quad \Gamma_1 \phi \qquad (A-21)$$

Therefore, isosteric measurements of size changes should be feasible. The literature now abounds with them. The surface tensions of the pure solids have been obtained in some cases by heats of solution of various areas extrapolated to zero area. Otherwise the third law of thermodynamics is used to measure s and h by means of the ΔC_p of the elements. Apply Equation (A-16)

to the pure solid alone. The Δ sign signifies formation from the elements, and Γ_1 becomes the specific surface area,

$$T\Delta s = \Delta h - \gamma_0 \Gamma_1 \qquad (A-22)$$

$$\gamma_0 \Gamma_1 = \Delta h - T\Delta s \qquad (A-23)$$

where ϕ has now been replaced by γ_0. Equation $(A-23)$ is the basis of the Jura-Garland method.

The above exhausts what thermodynamics can supply in the way of measurement elucidation. Mobility on the surface may be deduced from the measurements described by Equations $(A-11)$ and $(A-12)$. The importance for bed studies has been expounded in the technical section.

To detect the condition of the surface groups of the solid that because of their unsaturated valences or defects possess permanent magnetic moments, magnetic resonance techniques are finding increasing use. The changes in the gaseous adsorbate upon its condensation are now being studied by infrared absorption spectrometry. The nature of the adsorption forces for physical adsorption can then be characterized more fully and a better formulation made of the van der Waal's forces.

FUNDAMENTALS OF MASS BALANCES AND THEIR SIMPLIFICATION

Partial Molal Volumes and Their Possible Simplification of the Diffusion Equation

$$dV = \left(\frac{\partial V}{\partial T}\right)_{P,N_i} dt + \left(\frac{\partial V}{\partial P}\right)_{T,N_i} dP + \left(\frac{\partial V}{\partial N_i}\right)_{T,P,N_j \atop j \neq i} dN_i \qquad (B-1)$$

Let $\qquad \overline{V}_i = \dfrac{\partial V}{\partial N_i}$

(Note: A subscript that appears twice in a product implies a summation.)

Assume an infinitesimal change $d\eta$, all else constant such as

$$dV = V d\eta \qquad dN_i = N_i d\eta$$

The change is made holding all else constant

$$V d\xi = \overline{V}_i N_i d\eta$$

or $\qquad V = \overline{V}_i N_i \qquad\qquad\qquad\qquad (B-2)$

The following Gibbs-Duhem relation then can be applied

$$\left(\frac{\partial V}{\partial T}\right)_{P,N_i} dT + \left(\frac{\partial V}{\partial P}\right)_{t,N_i} dP + \overline{V}_i dN_i = \overline{V}_i dN_i + N_i d\overline{V}_i$$

or $\qquad \left(\dfrac{\partial V}{\partial T}\right)_{P,N_i} dT + \left(\dfrac{\partial V}{\partial T}\right)_{T,N_i} dP = N_i d\overline{V}_i \qquad (B-3)$

Equation (B-2) can be rewritten as follows:

Let m_i be the mass of species i, and M the mol. wt.

$$V = \overline{V}_i \frac{m_i}{M_i}$$

Then, if

$$\rho_i = \frac{m_i}{V}$$

$$1 = \frac{\bar{V}_i}{M_i} \rho_i \tag{B-4}$$

which is the relation that is desired.

For a binary system

$$1 = \frac{\bar{V}_A}{M_A} \rho_A + \frac{\bar{V}_B}{M_B} \rho_B \tag{B-5}$$

Another relation that is needed is

$$\frac{\partial \rho_A}{\partial \omega_A}$$

where

$$\omega_A = \frac{\rho_A}{\rho}$$

since

$$\nabla \rho_A = \frac{\partial \rho_A}{\partial \omega_A} \nabla \omega_A \tag{B-6}$$

From Equation (B-2) for binary system

$$V = \bar{V}_A N_A + \bar{V}_B N_B$$

$$V = \frac{\bar{V}_A}{M_A} m_A + \frac{V_\ell}{M_\ell} m_B$$

If the preceding equation is divided by m, the total mass,

$$\frac{1}{\rho} = \frac{\bar{V}_A}{M_A} \omega_A + \frac{\bar{V}_B}{M_B} \omega_B \tag{B-7}$$

The same result also follows from Equation (B-5)

$$d\left(\frac{1}{\rho}\right) = \frac{\bar{V}_A}{M_A} d\omega_A + \frac{\bar{V}_B}{M_B} d\omega_B$$

But
$$\omega_A + \omega_B = 1$$

$$d\omega_A = -d\omega_B$$

$$d\left(\frac{1}{\rho}\right) = \left(\frac{\overline{V}_A}{M_A} - \frac{\overline{V}_B}{M_B}\right) d\omega_A \qquad (B-8)$$

$$-\frac{1}{\rho^2}\frac{d\rho}{d\omega_A} = \frac{\overline{V}_A}{M_A} - \frac{\overline{V}_B}{M_B}$$

$$\frac{1}{\rho^2}\frac{d\rho}{d\omega_A} = \frac{\overline{V}_B}{M_B} - \frac{\overline{V}_A}{M_A}$$

$$\frac{d\rho}{d\omega_A} = \rho^2\left(\frac{\overline{V}_B}{M_B} - \frac{\overline{V}_A}{M_A}\right)$$

$$\rho_A = \rho\,\omega_A$$

$$\frac{d\rho_A}{d\omega_A} = \omega_A\frac{d\rho}{d\omega_A} + \rho$$

$$\frac{d\rho_A}{d\omega_A} = \rho + \rho^2\omega_A\left(\frac{\overline{V}_B}{M_B} - \frac{\overline{V}_A}{M_A}\right)$$

$$\frac{d\rho_A}{d\omega_A} = \rho\left[1 + \rho_A\left(\frac{\overline{V}_B}{M_B} - \frac{\overline{V}_A}{M_A}\right)\right]$$

$$\frac{d\rho_A}{d\omega_A} = \rho\left(\rho_A\frac{V_A}{M_A} + \rho_B\frac{\overline{V}_B}{M_B} + \rho_A\frac{\overline{V}_B}{M_B} - \rho_A\frac{\overline{V}_A}{M_A}\right)$$

Thus,
$$\frac{d\rho_A}{d\omega_A} = \rho^2\frac{\overline{V}_B}{M_B} \qquad (B-9)$$

Now the relation between the following is desired

$$\vec{j}_A \quad \text{and} \quad \vec{j}_A^{\,0}$$

where $\quad \vec{j_A} = \rho_A(\vec{v_A} - \vec{v})$ $\qquad \vec{v} = \omega_A \vec{v_A} + \omega_B \vec{v_B}$ $\qquad$ (B-10)

and $\quad \vec{j_A^o} = \rho_A(\vec{v_A} - \vec{v^o})$ $\qquad \vec{v^o} = \rho_A \vec{v_A} \dfrac{\bar{V_A}}{M_A} + \rho_B \vec{v_B} \dfrac{\bar{V_B}}{M_B}$ $\qquad$ (B-11)

If the following is considered

$$\rho \vec{j_A} = \rho \left[\rho_A \vec{v_A} - \rho_A \omega_A \vec{v_A} - \rho_A \omega_B \vec{v_B} \right]$$

$$= \rho \left[\rho_A \vec{v_A}(1 - \omega_A) - \rho_A \vec{v_B} \omega_B \right]$$

$$= \rho \left[\rho_A \omega_B (\vec{v_A} - \vec{v_B}) \right]$$

$$= \rho_A \rho_B (\vec{v_A} - \vec{v_B}) \qquad (B-12)$$

and it $\qquad \vec{j_A^o} = \rho_A \left[\vec{v_A} - \rho_A \vec{v_A} \dfrac{V_A}{M_A} - \rho_B \vec{v_B} \dfrac{\bar{V_B}}{M_B} \right]$

$$= \rho_A \left[\rho_A \dfrac{\bar{V_A}}{M_A} \vec{v_A} + \rho_B \dfrac{\bar{V_B}}{M_B} \vec{v_A} - \rho_A \dfrac{\bar{V_A}}{M_A} \vec{v_A} - \rho_B \vec{v_B} \dfrac{\bar{V_B}}{M_B} \right]$$

$$= \rho_A \rho_B \dfrac{\bar{V_B}}{M_B} (\vec{v_A} - \vec{v_B}) \qquad (B-13)$$

$$\therefore \vec{j_A} = \rho \dfrac{V_B}{M_B} \vec{j_A} \qquad (B-14)$$

Fick's first law of diffusion is commonly written

$$\vec{j_A} = -\rho D_{AB} \nabla \omega_A \qquad (B-15)$$

From Equation (B-6)

$$\nabla \omega_A = \frac{1}{\partial \rho_A / \omega_A} \nabla \rho_A$$

From Equation (B-9)

$$\nabla \omega_A = \frac{1}{\rho^2 \frac{\overline{V}_B}{M_B}} \nabla \rho_A$$

Therefore, the following is obtained

$$\vec{j}_A = \frac{D_{AB}}{\rho \frac{V_B}{M_B}} \nabla \rho_A$$

and, by substitution from Equation (B-14), the following expression results:

$$\vec{j}_A^o = -D_{AB} \nabla \rho_A \qquad (B-16)$$

This last expression is more suitable, since it shows that the concentration gradient rather than the mass fraction gradient can be used as the "driving force for diffusion."

Utilization of the Preceding Expression in the Equation of Mass Transport With Chemical, Mechanical, and Thermal Equilibrium

The total material balance is

$$\frac{\partial \rho_i}{\partial t} = -\nabla \cdot (\rho_i \vec{v}_i) \qquad (B-17)$$

where $\rho_i v_i$ represents the total mass flux due to each of the components

$$\rho_i \vec{v}_i = \rho_i (\vec{v}_i - \vec{v}^o) + \rho_i \vec{v}^o$$

$$\rho_i \vec{v}_i = \vec{j}_i^o + \rho_i \vec{v}^o \qquad (B-18)$$

$$\frac{\partial \rho_i}{\partial t} = \nabla \cdot \vec{j}_i^o + \nabla \cdot (\rho_i \vec{v}^o)$$

$$\nabla \cdot (\rho_i \vec{v}^o) = \rho_i (\nabla \cdot \vec{v}^o) + (\vec{v}^o \cdot \nabla) \rho_i$$

The equality $\nabla \cdot \vec{v}^o = 0$ must be demonstrated. For this purpose,

Let
$$\hat{V}_i = \frac{V_i}{M_i}$$

then
$$\sum \rho_i \hat{V}_i = 1 \tag{B19}$$

$$\sum \left(\hat{V}_i \frac{\partial \rho_i}{\partial t} + \rho_i \frac{\partial \hat{V}_i}{\partial t} \right) = 0$$

and

$$\frac{\partial \rho_i}{\partial t} = - \nabla \cdot (\rho_i \vec{v}_i)$$

Equation (B-19) then becomes

$$\sum \left[-\hat{V}_i \nabla \cdot (\rho_i \vec{v}_i) + \rho_i \frac{\partial \hat{V}_i}{\partial t} \right] = 0$$

$$\nabla \cdot (\rho_i \vec{v}_i) = \rho_i \nabla \cdot \vec{v}_i + (\vec{v}_i \cdot \nabla) \rho_i$$

$$-V_i \nabla \cdot (\rho_i v_i) = -\nabla \cdot (\rho_i \hat{V}_i \vec{v}) + \rho_i \vec{v}_i \cdot \nabla \hat{V}_i$$

but

$$\sum \nabla \cdot (\rho_i \hat{V}_i \vec{v}) = \nabla \cdot \vec{v}^{\circ}$$

and consequently

$$\nabla \cdot \vec{v}^{\circ} = \sum \rho_i \left(\frac{\partial \hat{V}_i}{\partial t} + \vec{v}_i \cdot \nabla \hat{V}_i \right) \tag{B-20}$$

Assuming that $\hat{V}_i$ are uniform and that there is no acceleration, it then follows that

$$\nabla \cdot \vec{v}^{\circ} = 0 \tag{B-21}$$

It must be noticed that if in addition to the previous conditions, the pressure gradients are small, as would be the case for the motion through the pores of a bed particle, v° is zero as shown in Reference D9.

Application to the Fixed Bed Problem

Let

$$\vec{v}^{\circ} = \vec{k} v$$

where v is the superficial velocity through the bed, and if v is independent of concentration, it can be considered to be uniform over the bed length. In this equation k is a unit vector in the z direction.

Then if ϵ is the external void fraction in the bed, and considering mass transfer diffusion only,

$$\frac{\partial \rho_i}{\partial t} = -\nabla \cdot \vec{\jmath}_A^{\,0} - (\vec{v}^{\,0} \cdot \nabla) \rho_A \tag{B-22}$$

Using Equation (B-16)

$$\frac{\partial \rho_A}{\partial t} = -(v^i \cdot \nabla) \rho_A + D_{AB} \nabla \rho_A$$

Now let $v^0 = kv$ and $D_{AB} \cong E$, the diffusivity for both molecular and and eddy transport in the stream flowing in the external voids. Also, the concentration of mass A in the flowing stream will be denoted by C and that in the pores of the stationary bed by $\bar{C}$. The superficial motion is taken to occur in the z direction. The mass balance for the flowing stream then becomes

$$\epsilon \frac{\partial c}{\partial t} + (1-\epsilon) \frac{\partial \bar{c}}{\partial t} = -v \frac{\partial c}{\partial z} + \epsilon \frac{\partial^2 c}{\partial z^2}$$

or

$$E \frac{\partial^2 c}{\partial z^2} = v \frac{\partial c}{\partial z} + \epsilon \frac{\partial c}{\partial t} + (1-\epsilon) \frac{\partial \bar{c}}{\partial t} \tag{B-22}$$

Here it has been assumed that pore diffusion is the sole mode of disappearance of mass A from the flowing stream.

By virtue of the remarks following Equation (B-21) there is no convective velocity term for pore diffusion and Equation (4-19) of Section 4 applies.

The interfacial concentrations are related by

$$\bar{C} = f(\omega)$$

where w is obtained from the process occurring on the surfaces of the solid pores.

APPENDIX C

RESULTS OF LABORATORY
ADSORPTION AND DESORPTION OF CO_2
ON MOLECULAR SIEVE AND H_2O
ON SILICA GEL
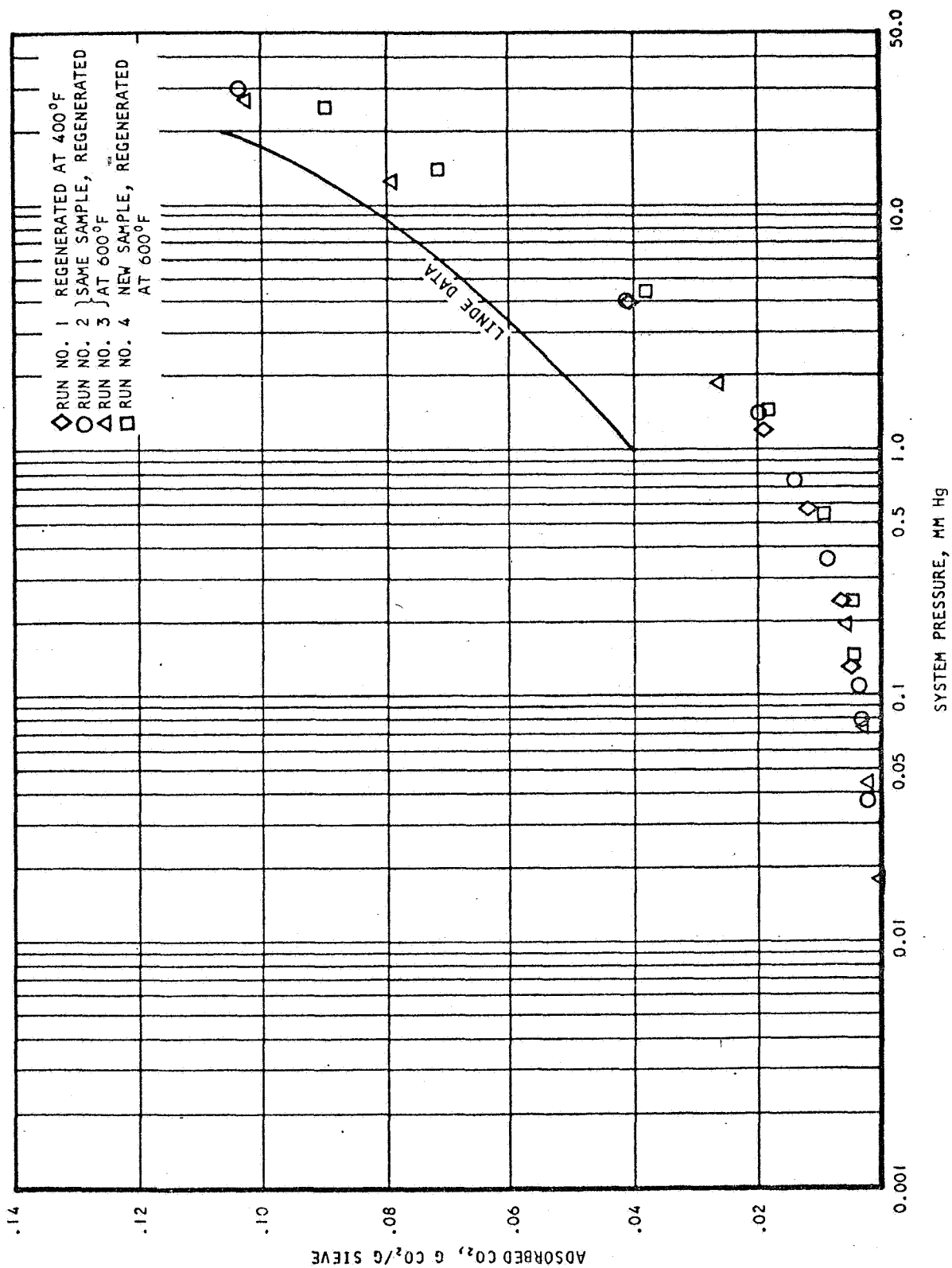
Figure C-1. Equilibrium Isotherms of Carbon Dioxide Adsorption on Linde Type 5A, 1/16 in. Diameter Pellets at 25°C
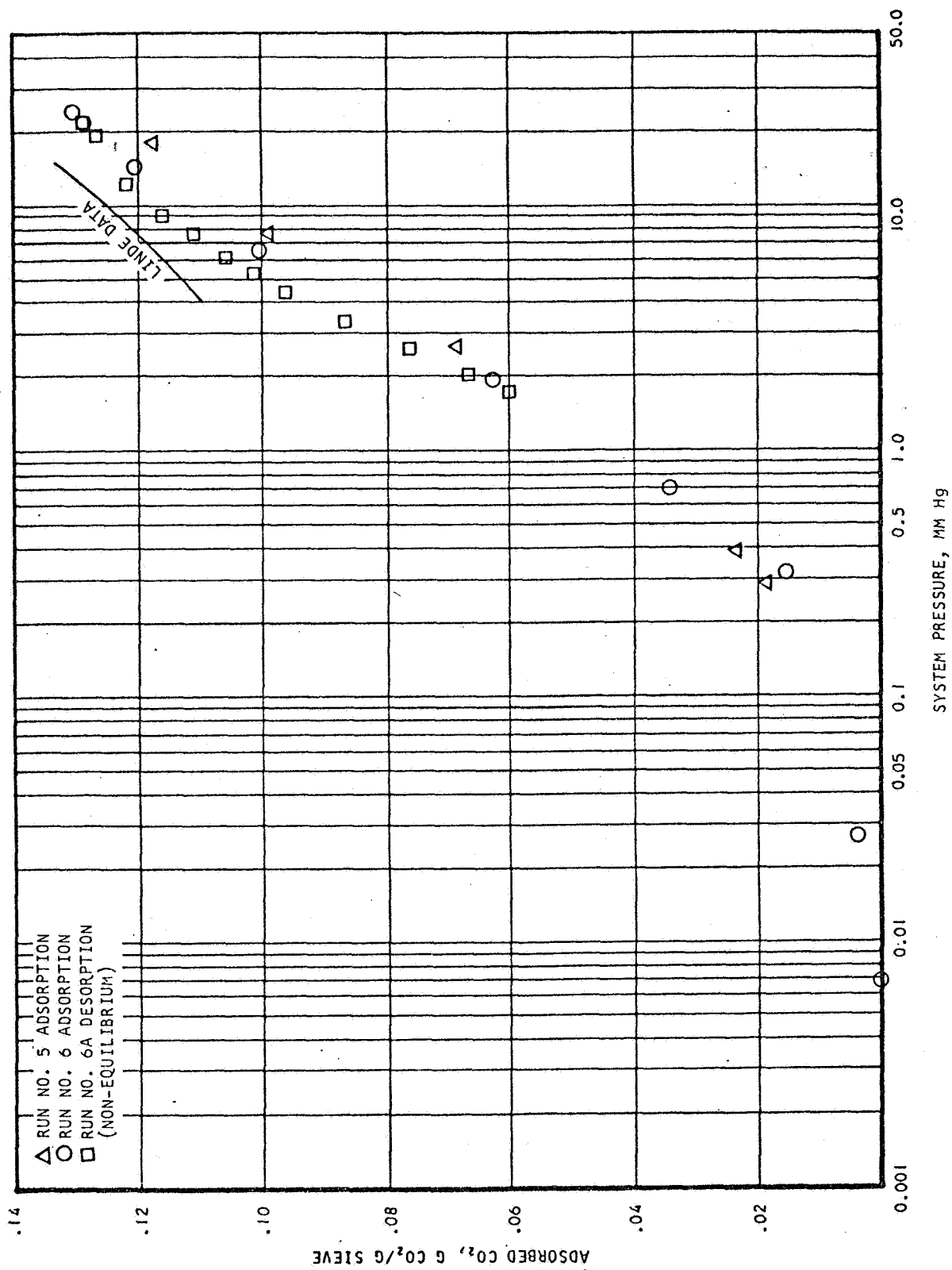
A-21997

Figure C-2. Equilibrium and Non-Equilibrium Isotherms of Carbon Dioxide during Adsorption and Desorption on Linde Type 5A, 1/16 in. Diameter Pellets at 0°C

A-22000
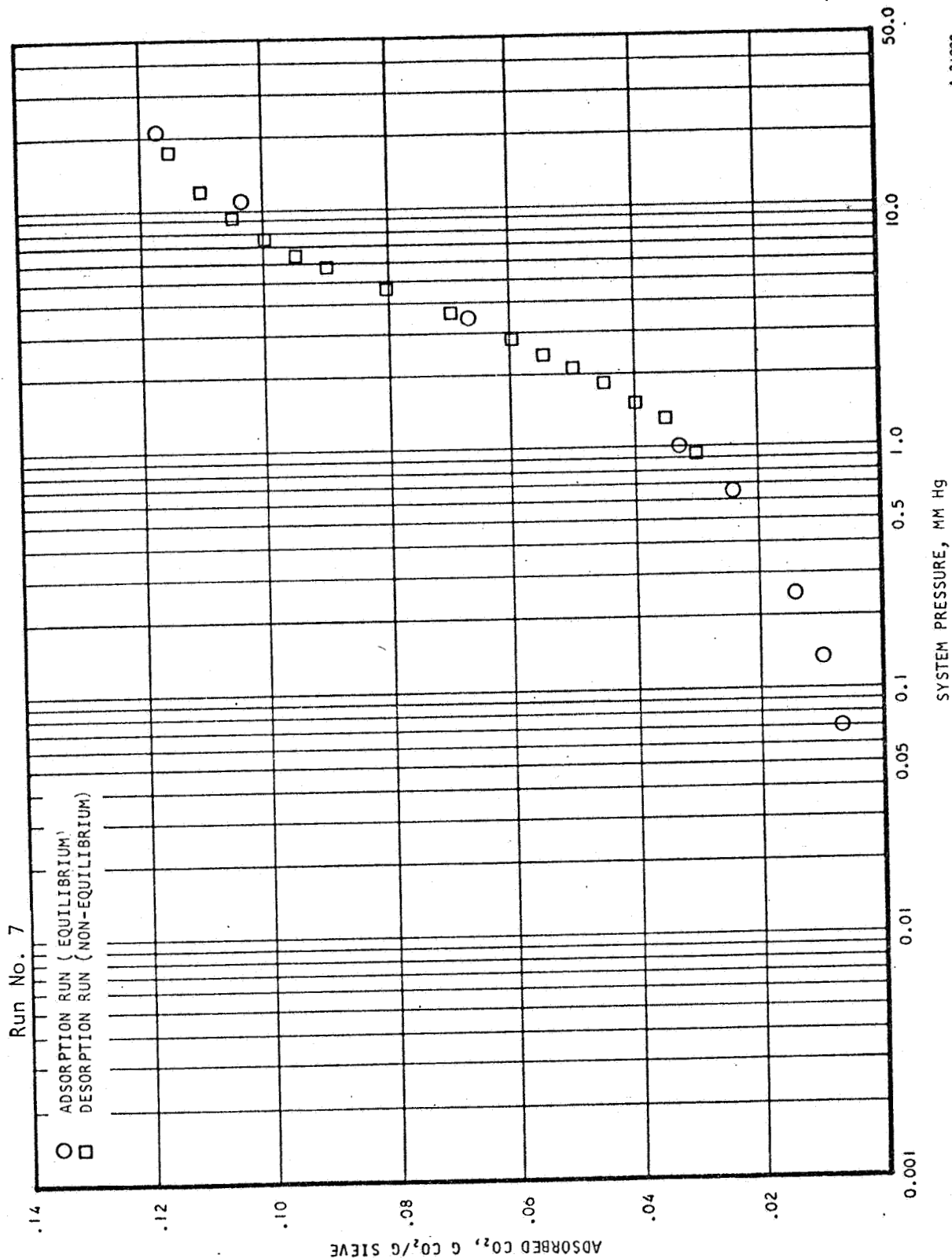
Figure C-3. Equilibrium and Non-Equilibrium Isotherms of Carbon Dioxide Adsorption and Desorption on Linde Type 5A, 1/16 in. Diameter Pellets at 10.5°C
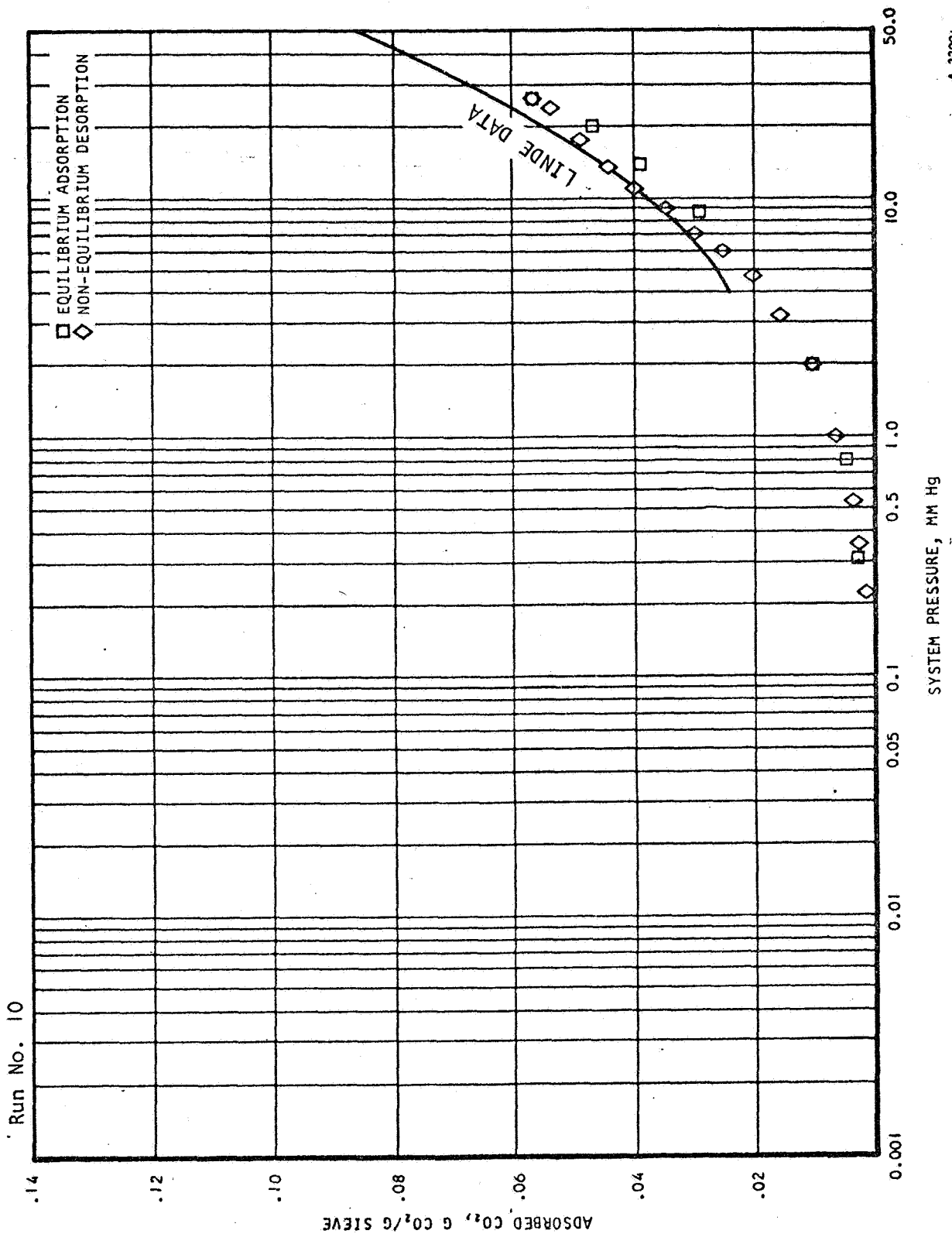
Figure C-4. Equilibrium and Non-Equilibrium Isotherms of Carbon Dioxide Adsorption and Desorption on Linde Type 5A, 1/16 in. Diameter Pellets at 50°C

A-22001
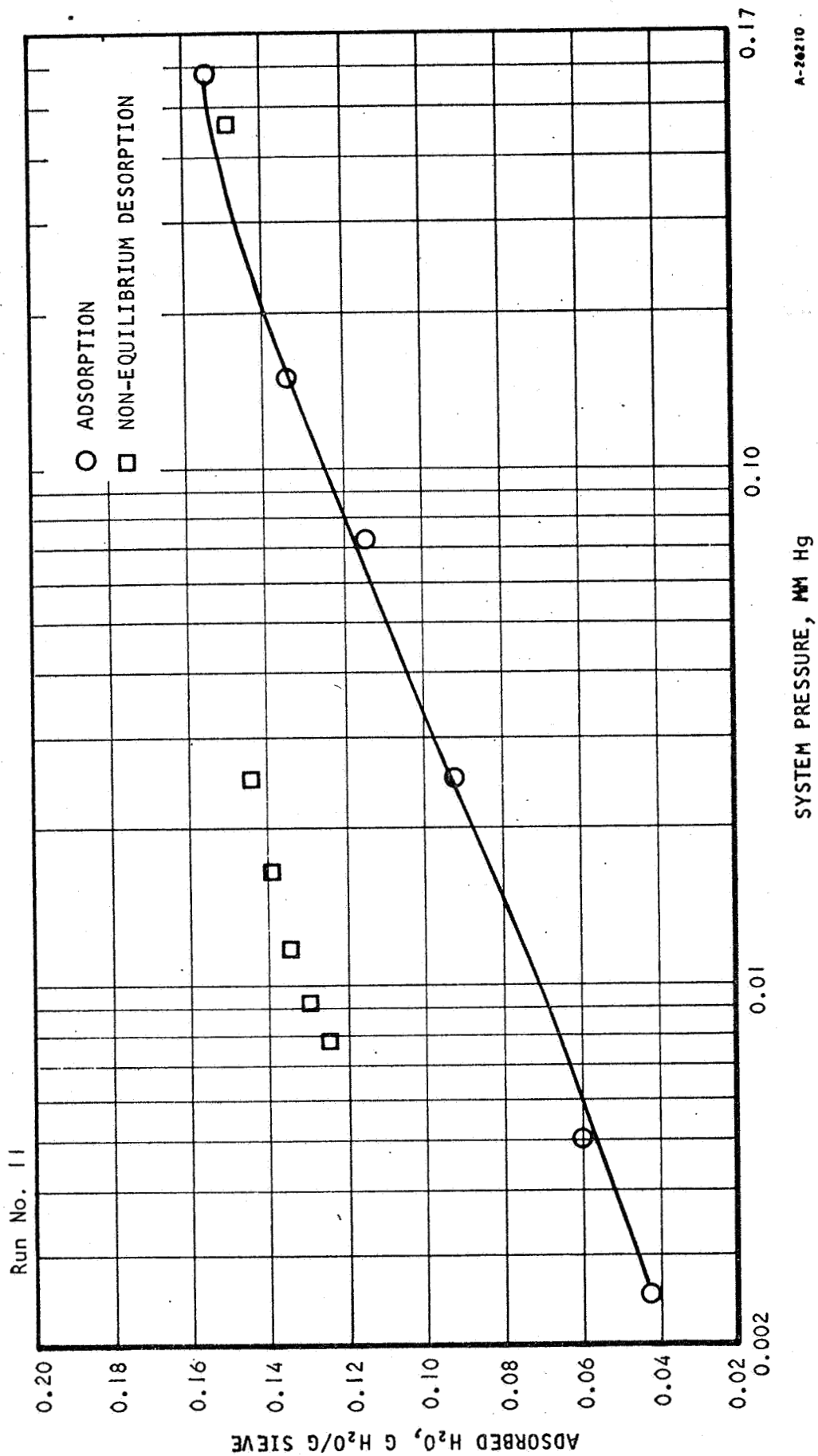
Figure C-5. Equilibrium and Non-Equilibrium Isotherms of Water Vapor Adsorption and Desorption on Linde Type 5A, 1/16 in. Diameter Pellets at 25°C
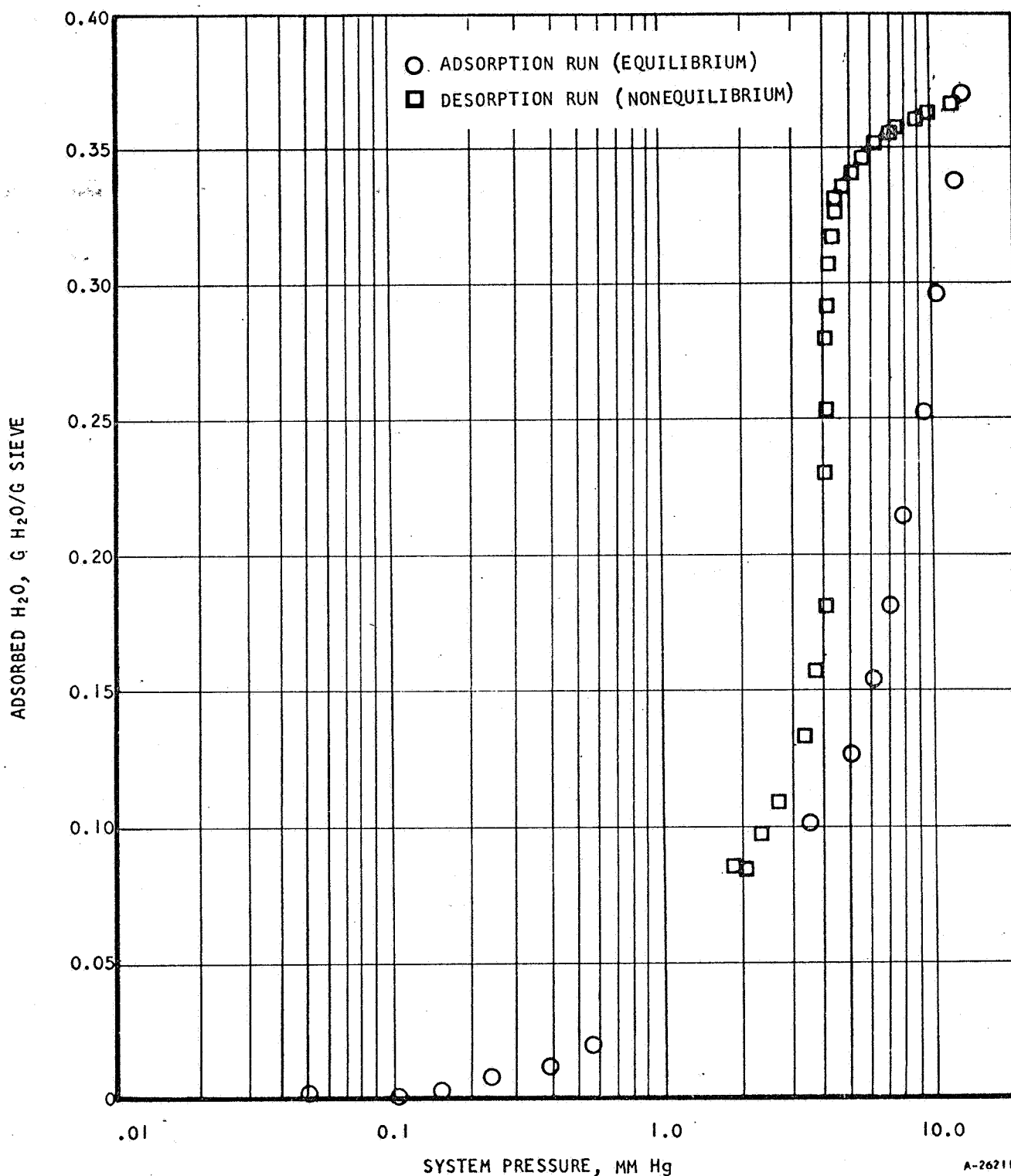
Figure C-6.   Equilibrium and Nonequilibrium Isotherms of Water Vapor Adsorption
and Desorption on Davison Type 05, 6-16 Mesh Silical Gel at 25°C

Run No. 2

CARRIER GAS = DRY NITROGEN
AVERAGE FLOW = 1.265 L/MIN (STD)
AVERAGE CO_2 INLET CONCENTRATION = 2.73 PERCENT = 7.15 mm Hg
BED WEIGHT = 24.5g
BED HEIGHT = 7.2 IN., BED I.D. = 5/8 IN.
AVERAGE SYSTEM PRESSURE = 10.32 IN. Hg = 5.07 PSIA
DESORBED AT 600°F UNDER VACUUM
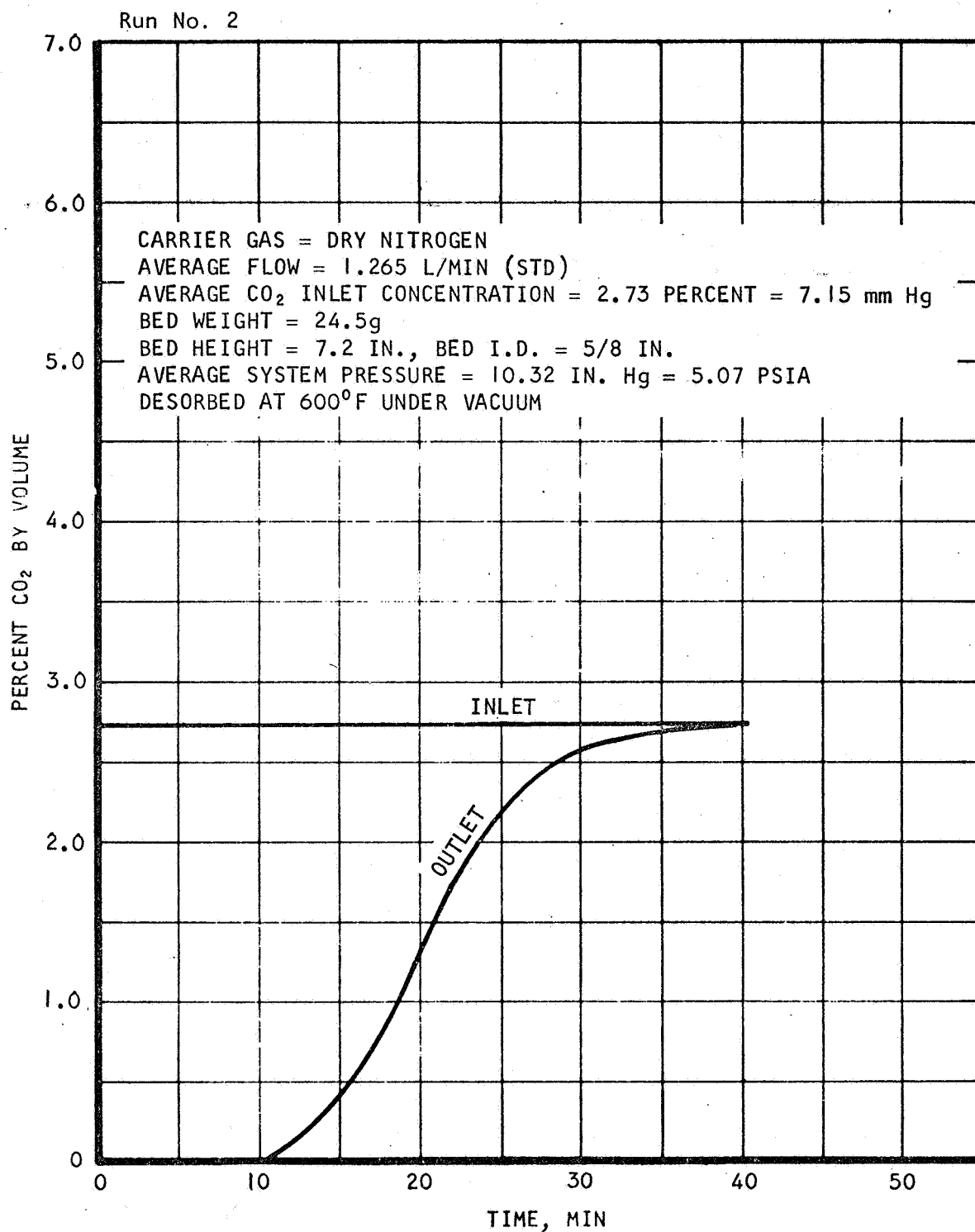
A-22022

Figure C-7. Dynamic Adsorption of CO_2 on Linde Molecular Sieve,
Type 5A, 1/16 in. Diameter Pellets at 25°C

Run No. 2

CARRIER GAS = DRY NITROGEN
AVERAGE FLOW = 1.265 L/MIN (STD)
AVERAGE CO_2 INLET CONCENTRATION = 2.73 PERCENT = 7.15 MM Hg
BED WEIGHT = 24.5g
BED HEIGHT = 7.2 IN., BED I.D. = 5/8 IN.
AVERAGE SYSTEM PRESSURE = 10.32 IN. Hg = 5.07 PSIA
DESORBED AT 600°F UNDER VACUUM

PERCENT BREAKTHROUGH

TIME, MIN
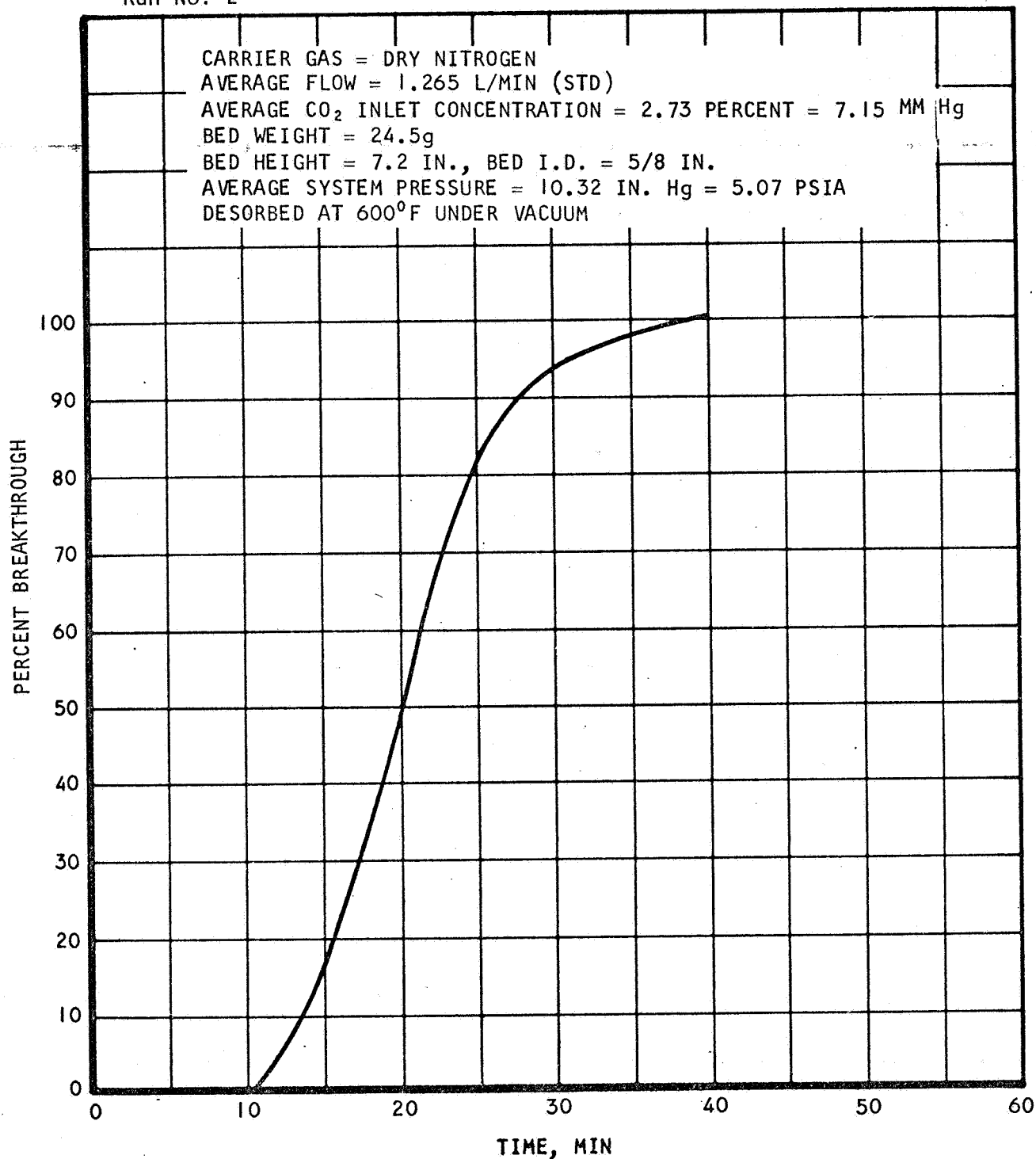
A-22003

Figure C-8. Breakthrough of CO_2 from Linde Molecular Sieve, Type 5A,
1/16 in. Diameter Pellets at 25°C

Run No. 3

CARRIER GAS = DRY NITROGEN
AVERAGE FLOW = 0.557 L/MIN (STD)
AVERAGE CO$_2$ INLET CONCENTRATION = 2.70 PERCENT = 7.13 mm Hg
BED WEIGHT = 24.5g
BED HEIGHT = 7.2 IN., BED I.D. = 5/8 IN.
AVERAGE SYSTEM PRESSURE = 10.39 IN. Hg = 5.10 PSIA
DESORBED AT 600°F UNDER VACUUM

INLET

OUTLET

PERCENT CO$_2$ BY VOLUME

TIME, MIN
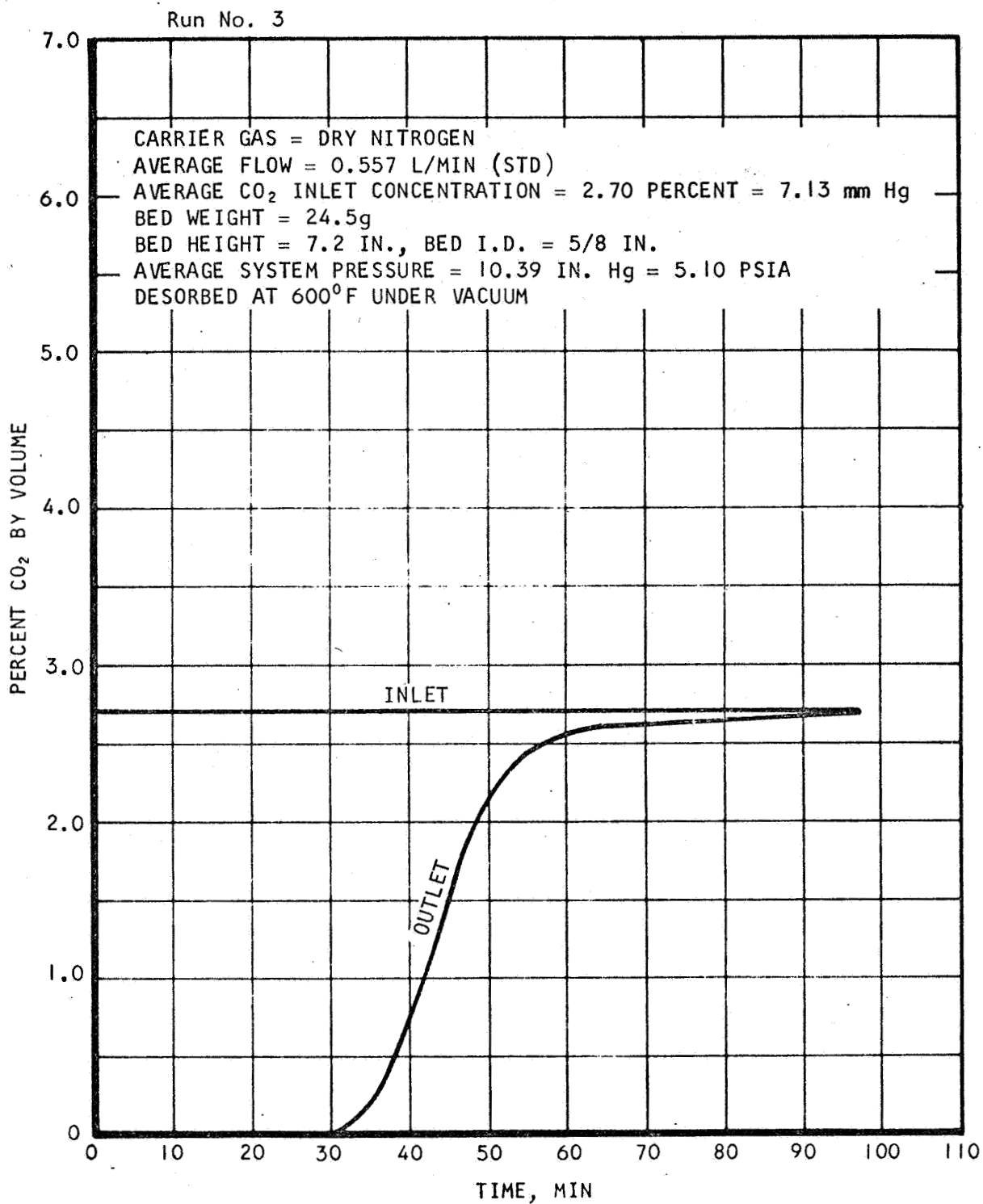
A-22021

Figure C-9.   Dynamic Adsorption of CO$_2$ on Linde Molecular Sieve
Type 5A, 1/16 in. Diameter Pellets at 25°C

Run No. 3

CARRIER GAS = DRY NITROGEN
AVERAGE FLOW = 0.557 L/MIN (STD)
AVERAGE CO_2 INLET CONCENTRATION = 2.70 PERCENT = 7.13 mm Hg
BED WEIGHT = 24.5g
BED HEIGHT = 7.2 IN., BED I.D. = 5/8 IN.
AVERAGE SYSTEM PRESSURE = 10.39 IN. Hg = 5.10 PSIA
DESORBED AT 600°F UNDER VACUUM

PERCENT BREAKTHROUGH

TIME, MIN
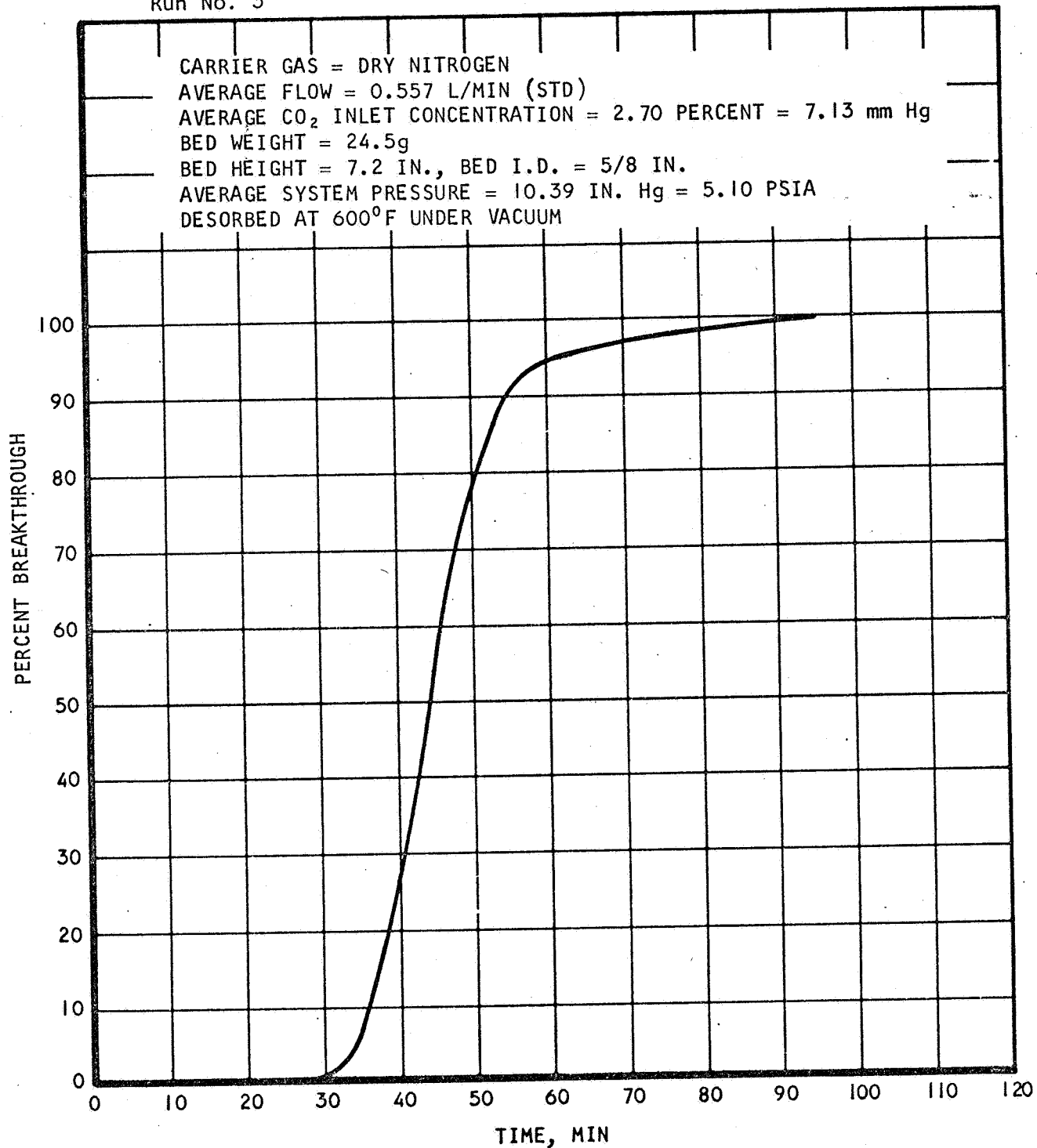
A-22005

Figure C-10. Breakthrough of CO_2 from Linde Molecular Sieve, Type 5A, 1/16 in. Diameter Pellets at 25°C

Run No. 4

CARRIER GAS = DRY NITROGEN
AVERAGE FLOW = 1.275 L/MIN (STD)
AVERAGE CO_2 INLET CONCENTRATION = 2.71 PERCENT = 7.12 mm Hg
BED WEIGHT = 24.5g
BED HEIGHT = 7.2 IN., BED I.D. = 5/8 IN.
AVERAGE SYSTEM PRESSURE = 10.35 IN. Hg = 5.08 PSIA
DESORBED AT 600°F UNDER VACUUM

INLET
OUTLET

PERCENT CO_2 BY VOLUME

TIME, MIN
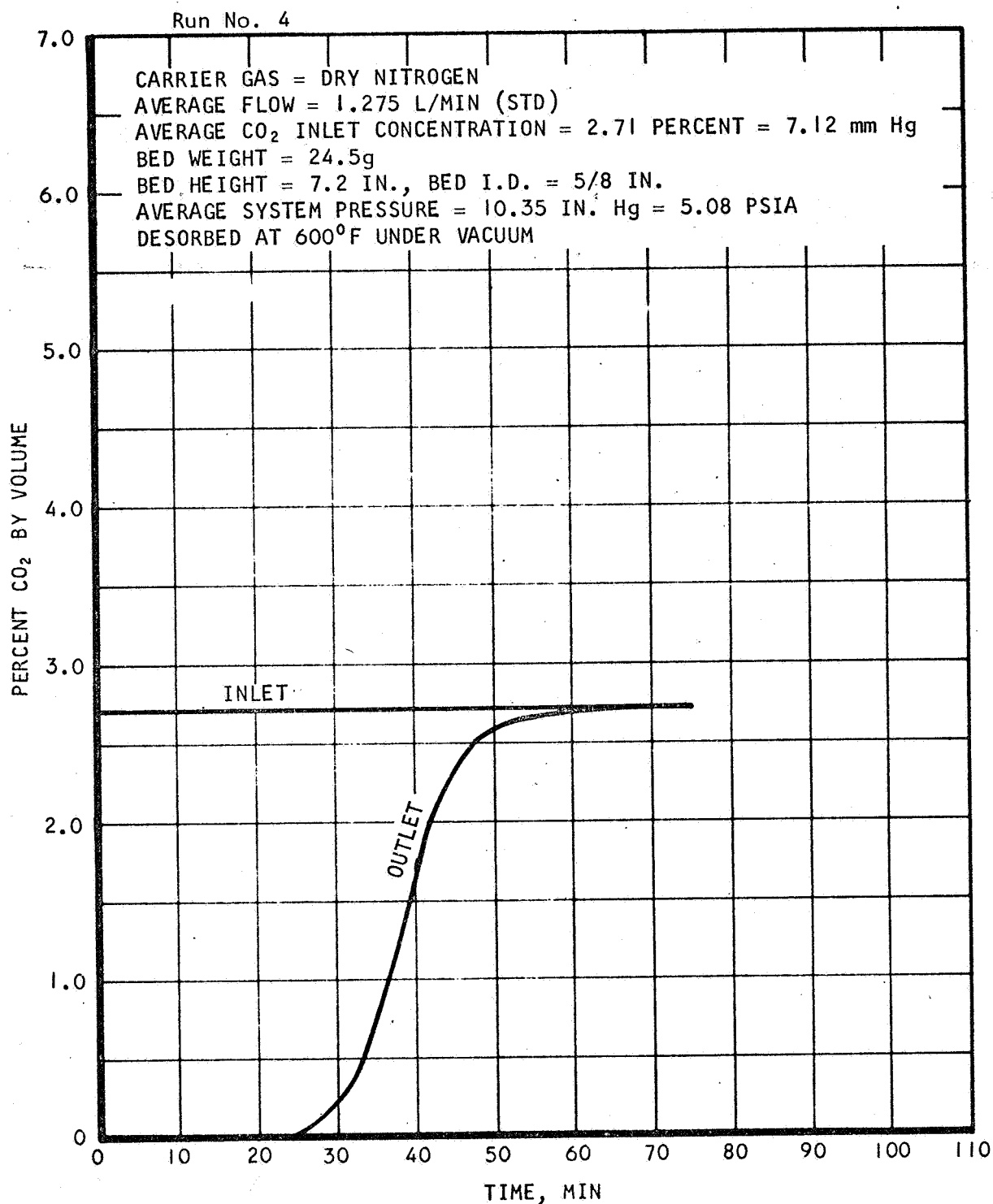
A-22023

Figure C-11.   Dynamic Adsorption of CO_2 on Linde Molecular Sieve
Type 5A, 1/16 in. Diameter Pellets at 0°C

Run No. 4

CARRIER GAS = DRY NITROGEN
AVERAGE FLOW = 1.275 L/MIN (STD)
AVERAGE CO_2 INLET CONCENTRATION = 2.71 PERCENT = 7.12 mm Hg
BED WEIGHT = 24.5g
BED HEIGHT = 7.2 IN., BED I.D. = 5/8 IN.
AVERAGE SYSTEM PRESSURE = 10.35 IN. Hg = 5.08 PSIA
DESORBED AT 600°F UNDER VACUUM

PERCENT BREAKTHROUGH

TIME, MIN
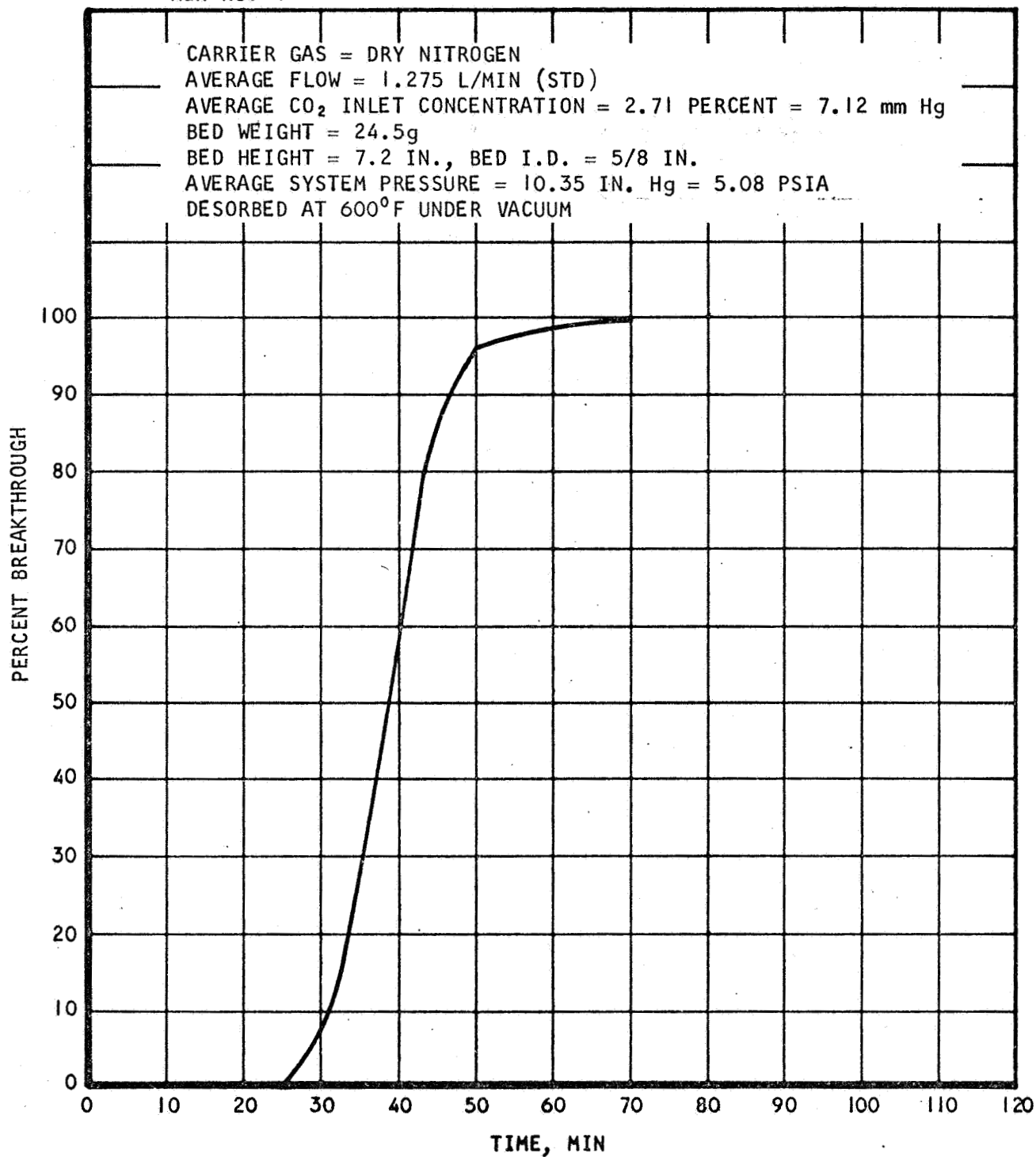
A-22006

Figure C-12.   Breakthrough of CO_2 from Linde Molecular Sieve, Type 5A,
1/16 in. Diameter Pellets at 0°C

Run No. 5

CARRIER GAS = DRY NITROGEN
AVERAGE FLOW = 0.561 L/MIN (STD)
AVERAGE CO_2 INLET CONCENTRATION = 1.93 PERCENT = 7.03 mm Hg
BED WEIGHT = 24.5g
BED HEIGHT = 7.2 IN., BED I.D. = 5/8 IN.
AVERAGE SYSTEM PRESSURE = 14.35 IN. Hg = 7.05 PSIA
DESORBED AT 600°F UNDER VACUUM
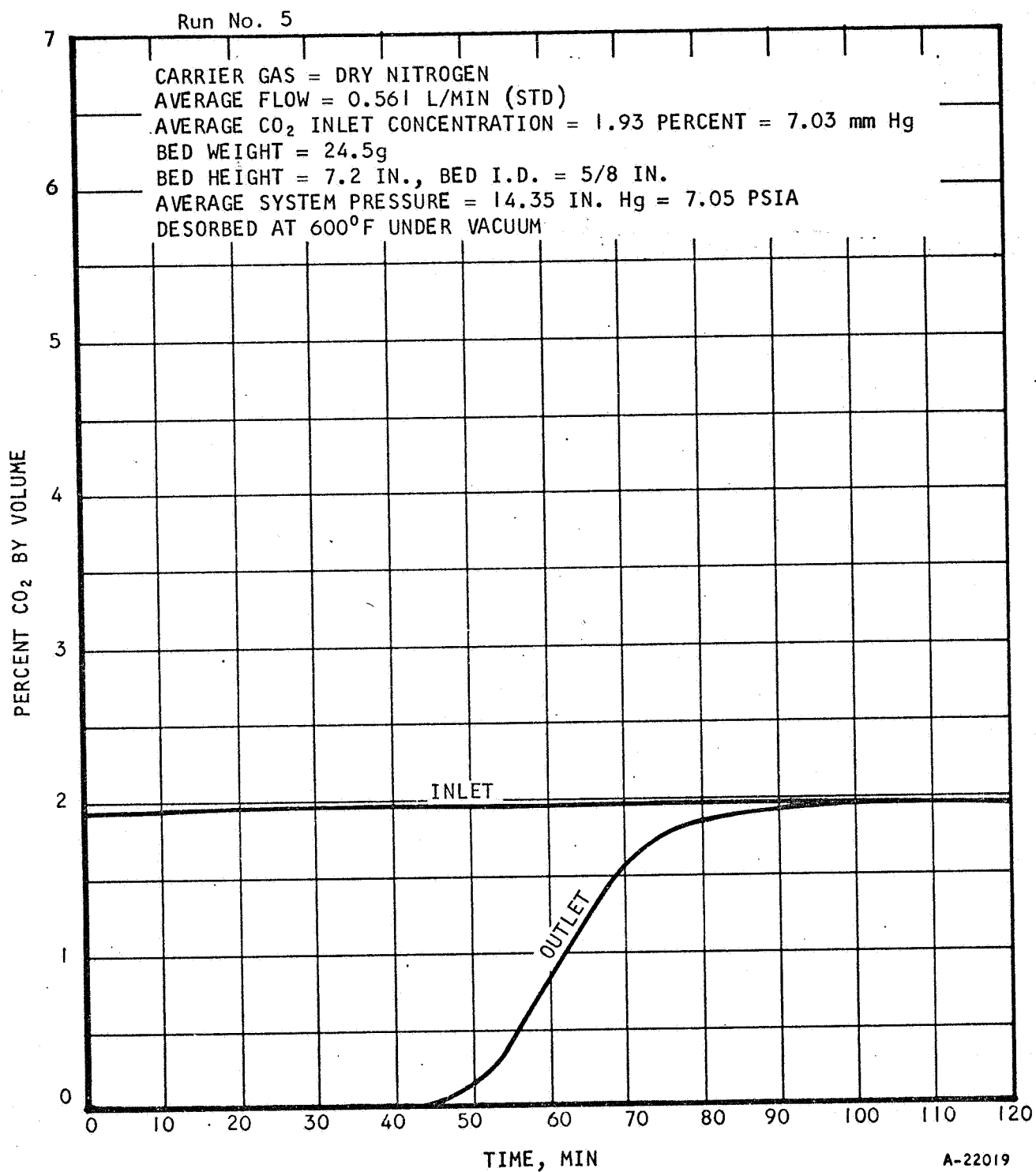
Figure C-13.   Dynamic Adsorption of CO_2 on Linde Molecular Sieve
Type 5A, 1/16 in. Diameter Pellets at 25°C

AIRESEARCH MANUFACTURING DIVISION
Los Angeles, California

Run No. 5
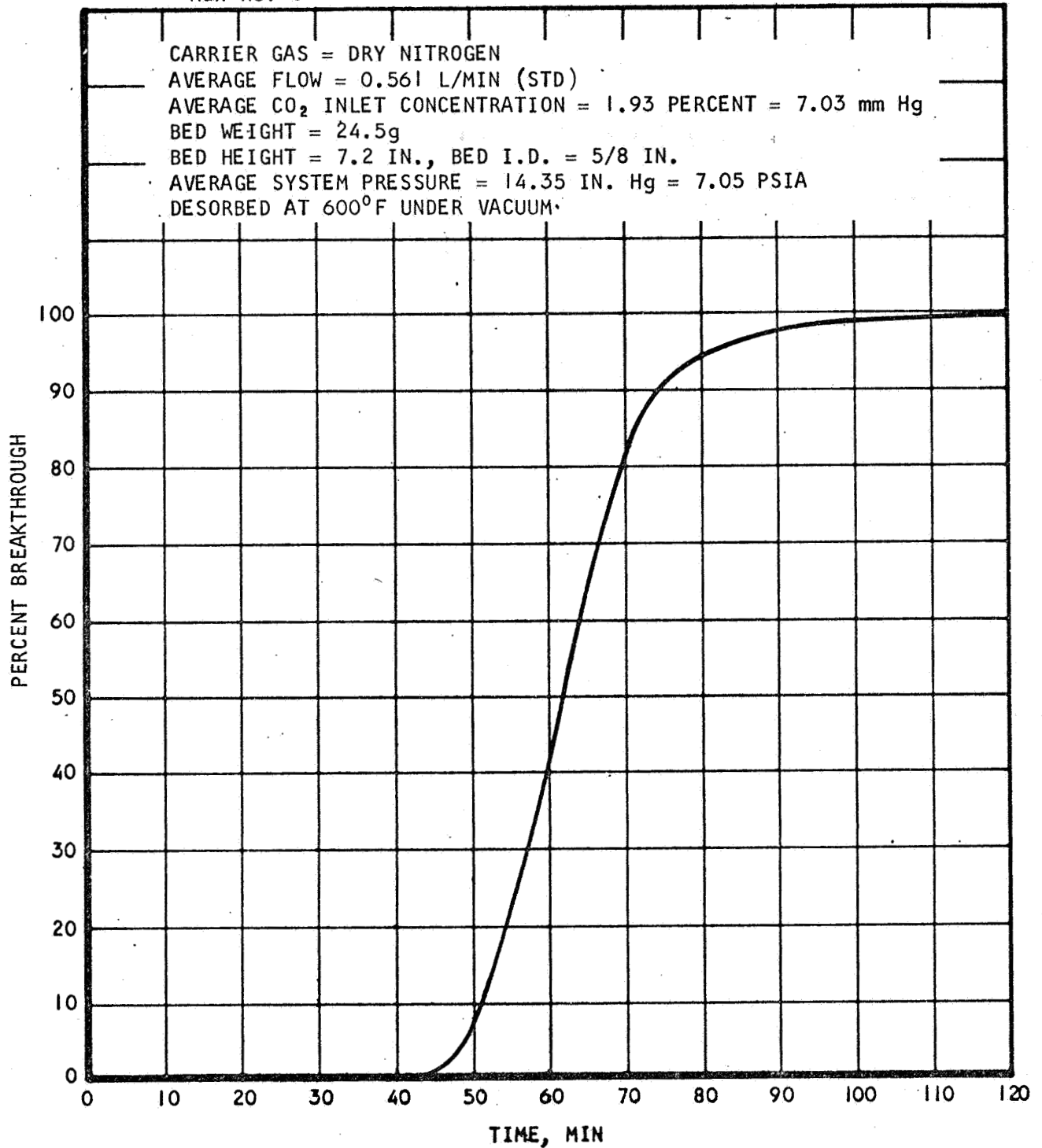
Figure C-14. Breakthrough of CO_2 from Linde Molecular Sieve, Type 5A, 1/16 in. Diameter Pellets at 25°C

CARRIER GAS = DRY NITROGEN
AVERAGE FLOW = 0.561 L/MIN (STD)
AVERAGE CO_2 INLET CONCENTRATION = 1.93 PERCENT = 7.03 mm Hg
BED WEIGHT = 24.5g
BED HEIGHT = 7.2 IN., BED I.D. = 5/8 IN.
AVERAGE SYSTEM PRESSURE = 14.35 IN. Hg = 7.05 PSIA
DESORBED AT 600°F UNDER VACUUM·

PERCENT BREAKTHROUGH

TIME, MIN

A-22007

Run No. 6

CARRIER GAS = NITROGEN
AVERAGE FLOW = 1.265 L/MIN
AVERAGE CO_2 INLET CONCENTRATION = 2.73 PERCENT = 7.18 mm Hg
BED WEIGHT = 35.4g
BED HEIGHT = 10.1 IN., BED I.D. = 5/8 IN.
AVERAGE SYSTEM PRESSURE = 10.35 IN. Hg = 5.08 PSIA
DESORBED AT 600°F UNDER VACUUM

INLET

OUTLET

PERCENT CO_2 BY VOLUME

TIME, MIN
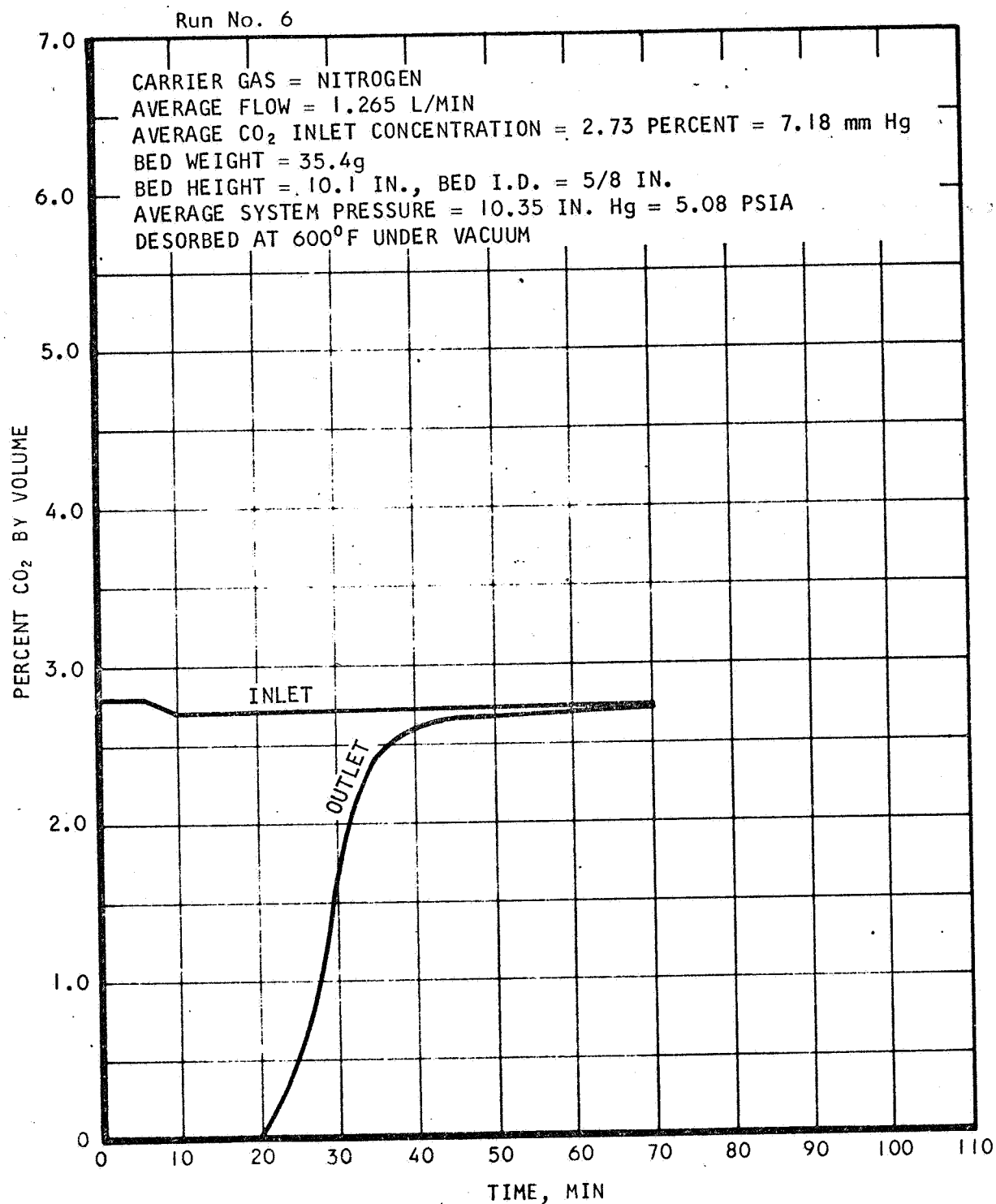
A-22024

Figure C-15.   Dynamic Adsorption of CO_2 on Linde Molecular Sieve
Type 5A, 1/16 in. Diameter Pellets at 25°C

Run No. 6

CARRIER GAS = DRY NITROGEN
AVERAGE FLOW = 1.265 L/MIN (STD)
AVERAGE CO_2 INLET CONCENTRATION = 2.73 PERCENT = 7.18 mm Hg
BED WEIGHT = 35.4g
BED HEIGHT = 10.1 IN., BED I.D. = 5/8 IN.
AVERAGE SYSTEM PRESSURE = 10.35 IN. Hg = 5.08 PSIA
DESORBED AT 600°F UNDER VACUUM

PERCENT BREAKTHROUGH

TIME, MIN
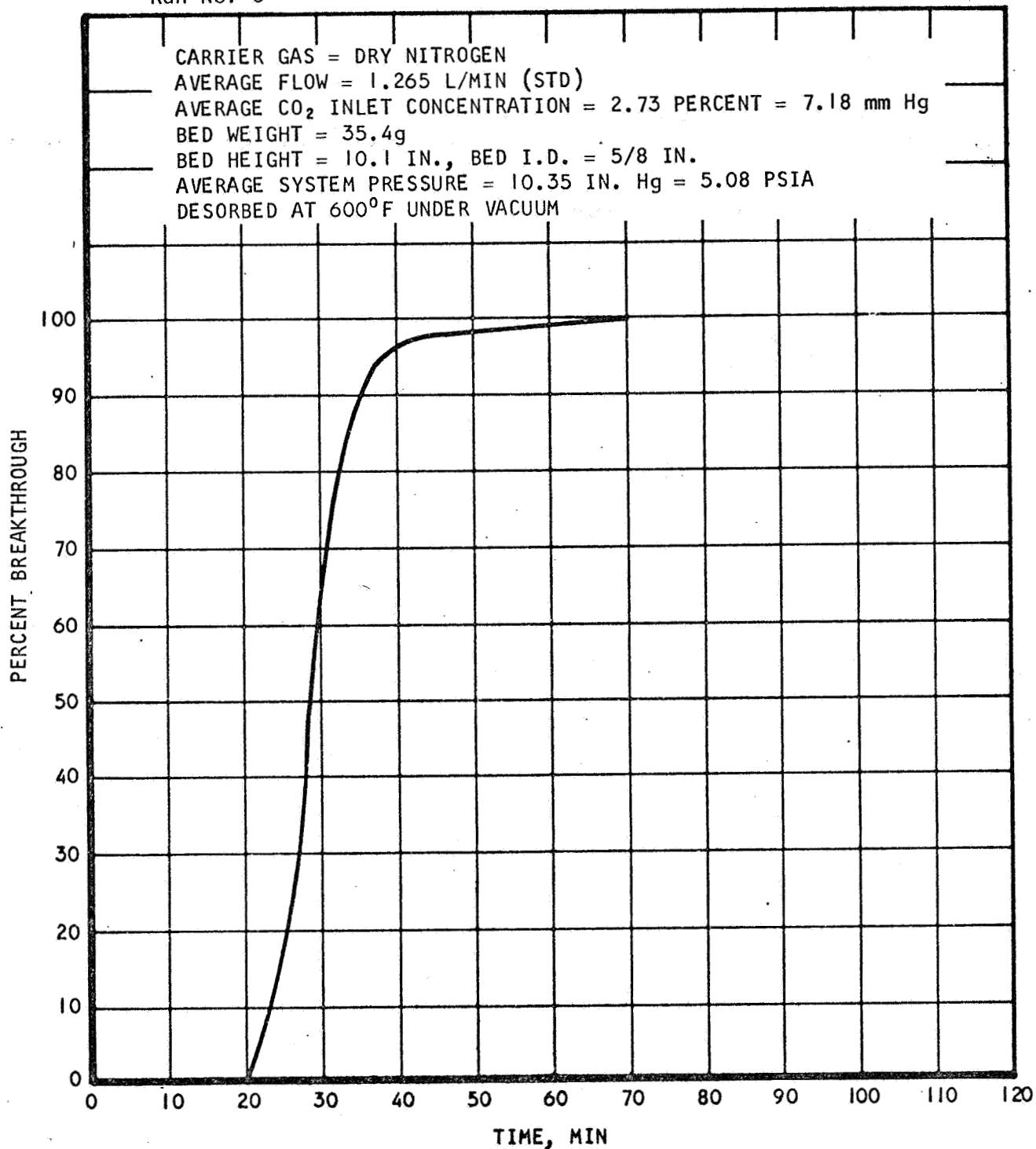
A-22004

Figure C-16.   Breakthrough of CO_2 from Linde Molecular Sieve, Type 5A,
1/16 in. Diameter Pellets at 25°C

Run No. 7

CARRIER GAS = DRY NITROGEN
AVERAGE FLOW = 0.565 L/MIN (STD)
AVERAGE CO_2 INLET CONCENTRATION = 2.72 PERCENT = 7.14 mm Hg
BED WEIGHT = 35.4g
BED HEIGHT = 10.1 IN., BED I.D. = 5/8 IN.
AVERAGE SYSTEM PRESSURE = 10.35 In. Hg = 5.08 PSIA
DESORBED AT 600°F UNDER VACUUM

INLET

OUTLET

PERCENT CO_2 BY VOLUME

TIME, MIN
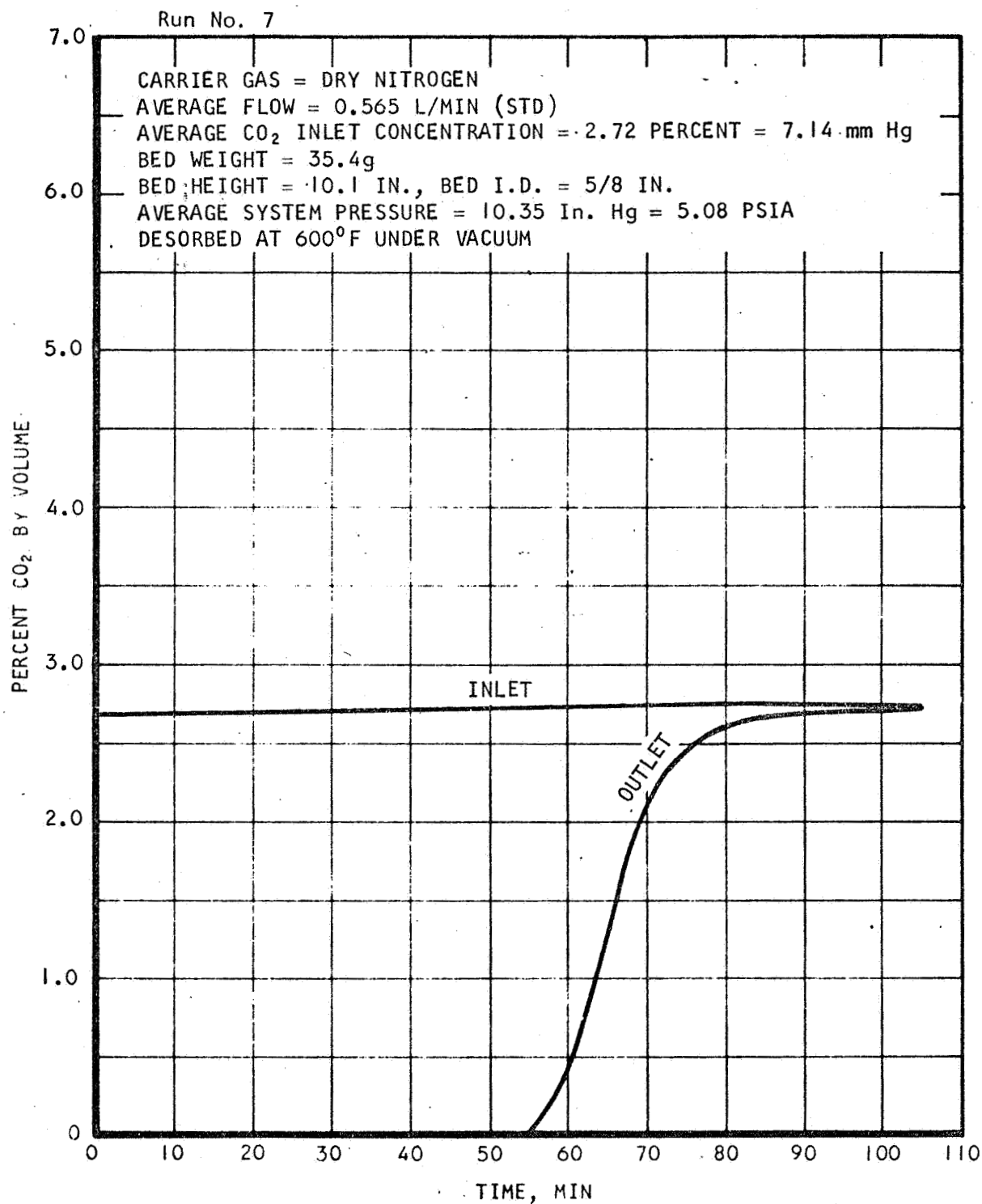
A-22026

Figure C-17. Dynamic Adsorption of CO_2 on Linde Molecular Sieve
Type 5A, 1/16 in. Diameter Pellets at 25°C

Run No. 7

CARRIER GAS = DRY NITROGEN
AVERAGE FLOW = 0.565 L/MIN (STD).
AVERAGE CO_2 INLET CONCENTRATION = 2.72 PERCENT = 7.14 mm Hg
BED WEIGHT = 35.4g
BED HEIGHT = 10.1 IN., BED I.D. = 5/8 IN.
AVERAGE SYSTEM PRESSURE = 10.35 IN. Hg = 5.08 PSIA
DESORBED AT 600°F UNDER VACUUM
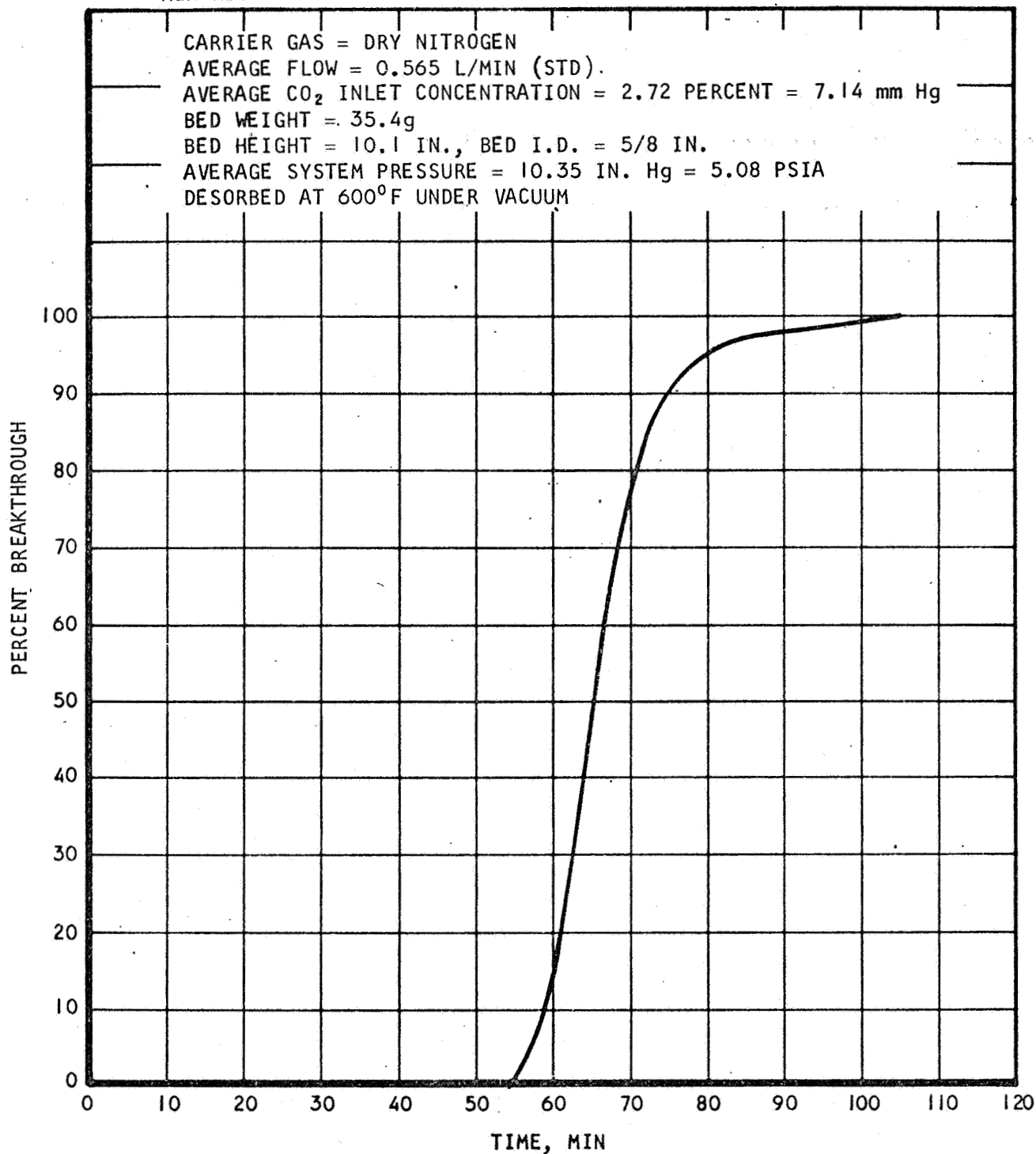
A-22010

Figure C-18.   Breakthrough of CO_2 from Linde Molecular Sieve, Type 5A,
1/16 in. Diameter Pellets at 25°C

Run No. 8

CARRIER GAS = DRY NITROGEN
AVERAGE FLOW = 1.264 L/MIN (STD)
AVERAGE CO_2 INLET CONCENTRATION = 2.71 PERCENT = 7.13 mm Hg
BED WEIGHT = 35.4g
BED HEIGHT = 10.1 IN., BED I.D. = 5/8 IN.
AVERAGE SYSTEM PRESSURE = 10.35 IN. Hg = 5.08 PSIA
DESORBED AT 600°F UNDER VACUUM

PERCENT CO_2 BY VOLUME

INLET

OUTLET

TIME, MIN
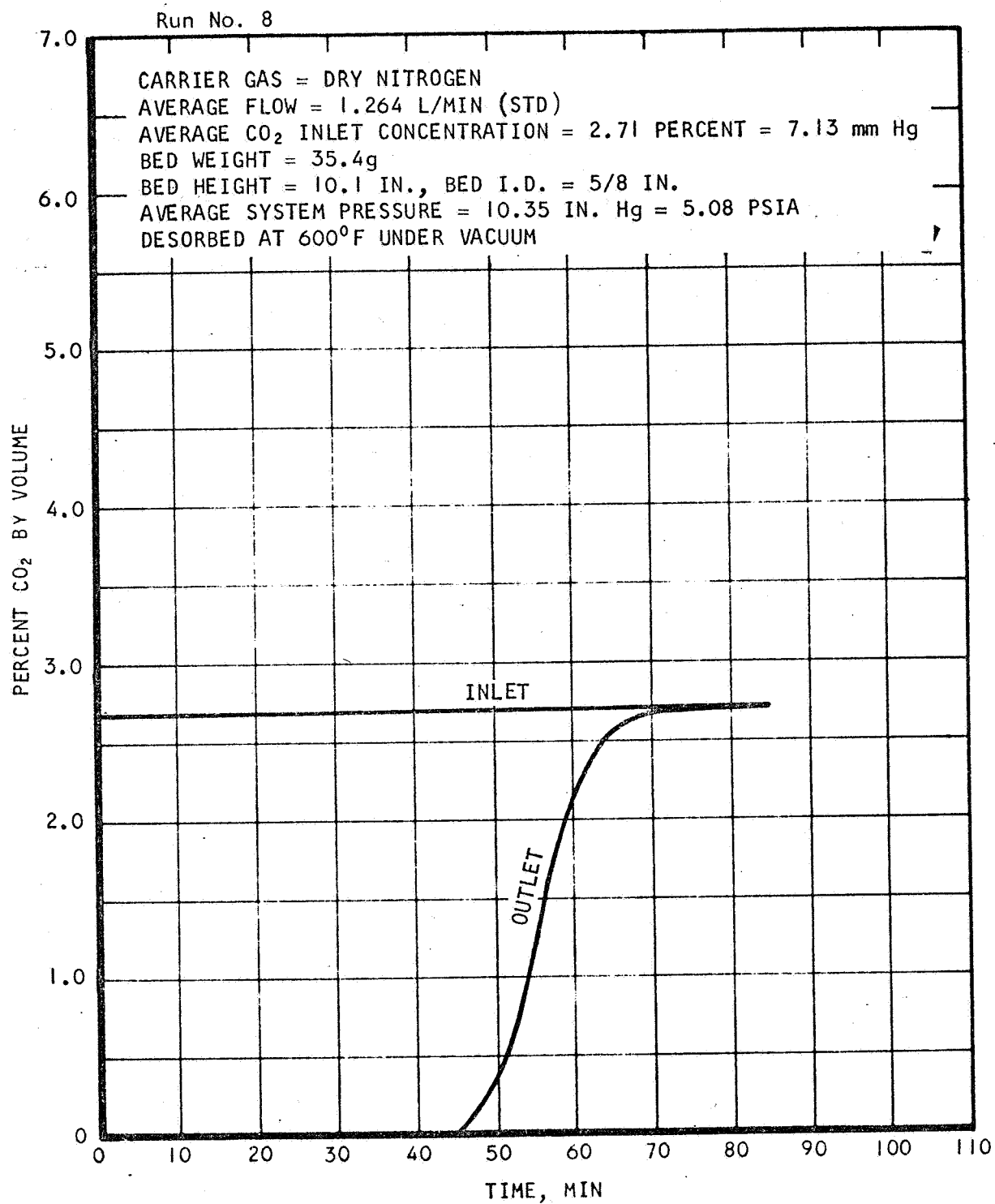
A-22025

Figure C-19.   Dynamic   Adsorption of CO_2 on Linde Molecular Sieve
Type 5A, 1/16 in. Diameter Pellets at 0°C

Run No. 8

CARRIER GAS = DRY NITROGEN
AVERAGE FLOW = 1.264 L/MIN (STD)
AVERAGE CO_2 INLET CONCENTRATION = 2.71 PERCENT = 7.13 mm Hg
BED WEIGHT = 35.4g
BED HEIGHT = 10.1 IN., BED I.D. = 5/8 IN.
AVERAGE SYSTEM PRESSURE = 10.35 IN. Hg = 5.08 PSIA
DESORBED AT 600^0F UNDER VACUUM
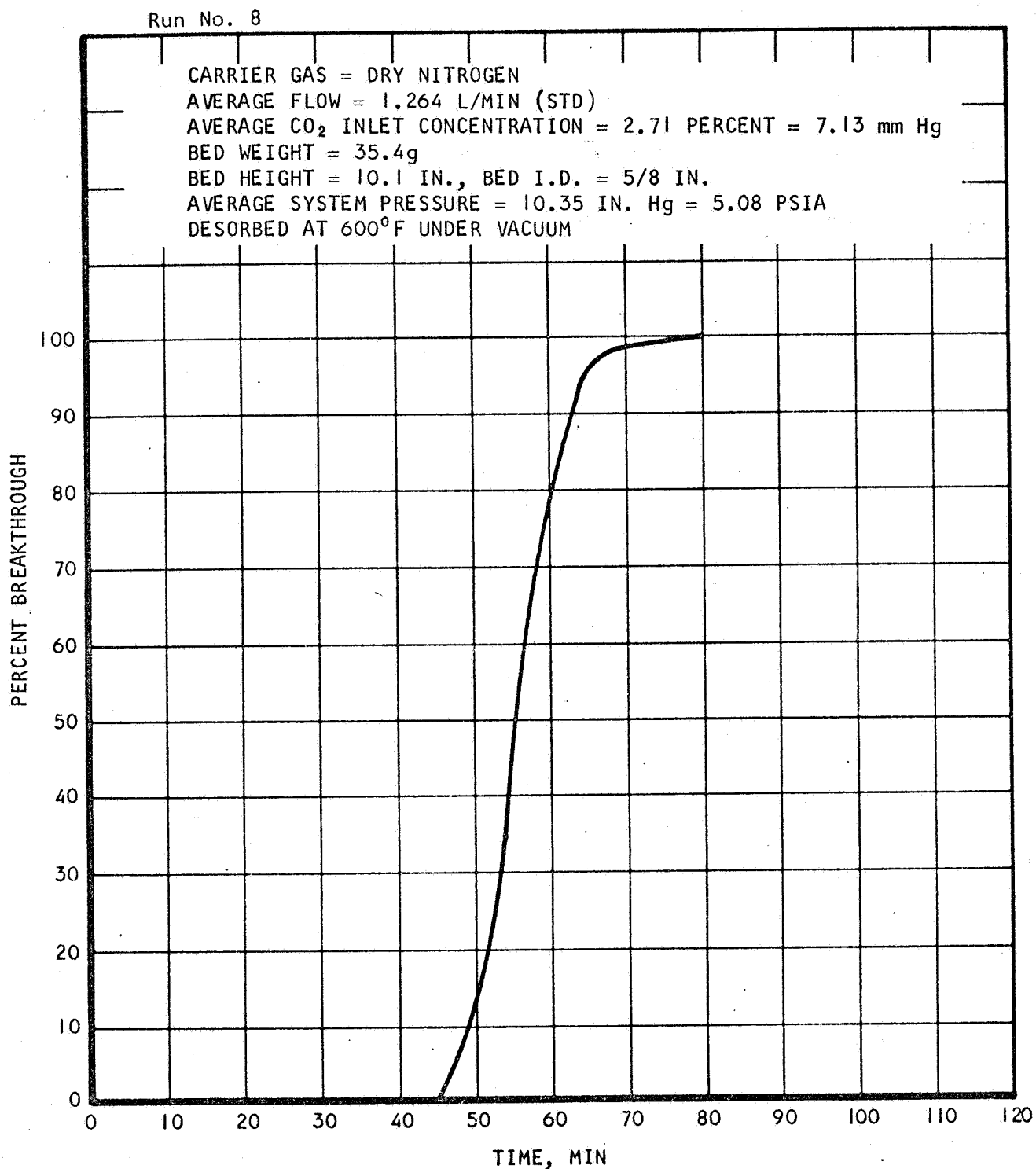
A-22008

Figure C-20.   Breakthrough of CO_2 from Linde Molecular Sieve, Type 5A,
1/16 in. Diameter Pellets at 0^0C

Run No. 9

CARRIER GAS = DRY OXYGEN
AVERAGE FLOW = 1.26 L/MIN (STD)
AVERAGE CO_2 INLET CONCENTRATION = 2.74 PERCENT = 7.19 mm Hg
BED WEIGHT = 35.4g
BED HEIGHT = 10.1 IN., BED I.D. = 5/8 IN.
AVERAGE SYSTEM PRESSURE = 10.35 IN. Hg = 5.08 PSIA
DESORBED AT 600°F UNDER VACUUM

INLET

OUTLET

PERCENT CO_2 BY VOLUME

TIME, MIN
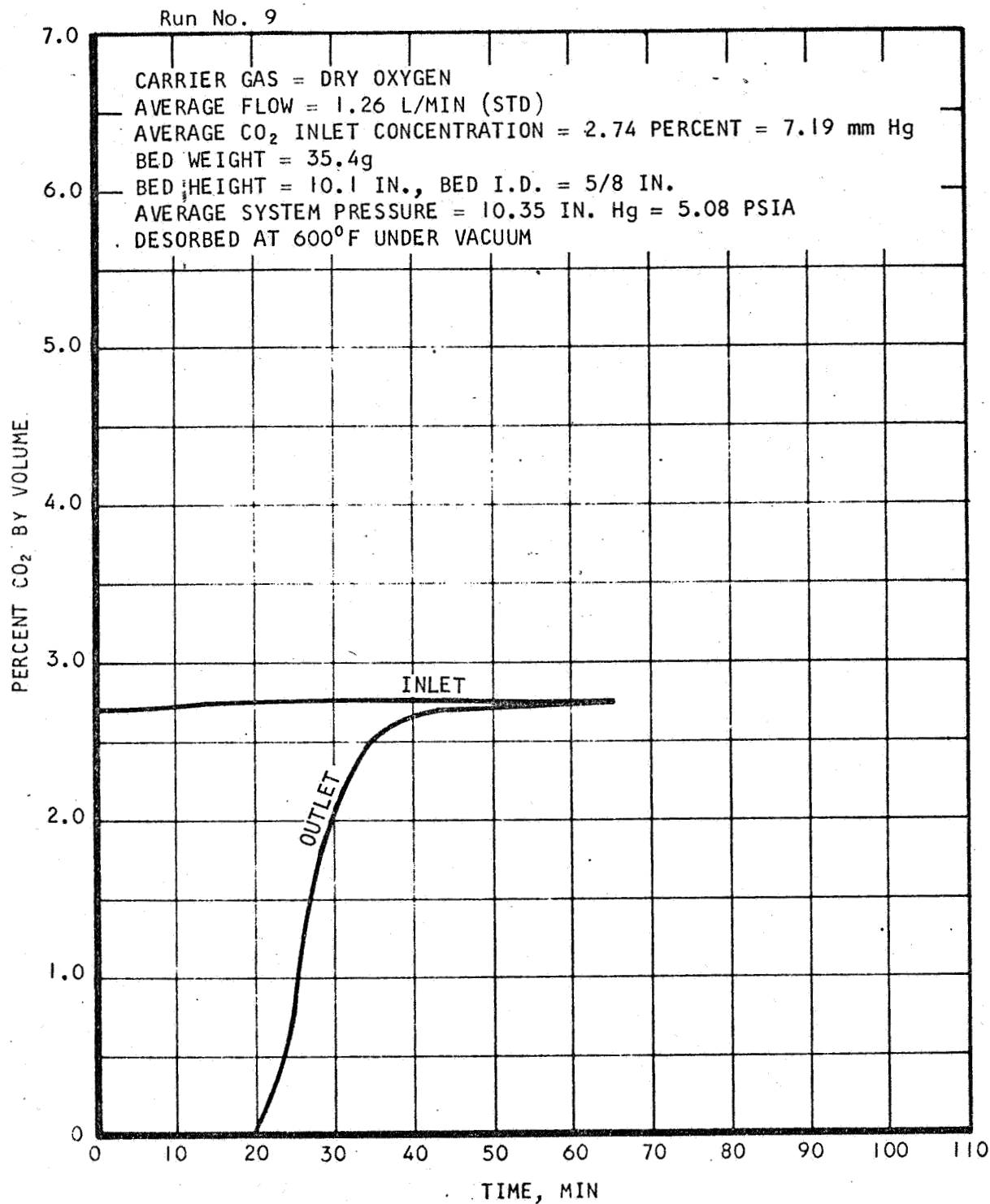
A-22027

Figure C-21. Dynamic Adsorption of CO_2 on Linde Molecular Sieve
Type 5A, 1/16 in. Diameter Pellets at 25°C

Run No. 9

CARRIER GAS = DRY OXYGEN
AVERAGE FLOW = 1.26 L/MIN (STD)
AVERAGE CO_2 INLET CONCENTRATION = 2.74 PERCENT = 7.19 mm Hg
BED WEIGHT = 35.4g
BED HEIGHT = 10.1 IN., BED I.D. = 5/8 IN.
AVERAGE SYSTEM PRESSURE = 10.35 IN. Hg = 5.08 PSIA
DESORBED AT 600°F UNDER VACUUM
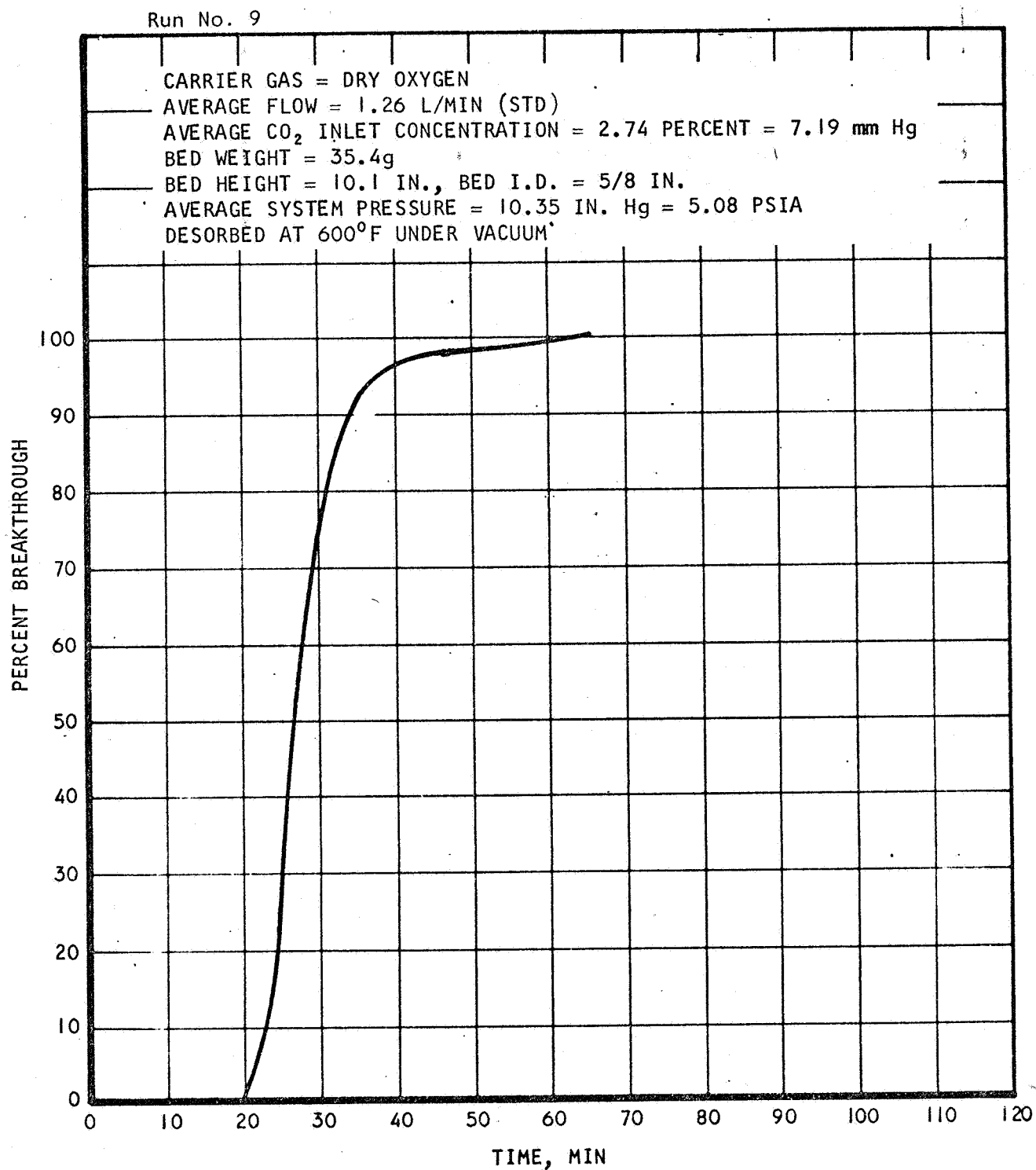
A-22009

Figure C-22.   Breakthrough of CO_2 from Linde Molecular Sieve, Type 5A,
1/16 in. Diameter Pellets at 25°C

Run No. 10

CARRIER GAS = DRY OXYGEN
AVERAGE FLOW = 1.26 L/MIN (STD)
AVERAGE CO_2 INLET CONCENTRATION = 2.76 PERCENT = 7.25 mm Hg
BED WEIGHT = 35.4g
BED HEIGHT = 10.1 IN., BED I.D. = 5/8 IN.
AVERAGE SYSTEM PRESSURE = 10.35 IN. Hg = 5.08 PSIA
DESORBED AT 600°F UNDER VACUUM

INLET

OUTLET

PERCENT CO_2 BY VOLUME

TIME, MIN
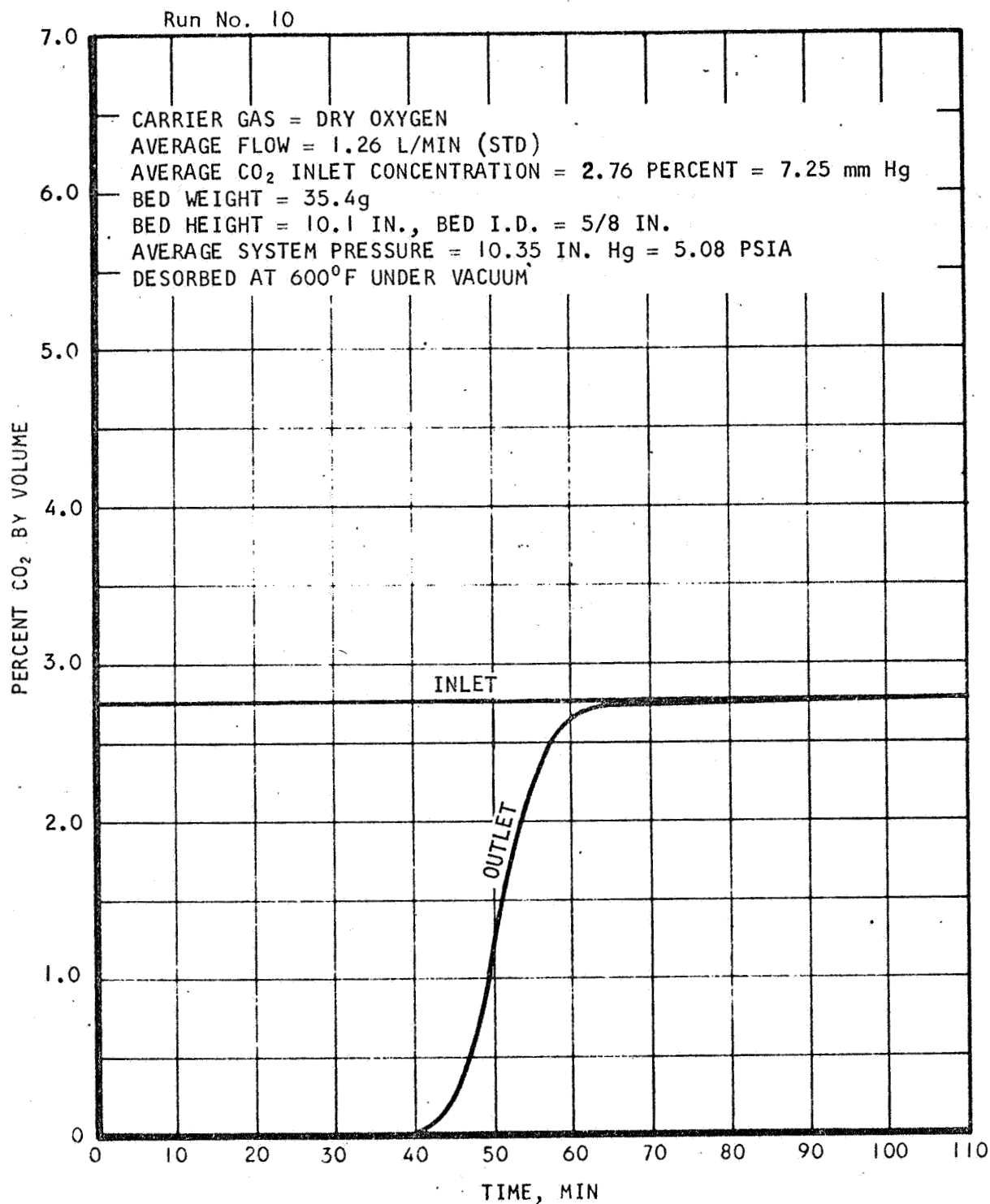
A-22028

Figure C-23. Dynamic Adsorption of CO_2 on Linde Molecular Sieve
Type 5A, 1/16 in. Diameter Pellets at 0°C

Run No. 10

CARRIER GAS = DRY OXYGEN
AVERAGE FLOW = 1.26 L/MIN (STD)
AVERAGE CO_2 INLET CONCENTRATION = 2.76 PERCENT = 7.25 mm Hg
BED WEIGHT = 35.4g
BED HEIGHT = 10.1 IN., BED I.D. = 5/8 IN.
AVERAGE SYSTEM PRESSURE = 10.35 IN. Hg = 5.08 PSIA
DESORBED AT 600°F UNDER VACUUM
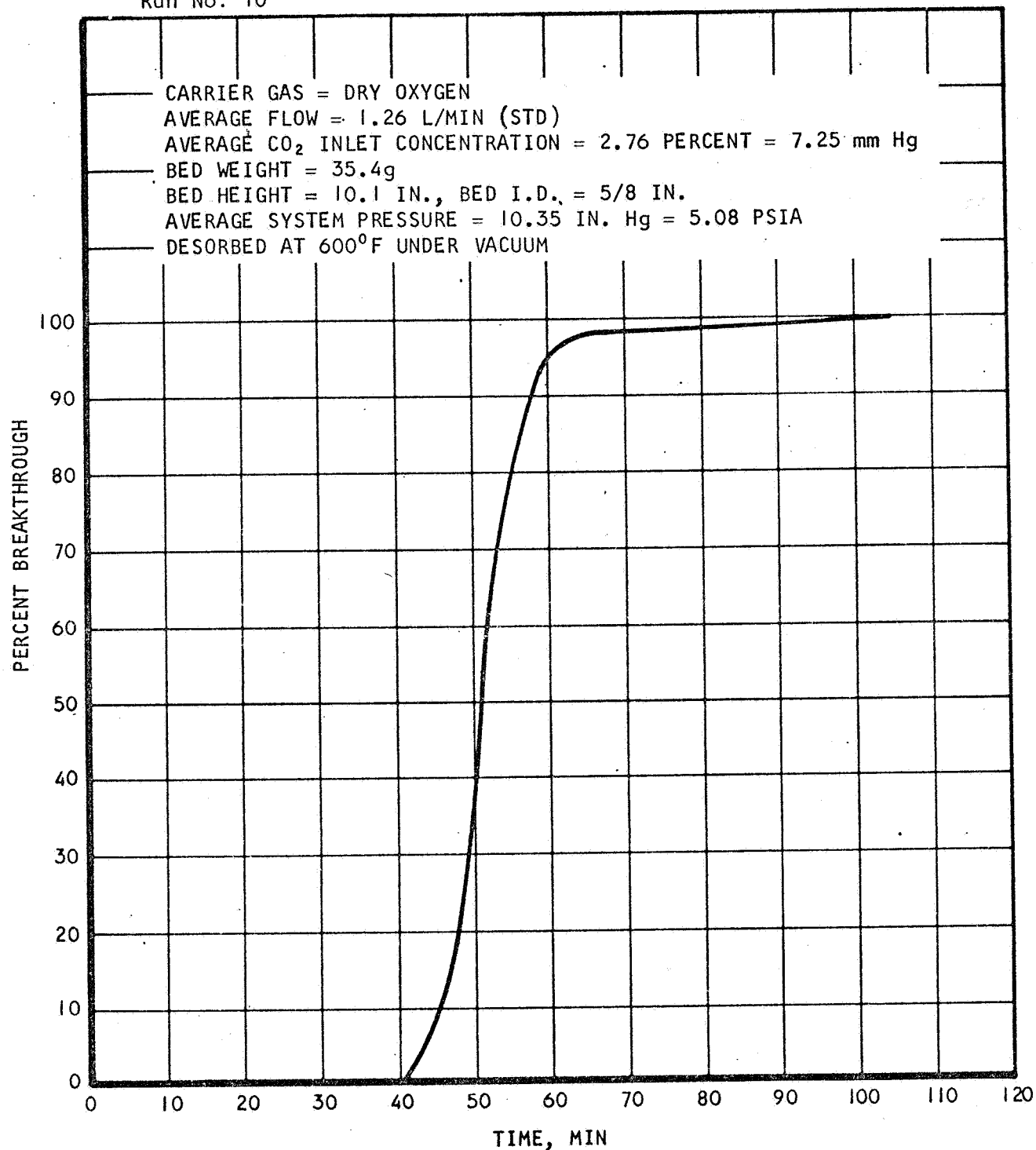
A-22011

Figure C-24.   Breakthrough of CO_2 from Linde Molecular Sieve, Type 5A,
1/16 in. Diameter Pellets at 0°C

Run No. 11

CARRIER GAS = HELIUM
AVERAGE FLOW = 1.30 L/MIN (STD)
AVERAGE CO_2 INLET CONCENTRATION = 2.74 PERCENT = 7.20 mm Hg
BED WEIGHT 35.4g
BED HEIGHT = 10.1 IN., BED I.D. = 5/8 IN.
AVERAGE SYSTEM PRESSURE = 10.35 IN. Hg = 5.08 PSIA
DESORBED AT 600°F UNDER VACUUM

INLET

OUTLET

PERCENT CO_2 BY VOLUME

TIME, MIN
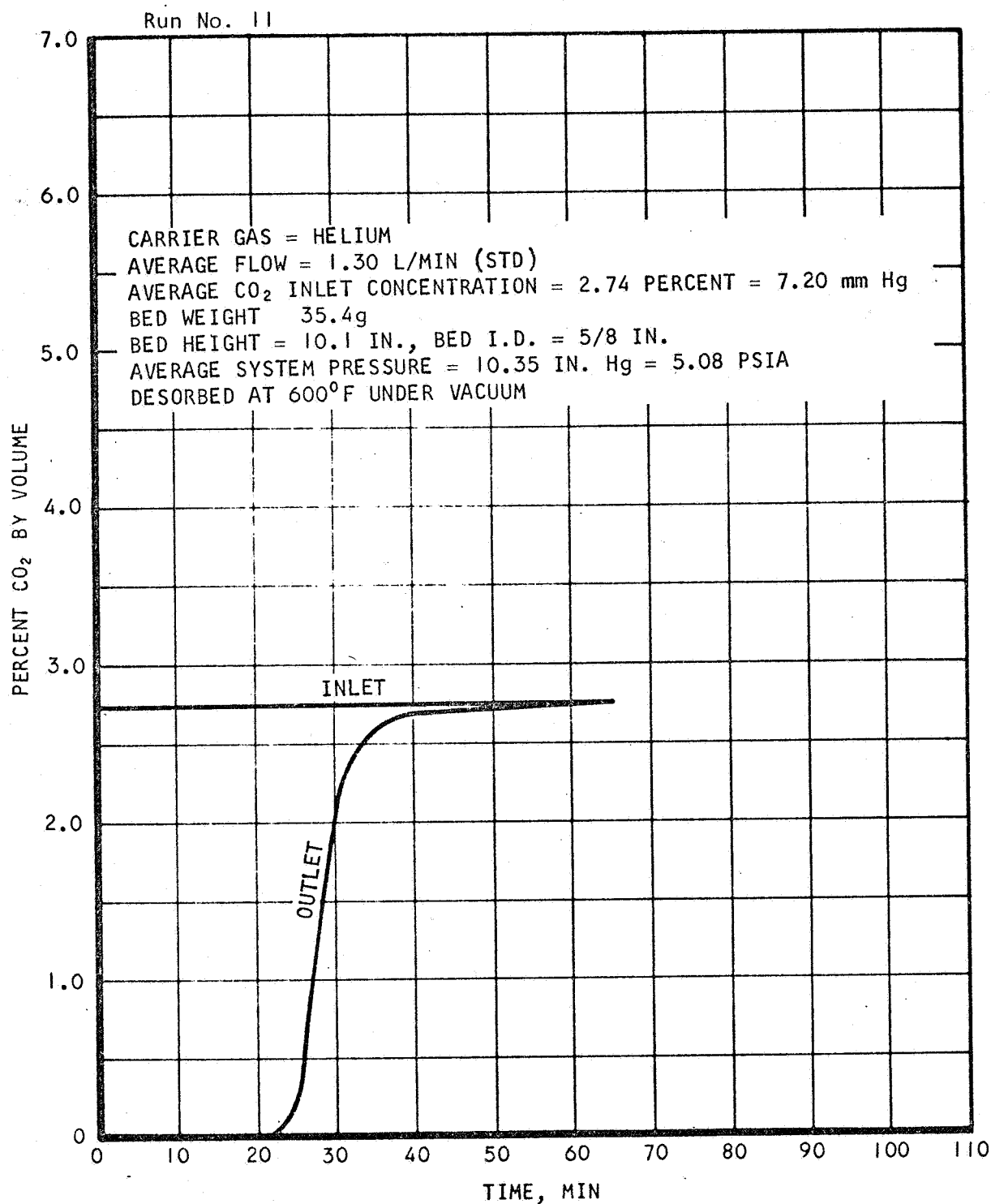
A-22029

Figure C-25.   Dynamic Adsorption of CO_2 on Linde Molecular Sieve
Type 5A, 1/16 in. Diameter Pellets at 25°C

Run No. 11

CARRIER GAS = HELIUM
AVERAGE FLOW = 1.30 L/MIN (STD)
AVERAGE CO_2 INLET CONCENTRATION = 2.74 PERCENT = 7.20 mm Hg
BED WEIGHT = 35.4g
BED HEIGHT = 10.1 IN., BED I.D. = 5/8 IN.
AVERAGE SYSTEM PRESSURE = 10.35 IN. Hg = 5.08 PSIA
DESORBED AT 600°F UNDER VACUUM
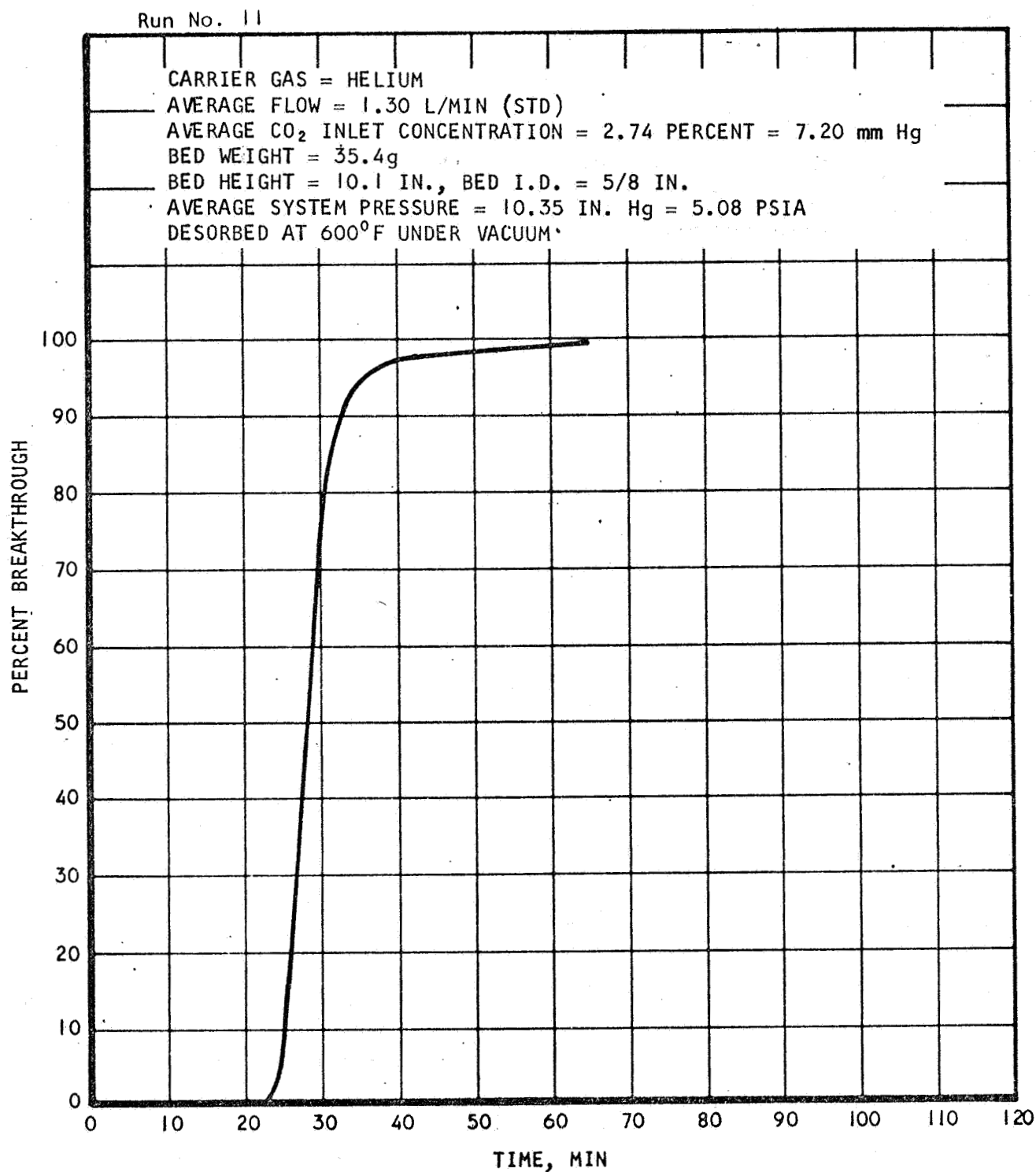
A-22012

Figure C-26. Breakthrough of CO_2 from Linde Molecular Sieve, Type 5A,
1/16 in. Diameter Pellets at 25°C

AIRESEARCH MANUFACTURING DIVISION
Los Angeles, California

CARRIER GAS = NITROGEN
AVERAGE FLOW = 0.561 L/MIN (STD)
AVERAGE CO_2 INLET CONCENTRATION = 1.89 PERCENT = 6.91 mm Hg
BED WEIGHT = 35.4g
BED HEIGHT = 10.1 IN., BED I.D. = 5/8 IN.
AVERAGE SYSTEM PRESSURE = 14.39 IN. Hg = 7.07 PSIA
DESORBED AT 600°F UNDER VACUUM

Run No. 12
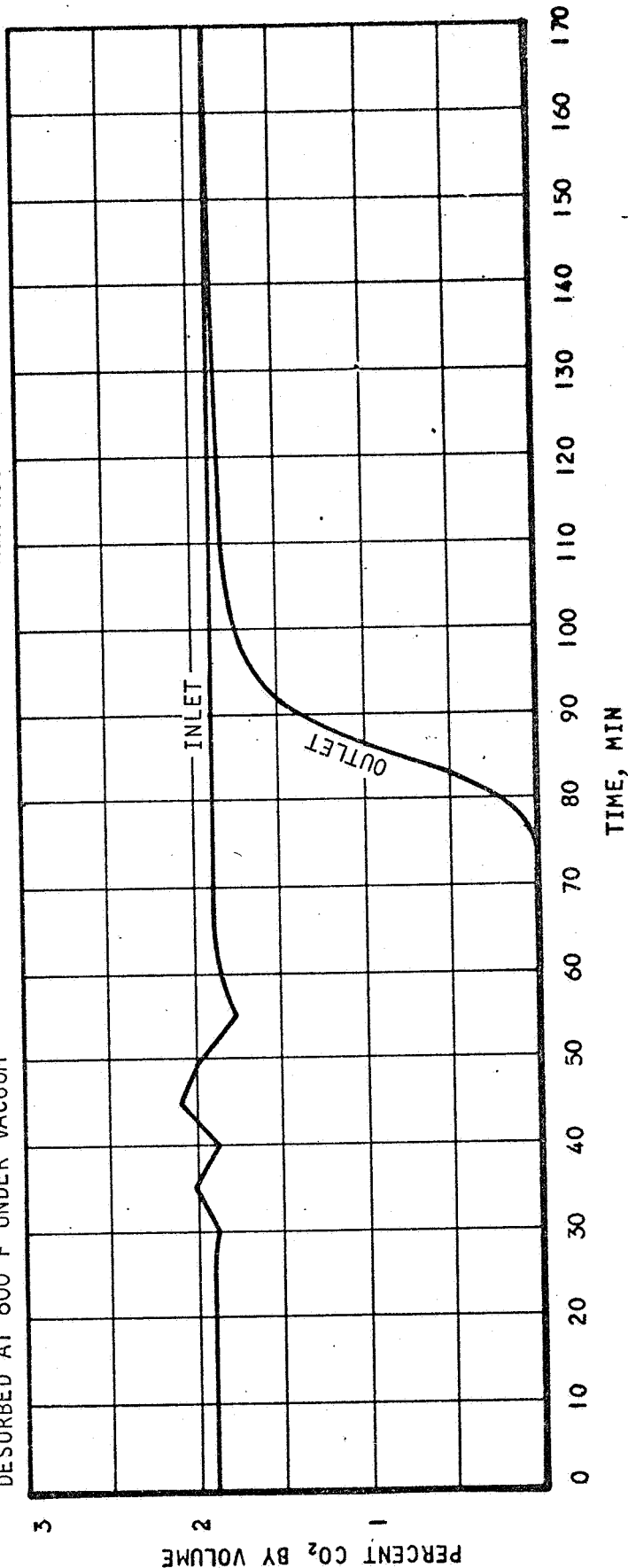
Figure C-27. Dynamic Adsorption of CO_2 on Linde Molecular Sieve
Type 5A, 1/16 in. Diameter Pellets at 25°C

A-22044

Run No. 12

CARRIER GAS = NITROGEN
AVERAGE FLOW = 0.561 L/MIN
AVERAGE CO_2 INLET CONCENTRATION = 1.89 PERCENT
= 6.91 mm Hg

BED WEIGHT = 35.4g
BED HEIGHT = 10.1 IN., BED I.D. = 5/8 IN.
AVERAGE SYSTEM PRESSURE = 14.39 IN Hg = 7.07 PSIA
DESORBED AT 600°F UNDER VACUUM

PERCENT BREAKTHROUGH

TIME , MIN
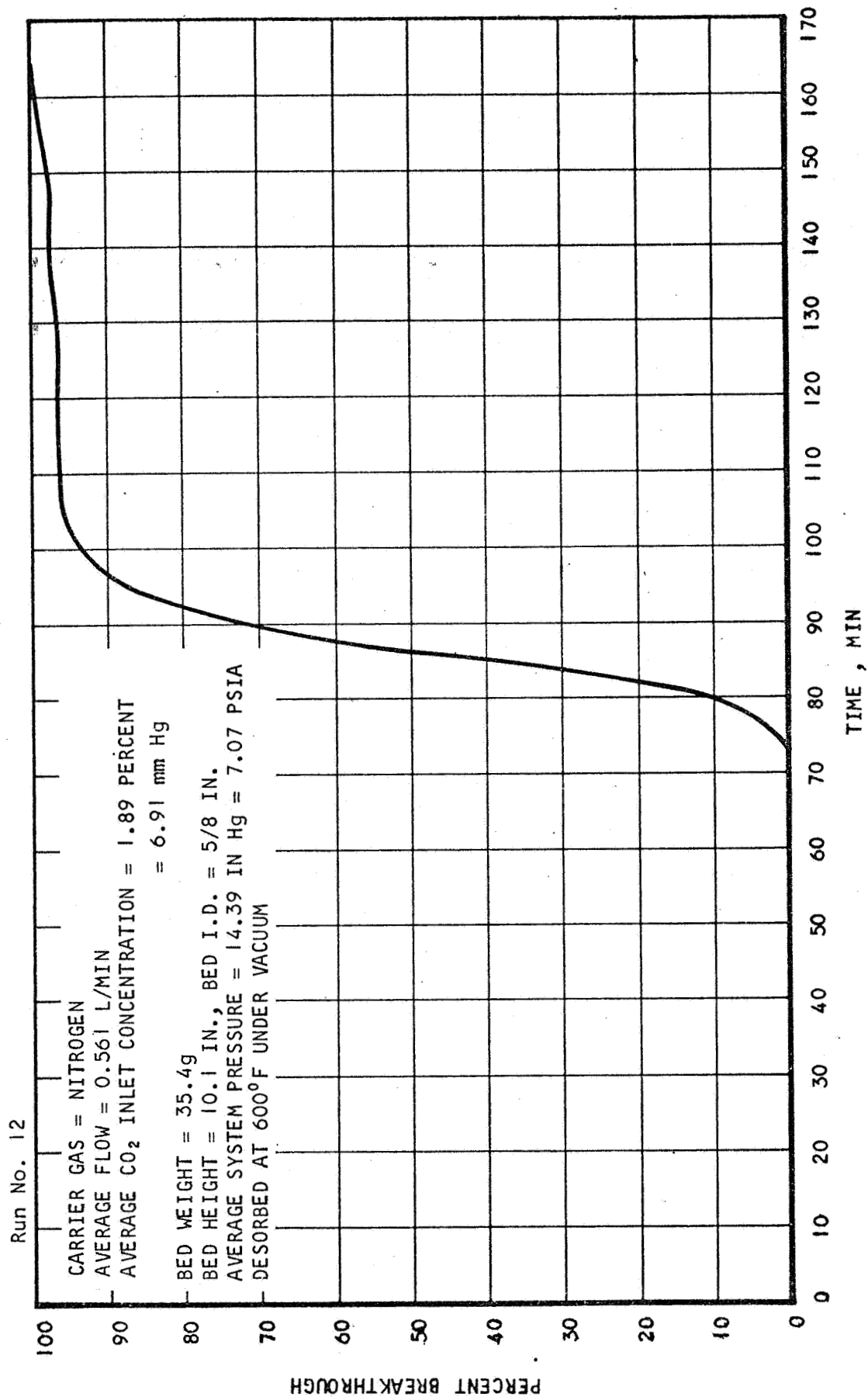
A-22036

Figure C-28. Breakthrough of CO_2 from Linde Molecular Sieve, Type 5A
1/16 in. Diameter Pellets at 25°C

Run No. 13

CARRIER GAS = NITROGEN
AVERAGE FLOW = 0.556 L/MIN (STD)
AVERAGE CO_2 INLET CONCENTRATION = 2.74 PERCENT = 7.21 mm Hg
BED WEIGHT = 35.4g
BED HEIGHT = 10.1 IN., BED I.D. = 5/8 IN.
AVERAGE SYSTEM PRESSURE = 10.35 IN. Hg = 5.08 PSIA
DESORBED AT 600°F UNDER VACUUM
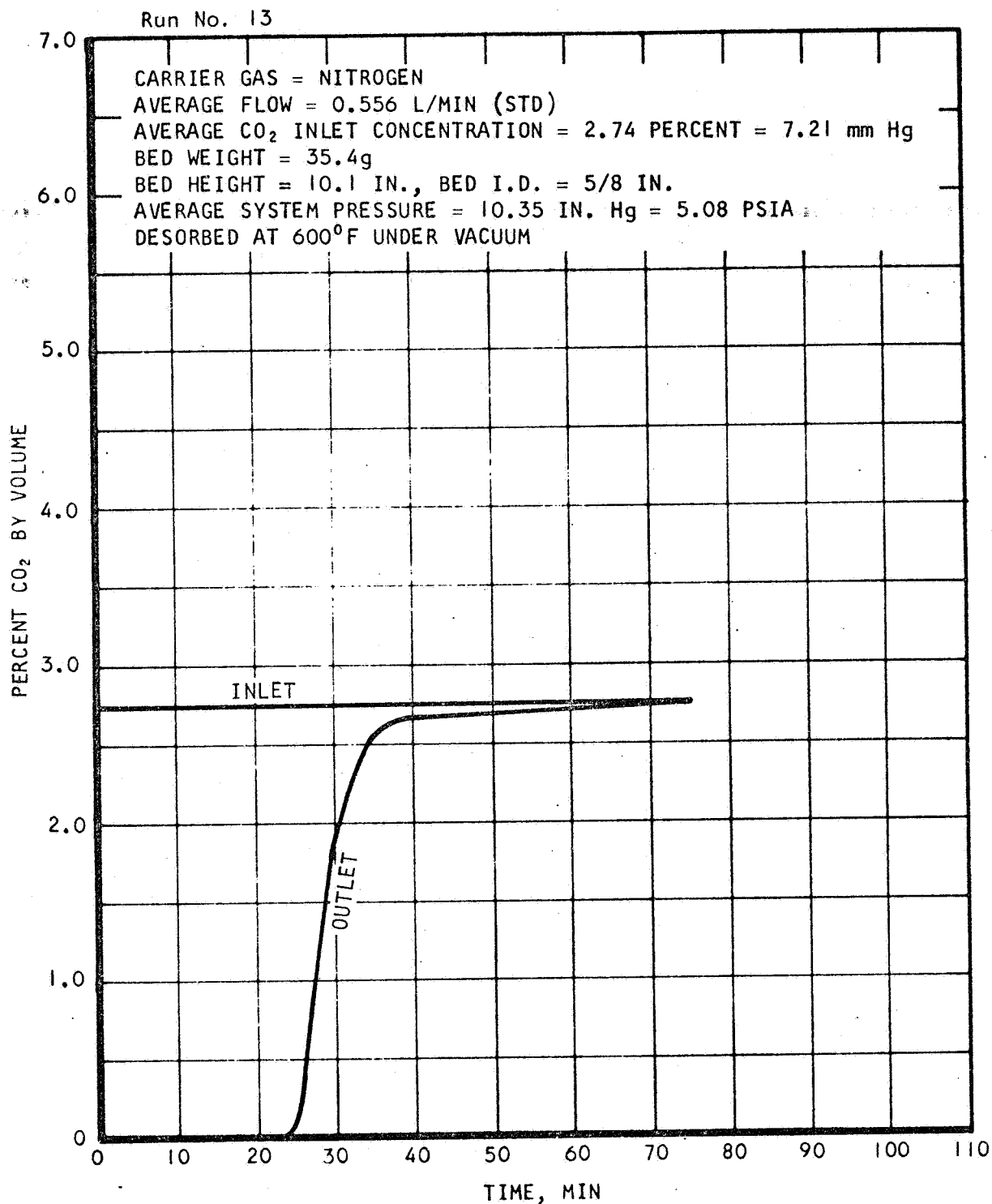
A-22030

Figure C-29. Dynamic Adsorption of CO_2 on Linde Molecular Sieve
Type 5A, 1/16 in. Diameter Pellets at 50°C

Run No. 13

CARRIER GAS = NITROGEN
AVERAGE FLOW = 0.556 L/MIN (STD)
AVERAGE CO_2 INLET CONCENTRATION = 2.74 PERCENT = 7.21 mm Hg
BED WEIGHT = 35.4g
BED HEIGHT = 10.1 IN., BED I.D. = 5/8 IN.
AVERAGE SYSTEM PRESSURE = 10.35 IN! Hg = 5.08 PSIA
DESORBED AT 600°F UNDER VACUUM
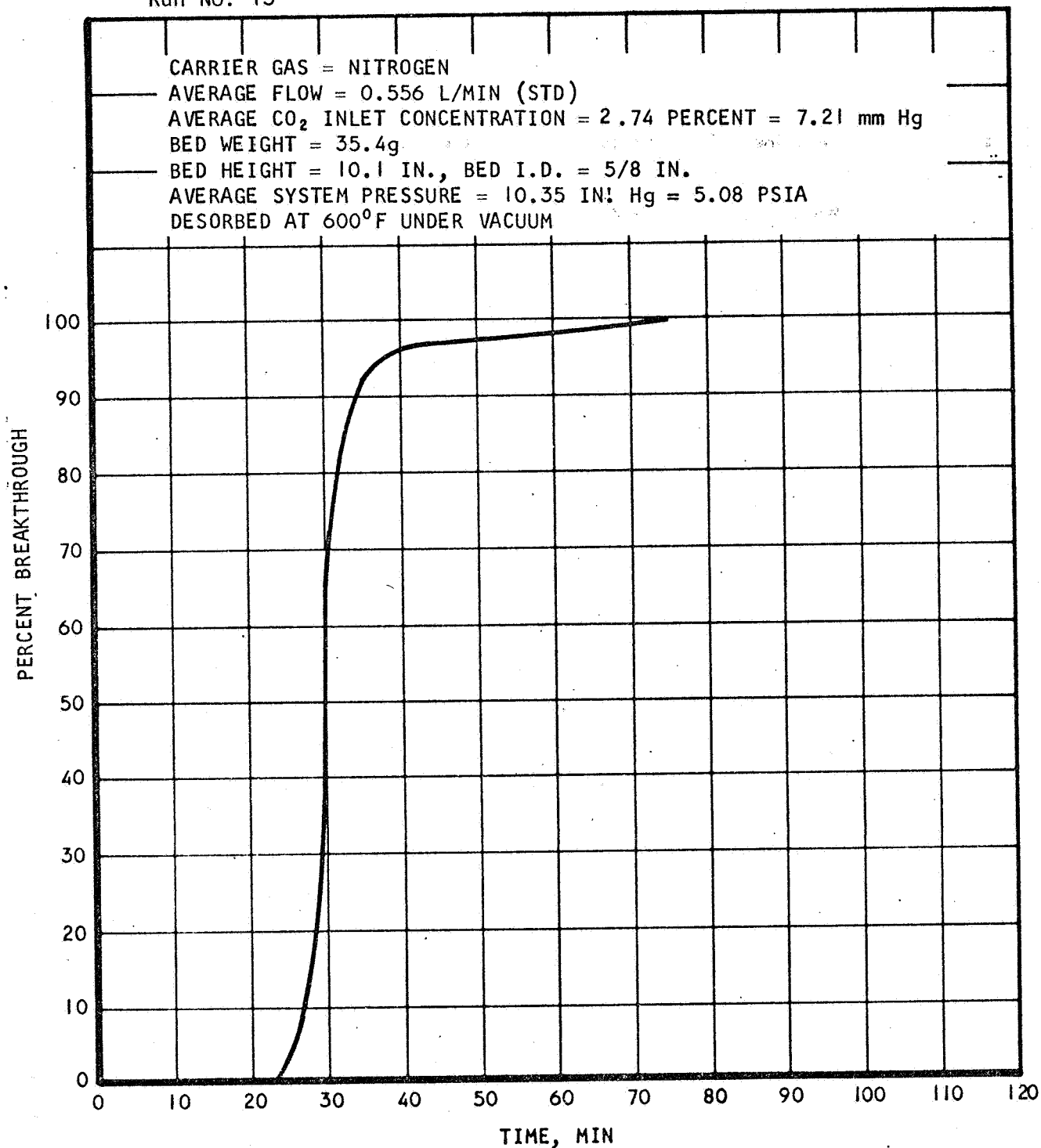
A-22013

Figure C-30.   Breakthrough of CO_2 from Linde Molecular Sieve, Type 5A, 1/16 in. Diameter Pellets at 50°C

Run No. 14

CARRIER GAS = NITROGEN
AVERAGE FLOW = 1.264 L/MIN (STD)
AVERAGE CO_2 INLET CONCENTRATION = 2.67 PERCENT = 7.01 mm Hg
BED WEIGHT = 35.4g
BED HEIGHT = 10.1 IN., BED I.D. = 5/8 IN.
AVERAGE SYSTEM PRESSURE = 10.35 IN. Hg = 5.08 PSIA
DESORBED AT 600°F UNDER VACUUM
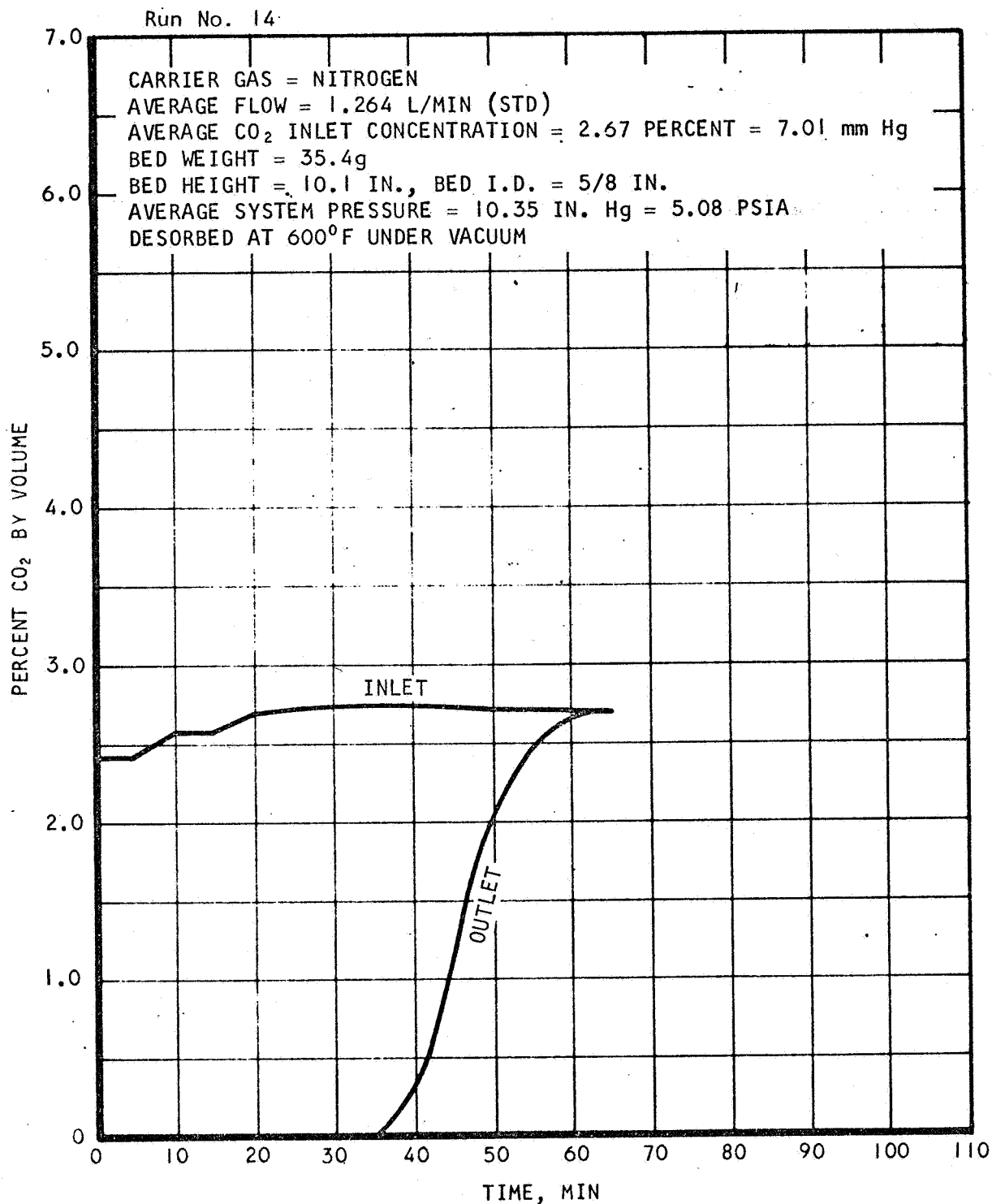
A-22031

Figure C-31.   Dynamic Adsorption of CO_2 on Linde Molecular Sieve
Type 5A, 1/16 in. Diameter Pellets at 9.1°C

Run No. 14

CARRIER GAS = NITROGEN
AVERAGE FLOW = 1.264 L/MIN (STD)
AVERAGE CO_2 INLET CONCENTRATION = 2.67 PERCENT = 7.01 mm Hg
BED WEIGHT = 35.4g
BED HEIGHT = 10.1 IN., BED I.D. = 5/8 IN.
AVERAGE SYSTEM PRESSURE = 10.35 IN. Hg = 5.08 PSIA
DESORBED AT 600°F UNDER VACUUM

A-22014
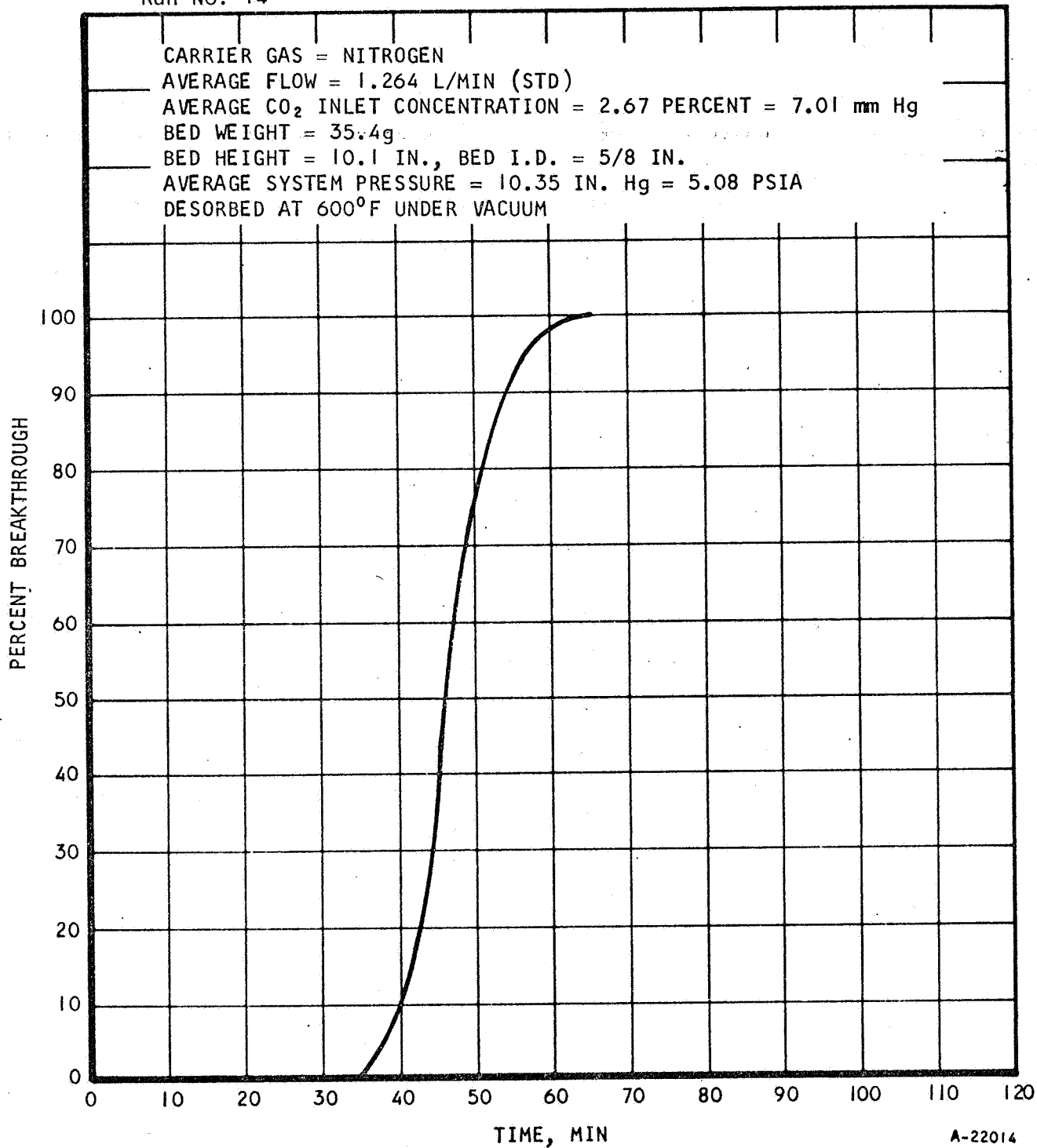
Figure C-32. Breakthrough of CO_2 from Linde Molecular Sieve, Type 5A,
1/16 in. Diameter Pellets at 9.1°C
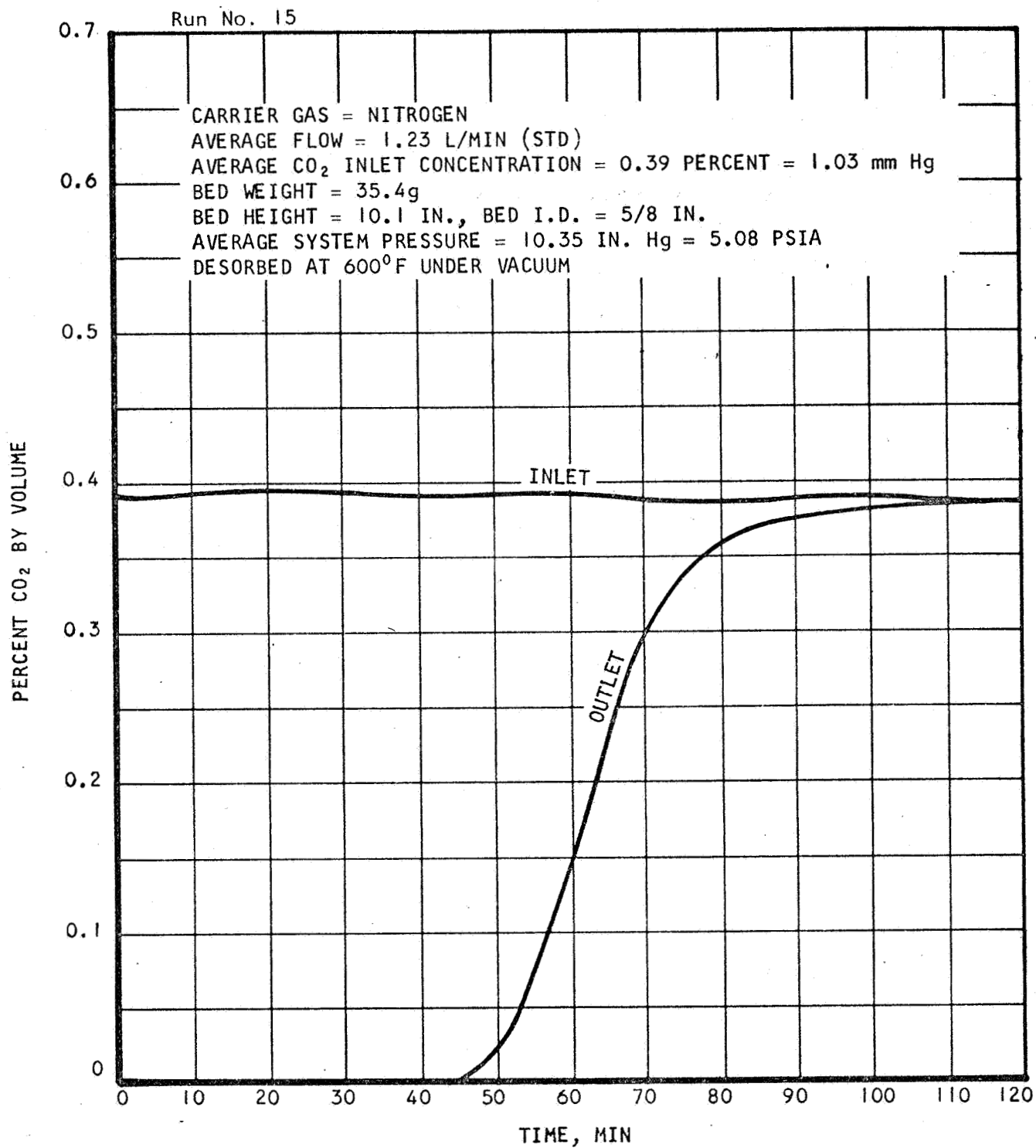
Figure C-33. Dynamic Adsorption of CO_2 on Linde Molecular Sieve Type 5A, 1/16 in. Diameter Pellets at 25°C

Run No. 15

CARRIER GAS = NITROGEN
AVERAGE FLOW = 1.23 L/MIN (STD)
AVERAGE CO_2 INLET CONCENTRATION = 0.39 PERCENT = 1.03 mm Hg
BED WEIGHT = 35.4g
BED HEIGHT = 10.1 IN., BED I.D. = 5/8 IN.
AVERAGE SYSTEM PRESSURE = 10.35 IN. Hg = 5.08 PSIA
DESORBED AT 600°F UNDER VACUUM
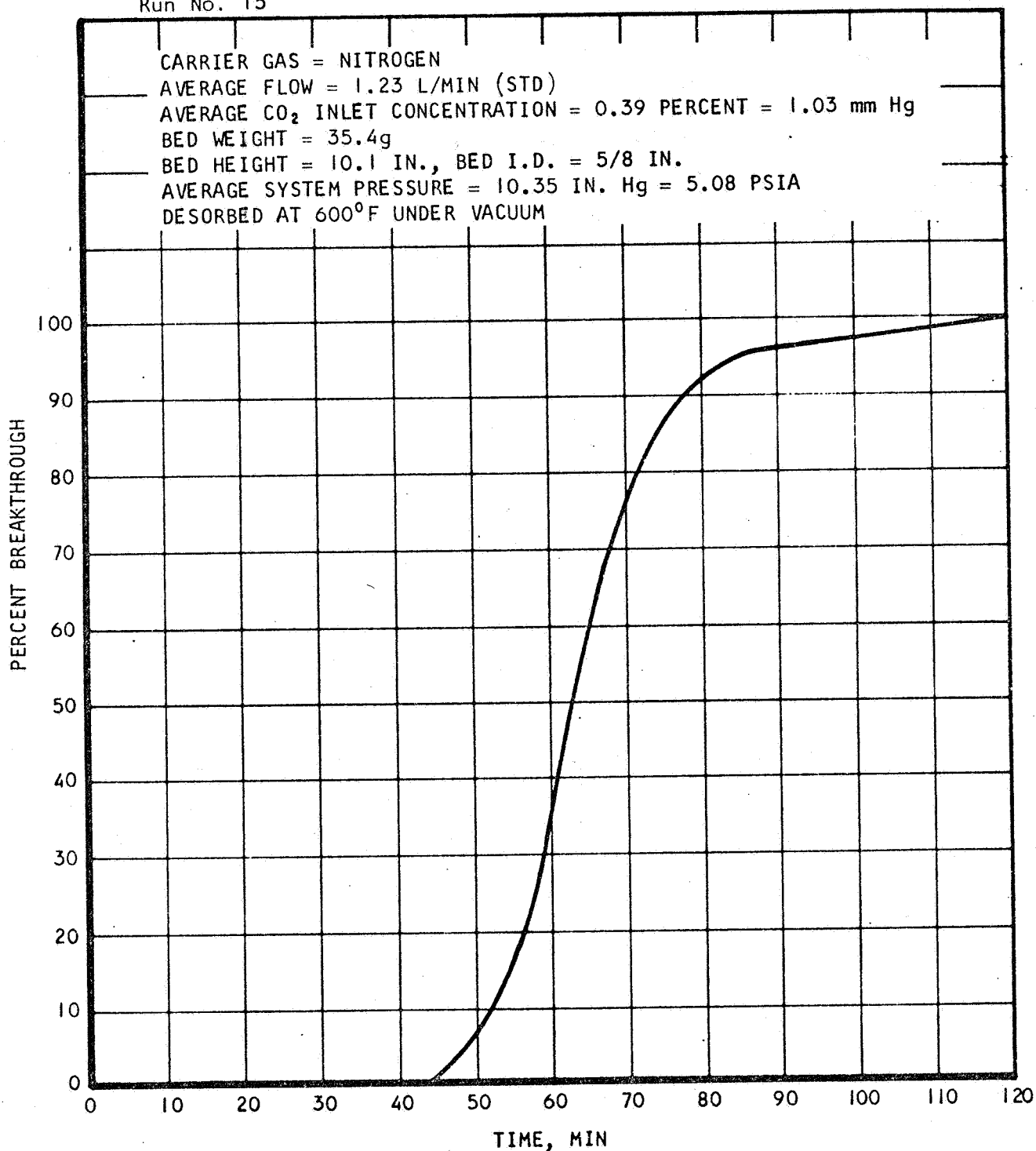
A-22015

Figure C-34. Breakthrough of CO_2 from Linde Molecular Sieve, Type 5A, 1/16 in. Diameter Pellets at 25°C

Run No. 16

CARRIER GAS = NITROGEN
AVERAGE FLOW = 1.24 L/MIN (STD)
AVERAGE CO_2 INLET CONCENTRATION = 0.395 PERCENT = 1.04 mm Hg
BED WEIGHT = 35.4g
BED HEIGHT = 10.1 IN., BED I.D. = 5/8 IN.
AVERAGE SYSTEM PRESSURE = 10.33 IN. Hg = 5.07 PSIA
DESORBED AT 600°F UNDER VACUUM

INLET

OUTLET

PERCENT CO_2 BY VOLUME

TIME, MIN
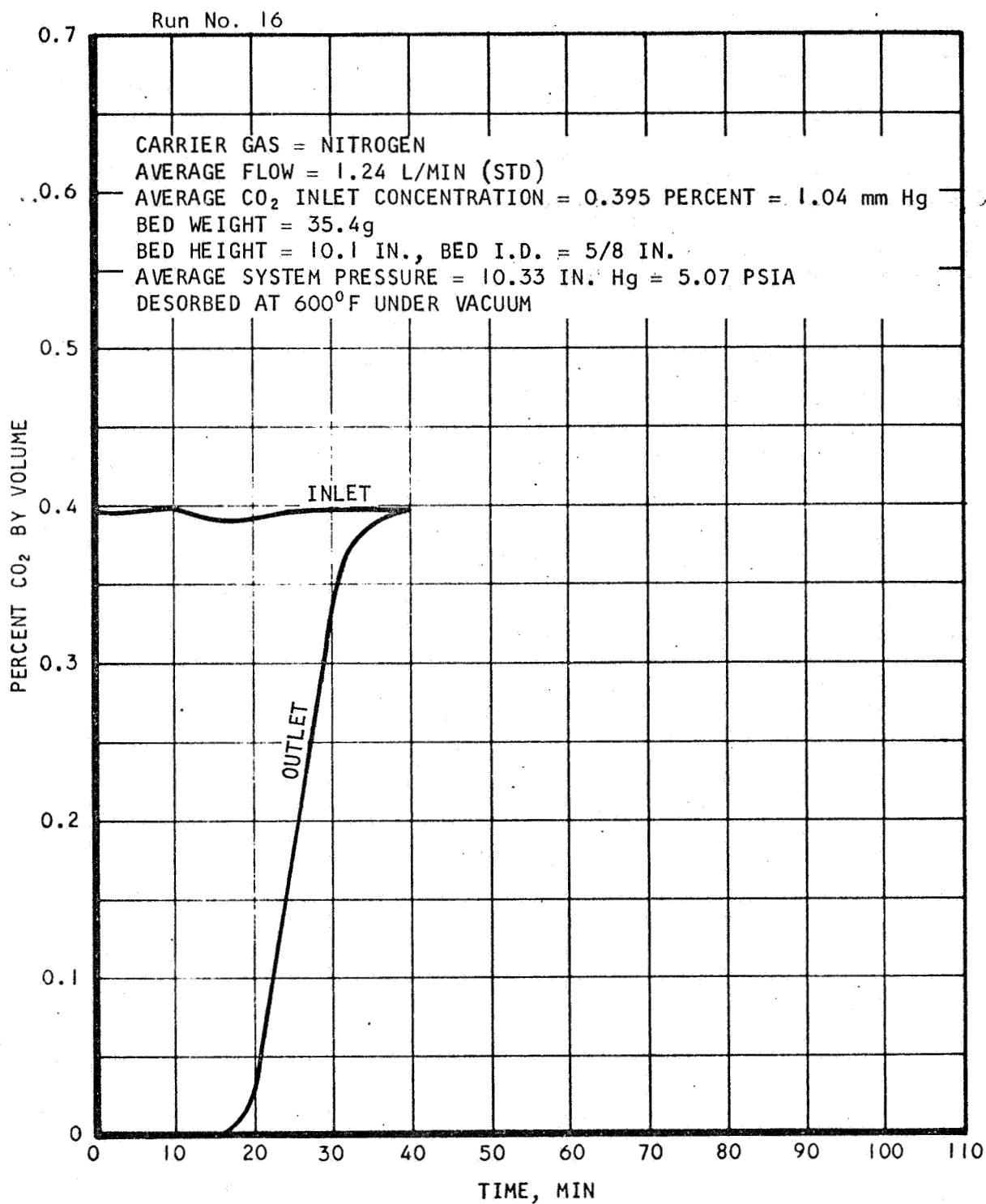
A-22018

Figure C-35.   Dynamic Adsorption of CO_2 on Linde Molecular Sieve
Type 5A, 1/16 in. Diameter Pellets at 50°C

Run No. 16

CARRIER GAS = NITROGEN
AVERAGE FLOW = 1.24 L/MIN (STD)
AVERAGE CO_2 INLET CONCENTRATION = 0.395 PERCENT = 1.04 mm Hg
BED WEIGHT = 35.4g
BED HEIGHT = 10.1 IN., BED I.D. = 5/8 IN.
AVERAGE SYSTEM PRESSURE = 10.33 IN. Hg = 5.07 PSIA
DESORBED AT 600^0F UNDER VACUUM
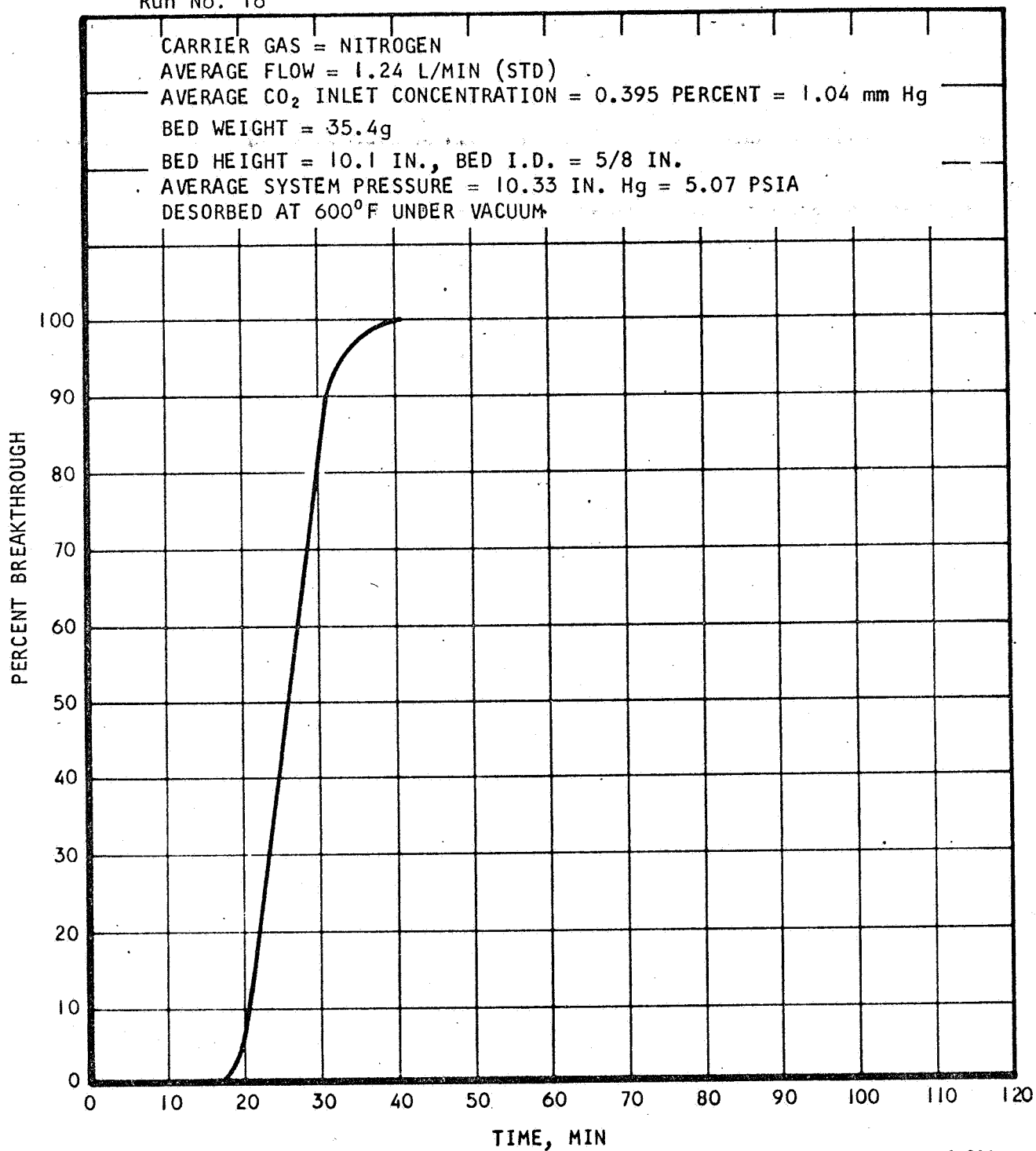
A-22016

Figure C-36.   Breakthrough of CO_2 from Linde Molecular Sieve, Type 5A,
1/16 in. Diameter Pellets at 50^0C

Run No. 17

CARRIER GAS = NITROGEN
AVERAGE FLOW = 1.223 L/MIN (STD)
AVERAGE CO_2 INLET CONCENTRATION = 0.384 PERCENT = 1.01 mm Hg
BED WEIGHT 35.4g
BED HEIGHT = 10.1 IN., BED I.D. = 5/8 IN.
AVERAGE SYSTEM PRESSURE = 10.34 IN. Hg = 5.08 PSIA
DESORBED AT 600°F UNDER VACUUM

INLET

OUTLET

PERCENT CO_2 BY VOLUME

TIME, MIN
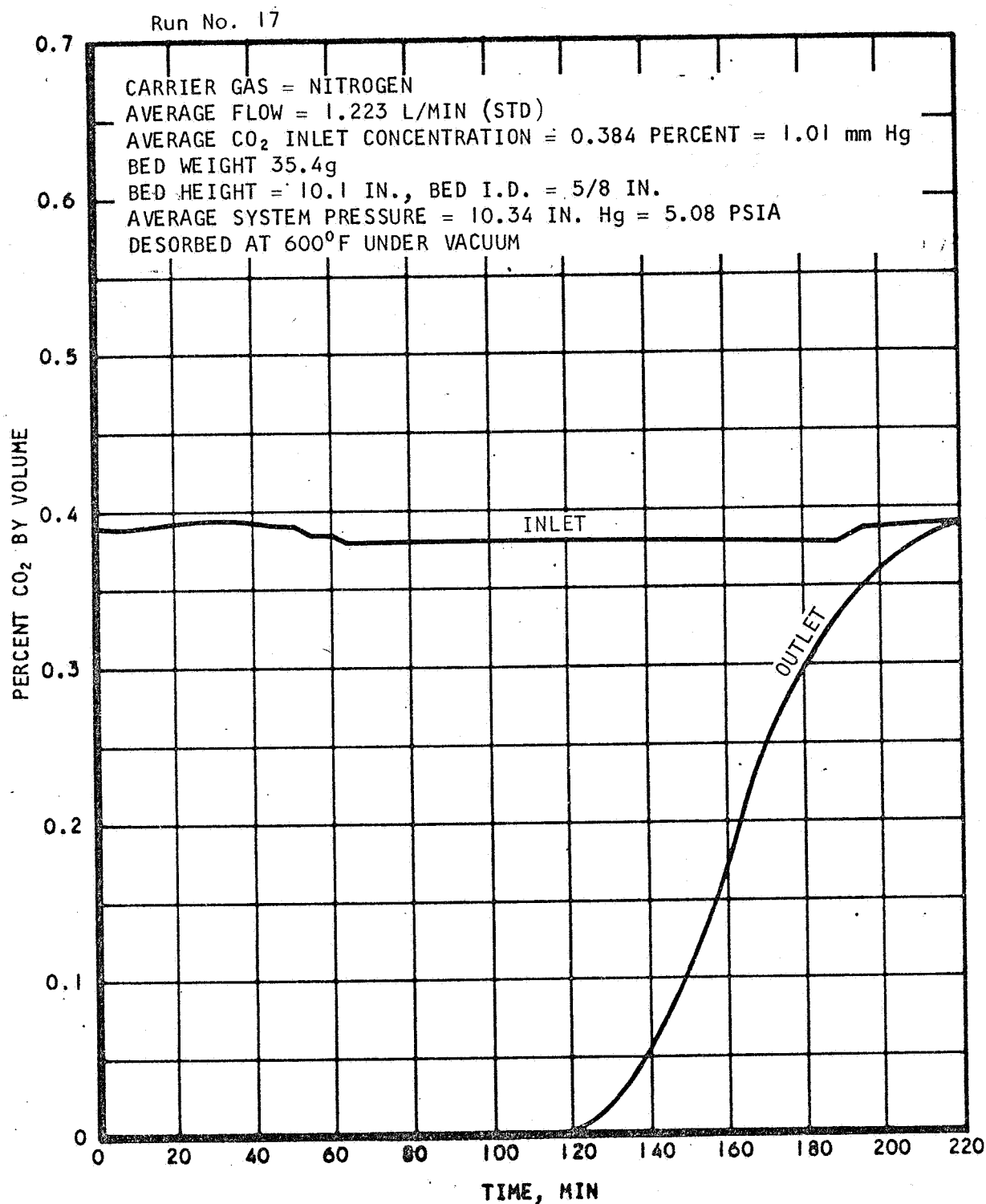
A-22017

Figure C-37. Dynamic Adsorption of CO_2 on Linde Molecular Sieve
Type 5A, 1/16 in. Diameter Pellets at 0°C

Run No. 17

CARRIER GAS = NITROGEN
AVERAGE FLOW = 1.223 L/MIN (STD)
AVERAGE CO_2 INLET CONCENTRATION = 0.384 PERCENT = 1.01 mm Hg
BED WEIGHT = 35.4g
BED HEIGHT = 10.1 IN., BED I.D. = 5/8 IN.
AVERAGE SYSTEM PRESSURE = 10.34 IN. Hg = 5.08 PSIA
DESORBED AT 600°F UNDER VACUUM

PERCENT BREAKTHROUGH

TIME, MIN
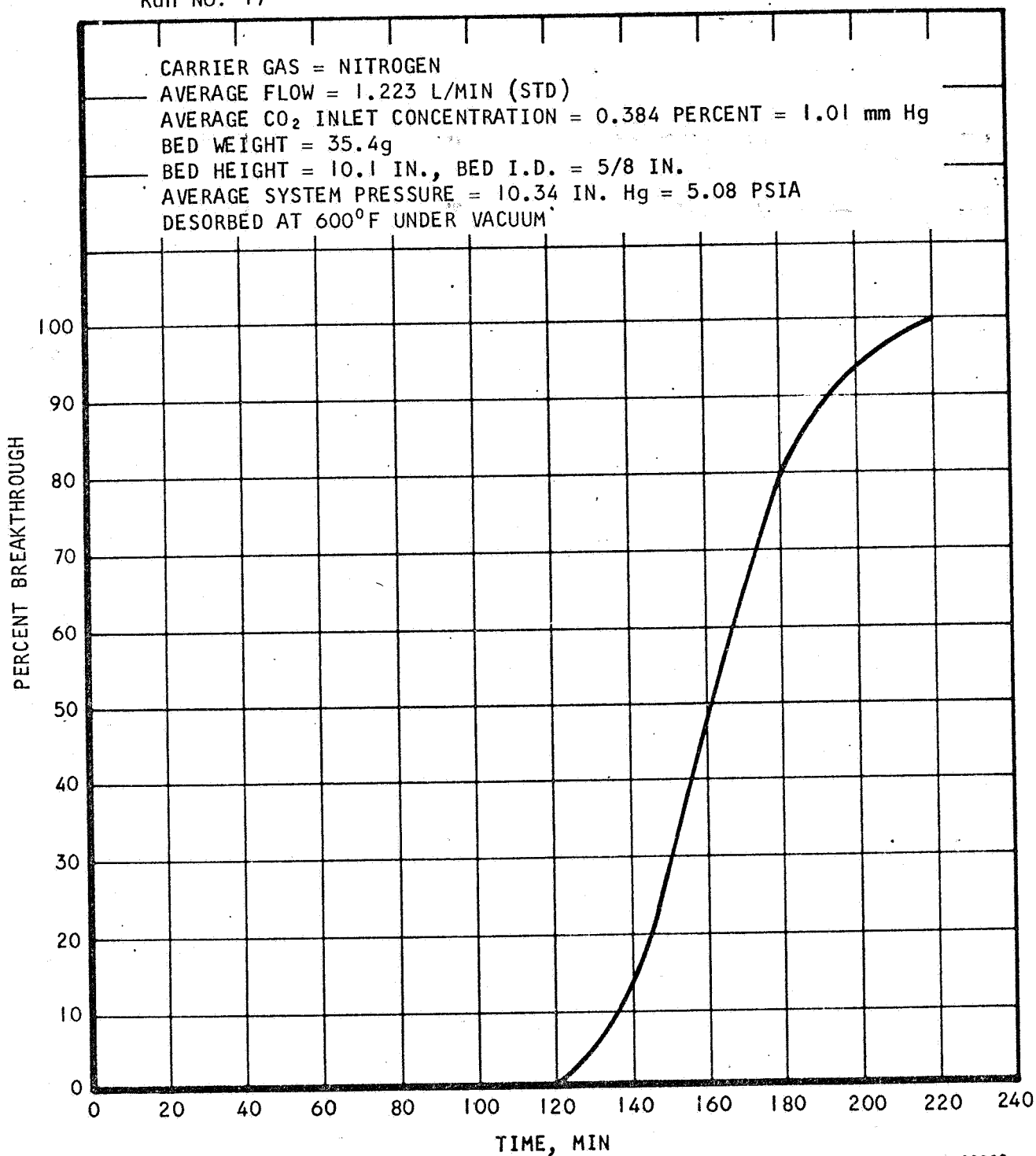
A-22002

Figure C-38.   Breakthrough of CO_2 from Linde Molecular Sieve, Type 5A,
1/16 in. Diameter Pellets at 0°C

RUN NO. IW
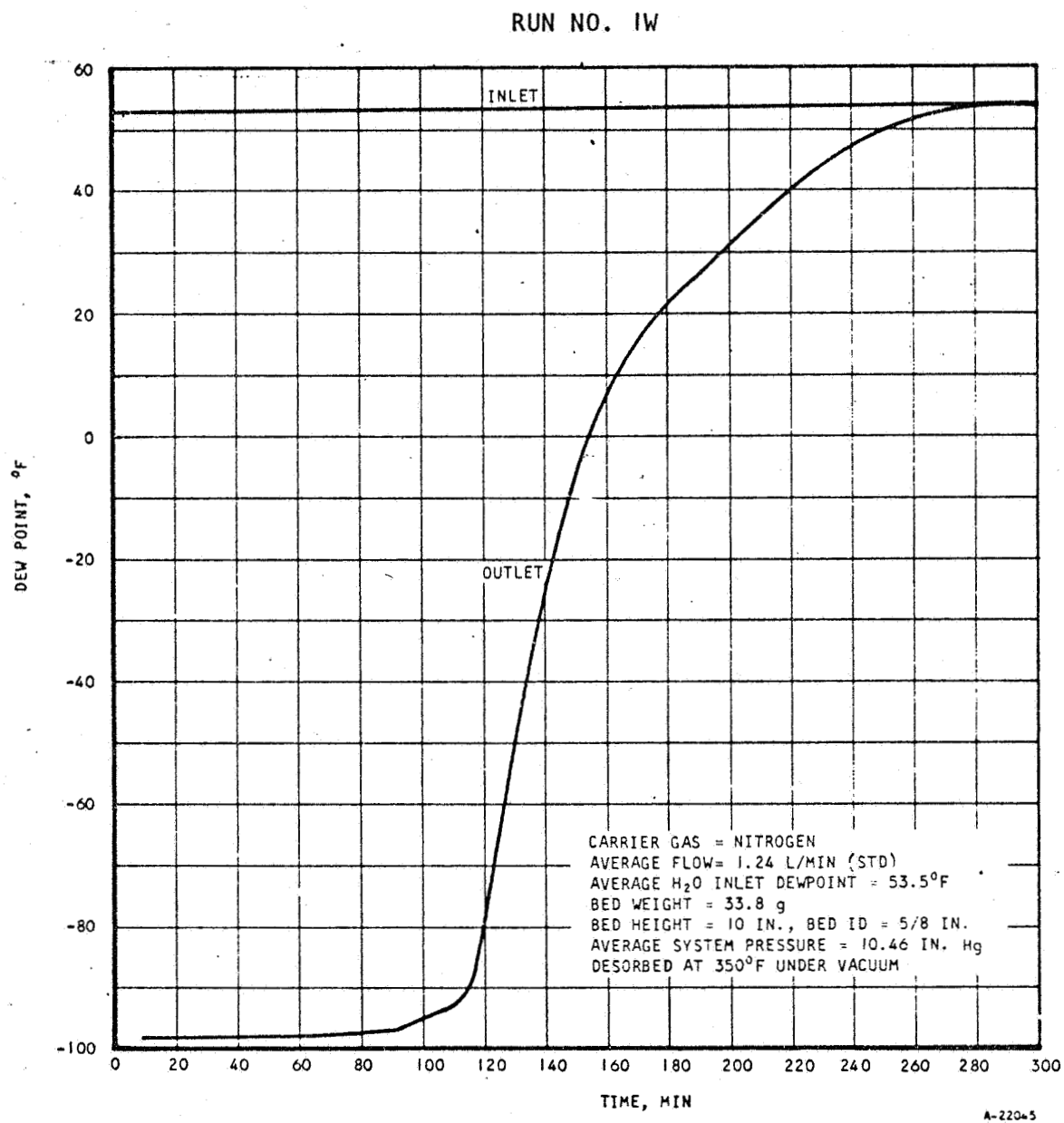
Figure C-39. Dynamic Adsorption of H_2O Vapor on Davison Silica Gel, Grade 05, 6-16 Mesh Granules at 25°C

AIRESEARCH MANUFACTURING DIVISION
Los Angeles, California

RUN NO. 1W

CARRIER GAS = NITROGEN
AVERAGE FLOW = 1.24 L/MIN (STD)
AVERAGE H_2O INLET DEWPOINT = 53.5°F
BED WEIGHT = 33.8 g
BED HEIGHT = 10 IN., BED ID = 5/8 IN.
AVERAGE SYSTEM PRESSURE = 10.46 IN. Hg
DESORBED AT 350°F UNDER VACUUM

PERCENT BREAKTHROUGH

TIME, MIN
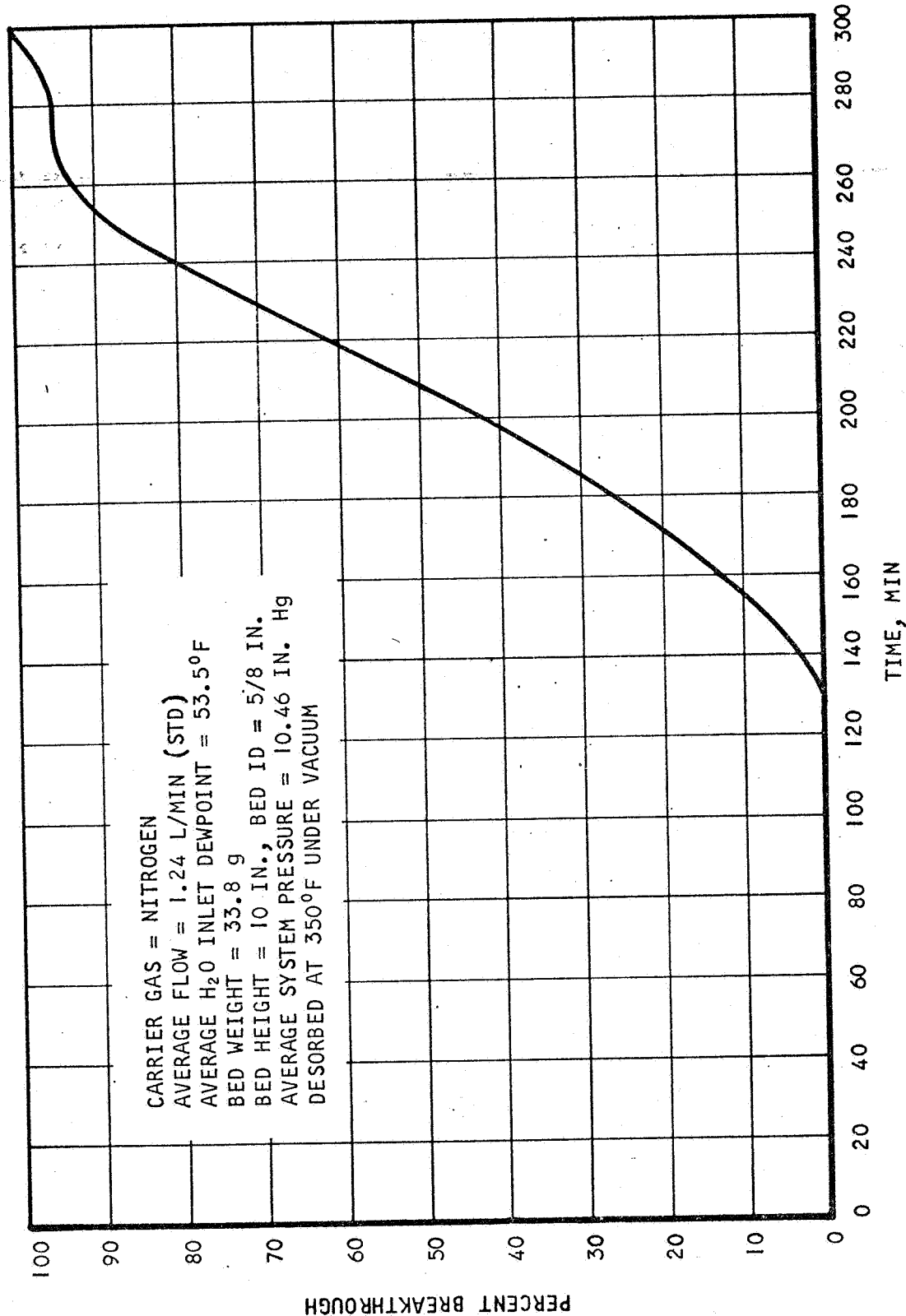
A-22034

Figure C-40. Breakthrough of Water Vapor From Davison Silica Gel, Grade 05, 6-16 Mesh Granules at 25°C

GARRETT AIRESEARCH MANUFACTURING DIVISION
Los Angeles, California

67-1751
Page C-40

RUN NO. 4W

CARRIER GAS = NITROGEN
AVERAGE FLOW = 1.22 L/MIN (STD)
AVERAGE H_2O INLET DEWPOINT = 49.3°F
BED WEIGHT = 33.8 g
BED HEIGHT = 10 IN., BED ID = 5/8 IN.
AVERAGE SYSTEM PRESSURE = 10.35 IN. Hg
DESORBED AT 350°F UNDER VACUUM
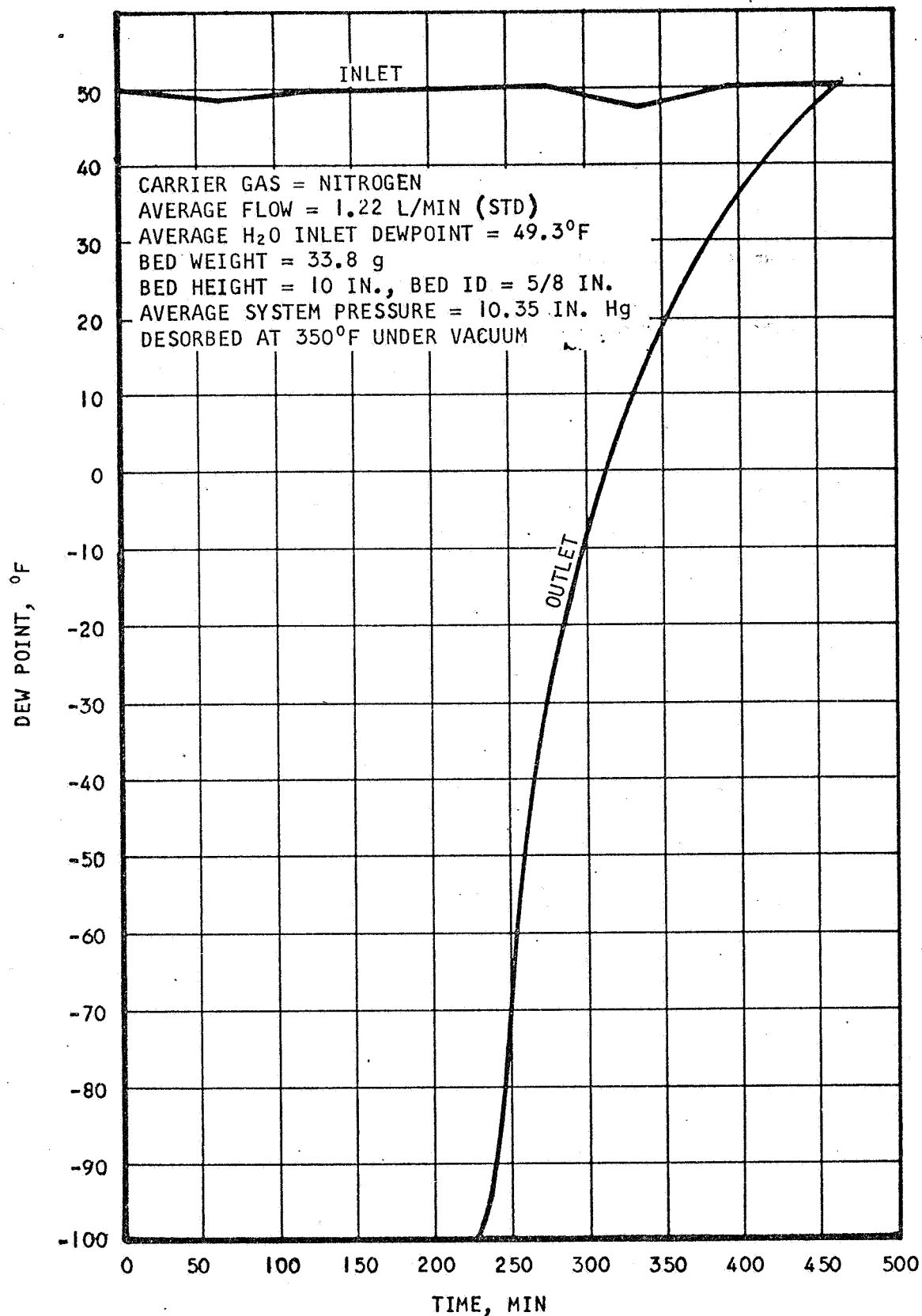
A-22037

Figure C-41.   Dynamic Adsorption of H_2O Vapor on Davison Silica Gel Grade 05, 6-16 Mesh Granules at 15.56°C (60°F)

RUN NO. 4W

CARRIER GAS = NITROGEN
AVERAGE FLOW = 1.22 L/MIN (STD)
AVERAGE H_2O INLET DEWPOINT = 49.3°F
BED WEIGHT = 33.8 g
BED HEIGHT = 10 IN., BED ID = 5/8 IN.
AVERAGE SYSTEM PRESSURE = 10.35 IN. Hg
DESORBED AT 350°F UNDER VACUUM

PERCENT BREAKTHROUGH

TIME, MIN
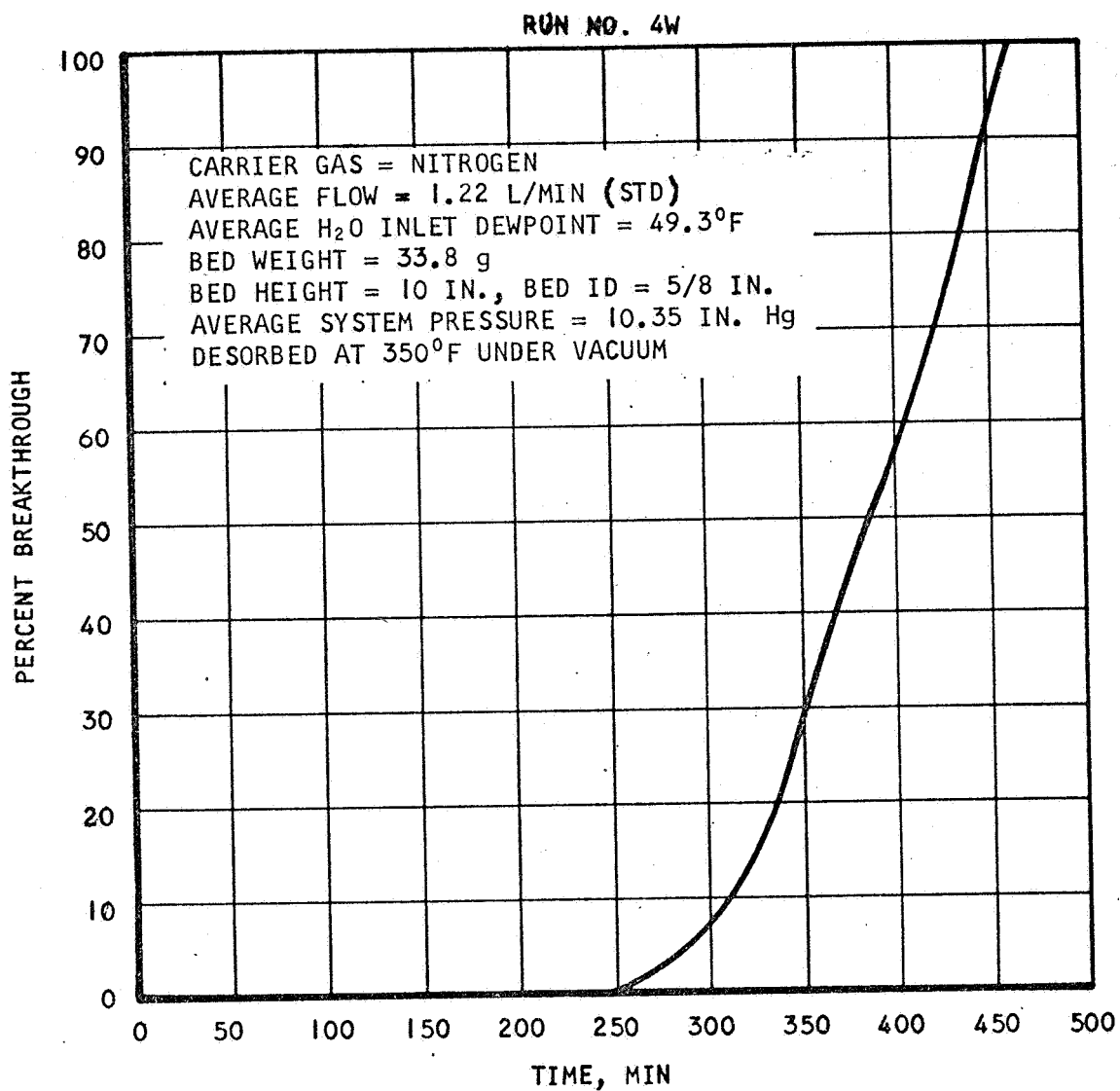
A-22038

Figure C-42. Breakthrough of Water Vapor From Davison Silica Gel, Grade 05, 6-16 Mesh Granules at 15.56°C (60°F)

RUN NO. 1

RUN NO.	EQUILIBRIUM CO_2 LOADING $\dfrac{g\ CO_2}{g\ SIEVE}$ (MM Hg)	
	INITIAL	FINAL
1	0.062, (7.98)	0.007, (0.241)
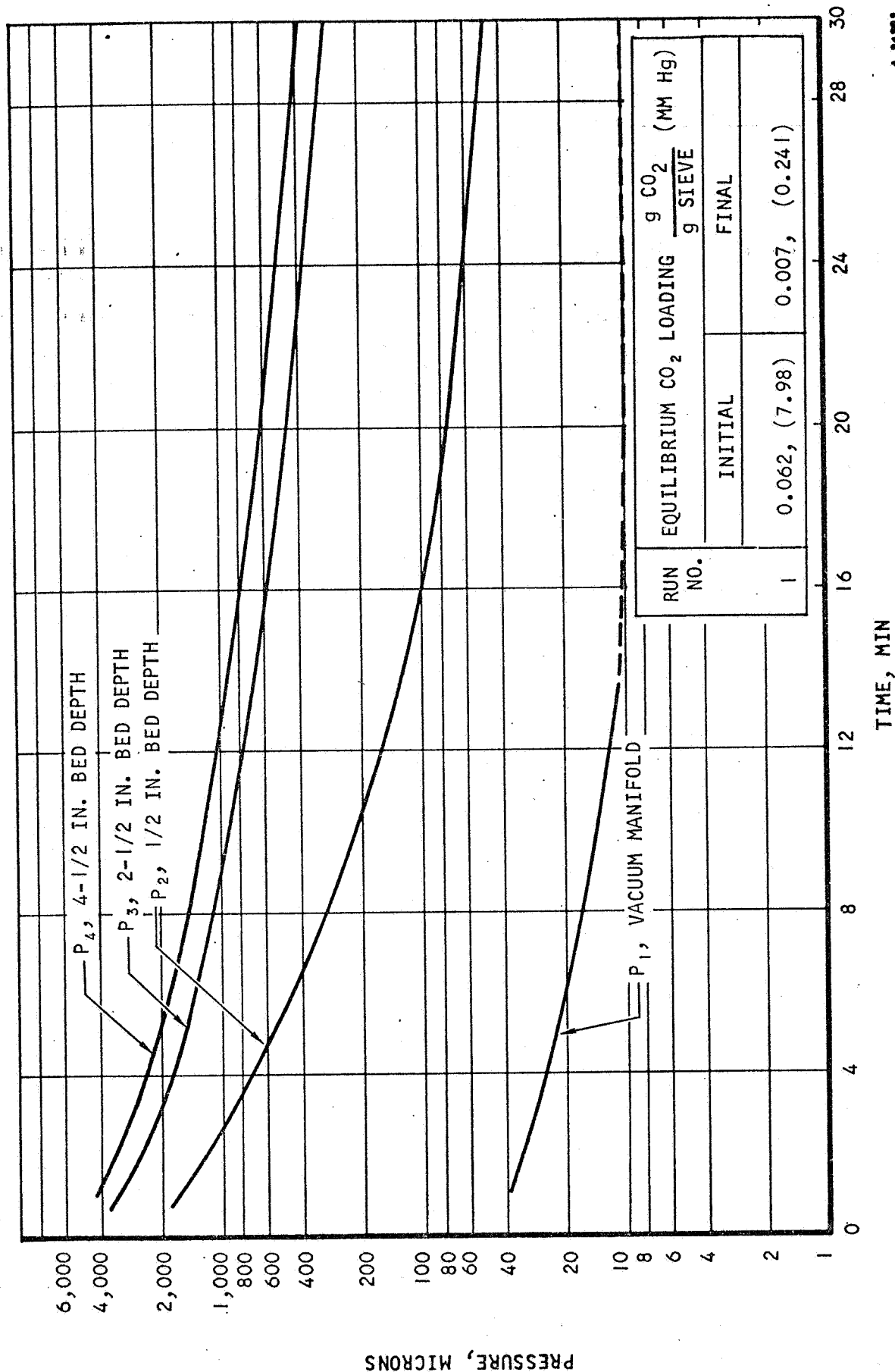
Figure C-43. Vacuum Desorption of CO_2 from Linde Molecular Sieve, Type 5A, 1/16 in. Diameter Pellets at 25°C

GARRETT AIRESEARCH MANUFACTURING DIVISION
Los Angeles, California

A-36892
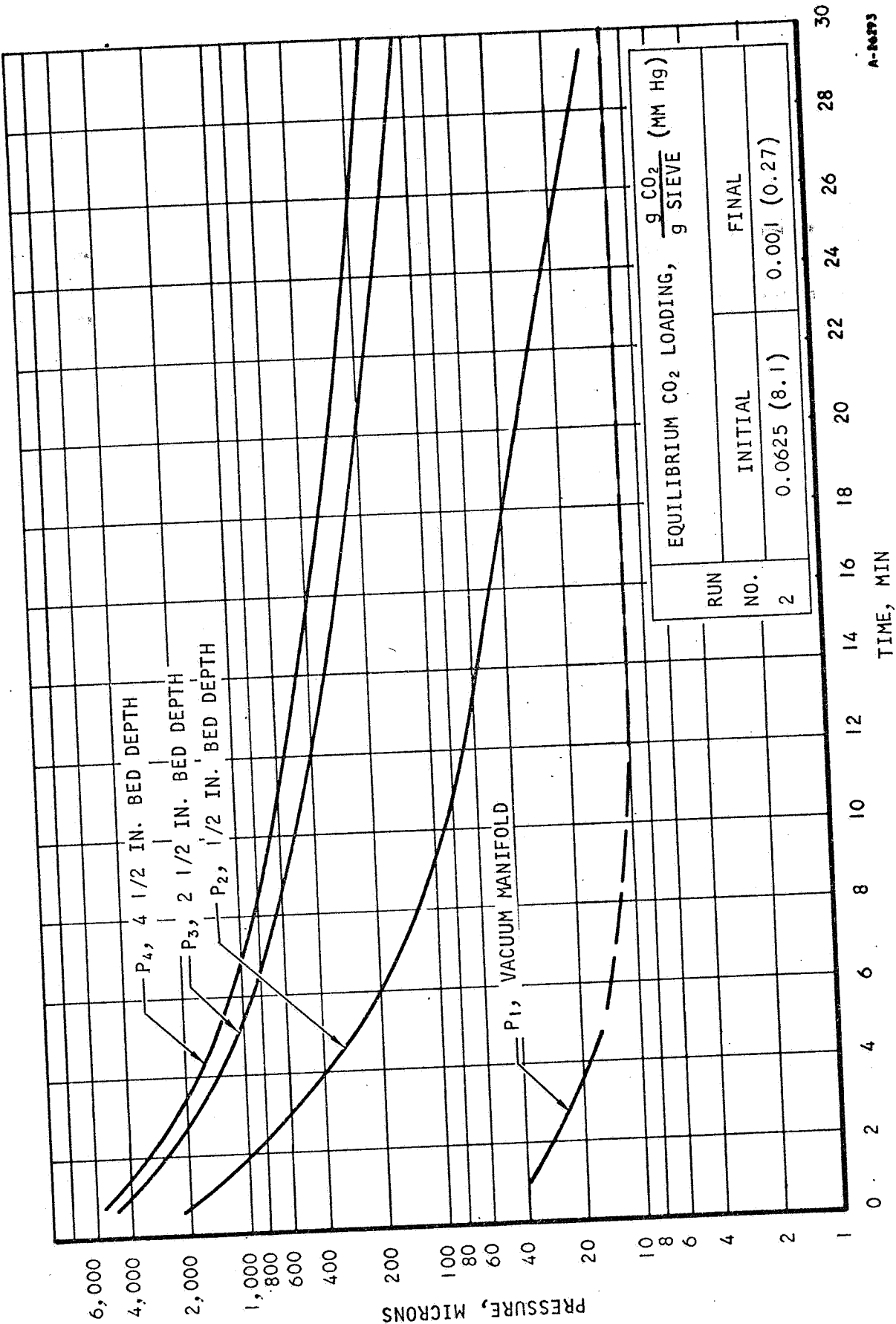
Figure C-44. Vacuum Desorption of CO_2 from Linde Molecular Sieve, Type 5A, 1/16 in. Diameter Pellets at 50°C
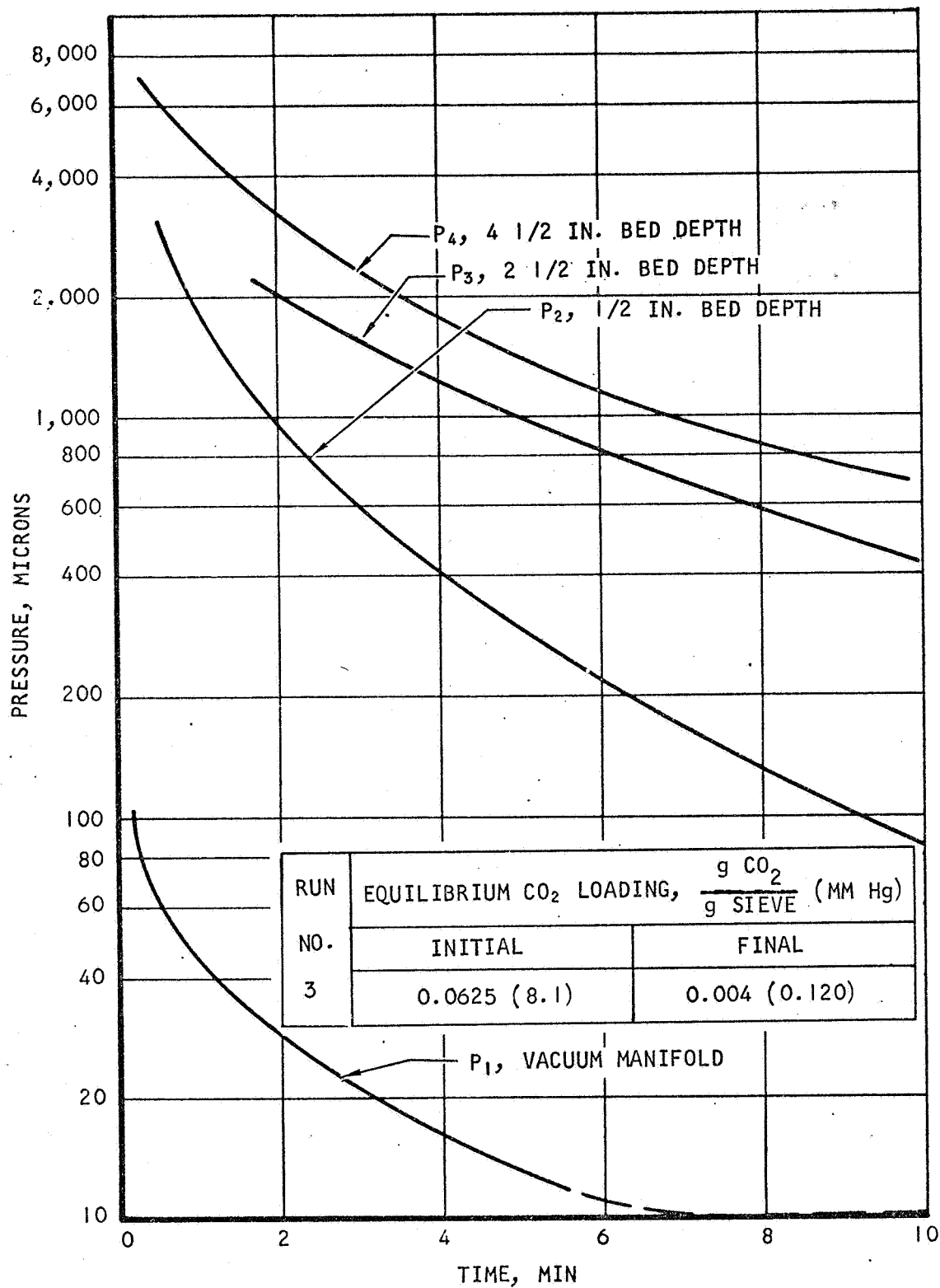
Figure C-45. Vacuum Desorption of CO_2 from Linde Molecular Sieve, Type 5A, 1/16 in. Diameter Pellets at $50°C$

GARRETT AIRESEARCH MANUFACTURING DIVISION
Los Angeles, California
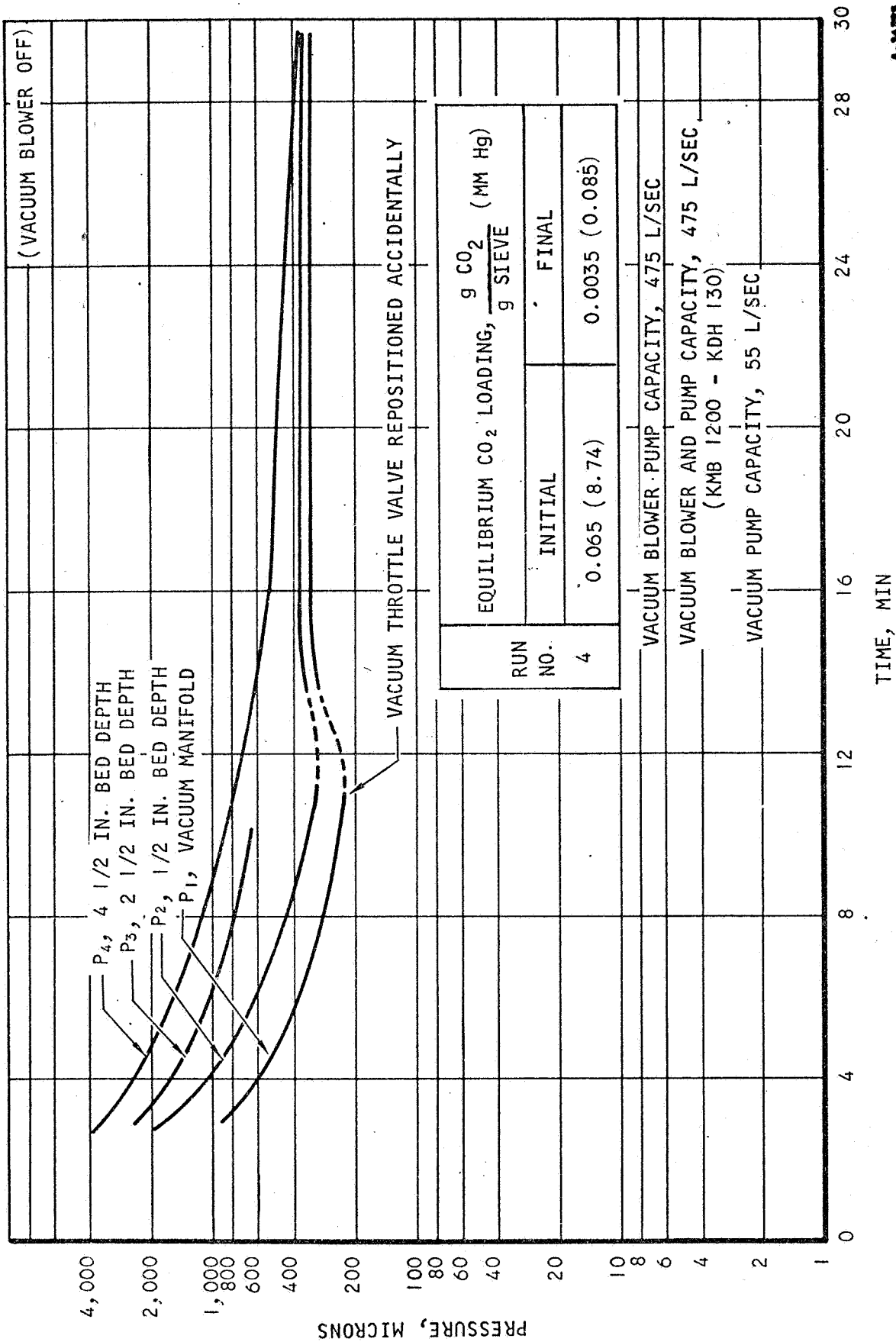
Figure C-46. Vacuum Desorption of CO_2 from Linde Molecular Sieve, Type 5A, 1/16 in. Diameter Pellets at 50^0C with Throttled Vacuum

AIRESEARCH MANUFACTURING DIVISION
Los Angeles, California
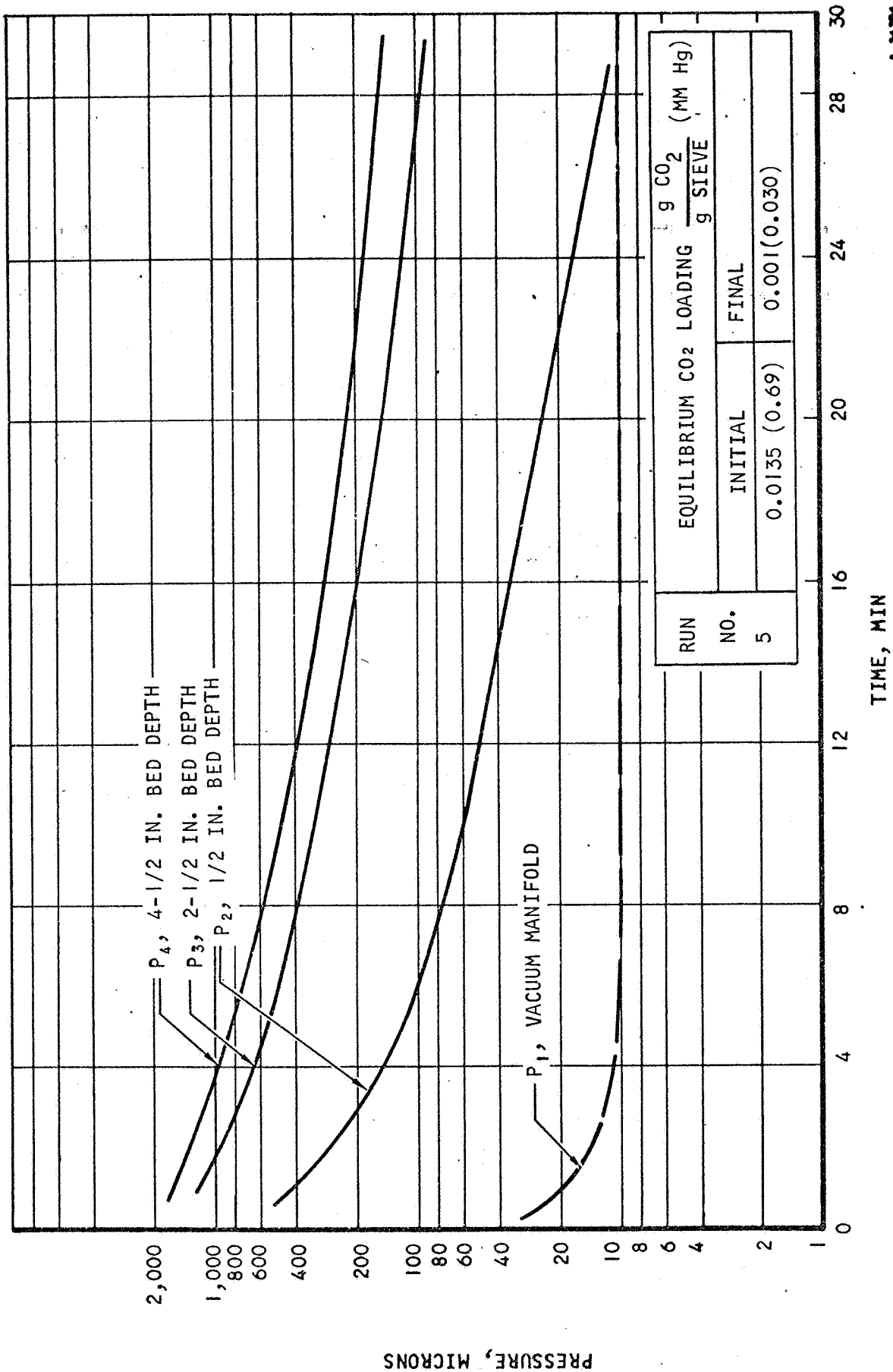
Figure C-47. Vacuum Desorption of CO_2 from Linde Molecular Sieve, Type 5A, 1/16 in. Diameter Pellets at 50°C

RUN NO. 5

	EQUILIBRIUM CO_2 LOADING $\frac{g\ CO_2}{g\ SIEVE}$ (MM Hg)	
RUN NO.	INITIAL	FINAL
5	0.0135 (0.69)	0.001 (0.030)

P_4, 4-1/2 IN. BED DEPTH
P_3, 2-1/2 IN. BED DEPTH
P_2, 1/2 IN. BED DEPTH

P_1, VACUUM MANIFOLD

TIME, MIN

PRESSURE, MICRONS

A-26376
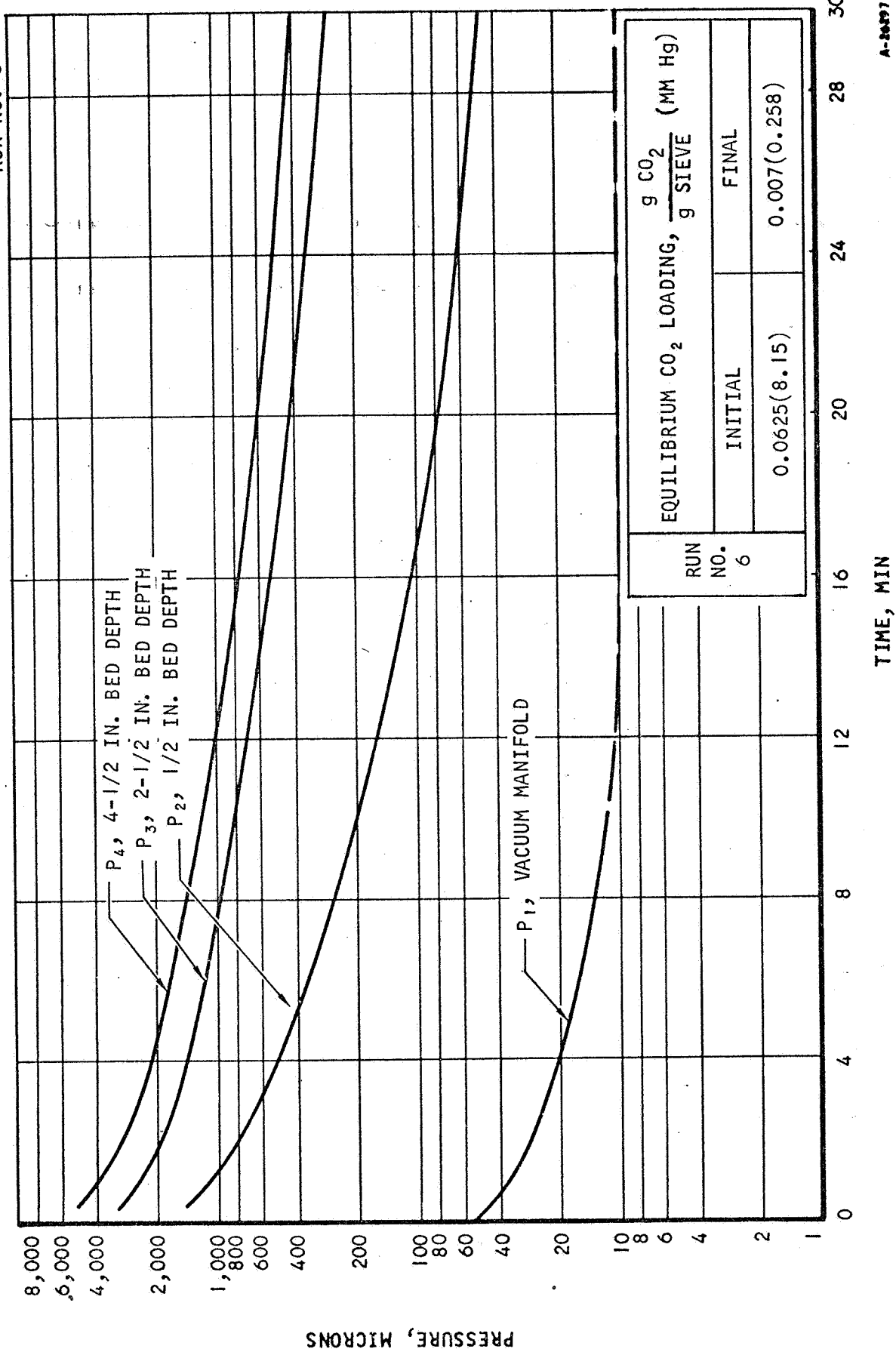
Figure C-48. Vacuum Desorption of CO_2 from Linde Molecular Sieve, Type 5A, 1/16 in. Diameter Pellets at Ambient Adiabatic Conditions
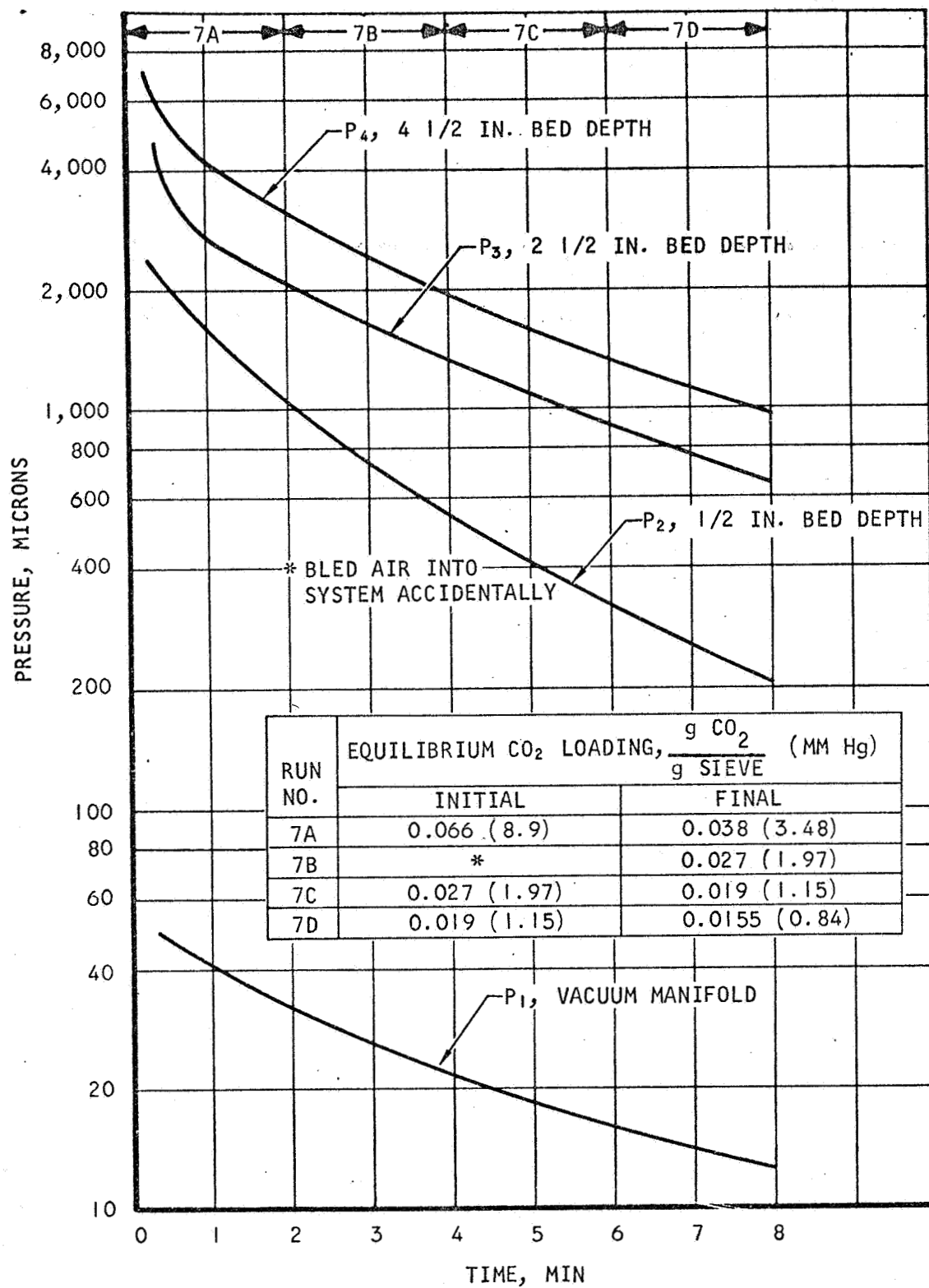
Figure C-49. Vacuum Desorption of CO_2 from Linde Molecular Sieve, Type 5A, 1/16 in. Diameter Pellets at 25°C

A-26298

The graph shows PRESSURE, MICRONS (vertical axis, from 10 to 8,000) versus TIME, MIN (horizontal axis, 0 to 8), with curves labeled:

- P_4, 4 1/2 IN. BED DEPTH
- P_3, 2 1/2 IN. BED DEPTH
- P_2, 1/2 IN. BED DEPTH
- P_1, VACUUM MANIFOLD
- * BLED AIR INTO SYSTEM ACCIDENTALLY

Top regions labeled 7A, 7B, 7C, 7D.

RUN NO.	EQUILIBRIUM CO_2 LOADING, $\frac{g\ CO_2}{g\ SIEVE}$ (MM Hg)	
	INITIAL	FINAL
7A	0.066 (8.9)	0.038 (3.48)
7B	*	0.027 (1.97)
7C	0.027 (1.97)	0.019 (1.15)
7D	0.019 (1.15)	0.0155 (0.84)

RUN NO. 8

RUN NO.	EQUILIBRIUM CO_2 LOADING, $\dfrac{g\ CO_2}{g\ SIEVE}$ (MM Hg)			
	INITIAL		FINAL	
8A	0.0625	(8.17)	0.025	(1.74)
8B	0.025	(1.74)	0.007	(0.251)

TIME, MIN

PRESSURE, MICRONS

Figure C-50. Vacuum Desorption of CO_2 from Linde Molecular Sieve, Type 5A, 1/16 in. Diameter Pellets at 25°C with Throttled Vacuum

A-26399

Figure C-51. Vacuum Desorption of CO_2 from Linde Molecular Sieve,
Type 5A, 1/16 in. Diameter Pellets at 25°C

| RUN NO. | EQUILIBRIUM CO_2 LOADING, $\dfrac{g\ CO_2}{g\ SIEVE}$ (MM Hg) | |
	INITIAL	FINAL
9A	0.0625 (8.15)	0.0175 (1.04)
9B	0.0175 (1.04)	0.010 (0.399)
9C	0.010 (0.399)	0.0055 (0.188)
9D	0.0055 (0.188)	0.0035 (0.094)

The chart is titled with axes PRESSURE, MICRONS (vertical) and TIME, MIN (horizontal), labeled RUN NO. 10.

Curve labels:
- P_4, 4-1/2 IN. BED DEPTH
- P_3, 2-1/2 IN. BED DEPTH
- P_2, 1/2 IN. BED DEPTH
- P_1, VACUUM MANIFOLD

RUN NO.	EQUILIBRIUM CO_2 LOADING, $\dfrac{g\ CO_2}{g\ SIEVE}$ (MM Hg)	
	INITIAL	FINAL
10	0.062(8.0)	0.001 (0.025)
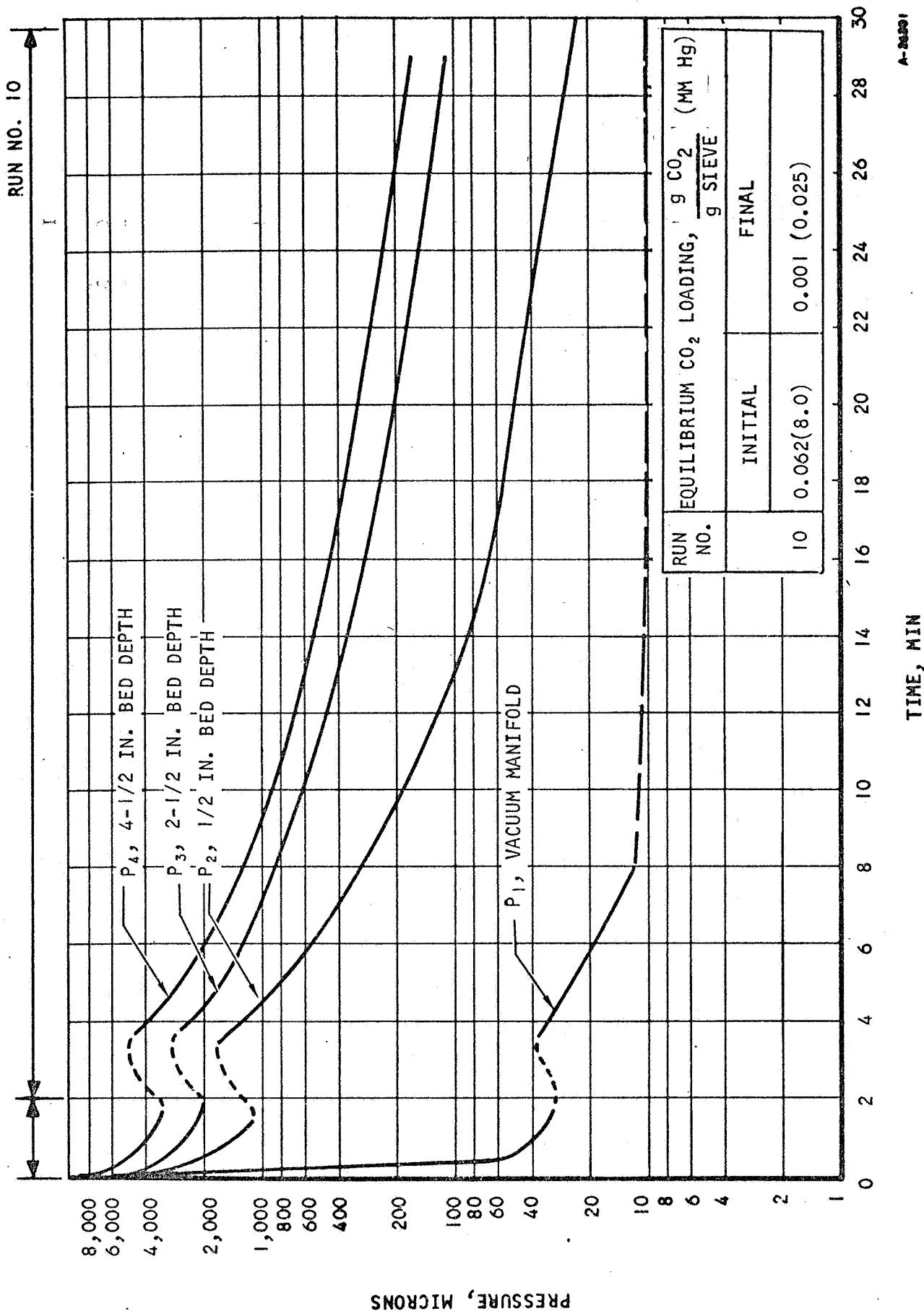
Figure C-52.   Vacuum Desorption of CO_2 from Linde Molecular Sieve, Type 5A, 1/16 In. Diameter Pellets at 25°C for 2 Min and 50°C for 28 Min

A-26291

GARRETT AIRESEARCH MANUFACTURING DIVISION
Los Angeles, California

67-1751
Page C-52

	EQUILIBRIUM CO_2 LOADING, $\frac{g\ CO_2}{g\ SIEVE}$ (mm Hg)	
RUN NO.	INITIAL	FINAL
11A	0.0625 (8.15)	0.035 (3.04)
11B	0.035 (3.04)	0.013 (0.64)
11C	0.013 (0.64)	0.007 (0.258)
11D	0.007 (0.258)	0.0037 (0.109)

A-33894
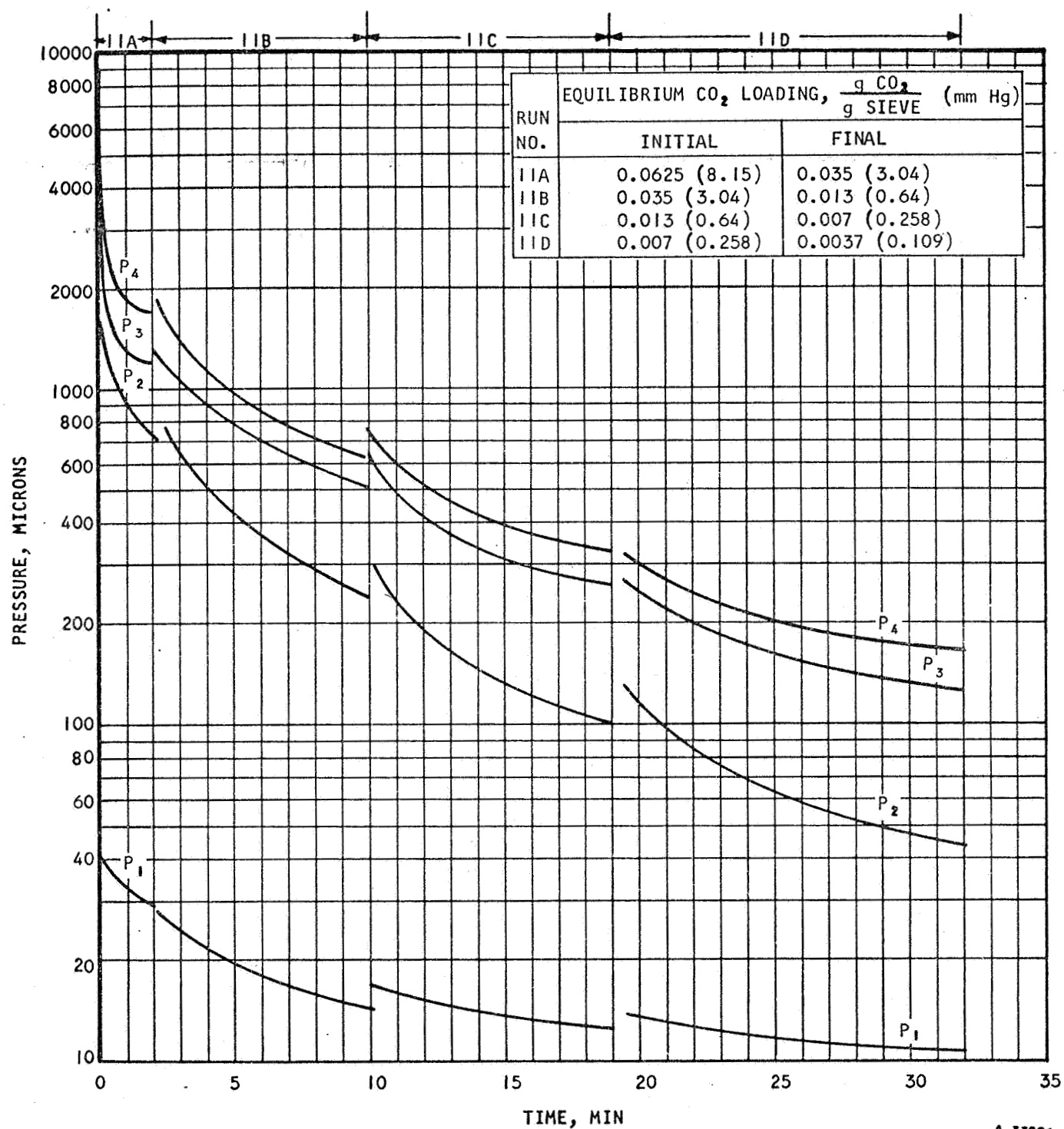
Figure C-53.   Vacuum Desorption of CO_2 from Linde Molecular Sieve,
Type 5A, 1/8 in. Diameter Pellets at 25°C
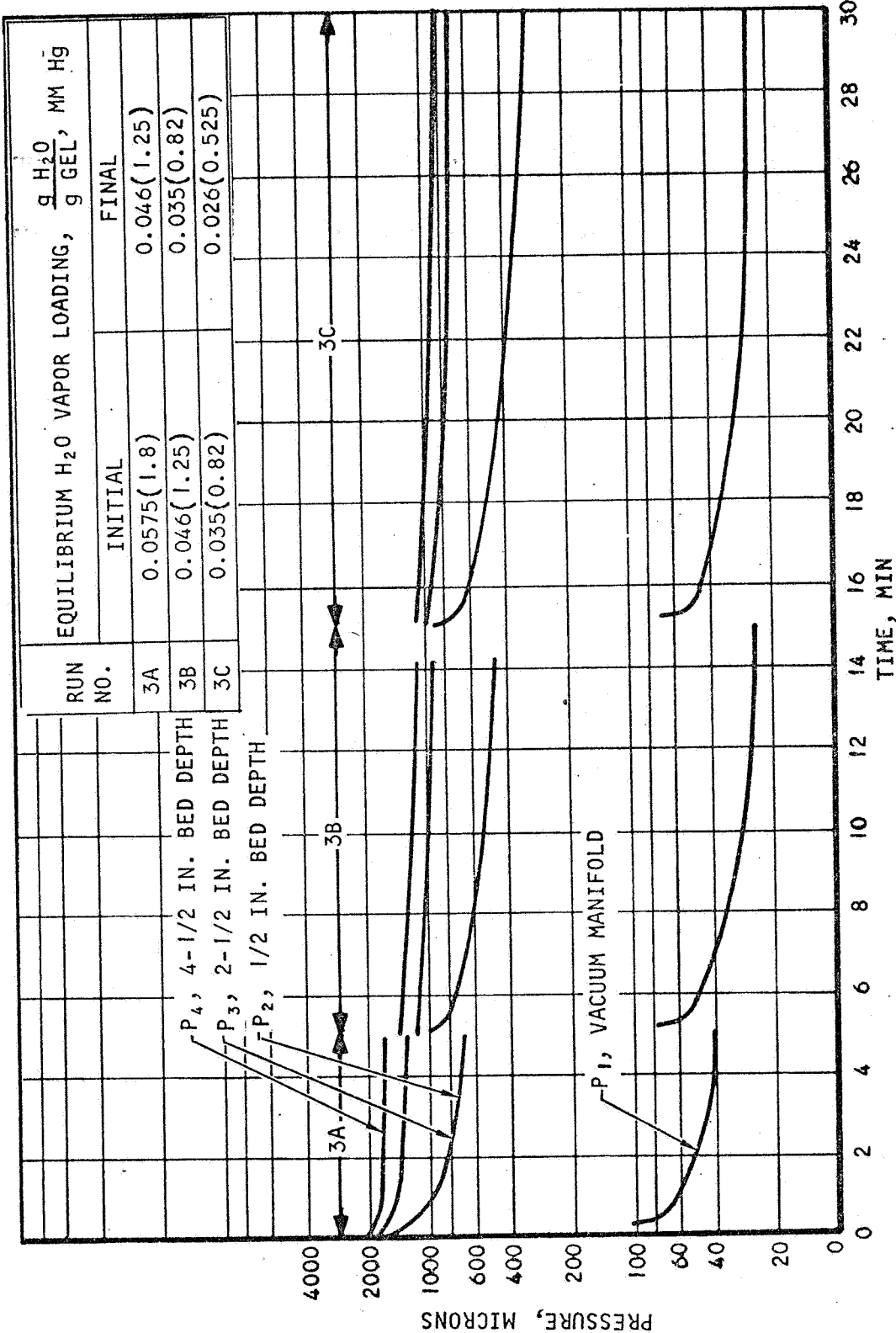
Figure C-54. Vacuum Desorption of H_2O Vapor from Davison Silica Gel, Grade 05, 6-16 Mesh Granules at 25°C

Figure C-55. Vacuum Desorption of H_2O Vapor from Davison Silica Gel, Grade 05, 6-16 Mesh Granules at 50°C

RUN NO.	EQUILIBRIUM H_2O VAPOR LOADING, $\frac{g\ H_2O}{g\ GEL}$, MM Hg	
	INITIAL	FINAL
5A	0.062(1.94)*	0.033(3.6)***
5B	0.033(3.6)***	0.0155(1.13)***
5C	0.0155(1.13)***	<0.007(0.050)*

*EQUILIBRIUM AT 25°C
***EQUILIBRIUM AT 50°C

P_4, 4-1/2 IN. BED DEPTH
P_3, 2-1/2 IN. BED DEPTH
P_2, 1/2 IN. BED DEPTH
P_1, VACUUM MANIFOLD

RUN NO. 5

PRESSURE, MICRONS

TIME, MIN
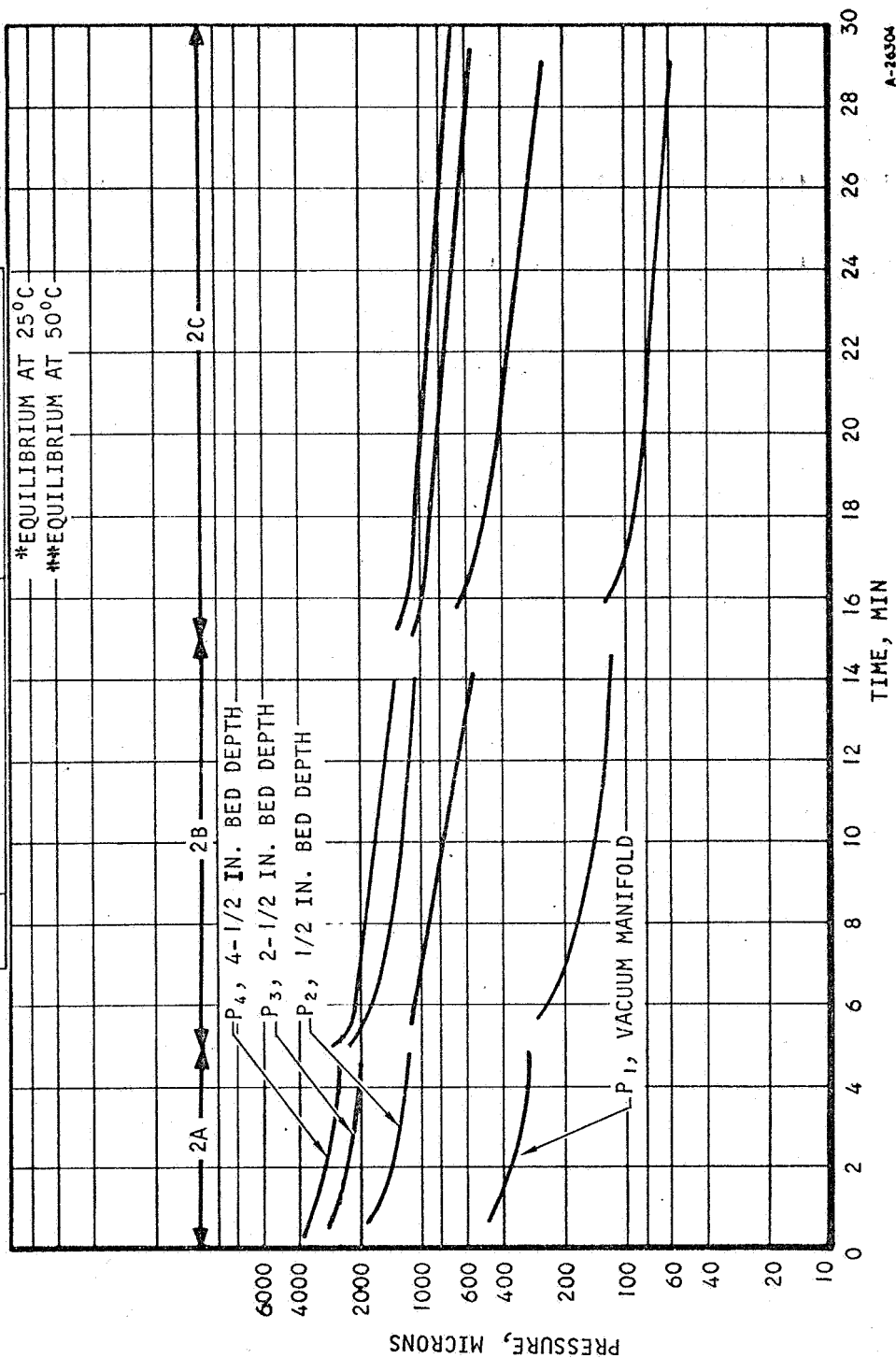
A-26304

Figure C-56. Vacuum Desorption of H_2O Vapor from Davison Silica Gel, Grade 05, 6-16 Mesh Granules at 50°C at Throttled Vacuum
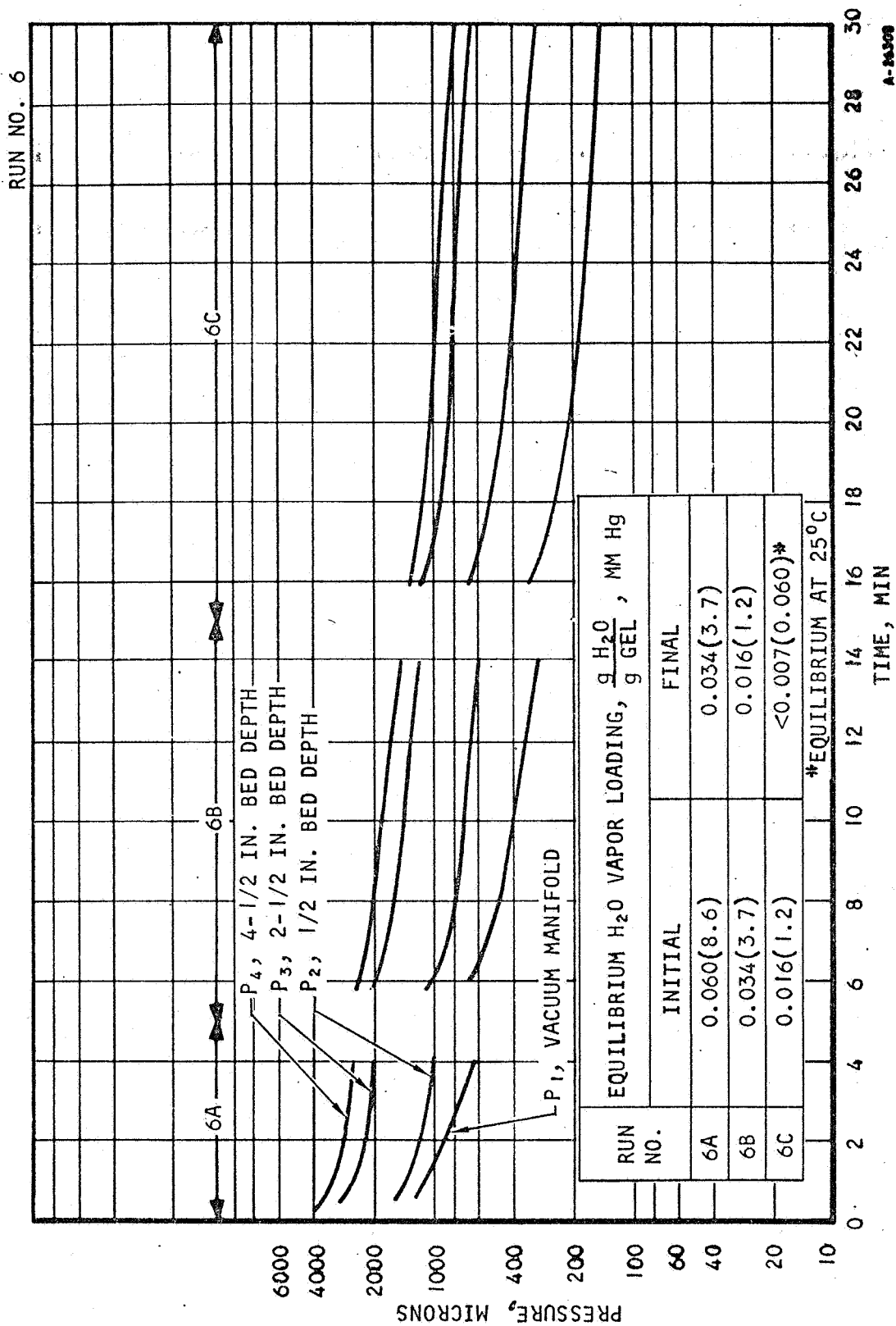
Figure C-57. Vacuum Desorption of H_2O Vapor from Davison Silica Gel, Grade 05, 6-16 Mesh Granules at 50°C at Throttled Vacuum

RUN NO. 6

EQUILIBRIUM H_2O VAPOR LOADING, $\dfrac{g\ H_2O}{g\ GEL}$, MM Hg		
RUN NO.	INITIAL	FINAL
6A	0.060(8.6)	0.034(3.7)
6B	0.034(3.7)	0.016(1.2)
6C	0.016(1.2)	<0.007(0.060)*

*EQUILIBRIUM AT 25°C

P_4, 4-1/2 IN. BED DEPTH
P_3, 2-1/2 IN. BED DEPTH
P_2, 1/2 IN. BED DEPTH
P_1, VACUUM MANIFOLD

A-24308

Figure C-58. Vacuum Desorption of H_2O Vapor from Davison Silica·Gel, Grade 05, 6-16 Mesh Granules at 38°C

Figure C-59. Vacuum Desorption of H_2O Vapor from Davison Silica Gel, 67-1751 Grade 05, 6-16 Mesh Granules at Ambient Adiabatic Conditions

RUN NO.	EQUILIBRIUM H_2O VAPOR LOADING $\frac{g\ H_2O}{g\ GEL}$, MM Hg	
	INITIAL	FINAL
9A	0.059(8.5)	0.0445(5.6)
9B	0.0445(5.6)	0.0208(1.82)
9C	0.0208(1.82)	0.0085(0.425)
9D	0.0085(0.425)	<0.003(0.015)*

*EQUILIBRIUM H_2O LOADING AT 25°C

RUN NO. 9

A-26308

P_4, 4-1/2 IN. BED DEPTH
P_3, 2-1/2 IN. BED DEPTH
P_2, 1/2 IN. BED DEPTH
P_1, VACUUM MANIFOLD

TIME, MIN

PRESSURE, MICRONS
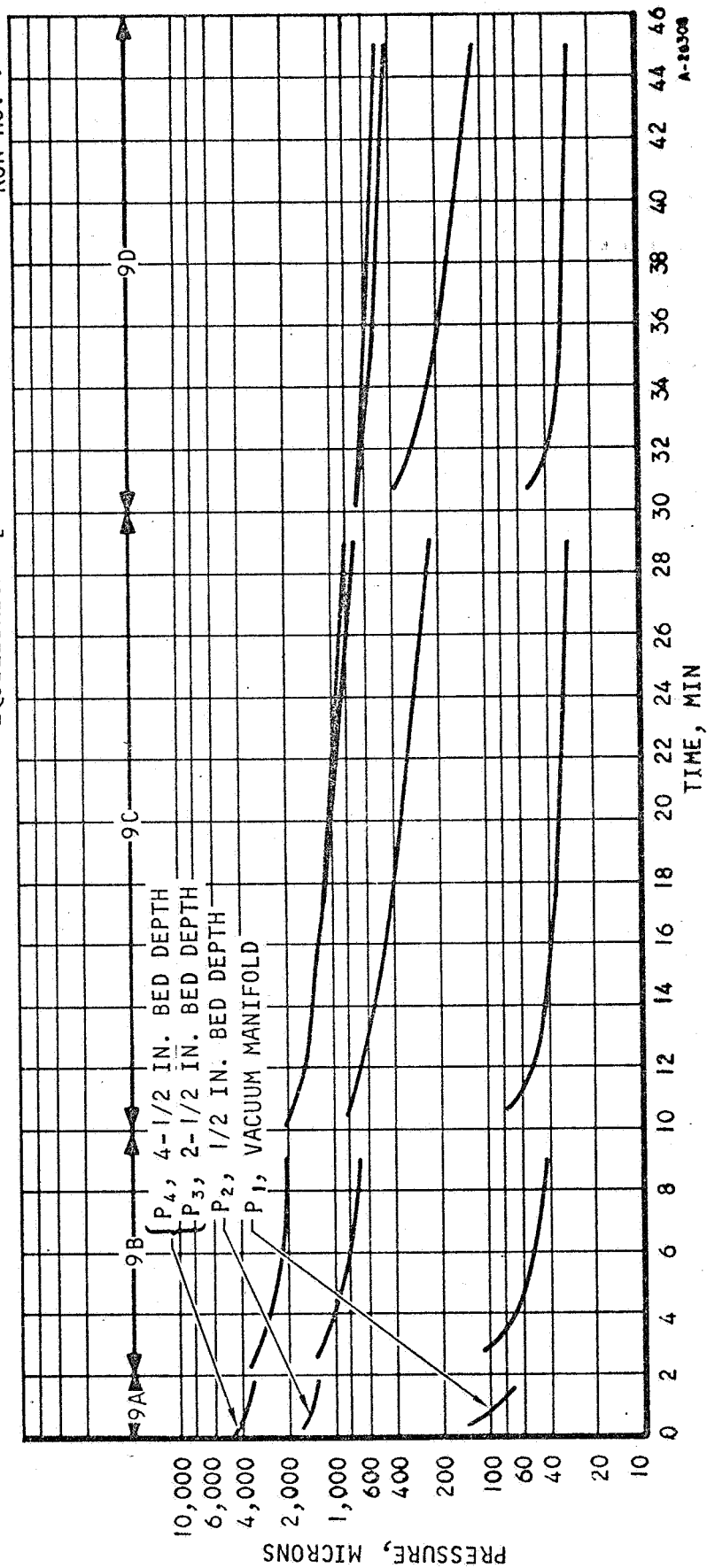
Figure C-60. Vacuum Desorption of H_2O Vapor from Davison Silica Gel, Grade 05, 6-16 Mesh Granules at 50°C

GARRETT | AIRESEARCH MANUFACTURING DIVISION
Los Angeles, California
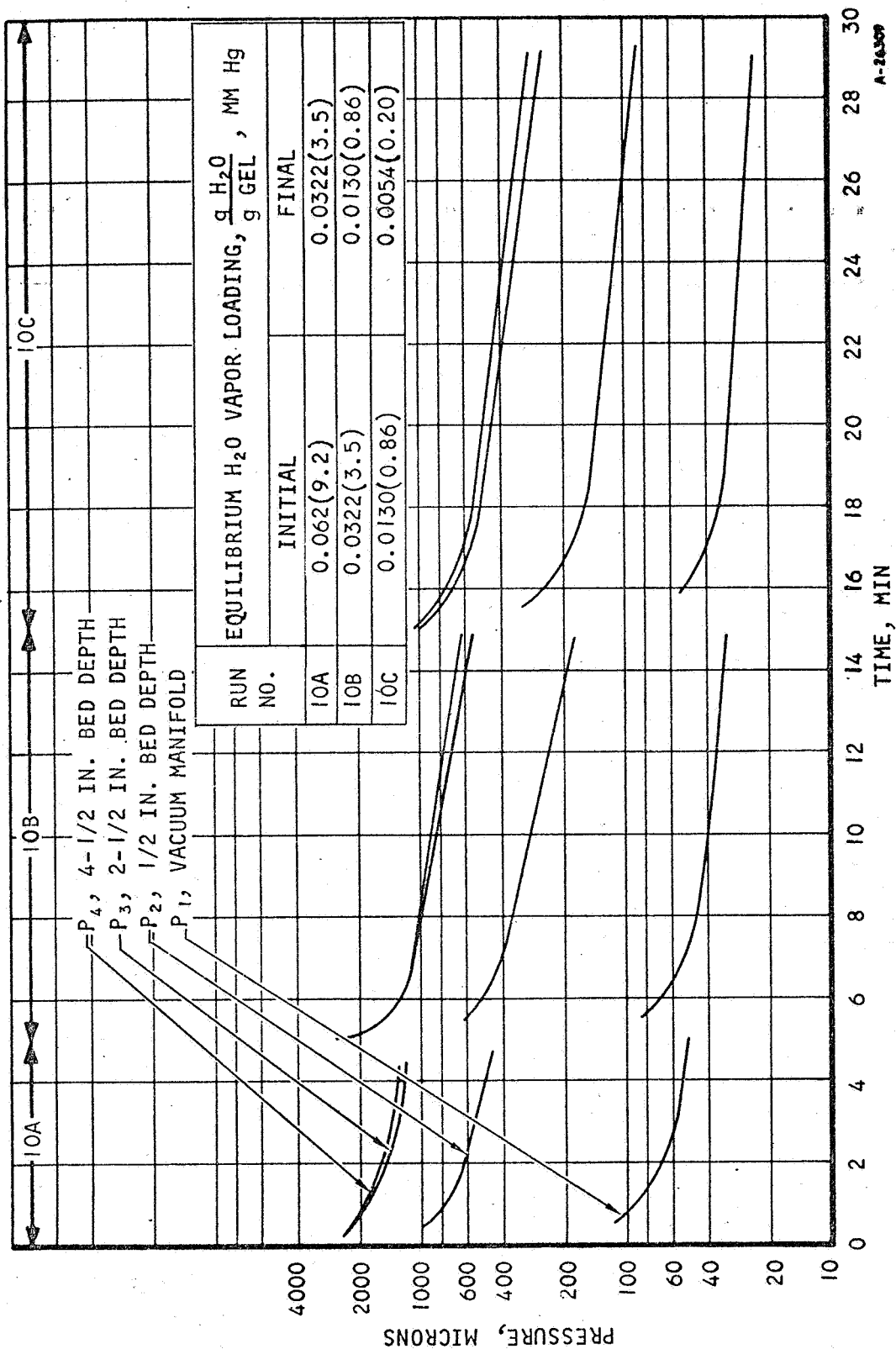
Figure C-61. Vacuum Desorption of H_2O Vapor from Davison Silica Gel, Grade 05, 3-8 Mesh Granules at 50°C

A-26369
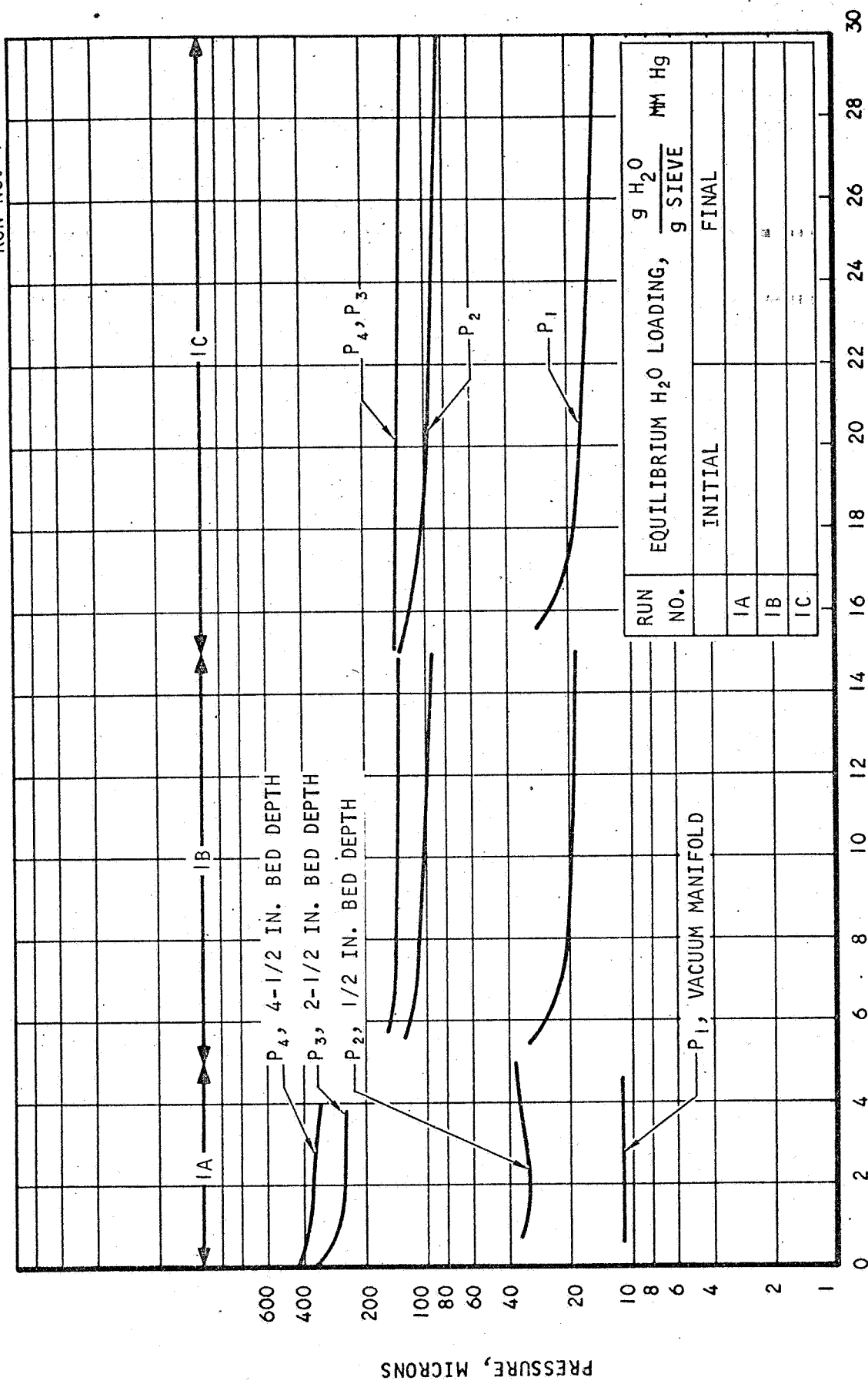
Figure C-62. Vacuum Desorption of H_2O Vapor from Linde Type 5A, 1/16 in. Diameter Pellets at 200°F

A-26310

RUN NO. 2

RUN NO.	EQUILIBRIUM H₂O VAPOR LOADING, $\frac{g\ H_2O}{g\ SIEVE}$ (MM Hg)	
	INITIAL	FINAL
2A	0.082 (14.18)	0.053 (3.55)
2B	0.053 (3.55)	0.043 (1.8)
2C	0.043 (1.8)	0.035 (1.02)

P₄, 4-1/2 IN. BED DEPTH
P₃, 2-1/2 IN. BED DEPTH
P₂, 1/2 IN. BED DEPTH

P₁, VACUUM MANIFOLD

PRESSURE, MICRONS

TIME, MIN
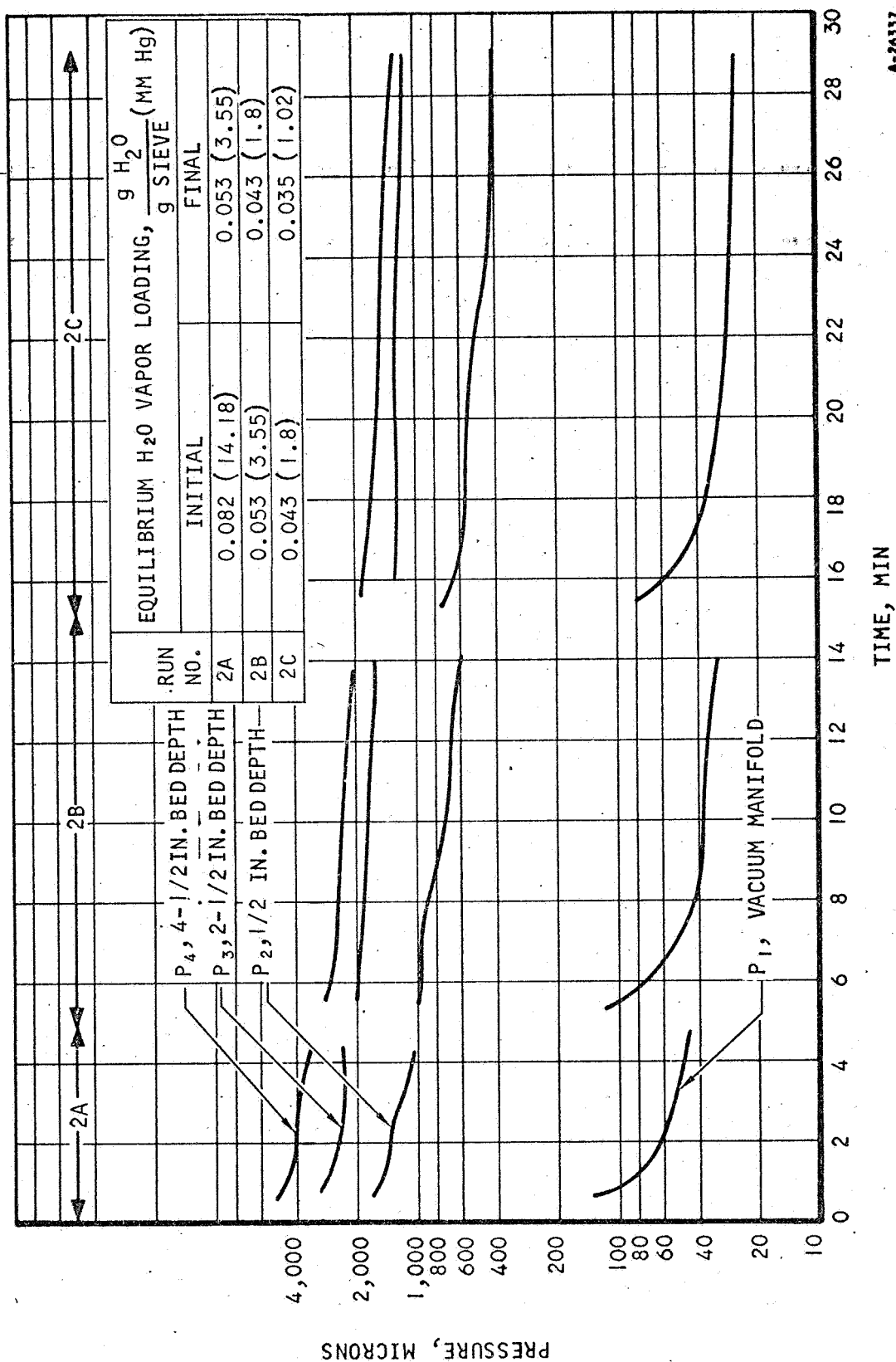
Figure C-63. Vacuum Desorption of H₂O from Linde Molecular Sieve,
Type 5A, 1/16 in. Diameter Pellets at 150°C

A-26357
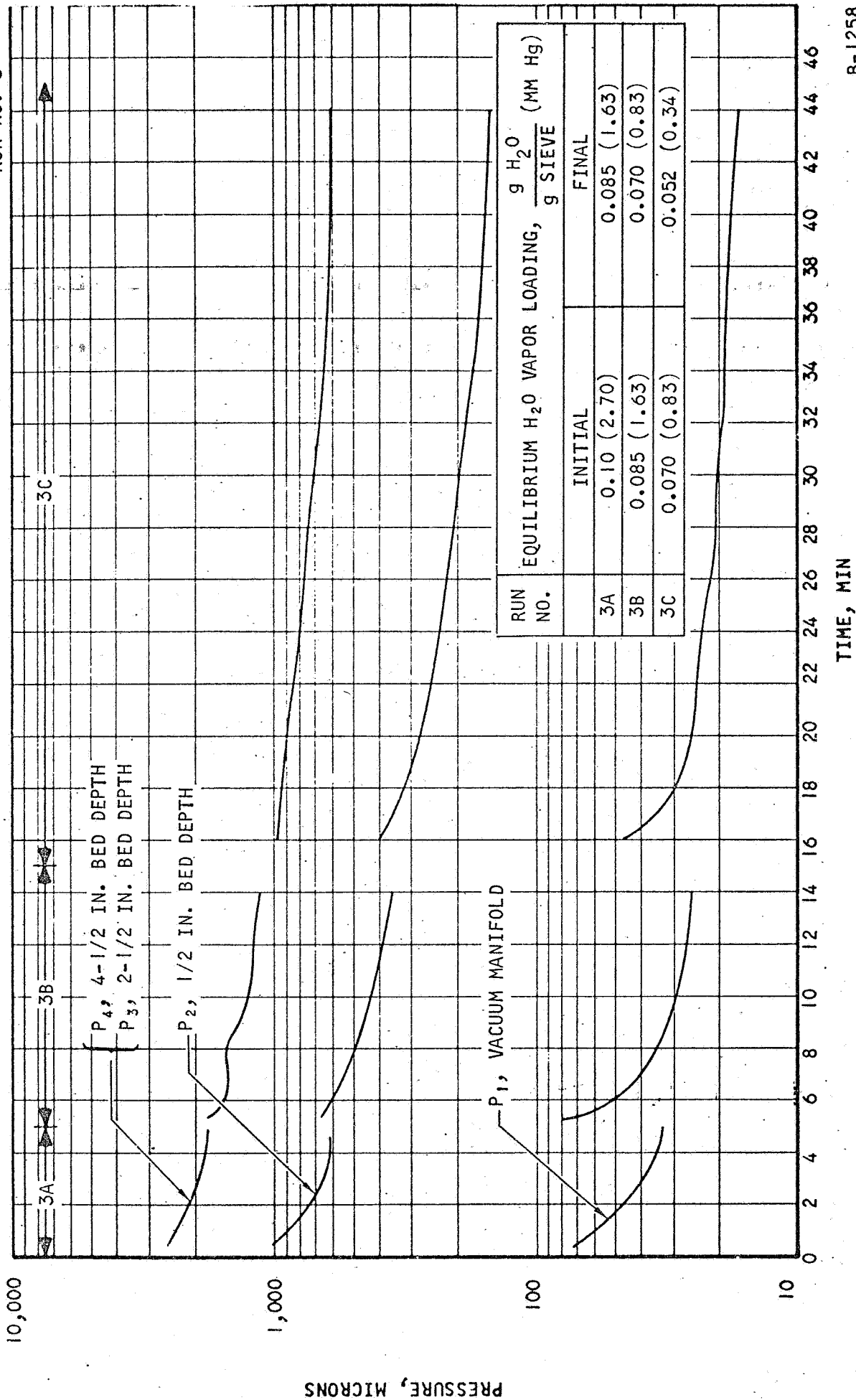
Figure C-64. Vacuum Desorption of H2O Vapor from Linde Type 5A, 1/16 in. Diameter Pellets at 100°C

RUN NO. 3

RUN NO.	EQUILIBRIUM H₂O VAPOR LOADING, $\frac{g\ H_2O}{g\ SIEVE}$ (MM Hg)	
	INITIAL	FINAL
3A	0.10 (2.70)	0.085 (1.63)
3B	0.085 (1.63)	0.070 (0.83)
3C	0.070 (0.83)	0.052 (0.34)

PRESSURE, MICRONS

TIME, MIN

P₄, 4-1/2 IN. BED DEPTH
P₃, 2-1/2 IN. BED DEPTH
P₂, 1/2 IN. BED DEPTH
P₁, VACUUM MANIFOLD

B-1258
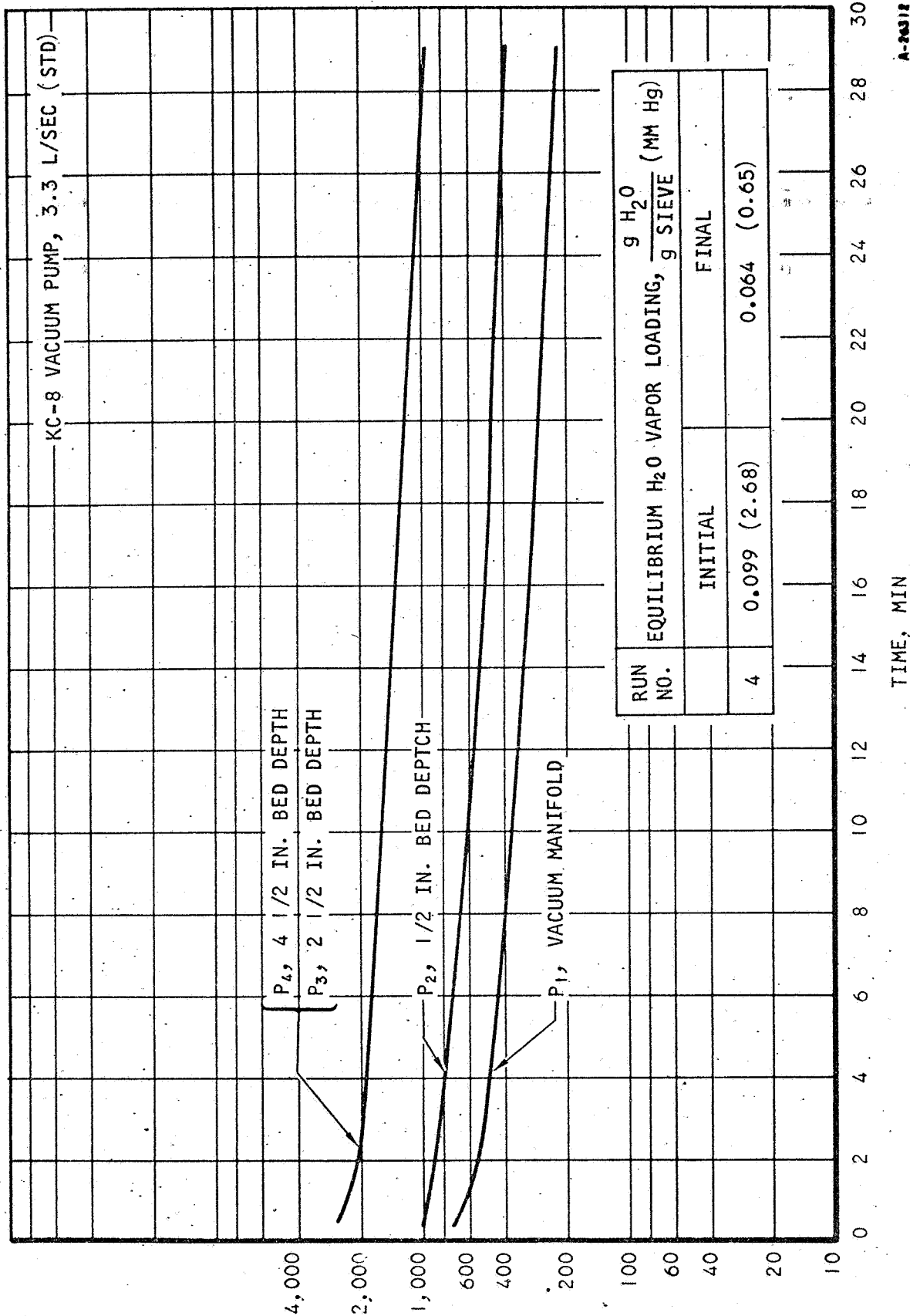
Figure C-65. Vacuum Desorption of H_2O Vapor from Linde Molecular Sieve, Type 5A, 1/16 in. Diameter Pellets at 100°C at Throttled Vacuum

RUN NO. 4

KC-8 VACUUM PUMP, 3.3 L/SEC (STD)

P_4, 4 1/2 IN. BED DEPTH
P_3, 2 1/2 IN. BED DEPTH
P_2, 1/2 IN. BED DEPTCH
P_1, VACUUM MANIFOLD

RUN NO.	EQUILIBRIUM H_2O VAPOR LOADING, $\frac{g\ H_2O}{g\ SIEVE}$ (MM Hg)	
	INITIAL	FINAL
4	0.099 (2.68)	0.064 (0.65)

TIME, MIN

PRESSURE, MICRONS

A-26312

AIRESEARCH MANUFACTURING DIVISION
Los Angeles, California
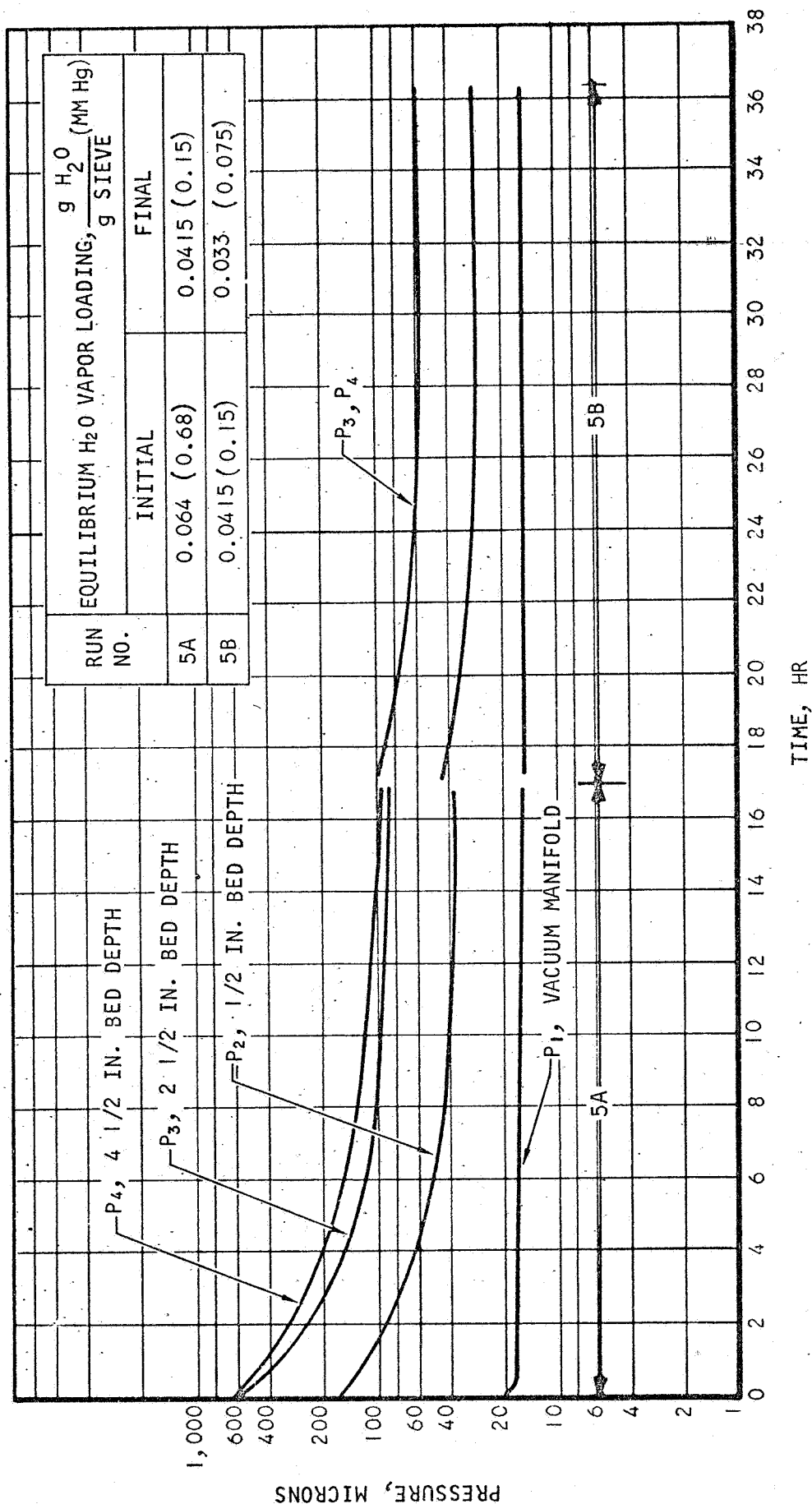
Figure C-66. Vacuum Desorption of H_2O Vapor from Linde Molecular Sieve, Type 5A, 1/16 in. Diameter Pellets at 100°C

GARRETT AIRESEARCH MANUFACTURING DIVISION
Los Angeles, California
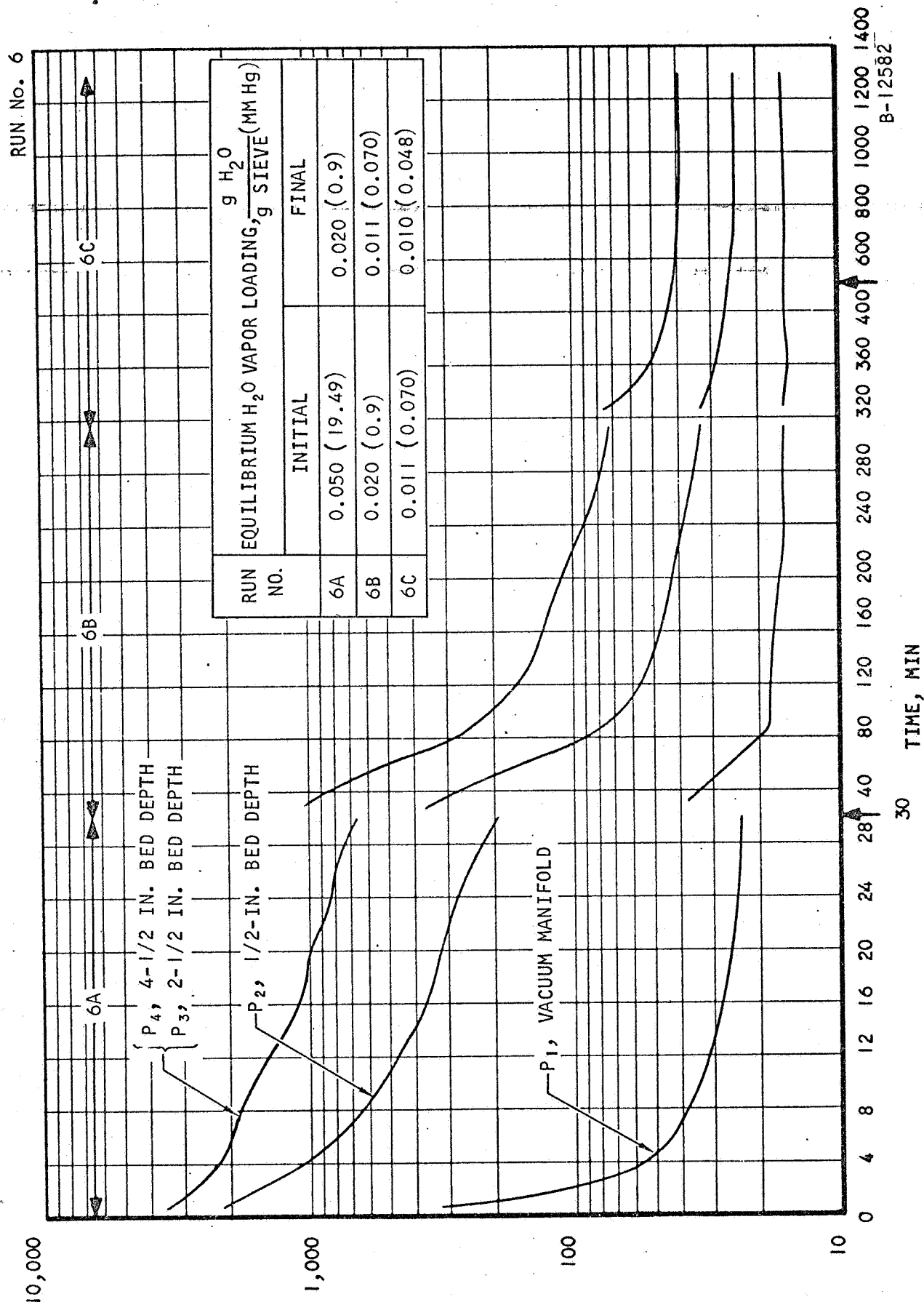
Figure C-67. Vacuum Desorption of H_2O Vapor from Linde Molecurar Sieve, Type 5A, 1/16 In. Diameter Pellets at 200°C

RUN No. 6

RUN NO.	EQUILIBRIUM H_2O VAPOR LOADING, $\dfrac{g\ H_2O}{g\ SIEVE}$ (MM Hg)	
	INITIAL	FINAL
6A	0.050 (19.49)	0.020 (0.9)
6B	0.020 (0.9)	0.011 (0.070)
6C	0.011 (0.070)	0.010 (0.048)

P_4, 4-1/2 IN. BED DEPTH
P_3, 2-1/2 IN. BED DEPTH
P_2, 1/2-IN. BED DEPTH
P_1, VACUUM MANIFOLD

TIME, MIN

PRESSURE, MICRONS

B-12582
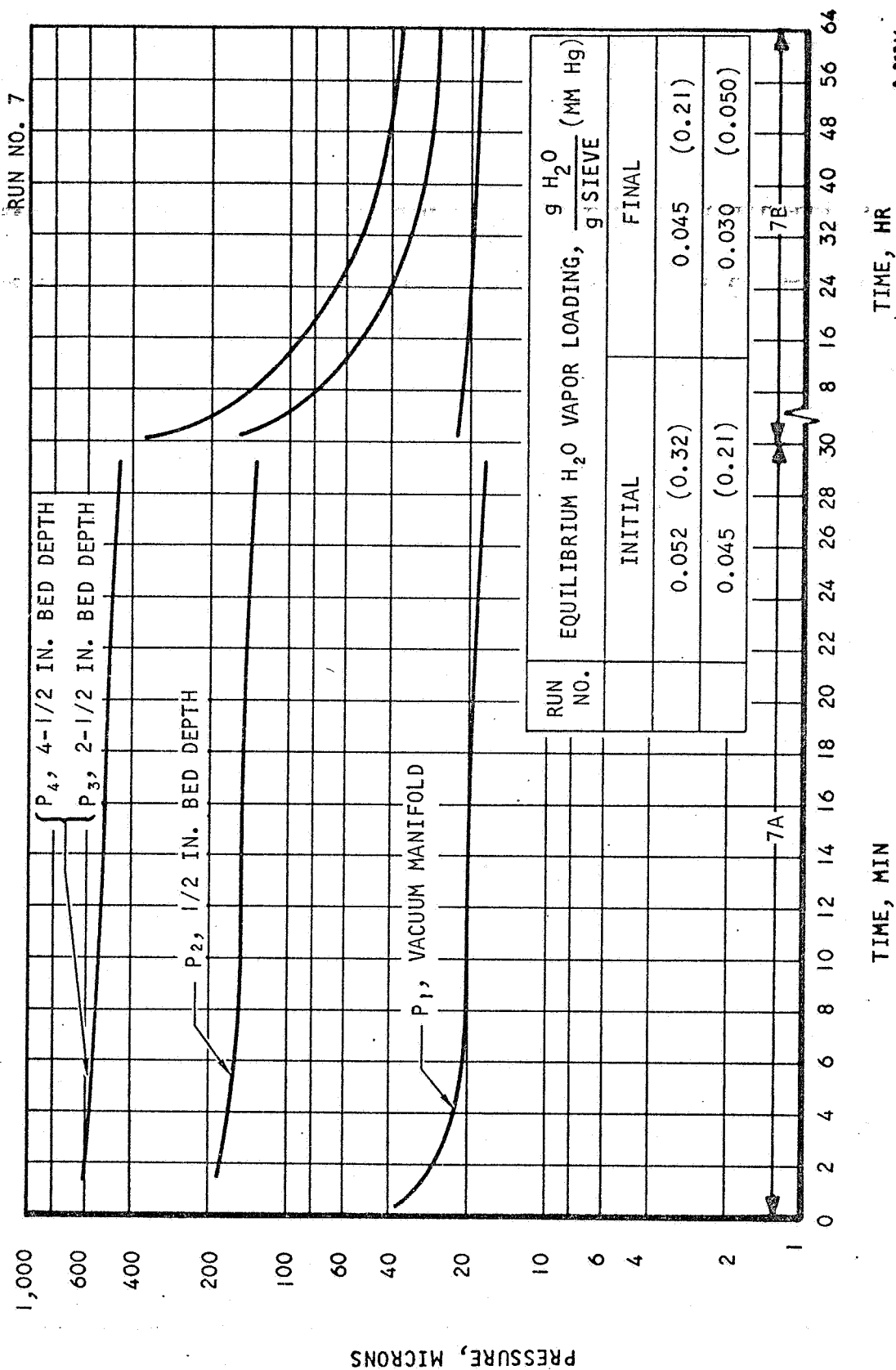
Figure C-68. Vacuum Desorption of H_2O Vapor from Linde Molecular Sieve, Type 5A, 1/16 in. Diameter Pellets at 100°C

A-20314

Figure C-69. Vacuum Desorption of H_2O Vapor from Linde Molecular Sieve, Type 5A, 1/16 in. Diameter Pellets at 100°C, after a Dry N_2 Purge
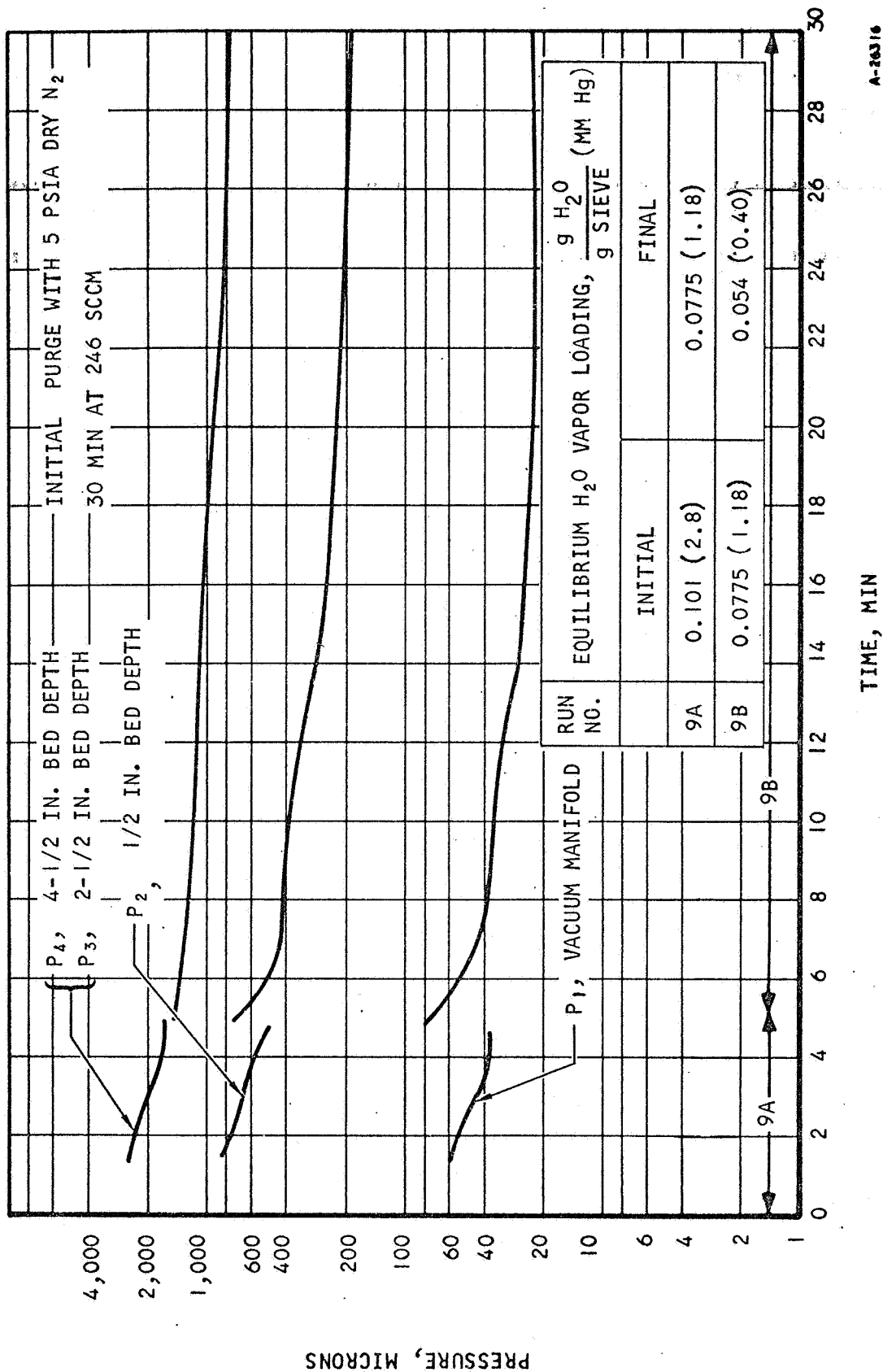
Figure C-70. Vacuum Desorption of H_2O Vapor from Linde Molecular Sieve, Type 5A, 1/16 in. Diameter Pellets at 100°C after a Dry N_2 Purge

The figure contains the following data table:

| RUN NO. | EQUILIBRIUM H_2O VAPOR LOADING, $\dfrac{g\ H_2O}{g\ SIEVE}$ (MM Hg) | | |
	INITIAL	FINAL
9A	0.101 (2.8)	0.0775 (1.18)
9B	0.0775 (1.18)	0.054 (0.40)

RUN NO. 9

INITIAL PURGE WITH 5 PSIA DRY N_2

30 MIN AT 246 SCCM

P_4, 4-1/2 IN. BED DEPTH
P_3, 2-1/2 IN. BED DEPTH
P_2, 1/2 IN. BED DEPTH
P_1, VACUUM MANIFOLD

TIME, MIN

PRESSURE, MICRONS

A-28316
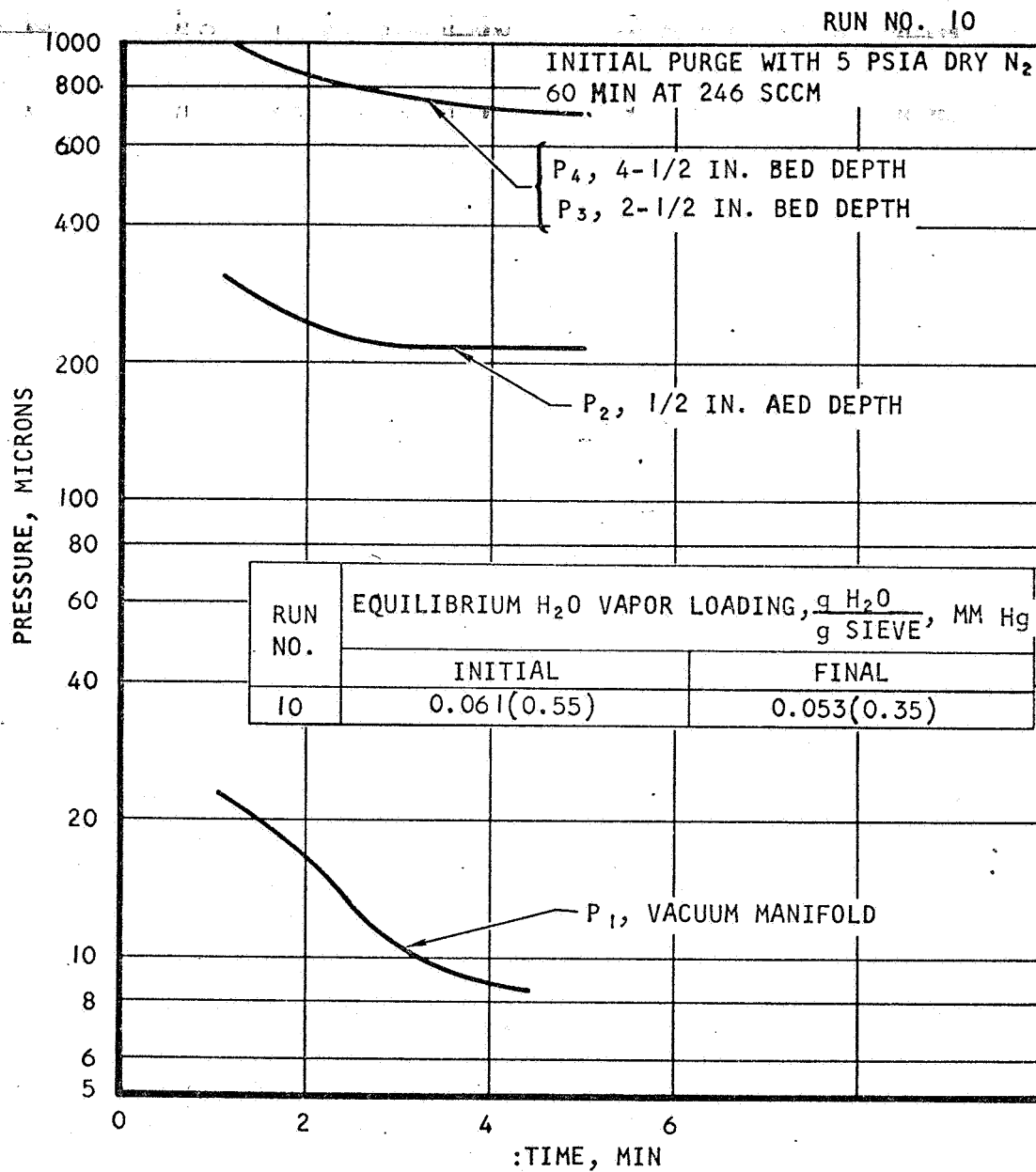
Figure C-71. Vacuum Desorption of H_2O Vapor from Linde Molecular Sieve, Type 5A, 1/16 in. Diameter Pellets at $100°C$ after a Dry N_2 Purge

APPENDIX D

INPUT DATA FOR
SIMULATING COMPOSITE BED DESCRIBED
IN SECTION 8

```
-A RUN  9S?960.079046.6.300
-R ASG A=387
- XQT CUR
 IN A
 TRI A
-I    FOR S9973.S9973
      BLOCK DATA
C
C     THESE ARE INPUT DATA TO ABSORB
C
      COMMON /BLOK2/ AMED(41). A(41). AVC(41).CPG(41).RHOG(41).
     1HXG(41).HXS(41).HXC(41).DIF(41).F(41).C(41).VS(2).DVS(2).DVSI(2).R
     2S1(2.41).RHOS(2).UG(41).WM(2).UC(41).NDXM.PS(41).RHOSB(41).DS(41).
     3CS1(41).CS2(41).C1(21.41).C2(21.41).D1(21.41).D2(41).PC1(41).PC2(4
     41).PC3(41).ASG(41).ASX(41).AGX(41).C1P(41).C2P(41).C3P(41).D1P(41)
     5.FR(2.41).PS(2).NDX1.NDR4.DX.DT.GK(41).DH(41).SK(41).P1(41).P2(41)
     6.P3(41).WS(41).CR1(2.21).CR2(2.21).CR3(2.21).C3(21.41).B(21.41).
     70(21.41).CP1(41).CP2(41).X(41).VOIDF(41).TIME
     8.AXC(41).RHOC(41).CPC(41).T268.AVX(41).TKX(41).CPX(41).RHOX(41)
     9.NOG.PX(2.41).PCO2I.PH2OI.  GMR.GMW.TGI.PA.PT(41).CPS(41).HSG(41)
      COMMON /BLOK3/ W(21.41).TG(41).TS(41).TC(41).TX(41).CYCLE
      COMMON /BLOK6/ NCYCLT
      COMMON /BLOK10/ NPRINT.DTMAX
      COMMON /BLOK12/ NTEMP
      COMMON /BLOK13/ WI. TI
      COMMON /BLOK16/ NDXMAC
      DATA WI. TI/ 0.01. 2./
      DATA NDXMAC/ 14 /
      DATA RHOS / 64..75. /
      DATA WM / 44..18. /
      DATA RHOSB / 3*45..14*36.0.1*45..5*37..18*0.0 /
      DATA W/ 861*1.E-6 /
      DATA TG. TS. TC. TX / 164*58. /
      DATA NPRINT. DTMAX/ 10. 0.005 /
      DATA NTEMP / 1 /
      DATA AVC / 18*0.0.5*521..18*0.0 /
      DATA GMR.GMW.PA / 10..31..259. /
      DATA APED / 3*0.424.14*0.386.1*0.424.5*0.350.18*0.0 /
      DATA AVX / 3*0.0.14*220..1*0.0.5*328..18*0.0 /
      DATA CPX / 41*0.11 /
      DATA RHOX / 41*490. /
      DATA HSG / 18*23.0.5*35.0.18*0.0 /
      DATA HXC / 18*0.0.5*180..18*0.0 /
      DATA HXS / 3*0.0.14*9.6.1*0.0.5*9.6.18*0.0 /
      DATA ASX / 3*0.0.14*28.2.1*0.0.5*40.2.18*0.0 /
      DATA AGX / 3*0.0.14*28.2.1*0.0.5*40.2.18*0.0 /
      DATA CPG / 41*0.23 /
      DATA NDXM.NDX1.NDR4.DX.DT / 18.23.4.0.0353.1.E-5 /
      DATA UC / 41*80.0 /
      DATA CPC / 41*0.75 /
      DATA RHOC / 41*67.0 /
      DATA T268 / 58. /
      DATA DH / 18*400..5*1400..18*0.0 /
      DATA PCO2I.PH2OI / 7.0.10.0 /
      DATA DIF / 18*40.0E-6.5*1.E-5.18*0.0 /
      DATA CPS / 18*0.25.5*0.22.18*0.0 /
      DATA ASG /3*658..14*526..1*658..5*700..18*0.0/
      DATA TKX/ 0.. 17*9.0. 0.45. 4*9.0. 18*0.0 /
```

```
      DATA SK/ 41*0.100 /
      DATA NOG / 19 /
      DATA HXG / 3*0.0,14*66.0,1*0.0,5*95.0,18*0.0 /
      DATA TGI / 58. /
      DATA PHOX/ 3*49.,14*490.,,49., 23*490. /
      DATA CYCLE / 0.33333333/
      DATA NCYCLT / 4 /
      DATA GK/ 14*0.60E-4, 4*0.00, 5*0.2E-3, 18*0.0 /
      END
  -I  FOR S9993, S9993
      BLOCK DATA
   C
   C  INPUT DATA TO DESORB
   C
      COMMON /BLOK1/ ABED(41), A(41), AVC(41),CPG(41),RHOG(41),
     1HXG(41),HXS(41),HXC(41),DIF(41),F(41),C(41),VS(2),DVS(2),DVS1(2),R
     2S1(2,41),RHOS(2),UG(41),WM(2),UC(41),NDXM,PS(41),RHOSB(41),DS(41),
     3CS1(41),CS2(41),C1(21,41),C2(21,41),D1(21,41),D2(41),PC1(41),PC2(4
     41),PC3(41),ASG(41),ASX(41),AGX(41),C1P(41),C2P(41),C3P(41),D1P(41)
     5,FR(2,41),RS(2),NDX1,NDR4,DX,DT,GK(41),DH(41),SK(41),P1(41),P2(41)
     6,P3(41),WS(41),CR1(2,21),CR2(2,21),CR3(2,21),C3(21,41),B(21,41),
     7Q(21,41),CP1(41),CP2(41),X(41),VOIDF(41),TIME
     8,AXC(41),RHOC(41),CPC(41),T268,AVX(41),TKX(41),CPX(41),RHOX(41)
     9,NOG,PK(2,41),PCO2I,PH2OI,  GMR,GMW,TGI,PA,PT(41),CPS(41),HSG(41)
      COMMON /BLOK4/ PCUT(10),TIMET(10),NBCOUT
      COMMON /BLOK13/ WI, TI
      COMMON /BLOK16/ NDXMAC
      DOUBLE PRECISION C1P,C2P,C3P,D1P
      DIMENSION AXS(41),AXG(41),AGS(41),HSX(41),HGX(41),HGS(41),ACX(41),
     1HCX(41)
      EQUIVALENCE (ASX,AXS),(AGX,AXG),(ASG,AGS),(HXS,HSX),(HXG,HGX),(HSG
     1,HGS),(AXC,ACX),(HXC,HCX)
      DATA GMR / 64.,,75. /
      DATA WM / 44.,18. /
      DATA CPG / 41*0.23 /
      DATA HXS / 3*0.0,14*9.6,1*0.0,5*9.6,18*0.0 /
      DATA HXC / 18*0.0, 5*46.,18*0.0 /
      DATA NBCOUT / 1 /
      DATA ABED / 3*0.424,14*0.386,1*0.424,5*0.350,18*0.0 /
      DATA AVX / 3*0.0,14*220.,1*0.0,5*328.,18*0.0 /
      DATA TKX / 3*0.0,14*9.0,1*0.0,5*9.0,18*0.0 /
      DATA CPX / 41*0.11 /
      DATA RHOX / 41*400. /
      DATA CPS / 18*0.25,5*0.22,18*0.0 /
      DATA RHOSB / 3*45.,14*34.2,1*45.,5*37.,18*0.0 /
      DATA ASG /3*658.,14*526.,1*658.,5*700.,18*0.0/
      DATA ASX / 3*0.0,14*28.2,1*0.0,5*40.2,18*0.0 /
      DATA AGX / 3*0.0,14*28.2,1*0.0,5*40.2,18*0.0 /
      DATA NDXM,NDX1,NDR4,DX,DT / 18,23,4,0.0353,1.E-5 /
      DATA DH / 18*400.,5*1400.,18*0.0 /
      DATA UC / 41*8.0 /
      DATA RHOC / 41*67.0 /
      DATA CPC / 41*0.75 /
      DATA T268 / 120. /
      DATA DIF / 18*40.0E-6,5*1.E-5,18*0.0 /
      DATA AVC / 18*0.0,5*521.,18*0.0 /
      DATA HXG / 3*0.0,14*9.50,1*0.0,5*6.00,18*0.0 /
      DATA HSG / 18*3.02, 5*1.87, 18*0. /
```

```
      DATA HXC / 18*0.0,5*46.,18*0.0 /
      DATA NOG / 19 /
      DATA SK/ 41* 0.08 /
      DATA TKX/ 0., 17*9.0, 0.45, 4*9.0, 18*0.0 /
      DATA RHOX/ 3*49., 14*490., 49., 23*490. /
      DATA GK/ 14*5.00E-4, 4*0.00, 5*1.E-3, 18*0.00 /
      END
   - XQT S9960
   - FIN
```

APPENDIX E

EXAMPLE PRINTOUT
DURING ADSORPTION PERIOD

TOTAL VOLUME OF M.S. BED = .2506 CU FT

TOTAL WT OF M.S. BED = 9.561 LB

TOTAL VOLUME OF S.G. BED = .6177-01 CU FT

TOTAL WT OF S.G. BED = 2.286 LB

TOTAL WT OF ACTIVE M.S. BED = 7.416 LB

```
22    .0518    .0439    .0513    .0541    .0564
23    .0971    .0839    .0963    .1008    .1045
```

AVG CO2 LOADING IN M.S. BED = .0277 LB/LB   AVG H2O LOADING IN S.G. BED = .0390 LB/LB

TIME AVG CO2 ADSORP RATE = .3396 LB/HR   TIME AVG H2O ADSORP RATE = .2184 LB/HR

TIME AVG EXIT PH2O = .2603 MM   TIME AVG RATE OF M.S. POISONING BY H2O = .5835-02 LB/HR

GARRETT AIRESEARCH MANUFACTURING DIVISION
Los Angeles, California

ADSORPTION CYCLE 2
TIME= .33333 HR   TIME INCREMENT= .00462 HR   20.000 MIN

AXIAL NODE	PCO2 MM	PH2O MM	GAS TEMP, F	SORBENT TEMP, F	GLYCOL TEMP, F	HX CORE TEMP, F
1	1.3436	.3659	79.3117	79.3026	.0000	80.5082
2	1.6198	.3659	80.0493	80.0415	.0000	80.5413
3	1.9543	.3659	80.6819	80.6824	.0000	80.6075
4	2.3469	.3659	80.8055	80.8170	.0000	80.7068
5	2.6724	.3659	81.0425	81.0589	.0000	80.9124
6	3.0303	.3659	81.2824	81.3044	.0000	81.1269
7	3.4174	.3659	81.4356	81.4635	.0000	81.2577
8	3.8286	.3659	81.4907	81.4344	.0000	81.2088
9	4.2535	.3659	81.0956	81.1351	.0000	80.8974
10	4.7024	.3659	80.4538	80.4985	.0000	80.2565
11	5.1563	.3659	79.4269	79.4761	.0000	79.2372
12	5.6173	.3659	77.9870	78.0399	.0000	77.8117
13	6.0625	.3659	76.1290	76.1840	.0000	75.9767
14	6.5468	.3659	73.8652	73.9194	.0000	73.7619
15	7.0000	.3659	71.1249	71.1323	.0000	71.2736
16	7.0000	.3659	69.9567	68.9602	.0000	69.1292
17	7.0000	.3659	66.8188	66.8088	.0000	67.3852
18	7.0000	.3659	61.2984	61.3166	.0000	66.9603
19	7.0000	.3659	58.7630	58.8022	58.2173	58.4826
20	7.0000	.7696	59.4195	59.4953	58.5155	58.8794
21	7.0000	1.6732	60.6435	60.7857	59.0306	59.6572
22	7.0000	3.0932	62.4760	62.7232	59.8386	60.8185
23	7.0000	5.7631	64.2569	64.6577	60.9223	62.0109

LOADING AT INTERIOR OF SORBENT, LB/LB

SORB NODE AXIAL NODE	AVG	1	2	3	4	5	6	7	8	9	10	11
1	.0141	.0134	.0141	.0143	.0145							
2	.0155	.0146	.0154	.0157	.0160							
3	.0173	.0162	.0172	.0176	.0179							
4	.0197	.0184	.0196	.0200	.0204							
5	.0214	.0201	.0213	.0218	.0222							
6	.0234	.0219	.0233	.0238	.0242							
7	.0256	.0240	.0255	.0260	.0265							
8	.0280	.0263	.0279	.0285	.0290							
9	.0306	.0288	.0305	.0312	.0317							
10	.0336	.0317	.0335	.0341	.0345							
11	.0369	.0349	.0367	.0374	.0379							
12	.0405	.0386	.0404	.0411	.0416							
13	.0448	.0427	.0447	.0453	.0459							
14	.0497	.0477	.0496	.0503	.0508							
15	.0000	.0000	.0000	.0000	.0000							
16	.0000	.0000	.0000	.0000	.0000							
17	.0000	.0000	.0000	.0000	.0000							
18	.0000	.0000	.0000	.0000	.0000							
19	.0063	.0052	.0063	.0067	.0070							
20	.0132	.0109	.0130	.0138	.0145							
21	.0266	.0222	.0263	.0278	.0292							

APPENDIX F

EXAMPLE PRINTOUT
DURING DESORPTION PERIOD

67-1751

DESORPTION CYCLE 2
TIME= .33333 HR   20.000 MIN   TIME INCREMENT= .00214 HR

AXIAL NODE	TOTAL PRESS,MM	GAS TEMP,DEG F	SORBENT TEMP, DEG F	GLYCOL TEMP, DEG F	HX CORE TEMP, DEG F
1	.7987	79.6119	79.6119	.0000	72.4837
2	.7957	79.5525	78.5625	.0000	72.4658
3	.7824	76.3508	76.3605	.0000	72.4299
4	.7424	72.7350	72.7946	.0000	72.3759
5	.7746	71.9571	71.9633	.0000	71.9192
6	.7651	71.2344	71.2282	.0000	71.2696
7	.7538	70.3890	70.3703	.0000	70.4877
8	.7405	69.4564	69.4259	.0000	69.6348
9	.7243	68.5139	68.4674	.0000	68.7861
10	.7069	67.6522	67.5877	.0000	68.0314
11	.6859	66.9773	66.8935	.0000	67.4710
12	.6615	66.6050	66.5024	.0000	67.2114
13	.6311	66.6576	66.5400	.0000	67.3554
14	.6008	67.2854	67.1673	.0000	67.9872
15	.5636	68.9526	68.9256	.0000	69.1253
16	.5258	70.2790	70.2529	.0000	70.4369
17	.4873	71.4078	71.3233	.0000	71.9176
18	.4420	69.0569	69.0545	.0000	75.7951
19	.3925	110.2509	110.0860	114.2129	111.5116
20	.3450	107.0605	106.7204	110.5251	108.8420
21	.2903	100.3900	100.3691	105.2291	104.2942
22	.2200	92.3520	91.1654	101.0077	98.6783
23	.1117	82.4996	80.3935	95.9454	93.7292

CO2 DESORPTION RATE= .1197 LB/HR   H2O DESORPTION RATE= .1230 LB/HR

AXIAL NODE	MOLE FRAC	CO2 RATE,M/HR	H2O RATE,M/HR
1	1.000000	.000159	.000000
2	1.000000	.000314	.000000
3	1.000000	.000476	.000000
4	1.000000	.000597	.000000
5	1.000000	.000724	.000000
6	1.000000	.000862	.000000
7	1.000000	.001013	.000000
8	1.000000	.001183	.000000
9	1.000000	.001374	.000000
10	1.000000	.001590	.000000
11	1.000000	.001835	.000000
12	1.000000	.002109	.000000
13	1.000000	.002408	.000000
14	1.000000	.002720	.000000
15	1.000000	.002720	.000000
16	1.000000	.002720	.000000
17	1.000000	.002720	.000000
18	.065047	.002720	.000175
19	.165788	.002720	.000540
20	.330092	.002720	.001346
21	.530498	.002720	.003111
22	.708956	.002720	.006831
23		.002720	

LOADING AT INTERIOR OF SCREEN

SORB NODE AXIAL NODE	AVG	1	2	3	4	5	6	7	8	9	10	11
1	.0154	.0158	.0155	.0153	.0152							
2	.0157	.0161	.0157	.0156	.0155							
3	.0163	.0167	.0163	.0162	.0161							
4	.0174	.0178	.0174	.0173	.0171							
5	.0176	.0180	.0176	.0175	.0174							
6	.0178	.0182	.0178	.0176	.0175							
7	.0180	.0185	.0180	.0178	.0177							
8	.0182	.0168	.0183	.0181	.0179							
9	.0185	.0191	.0185	.0183	.0181							
10	.0187	.0194	.0187	.0185	.0183							
11	.0188	.0197	.0189	.0186	.0184							
12	.0186	.0197	.0188	.0195	.0193							
13	.0185	.0136	.0146	.0182	.0173							
14	.0179	.0190	.0179	.0176	.0173							
15	.0000	.0000	.0000	.0000	.0000							
16	.0000	.0000	.0000	.0000	.0000							
17	.0000	.0000	.0000	.0000	.0000							
18	.0000	.0021	.0016	.0014	.0013							
19	.0015	.0043	.0031	.0028	.0025							
20	.0031	.0087	.0063	.0055	.0050							
21	.0062	.0175	.0124	.0107	.0095							
22	.0122	.0344	.0242	.0207	.0141							
23	.0237											

AVG CO2 LOADING IN H.S. BED = .0149 LB/LB   AVG H2O LOADING IN S.G. BED = .0094 LB/LB

TIME AVG CO2 DESORP RATE = .2253 LB/HR   TIME AVG H2O DESORP RATE = .2034 LB/HR

APPENDIX G

SOURCE PROGRAM LISTING

```
      -A RUN  9S9960,079046,2,100                          GAR93      K C HWANG          1
      -R ASG B=387                                                                       1
      - XQT CUR                                                                          1
       IN B                                                                              1
       TRI B                                                                             1
      -I    FOR S9960,S9960                                                              1
      C     MAIN PROGRAM FOR COMBINED ADSORPTION/DESORPTION PROGRAM -- DEVELOPED         1
      C     BY K C HWANG, AIRESEARCH , LOS ANGELES                                       1
      C                                                                                  1
            COMMON /BLOK3/ W(21,41),TG(41),TS(41),TC(41),TX(41),CYCLE                    1
            COMMON /BLOK6/ NCYCLT                                                        1
            COMMON /BLOK14/ NCYCLE                                                       1
            NCYCLE=1                                                                     1
         11 CONTINUE                                                                     1
            WRITE (6,300)                                                                1
            CALL MADSOR                                                                  1
            WRITE (6,400)                                                                1
            CALL MDESOR                                                                  1
            NCYCLE=NCYCLE+1                                                              1
            IF(NCYCLE .LE. NCYCLT) GO TO 11                                              1
            CALL EXIT                                                                    1
        300 FORMAT(24H1 START ADSORPTION CYCLE )                                         1
        400 FORMAT(24H1 START DESORPTION CYCLE )                                         1
            END                                                                          1
      C                                                                                  1
      C                                                                                  1
      -I    FOR S9950, S9950                                                             1
            CALL MADSOR                                                                  1
            END                                                                          1
      -I    FOR S9951, S9951                                                             1
            CALL MDESOR                                                                  1
            END                                                                          1
      -I    FOR S9970,S9970                                                              1
            SUBROUTINE MADSOR                                                            1
      C                                                                                  1
            COMMON /BLOK2/ ABED(41), A(41), AVC(41),CPG(41),RHOG(41),                    1
           1HXG(41),HXS(41),HXC(41),DIF(41),F(41),C(41),VS(2),DVS(2),DVS1(2),R           1
           2S1(2,41),RHOS(2),UG(41),WM(2),UC(41),NDXM,PS(41),RHOSB(41),DS(41),           1
           3CS1(41),CS2(41),C1(21,41),C2(21,41),D1(21,41),D2(41),PC1(41),PC2(4           1
           41),PC3(41),ASG(41),ASX(41),AGX(41),C1P(41),C2P(41),C3P(41),D1P(41)           1
           5,FR(2,41),RS(2),NDX1,NDR4,DX,DT,GK(41),DH(41),SK(41),P1(41),P2(41)           1
           6,P3(41),WS(41),CR1(2,21),CR2(2,21),CR3(2,21),C3(21,41),B(21,41),             1
           7Q(21,41),CP1(41),CP2(41),X(41),VOIDF(41),TIME                               1
           8,AXC(41),RHOC(41),CPC(41),T268,AVX(41),TKX(41),CPX(41),RHOX(41)              1
           9,NOG,PK(2,41),PCO2I,PH2OI,   GMR,GMW,TGI,PA,PT(41),CPS(41),HSG(41)           1
            COMMON /BLOK3/ W(21,41),TG(41),TS(41),TC(41),TX(41),CYCLE                    1
            COMMON /BLOK8/ DTO,TS1(41),TS2(41),TX1(41),TX2(41),TC1(41),TC2(41)           1
            COMMON /BLOK10/ NPRINT,DTMAX                                                 1
            COMMON /BLOK11/ TOTCO2,TOTH2O,SUMPTM,WTACMS,WTSG                             1
            COMMON /BLOK13/ WI, TI                                                       1
            COMMON /BLOK14/ NCYCLE                                                       1
            COMMON /BLOK16/ NDXMAC, PCO2C, VOLCAB, RCO2C                                 1
      C                                                                                  1
            SUMPTM=0.                                                                    1
            N1=NDXM+1                                                                    1
            VMS = 0.0                                                                    1
            WTMS=0.0                                                                     1
            VSG=0.0                                                                      1
```

```
       WTSG=0.0
       DO 10 N= 1, NDXM
       VMS=VMS+DX*ABED(N)
       WTMS=WTMS+DX*ABED(N)*RHOSB(N)
   10  CONTINUE
       DO 30 N= N1,NDX1
       VSG=VSG+DX*ABED(N).
       WTSG=WTSG+DX*ABED(N)*RHOSB(N)
   30  CONTINUE
       WRITE(6,500) VMS, WTMS, VSG, WTSG
  500  FORMAT( 28H1TOTAL VOLUME OF M.S. BED = G10.4,2X,5HCU FT//
      123H TOTAL WT OF M.S. BED =  G10.4,2X, 2HLB//
      228H TOTAL VOLUME OF S.G. BED =  G10.4,2X,5HCU FT//
      323H TOTAL WT OF S.G. BED =   G10.4, 2X,2HLB)
       WTACMS=0.0
       DO 70 N= 1, NDXMAC
   70  WTACMS=WTACMS + DX*ABED(N)*RHOSB(N)
       WRITE(6,501) WTACMS
  501  FORMAT( /  30H TOTAL WT OF ACTIVE M.S. BED =  , G10.4,3H LB )
       TIME = 0.0
       DT = 1.E-5
       DTO =0.0
       TOTCO2=0.0
       TOTH2O=0.0
       DO 20 N=1,NDX1
       TS1(N)= TS(N)
       TS2(N)= TS(N)
       TX1(N)=TX(N)
       TX2(N)=TX(N)
       TC1(N)=TC(N)
       TC2(N)=TC(N)
   20  CONTINUE
       CALL STARTA
       NPR=NPRINT - 1
       GO TO 3
    2  CALL PRADSB
       NPR = 0
    4  CONTINUF
       IF( TIME .GE. CYCLE) CALL PRADSB
       IF( TIME .GE. CYCLE) GO TO 9999
       ADT=DTMAX
       DO 60 N=1,NDX1
       ADT2=WI      /(ABS(W(NDR4,N)-WS(N))+1.E-9)*DT
       IF(ADT2.LT. ADT) ADT=ADT2
       ADT2=TI/(ABS(TS1(N)-TS2(N))+1.E-9)*DT
       IF(ADT2.LT. ADT) ADT=ADT2
       ADT2=TI/(ABS(TX1(N)-TX2(N))+1.E-9)*DT
       IF(ADT2.LT. ADT) ADT=ADT2
   60  CONTINUE
       DTO=DT
       DT=ADT
    3  CONTINUE
       IF((TIME+DT) .GT. CYCLE) DT = CYCLE-TIME
       PCO2I = PCO2C
       CALL ADSORB(DT)
       DPCO2C = DT*(RCO2C - GMR*
      1                (PCO2I-PK(1,1))*44./(PA*GMW))*554.*530./(44.*
      2VOLCAB)
```

```
       PCO2C= PCO2C+DPCO2C                                                         1
       TOTCO2=TOTCO2+GMR*DT*(PCO2I-PK(1,1))*44./(PA*GMW)                           1
       TOTH2O=TOTH2O+GMR*DT*(PH2OI-PK(2,1))*18./(PA*GMW)                           1
       SUMPTM= SUMPTM+PK(2,1)*DT                                                   1
       DO 21 N=1,NDX1                                                              1
       TS2(N)=TS1(N)                                                               1
       TS1(N)=TS(N)                                                                1
       TX2(N)=TX1(N)                                                               1
       TX1(N)=TX(N)                                                                1
       TC2(N)=TC1(N)                                                               1
       TC1(N)=TC(N)                                                                1
   21  CONTINUE                                                                    1
       TIME=TIME+DT                                                                1
       NPR = NPR+1                                                                 1
       IF (NPR .GE. NPRINT) GO TO 2                                                1
       GO TO 4                                                                     1
 9999  CONTINUE                                                                    1
       RETURN                                                                      1
       END                                                                        1
    C                                                                             1
    C                                                                             1
  -I       FOR S9978,S9978                                                        1
          SUBROUTINE STARTA                                                       1
    C                                                                             1
          COMMON /BLOK2/ ABED(41), A(41), AVC(41),CPG(41),RHOG(41),               1
         1HXG(41),HXS(41),HXC(41),DIF(41),F(41),C(41),VS(2),DVS(2),DVS1(2),R      1
         2S1(2,41),RHOS(2),UG(41),WM(2),UC(41),NDXM,PS(41),RHOSB(41),DS(41),      1
         3CS1(41),CS2(41),C1(21,41),C2(21,41),D1(21,41),D2(41),PC1(41),PC2(4      1
         41),PC3(41),ASG(41),ASX(41),AGX(41),C1P(41),C2P(41),C3P(41),D1P(41)      1
         5,FR(2,41),RS(2),NDX1,NDR4,DX,DT,GK(41),DH(41),SK(41),P1(41),P2(41)      1
         6,P3(41),WS(41),CR1(2,21),CR2(2,21),CR3(2,21),C3(21,41),B(21,41),        1
         7Q(21,41),CP1(41),CP2(41),X(41),VOIDF(41),TIME                           1
         8,AXC(41),RHOC(41),CPC(41),T268,AVX(41),TKX(41),CPX(41),RHOX(41),        1
         9,NOG,PK(2,41),PCO2I,PH2OI,  GMR,GMW,TGI,PA,PT(41),CPS(41),HSG(41)       1
          COMMON /BLOK3/ W(21,41),TG(41),TS(41),TC(41),TX(41),CYCLE               1
          DO 115 N=1,NDX1                                                         1
   115  A(N)= GMR/ABED(N)/PA/GMW                                                  1
    C                                                                             1
    C                                                                             1
          RS(1)=RHOSB(1)*3./RHOS(1)/ASG(1)                                        1
          RS(2)=RHOSB(NDX1)                                                       1
         1                 *3./RHOS(2)/ASG(NDX1)                                  1
          NDR=NDR4-1                                                              1
          NDR2=2.*NDR                                                             1
          NDR3=NDR2+1                                                             1
          DO 10 I=1,2                                                             1
          VS(I)=4./3.*3.1416*RS(I)**3                                            1
          DVS(I)=VS(I)/NDR                                                        1
          DVS1(I)=DVS(I)/2                                                        1
          RS1(I,1)=0.                                                            1
          DO 10 K=2,NDR3                                                          1
    10  RS1(I,K)=CBRT(3./4./3.1416*(4./3.*3.1416*RS1(I,K-1)**3+DVS1(I)))          1
```

168

```
      DO 11 I=1,2                                                          1
      IF(I.EQ.1) DIF1=DIF(1)                                               1
      IF (I.EQ. 2) DIF1=DIF(NDX1)                                          1
      CR1(I,1)=DVS1(I)*RHOS(I)                                             1
      CR2(I,1)=0.                                                          1
      CR3(I,1)=4.*3.1416*RS1(I,2)**2*DIF1   /(RS1(I,3)-RS1(I,1))*RHOS(I)   1
      DO 11 K=2,NDR4                                                       1
      CR1(I,K)=DVS(I)*RHOS(I)                                              1
      CR2(I,K)=4.*3.1416*RS1(I,2*K-2)**2*DIF1   /(RS1(I,2*K-1)-RS1(I,2*K-  1
     13))*RHOS(I)                                                          1
   11 CR3(I,K)=4.*3.1416*RS1(I,2*K)**2*DIF1   /(RS1(I,2*K+1)-RS1(I,2*K-1)  1
     1)*RHOS(I)                                                            1
      CR1(1,NDR4)=CR1(1,1)                                                 1
      CR1(2,NDR4)=CR1(2,1)                                                 1
      RETURN                                                              1
      END                                                                 1
C                                                                         1
C                                                                         1
-I    FOR S9971,S9971                                                     1
      SUBROUTINE ADSORB(DELT)                                             1
      COMMON /BLOK2/ ABED(41), A(41), AVC(41),CPG(41),RHOG(41),           1
     1HXG(41),HXS(41),HXC(41),DIF(41),F(41),C(41),VS(2),DVS(2),DVS1(2),R  1
     2S1(2,41),RHOS(2),UG(41),WM(2),UC(41),NDXM,PS(41),RHOSB(41),DS(41),  1
     3CS1(41),CS2(41),C1(21,41),C2(21,41),D1(21,41),D2(21,41),PC1(41),PC2(4 1
     41),PC3(41),ASG(41),ASX(41),AGX(41),C1P(41),C2P(41),C3P(41),D1P(41)  1
     5,FR(2,41),RS(2),NDX1,NDR4,DX,DT,GK(41),DH(41),SK(41),P1(41),P2(41)  1
     6,P3(41),WS(41),CR1(2,21),CR2(2,21),CR3(2,21),C3(21,41),B(21,41),    1
     7Q(21,41),CP1(41),CP2(41),X(41),VOIDF(41),TIME                       1
     8,AXC(41),RHOC(41),CPC(41),T268,AVX(41),TKX(41),CPX(41),RHOX(41)     1
     9,NOG,PK(2,41),PCO2I,PH2OI,  GMR,GMW,TGI,PA,PI(41),CPS(41),HSG(41)   1
      COMMON /BLOK3/ W(21,41),TG(41),TS(41),TC(41),TX(41),CYCLE           1
      COMMON /BLOK12/ NTEMP                                               1
      DIMENSION AS(2)                                                     1
      EQUIVALENCE (ASX,AXS),(AGX,AXG),(ASG,AGS),(HXS,HSX),(HXG,HGX),(HSG  1
     1,HGS)                                                               1
      DT = DELT                                                           1
      AS(1)=4.*3.1416*RS(1)**2                                            1
      AS(2)=4.*3.1416*RS(2)**2                                            1
C                                                                         1
C                                                                         1
C                                                                         1
      DATA RGAS/554./                                                     1
C                                                                         1
      NDR=NDR4-1                                                          1
      DO 21 N=1,NDX1                                                      1
      I=IFN(N,NDXM)                                                       1
      DO 20 NR=1,NDR4                                                     1
      C1(NR,N)=-CR2(I,NR)                                                 1
      C2(NR,N)=CR1(I,NR)/DT+CR2(I,NR)+CR3(I,NR)                           1
   20 C3(NR,N)=-CR3(I,NR)                                                 1
C                                                                         1
C                                                                         1
      B(1,N)=C3(1,N)/C2(1,N)                                             1
      DO 21 J=2,NDR                                                       1
   21 B(J,N)=C3(J,N)/(C2(J,N)-C1(J,N)*B(J-1,N))                          1
      NDX=NDX1-1                                                          1
C     TO TEMPORARILY STORE SURFACE LOADING                               1
      DO 50 N=1,NDX1                                                      1
```

```
   50  WS(N)=W(NDR4,N)                                                            1
       IF (NTEMP .EQ. 0.) GO TO 111                                              1
C                                                                                1
C      TO CALCULATE CS1,CS2,DS FOR SORBENT HEAT BALANCE EQUATION                 1
       DO 12 N=1,NDX1                                                            1
       I=IFN(N,NDXM)                                                             1
       CS2(N)=DT/CPS(N)/RHOSB(N)*ASG(N)*GK(N)*WM(I)*DH(N)                        1
       CS1(N) = CS2(N)                                                           1
       IF (N.EQ.1) GO TO 13                                                      1
       IF (N.EQ.NDX1) GO TO 14                                                   1
       S1=SK(N)/DX**2*(TS(N-1)-2.*TS(N)+TS(N+1))                                 1
       GO TO 15                                                                  1
   13  S1=SK(1)/DX**2*(TS(2)-TS(1))                                              1
       GO TO 15                                                                  1
   14  S1=SK(NDX1)/DX**2*(TS(NDX)-TS(NDX1))                                      1
   15  DS(N)=DT/CPS(N)/RHOSB(N)*(S1+ASG(N)*HSG(N)*(TG(N)-TS(N))+ASX(N)*HX        1
      1S(N)*(TX(N)-TS(N)))                                                       1
   12  CONTINUE                                                                  1
       GO TO 110                                                                 1
  111  DO 112 N= 1, NDX1                                                         1
       CS1(N)=0.                                                                 1
       CS2(N)=0.                                                                 1
       DS(N)=0.                                                                  1
       TS(N)=T268                                                                1
       TC(N)=T268                                                                1
       TX(N)=T268                                                                1
       TG(N)=T268                                                                1
  112  CONTINUE                                                                  1
  110  CONTINUE                                                                  1
C                                                                                1
C      TO CALCULATE PARTIAL PRESSURE OF ADSORBATE IN GAS STREAM                  1
C                                                                                1
       DO 24 N=1,NDX1                                                            1
       I=IFN(N,NDXM)                                                             1
C      TO CALCULATE P1,P2,P3                                                     1
       DPKDTS=                                                                   1
      1      (PKEQ(I,W(NDR4,N),(TS(N)+0.001))-PKEQ(I,W(NDR4,N),TS(N)))/          1
      20.001                                                                     1
       DPKDWK=(PKEQ(I,(W(NDR4,N)+1.E-6),TS(N))-PKEQ(I,W(NDR4,N),TS(N)))/1        1
      1.E-6                                                                      1
       G=1.+CS2(N)*DPKDTS                                                        1
       P1(N)=(PKEQ(I,W(NDR4,N),TS(N))+DS(N)*DPKDTS)/G                            1
       P2(N)=DPKDWK/G                                                            1
       P3(N)=CS1(N)/G*DPKDTS                                                     1
C                                                                                1
       C2(NDR4,N)=CR1(I,NDR4)/DT+CR2(I,NDR4)+WM(I)*GK(N)*P2(N)*AS(I)             1
       C3(NDR4,N)=0.0                                                            1
       DO 23 NR=1,NDR4                                                           1
   23  D1(NR,N)=CR1(I,NR)/DT*W(NR,N)                                             1
       D1(NDR4,N)=D1(NDR4,N)-WM(I)*GK(N)*(P1(N)-P2(N)*W(NDR4,N))*AS(I)           1
       D2(N)=AS(I)*WM(I)*GK(N)*( 1.     -P3(N))                                  1
       D2(N)=D2(N)/(C2(NDR4,N)-C1(NDR4,N)*B(NDR4-1,N))                           1
       Q(1,N)=D1(1,N)/C2(1,N)                                                    1
       DO 24 J=2,NDR4                                                           1
   24  Q(J,N)=(D1(J,N)-C1(J,N)*Q(J-1,N))/(C2(J,N)-C1(J,N)*B(J-1,N))             1
C                                                                                1
       DO 25 N=1,NDX1                                                            1
       I=IFN(N,NDXM)                                                             1
```

GARRETT AIRESEARCH MANUFACTURING DIVISION
Los Angeles, California

```
        CP1(N)=ASG(N)*GK(N)*(P1(N)+P2(N)*(Q(NDR4,N)-W(NDR4,N)))
     25 CP2(N)=ASG(N)*GK(N)*(P2(N)*D2(N)+P3(N)-1.0)
        PK(1,NDX1+1) = PCO2I
        PK(2,NDX1+1) = PH2OI
        DO 26 N=1,NDX1
        N1=NDX1+1-N
        I=IFN(N1,NDXM)
        PK(I,N1) = (PK(I,N1+1)/DX+CP1(N1)/A(N1))
     1                                   /(1./DX-CP2(N1)/A(N1))
        IF (I.EQ.1)J=2
        IF(I.EQ.2)J=1
        PK(J,N1)=PK(J,N1+1)
     26 CONTINUE
C
C
C
C       TO CALCULATE SORBENT LOADING
C
        DO 30 N=1,NDX1
        I=IFN(N,NDXM)
        W(NDR4,N)=Q(NDR4,N)+D2(N)*PK(I,N)
        DO 30 J=2,NDR4
        L=NDR4+1-J
     30 W(L,N)=Q(L,N)-B(L,N)*W(L+1,N)
C
C
        IF( NTEMP .EQ. 0) RETURN
C       TO CALCULATE SORBENT,GLYCOL,HX CORE AND GAS TEMPERATURES
C
        CALL TSORBA
        CALL TGLCOL(TC,NDX1,UC,RHOC,CPC,CX,AXC,HXC,T268,TX,DX,DT,AVC,NOG)
        CALL HXCORE(TX,TC,TS,TG,HXC,HXS,HXG,RHOX,CPX,TKX,DX,DT,NDX1,AVX,
     1NDXM)
        CALL GASTA(GMR,CPG,ABED,NDX1,TGI,ASG,HSG,AXG,HXG,DX,TG,TS,TX)
        RETURN
        END
C
C
C
C
     -I  FOR S9977,S9977
        SUBROUTINE TSORBA
        COMMON /BLOK2/ ABED(41), A(41), AVC(41),CPG(41),RHOG(41),
     1HXG(41),HXS(41),HXC(41),DIF(41),F(41),C(41),VS(2),DVS(2),DVS1(2),R
     2S1(2,41),RHOS(2),UG(41),WM(2),UC(41),NDXM,PS(41),RHOSB(41),DS(41),
     3CS1(41),CS2(41),C1(21,41),C2(21,41),D1(21,41),D2(41),PC1(41),PC2(4
     41),PC3(41),ASG(41),ASX(41),AGX(41),C1P(41),C2P(41),C3P(41),D1P(41)
     5,FR(2,41),RS(2),NDX1,NDR4,DX,DT,GK(41),DH(41),SK(41),P1(41),P2(41)
     6,P3(41),WS(41),CR1(2,21),CR2(2,21),CR3(2,21),C3(21,41),B(21,41),
     7Q(21,41),CP1(41),CP2(41),X(41),VOIDF(41),TIME
     8,AXC(41),RHOC(41),CPC(41),T268,AVX(41),TKX(41),CPX(41),RHOX(41)
     9,NOG,PK(2,41),PCO2I,PH2OI,  GMR,GMW,TGI,PA,PT(41),CPS(41),HSG(41)
        COMMON /BLOK3/ W(21,41),TG(41),TS(41),TC(41),TX(41),CYCLE
        COMMON /BLOK8/ DTO,TS1(41),TS2(41),TX1(41),TX2(41),TC1(41),TC2(41)
        DIMENSION S1(41),S2(41),S3(41),B1(41)
        RATIO = (DT+DTO)/DT
        DO 10 N=1,NDX1
        CS1(N)=RATIO*CS1(N)
```

```
        CS2(N)=RATIO*CS2(N)
        T=(DT+DTO)/CPS(N)/RHOSB(N)
        T1=0.5*T*(ASG(N)*HSG(N)+ASX(N)*HXS(N))
        I=IFN(N,NDXM)
        TGAVG1=TG(N)
        B1(N) =TS2(N)+CS1(N)*
     1PK(I,N)
     2                          -CS2(N)*(P1(N)+P2(N)*(W(NDR4,N)-WS(N))+
     1P3(N)*
     2PK(I,N)
     3           )+T*(ASG(N)*HSG(N)*TGAVG1+
     4ASX(N)*HXS(N)*TX1(N))-T1*TS2(N)
        S1(N)=-T*SK(N)/DX/DX
        S2(N)=1.-2.*S1(N)+T1
        S3(N)=S1(N)
   10 CONTINUE
        S2(1)=S2(1)+S1(1)
        S1(1)=0.0
        S2(NDX1)=S2(NDX1)+S3(NDX1)
        S3(NDX1)=0.
        NSG=NDXM+1
        S2(NDXM)=S2(NDXM)+S3(NDXM)
        S3(NDXM)=0.
        S2(NSG)= S2(NSG)+S1(NSG)
        S1(NSG)=0.0
        CALL FDEQIM(S1,S2,S3,B1,TS,NDX1)
        RETURN
        END
C
C
C
-I      FOR S9976,S9976
        SUBROUTINE GASTA(GMR,CPG,ABED,NDX1,TGI,ASG,HSG,AXG,HXG,DX,TG,TS,TX
     1)
C
C       GAS TEMPERATURE CALCULATIONS FOR ADSORPTION
C
        DIMENSION CPG(1),ASG(1),HSG(1),HXG(1),TG(1),TS(1),TX(1),ABED(1),
     1AXG(1)
C
        TG(NDX1+1) = TGI
        DO 10 N=1,NDX1
        C=GMR*CPG(N)/ABED(N)
        N1=NDX1+1-N
        C1=ASG(N1)*HSG(N1)+AXG(N1)*HXG(N1)
   10   TG(N1) = (TG(N1+1)/DX+(ASG(N1)*HSG(N1)*TS(N1)+AXG(N1)
     1                          *HXG(N1)*TX(N1))/
     1C)/(1./DX+C1/C)
        RETURN
        END
C
C
C
-I      FOR S9979,S9979
        SUBROUTINE PRADSB
C
        COMMON /BLOK2/ ABED(41), A(41), AVC(41),CPG(41),RHOG(41),
     1HXG(41),HXS(41),HXC(41),DIF(41),F(41),C(41),VS(2),DVS(2),DVS1(2),R
     2S1(2,41),RHOS(2),UG(41),WM(2),UC(41),NDXM,PS(41),RHOSB(41),DS(41),
```

```
      3CS1(41),CS2(41),C1(21,41),C2(21,41),D1(21,41),D2(41),PC1(41),PC2(4       1
      41),PC3(41),ASG(41),ASX(41),AGX(41),C1P(41),C2P(41),C3P(41),D1P(41)        1
      5,FR(2,41),RS(2),NDX1,NDR4,DX,DT,GK(41),DH(41),SK(41),P1(41),P2(41),       1
      6,P3(41),WS(41),CR1(2,21),CR2(2,21),CR3(2,21),C3(21,41),B(21,41),          1
      70(21,41),CP1(41),CP2(41),X(41),VOIDF(41),TIME                            1
      8,AXC(41),RHOC(41),CPC(41),T268,AVX(41),TKX(41),CPX(41),RHOX(41)          1
      9,NOG,PK(2,41),PCO2I,PH2OI,  GMR,GMW,TGI,PA,PT(41),CPS(41),HSG(41)        1
      COMMON /BLOK3/ W(21,41),TG(41),TS(41),TC(41),TX(41),CYCLE                 1
      COMMON /BLOK11/ TOTCO2,TOTH2O,SUMPTM,WTACMS,WTSG                          1
      COMMON /BLOK16/ NDXMAC                                                    1
      COMMON /BLOK14/ NCYCLE                                                    1
      DIMENSION AVLD(41)                                                        1
      EQUIVALENCE(NDX,NDX1)                                                     1
      AVPH2O = SUMPTM/TIME                                                      1
      AVH2OP=GMR*AVPH2O*18./(PA*GMW)                                            1
   C                                                                            1
      TIMEM=60.*TIME                                                            1
      WRITE (6,100) NCYCLE, TIME, TIMEM, DT                                     1
      WRITE (6,101)                                                             1
      WRITE(6,102)(N,PK(1,N),PK(2,N),                                           1
     1                    TG(N),TS(N),TC(N),TX(N),N=1,NDX)                      1
      WRITE (6,202)                                                             1
      N1=NDXM+1                                                                 1
      NDR3=NDR4-1                                                               1
      DO 20 N= 1, NDXM                                                          1
      SUMMS=0.0                                                                 1
      SUMMS=SUMMS+0.5*(W(1,N)+W(NDR4,N))                                        1
      DO 22 NR=2,NDR3                                                           1
   22 SUMMS=SUMMS+W(NR,N)                                                       1
      AVLD(N)=SUMMS/NDR3                                                        1
   20 CONTINUE                                                                  1
      DO 30 N= N1,NDX1                                                          1
      SUMMS=0.0                                                                 1
      SUMMS=SUMMS+0.5*(W(1,N)+W(NDR4,N))                                        1
      DO 33 NR=2, NDR3                                                          1
   33 SUMMS=SUMMS+W(NR,N)                                                       1
      AVLD(N)=SUMMS/NDR3                                                        1
   30 CONTINUE                                                                  1
      SUM=0.                                                                    1
      DO 31 N= 1, NDXMAC                                                        1
   31 SUM= SUM+AVLD(N)*ABED(N)*DX*RHOSB(N)                                      1
      AVMSLD = SUM/WTACMS                                                       1
      SUM=0.                                                                    1
      DO 32 N= N1,NDX1                                                          1
   32 SUM = SUM+AVLD(N)*ABED(N)*DX*RHOSB(N)                                     1
      AVSGLD=SUM/WTSG                                                           1
      DO 10 N=1,NDX                                                            1
   10 WRITE (6,203)N, AVLD(N)                                                   1
     1              ,(W(NR,N),NR=1,NDR4)                                        1
      WRITE (6,205) AVMSLD, AVSGLD                                              1
      AVRCO2=TOTCO2/TIME                                                        1
      AVRH2O=TOTH2O/TIME                                                        1
      WRITE(6,204) AVRCO2,AVRH2O                                                1
      WRITE(6, 206) AVPH2O, AVH2OP                                              1
      RETURN                                                                    1
  100 FORMAT (1H1,16HADSORPTION CYCLE  I3/                                      1
     1           3X,5HTIME=,F9.5,1X2HHR,F12.3,1X,3HMIN,                         1
     1                                  5X,15HTIME INCREMENT=F7.5,1X2HHR)       1
```

```
101 FORMAT (//2X,10HAXIAL NODE,3X,7HPCO2,MM,5X,7HPH2O,MM,8X,
   1                                        11HGAS-TEMP, F
   1   ,8X,15HSORBENT TEMP, F     ,6X,14HGLYCOL TEMP, F    ,7X,15HHX_CO
   2RE TEMP, F   )
102 FORMAT(//(I9,2F12.4,5X,4(F14.4,6X)))
202 FORMAT (//  38HOLOADING AT INTERIOR OF SORBENT, LB/LB
   1                                        //4X,4HSORB/4X,4HNOD
   1E,3X, 3HAVG, 9X,
   1       1H1,9X,1H2,9X,1H3,9X,1H4,9X,1H5,9X,1H6,9X,1H7,9X,
   21H8,9X,1H9,8X,2H10,
   28X,2H11/6H AXIAL/5H NODE)
203 FORMAT ( I5,4X,12(F6.4,4X))
204 FORMAT(//27HOTIME AVG CO2 ADSORP RATE =
   1    F8.4, 6H LB/HR ,10X,
   227H TIME AVG H2O ADSORP RATE =
   3 F8.4, 7H LB/HR          )
205 FORMAT(/// 30H AVG CO2 LOADING IN M.S. BED = F8.4,1X,5HLB/LB,7X,
   130H AVG H2O LOADING IN S.G. BED = F8.4, 6H LB/LB)
206 FORMAT( //21H TIME AVG EXIT PH2O =  , F10.4, 3H MM ,18X,
   140HTIME AVG RATE OF M.S. POISONING BY H2O.= , G8.4,6H LB/HR )
    END
C
C
TI    FOR S9980,S9980
    SUBROUTINE MDESOR
C   MAIN PROGRAM FOR TRANSIENT DESORPTION BED CALCULATIONS
C
    COMMON /BLOK1/ ABED(41), A(41), AVC(41),CPG(41),RHOG(41),
   1HXG(41),HXS(41),HXC(41),DIF(41),F(41),C(41),VS(2),DVS(2),DVS1(2),R
   2S1(2,41),RHOS(2),UG(41),WM(2),UC(41),NDXM,PS(41),RHOSB(41),DS(41),
   3CS1(41),CS2(41),C1(21,41),C2(21,41),D1(21,41),D2(41),PC1(41),PC2(4
   41),PC3(41),ASG(41),ASX(41),AGX(41),C1P(41),C2P(41),C3P(41),D1P(41)
   5,FR(2,41),RS(2),NDX1,NDR4,DX,DT,GK(41),DH(41),SK(41),P1(41),P2(41)
   6,P3(41),WS(41),CR1(2,21),CR2(2,21),CR3(2,21),C3(21,41),B(21,41),
   7Q(21,41),CP1(41),CP2(41),X(41),VOIDF(41),TIME
   8,AXC(41),RHOC(41),CPC(41),T268,AVX(41),TKX(41),CPX(41),RHOX(41)
   9,NOG,PK(2,41),PCO2I,PH2OI,  GMR,GMW,TGI,PA,PT(41),CPS(41),HSG(41)
    DOUBLE PRECISION C1P,C2P,C3P,D1P
    COMMON /BLOK3/ W(21,41),TG(41),TS(41),TC(41),TX(41),CYCLE
    COMMON /BLOK8/ DTO,TS1(41),TS2(41),TX1(41),TX2(41),TC1(41),TC2(41)
    COMMON /BLOK10/ NPRINT,DTMAX
    COMMON /BLOK11/ TOTCO2,TOTH2O
    COMMON /BLOK13/ WI, TI
C
    TIME = 0.0
    DT = 1.E-5
    DTO =0.0
    TOTCO2=0.0
    TOTH2O=0.0
    DO 20 N=1,NDX1
    TS1(N)= TS(N)
    TS2(N)= TS(N)
    TX2(N)=TX(N)
    TX1(N)=TX(N)
    TC1(N)=TC(N)
    TC2(N)=TC(N)
 20 CONTINUE
    CALL START
```

```
        CALL PRDESB                                                          1
        NPR = 0                                                              1
        GO TO 3                                                              1
    2 CALL PRDESB                                                            1
        IF( TIME .GE. CYCLE) GO TO 9999                                      1
        NPR = 0                                                              1
    4 CONTINUE                                                               1
        IF( TIME  .LT.0.5E-4) GO TO 3                                        1
        ADT=DTMAX                                                            1
        DO 60 N= 1, NDX1                                                     1
        ADT2=WI       /(ABS(W(NDR4,N)-WS(N))+1.E-9)*DT                       1
        IF(ADT2.LT. ADT) ADT=ADT2                                            1
        ADT2=TI/(ABS(TS1(N)-TS2(N))+1.E-9)*DT                               1
        IF(ADT2.LT. ADT) ADT=ADT2                                            1
        ADT2=TI/(ABS(TX1(N)-TX2(N))+1.E-9)*DT                               1
        IF(ADT2.LT. ADT) ADT=ADT2                                            1
   60 CONTINUE                                                               1
        DTO=DT                                                               1
        DT=ADT                                                               1
        IF((TIME+DT) .GT. CYCLE) DT = CYCLE-TIME                             1
    3 CONTINUE                                                               1
        CALL DESORB(DT)                                                      1
        TOTCO2=TOTCO2+DT*FR(1,NDX1)*WM(1)                                    1
        TOTH2O=TOTH2O+DT*FR(2,NDX1)*WM(2)                                    1
        DO 21 N=1,NDX1                                                       1
        TS2(N)=TS1(N)                                                        1
        TS1(N)=TS(N)                                                         1
        TX2(N)=TX1(N)                                                        1
        TX1(N)=TX(N)                                                         1
        TC2(N)=TC1(N)                                                        1
        TC1(N)=TC(N)                                                         1
   21 CONTINUE                                                               1
        TIME=TIME+DT                                                         1
        NPR=NPR+1                                                            1
        IF (NPR .GE. NPRINT) GO TO 2                                         1
        IF(TIME .GE. CYCLE) GO TO 2                                          1
        GO TO 4                                                              1
 9999 CONTINUE                                                               1
        RETURN                                                               1
        END                                                                 1
  C                                                                          1
  C                                                                          1
 -TI    FOR S9988,S9988                                                      1
        SUBROUTINE START                                                     1
  C                                                                          1
        COMMON /BLOK1/ ABED(41), A(41), AVC(41),CPG(41),RHOG(41),           1
       1HXG(41),HXS(41),HXC(41),DIF(41),F(41),C(41),VS(2),DVS(2),DVS1(2),R   1
       2S1(2,41),RHOS(2),UG(41),WM(2),UC(41),NDXM,PS(41),RHOSB(41),DS(41),   1
       3CS1(41),CS2(41),C1(21,41),C2(21,41),D1(21,41),D2(41),PC1(41),PC2(4   1
       41),PC3(41),ASG(41),ASX(41),AGX(41),C1P(41),C2P(41),C3P(41),D1P(41)   1
       5,FR(2,41),RS(2),NDX1,NDR4,DX,DT,GK(41),DH(41),SK(41),P1(41),P2(41)   1
       6,P3(41),WS(41),CR1(2,21),CR2(2,21),CR3(2,21),C3(21,41),B(21,41),     1
       7Q(21,41),CP1(41),CP2(41),X(41),VOIDF(41),TIME                        1
       8,AXC(41),RHOC(41),CPC(41),T268,AVX(41),TKX(41),CPX(41),RHOX(41)      1
       9,NOG,PK(2,41),PCO2I,PH2OI,  GMR,GMW,TGI,PA,PT(41),CPS(41),HSG(41)    1
        COMMON /BLOK3/ W(21,41),TG(41),TS(41),TC(41),TX(41),CYCLE            1
        DOUBLE PRECISION C1P,C2P,C3P,D1P                                     1
  C                                                                          1
```

```
      RS(1)=RHOSB(1)*3./RHOS(1)/ASG(1)
      RS(2)=RHOSB(NDX1)
     1                   *3./RHOS(2)/ASG(NDX1)
      DO 30 N=1,NDX1
      RHOG(N) = 0.0003
      X(N) = 0.5
      C(N) = 0.2E-3
      PT(N) = 3.0
      I=IFN(N,NDXM)
   30 VOIDF(N) = 1. - RHOSB(N)/RHOS(I)
      NDR=NDR4-1
      NDR2=2.*NDR
      NDR3=NDR2+1
      DO 10 I=1,2
      VS(I)=4./3.*3.1416*RS(I)**3
      DVS(I)=VS(I)/NDR
      DVS1(I)=DVS(I)/2
      RS1(I,1)=0.
      DO 10 K=2,NDR3
   10 RS1(I,K)=CBRT(3./4./3.1416*(4./3.*3.1416*RS1(I,K-1)**3+DVS1(I)))
      DO 11 I=1,2
      IF(I.EQ.1) DIF1=DIF(1)
      IF(I.EQ.2) DIF1=DIF(NDX1)
      CR1(I,1)=DVS1(I)*RHOS(I)
      CR2(I,1)=0.
      CR3(I,1)=4.*3.1416*RS1(I,2)**2*DIF1   /(RS1(I,3)-RS1(I,1))*RHOS(I)
      DO 11 K=2,NDR4
      CR1(I,K)=DVS(I)*RHOS(I)
      CR2(I,K)=4.*3.1416*RS1(I,2*K-2)**2*DIF1   /(RS1(I,2*K-1)-RS1(I,2*K-
     13))*RHOS(I)
   11 CR3(I,K)=4.*3.1416*RS1(I,2*K)**2*DIF1   /(RS1(I,2*K+1)-RS1(I,2*K-1)
     1)*RHOS(I)
      CR1(1,NDR4)=CR1(1,1)
      CR1(2,NDR4)=CR1(2,1)
      RETURN
      END
C
C
-I    FOR S9983,S9983
      SUBROUTINE DESORB(DELT)
C
      COMMON /BLOK1/ ABED(41), A(41), AVC(41),CPG(41),RHOG(41),
     1HXG(41),HXS(41),HXC(41),DIF(41),F(41),C(41),VS(2),DVS(2),DVS1(2),R
     2S1(2,41),RHOS(2),UG(41),WM(2),UC(41),NDXM,PS(41),RHOSB(41),DS(41),
     3CS1(41),CS2(41),C1(21,41),C2(21,41),D1(21,41),D2(41),PC1(41),PC2(4
     41),PC3(41),ASG(41),ASX(41),AGX(41),C1P(41),C2P(41),C3P(41),D1P(41)
     5,FR(2,41),RS(2),NDX1,NDR4,DX,DT,GK(41),DH(41),SK(41),P1(41),P2(41)
     6,P3(41),WS(41),CR1(2,21),CR2(2,21),CR3(2,21),C3(21,41),B(21,41),
     7Q(21,41),CP1(41),CP2(41),X(41),VOIDF(41),TIME
     8,AXC(41),RHOC(41),CPC(41),T268,AVX(41),TKX(41),CPX(41),RHOX(41)
     9,NOG,PK(2,41),PCO2I,PH2OI,   GMR,GMW,TGI,PA,PT(41),CPS(41),HSG(41)
      COMMON /BLOK3/ W(21,41),TG(41),TS(41),TC(41),TX(41),CYCLE
      COMMON /BLOK4/ POUT(10),TIMET(10),NBCOUT
      COMMON /BLOK12/ NTEMP
      DIMENSION AS(2),PD(41)
      DIMENSION P4(41),VIST(2)
      DOUBLE PRECISION PD
      DOUBLE PRECISION C1P,C2P,C3P,D1P
```

```
      EQUIVALENCE (ASX,AXS),(AGX,AXG),(ASG,AGS),(HXS,HSX),(HXG,HGX),(HSG
     1,HGS)
      DATA VIST/ 0.015, 0.0150 /
      DT=DELT
      AS(1)=4.*3.1416*RS(1)**2
      AS(2)=4.*3.1416*RS(2)**2
C
C
C
      DATA RGAS/554./
C
      NDR=NDR4-1
      DO 21 N=1,NDX1
      J=2
      P4(N)=PT(N)
      I=IFN(N,NDXM)
      IF( I .EQ. 2) J=1
      VIS= X(N)*VIST(I)+(1.-X(N))*VIST(J)
      F(N)=2.494E-4*PT(N)**0.795*(VIS/0.0174)
      DO 20 NR=1,NDR4
      C1(NR,N)=-CR2(I,NR)
      C2(NR,N)=CR1(I,NR)/DT+CR2(I,NR)+CR3(I,NR)
   20 C3(NR,N)=-CR3(I,NR)
C
C
      B(1,N)=C3(1,N)/C2(1,N)
      DO 21 J=2,NDR
   21 B(J,N)=C3(J,N)/(C2(J,N)-C1(J,N)*B(J-1,N))
      NDX=NDX1-1
C     TO TEMPORARILY STORE SURFACE LOADING
      DO 50 N=1,NDX1
   50 WS(N)=W(NDR4,N)
C
C     TO CALCULATE CS1,CS2,DS FOR SORBENT HEAT BALANCE EQUATION
      IF (NTEMP .EQ. 0.) GO TO 111
      DO 12 N=1,NDX1
      I=IFN(N,NDXM)
      CS2(N)=DT/CPS(N)/RHOSB(N)*ASG(N)*GK(N)*WM(I)*DH(N)
      CS1(N) = CS2(N)*X(N)
      IF (N.EQ.1) GO TO 13
      IF (N.EQ.NDX1) GO TO 14
      S1=SK(N)/DX**2*(TS(N-1)-2.*TS(N)+TS(N+1))
      GO TO 15
   13 S1=SK(1)/DX**2*(TS(2)-TS(1))
      GO TO 15
   14 S1=SK(NDX1)/DX**2*(TS(NDX)-TS(NDX1))
   15 DS(N)=DT/CPS(N)/RHOSB(N)*(S1+ASG(N)*HSG(N)*(TG(N)-TS(N))+ASX(N)*HX
     1S(N)*(TX(N)-TS(N)))
   12 CONTINUE
      GO TO 110
  111 DO 112 N=1,NDX1
      CS1(N)=0.
      CS2(N)=0.
      DS(N)=0.
      TS(N)=T268
      TC(N)=T268
      TX(N)=T268
      TG(N)=T268
```

```
    112 CONTINUE                                                                        1
    110 CONTINUE                                                                         1
    C                                                                                    1
    C     TO CALCULATE TOTAL PRESSURE                                                    1
    C                                                                                    1
          DO 24 N=1,NDX1                                                                 1
          I=IFN(N,NDXM)                                                                  1
    C     TO CALCULATE P1,P2,P3                                                          1
          DPKDTS=                                                                        1
         1     (PKEQ(I,W(NDR4,N),(TS(N)+0.001))-PKEQ(I,W(NDR4,N),TS(N)))/                1
          20.001                                                                         1
          DPKDWK=(PKEQ(I,(W(NDR4,N)+1.E-6),TS(N))-PKEQ(I,W(NDR4,N),TS(N)))/1             1
          1.E-6                                                                          1
          G=1.+CS2(N)*DPKDTS                                                             1
          P1(N)=(PKEQ(I,W(NDR4,N),TS(N))+DS(N)*DPKDTS)/G                                 1
          P2(N)=DPKDWK/G                                                                 1
          P3(N)=CS1(N)/G*DPKDTS                                                          1
    C                                                                                    1
          C2(NDR4,N)=CR1(I,NDR4)/DT+CR2(I,NDR4)+WM(I)*GK(N)*P2(N)*AS(I)                  1
          C3(NDR4,N)=0.0                                                                 1
          DO 23 NR=1,NDR4                                                                1
       23 D1(NR,N)=CR1(I,NR)/DT*W(NR,N)                                                  1
          D1(NDR4,N)=D1(NDR4,N)-WM(I)*GK(N)*(P1(N)-P2(N)*W(NDR4,N))*AS(I)                1
          D2(N)=AS(I)*WM(I)*GK(N)*(X(N)   -P3(N))                                        1
          D2(N)=D2(N)/(C2(NDR4,N)-C1(NDR4,N)*B(NDR4-1,N))                                1
          Q(1,N)=D1(1,N)/C2(1,N)                                                         1
          DO 24 J=2,NDR4                                                                 1
       24 Q(J,N)=(D1(J,N)-C1(J,N)*Q(J-1,N))/(C2(J,N)-C1(J,N)*B(J-1,N))                   1
    C                                                                                    1
    C     COEFFICIENTS FOR P-EQUATION                                                    1
          DO 25 N=2,NDX                                                                  1
       25 PC2(N) = PT(N)/(VOIDF(N)*C(N)*ABED(N))*(VOIDF(N+1)*C(N+1)*ABED(N+1            1
         1)/F(N+1) - VOIDF(N-1)*C(N-1)*ABED(N-1)/F(N-1))/(2.*DX)                        1
          N=1                                                                            1
          PC2(N) = PT(N)/(VOIDF(N)*C(N)*ABED(N))*(VOIDF(N+1)*C(N+1)*ABED(N+1            1
         1)/F(N+1) - VOIDF(N  )*C(N  )*ABED(N  )/F(N  ))/(1.*DX)                        1
          N= NDX1                                                                        1
          PC2(N) = PT(N)/(VOIDF(N)*C(N)*ABED(N))*(VOIDF(N  )*C(N  )*ABED(N             1
         1)/F(N  ) - VOIDF(N-1)*C(N-1)*ABED(N-1)/F(N-1))/(1.*DX)                        1
          DO 26 N=1,NDX1                                                                 1
          PC1(N)=PT(N)/F(N)                                                              1
       26 PC3(N)=PT(N)/C(N)/VOIDF(N)*ASG(N)*GK(N)                                        1
    C                                                                                    1
          DO 27 N=1,NDX1                                                                 1
          CP1(N)=PC3(N)*(P1(N)+P2(N)*(Q(NDR4,N)-W(NDR4,N)))                              1
          CP2(N)=PC3(N)*(P2(N)*D2(N)+P3(N)     -X(N))                                    1
          C1P(N)=-PC1(N)/DX/DX+PC2(N)/2./DX                                              1
          C2P(N)=1./DT+2.*PC1(N)/DX/DX-CP2(N)                                            1
          C3P(N)=-PC1(N)/DX/DX-PC2(N)/2./DX                                             1
       27 D1P(N)=PT(N)/DT+CP1(N)                                                         1
    C                                                                                    1
    C     BOUNDARY CONDITION FOR P-EQUATION                                              1
    C                                                                                    1
          C2P(1)=C2P(1)+C1P(1)                                                           1
          C1P(1)=0.                                                                      1
          GO TO (55,56), NBCOUT                                                          1
       55 CONTINUE                                                                       1
          CEXIT = 11.2*PT(NDX1)**0.715/(VOIDF(NDX1)*RHOG(NDX1)*ABED(NDX1))               1
```

```
      C2P(NDX1) = C2P(NDX1)+C3P(NDX1)*(1.-DX*F(NDX1)*CEXIT)          1
      C3P(NDX1)=0.0                                                   1
      GO TO 57                                                        1
   56 C1P(NDX1)=0.                                                    1
      C2P(NDX1)=1.0                                                   1
      C3P(NDX1)=0.0                                                   1
      CALL LAGIN2(10,TIMET,10,2,TIME,D1PPT,POUT)                      1
      D1P(NDX1)=D1PPT                                                 1
   57 CONTINUE                                                        1
      CALL FDEQID(C1P,C2P,C3P,D1P,PD,NDX1)                            1
      DO 34 N=1,NDX1                                                  1
      IF(PD(N) .LE. 0.) PD(N) = 1.E-3                                 1
   34 PT(N)=PD(N)                                                     1
    C                                                                 1
    C  TO CALCULATE SORBENT LOADING                                   1
    C                                                                 1
      DO 30 N=1,NDX1                                                  1
      W(NDR4,N)=Q(NDR4,N)+D2(N)*PT(N)                                 1
      DO 30 J=2,NDR4                                                  1
      L=NDR4+1-J                                                      1
   30 W(L,N)=Q(L,N)-B(L,N)*W(L+1,N)                                   1
    C                                                                 1
    C  TO CALCULATE STREAM COMPOSITION                                1
    C                                                                 1
      FR(1,1) = 0.0                                                   1
      FR(2,1)=0.                                                      1
      DO 31 N=1,NDX1                                                  1
      I=IFN(N,NDXM)                                                   1
      TEMP    =C(N)*VOIDF(N)                                          1
     1/P4(N)*ABED(N)              *DX*(CP1(N)+CP2(N)*PT(N))           1
      IF(I.EQ.1)J=2                                                   1
      IF(I.EQ.2)J=1                                                   1
      IF(N . EQ. 1) GO TO 200                                         1
      FR(J,N)=FR(J,N-1)                                               1
      FR(I,N)=TEMP+FR(I,N-1)                                          1
      IF( NDXM .EQ. 0) GO TO 202                                      1
      IF (I .EQ. 1) GO TO 202                                         1
      GO TO 201                                                       1
  200 FR(I,1) = TEMP                                                  1
  202 X(N) = 1.0                                                      1
      GO TO 31                                                        1
  201 CONTINUE                                                        1
      CT=ABED(N)*DX*ASG(N)*GK(N)                                      1
      FRT = FR(1,N) + FR(2,N) +1.E-10                                 1
      X(N)=(( FR(2,N-1)+CT*PKEQ(2,W(NDR4,N),(TS(N)+0.001)))/FRT/      1
     1(1. + CT*PT(N)/FRT)+X(N))/2.                                    1
   31 CONTINUE                                                        1
      DO 33 N=1,NDX1                                                  1
      C(N) = (PT(N)/RGAS/(TG(N)+460)+C(N))/2.0                        1
      I = IFN (N,NDXM)                                                1
      IF (I.EQ.1) J=2                                                 1
      IF (I.EQ.2) J=1                                                 1
      RHOG(N)=C(N)*(X(N)*WM(I)+(1.-X(N))*WM(J))                       1
      UG(N)=(FR                                                       1
     1       (1,N)*WM(1)+FR(2,N)*WM(2))/RHOG(N)/ABED(N)/VOIDF(N)      1
   33 CONTINUE                                                        1
      IF( NTEMP .EQ. 0) RETURN                                        1
    C                                                                 1
```

```fortran
C     TO CALCULATE SORBENT TEMPERATURES
C
      CALL TSORB
      CALL TGLCOL(TC,NDX1,UC,RHOC,CPC,CX,AXC,HXC,T268,TX,DX,DT,AVC,NOG)
      CALL HXCORE(TX,TC,TS,TG,HXC,HXS,HXG,RHOX,CPX,TKX,DX,DT,NDX1,AVX,
     1NDXM)
      CALL GAST(DX,RHOG,CPG,UG,TS,TX,NDX1,ASG,HSG,AXG,HXG,TG,VOIDF)
  100 FORMAT(8G12.3)
      RETURN
      END
C
C
C
C
C
C
 -TI     FOR S9989,S9989
C
      SUBROUTINE PRDESB
C
      COMMON /BLOK1/ ABED(41), A(41), AVC(41),CPG(41),RHOG(41),
     1HXG(41),HXS(41),HXC(41),DIF(41),F(41),C(41),VS(2),DVS(2),DVS1(2),R
     2S1(2,41),RHOS(2),UG(41),WM(2),UC(41),NDXM,PS(41),RHOSB(41),DS(41),
     3CS1(41),CS2(41),C1(21,41),C2(21,41),D1(21,41),D2(41),PC1(41),PC2(4
     41),PC3(41),ASG(41),ASX(41),AGX(41),C1P(41),C2P(41),C3P(41),D1P(41)
     5,FR(2,41),RS(2),NDX1,NDR4,DX,DT,GK(41),DH(41),SK(41),P1(41),P2(41)
     6,P3(41),WS(41),CR1(2,21),CR2(2,21),CR3(2,21),C3(21,41),B(21,41),
     7Q(21,41),CP1(41),CP2(41),X(41),VOIDF(41),TIME
     8,AXC(41),RHOC(41),CPC(41),T268,AVX(41),TKX(41),CPX(41),RHOX(41)
     9,NOG,PK(2,41),PCO2I,PH2OI,   GMR,GMW,TGI,PA,PT(41),CPS(41),HSG(41)
      COMMON /BLOK3/ W(21,41),TG(41),TS(41),TC(41),TX(41),CYCLE
      COMMON /BLOK11/ TOTCO2,TOTH2O,SUMPTM,WTACMS,WTSG
      COMMON /BLOK14/ NCYCLE
      COMMON /BLOK16/ NDXMAC
      DIMENSION AVLD(41)
      DOUBLE PRECISION C1P,C2P,C3P,D1P
      EQUIVALENCE(NDX,NDX1)
C
      TIMEM=60.*TIME
      WRITE (6,100) NCYCLE, TIME, TIMEM, DT
      WRITE (6,101)
      WRITE (6,102)(N,PT(N),TG(N),TS(N),TC(N),TX(N),N=1,NDX)
      FR1=FR(1,NDX)*WM(1)
      FR2=FR(2,NDX)*WM(2)
      WRITE (6,103)FR1,FR2
      WRITE (6,200)
      WRITE (6,201)(N,X(N),FR(1,N),FR(2,N),N=1,NDX)
      WRITE (6,202)
      N1=NDXM+1
      NDR3=NDR4-1
      DO 20 N= 1, NDXM
      SUMMS=0.0
      SUMMS=SUMMS+0.5*(W(1,N)+W(NDR4,N))
      DO 22 NR=2,NDR3
   22 SUMMS=SUMMS+W(NR,N)
      AVLD(N)=SUMMS/NDR3
   20 CONTINUE
      DO 30 N= N1,NDX1
```

```
      SUMMS=0.0                                                    1
      SUMMS=SUMMS+0.5*(W(1,N)+W(NDR4,N))                           1
      DO 33 NR=2, NDR3                                             1
   33 SUMMS=SUMMS+W(NR,N)                                          1
      AVLD(N)=SUMMS/NDR3                                           1
   30 CONTINUE                                                     1
      SUM=0.                                                       1
      DO 31 N= 1, NDXMAC                                           1
   31 SUM= SUM+AVLD(N)*ABED(N)*DX*RHOSB(N)                         1
      AVMSLD = SUM/WTACMS                                          1
      SUM=0.                                                       1
      DO 32 N= N1,NDX1                                             1
   32 SUM = SUM+AVLD(N)*ABED(N)*DX*RHOSB(N)                        1
      AVSGLD=SUM/WTSG                                              1
      DO 10 N=1,NDX                                                1
   10 WRITE (6,203)N, AVLD(N)                                      1
     1              ,(W(NR,N),NR=1,NDR4)                           1
      WRITE (6,205) AVMSLD, AVSGLD                                 1
      AVRCO2=TOTCO2/TIME                                           1
      AVRH2O=TOTH2O/TIME                                           1
      WRITE(6,204) AVRCO2,AVRH2O                                   1
      RETURN                                                       1
    C                                                              1
  100 FORMAT (1H1,16HDESORPTION CYCLE  I3/                         1
     1        3X,5HTIME=,F9.5,1X2HHR,F12.3,1X,3HMIN,               1
     1                 5X,15HTIME INCREMENT=F7.5,1X2HHR)           1
  101 FORMAT (//2X,10HAXIAL NODE,10X,14HTOTAL PRESS,MM,6X,14HGAS TEMP,DE 1
     1G F,5X,19HSORBENT TEMP, DEG F,2X,18HGLYCOL TEMP, DEG F,3X,19HHX CO 1
     2RE TEMP, DEG F  )                                            1
  102 FORMAT(/(I9,11X,5(F14.4,6X)))                                1
  103 FORMAT (/21H0CO2 DESORPTION RATE=F7.4,1X5HLB/HR,5X,20HH2O DESORPTI 1
     1ON RATE=F7.4,1X5HLB/HR)                                      1
  200 FORMAT (1H0/2X,10HAXIAL NODE,13X,9HMOLE FRAC,7X,             1
     1      12X,13HCO2 RATE,M/HR,6X,13HH2O RATE,M/HR)              1
  201 FORMAT(/(I9,11X,3(4X,F12.6,4X)))                             1
  202 FORMAT (//  31H0LOADING AT INTERIOR OF SORBENT//4X,4HSORB/4X,4HNOD 1
     1E,3X, 3HAVG, 9X,                                             1
     1     1H1,9X,1H2,9X,1H3,9X,1H4,9X,1H5,9X,1H6,9X,1H7,9X,       1
     21H8,9X,1H9,8X,2H10,                                          1
     28X,2H11/6H AXIAL/5H NODE)                                    1
  203 FORMAT ( I5,4X,12(F6.4,4X))                                  1
  204 FORMAT(/27H0TIME AVG CO2 DESORP RATE =                       1
     1    F8.4, 6H LB/HR ,10X,                                     1
     227H TIME AVG H2O DESORP RATE =                               1
     3   F8.4, 7H LB/HR        )                                   1
  205 FORMAT(/// 30H AVG CO2 LOADING IN M.S. BED = F8.4,1X,5HLB/LB,7X,   1
     130H AVG H2O LOADING IN S.G. BED = F8.4, 6H LB/LB)            1
      END                                                          1
    C                                                              1
    C                                                              1
    C                                                              1
 -I FOR S9997,S9997                                                1
      SUBROUTINE TSORB                                             1
      COMMON /BLOK1/ ABED(41), A(41), AVC(41),CPG(41),RHOG(41),    1
     1HXG(41),HXS(41),HXC(41),DIF(41),F(41),C(41),VS(2),DVS(2),DVS1(2),R 1
     2S1(2,41),RHOS(2),UG(41),WM(2),UC(41),NDXM,PS(41),RHOSB(41),DS(41), 1
     3CS1(41),CS2(41),C1(21,41),C2(21,41),D1(21,41),D2(41),PC1(41),PC2(4 1
     41),PC3(41),ASG(41),ASX(41),AGX(41),C1P(41),C2P(41),C3P(41),D1P(41) 1
```

```
       5,FR(2,41),RS(2),NDX1,NDR4,DX,DT,GK(41),DH(41),SK(41),P1(41),P2(41)           1
       6,P3(41),WS(41),CR1(2,21),CR2(2,21),CR3(2,21),C3(21,41),B(21,41),             1
       70(21,41),CP1(41),CP2(41),X(41),VOIDF(41),TIME                               1
       8,AXC(41),RHOC(41),CPC(41),T268,AVX(41),TKX(41),CPX(41),RHOX(41)             1
       9,NOG,PK(2,41),PCO2I,PH2OI,   GMR,GMW,TGI,PA,PT(41),CPS(41),HSG(41)          1
       COMMON /BLOK3/ W(21,41),TG(41),TS(41),TC(41),TX(41),CYCLE                    1
       COMMON /BLOK8/ DTO,TS1(41),TS2(41),TX1(41),TX2(41),TC1(41),TC2(41)           1
       DOUBLE PRECISION C1P,C2P,C3P,D1P                                            1
       DIMENSION S1(41),S2(41),S3(41),B1(41)                                       1
       RATIO = (DT+DTO)/DT                                                         1
       DO 10 N=1,NDX1                                                              1
       CS1(N)=RATIO*CS1(N)                                                         1
       CS2(N)=RATIO*CS2(N)                                                         1
       T=(DT+DTO)/CPS(N)/RHOSB(N)                                                  1
       T1=0.5*T*(ASG(N)*HSG(N)+ASX(N)*HXS(N))                                      1
       B1(N) =TS2(N)+CS1(N)*PT(N)-CS2(N)*(P1(N)+P2(N)*(W(NDR4,N)-WS(N))+           1
      1P3(N)*PT(N))+T*(ASG(N)*HSG(N)*TG (N)+ASX(N)*HXS(N)*                         1
      2                                        TX1(N))-T1*TS2(N)                   1
       S1(N)=-T*SK(N)/DX/DX                                                        1
       S2(N)=1.-2.*S1(N)+T1                                                        1
       S3(N)=S1(N)                                                                 1
   10  CONTINUE                                                                    1
       S2(1)=S2(1)+S1(1)                                                           1
       S1(1)=0.0                                                                   1
       S2(NDX1)=S2(NDX1)+S3(NDX1)                                                  1
       S3(NDX1)=0.                                                                 1
       NSG=NDXM+1                                                                  1
       S2(NDXM)=S2(NDXM)+S3(NDXM)                                                  1
       S3(NDXM)=0.                                                                 1
       S2(NSG)= S2(NSG)+S1(NSG)                                                    1
       S1(NSG)=0.0                                                                 1
       CALL FDEQIM(S1,S2,S3,B1,TS,NDX1)                                            1
       RETURN                                                                      1
       END                                                                        1
  -1     FOR S9986,S9986                                                          1
       SUBROUTINE GAST (DX,RHOG,CPG,U,TS,TX,NDX1,ASG,HSG,AXG,HXG,TG,VOIDF          1
      1)                                                                          1
       DIMENSION RHOG(1),CPG(1),U(1),TS(1),TX(1),TG(1),ASG(1),HSG(1),HXG(         1
      11),VOIDF(1),AXG(1)                                                         1
       W=1.0                                                                       1
       N2= NDX1-1                                                                  1
       TG(1)=TS(1)                                                                 1
       DO 10 N= 1, N2                                                              1
       F= 0.5*(VOIDF(N)+ VOIDF(N+1))                                              1
       AS1=ASG(N+1)                                                               1
       HS1=HSG(N+1)                                                               1
       AX1=AXG(N+1)                                                               1
       HX1=HXG(N+1)                                                               1
       CP1=CPG(N)                                                                 1
       RO = 0.5*(RHOG(N)+RHOG(N+1))                                               1
       U1= 0.5*( U(N)+U(N+1))                                                     1
       TS1=TS(N+1)                                                                1
       TX1=TX(N+1)                                                                1
       C1=1./(F*RO*CP1*U1)                                                        1
       D=C1*(AS1*HS1*TS1+AX1*HX1*TX1)                                             1
       A=(AS1*HS1+AX1*HX1)*C1                                                     1
   10  TG(N+1)=((1./DX-A*(1.-W))*TG(N)+D)/(1./DX+A*W)                             1
       RETURN                                                                      1
```

```
              END
        C
        C
        C
-TI     FOR    S9992,S9992
        FUNCTION PKEQ(ID,W,T)
C       PKEQ=EQUILIBRIUM PRESSURE IN MM HG
C       ID=2,H2O ON SILICA GEL
C       ID=1,CO2 ON MOLECULAR SIEVE
C       W=LOADING IN LB ADSORBATE PER LB ADSORBENT
C       T=TEMP IN DEG F
C
C
        IF (W .LE. 0. ) W= 1.E-5
        GO TO (1,2),ID
      1 PKEQ=EXP(-9166.56/(T+460.)+1.678*ALOG(W)+23.823)
        RETURN
      2 CONTINUE
        SLOG = ALOG(W)
        P1= -1.075E4*(0.852-0.03215*SLOG)/(T+460.) + (-0.0592*SLOG+0.394)
      1 *SLOG+21.08
        PKEQ=EXP(P1)
        RETURN
        END
        C
        C
-TI       FOR S9991,S9991
        SUBROUTINE HXCORE(TX,TC,TS,TG,HXC,HXS,HXG,RHOX,CPX,TKX,DX,DT,NDX,A
       1VX,NDXM)
        C
        DIMENSION TX(1),TC(1),TS(1),TG(1),HXC(1),HXS(1),HXG(1),RHOX(1),
       1CPX(1),TKX(1),AVX(1)
        DIMENSION C1(41),C2(41),C3(41),D1(41)
        COMMON /BLOK8/ DTO,TS1(41),TS2(41),TX1(41),TX2(41),TC1(41),TC2(41)
        DN=DT+DTO
        DO 10 N=1,NDX
        T1= AVX(N)*(HXC(N)+HXS(N)+HXG(N))*0.5
        C1(N)=-TKX(N)/DX/DX
        C3(N)= -TKX(N+1)/DX/DX
        C2(N)= RHOX(N)*CPX(N)/DN -C1(N) - C3(N) + T1
     10 D1(N) = RHOX(N)*CPX(N)/DN*TX2(N) + AVX(N)*(HXC(N)
       1*TC1(N) + HXS(N)*TS1(N)+HXG(N)*TG(N)) - T1*TX2(N)
        C2(1)=C2(1)+C1(1)
        C1(1)=0.
        C2(NDX)=C2(NDX)+C3(NDX)
        C3(NDX)=0.0
        CALL FDEQIM(C1,C2,C3,D1,TX,NDX)
        RETURN
        END
        C
        C
        C
-I        FOR S9987,S9987
        SUBROUTINE TGLCOL(TC,NDXMAX,UC,RHOC,CPC,CX,AXC,HXC,T268,TX,DX,DT,
       1AVC, NOGLIN)
        DIMENSION C1(30),C2(30),C3(30),D(30),TC(1),TX(1),HXC(1),AVC(1)
        DIMENSION UC(1),RHOC(1),CPC(1),AXC(1)
        COMMON /BLOK8/ DTO,TS1(41),TS2(41),TX1(41),TX2(41),TC1(41),TC2(41)
```

```
          DN=DT+DTO
          DO 10 N=1,NDXMAX
          CC1=-UC(N)
          CC2=HXC(N)/(CPC(N)*RHOC(N))*AVC(N)*0.5
          IF( UC(N) .GT. 0.) GO TO 5
          C3(N)=-CC1/DX
          C2(N)=1./DN+CC2-C3(N)
          C1(N)=0.0
          GO TO 10
       5  C1(N) = CC1/DX
          C2(N) = 1./DN + CC2 - C1(N)
          C3(N) = 0.0
      10  D(N)=TC2(N)/DN+CC2*TX1(N)*2. - CC2*TC2(N)
          C1(NOGLIN) = 0.
          C3(NOGLIN) = 0.
          D(NOGLIN)=D(NOGLIN) +ABS(UC(NOGLIN))/DX*T268
          CALL FDEQIM(C1,C2,C3,D,TC,NDXMAX)
          RETURN
          END
      C
      C
      C
      -TI    FOR S9981,S9981
          FUNCTION IFN(N,NDXM)
          IFN=1
          IF(N.GT.NDXM)IFN=2
          RETURN
          END
      C
      C
      C
      -LI    FOR S9984,S9984
          SUBROUTINE FDEQIM(C1,C2,C3,D,VAR,NN)
          DIMENSION C1(1),C2(1),C3(1),D(1),VAR(1),B(30),Q(30)
          NN1=NN-1
          B(1)=C3(1)/C2(1)
          DO 41 J=2,NN1
      41  B(J)=C3(J)/(C2(J)-C1(J)*B(J-1))
          Q(1)=D(1)/C2(1)
          DO 42 J=2,NN
      42  Q(J)=(D(J)-C1(J)*Q(J-1))/(C2(J)-C1(J)*B(J-1))
          VAR(NN)=Q(NN)
          DO 43 J=2,NN
          L=NN+1-J
      43  VAR(L)=Q(L)-B(L)*VAR(L+1)
          RETURN
          END
      C
      C
      C
      -TI    FOR S9985,S9985
          SUBROUTINE FDEQID(C1,C2,C3,D,VAR,NN)
          DIMENSION C1(1),C2(1),C3(1),D(1),VAR(1),B(30),Q(30)
          DOUBLE PRECISION C1,C2,C3,D,VAR,B,Q
          NN1=NN-1
          B(1)=C3(1)/C2(1)
          DO 41 J=2,NN1
      41  B(J)=C3(J)/(C2(J)-C1(J)*B(J-1))
```

```
        Q(1)=D(1)/C2(1)                                                        1
        DO 42 J=2,NN                                                           1
   42   Q(J)=(D(J)-C1(J)*Q(J-1))/(C2(J)-C1(J)*B(J-1))                          1
        VAR(NN)=Q(NN)                                                          1
        DO 43 J=2,NN                                                           1
        L=NN+1-J                                                               1
   43   VAR(L)=Q(L)-B(L)*VAR(L+1)                                              1
        RETURN                                                                 1
        END                                                                    1
     C                                                                         1
     C                                                                         1
     C                                                                         1
  -I    FOR S9996, S9996                                                       1
        SUBROUTINE  LAGIN2(ID,X,NP,ND,XO,YO,Y)                                 1
     C  REVISED FOR FORTRAN IV 8-8-65  S. WONG                                 1
        DIMENSION  X(2), Y(2)                                                  1
     C                                                                         1
        ILO=1                                                                  1
        IF(XO-X(1))10,16,4                                                     1
    4   IF(XO-X(NP))19,13,7                                                    1
    7   ILO=NP-1                                                               1
   10   IHI=ILO+1                                                              1
        WRITE (6,1) ID,XO                                                      1
        GO TO 46                                                               1
   13   ILO=NP                                                                 1
   16   YO=Y(ILO)                                                              1
        RETURN                                                                 1
   19   DO 22 ILO=2,NP                                                         1
        ILO=ILO                                                               1
        IF(XO-X(ILO))25,16,22                                                  1
   22   CONTINUE                                                               1
   25   IHI=ILO                                                                1
        ILO=IHI-1                                                              1
        IF(ND-2)46,46,28                                                       1
   28   DO 43 I=3,ND                                                           1
        IF(ILO-1)40,40,31                                                      1
   31   IF(IHI-NP)34,37,37                                                     1
   34   IF (2.*XO-X(ILO-1)-X(IHI+1)) 37,37,40                                  1
   37   ILO=ILO-1                                                              1
        GO TO 43                                                               1
   40   IHI=IHI+1                                                              1
   43   CONTINUE                                                               1
   46   YO=0.0                                                                 1
        PN=1.0                                                                 1
        DO 49 I=ILO,IHI                                                        1
   49   PN=PN*(XO-X(I))                                                        1
        DO 58 I=ILO,IHI                                                        1
        P=PN/(XO-X(I))                                                         1
        DO 55 J=ILO,IHI                                                        1
        IF(J-I)52,55,52                                                        1
   52   P=P/(X(I)-X(J))                                                        1
   55   CONTINUE                                                               1
        YO=YO+P*Y(I)                                                           1
   58   CONTINUE                                                               1
        RETURN                                                                 1
    1   FORMAT (97X,7HLAGIN2 ,I4,E12.5)                                        1
        END                                                                    1
```